PNWD-3369
WTP-RPT-085, Rev 0

Liquidus Temperature Testing and Model Evaluation Results

J. D. Vienna[a]
S. K. Cooley[a]
J. V. Crum[a]
T. B. Edwards[b]
J. Matyas[a]
D. K. Peeler[b]
G. F. Piepel[a]
D. E. Smith[a]

(a) Battelle—Pacific Northwest Division, Richland, Washington
(b) Westinghouse Savannah River Company, Aiken, South Carolina

December 2003

Prepared for Bechtel National, Inc.
under Contract 24590-101-TSA-W000-0004

LEGAL NOTICE

This report was prepared by Battelle Memorial Institute (Battelle) as an account of sponsored research activities. Neither Client nor Battelle nor any person acting on behalf of either:

MAKES ANY WARRANTY OR REPRESENTATION, EXPRESS OR IMPLIED, with respect to the accuracy, completeness, or usefulness of the information contained in this report, or that the use of any information, apparatus, process, or composition disclosed in this report may not infringe privately owned rights; or

Assumes any liabilities with respect to the use of, or for damages resulting from the use of, any information, apparatus, process, or composition disclosed in this report.

Reference herein to any specific commercial product, process, or service by trade name, trademark, manufacturer, or otherwise, does not necessarily constitute or imply its endorsement, recommendation, or favoring by Battelle. The views and opinions of authors expressed herein do not necessarily state or reflect those of Battelle.

Liquidus Temperature Testing and Model Evaluation Results

J. D. Vienna[(a)]
S. K. Cooley[(a)]
J. V. Crum[(a)]
T. B. Edwards[(b)]
J. Matyas[(a)]
D. K. Peeler[(b)]
G. F. Piepel[(a)]
D. E. Smith[(a)]

(a) Battelle—Pacific Northwest Division, Richland, Washington
(b) Westinghouse Savannah River Company, Aiken, South Carolina

December 2003

Test specification: *24590-HLW-TSP-RT-02-002*
Test plan: *TP-RPP-WTP-182*
Test exceptions: *24590- HLW-TEF-RT-03-001*
R&T focus area: *Vitrification/WFQ*
Test Scoping Statement(s): *B-75*

ACCEPTED FOR
WTP PROJECT USE

for W. L. Tamosaitis
12/16/03

Battelle—Pacific Northwest Division
Richland, WA 99352

COMPLETENESS OF TESTING

This report describes the results of work and testing specified by Test Specification 24590-HLW-TSP-RT-02-002, Rev. 0 and Test Plan TP-RPP-WTP-182, Rev. 0. The work and any associated testing followed the quality assurance requirements outlined in the Test Specification/Plan. The descriptions provided in this test report are an accurate account of both the conduct of the work and the data collected. Test plan results are reported. Also reported are any unusual or anomalous occurrences that are different from expected results. The test results and this report have been reviewed and verified.

Approved:

Paul B for GHB — 12/4/03

Gordon H. Beeman, Manager — Date
WTP R&T Support Project

Summary

Objectives

The objectives of this study as described in the Test Specification (Nelson 2002) and Test Plan (Vienna 2002) were to: 1) develop glass-composition and liquidus-temperature (T_L) data for use in model development for Waste Treatment and Immobilization Plant (WTP) high-level waste (HLW) glass melts and 2) evaluate available models relating T_L to HLW glass composition. Liquidus temperature can be defined as the highest temperature at which a melt is in thermodynamic equilibrium with its primary crystalline phase. It is important to WTP HLW glass processing because the dilaterious effects of crystal accumulation in the melter may be avoided if the melter is operated at a temperature above T_L. The data and models are required for formulation of optimized HLW glass compositions, process modeling, process control, and rapid adjustments to HLW composition changes.

Conduct of Testing

A statistically designed matrix of 31 simulated HLW glasses was developed to optimally augment a set of 35 existing compositions within the initial WTP HLW glass-composition region. Test glasses were fabricated from reagent-grade chemicals in platinum alloy crucibles, and equilibrium crystal fractions were measured as a function of temperature for each glass/melt. Uniform temperature furnaces were used to heat-treat glass samples for typically 24±2 hours followed by optical microscopy (OM), X-ray diffraction, and scanning electron microscopy (SEM) with energy-dispersive spectroscopy analyses. T_L was measured primarily using OM and SEM. Crystal fractions were interpolated to the temperature at 1 vol% of crystal, denoted $T_{0.01}$. $T_{0.01}$ is described by Kot and Pegg (2001) as the appropriate constraint to use in limiting the possible adverse effects of crystallinity in the WTP HLW melter. Existing T_L-composition model forms from the literature were fitted to subsets of new and existing T_L and $T_{0.01}$ data within the appropriate composition region. These models were evaluated for their relative capability to predict the T_L and $T_{0.01}$[(a)] of glasses not used in their fitting (e.g., validation data). A number of statistical measures were used to compare the models.

Results and Performance against Objectives

The T_L values of 25 glasses in the spinel primary phase field were measured and combined with T_L data from 135 glasses found in the literature.[(b)] The T_L values ranged from 780°C to 1306°C for the new data set and from 811°C to 1350°C for the literature data set. The $T_{0.01}$ of 14 glasses in the spinel primary phase field were measured[(c)] and combined with $T_{0.01}$ data from 31 glasses found in the literature. The $T_{0.01}$ values for the new glasses ranged from 740°C to 1180°C and from 633°C to 1158°C for the literature data set. The lower temperatures were expected for $T_{0.01}$ and will afford greater composition flexibility if used to constrain WTP HLW glass compositions.

(a) Note, models designed specifically for $T_{0.01}$ were not found, so those models designed for T_L were fitted to $T_{0.01}$ data to determine if they could be extended to its prediction.

(b) After the matrix was designed, the composition region of interest was expanded (Westsik 2003), which allowed for a larger number of literature data to be used in model evaluation.

(c) There were difficulties in obtaining $T_{0.01}$ in a number of glasses as described in Section 3.2.

Six different models:

- Defense Waste Processing Facility model [DWPFM]
- ion potential model [IPM]
- two solubility product models [SPMs]
- sub-lattice model [SLM]
- linear mixture model [LMM].

were fitted to the same model-development data sets and used to predict the same validation data sets. The six model forms were fitted to both T_L and $T_{0.01}$. It was found that all six of the models had difficulty in predicting $T_{0.01}$ with good precision; those results are likely due to the small available data set or the fact that the model forms were not specifically developed for $T_{0.01}$. Of all the models, the LMM was found to predict the $T_{0.01}$ of validation glasses with the best precision. The IPM and LMM models were found to most consistently predict the T_L of the model development and validation data sets with the smallest prediction uncertainties and the most favorable responses to other statistical measures for comparing models. The SLM also performed reasonably well. The LMM and SLM have more coefficients determined by the data and thus were more sensitive to outliers and influential data points in the modeling and validation data sets.

The LMM for $T_{0.01}$ and the IPM and LMM for T_L represent the best current models for predicting the $T_{0.01}$ and T_L of WTP HLW glasses. These models performed the best at predicting glasses not used to fit them and incorporating all the published data found in this composition region. In the future, these models can be improved by adding more data, and other model forms may be developed that give better performance.

Quality Requirements

The testing conducted under this activity was performed under the quality assurance program of the Battelle—Pacific Northwest Division's WTP Support Project (WTPSP). This quality-assurance program complies with the DOE Office of Civilian Radioactive Waste Management, Quality Assurance Requirements and Description document (DOE/RW-0333P, Rev. 11) (DOE 2002). Model evaluation was performed under the Westinghouse Savannah River Company (WSRC) Quality Assurance Programs as defined in the WSRC Quality Assurance Management Plan, WSRC-RP-92-225, the WSRC Quality Assurance Manual 1Q, and the SRTC Procedures Manual L1, which are responsive to the requirements of DOE Quality Assurance Orders, 10 CFR 830 Subpart A, NQA-1-1989, Part 1, Basic and Supplementary Requirements and NQA-2A-1990, Subpart 2.7, and the Office of Civilian Radioactive Quality Assurance Requirements Document (QARD), RW-0333P.

Issues

A significant issue was identified regarding the inability for models developed with the current data set to reliably predict $T_{0.01}$. It was found that either the model forms are ineffective for predicting $T_{0.01}$ or that the data set is too small to adequately fit the models. It is recommended that the WTP evaluate the impacts of using a $T_{0.01}$ model with low precision or constraining glass composition based on T_L (using higher precision models). If the former is determined to be more beneficial, then we recommend further

development of the $T_{0.01}$ database and, if necessary to obtain adequate prediction precision, further development of model forms specifically for $T_{0.01}$.

List of Symbols, Acronyms, and Abbreviations

a	fit parameter in solubility product model (Equation 4.5)
a_{sp}	chemical activity of spinel species (Equations 4.6 and 4.7)
$a(P_{(l)})$	activity of P in the liquid (Equations 4.12 and 4.14)
ACED	commercial software used to select candidate points for a mixture experimental design
APU	average prediction uncertainty (Equation 4.25)
b	slope of linear relationship between c and T (Equation 3.1)
b	fit parameter in solubility product model (Equation 4.5)
B_L	coefficient in non-linear relationship between c and T (Equation 2.1)
B_{sp}	a SLM proportionality factor (Equation 4.8
c	fraction of crystals in equilibrium with melt (used to represent either mass or volume fraction depending on application) (Equations 2.1 and 3.1)
c_0	coefficient in non-linear relationship between c and T (Equation 2.1)
c-T	crystal fraction – temperature relationship
C_i	SLM fit parameters, i = null, 0, 1, 2, 3, and sp (Equations 4.7, 4.8 and 4.9)
D_0	SLM intercept (Equation 4.11)
D_i	SLM model coefficient for the i^{th} component (Equations 4.11)
D_{sp}	SLP coefficient (Equation 4.11)
DOE	U.S. Department of Energy
DWPF	Defense Waste Processing Facility
DWPFM	DWPF model
EDS	energy dispersive spectroscopy
g_i	mass fraction or mass percent of i^{th} glass component (Equations 4.1, 4.2, 4.5, 4.10, and 4.11)
g_i	normalized mass fraction of i^{th} glass component (Equation 4.2)
HLW	high-level waste

HW	half-width (Equation 4.24)
IHLW	immobilized high-level waste
IPM	ion potential model
JMP	commercial software used in model fitting and evaluation (SAS institute)
K_P	DWPF model reaction constant (Equations 4.14, 4.16 and 4.17)
LAW	low-activity waste
LMM	linear mixture model
LOF	lack of fit
MCCVRT	a subroutine in MIXSOFT commercial software for the generation of extreme vertices of a constrained mixture experimental region
MIXSOFT	commercial software used to design mixture and other constrained region experiments
n	number of data points in a given model (Equations 4.19, 4.20, 4.21, and 4.22)
OM	optical (light) microscopy
OM T_L	T_L values determined using OM/SEM methods
p	number of model coefficients (Equations 4.20 and 4.22)
PDF	powder diffraction files
p_i	$1/T_L$ coefficient for ith glass component (Equation 4.9)
P_i	electric potential of ith electropositive glass component, $P_i = Z_i/r_i$ (Equation 4.3)
PNWD	Battelle—Pacific Northwest Division
PQM	partial quadratic mixture
PRESS	predicted error sums of squares (Equation 4.21)
q	number of component coefficients in a LMM (Equation 4.2)
QA	quality assurance
QAPjP	Waste Treatment Plant Support Project quality assurance project plan
QARD	Quality Assurance Requirements Document
r_i	ionic radius of component i

R	universal gas constant (Equations 4.6, 4.7, 4.8, 4.12, and 4.17)
R^2	coefficient of determination or coefficient of multiple determinations (Equation 4.19)
R^2_{adj}	adjusted coefficient of determination or multiple determinations (Equation 4.20)
RIQAS	commercial software used to perform crystal cell refinements
RPP	River Protection Project
R&T	Research and Technology
s	root mean squared error (Equations 4.22 4.24 and 4.25)
SEM	scanning electron microscopy
SLM	sub-lattice model
SLP	sub-lattice parameter (Equations 4.10 and 4.11)
SRM	standard reference material
SPM	solubility product model
T	temperature (Equation 2.1)
T_0	temperature at zero crystallinity, extrapolated from c-T data (Equation 3.1)
$T_{0.01}$	temperature at one mass percent crystal in glass, interpolated or extrapolated from c-T data
T_A	lowest temperature at which no crystals were identified
T_c	temperature at equilibrium fraction of crystals c
T_C	highest temperature at which crystals were identified
t_{cov}	intercept of the $T_i - P_i$ line for the remaining components (Equation 4.3)
t_{ion}	intercept of the $T_i - P_i$ line for the ionic components (Equation 4.3)
T_i	LMM coefficient for i^{th} glass component (Equation 4.1 and 4.3)
T_L	liquidus temperature
T_P	melting point of component P (Equations 4.12 and 4.17)
TRU	transuranic
UVESS	uncertainty-weighted validation error sum of squares
VESS	validation error sum of squares

VSL	Vitreous State Laboratory
WSRC	Westinghouse Savannah River Company
WTP	Waste Treatment and Immobilization Plant
WTPSP	WTP Support Project
x_i	mole fraction of the i^{th} electropositive element in glass (Equation 4.3)
x_j	concentration of j^{th} glass component (in model units) (Equations 4.24 and 4.25)
x_j, x'_j	concentration of j^{th} glass component (in model units) (Equations 4.24 and 4.25)
X	matrix of independent variables for all model data (in model units) (Equations 4.24 and 4.25)
X'	transpose of matrix X (Equations 4.24 and 4.25)
X_{sp}	molar fraction of spinel species in the melt (Equations 4.7, 4.9 and 4.10)
XRD	X-ray diffraction
y_i	measured T_L or $T_{0.01}$ for the i^{th} data point (Equations 4.19, 4.20, 4.21, 4.22, 4.23, and 4.26)
$\hat{y}_i$	predicted T_L or $T_{0.01}$ for the i^{th} data point (Equations 4.19, 4.20, 4.22, 4.23, and 4.26)
$\overline{y}_i$	average of the n measured T_L or $T_{0.01}$ values (Equations 4.19 and 4.20)
$\hat{y}_{(i)}$	predicted T_L or $T_{0.01}$ for the i^{th} data point without using the i^{th} data point in the model fit (Equation 4.21)
Z_i	formal valance of electropositive component i
z_j	total moles of j^{th} component in 100 g of glass
$\Delta H_{fus,P}$	standard Enthalpy change of fusion for component P
$\Delta\mu^\circ$	chemical potential difference between two states (Equation 4.6)
Θ_{cov}	slope of $T_i - P_i$ line for the remaining components (Equation 4.3)
Θ_{ion}	slope of $T_i - P_i$ line for the ionic components (Equation 4.3)
μ_P	chemical potential of component P
Σ_i	molar site distribution in site i=MT, M1, M2, T1, N1 (Equation 4.15)
$\varphi_{i,j}$	fraction of the moles of j associated with the ith site

Contents

Figures

Tables

1.0 Introduction

The high-level waste (HLW) glass that will be produced by the Waste Treatment and Immobilization Plant (WTP) is required to meet a number of performance, regulatory, processability, and cost-related requirements. To meet these requirements, glass property-composition models will be developed and used to relate key glass properties (e.g., melt viscosity and product consistency test response) to the composition of the HLW glass melter feed (Arakali et al. 2003). The processing-related constraint used to avoid the deleterious effects of solids accumulation in HLW melters—the liquidus temperature (T_L) constraint—is one of the most restrictive constraints on the loading of HLWs to be processed in the WTP (Hrma et al. 1996; Hrma and Vienna 2001; Kot and Pegg 2001; Perez et al. 2001; Vienna et al. 2002). The T_L of the glass melt, or more specifically, the model-predicted T_L of the glass melt plus the prediction uncertainties, directly impacts waste loading, compliance with the Contract (DOE 2003), and the cost of HLW immobilization. Therefore, the cost of immobilization of HLW in the WTP is directly related to the T_L of the glass and the precision of the T_L-composition model.

To meet or exceed the minimum HLW loading specified in 1.2.2.1.6 of the Contract (DOE 2003), glass composition must be optimized for minimum T_L with each HLW while maintaining other properties within an adequate range. For this reason, the Contract specifies in Requirement (3), Required Research and Technology Testing, Part (vii) of Standard 2 – Research, Technology, and Modeling (DOE 2003) that:

> The Contractor shall provide IHLW[(a)] glass properties data and information in a form that allows DOE to further develop glass properties models. These models will include: (1) liquidus temperature; (2) volume fraction of crystals below the liquids temperature;…"

The T_L-composition model is required to develop glass formulations and glass-composition envelopes for each HLW feed. The glass formulations are required for many WTP activities, including 1) HLW form qualification and delisting, 2) radioactive HLW vitrification tests, 3) physical and rheological properties testing of HLW melter feed, 4) HLW flowsheet demonstrations, 5) glass-former selection, and 6) blending/transport testing (Arakali et al. 2003).

Liquidus temperature is defined as the highest temperature at which a melt is in thermodynamic equilibrium with its primary crystalline phase. However, Hrma and colleagues (Hrma et al. 2001; Schill et al. 2001) have used models of crystal settling in a waste-glass melter to show that crystal layer growth at the melter bottom is much less sensitive to T_L than crystal size and fraction. Kot and Pegg (2001) state that "The amount [of crystals] that is acceptable will depend on the density and particle size of the phase in question, since the primary concern is sedimentation." Note that the considerations were validated over many years of melter testing and operation at the Vitreous State Laboratory (VSL) and Duratek. For this reason, the WTP "T_L constraint" is that the melt must contain less than 1 vol% of solid phases at 950°C[(b)] and that these phases must not settle rapidly (Kot and Pegg 2001).

(a) IHLW = immobilized high-level waste.

(b) $T_{0.01}$ is defined in this report as the temperature at which 1 vol% of spinel crystals are in equilibrium with the glass melt.

1.1 Objectives

The objectives of this study are two fold: 1) develop glass composition and T_L data for use in model development for the WTP HLW glass melts and 2) evaluate available T_L-composition model forms for use by WTP. The data collected in this study will be used to augment T_L data being collected under other tasks of the WTP Research and Technology (R&T) Program for use in T_L-composition modeling efforts. These data are expected to form a link between the vast data available in literature and the data being developed by the WTP R&T Program. Model comparisons are performed to determine which of the current candidate T_L-composition model forms will yield the lowest prediction uncertainties for glasses within the expected composition region of WTP HLW glasses. The model form(s) with the best predictive performances and lowest uncertainties will be recommended for fitting with future databases of T_L-composition data, including the appropriate data reported in literature, the data collected in this study, and the future data collected by the WTP R&T Program.

1.2 Program References

This study was performed according to the test plan *TP-RPP-WTP-182* (Vienna 2002), the test specification *24590-HLW-TSP-RT-02-002* (Nelson 2002), and test scoping statement *B-75* (Arakali et al. 2003). Additionally, test exception *24590-HLW-TEF-RT-03-001* was issued to modify the testing by updating the composition region of expected WTP HLW glasses (Westsik 2003).

2.0 Experimental Approach

Section 2.1 describes how the glass composition region of initial interest for this study was selected. Section 2.2 describes how a new test matrix of 31 glasses was selected to augment 35 existing glasses within the initial glass-composition region of interest. Sections 2.3 and 2.4, respectively, discuss how the new test-matrix glasses were fabricated, and spinel crystallinity versus temperature data were collected. Section 2.5 describes how the initial glass-composition region of interest was expanded based on WTP Project decisions after the work in Sections 2.1 and 2.2 was completed. Finally, Section 2.6 describes the quality assurance (QA) program and procedures under which the work described in this report was performed.

2.1 Initial Composition Region for Study

The composition region of interest was initially defined to include the IHLW glasses that the WTP anticipates processing from wastes in AZ-101, AZ-102, AY-101/C-104, and AY-102/C-106 tanks (DOE 2003). To determine the glass-composition region, the component concentration ranges of glasses currently available were first considered. Table 2.1 lists the concentration ranges of key HLW glass components from previous WTP studies, radioactive waste vitrification and product testing efforts, Contract limits, and the AZ-101 tank current baseline glass composition. Table 2.2 lists the subset of the composition regions given in Table 2.1 that was selected for data collection in this study. It was expected that this composition region would appropriately cover the glasses that are expected to be produced from the first four HLW streams.

Other components present in pretreated HLW in significant concentrations to influence T_L of the HLW glasses were added to each test glass at a fixed concentration. Examples of these other components are Ag_2O (0.08%), As_2O_5 (0.08%) and BaO (0.01%). Table 2.3 lists the compositions of each of the four nominal HLW feeds plus one nominal feed with pretreatment products added, scaled to a minimum waste loading that is required to meet one Contract specification (Fe_2O_3 for AZ-101, AZ-102, and C-106/AY-102; ThO_2 for C-104/AY-101; given in bold italics in the table) (DOE 2003). The mean value for each of the non-varied components (the "Others" component) used in test glasses from this study is also listed. The "Others" component makes up 1.94 mass percent of all test glasses, leaving 98.06% to be comprised by the systematically varied components.

Table 2.1. Concentration Ranges of Key Glass Components in Prior WTP HLW Glasses and Studies (in mass percent)

	VSL Statistical HLW Glass Matrix (Kot and Pegg 2001)			VSL Supplemental HLW Glass Matrix (Kot and Pegg 2001)			Contract Min. (DOE 2003)[c]	Glasses for Radioactive HLW Samples		Baseline Glass (Perez et al. 2001)[d]
	Min	Max	Comment	Min	Max	Comment	Min	Min	Max	AZ-101
Ag_2O	0.25	0.25	-	0.25	0.25	-	0.25	-	-	-[e]
Al_2O_3	0	11	-	7	7	-	11	2.4	7.8	5.2
B_2O_3	5	20	-	10	10	-	-	3.8	9.2	11.9
BaO	-	-	up to 4[a]	-	-	up to 4[a]	4	-	-	0
Bi_2O_3	-	-	up to 2[a]	-	-	up to 2[a]	2	-	-	0
CaO	0	7	-	2	2	-	7	0.3	0.7	0.3
CdO	-	-	up to 3[a]	-	-	up to 3[a]	3	-	-	0.1
Cr_2O_3	-	-	up to 0.5[a]	0.2	0.2	-	0.5	-	-	0
F	0.2	0.2	-	0.2	0.2	-	1.7	-	-	0
Fe_2O_3	2	12.5	-	2	12.5	-	12.5	4.5	12.6	12.2
K_2O	1	1	-	1	1	-	15	0	0.3	0
Li_2O	0	7	-	3	3	-	-	4.1	5.6	3.5
MgO	-	-	up to 2[a]	-	-	up to 2[a]	5	0.1	0.2	0.1
MnO_2	0.2	0.2	-	3.6	8.7	[b]	-	1	3.5	0.2
Na_2O	5	20	-	5	12	-	15	8.6	13.9	11.7
NiO	-	-	up to 3[a]	-	-	up to 3[a]	3	0.2	0.8	0.6
P_2O_5	-	-	up to 3[a]	0.25	0.25	-	3	0.3	0.6	0
PbO	-	-	up to 1[a]	-	-	up to 1[a]	1	-	-	0
SiO_2	30	50	-	30	47.8	-	-	44.3	47.8	47.4
SO_3	-	-	up to 0.5[b]	0.25	0.25	-	0.5	0	0	0.1
SrO	0.2	0.2	-	5.4	13.3	[b]	-	-	-	0
ThO_2	-	-	up to 0.2[a]	-	-	-	4	0	4.1	0
TiO_2	-	-	up to 1[a]	-	-	up to 1[a]	1	-	-	0
UO_2	-	-	up to 8[a]	-	-	-	8	0	3.9	0
ZnO	2	2	-	2	2	-	-	0	2	2
ZrO_2	0	10	-	3	3	-	10	0.1	4.9	3.8

(a) There were two sets of grouped components (Others1 and Others2) that were varied in the VSL statistical and supplemental studies. The components Cr_2O_3, P_2O_5, SO_3, ThO_2, and UO_2 were found in Others1 while BaO, Bi_2O_3, CdO, MgO, NiO, PbO, and TiO_2 were found in Others2. Their maximum concentrations in glass are listed.

(b) The concentrations of SrO and MnO_2 were varied according to $[SrO]=1.53\times[MnO_2]$ in the VSL supplemental study to reflect the ratio of these components coming from the strontium/transuranic precipitation process applied to selected low-activity waste (LAW) streams.

(c) Only one of the minimum concentrations listed must be met to obtain the minimum loading specified in the Contract.

(d) At the time testing was planned, baseline glass compositions for the current estimates of other HLW feed compositions were not available.

(e) "-" signifies an empty data field.

Table 2.2. Component Concentration Constraints for New T_L Data Collection (in mass percent)

Component	Min	Max	Component	Min	Max	Component	Min	Max
Al_2O_3	2	11	Li_2O	0	6	SrO	0	8.5
B_2O_3	4	15	MnO[(a)]	0	5	ThO_2	0	4
CdO	0	1	Na_2O	4	15	U_3O_8[(a)]	0	4
Cr_2O_3	0	0.5	NiO	0	1	ZnO	0	2.5
Fe_2O_3	3	13	SiO_2	38	53	ZrO_2	0	6
Fe_2O_3+ZrO_2	5	19	-[(b)]	-	-	-	-	-

(a) Note the change in reported oxidation states for Mn and U in this table.
(b) "-" signifies empty data field.

Table 2.3. Estimates of Feed and Other Non-Glass Former Constituents in the HLW Glasses (mass percent)

	Limit	AZ101	AZ102	C106/ AY102	C106/AY102 +Sr/TRU[(a)] ppt	C104/ AY101	Others[(b)]
Ag_2O	0.25	0.02	0.03	0.15	0.15	0.03	0.08
Al_2O_3	11	5.32	5.58	1.40	3.52	3.32	-[(c)]
As_2O_5	-	0.01	0.00	0.20	0.19	-	0.08
B_2O_3	-	0.18	0.52	0.15	0.14	0.10	-
BaO	4	0.02	0.01	0.01	0.01	0.00	0.01
BeO	-	0.00	0.00	-	-	0.01	-
Bi_2O_3	2	0.01	0.00	0.00	0.00	0.01	-
CaO	7	0.29	0.23	0.66	0.30	0.45	0.38
CdO	3	0.07	0.11	-	-	0.00	-
Ce_2O_3	-	0.01	0.00	0.00	0.00	0.00	
Cl	-	-	0.00	0.14	0.11	0.00	0.05
CoO	-	-	0.00	-	-	-	-
Cr_2O_3	0.5	0.01	0.02	0.04	0.08	0.06	-
Cs_2O	-	0.01	0.00	-	-	-	-
CuO	-	0.04	0.01	0.05	0.04	0.03	0.03
F	1.7	0.04	0.00	-	-	0.11	0.03
Fe_2O_3	12.5	***12.50***	***12.50***	***12.50***	***12.50***	8.83	-
K_2O	15	0.06	0.03	0.00	0.01	0.01	0.02
La_2O_3	-	0.42	0.38	0.24	0.24	0.15	0.28
Li_2O	-	0.02	0.01	0.00	0.01	0.09	-
MgO	5	0.11	0.07	0.55	1.16	-	0.38
MnO_2	-	0.17	0.36	2.98	3.97	1.41	-
MoO_3	-	0.01	0.01	0.01	0.01	-	0.01
Na_2O	15	1.47	0.77	0.47	0.58	1.47	-
Nd_2O_3	-	0.26	0.14	0.15	0.15	0.08	0.15
NiO	3	0.63	0.45	0.37	0.17	0.43	-
PbO	1	0.04	0.07	0.25	0.14	0.11	0.12
PdO	-	-	0.00	-	-	-	-[(d)]
P_2O_5	3	0.00	0.02	0.10	0.09	0.04	0.05
Pr_2O_3	-	-	0.03	-	-	0.02	0.01

Table 2.3 (cont'd)

	Limit	AZ101	AZ102	C106/ AY102	C106/AY102 +Sr/TRU[(a)] ppt	C104/ AY101	Others[(b)]
PuO_2	-	-	-	-	-	0.01	-
Rb_2O	-	0.00	-	-	-	0.02	0.01
Rh_2O_3	-	0.02	0.00	-	-	-	-[(d)]
RuO_2	-	-	-	-	-	-	-[(d)]
Sb_2O_3	-	-	-	0.11	0.25	-	0.07
SeO_2	-	-	-	0.21	0.37	-	0.12
SiO_2	-	0.42	1.01	2.09	2.03	2.30	-
SO_3	0.5	0.08	0.04	0.00	0.00	0.02	0.03
SrO	-	-	0.01	-	0.91	0.02	-
Tc_2O_7	-	0.03	-	0.04	-	-	-
ThO_2	4	-	-	-	-	***4.00***	-
TiO_2	1	0.01	0.00	0.03	0.14	0.02	0.04
UO_2	8	0.01	0.00	-	-	2.40	-
V_2O_5	-	-	-	-	-	0.01	-
Y_2O_3	-	-	-	-	-	0.01	-
ZnO	-	0.02	0.01	0.02	0.07	0.02	-
ZrO_2	10	3.89	1.77	0.12	0.26	8.73	-
Total	-	26.19	24.22	23.07	27.63	34.31	1.94

(a) TRU = transuranic.

(b) The component concentrations in "Others" are the average concentrations for the components in glass for the five wastes listed. Components were not included in others if 1) they are being systematically varied in the study, 2) there is no non-radioactive isotope, or 3) the concentration in glass would be less than 0.01%. There is only a single "Others" in this study instead of the two groups of others listed in Table 2.1.

(c) "-" signifies an empty data field.

(d) Recent data (personal communication from I. L. Pegg, Catholic University of America, Washington, D.C.) suggests that noble metals concentrations may be significant in spinel crystals from WTP HLW glass melts, and their concentration in the melt may influence T_L and/or $T_{0.01}$. However, noble metals were not included in the test-matrix glasses due to the low (generally zero) concentrations in the waste-composition estimates available at the time of this study.

2.2 Test-Matrix Design

One objective of this work was to generate additional T_L-composition data to augment existing literature data. The existing data were obtained from Vienna et al. (2002) by sorting all the T_L data in the spinel primary phase field by composition and selecting those glasses in the initial HLW glass-composition region of interest (as defined in Table 2.2). A total of 35 glasses met these criteria, with their compositions and T_L values listed in Table A.1 of Appendix A with a "Y" in the "matrix" column. These 35 glass compositions were augmented with new test-matrix glasses selected as described below.

There are a number of methods for developing a test matrix of glasses to augment existing data. For this study, the 35 existing glasses were augmented in a layered design (Piepel et al. 1993; Piepel et al. 2002a)

with a centroid, an outer layer, and an inner layer. In addition, three existing glasses were added to the matrix to assure the reproducibility of results from previous studies to this study. Finally, the new test matrix was developed in two parts: the first part contained radioactive components (Th and U) while the second did not. The inner layer was defined by adding 25% of the range of component concentrations to the minimum and, likewise, 25% subtraction from the maximum. This method provided for evenly distributing data across the range of component concentrations with most points at the minimum concentration plus 0, 25%, 50%, 75%, and 100% of the range.

Table 2.4 lists the 31 new glasses that were fabricated and tested: 10 with U and/or Th and 21 without. These glasses are designated WTP-TL-01 to WTP-TL-31. The first three glasses, WTP-TL-01 to WTP-TL-03, are replicates of three VSL glasses (HLW99-73, HLW99-86, and HLW99-85, respectively). WTP-TL-04 is a centroid glass with U and Th, whereas WTP-TL-05 is a centroid glass without U and Th. WTP-TL-31 is a replicate of WTP-TL-05, the nonradioactive centroid glass. The remaining glass compositions were then selected to augment the 41 compositions determined so far (namely, the existing 35 glass compositions listed in Appendix A and the 6 pre-selected glasses denoted WTP-TL-01 to WTP-TL-05 and WTP-TL-31). The steps to select the remaining 25 glass compositions proceeded as follows.

Step 1: Existing Glass Compositions Normalized

The ACED[(a)] optimal experimental design software (Welch 1987), which was used to select the 25 remaining glass compositions, requires that the proportions of mixture components used as design factors sum to 1.0. Hence, the mass fractions of the 15 components listed in Table 2.2 were normalized to sum to 1.0 for the 35 existing glass compositions and the 6 pre-selected compositions. Before normalization, the mass fractions of the 15 components listed in Table 2.2 totaled from 0.9020 to 0.9943 for the 35 existing glass compositions. For the 6 pre-selected glass compositions, the mass fractions totaled 0.9806 (as discussed in Section 2.1). The normalized compositions were used only for design selection purposes by ACED and are not the actual glass compositions to be tested.

Step 2: Outer-Layer Glasses with U and Th Generated and Four Selected

The 81,103 vertices of the outer layer with U and Th were generated using the MCCVRT[(b)] routine in MIXSOFT[(c)] (Piepel 1999). Then, ACED was used to select 4 glasses to augment the previous 35 + 6 = 41 glasses. Optimal experimental design software can converge to local optima, so multiple "tries" are recommended. ACED was used to generate 10 tries (sets of 4 glasses) using each of three design criteria referred to as D-, G-, and V-optimality.[(d)] A linear mixture model (See Section 4.1.1) was assumed for use with these optimality criteria. Various design summary statistics in the ACED output were compared, and one set of 4 outer-layer (with U and Th) glasses was selected. These glasses are listed as WTP-TL-06 to WTP-TL-09 in Table 2.4.

(a) ACED = commercial software used to select candidate points for a mixture experimental design.
(b) MCCVRT = a subroutine in MIXSOFT commercial software for the generation of extreme vertices of a constrained mixture experimental region.
(c) MIXSOFT = commercial software used to design mixture and other constrained region experiments.
(d) The three different criteria can be described as: D-optimal minimizes the uncertainties in model coefficients, G-optimal minimizes the maximum uncertainty model predictions, and V-optimal minimizes the average uncertainty in model predictions (see Welch 1987 for further discussion of these criteria).

Step 3: Inner-Layer Glasses with U and Th Generated and Five Selected

The 55,161 vertices of the inner layer with U and Th were generated using the MCCVRT routine in MIXSOFT. ACED was used to select 5 of these vertices to optimally augment the existing 35 glasses, the pre-selected 6 glasses, and the 4 glasses selected in Step 2. Again, 10 tries were made with each of the three design criteria, based on a linear-mixture model. The design summary statistics for the 30 tries were compared, and a set of 5 inner layer (with U and Th) glasses was selected. These glasses are listed as WTP-TL-10 to WTP-TL-14 in Table 2.4.

Step 4: Outer-Layer Glasses Without U and Th Generated and Eight Selected

The 15,024 vertices of the outer layer without U and Th were generated using the MCCVRT routine in MIXSOFT. ACED was used to select 8 of these vertices to optimally augment the existing 35 glasses, the pre-selected 6 glasses, the 4 glasses selected in Step 2, and the 5 glasses selected in Step 3. Again, 10 tries were made with each of the three design criteria, based on a linear-mixture model. The design summary statistics for the 30 tries were compared, and a set of 8 outer layer (without U and Th) glasses was selected. These glasses are listed as WTP-TL-15 to WTP-TL-22 in Table 2.4.

Step 5: Inner-Layer Glasses Without U and Th Generated and Five Selected

The 11,432 vertices of the inner layer without U and Th were generated using the MCCVRT routine in MIXSOFT. ACED was used to select 8 of these vertices to optimally augment the existing 35 glasses, the pre-selected 6 glasses, the 4 glasses selected in Step 2, the 5 glasses selected in Step 3, and the 8 glasses selected in Step 4. Again, 10 tries were made with each of the three design criteria, based on a linear-mixture model. The design-summary statistics for the 30 tries were compared, and a set of 8 inner layer (without U and Th) glasses was selected. These glasses are listed as WTP-TL-23 to WTP-TL-30 in Table 2.4.

Glasses WTP-TL-01 through -31 (listed in Table 2.4), when combined with the initial 35 glasses listed in Appendix A, yield a data set with low correlations between pairs of the 15 systematically varied components as shown by the correlation coefficients in Table 2.5 and the scatter-plot matrix in Figure 2.1. Low correlations are good in that the data will support fitting models in which the effects of glass components on T_L can be properly estimated.

Table 2.4. Test Matrix Glasses for T_L Data Collection

Glass	Comment	Al_2O_3	B_2O_3	CdO	Cr_2O_3	Fe_2O_3	Li_2O	MnO	Na_2O	NiO	SiO_2	SrO	ThO_2	U_3O_8	ZnO	ZrO_2
WTP-TL-01	HLW99-73	7.41	5.29	0.00	0.21	2.11	3.17	3.07	14.22	0.00	46.19	5.77	0.00	0.00	2.11	3.17
WTP-TL-02	HLW99-86	7.05	10.06	0.00	0.20	2.01	3.02	2.92	9.50	0.00	48.07	5.49	0.00	0.00	2.01	3.02
WTP-TL-03	HLW99-85	7.04	10.06	0.95	0.20	7.30	3.02	2.92	7.44	0.95	39.81	5.48	0.00	0.00	2.01	3.02
WTP-TL-04	rad cent	6.49	9.48	0.50	0.25	7.98	2.99	2.50	9.48	0.50	45.41	4.24	2.00	2.00	1.25	2.99
WTP-TL-05	norad cent	6.76	9.88	0.52	0.26	8.32	3.12	2.60	9.88	0.52	47.34	4.42	0.00	0.00	1.30	3.12
WTP-TL-06	rad outer	2.00	15.00	0.00	0.00	13.00	0.00	0.00	15.00	0.00	38.00	2.56	4.00	0.00	2.50	6.00
WTP-TL-07	rad outer	11.00	4.00	1.00	0.50	5.00	6.00	5.00	4.00	1.00	48.06	8.50	4.00	0.00	0.00	0.00
WTP-TL-08	rad outer	10.56	4.00	1.00	0.00	3.00	6.00	5.00	15.00	1.00	38.00	8.50	0.00	4.00	0.00	2.00
WTP-TL-09	rad outer	11.00	4.00	1.00	0.00	3.00	6.00	5.00	15.00	1.00	39.56	0.00	4.00	4.00	2.50	2.00
WTP-TL-10	rad inner	8.75	12.25	0.25	0.38	10.50	4.50	1.25	6.75	0.25	41.75	2.12	1.00	3.00	1.88	3.43
WTP-TL-11	rad inner	4.25	12.25	0.75	0.38	5.50	1.50	3.75	12.25	0.25	48.94	2.12	1.00	3.00	0.62	1.50
WTP-TL-12	rad inner	8.75	12.25	0.25	0.38	5.50	1.50	1.25	11.18	0.75	41.75	6.38	3.00	3.00	0.62	1.50
WTP-TL-13	rad inner	7.18	12.25	0.75	0.38	5.50	4.50	3.75	12.25	0.25	41.75	2.12	3.00	1.00	1.88	1.50
WTP-TL-14	rad inner	4.25	6.75	0.25	0.12	10.50	2.81	3.75	6.75	0.25	45.13	6.38	3.00	3.00	0.62	4.50
WTP-TL-15	norad outer	2.00	15.00	0.00	0.50	13.00	6.00	0.00	15.00	0.00	38.06	8.50	0.00	0.00	0.00	0.00
WTP-TL-16	norad outer	11.00	15.00	1.00	0.50	13.00	6.00	5.00	4.00	0.00	40.06	0.00	0.00	0.00	2.50	0.00
WTP-TL-17	norad outer	11.00	15.00	0.00	0.50	6.56	0.00	0.00	15.00	1.00	38.00	8.50	0.00	0.00	2.50	0.00
WTP-TL-18	norad outer	2.00	15.00	1.00	0.00	9.06	6.00	0.00	15.00	1.00	38.00	8.50	0.00	0.00	2.50	0.00
WTP-TL-19	norad outer	2.00	15.00	1.00	0.50	3.00	0.00	5.00	15.00	1.00	49.56	0.00	0.00	0.00	0.00	6.00
WTP-TL-20	norad outer	2.00	4.00	1.00	0.50	13.00	6.00	0.00	4.00	1.00	49.56	8.50	0.00	0.00	2.50	6.00
WTP-TL-21	norad outer	2.00	4.00	1.00	0.50	13.00	0.02	5.00	15.00	0.00	53.00	2.04	0.00	0.00	2.50	0.00
WTP-TL-22	norad outer	7.52	15.00	1.00	0.00	13.00	0.04	5.00	4.00	0.00	38.00	8.50	0.00	0.00	0.00	6.00
WTP-TL-23	norad inner	8.75	6.75	0.75	0.38	7.93	4.50	3.75	6.75	0.75	49.25	6.38	0.00	0.00	0.62	1.50
WTP-TL-24	norad inner	4.25	6.75	0.25	0.12	10.50	1.50	3.75	11.18	0.75	49.25	6.38	0.00	0.00	1.88	1.50
WTP-TL-25	norad inner	4.25	12.25	0.75	0.12	5.50	4.50	3.75	12.25	0.25	42.94	6.38	0.00	0.00	0.62	4.50

Table 2.4 (cont'd)

Glass	Comment	Al_2O_3	B_2O_3	CdO	Cr_2O_3	Fe_2O_3	Li_2O	MnO	Na_2O	NiO	SiO_2	SrO	ThO_2	U_3O_8	ZnO	ZrO_2
WTP-TL-26	norad inner	4.25	12.25	0.75	0.38	5.50	4.50	3.75	12.25	0.25	42.68	6.38	0.00	0.00	0.62	4.50
WTP-TL-27	norad inner	8.75	12.25	0.25	0.12	10.50	4.50	3.75	6.75	0.25	42.44	2.12	0.00	0.00	1.88	4.50
WTP-TL-28	norad inner	4.25	6.75	0.25	0.12	10.50	4.50	3.75	6.75	0.25	48.18	6.38	0.00	0.00	1.88	4.50
WTP-TL-29	norad inner	4.25	12.25	0.75	0.38	10.50	1.50	3.75	6.75	0.25	49.25	5.20	0.00	0.00	0.62	2.61
WTP-TL-30	norad inner	8.75	12.25	0.25	0.38	5.50	4.50	1.58	6.75	0.75	48.85	2.12	0.00	0.00	1.88	4.50
WTP-TL-31	norad cent dup	6.76	9.88	0.52	0.26	8.32	3.12	2.60	9.88	0.52	47.34	4.42	0.00	0.00	1.30	3.12

Table 2.5. Pair-Wise Correlations for Augmented Data set Major Component Concentrations

	Al_2O_3	B_2O_3	CdO	Cr_2O_3	Fe_2O_3	Li_2O	MnO	Na_2O	NiO	SiO_2	SrO	ThO_2	U_3O_8	ZnO	ZrO_2
Al_2O_3	1.000	-0.249	0.024	-0.001	-0.139	0.168	0.006	0.010	0.117	-0.240	-0.169	0.073	0.141	-0.098	-0.026
B_2O_3	-[(a)]	1.000	-0.006	-0.022	-0.073	-0.241	-0.146	-0.180	-0.202	-0.259	0.065	-0.037	-0.127	0.080	-0.090
CdO	-	-	1.000	0.066	-0.075	-0.018	0.119	-0.214	-0.052	-0.109	0.189	0.100	0.095	0.117	-0.111
Cr_2O_3	-	-	-	1.000	-0.017	-0.004	0.176	-0.055	0.032	-0.033	0.220	0.046	-0.039	0.205	0.038
Fe_2O_3	-	-	-	-	1.000	-0.014	-0.214	0.005	0.041	0.032	-0.294	-0.180	-0.253	-0.239	-0.063
Li_2O	-	-	-	-	-	1.000	0.007	-0.141	0.219	-0.092	-0.017	-0.019	0.113	-0.069	-0.052
MnO	-	-	-	-	-	-	1.000	-0.206	0.065	-0.150	0.270	0.179	0.249	0.220	0.040
Na_2O	-	-	-	-	-	-	-	1.000	0.120	-0.159	-0.295	-0.069	-0.003	-0.195	0.025
NiO	-	-	-	-	-	-	-	-	1.000	-0.038	-0.078	-0.001	0.067	-0.183	0.047
SiO_2	-	-	-	-	-	-	-	-	-	1.000	-0.389	-0.275	-0.239	-0.315	-0.160
SrO	-	-	-	-	-	-	-	-	-	-	1.000	0.170	0.126	0.483	-0.041
ThO_2	-	-	-	-	-	-	-	-	-	-	-	1.000	0.527	0.237	-0.039
U_3O_8	-	-	-	-	-	-	-	-	-	-	-	-	1.000	0.087	-0.140
ZnO	-	-	-	-	-	-	-	-	-	-	-	-	-	1.000	-0.039
ZrO_2	-	-	-	-	-	-	-	-	-	-	-	-	-	-	1.000

(a) "-" signifies an empty data field.

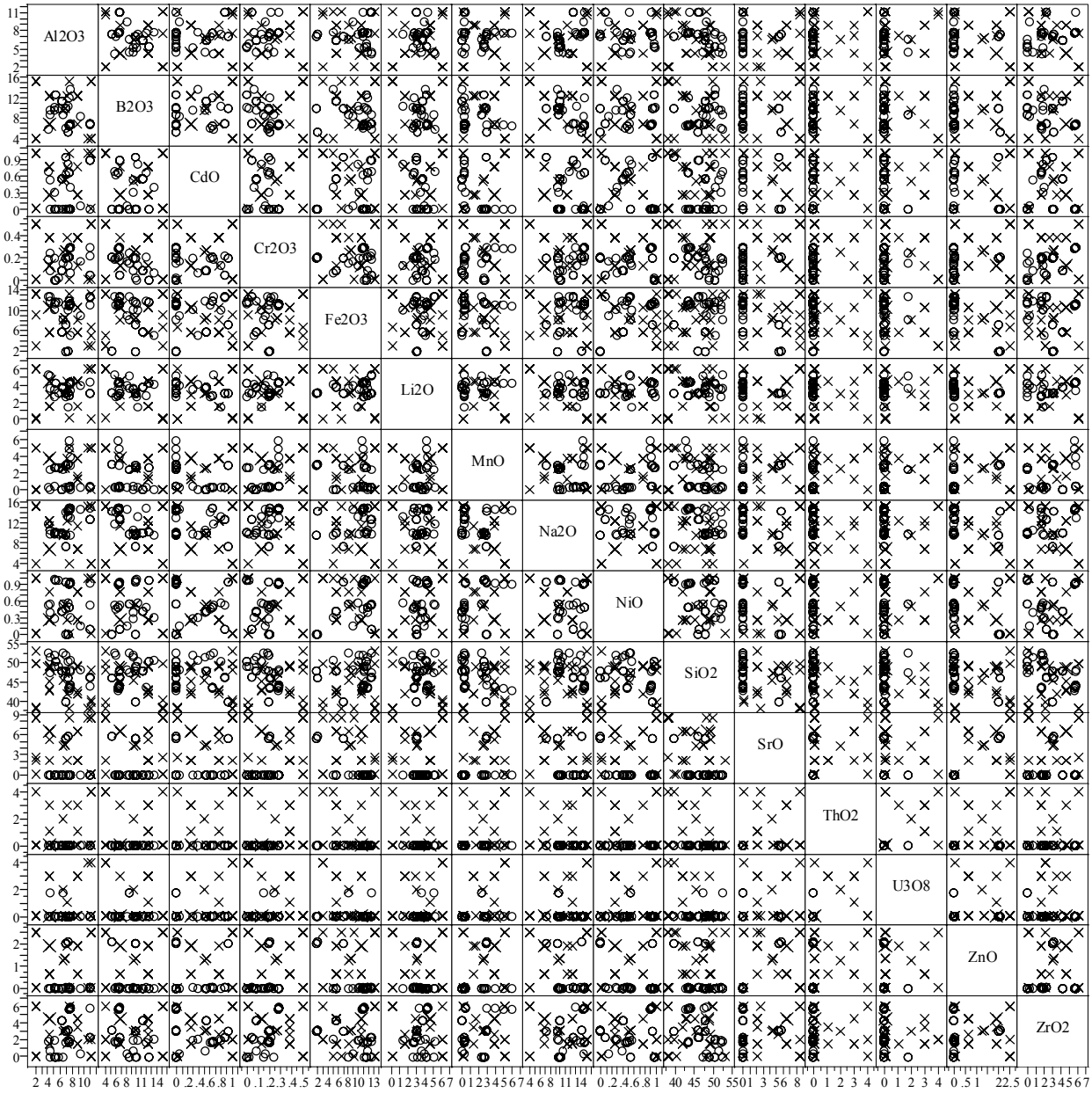

Figure 2.1. Scatterplot Matrix of Component Concentrations of Augmented Data Set
(in mass percent, × represents new test-matrix glasses and ○ represents previous literature data.)

2.3 Glass Fabrication

Glasses were fabricated in batches of 200 g using approved procedures (Schweiger 2002). Single-metal oxides and carbonates along with Na_2SO_4, NaF, NaCl, H_3BO_3, and $NaPO_3$ were used as source chemicals. The reagent grade or better raw materials were weighed in the proper proportions, thoroughly mixed in an agate mill, and melted in a covered Pt/Rh crucible for 1 hour. The melts were quenched on a clean stainless-steel plate, ground in a tungsten carbide mill (to roughly 1-μm particles) to assure homogeneity, remelted for 1 hour, and again quenched. The glasses were examined for the presence of precipitated crystalline material and undissolved solids after each melt using optical (light) microscopy (OM), X-ray diffraction (XRD), and/or scanning electron microscopy (SEM) with energy dispersive spectroscopy (EDS) when necessary. If solid materials other than noble metals and their oxides were present after the first melt, the second melt was performed at a higher temperature (typically 50°C higher, determined by examination of the sample). If solid materials were present after the second melt, a third melt was made to dissolve the material. The glasses from the crucible walls and the pour patty (the glass cast on the steel plate) were examined. Following the final melt, the pour-patty glass was segregated from the glass remaining on the crucible wall and was then used for testing as described below. A few glasses crystallized upon cooling after they were poured onto the stainless steel plate (evident by the size and distribution of crystals in the pour patty). For these glasses, increasing the melting temperature would not change the outcome because they are single phased at the melting temperature and only crystallize upon cooling. In these cases, a homogenous sample was obtained by grinding the glass in a tungsten-carbide mill to a fine powder (roughly 10-μm particles).

2.4 Testing

Matrix glasses were tested according to approved procedures previously published (Vienna et al. 2001). The T_L was determined using the uniform-temperature method where glass is ground, sized, and washed of contamination and fines, except for glasses that crystallized upon quenching. As stated above for these glasses, the entire batch was milled to a fine powder to assure that a homogenous sample was used for T_L testing. The sized or powdered glass was loaded into Pt/Au or Pt/Rh crucibles with very tight-fitting lids and heat treated in a uniform-temperature furnace for a fixed time. The nominal heat-treatment time of 24±2 hours was typically used unless there were signs of complication due to not obtaining equilibrium or excessive volatility. In the case of such complications, the heat-treatment times were adjusted accordingly. At the completion of heat treatment, the samples were quenched by placing the crucible, containing glass, on a steel plate or refractory block unless crystallization occurred upon quenching in which case the outer crucible surfaces were quenched in water. Each specimen was examined using an optical microscope at a minimum magnification of 70×. Select samples were thin-sectioned and examined from 100× up to 2000×. Select samples were also analyzed by XRD to determine the structure and concentration of crystalline phases in the glass.

For the non-radioactive and a few select radioactive glasses, XRD samples were prepared and analyzed according to procedure GDL-XRD Rev. 0. One- to 2-gram samples of glass plus CaF_2 (an internal standard) were weighed out to a tenth of a milligram and then milled for 2 minutes in a tungsten-carbide mill to assure a homogenous powdered sample for mounting in the XRD holder. Samples were scanned using a step size of 0.04° 2-Θ over a scan range of 10 to 70° 2-Θ with a hold time of 4 seconds at each step. Crystalline phases were identified using Jade 6.0 software (MDI 2001a) equipped with search match capabilities and PDF (powder diffraction file, release 1999) database. Whole-pattern fitting to each pattern was performed to determine the concentration of each identified crystalline phase using RIQAS 4.0 software (MDI 2001b). The ratio was then used to determine the mass fraction of spinel in the

sample. The technique was confirmed using samples with known spinel spikes. The confirmation samples suggested a precision of roughly 0.1 mass% for this technique.[(a)]

The equilibrium crystal fraction (c) versus temperature (T) curves were generated, such as the example shown in Figure 2.2 (for a previously tested high-temperature melter glass). The number of c-T datapoints measured per glass ranged from 6 to 15. These data were fitted to an equation derived by Vienna et al. (1997) using ideal-solution assumptions:

$$c = c_0 \left\{ 1 - \exp\left[-B_L \left(\frac{1}{T} - \frac{1}{T_L} \right) \right] \right\} \tag{2.1}$$

where c is the equilibrium fraction of crystal, c_0 is the maximum crystal fraction as T approaches 0 K, and B_L is a temperature-independent parameter related to the enthalpy of crystal formation divided by the gas constant. If the data were insufficient to fit this non-linear model, a linear approximation was used. For example, if a secondary phase formed before the curvature (related to B_L) could be precisely estimated, then a linear approximation was used. These models were then used to interpolate to the T at 1 vol% spinel ($T_{0.01}$).

The polished thin sections were examined by OM and/or SEM to determine if crystalline material (e.g., spinel) was present in the sample and to estimate (qualitatively) the concentration and type of phase present. The heat treatments were conducted at different temperatures in a manner to narrow the gap between the highest temperature at which crystals were present in the melt (T_C) and the lowest temperature at which no crystals were present in the melt (T_A). The range of temperatures, between T_A and T_C, was progressively reduced until less than or equal to roughly 10°C, and the T_L is estimated within that 10°C range (usually as the center of the range).

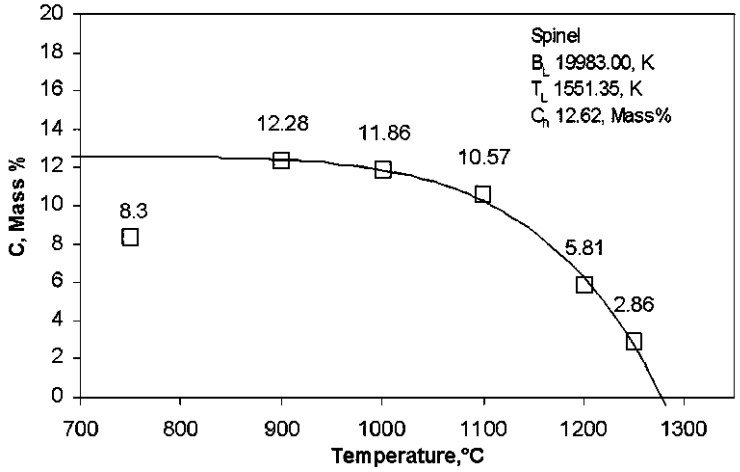

Figure 2.2. Example c – T Curve for a Simulated HLW Glass

(a) The precision in vol% is dependent on the densities of spinel and glass/melt phase.

2.5 Expanded Composition Region and Additional Literature Data

After the matrix design and start of testing, a revised estimate of the HLW-glass-composition region of interest to WTP was defined (Westsik 2003). The new HLW-glass-composition region (as defined in Table 2.6) is larger than the initial composition region (as defined in Table 2.2). An additional 103 existing T_L-composition data points were identified as lying within the expanded composition region and are listed in Table A.1 in Appendix A. A scatterplot matrix (for components listed in Table 2.6) of the new, combined, data is shown in Figure 2.3, and correlation coefficients for the same components are listed in Table 2.7.

Table 2.6. Expanded Glass Composition Region of Interest (mass percent oxides)[(a)]

Combined	Min	Max
Al_2O_3	***1.92%***	11.00%
B_2O_3	4.00%	15.00%
CdO	0.00%	***1.60%***
Cr_2O_3	0.00%	0.50%
Fe_2O_3	***1.92%***	***14.00%***
Li_2O	0.00%	6.00%
MnO	0.00%	***6.96%***
Na_2O	***3.91%***	15.00%
NiO	0.00%	1.00%
SiO_2	***34.81%***	53.01%
SrO	0.00%	***9.95%***
ThO_2	0.00%	***5.97%***
U_3O_8	0.00%	***6.20%***
ZnO	0.00%	***3.98%***
ZrO_2	0.00%	***9.67%***

(a) Bold and italic numbers represent changes from previous ranges.

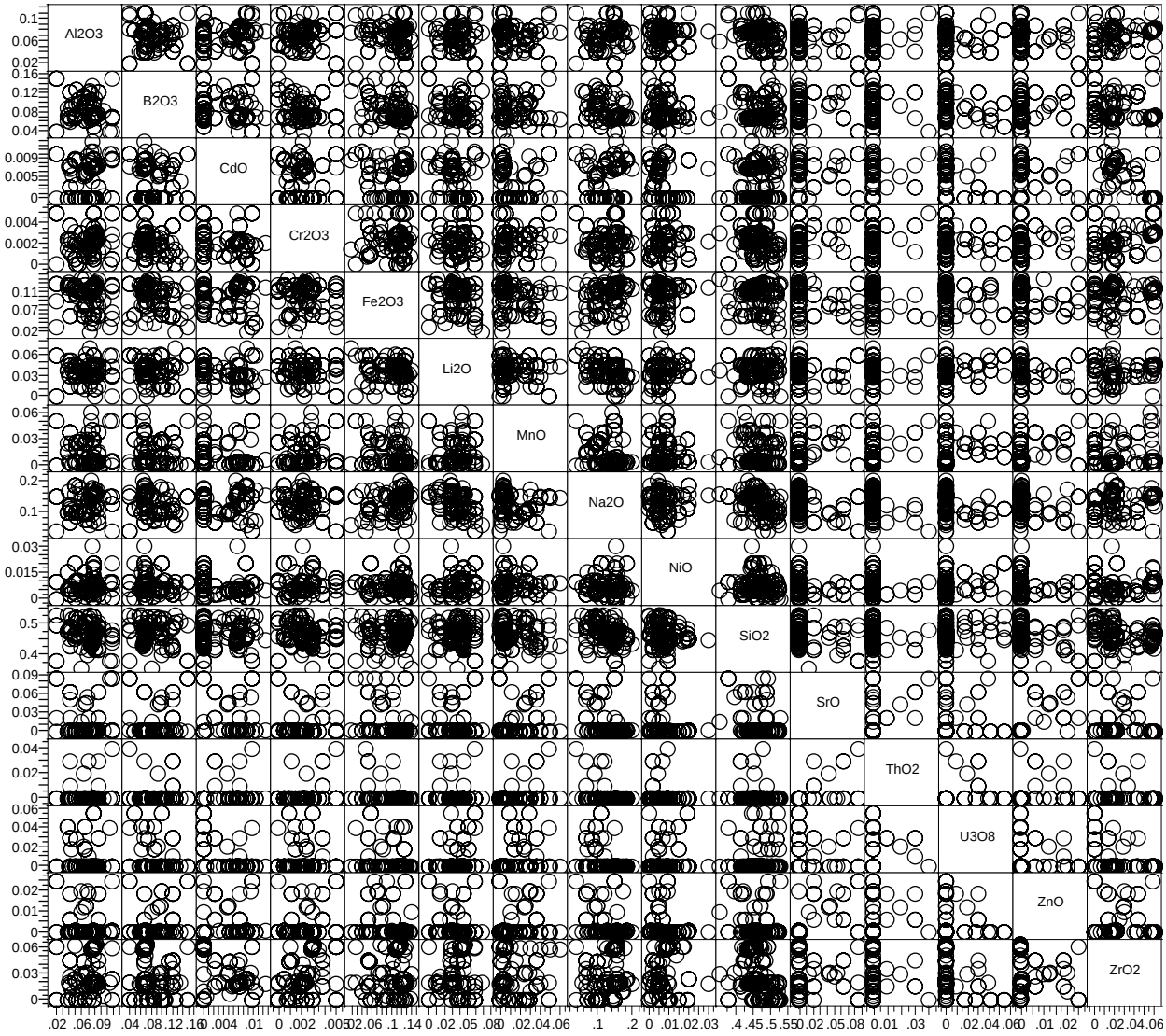

Figure 2.3. Scatter-Plot Matrix of Major Component in New Combined Data Set (in mass fractions)

Table 2.7. Correlation Coefficients for New Combined Data Set

	Al_2O_3	B_2O_3	CdO	Cr_2O_3	Fe_2O_3	Li_2O	MnO	Na_2O	NiO	SiO_2	SrO	ThO_2	U_3O_8	ZnO	ZrO_2
Al_2O_3	1.00	-0.29	-0.01	0.04	0.00	0.01	-0.25	0.20	0.09	-0.24	-0.24	0.05	-0.13	-0.27	0.15
B_2O_3	-[(a)]	1.00	-0.04	-0.06	-0.47	-0.04	0.11	-0.32	-0.09	-0.08	0.26	0.08	-0.01	0.30	-0.18
CdO	-	-	1.00	-0.24	-0.02	-0.40	-0.13	0.11	-0.33	0.01	0.17	0.08	-0.27	0.12	-0.29
Cr_2O_3	-	-	-	1.00	-0.05	0.02	0.09	0.06	0.09	-0.18	0.17	0.18	-0.06	0.17	0.37
Fe_2O_3	-	-	-	-	1.00	-0.24	-0.37	0.41	-0.10	-0.08	-0.32	-0.27	-0.27	-0.20	0.06
Li_2O	-	-	-	-	-	1.00	0.10	-0.38	0.28	0.02	0.06	0.00	0.22	-0.13	0.14
MnO	-	-	-	-	-	-	1.00	-0.40	0.04	0.01	0.39	0.30	0.29	0.32	-0.11
Na_2O	-	-	-	-	-	-	-	1.00	0.00	-0.42	-0.38	-0.29	-0.37	-0.31	0.22
NiO	-	-	-	-	-	-	-	-	1.00	-0.07	-0.13	-0.09	0.18	-0.16	0.05
SiO_2	-	-	-	-	-	-	-	-	-	1.00	-0.30	-0.11	0.12	-0.23	-0.26
SrO	-	-	-	-	-	-	-	-	-	-	1.00	0.41	0.08	0.65	-0.07
ThO_2	-	-	-	-	-	-	-	-	-	-	-	1.00	0.21	0.21	-0.07
U_3O_8	-	-	-	-	-	-	-	-	-	-	-	-	1.00	-0.01	-0.36
ZnO	-	-	-	-	-	-	-	-	-	-	-	-	-	1.00	-0.05
ZrO_2	-	-	-	-	-	-	-	-	-	-	-	-	-	-	1.00

(a) "-" indicates an empty data field. This matrix is symmetric and only the upper right half is shown.

2.6 Quality Assurance

Battelle—Pacific Northwest Division (PNWD) implements the River Protection Project (RPP)-WTP quality requirements by performing work in accordance with the PNWD Waste Treatment Plant Support Project QA project plan (QAPjP) approved by the RPP-WTP QA organization. This work was performed to the quality requirements of NQA-1-1989 Part I, Basic and Supplementary Requirements, and NQA-2a-1990, Part 2.7. These quality requirements are implemented through PNWD's *Waste Treatment Plant Support Project (WTPSP) Quality Assurance Requirements and Description Manual*. The analytical requirements are implemented through PNWD's *Conducting Analytical Work in Support of Regulatory Programs*.

The data-collection part of this study was performed under the additional QA requirements of DOE/RW-0333P, Rev. 11, *Quality Assurance Requirements and Description* (DOE 2002), which were met as described in TP-RPP-WTP-182 Rev. 0. Additional data were collected from literature for use in model evaluation. The QA program used in developing the literature data was identified for each data set. Those data sets without a QA Program specifically reported in the source documents were labeled as "unknown" for QA.

A listing of the procedures implementing the DOE/RW-0333P QA requirements (DOE 2002) is included in Table 2.8.

Table 2.8. QA Implementing Procedures Used in this Study

QARD Section	Yes	No	Implementing Procedure Title	Justification for Exclusion
1	X		WTPSP Manual Section 1.1, Organization QA-RPP-WTP-101, Communication and Commitment (Interface) Control QA-RPP-WTP-1501, Nonconforming Items	
2	X		WTPSP Manual Section 2.1, Quality Assurance Program QA-RPP-WTP-205, Quality Assurance Plans QA-RPP-WTP-208, Applying QA Controls (Grading) WTPSP Manual Section 18.1, Audits QA-RPP-WTP-1801, Internal Audits QA-RPP-WTP-201, Indoctrination and Training	
3		X	WTPSP Manual Section 3.1 QA-RPP-WTP-301, Hand Calculations QA-RPP-WTP-302, Design Control	Design activities will not be performed; however, hand calculations may be performed as per procedure QA-RPP-WTP-301.
4	X		WTPSP Manual Section 4.1 QA-RPP-WTP-401, Purchase Requisitions QA-RPP-WTP-404, Procurement of Internal Quality Affecting Services	Internal, quality-affecting services will not be needed for model evaluation work scope so that QA-RPP-WTP-404 will not be needed.
5	X		WTPSP Manual Section 5.1 QA-RPP-WTP-501, Preparation, Review, and Approval of QA Implementing Procedures	
6	X		WTPSP Manual Section 6.1 QA-RPP-WTP-601, Document Control QA-RPP-WTP-602, Document Change Control	
7	X		WTPSP Manual Section 7.1 QA-RPP-WTP-401, Purchase Requisitions QA-RPP-WTP-404, Procurement of Internal Quality Affecting Services	Internal, quality-affecting services will not be needed for model evaluation work scope so that QA-RPP-WTP-404 will not be needed.
8		X	WTPSP Manual Section 8.1 QA-RPP-WTP-801, Sample Control	Model-evaluation work will not involve working with samples.
9		X	WTPSP Manual Section 9.1 QA-RPP-WTP-902, Control of Special Processes	No special processes will be used.
10		X	WTPSP Manual Section 10.1	Inspections will not be performed as part of this test plan.
11	X		WTPSP Manual Section 11.1 QA-RPP-WTP-1101, Scientific Investigation QA-RPP-WTP –604, Independent Technical Review	
12		X	WTPSP Manual Section 12.1 QA-RPP-WTP-1201, Calibration Control System	Model-evaluation work will not involve the use of calibrated equipment.
13		X	WTPSP Manual Section 13.1 QA-RPP-WTP-1301, Handling, Storage, and Shipping	Model-evaluation work will not involve the handling, storage, or shipment of materials.

Table 2.8 (Contd)

QARD Section	Yes	No	Implementing Procedure Title	Justification for Exclusion
14		X	WTPSP Manual Section 14.1 QA-RPP-WTP-1401, Inspection and Test Status and Tagging	Model-evaluation work will not involve the use of items that require inspection, testing, or operational statusing.
15	X		WTPSP Manual Section 15.1 QA-RPP-WTP-1501, Nonconforming Items	
16	X		WTPSP Manual Section 16.1 QA-RPP-WTP-1601, Trend Analysis QA-RPP-WTP-1602, Corrective Action	
17	X		WTPSP Manual Section 17.1 QA-RPP-WTP-1701, Records System QA-RPP-WTP-1704, Laboratory Record Books	Laboratory Record Books will not be needed or used for model-evaluation work.
18	X		WTPSP Manual Section 18.1 QA-RPP-WTP-1801, Internal Audits	

QARD Supplement	Yes	No	Implementing Procedure Title	Justification for Exclusion
I	X		QA-RPP-WTP-SCP, Software Control QA-RPP-WTP-604, Independent Technical Review QA-RPP-WTP-401, Purchase Requisitions QA-RPP-WTP-1701, Records System	
II		X	WTPSP Manual Section 8.1 QA-RPP-WTP-801, Sample Control	Model-evaluation work will not involve working with samples.
III	X		WTPSP Manual Section 11.1 QA-RPP-WTP-1101, Scientific Investigation QA-RPP-WTP –604, Independent Technical Review	
IV		X	PNWD has no Field Surveying responsibilities.	Not applicable.
V	X		QA-RPP-WTP-SV, Control of the Electronic Management of Data	

Model evaluation was performed under the WSRC QA Programs as defined in the WSRC QA Management Plan, WSRC-RP-92-225, the WSRC QA Manual 1Q and SRTC Procedures Manual L1, which are responsive to the requirements of DOE QA Orders, 10 CFR 830 Subpart A, NQA-1-1989, Part 1, Basic and Supplementary Requirements and NQA-2A-1990, Subpart 2.7, and the Office of Civilian Radioactive QARD, RW-0333P.

3.0 Testing Results

The data collected from the new test-matrix glasses discussed in Section 2.2 are presented and discussed in this section. Section 3.1 presents the T_L results, while Section 3.2 discusses the crystalline-fraction-data collected. Section 3.3 discusses the measurement results on a standard glass for which measurements were made along with the new test-matrix glasses.

3.1 Liquidus Data

Data gathered for each glass heat treatment are summarized in Appendix B. The T_L values of test glasses are summarized in Table 3.1. These values span the range from 780°C to 1306°C for those glasses in the spinel primary phase field. Glasses WTP-TL-01, -02, -06, -09, and -22 were found to be in a different primary phase field (as described in Appendix B). WTP-TL-16 was found to show excessive volatility at temperatures near T_L, so T_L could not be accurately determined. The T_L values of these six glasses were not used in model development or validation.

Table 3.1. Summary of T_L Values for Glasses Listed in Table 2.4 (determined by OM/SEM method)

Glass ID	OM T_L	Phase	Glass ID	OM T_L	Phase	Glass ID	OM T_L	Phase
WTP-TL-01	760	Crystobalite	WTP-TL-12	1,306	Spinel	WTP-TL-23	1,219	Spinel
WTP-TL-02	711	Albite	WTP-TL-13	1,006	Spinel	WTP-TL-24	1,071	Spinel
WTP-TL-03	1,191	Spinel	WTP-TL-14	1,195	Spinel	WTP-TL-25	820	Spinel
WTP-TL-04	1,117	Spinel	WTP-TL-15	780	Spinel	WTP-TL-26	972	Spinel
WTP-TL-05	1,107	Spinel	WTP-TL-16	(a)	Spinel	WTP-TL-27	1,165	Spinel
WTP-TL-06	898	Clinopyroxene	WTP-TL-17	1,197	Spinel	WTP-TL-28	1,064	Spinel
WTP-TL-07	1,296	Spinel	WTP-TL-18	852	Spinel	WTP-TL-29	1,254	Spinel
WTP-TL-08	1,029	Spinel	WTP-TL-19	1,070	Spinel	WTP-TL-30	1,257	Spinel
WTP-TL-09	1,289	Thorianite	WTP-TL-20	1,259	Spinel	WTP-TL-31	1,119	Spinel
WTP-TL-10	1,194	Spinel	WTP-TL-21	1,181	Spinel	-(b)	-	-
WTP-TL-11	1,070	Spinel	WTP-TL-22	1,249	Zircon	-	-	-

(a) T_L could not be determined due to excessive volatility at T near T_L.
(b) "-" signifies an empty data field.

Samples of WTP-TL-01 and -30 were analyzed using SEM/EDS to determine the presence and chemistry of phases other than glass in the samples. WTP-TL-01 in particular was analyzed to determine if the irregular-shaped particles in the glass were spinels or undissolved noble metals. Figure 3.1 shows micrographs of the irregular-shaped Ru-rich particles as determined by EDS with compositions listed in Table 3.2. No spinels were found in the SEM sample or samples analyzed by XRD. Figure 3.2 shows spinel crystals with their composition listed in Table 3.3. Table 3.4 compares the composition of WTP-TL-30 glass with its target value.

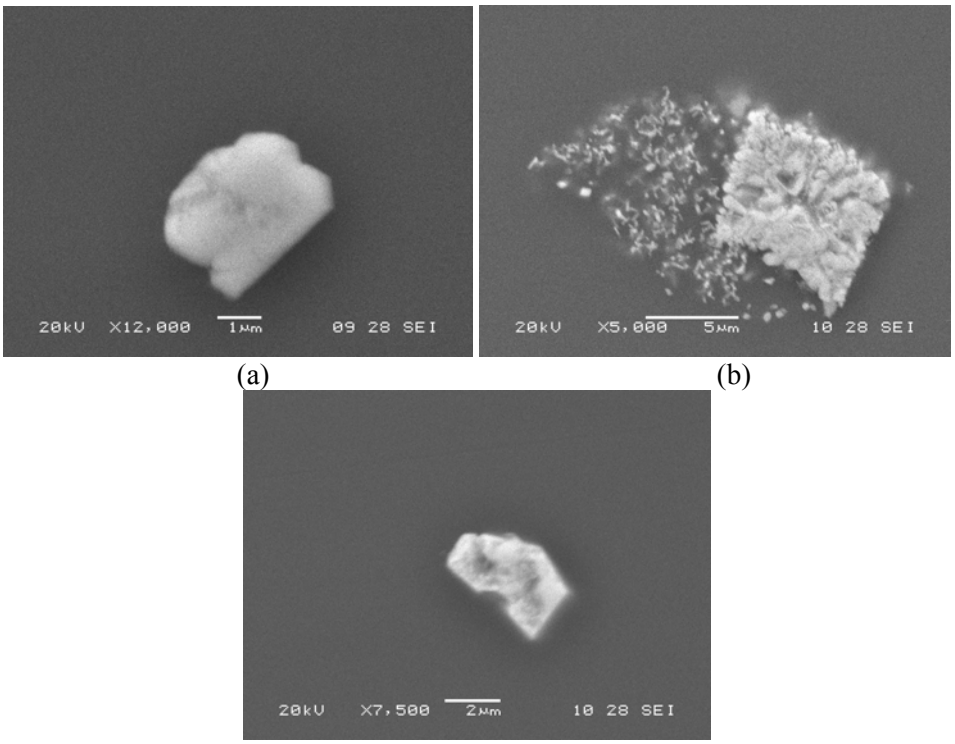

(a) (b)

(c)

Figure 3.1. Scanning Electron Micrographs of Ru-Rich Particles in WTP-TL-01 Glass Heat Treated at 1001°C for 24 Hours

Table 3.2. Elemental Concentrations of Particles in WTP-TL-01 Heat Treated at 1001°C for 24 hours, mass%

Element	Particle 1 (a)	Particle 2 (b)	Particle 3 (c)
O	30.65	16.93	17.06
Na	3.83	0.00	0.00
Al	1.25	0.00	0.00
Si	6.69	2.10	0.00
Ru	57.58	80.97	82.94
Total	100.00	100.00	100.00

WTP-TL-30 heat treated at 1226°C for 24 hours was also examined by SEM/EDS to determine the morphology and chemistry of the crystalline phase present in the sample. SEM micrographs show areas of agglomerated spinels with varying shapes. Measured EDS data on the crystals indicate that the crystals are spinel. The crystals contain high concentrations of Cr, Fe, Ni, Zn, Mn, and O.

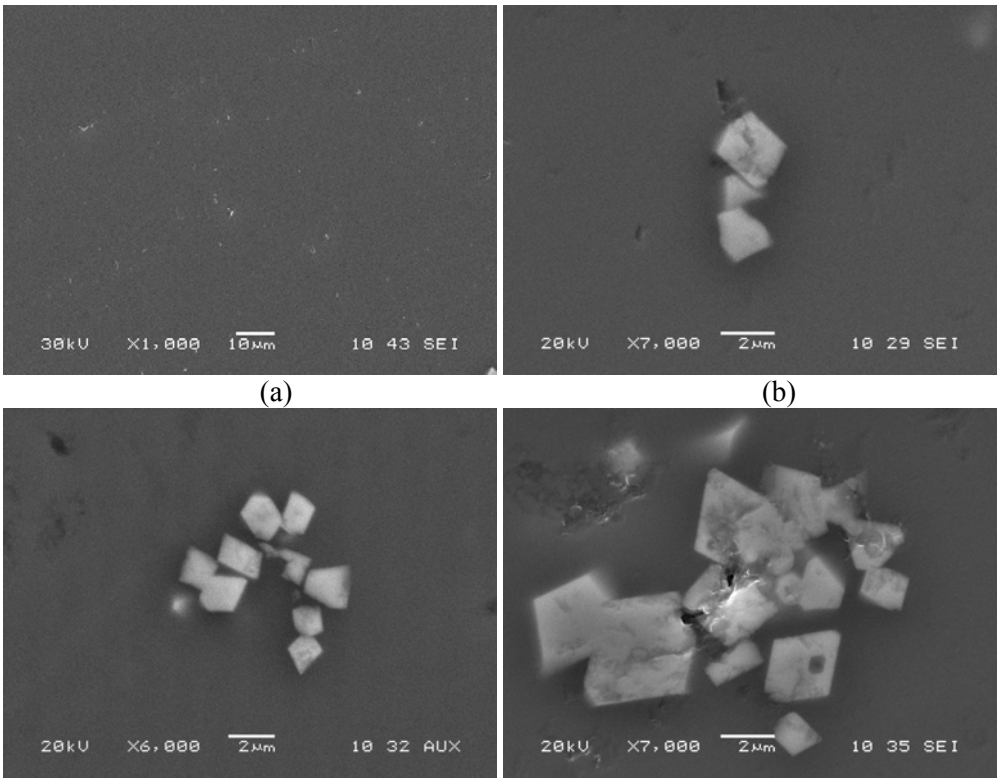

Figure 3.2. Scanning Electron Micrographs of Ru-Rich Particles in WTP-TL-30 Glass Heat Treated at 1226°C for 24 hours

Table 3.3. Elemental Concentrations of Particles in WTP-TL-30 Heat Treated at 1226°C for 24 hours

	Wt%
O	20.54
Na	7.49
Mg	0.63
Al	1.54
Si	3.72
Cr	34.65
Mn	2.87
Fe	10.21
Ni	5.23
Zn	13.14
Total	100

Table 3.4. Comparison of Measured and Target Glass Compositions of WTP-TL-30 Heat Treated at 1226°C for 24 hours, wt%

Component	Measured	Target[(a)]
Al_2O_3	10.25	10.66
B_2O_3	NA	0.00
CaO	0.47	0.46
CdO	NA	0.30
Cr_2O_3	0.31	0.46
Fe_2O_3	7.13	6.70
Li_2O	NA	0.00
MgO	0.38	0.46
MnO	1.97	1.93
Na_2O	5.94	8.22
NiO	0.79	0.91
SiO_2	58.80	59.52
SrO	3.21	2.58
ZnO	2.80	2.29
ZrO_2	7.96	5.48
Total	100.01	99.97

(a) Renormalized to exclude B_2O_3, Li_2O, and Others to compare with limitations of EDS system.

3.2 Crystal-Fraction Data

The crystal fractions measured in test samples are listed in Appendix B and summarized in Table 3.5. The crystal fractions for literature data are tabulated in Appendix A. An example of a whole pattern fit to a scan is shown in Figure 3.3. Shown in the plot are the following: XRD pattern in red, refined pattern in green, difference pattern in black, fitted background in blue, red vertical lines and peak fit at each peak for Fluorite, and blue line for Magnetite (spinel). From this fit, RIQAS calculates the concentration of each crystalline phase as shown in Figure 3.4.

Few of the glasses had sufficient data to accurately determine c_0, T_L, and B_L coefficients (from Equation 2.1). The primary reasons for this discrepancy were that the data largely appeared to be linear in the region of $T_{0.01}$, and secondary-phase in-growth at lower temperatures limited the temperature range of testing. Therefore, the data were fit using a linear relationship according to:

$$T = T_0 + bc \tag{3.1}$$

where T_0 and b are fit parameters, with T_0 being the estimated temperature for zero fraction of spinel (i.e., T_L). Any samples that showed non-linearity at lower temperatures were excluded from the fit to give the best approximation of T_0 and $T_{0.01}$ (only six data points were removed).

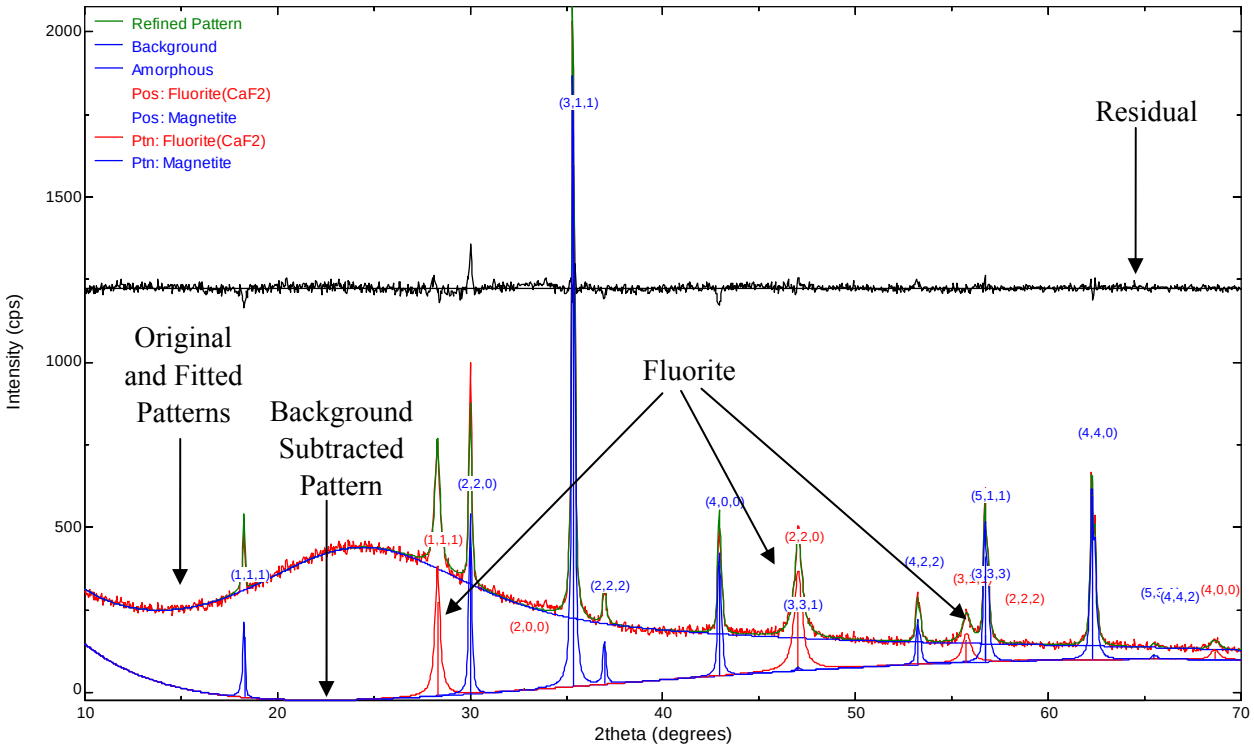

Figure 3.3. Example XRD Pattern with Cell Refinement

```
* *  QUANTITATIVE PHASE ANALYSIS:

Job Title:
  File: C:\XRD patterns\WTP-tl\EXAMPLE SCAN.DIF
  Title:
  Range: 10 - 70, Inc: 0.04, Time: 4,  NPts: 1501.

  Quantitative results based on all phases used in the refinement.
  The sum of the weight fractions is normalized to 1.0
  ---------------------------------------------------------------
        Phases                          wt%    (ESD)   Size(A)
  ---------------------------------------------------------------
   1: Fluorite(CaF2)                   39.1   ( 1.8)      203
   2: Magnetite                        60.9   ( 1.2)      575
  ---------------------------------------------------------------

  Quantitative results scaled to the internal standard.
  The values in () are calculated excluding the internal standard.
  Internal Std Phase:  1,  wgt: 5.00%,  Wgt.Scale=7.82, K*RHO(M)/U(M): 2183.79
  ---------------------------------------------------------------
        Phases                          wt%  (No Std)  Size(A)
  ---------------------------------------------------------------
   1: Fluorite(CaF2)                    5.0  (  0.0)      203
   2: Magnetite                         7.8  (  8.2)      575
  ---------------------------------------------------------------
       Total weight %:                 12.8  (  8.2)
```

Figure 3.4. Example Mass% Determination from RIQAS

To convert the measured mass fraction of spinel to a volume fraction, the densities of both the crystal and melt phases are required. Because the densities of both phases are unknown functions of temperature and composition, gross estimates of densities based on values at room temperature were assumed. The spinel density assumed was 5.29 g/cm^3 (based on cell refinements performed as described in Appendix B). The densities of the glasses, which averaged roughly 2.7 g/cm^3, were calculated according to the model reported by Vienna et al. (2002). Because the thermal expansion of the liquid phase is greater than that of the solid phase, it is expected that the actual volume fractions of crystal at melt temperature is lower than estimated by this method—thus providing some degree of conservatism in this assessment. It is difficult to assess how composition impacts the thermal expansion of the melt and therefore the melt density at T_L with current tools. No assessment is made as to how these assumptions impact the outcome.

Table 3.5. Summary of *c*-*T* Data for Test Glasses Containing Spinel[(a)]

ID	*T*	*c*	ID	*T*	*c*	ID	*T*	*c*	ID	*T*	*c*	ID	*T*	*c*
-03	900	2.2	-16	1251	0.9	-20	900	3.4	-23	1140	0.2	-27	1000	2.1
-03	1000	1.2	-16	1275	0.7	-20	1000	2.2	-23	1176	0.1	-27	1100	0.7
-03	1100	0.6	-17	894	1.1	-20	1100	1.4	-24	900	1.7	-29	900	2.7
-05	800	1.6	-17	1000	0.6	-20	1200	0.5	-24	1000	0.4	-29	1000	1.5
-05	900	1.2	-17	1100	0.2	-21	802	1.7	-24	1025	0.2	-29	1100	0.9
-05	1025	0.5	-17	1140	0.1	-21	900	1.2	-26	750	0.4	-29	1200	0.6
-05	1050	0.3	-18	750	0.2	-21	1000	0.7	-26	800	0.3	-30	900	1.8
-16	1002	4.5	-19	900	1.7	-21	1100	0.4	-26	900	0.2	-30	1000	1.2
-16	1101	3	-19	1000	0.5	-23	1100	0.4	-26	916	0.1	-30	1100	0.8
-16	1200	1.8	-19	1025	0.4	-23	1126	0.3	-27	900	5.3	-30	1200	0.3

(a) Glass IDs are given by WTP-TL-×× with -×× listed in the table, *T*'s are in °C, and *c*'s are reported in mass %.

The T_L and *c*-*T* data were evaluated for self consistency and consistency with other data in the same composition region. A slightly different set of T_0 values (Equation 3.1) was fit to the *c*-*T* data as an estimate of T_L (e.g., extrapolation of *c*-*T* data to *c*=0).[(a)] This revised set of T_0, focused on a very low concentration region, will be called XRD T_L to set them aside from the T_0 values aimed at defining $T_{0.01}$ and OM T_L values. The XRD T_L value from each test glass that had sufficient data (including literature data) was compared to the T_L measured using OM (denoted as OM T_L). A summary of the results is listed in Table 3.6. Figure 3.5 shows this comparison of OM T_L and XRD T_L. All XRD T_L values were within 50°C of the OM T_L values with the exception of three samples (Sp-Na-1, Sp-Na-3, and Sp-Cr-1 from literature), showing excellent agreement. The measurement uncertainty from the OM method is estimated at 12°C (Vienna et al. 2001, for example). The three glasses with greater than 50°C differences in OM T_L and XRD T_L measurements are labeled in the figure and were not used in model evaluations. To help determine the cause for the relatively large differences in T_L and T_0, one of the three glasses, Sp-Cr-1, was re measured by both techniques—yielding virtually the same results, as shown in the figure. This suggests that the cause of the differences is likely not random experimental error.

(a) With data that were not quite linear, a portion of the data surrounding the 0.01 volume fraction was used to interpolate to $T_{0.01}$ while only the higher temperature data were used to extrapolate to T_L.

Table 3.6. Summary of Spinel Fraction Data (with *T* in °C and *c* in volume fraction)

Glass ID	OM T_L	Phase[1]	*b* (slope)	T_0 (int)	XRD T_L	$T_{0.01}$	Comments
WTP-TL-01	760	si	-[b]	-	-	-	Crystobalite
WTP-TL-02	771	ab	-	-	-	-	Albite
WTP-TL-03	1,191	sp	-23,256	1,164	1,167	932	-
WTP-TL-04	1,117	sp	-	-	-	-	XRD performed on only one sample.
WTP-TL-05	1,107	sp	-37,037	1,088	1,115	740	-
WTP-TL-06	898	cl	-	-	-	-	Clinopyroxene
WTP-TL-07	1,296	sp	-	-	-	-	Thorianite is secondary phase.
WTP-TL-08	1,029	sp	-	-	-	-	Thorianite is secondary phase.
WTP-TL-09	1,289	th	-	-	-	-	Thorianite is primary phase and spinel is secondary phase.
WTP-TL-10	1,194	sp	-	-	-	-	XRD not Performed.
WTP-TL-11	1,070	sp	-	-	-	-	XRD not performed.
WTP-TL-12	1,306	sp	-	-	-	-	XRD not performed.
WTP-TL-13	1,006	sp	-	-	-	-	XRD not performed.
WTP-TL-14	1,195	sp	-	-	-	-	XRD not performed.
WTP-TL-15	780	sp	-	-	-	-	Foaming caused loss of sample at lower temperatures.
WTP-TL-16	NA	sp	-14,085	1,320	1,316	1,180	Volatility caused crystallization to increase at temperatures near or above the XRD T_L.
WTP-TL-17	1,197	sp	-17,241	997	1,159	825	-
WTP-TL-18	852	sp	-	-	-	-	Crystallinity only detected at 750°C using XRD.
WTP-TL-19	1,070	sp	-18,182	1,058	1,051	876	-
WTP-TL-20a	1,259	sp	-19,231	1,252	1,247	1,068	$T_{0.01}$ includes both phases.
WTP-TL-20b	-	zs	-10,989	1,072	1,075	1,068	Zircon is secondary phase.
WTP-TL-21	1,181	sp	-43,478	1,198	1,192	764	-
WTP-TL-22a	1,249	zs	-19,608	1,401	1,365	-	Zircon is primary phase.
WTP-TL-22b	-	h	-6,135	1,160	1,177	-	Hematite is secondary phase.
WTP-TL-23	1,219	sp	-11,364	1,060	1,203	947	-
WTP-TL-24	1,071	sp	-15,385	1,045	1,036	891	-
WTP-TL-25	820	sp	-	-	-	-	Crystallinty below detection limits of xrd at temperatures tested.
WTP-TL-26	972	sp	-120,627	1,000	981	-	1 vol% crystallinity projected to be below Tg.
WTP-TL-27a	1,165	sp	-8,403	1,120	1,117	1,047	$T_{0.01}$ includes both phases.
WTP-TL-27b	-	zs	-140,252	1,200	-	1,047	Zircon is secondary phase.
WTP-TL-28	1,064	sp	-33,333	1,433	1433	1,100	-

Table 3.6 (Contd)

Glass ID	OM T_L	Phase[(1)]	*b* (slope)	T_0 (int)	XRD T_L	$T_{0.01}$	Comments
WTP-TL-22a	1,249	zs	-19,608	1,401	1,365	-	Zircon is primary phase.
WTP-TL-22b	-	h	-6,135	1,160	1,177	-	Hematite is secondary phase.
WTP-TL-23	1,219	sp	-11,364	1,060	1,203	947	-
WTP-TL-24	1,071	sp	-15,385	1,045	1,036	891	-
WTP-TL-25	820	sp	-	-	-	-	Crystallinty below detection limits of XRD at temperatures tested.
WTP-TL-26	972	sp	-120,627	1,000	981	-	1 vol% crystallinity projected to be below Tg.
WTP-TL-27a	1,165	sp	-8,403	1,120	1,117	1,047	$T_{0.01}$ includes both phases.
WTP-TL-27b	-	zs	-140,252	1,200	-	1,047	Zircon is secondary phase.
WTP-TL-28	1,064	sp	-33,333	1,433	1433	1,100	-
WTP-TL-29	1,254	sp	-27,778	1,251	1,257	973	-
WTP-TL-30a	1,257	sp	-40,683	1,259	1,259	974	$T_{0.01}$ includes both phases.
WTP-TL-30b	-	zs	-22306	1054	1,054	-	Zircon is secondary phase.
WTP-TL-31	1,119	sp	-	-	-	-	Very few crystals detected.

(a) sp–spinel, h--hematite, zs–zircon, th—thorianite, si–crystobalite, cl–clinopyroxene, ab–albite.
(b) "-" signifies an empty data field.

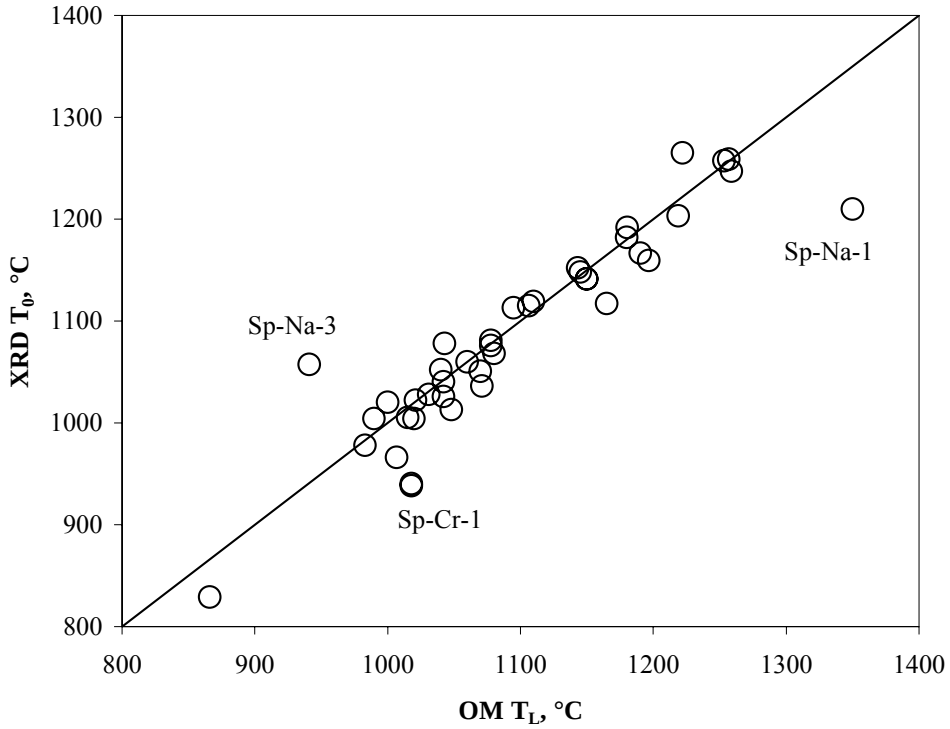

Figure 3.5. Comparison of OM T_L with T_0

3.3 Standard Glass-Measurement Results

The procedure used calls for a T_L determination of a standard glass with each batch of samples tested in each furnace used. For this study, the standard glass selected for verification of the measurement technique was the Liquidus Temperature Standard Reference Material 773 (SRM-773) (NBS 1980). This particular reference material has an average measured T_L of 991±5°C. The results for SRM-773 T_L measurement in each test furnace before and after testing were within 991±5°C, with the exception of furnace R1 (used for the measurement of all radioactive glasses). In Furnace R1, the measured T_L value of SRM-773 was within 5°C of 991°C before testing began. After the last sample heat treatment was performed, but before the final SRM-773 could be measured, the furnace elements were lost due to a crucible being placed too close to them, and the furnace was rebuilt. As measurement before and after was not a requirement of the procedure, no further actions were taken.

4.0 Model Evaluation

The models fitted to T_L and $T_{0.01}$ data, discussed in Section 3.0, are presented and compared in this section. Section 4.1 presents the various model forms. Section 4.2 explains the methods for model evaluation, Sections 4.3 and 4.4 discuss the selection and subsetting of data to be used in fitting and evaluation of models, and Sections 4.5 and 4.6 summarize the results of model fitting (including summary statistics) and model comparisons for the T_L and $T_{0.01}$ models, respectively.

4.1 Description of Evaluated Models

There are a host of models for predicting the T_L of commercially important glass melts and other solutions. However, we considered only those models thought to be successful in predicting the T_L in WTP HLW glasses. Several models proposed for use in predicting the T_L of HLW glass melts in the spinel primary phase field have been reported in literature, including:

1. Linear mixture model (LMM) (i.e., a first-order expansion of T_L data in composition) described in general by Cornell (2002) and applied to waste glass T_L by Hrma et al. (1999)
2. Ion potential model (IPM) described by Vienna et al. (2001)
3. Solubility-product models (SPM) described by Plodinec (1999)
4. Sub-lattice model (SLM) described by Gan and Pegg (2001)
5. Defense Waste Processing Facility (DWPF) T_L model (DWPFM) described by Brown et al. (2001).

The models are described in more detail in the following subsections.

Another model form that was considered but not included in this comparison is the partial quadratic mixture (PQM) model discussed by Piepel et al. (2002b). A PQM model consists of an LMM (Model #1 above) plus selected squares or crossproducts of components in the linear terms. It is reasonable that components of spinel (e.g., Fe, Cr, and Ni), or glass components that enhance or detract from the formation of spinel, could appear in such quadratic terms. PQM models with such terms could have improved prediction performance over LMMs over narrow composition regions. However, it was decided not to include PQM models in this comparison because of the extra effort required to develop such models for each of the five splits of the available data.

The models are described in more detail in the following subsections. Each model summary description is intended to provide some insight into the basis and background for that model. The end result is a description of each model form considered in the assessment. It was not the intent of this study to modify or revise the basic model form or to challenge the technical basis for the models. This was a conscious decision in an effort to avoid misrepresenting the model form as defined by its developers. The intent is to use each model form as is, refit the empirically derived parameters with the T_L data of interest to WTP HLW glasses (which places each model on a "level-playing field"), and perform the assessment using a constant database.

4.1.1 Linear-Mixture Model

The LMM form is based on the assumption that T_L can be adequately approximated by a first-order expansion of the form:

$$T_L = \sum_{i=1}^{N} T_i g_i \tag{4.1}$$

where, T_i and g_i are the coefficient and mass fraction of the i[th] oxide component in glass, and N is the number of components (and number of fit parameters) considered in the model. In a LMM, $\sum_{i=1}^{N} g_i = 1$, so that a constant term is not included in the model (Cornell 2002). The model in Equation 4.1 could be expressed just as easily by an LMM in mole fractions of oxide components or other component bases. However, for this treatment, we elected the simplest possible representation of mass fractions of single metal oxides and halogens.

According to the theory for mixture-experiment models (Cornell 2002), only the components having an effect on the response should be included in the number of components N in the LMM form given in Equation 4.1. Hence, the mass fractions g_i in Equation 4.1 should be based only on the N components affecting spinel T_L. Thus, one defensible approach for developing an LMM is to start with all components supported by the data set for potential inclusion in the model. Then, components found not to have statistically significant effects on spinel T_L are successively removed. However (per the statistical theory), at each step, the relative proportions of mass fractions for components still in the model must be re-normalized. That is, if components i = 1, 2, … , q (q < N) with mass fractions g_i are still in the model, then the re-normalized relative proportions of the component mass fractions are given by

$$g_i^* = \frac{g_i}{\sum_{i=1}^{q} g_i} \tag{4.2}$$

where q <N is the number of components in the LMM, and g_i^* are the renormalized relative proportions of component mass fractions. Note that $\sum_{i=1}^{q} g_i^* = 1$, the standard constraint for mixture experiment models. The successive reduction of mixture components appearing in a mixture-experiment model followed by re-normalizing the relative proportions is referred to as "backward elimination for LMMs." Standard forward, backward, and stepwise variable selection methods in statistical-regression software cannot be used to develop LMMs of the form in Equation 4.1 because those methods 1) do not properly assess whether mixture components have no effect on the response and 2) do not successively renormalize the mixture component proportions (i.e., mass fractions in this case) as components are dropped from the model. Piepel and Redgate (1997) and Cornell (2002) discuss methods for properly reducing the number of components in LMMs. The backward elimination method for LMMs is related to the methods discussed by these authors.

4.1.1.1 Linear-Mixture Model Form for T_L

Before applying the backward elimination method, the 163-point T_L data set used for model assessment (described in Section 4.3) was examined to determine the components varying over a sufficient range to support corresponding LMM terms. Starting with the 48 glass components (single metal oxides plus F

and Cl) in the database, the following 25 components were eliminated as having insignificant concentration ranges or variation: Ag_2O, As_2O_3, Bi_2O_3, Ce_2O_3, Cl, CoO, Cs_2O, CuO, La_2O_3, MoO_3, PbO, PdO, Pr_2O_3, Rb_2O, Rh_2O_3, RuO_2, Sb_2O_3, SeO_2, Sm_2O_3, TeO_2, TiO_2, Tl_2O, V_2O_5, WO_3, and Y_2O_3. The 23 remaining components (Al_2O_3, B_2O_3, BaO, CaO, CdO, Cr_2O_3, F, Fe_2O_3, K_2O, Li_2O, MgO, MnO, Na_2O, Nd_2O_3, NiO, P_2O_5, SiO_2, SO_3, SrO, ThO_2, U_3O_8, ZnO, and ZrO_2) had sufficient variation to be considered for possible inclusion in the LMM. In addition, a 24th component denoted "Others", with mass fraction calculated as $1-\sum_{i=1}^{23} g_i$, was considered for inclusion in the LMM. As part of the data assessment, the glasses CVS2-15, SP-Ca-2, SPA-18, SPA-32, WTP-TL-3, CVS2-1, and CVS2-46 were identified as having component values significantly different from the rest of the data. Also, there were questions about the accuracy of T_L values for glasses Sp-Na-1, Sp-Na-3, and Sp-Cr-1, as discussed in Section 3.2. Hence, these 10 glasses were removed from the data set before applying the backward-elimination method to develop an LMM for spinel T_L. This left a data set of 153 spinel T_L-composition data points.

The backward-elimination method for LMMs was applied to the set of 153 spinel T_L-composition data points. The method identified seven components as having nonsignificant effects on spinel T_L. These components, listed in the order they were removed, are as follows: Others, SrO, Nd_2O_3, CaO, BaO, SO_3, and ZnO. The removal of these seven components left the following 17 components as having effects on spinel T_L statistically significant at the 90% confidence level or greater: Al_2O_3, B_2O_3, CdO, Cr_2O_3, F, Fe_2O_3, K_2O, Li_2O, MgO, MnO, Na_2O, NiO, P_2O_5, SiO_2, ThO_2, U_3O_8, and ZrO_2. Hence, the LMM form considered in this report is of the form in Equation 4.1, using normalized mass fractions (per Equation 4.2) of these 17 components.

4.1.1.2 Linear-Mixture Model Form for $T_{0.01}$

An LMM form was selected for the $T_{0.01}$ response and data set in a similar fashion as for the T_L response and data set. An LMM form was selected for the $T_{0.01}$ response and data set in a similar fashion as for the T_L response and data set. The initial $T_{0.01}$ data set consisted of 43 glass compositions, but 2 of these (SP-Na-1 and SP-Na-3) were dropped due to questionable response values. Thus, 41 glass compositions remained for the $T_{0.01}$ LMM development. The 41 compositions were initially given in 48 components. However, 4 of these components (Sm_2O_3, ThO_2, U_3O_8, and Y_2O_3) were zero for all 41 glass compositions. These four components were therefore dropped before model development. Seven additional components (Bi_2O_3, Cs_2O, PdO, TeO_2, Tl_2O, V_2O_5, and WO_3) were zero for all 41 glass compositions with the exception of one or more of the three glasses SPA-18, SPA-32, and WTP-TL-03. These 7 components were also dropped before model development. Of the remaining 37 components, 22 had maximum values that were less than 0.5 wt% (mass fractions less than 0.005) when the three glasses SPA-18, SPA-32, and WTP-TL-03 were ignored. These 22 components with limited support were combined to form an "Others" component as was described in the previous section. The 22 components making up Others were Ag_2O, As_2O_5, BaO, Ce_2O_3, Cl, CoO, CuO, F, K_2O, La_2O_3, MoO_3, Nd_2O_3, P_2O_5, PbO, Pr_2O_3, Rb_2O, Rh_2O_3, RuO_2, Sb_2O_5, SeO_2, SO_3, and TiO_2. After forming Others from the 22 components listed, there were 16 components remaining for model development: Al_2O_3, B_2O_3, CaO, CdO, Cr_2O_3, Fe_2O_3, Li_2O, MgO, MnO, Na_2O, NiO, SiO_2, SrO, ZnO, ZrO_2, and Others.

As mentioned, the three glasses SPA-18, SPA-32, and WTP-TL-03 were outliers in various component distributions. This was apparent from viewing dotplots of the component distributions. The dotplots also revealed several other glasses as outliers in one or more component distributions. These additional outlying glasses were MS7-H-Mg and SP-Ni-3, which were a replicate pair.

Three separate model development approaches were attempted: 1) develop the $T_{0.01}$ LMM using all 41 glasses available, 2) develop the $T_{0.01}$ LMM using the 35 glasses that remained after dropping the outlying glasses (mentioned above) initially observed among the component distributions, and 3) develop the $T_{0.01}$ LMM, dropping the outlying glasses (mentioned above) initially observed among the component distributions, plus any additional glass compositions identified as outliers in $T_{0.01}$ property space as the model development progressed. The first model-development plan reflected the philosophy that because the data set is somewhat small to begin with, all available data should be retained for modeling. The second plan favored dropping a minimal number of glasses in order to develop a model that is not disproportionately influenced by these relatively few outlying glasses. The third plan allowed the freedom to pursue an optimal model fit by retaining only those points best suited for model development over a reasonably well-covered composition subregion.

The backward elimination method for LMMs was applied based on the three model-development approaches described above. In pursuing the third model-development approach, several glasses were identified as outliers in $T_{0.01}$ space and subsequently dropped from the model development. They were WTP-TL-05, SP-Mg-1, SP-Mn-1, and SP-Cr-1, the last of which occurred as a replicate pair. One point of the replicate pair had an outlying response, the other did not. Depending on whether one or both of the replicate points was dropped, the third model-development plan led to a model based on 30 or 31 glass compositions.

The model-development process proved to be robust to the outlying glasses in that all three approaches ultimately resulted in the same LMM form. The $T_{0.01}$ LMM form involved the following 11 components: Al_2O_3, B_2O_3, Cr_2O_3, Fe_2O_3, Li_2O, MnO, Na_2O, NiO, SiO_2, SrO, and ZrO_2. As discussed in Section 4.1.1, this model form is to be applied to glass compositions expressed in normalized mass fractions (as was the case with the T_L model from Section 4.1.1.1).

4.1.2 Ion Potential Model

The IPM is based on the hypothesis that the T_L within the spinel primary phase field is largely determined by Cr and Ni solubility in the melts. Vienna and colleagues (Vienna et al. 2001; Vienna 2002; Vienna et al. 2002) developed the IPM based on this assumption. Cr and Ni are bound in the glass in 6-fold coordination—in the cages and rings formed by the network-forming tetrahedra. They are low-field-strength components (0.76 and 0.46 for Cr^{3+} and Ni^{2+}, respectively) and thus have little control over their oxygen-coordination environment, which is controlled by smaller components with higher charges. So, other components affect the solubility of Cr and Ni in proportion to their relative ability to help Cr and Ni obtain their desired coordination environment in the melt. These components fall into two general categories, those bound in glass with high ionic character and those bound in glass with a high covalent character.

Ionic components, such as K^+, break up the connectivity of SiO_4^{4-} tetrahedral, changing the melt structure so that O^{2-} ions are better able to accommodate the coordination requirements of Cr and Ni. The degree to which components influence the O^{2-} configuration is determined by their ion potential, $P_i = Z_i/r_i$ (an indication of bond energy, with r_i and Z_i being the ionic radius and valance of the ith ion). The higher the P_i of these ionically-bonded components, the more tightly they are bound to the O^{2-} ions. Such components become less likely to accommodate the coordination requirements of Cr or Ni.

Components with a high covalent character also influence Cr solubility. The roles of these components include glass formers and 6-fold modifiers/intermediates[(a)] that compete with Cr and Ni for sites within O^{2-} cages that can conform to their coordination requirements. Adding different glass formers adds to the glass network more variety in cage structure to allow Cr and Ni to obtain their ideal coordination environment. The effects of these components on T_L are also dependent upon P_i.

This hypothesis suggests that the effects of components that are primarily ionically (alkali and alkaline earth) and those that are primarily covalently bound in the glass (e.g., Si^{4+}) on T_L will scale with P_i. Figure 4.1 shows how the first-order-expansion coefficients (T_i) of electropositive elements scale with P_i. These T_i values are the LMM coefficients fit by Vienna et al. (2001), based on mole fractions of electropositive elements in glass and T_L in °C.

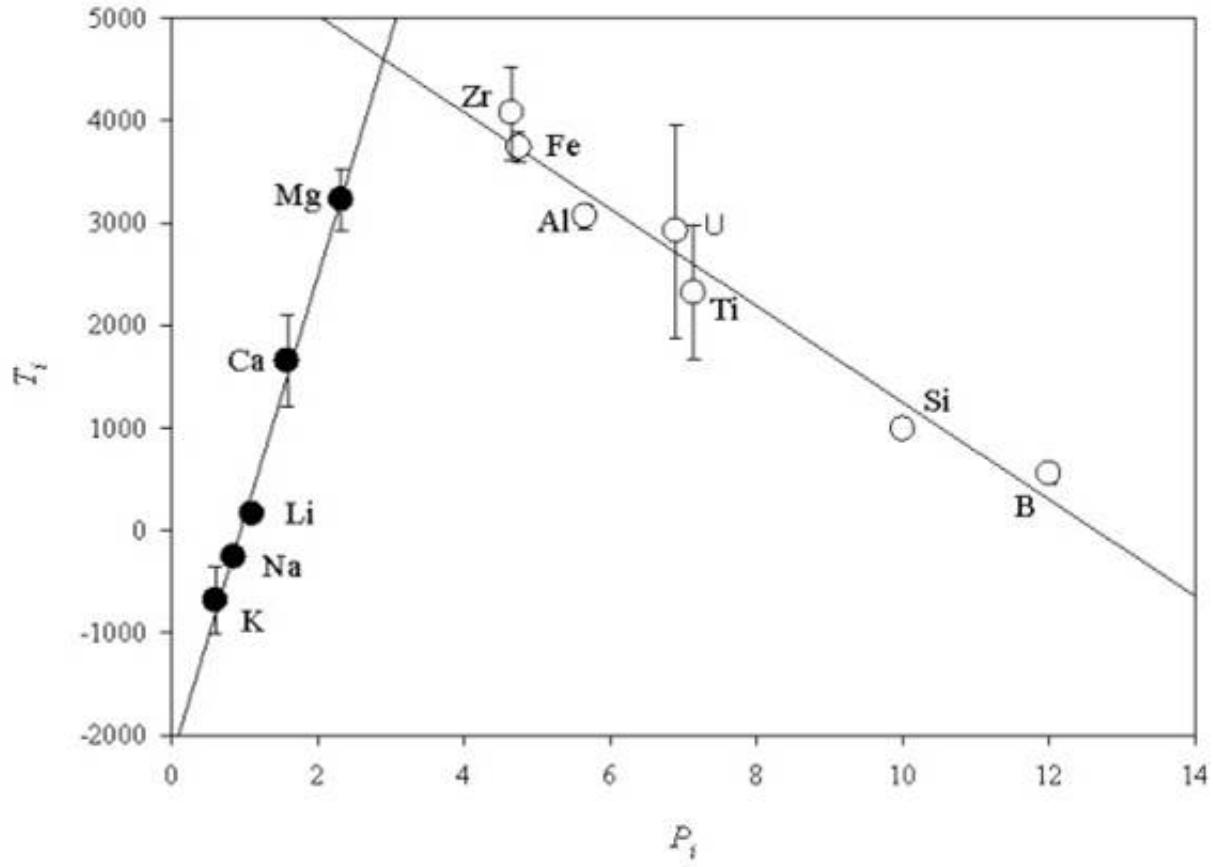

Figure 4.1. Comparison of Empirically Derived T_i Coefficients with P_i (from Vienna et al. 2001)

(a) Six-fold modifiers/intermediates are those components in glass that tend to be sourrounded by six oxygens (typically, but not always, in octahedral coordination).

This relationship leads directly to the IPM:

$$T_L = \sum_{Ni,Cr,Mn} T_i x_i + \sum_{Alk,AlkE} (t_{ion} + \Theta_{ion} P_i) x_i + \sum_{remaining} (t_{\mathrm{cov}} + \Theta_{\mathrm{cov}} P_i) x_i \qquad (4.3)$$

where T_i = coefficients for i=Ni, Mn, and Cr
t_{ion} and Θ_{ion} = intercept and slope of the $T_i - P_i$ line for ionic components
t_{cov} and Θ_{cov} = intercept and slope of the $T_i - P_i$ line for the remaining components
x_i = mole fraction of the i^{th} electropositive element.

To implement this model, the glass composition is first converted into mole fractions of electropositive elements (normalizing electronegative elements out of the composition). A P_i is then assigned based on the most likely valence state and coordination number as listed in Table 4.1. The fit parameters assumed for this study are T_{Cr}, T_{Mn}, T_{Ni}, t_{ion}, Θ_{ion}, t_{cov}, and Θ_{cov}.

It is interesting to note that the IPM in Equation 4.3 is a reduced form of an LMM similar to that given in Equation 4.1, except that mole fractions x_i of electropositive elements are used in place of mass fractions g_i of oxide components. Equation 4.3 is a reduced form of an LMM because of the special linear equations representing the coefficients for the "Alkalis + Alkaline Earths" ($t_{ion} + \Theta_{ion} P_i$) and "Remaining" ($t_{cov} + \Theta_{cov} P_i$) groups of components. These special coefficient expressions reduce the number of parameters to be estimated from data compared to an LMM. Reducing the number of parameters to be estimated from data can reduce prediction uncertainties, provided the model reductions do not have significant negative impacts on prediction accuracy. Work by Vienna et al. (2001) has compared the IPM in Equation 4.3 to unreduced LMMs in the x_i and found minimal impact to the quality of model predictions. However, the LMM in Equation 4.1 is in terms of mass fractions of oxides g_i rather than mole fractions of electropositive elements x_i, so there are potentials for different prediction performances.

Table 4.1. Z_i, r_i, and P_i Values for IPM

Element (i)	Z_i [(a)]	r_i [(b)] (Å)	P_i	Element (i)	Z_i	r_i (Å)	P_i
Ag	1	1.08	0.9259	P	5	0.31	16.1290
Al	3	0.53	5.6604	Pb	2	1.43	1.3986
As	5	0.475	10.5263	Pd	2	1	2.0000
B	3	0.25	12.0000	Pr	3	1.266	2.3697
Ba	2	1.56	1.2821	Rb	1	1.75	0.5714
Bi	3	1.17	2.5641	Rh	3	0.805	3.7267
Ca	2	1.26	1.5873	Ru	4	0.76	5.2632
Cd	2	1.09	1.8349	S	6	0.26	23.0769
Ce	4	1.01	3.9604	Sb	5	0.74	6.7568
Co	2	0.72	2.7778	Se	6	0.42	14.2857
Cr	3	0.755	3.9735	Si	4	0.4	10.0000
Cs	1	1.88	0.5319	Sm	3	1.219	2.4610
Cu	2	0.87	2.2989	Sr	2	1.4	1.4286
Fe	3	0.63	4.7619	Te	4	0.8	5.0000
K	1	1.65	0.6061	Th	4	1.08	3.7037
La	3	1.3	2.3077	Ti	4	0.56	7.1429
Li	1	0.9	1.1111	U	6	0.87	6.8966
Mg	2	0.86	2.3256	V	5	0.68	7.3529
Mn	2	0.97	2.0619	W	6	0.74	8.1081
Mo	6	0.73	8.2192	Y	3	1.159	2.5884
Na	1	1.16	0.8621	Zn	2	0.74	2.7027
Nd	3	1.249	2.4019	Zr	4	0.86	4.6512
Ni	2	0.83	2.4096				

(a) For multivalent components, the most abundant valence states were assumed.
(b) The crystal radii from Shannon (1976) were used, assuming the most abundant coordination environment.

4.1.3 Solubility Product Model

Plodinec (1999) developed a model for the T_L of waste glasses based on the hypothesis that the T_L was controlled by the solubility of Ni and Cr in the silicate melt (much like the IPM). This model further asserts that the relationship between the solubility of Ni and Cr can be approximated by a solubility product. The solubility-product relationship is given by first making use of the following assumed chemical reactions:

$$Fe_2O_3(m) + NiO(m) \leftrightarrow NiFe_2O_4(s) \quad (4.4a)$$

or

$$Cr_2O_3(m) + NiO(m) \leftrightarrow NiCr_2O_4(s) \quad (4.4b)$$

where (m) indicates a compound in the melt phase, and (s) indicates one in the solid phase. Assuming that the activities of spinel (trevorite and nichromite) are 1 and the activities of Cr_2O_3, NiO, and Fe_2O_3 can be approximated by mass% in the melt, then $K_{sp} = 1/g_{Fe2O3}g_{NiO}$ or $1/g_{Cr2O3}g_{NiO}$, respectively. Then the

reaction constant can be expressed as a function of temperature according to $\Delta G = -RT\ln[K]$. This is simplified to obtain a T_L model:

$$T_L = \frac{1000}{a + b\ln(g_{NiO} g_{Cr_2O_3})} \tag{4.5a}$$

or

$$T_L = \frac{1000}{a + b\ln(g_{NiO} g_{Fe_2O_3})} \tag{4.5b}$$

where a and b are fit parameters and g_{NiO}, g_{Fe2O3}, and g_{Cr2O3} are the mass% of NiO, Fe_2O_3, and Cr_2O_3 in glass, respectively.[(a)]

4.1.4 Sub-Lattice Model

The SLM was developed by Gan and Pegg (2001) to describe the relationship between T_L and the composition of Hanford HLW glasses. They begin by considering the reaction of spinel(m) ↔ spinel(s) and derive:

$$1/T_L = R \ln [a_{sp}(s) / a_{sp}(m)]/\Delta\mu° \tag{4.6}$$

where $a_{sp}(s)$ and $a_{sp}(m)$ are the activities of the spinel species in the solid and in the melt, respectively, and $\Delta\mu°$ is the chemical potential difference between the solid and liquid spinel phases in their reference state. By setting $a_{sp}(s)$ to 1 and assuming that the $\Delta\mu°$ is a temperature-independent constant, C, they obtain:

$$1/T_L = -R \ln[a_{sp}(m)]/C \tag{4.7}$$

Because the activity is the product of the mole fraction and the activity coefficient (Gan and Pegg 2001), $\ln[a_{sp}(m)]$ was approximated as a linear combination of temperature-independent coefficients P_i multiplied by the concentrations of various oxides in the melt to obtain:

$$1/T_L = -R\ln[B_{sp}]/C_1 - R\ln[X_{sp}]/C_2 - \sum_{i=1}^{N} P_i x_i /C_3 \tag{4.8}$$

where X_{sp} is an expression for molar fraction of spinel species in the melt, B_{sp} is a proportionality factor, and the C_i (i=1, 2, 3) are temperature-independent constants. This led directly to:

$$1/T_L = C_0 + C_{sp} \ln[X_{sp}] + \sum_{i=1}^{N} p_i x_i \tag{4.9}$$

(a) Equations (4.5a) and (4.5b) are non-linear in parameters a and b. However, for our work, the model was linearized by fitting $1000/T_L = a+b\ln[g_j g_k]$. Also note that g_i is used as mass% rather than mass fraction in this application.

The quantity X_{sp} is difficult to calculate because spinel is not typically a melt component, and the composition of spinel varies with temperature and melt composition. Gan and Pegg (2001), therefore, approximated $\ln[X_{sp}]$ by:

$$\ln[X_{sp}] = [g_{NiO}/(g_{NiO}+g_{MnO2}+0.03g_{Fe2O3})]\,[g_{Cr2O3}/(g_{Cr2O3}+0.97g_{Fe2O3})]2 = SLP \quad (4.10)$$

This led to the final form of the SLM given by:

$$1/T_L = D_0 + D_{sp}\,(SLP) + \sum_{i=1}^{N} D_i g_i \quad (4.11)$$

where D_0, D_{sp}, and D_i are fit parameters, and g_i are mass% of oxides. The final term in this model includes the following components: i=Al_2O_3, B_2O_3, CaO, Cr_2O_3, Fe_2O_3, K_2O, Li_2O, MgO, MnO_2, Na_2O, NiO, SiO_2, TiO_2, UO_2, ZnO, and ZrO_2. These are the components chosen in the work by Gan and Pegg (2001). They used a stepwise regression procedure to empirically select those components based on the data set they used for fitting. Using the method of LMM component selection discussed in Section 4.1.1 to select the components considered in the last term of the SLM (Equation 4.11) may yield an SLM with better prediction performance.

It should be noted that manganese and uranium oxides are assumed to be in a different oxidation state in this model than those listed in the data set, and so the compositions were adjusted and renormalized to account for this difference before model fitting.

4.1.5 Defense Waste Processing Facility Model

Jantzen (1991) summarized the original DWPF T_L model, which was based upon a pseudo-equilibrium constant describing the formation of trevorite spinel ($NiFe_2O_4$ was assumed) in a spinel-nepheline-amorphous silica system. In this model, only the concentrations of Fe_2O_3, Al_2O_3, and SiO_2 (representing spinel, nepheline, and amorphous silica, respectively) are needed to describe the simple relationship between T_L and the composition for the 22 T_L measurements available at the time of model development. However, as more data became available, an improved model for T_L of DWPF glasses was developed by Brown et al. (2001). As the latter model is currently being used by DWPF and thought to be applicable to a broader range of compositions than the initial model, it was evaluated as part of this study.

Brown et al. (2001) provide a detailed discussion of the model and its development. The salient points of the model are summarized here for the purposes of comparison with other possible T_L models for application to Hanford HLW glasses.

The basis for the DWPFM is that the T_L represents the equilibrium between liquid and the primary phase, P, controlling the onset of crystallization. At equilibrium, the chemical potentials, μ_P, of the pure crystalline (or solid) phase, P, and of P in the liquid (or melt) must be equal, at a given constant pressure and temperature (T_L). The chemical potentials are related by:

$$-R\ln\left\{a\left(P_{(l)}\right)\right\} \approx \Delta\overline{H}_{fus,P}\left(T_P^*\right)\left(\frac{1}{T_L}-\frac{1}{T_P^*}\right) \quad (4.12)$$

where $a(P_{(l)})$ represents the activity of P in the liquid (or melt) phase, *R* is the gas constant, and the asterisk (*) indicates a pure substance. The activity of P (assumed to be pyroxene for DWPF glasses) in the melt phase is an unknown. The pyroxene formula unit is:

$$(M2)_1(M1)_1(MT)_2O_6 \tag{4.13}$$

where M2 designates a distorted 6 to 8 coordination site and M1 and MT designate regular octahedral and tetrahedral coordination sites, respectively. Ideal cation site occupancies for pyroxene were presented by Brown et al. (2001), and after a number of assumptions, it was shown that the pyroxene liquid phase activity can be represented by:

$$a(P_{(l)}) \approx K_P\left[(M2)_2^{(VI)}O_{(l)}\right]^a\left[(M1)_2O_{3(l)}\right]^b\left[(MT)O_{2(l)}\right]^c \tag{4.14}$$

Brown et al. (2001) indicated that there is growing evidence that the cations that form crystalline material in DWPF glasses are not likely found in the melt as independent cations (e.g., Ni^{2+}, Fe^{2+}, Fe^{3+}, etc.) or in oxides (e.g., NiO, FeO, Fe_2O_3). These cations may be in the form of nano- or quasi-crystalline structures (e.g., $NiAl_2O_4$, $FeNi_2O_4$, $NaFeO_2$) that are analogous to the crystalline structures that ultimately form in the glass. Thus, at equilibrium and at a temperature just above T_L, it was assumed that if a cation is associated with a site in one melt-phase complex or precursor, it will not be available to another complex or precursor. However, it was noted that the latter statement did not mean that there is not some degree of interchange of cations as crystalline material begins to form at T_L (i.e., the system establishes a new equilibrium at the given temperature). It was mentioned that DWPF glasses are rich in modifier cation-tetrahedral groups, which suggests that the various cations are free to exchange sites with each other, depending on the favored energetics.

The following molar site distributions were suggested for the pyroxene-like complex or precursor:

$$\Sigma_{MT} \equiv \phi_{T,SiO_2}z_{SiO_2} + \phi_{T,Al_2O_3}z_{Al_2O_3} + \phi_{T,Fe_2O_3}z_{Fe_2O_3}$$

$$\Sigma_{M1} \equiv \phi_{M1,Al_2O_3}z_{Al_2O_3} + \phi_{M1,Fe_2O_3}z_{Fe_2O_3} + \phi_{M1,TiO_2}z_{TiO_2} + \phi_{M1,Cr_2O_3}z_{Cr_2O_3} + \phi_{M1,ZrO_2}z_{ZrO_2} + \phi_{M1,NiO}z_{NiO} + \phi_{M1,MgO}z_{MgO} + \phi_{M1,MnO}z_{MnO}$$

$$\Sigma_{M2} \equiv \phi_{M2,NiO}z_{NiO} + \phi_{M2,MgO}z_{MgO} + \phi_{M2,MnO}z_{MnO} + \phi_{M2,CaO}z_{CaO} + \phi_{M2,K_2O}z_{K_2O} + \phi_{M2,Li_2O}z_{Li_2O} + \phi_{M2,Na_2O}z_{Na_2O}$$

where $\varphi_{i,j}$ is the fraction of the moles of j associated with the i^{th} site, and z_j represents the total moles of j per 100 g of glass.

In the definition process, Brown et al. (2001) indicated that a term representing the ZnO concentration must be added to $\sum_{M2}$ when the T_L values of glasses containing significant concentrations of this oxide are to be predicted. Because DWPF glasses contain very little, if any, ZnO, this term was assumed to be zero.

A second melt complex or precursor, representing nepheline, was also described with a distribution of sites given by:

$$\Sigma_{T1} \equiv \phi_{T1,SiO_2} z_{SiO_2} + \phi_{T1,Al_2O_3} z_{Al_2O_3} + \phi_{T1,Fe_2O_3} z_{Fe_2O_3} + \phi_{T1,TiO_2} z_{TiO_2}$$

$$\Sigma_{N1} \equiv \phi_{N1,K_2O} z_{K_2O} + \phi_{N1,Li_2O} z_{Li_2O} + \phi_{N1,Na_2O} z_{Na_2O}$$

where $\varphi_{i,j}$ is the fraction of the moles of j associated with the i^{th} site, and z_j represents the total moles of j per 100 g of glass. The site occupancies ($\varphi_{i,j}$), which were determined through a combination of T_L data evaluation and glass-chemistry insight, are listed in Table 4.2. Although some empirical data were used in their determination, Brown et al. (2001) argue that these are to be considered fundamental parameters of the minerals used and should not be considered fit parameters. Those parameters were adopted for this study and not fit to the Hanford T_L data. However, one option for improvement of this model with respect to its applicability to the Hanford compositional region would be to modify these parameters (for example, add a zinc term as noted by Brown et al. [2001]).

The appropriate mole fractions to use in Equation 4.13 to represent the liquid-phase activities for the components comprising the proposed melt phase complexes or precursors were reported to be:

$$M_2 = \left[(M2)_2O_{(l)}\right] \equiv \frac{\Sigma_{M2}}{\Sigma}, \quad M_1 = \left[(M1)_2O_{3(l)}\right] \equiv \frac{\Sigma_{M1}}{\Sigma}, \text{ and } \quad M_T = \left[(MT)O_{2(l)}\right] \equiv \frac{\Sigma_{MT}}{\Sigma} \tag{4.15}$$

where

$$\Sigma \equiv \Sigma_{M2} + \Sigma_{M1} + \Sigma_{MT} + \Sigma_{T1} + \Sigma_{N1}$$

Brown et al. (2001) proposed that only the pyroxene-nepheline pseudo-binary is of concern in predicting T_L in the spinel primary phase field. The pyroxene melt phase precursor liquid activities were approximated by:

$$a\left(P_{(l)}\right) \approx K_P \left(M_2\right)^a \left(M_1\right)^b \left(M_T\right)^c \tag{4.16}$$

Then Equation (4.12), upon substitution and rearrangement, becomes the final model form:

$$\left(\frac{1}{T_L}\right) \approx -\frac{R}{\Delta\overline{H}_{fus,P}\left(T_P^*\right)} \ln\left\{M_2{}^a M_1{}^b M_T{}^c\right\} + \left\{\left(\frac{1}{T_P^*}\right) - \frac{R\ln\left(K_P\right)}{\Delta\overline{H}_{fus,P}\left(T_P^*\right)}\right\} \tag{4.17}$$

Equation (4.17) provides a way to estimate T_L as a function of the molar-melt-constituent concentrations and the basis for predicting T_L for DWPF glasses, assuming the presence of a pyroxene intermediate that then melts incongruently to spinel.

Table 4.2. Summary of $\varphi_{i,j}$ Factors Used in DWPFM (from Brown et al. [2001])

Speciation (Sp)	M2	M1	MT	N1	T1	SUM
Al_2O_3	0	0.0607	0.9393	0	0	1
B_2O_3	0	0	0	0	0	0
BaO						
HCOO						
CaO	0.029	0	0	0	0	0.029
Ce_2O_3						
NaCl						
Cr_2O_3	0	0.9202	0	0	0	0.9202
Cs_2O						
CuO						
NaF						
Fe_2O_3	0	0.1079	0.0193	0	0.6094	0.7366
K_2O	0.3041	0	0	0.1049	0	0.409
La_2O_3						
Li_2O	0.1745	0	0	0.1068	0	0.2813
MgO	0.0167	0.0223	0	0	0	0.039
MnO	0.994	0.00603	0	0	0	1
MoO_3						
NO_2						
NO_3						
Na_2O	0.1671	0	0	0.2518	0	0.4189
Na_2SO_4						
Nd_2O_3						
NiO	0	0.1079	0	0	0	0.1079
P_2O_5						
PbO						
SiO_2	0	0	0.0193	0	0.0133	0.0326
ThO_2						
TiO_2	0	0.0568	0	0	0.5667	0.6235
U_3O_8	0	0	0	0	0	0
Y_2O_3						
ZnO						
ZrO_2	0	0.0458	0	0	0	0.0458
Coeff	-0.0002597	-0.0005662	-0.0001525			-0.0014422

To predict the T_L for a given set of DWPF melt compositions, the enthalpy of fusion, melt temperature, distribution of cations among melt-phase complexes or precursors, and equilibrium constant and stoichiometry of the pertinent equilibrium reaction must be known. This information is clearly not available; therefore, T_L data were used to fit a group of related parameters. The following relationship between $(1/T_L)$ and composition was obtained using the DWPF T_L data:

$$\begin{aligned}\frac{1}{T_L(K)} &= -0.000260\ln(M_2) - 0.000566\ln(M_1) - 0.000153\ln(M_T) - 0.00144 \\ &= \ln\left\{(M_2)^{-0.000260}(M_1)^{-0.000566}(M_T)^{-0.000153}\right\} - 0.00144\end{aligned} \tag{4.18}$$

where the new coefficients were obtained from the multi-linear regression of ($1/T_L$) as the dependent variable and ln(M_2), ln(M_1), and ln(M_T) as the independent variables. This model has four fitted parameters and is the basis from which the T_L model assessment was performed. The basic model form can be represented as $1/T_L = a\ln(M2)+b\ln(M1) +c\ln(MT)+d$ where *a*, *b*, *c*, and *d* values were refitted with the WTP HLW data.

4.1.6 A Note on Temperature

The models described relate HLW glass composition to either T_L or $1/T_L$. Therefore, it is interesting to consider the relationship between absolute temperature and its inverse (*T* and 1/*T*) for the range of temperatures of interest. The interest is from two perspectives:

- Models relating composition to $1/T_L$ might fit better than models relating composition to T_L, or vice versa.

- The unweighted least-squares assumption of constant variance for the response variable across all data points might be more appropriate for T_L or $1/T_L$.

The data collected in this study produced T_L values ranging from 780 to 1306°C (1053 to 1579 K). As shown in Figure 4.2, the relationship between the absolute T and 1/T is very close to linear over that range. The deviation between a straight-line fit and 1/T is less than 35 K over the entire temperature span and less than 20 K from 820°C to 1250°C (1093 to 1523 K). This suggests that if there is any advantage to modeling $1/T_L$ versus T_L from either perspective above, the advantage will be small (i.e., of little practical concern).

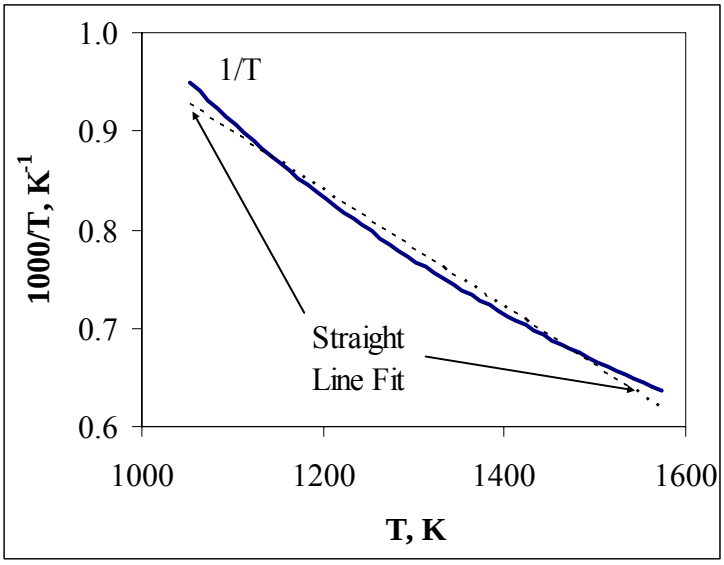

Figure 4.2. Comparison of *T* with 1/T

4.2 Model Evaluation Methods

All of the model forms being considered in this study fall within the class of semi-empirical model forms and, so, are strictly valid only over the region for which they are fit. For this task, the T_L and $T_{0.01}$ responses are modeled using two different data sets. One of these subsets has as its response the T_L while the second data set has as its response the $T_{0.01}$. Each of the model forms of interest was fit to each of these two subsets, and the assessment of their relative performances was conducted for each of the two data sets. The following subsections describe the systematic ways used to compare the candidate model forms for T_L and $T_{0.01}$ (hereafter simply referred to as models) for each of these two data sets. The comparisons are purely data driven and are based upon the T_L- and $T_{0.01}$-glass-composition databases generated to meet the objectives of the study. The data in each data set were divided into model-development data (~80% of the available data and hereafter referred to as model data) and model-validation data (the remaining ~20% of the available data and hereafter referred to as validation data). The model data were used in fitting the empirically derived coefficients (or fit parameters) for each of the candidate models. Thus, a consistent set of data was used to attune each of the candidate models to the HLW glass compositional region of interest for WTP for each of the two responses (T_L and $T_{0.01}$). The validation data then provided an independent set of results covering this same compositional region. The model and validation data sets allowed computing of goodness-of-fit measures for each of the candidate models. Several goodness-of-fit measures were suggested in Vienna (2002). Although many of these measures are related, it is possible that different models may be the best performers relative to different goodness-of-fit measures. A suggestion is offered for a single metric for use in selecting among the candidate models for each of the responses.

One could question the utility of the single metric in terms of its validity to summarize the individual criteria or responses. However, it is the belief of the authors that if one were to attempt an unbiased ranking of the models based on the individual criteria, the outcome or conclusions drawn would be identical to those based on the use of the single metric.

The following sub-sections discuss 1) the purpose of a T_L model for the WTP from a statistical perspective, 2) model development and region of validity, 3) associated measures of model goodness-of-fit, 4) the identification of outliers, 5) the role of the validation data, and 6) the suggested metric for use in selecting among the candidate models. An approach for assessing the sensitivity of a model's value for this metric to the splitting of the T_L-glass-composition database into the model-development and validation sets is also provided in this section. The use of this approach assures that the metric being used for model selection is robust (i.e., not overly sensitive) to different splits of the data into modeling data and validation data.

4.2.1 Purpose of the T_L Model

During the vitrification of HLW at the WTP, there will be a need to avoid the deleterious effects of crystal accumulation on the operation and useful life of the melter. The method used at other U.S. HLW vitrification facilities for avoiding these ill effects is to control the melt composition so that the T_L of the melt is below the temperatures that melt is likely to be exposed to for extended periods of time (e.g., a T_L limit or constraint on glass-melt composition). Since it is not currently possible to measure the T_L of the melt composition *in situ* to assure that the constraint is met, there is a need to predict the T_L for a given glass composition using a model. The WTP will likely use a finite crystal fraction restriction as discussed

in Section 1.0. For the purposes of this study, we have selected a *c* of 1 mass% to base the constraint. Like T_L, $T_{0.01}$ cannot be measured *in situ* and must be predicted using a model. This leads to prediction being the main purpose of the T_L or $T_{0.01}$ model that is to be selected by this study. Thus, the prediction uncertainties and predictive capabilities of the candidate T_L and $T_{0.01}$ models become important measures of goodness-of-fit that should be considered as part of the model assessments.

4.2.2 Model Development and Model Validity

As discussed above, six models have been identified in the literature that purport to be useful in predicting the T_L of nuclear waste glasses in the spinel primary phase field. Each of these models has been found by its developer(s) to adequately fit a set of relevant data for a study of interest to them. Two or more coefficients for each model were estimated by the developer(s) using this relevant data. To provide a consistent basis for comparison of the models, these coefficients (fit parameters) were re-estimated as part of this study using the same model-development data set for each response (i.e., a consistent data set for T_L and one for $T_{0.01}$). Section 4.1 identifies the specific coefficients to be re-estimated for each model.

As part of the original development of each model, some checks of the model's validity were made. Certainly, such checks should be made before the implementation of any model. For this study, these checks involved the results of the model-development effort and the performance of the model relative to the validation data. The important measures of goodness-of-fit determined for the model data are described in the next section. Of critical importance for WTP operation is the uncertainty of the predicted T_L or $T_{0.01}$ for an individual glass composition of a candidate model. This uncertainty, which is fully described in the next section, depends upon the desired confidence level, the number of glass compositions involved in the fitting process, the compositions themselves, the number of estimated parameters in the fitted model, the root mean square error of the fitted model, and the individual glass composition for which the prediction is to be made. If the T_L or $T_{0.01}$ constraint is to be met with sufficient confidence, this uncertainty must be accommodated. Having a consistent set of data over which each of the candidate models is fitted and validated provides a "level playing field" for comparing the prediction uncertainties of the resulting fitted models.

The second primary area for checking the validity of each of the models is centered on the validation data. Because the main purpose of any T_L or $T_{0.01}$ model is in predicting future T_L or $T_{0.01}$ values, how well the model performs in predicting the validation data plays a crucial role in the assessment of the candidate models. The use of a consistent set of data for this part of the assessment also contributes to the "level playing field" for the model comparisons. The measure of validation performance here is very straightforward. For each glass composition (x_i) in the validation set, a model's predictive performance is indicated by the difference between its predicted value [$\hat{y}_i$] and corresponding measured T_L or $T_{0.01}$ value (y_i) in the database. More will be said in the next section on the determination of an appropriate metric based upon these differences.

4.2.3 Measures of Goodness-of-Fit for Model Development

Several goodness-of-fit measures for model development and validation were included in the discussion of the test plan (Vienna 2002) for this study. For a more complete description of these measures, please see statistical references such as Cornell (2002), Snee (1977), and/or Draper and Smith (1998).

As part of the critique of the model-fitting process, the following measures of goodness-of-fit were computed for each fitted model: R^2 (the coefficient of multiple determination), R^2_{adj} (the adjusted R^2 value), and s (the root mean squared error). The intent was to conduct this model-fitting process over exactly the same set of data (i.e., the model-development data set) for each of the candidate models for each of the responses, T_L and $T_{0.01}$. (See the next section on how outliers, if identified, were to be handled.) Thus, differences that are seen in the goodness-of-fit measures among the fitted models are due strictly to the features of the models themselves.

A model's R^2 value, which must be between 0 and 1, represents the portion of the variation in the responses (i.e., the T_L or $T_{0.01}$ values) corresponding to the compositions in the data set that is accounted for by the model. It is a convenient and frequently used measure of the goodness-of-fit for a model. There is the potential, however, to increase a model's R^2 value by adding more terms to the model, even if the added terms do not significantly improve the fit. This lessens the utility of using R^2 values to compare two models that have different numbers of parameters. To help overcome this shortcoming, a related statistic, the adjusted R^2 (denoted here as R^2_{adj}) is available. Equations 4.19 and 4.20 provide formulas for computing these two statistics:

$$R^2 = 1 - \frac{\sum_{i=1}^{n}(y_i - \hat{y}_i)^2}{\sum_{i=1}^{n}(y_i - \bar{y})^2} \tag{4.19}$$

and

$$R^2_{adj} = 1 - \left(\frac{\sum_{i=1}^{n}(y_i - \hat{y}_i)^2 \Big/ (n-p)}{\sum_{i=1}^{n}(y_i - \bar{y})^2 \Big/ (n-1)} \right) \tag{4.20}$$

where n = number of data points used to fit the model
p = number of fitted parameters in the model
y_i = measured T_L or $T_{0.01}$ for the i^{th} data point
$\hat{y}_i$ = predicted T_L or $T_{0.01}$ value for the i^{th} data point made using the fitted model
$\bar{y}$ = average of the n measured T_L or $T_{0.01}$ values (i.e., the $y_1, y_2, y_3, \ldots, y_n$).

Another goodness-of-fit measure that is often used to assess the performance of a fitted model over the data set for which it is fitted is the predicted error sums of squares (PRESS) statistic. The formula for this statistic is given by:

$$PRESS = \sum_{i=1}^{n}(y_i - \hat{y}_{(i)})^2 \tag{4.21}$$

where the notation $\hat{y}_{(i)}$ represents the prediction of the i^{th} response value without using the i^{th} data point in the model fit. The value of the PRESS statistic may be used to replace the numerator of the second term of Equation 4.19 to calculate an additional goodness-of-fit measure, denoted as R^2_{PRESS}.

Another important measure of goodness-of-fit is the value for s, the root mean squared error, of the fitted model. It is a measure of the variability of the model-prediction errors, and using the notation above, its formula is given by:

$$s = \sqrt{\frac{\sum_{i=1}^{n}(y_i - \hat{y}_i)^2}{(n-p)}} \tag{4.22}$$

If a fitted model does not have a statistically significant lack-of-fit (LOF, discussed in the following paragraph), then s provides an unbiased estimate of the standard deviation of experimental and measurement uncertainty in determining T_L or $T_{0.01}$. Values for these statistics are provided in the discussion that follows for each fitted model for T_L or $T_{0.01}$. In comparing values for R^2, R^2_{adj}, and R^2_{PRESS} among the models, it should be noted that the rule is "the bigger the better." For PRESS and s, the comparison rule is "the smaller the better."

A statistical test for a significant LOF for each fitted model was conducted using available, replicate data to estimate the so-called "pure error" (measurement error) variation. This involves comparing the variation in model-prediction errors to the variation in data-measurement errors using an F-test. If the variation in prediction errors for a given fitted model is significantly larger (via a statistical F-test) than the variation in measurement errors, the model is said to have a statistically significant LOF. Technically, statistical interval methods for regression should not be applied for a model with statistically significant LOF. LOF testing is to be performed with the model-development data for both T_L and $T_{0.01}$.

4.2.4 Measures of Model-Validation Performance

As previously stated, the WTP will use a T_L or $T_{0.01}$ (or other T_c) model for prediction. Therefore, the crucial performance measure for each candidate model relative to the validation data is related to the differences between the model's predictions and the T_L or $T_{0.01}$ values for these data. Specifically, the validation error sums-of-squares (VESS) is an appropriate measure of model predictive performance. Its formula for a given candidate model is given by:

$$VESS = \sum_{j=1}^{m}(y_j - \hat{y}_j)^2 \tag{4.23}$$

where the notation is as defined earlier except that j and m are used to indicate that this summation is being conducted over the set of m data points in the validation data set. In comparing the VESS statistics among the models, the rule would be "the smaller the better." Values for this statistic are provided for each fitted model as part of the information generated for T_L or $T_{0.01}$.

An R^2 value for the validation data, denoted by R^2_{val}, is another measure of predictive performance that is provided as part of this study. It is computed from Equation 4.19 for the m y_js of the validation data. As with the other R^2-type measures, the comparison rule is the "bigger the better."

The VESS and R^2_{Val} statistics are useful measures of a model's predictive performance over the whole validation data set. However, it is also useful to be able to assess a model's predictive performance separately for each data point in the validation data set. A two-sided, prediction interval at 95% confidence can be used for this type of assessment of the candidate models for T_L and $T_{0.01}$. The half-width (HW) of this interval for the j^{th} validation point, x_j, is given by:

$$HW_{95\%} = t_{0.025,n-p} \cdot s \cdot \sqrt{1 + x_j (X'X)^{-1} x'_j} \tag{4.24}$$

where the additional notation is as follows:

$t_{0.025,n-p}$ = upper 2.5% tail of Student's t distribution with n-p degrees of freedom
x_j = vector of explanatory values for the j^{th} validation data point, with j going from 1 to m
X = matrix of explanatory (independent) variables used in fitting the model
X′ = transpose of X
$(X'X)^{-1}$ = inverse of the matrix X′X.

The percentage of the validation points for which the measured T_L or $T_{0.01}$ value is within the prediction interval (i.e., within the $HW_{95\%}$ of the predicted T_L or $T_{0.01}$) were determined for each model. This is the percentage of successfully predicted points, and the comparison rule is the "bigger the better." According to statistical theory, the $HW_{95\%}$ formula in Equation 4.24 should only be applied if the fitted model is adequate (i.e., does not have a statistically significant lack-of-fit). However, as is discussed in a subsequent section of the report, essentially all of the fitted models have a statistically significant lack-of-fit. The decision was made to proceed with using the $HW_{95\%}$ validation approach, but keeping in mind its limitations. For example, poor models may have $HW_{95\%}$ values so large that all or virtually all measured values are included. In such cases, the percentage of "successfully predicted" points will be a misleading statistic.

The average prediction uncertainty (at 95% confidence) for each model over all of the validation data will be computed as well. This statistic, denoted as average prediction uncertainty $(APU)_{95\%}$, is determined by the formula given by:

$$APU_{95\%} = \frac{\sum_{j=1}^{m} t_{0.025,n-p} \cdot s \cdot \sqrt{1 + x_j (X'X)^{-1} x'_j}}{m} \tag{4.25}$$

For the $APU_{95\%}$ statistic, the comparison rule is the "smaller the better."

4.2.5 Identification of Outliers

Concurrent with the model-development and validation process, there is a need for an assessment of each data point in the database. Even when care is taken in the preparation of such a database, there is a potential for one or more outliers to find their way into the set of values. Also, one or more data points

may be highly influential in determining the fits of one or more models. Including such data points in either the model development or validation activities may yield misleading measures of goodness-of-fit or validation performance for one or more of the models under consideration. As discussed in the test plan (Vienna 2002) for the study, caution was taken in identifying outliers during the model development and validation processes. There was a need to be consistent regarding the identification of outliers across the models and, to the extent possible, to gain a consensus for an outlier over all of the models. To that end, unless there was consensus regarding the status of a data point as an outlier, the data point remained a part of the development and validation process for all of the models.

Once again, the intent is to conduct the model-fitting and validation processes over exactly the same sets of data for each of the candidate models. Thus, differences that are seen in the resulting measures of goodness-of-fit among the fitted models then will be strictly due to the features of the models themselves.

4.2.6 Selecting Among the Candidate Models

If no other critical issues arise in fitting and validating the candidate models, then the goodness-of-fit measures for the model-development and validation processes discussed previously provide the starting place for selecting the T_L model for use by WTP. If a model has the best value for each of these measures, then that is the model that should be selected by the assessment process and recommended for further consideration. It is also possible that another model would consistently be a very close second in each of the measures. Such a close finish would suggest that this second model also should be kept on the short-list for possible use at WTP. This short list should be compared again when all the data collection for the project is complete and final models are fit. Whichever model performs better with the final data set would then be the leading candidate for use by the WTP.

However, it is probably more likely that different models may be best for different measures. In this case, there is a need for a single metric that would allow for meaningful comparisons among the models. This metric should be influenced by both the model-development and model-validation results. Such a metric is provided by an uncertainty-weighted validation-error sum of squares (UVESS) statistic as given by:

$$\text{UVESS} = \sum_{j=1}^{m} t_{0.025,n-p} \cdot s \cdot \sqrt{1 + x_j (X'X)^{-1} x_j'} \left(y_j - \hat{y}_j\right)^2 \tag{4.26}$$

The weights in this expression are the prediction uncertainties (at 95% confidence) for each of the validation data points.[(a)] Note that for each model, the weights 1) bring in the model's root mean squared error (s), 2) depend on the number of parameters in the model through the degrees of freedom of student's t statistic, and 3) are influenced by the X's (predictor variables) used in the model fitting. For this metric, the rule is "the smaller the better." In fact, a useful scale for comparisons is provided by dividing all of the UVESS values by the smallest value. Thus, the model with a value of 1 after this "normalization" is the best performer relative to this metric for T_L or $T_{0.01}$ being modeled. Once again, there is the possibility of a "close second" in such an assessment.

(a) Note that the weights used here are prediction uncertainties and not the reciprocals of the associated prediction variances. Snee (1977) discusses the use of the latter with the PRESS statistic.

4.3 Evaluation Data

The data nominally available for spinel T_L model evaluation included the initial 35 existing glasses (see Section 2.2), the 31 new test matrix glasses (see Section 2.2), and the additional 103 existing glasses for the expanded composition region of interest (see Section 2.5). However, spinel T_L values could not be obtained for 6 of the new test matrix glasses (see Section 3.1). This left a total of 163 spinel T_L-composition data points available for evaluating the models presented in Section 4.1. The compositions and spinel T_L values for these 163 data points are listed in Table A.2 of Appendix A. However, as discussed in Section 3.2, the spinel T_L values for glasses Sp-Na-1, Sp-Na-3, and Sp-Cr-1 are suspect. Hence, the data points for those three glasses were excluded from the model-evaluation process.

A total of 7 glasses (CVS2-1, CVS2-15, CVS2-46, SP-Ca-2, SPA-18, SPA-32, and WTP-TL-3), which had at least one component mass fraction significantly beyond the range of values for the remaining glasses, were not removed from the model-evaluation data set since the purpose of the study is to evaluate model predictions over the entire range of expected WTP HLW glass compositions. Hence, the model-evaluation results presented subsequently may be affected by these 7 potentially influential data points remaining in the model-evaluation data set.

During the model-evaluation process, certain data points were identified as outlying or influential for some models. However, there was no consensus across all the candidate model forms. The poor performance of the solubility product models made it difficult to declare points as outliers or influential, thereby making consensus difficult to obtain. Hence, outliers or influential data points remain in the evaluation data set and could impact the fitted candidate models in different ways. The LMM and the sub-lattice model may be more sensitive to outlying and influential data points because of their larger numbers of fitted parameters.

Some new test-matrix glasses (discussed in Section 2.2) were identified as outliers, influential points, or points having larger prediction uncertainties for some candidate model forms. Such results are likely due to the use of vertices in constructing the outer-layer portions of the test matrix with and without U and/or Th. Vertices are the most extreme points in a composition region of interest. The numbers of outer-layer radioactive vertices (4) and outer-layer nonradioactive vertices (8) in the test matrix were relatively small to begin with. Then two points from each of the two groups were lost due to the inability to determine spinel T_L. This left an even smaller number of outer layer points available for model evaluation. Further, in the model evaluation data set, a smaller number of the 160 glasses came from the new test matrix. The rest were from existing databases. Because the existing literature data are generally not nearly as extreme in composition space as the test matrix outer-layer vertices, the outer-layer vertices may be among the most outlying in multivariate composition space. Such glasses will tend to be more challenging for models to fit or predict when validating.

Pairwise correlation coefficients were calculated using the 160 data points over all pairs of 48 components in the database. Values greater in absolute value than 0.50 were observed only for the pair ZnO – SrO, which had a correlation coefficient of +0.65. This suggests that the effects of ZnO and SrO cannot be easily distinguished using this final T_L data set, and the correlation between all other pairs of components is within an acceptable range.

In summary, 160 data points were used in the model-evaluation process. Several outliers and potentially influential points remain in the data set and may affect different models in different ways. Models with more parameters fitted to the data will tend to be most affected by outliers and influential points.

The T0.01 data set was more limited. Measured $T_{0.01}$ data was available for only 14 of the 31 new formulations (given in Table 3.6) with spinel as the only crystalline phase. The $T_{0.01}$ was available for 31 additional literature glasses, with 26 unique compositions (listed in Appendix A). This leaves a total of 45 data points. However, four of the 45 glasses were found to be suspect data to inconsistencies between T_L and T_0 (SP-Na-1, SP-Na-3, SP-Cr-1-o, and SP-Cr-1-r). This left a data set of 41 points for fitting the $T_{0.01}$ model. As described in Section 4.1.1.2, this 41 glass data set is poorly designed to support multi-component modeling over the entire composition region.

4.4 Data-Set Splitting

There is a need to assess the sensitivity of a model's values for the various metrics to the splitting of the T_L-glass composition database into the model-development and validation sets. As anticipated in the test plan, the data set was sorted by T_L value and then every fifth data point removed for validation. Since about one-fifth of the data is to be used for validation, selecting these data starting at the first, second, third, fourth, or fifth values in the database provides five possible splitting outcomes. A similar process was used for the $T_{0.01}$ database, although it contains fewer data points as described in Section 3.2. The model-development and model-validation processes were conducted for each of these possible splitting outcomes (labeled as data groupings 1 through 5), and the goodness-of-fit and validation-performance metrics were computed for each. Comparisons among the fitted coefficients for each model were also provided. A consistent outcome for the model selected as best would assure that the metric being used for model selection is robust (i.e., not overly sensitive) to the way the splits have been generated. Results from these splitting options were included as part of the assessment study.

The five data groupings are explored for each of the two response variables (T_L and $T_{0.01}$) in the following sections.

4.5 T_L Model Fitting and Comparisons

Each of the six model forms were fitted to each of the five T_L data groupings. The summary statistics for the model fits and validation are tabulated in Table 4.3. JMP[(a)] Version 5.0 from SAS Institute, Inc. (2002) was used to fit all models. Appendix C provides additional details of the statistical analyses including tables of fitting results and exhibits with graphical results from the statistical analyses. Exhibits C.1 through C.6 provide the fits of each of the six models, respectively, to these data for each of the five data groupings. Included in the output generated by JMP are values for R^2 (denoted as RSquare), R^2_{adj} (denoted as Rsquare Adj), s (denoted as root mean square error), and the PRESS statistic (denoted by Press). In the graphical output from these fitting processes, an open, green diamond is used to represent a model-development data point and a closed, red circle is used to represent a model-validation data point. Note that the response variables for the models are not all the same. For example, some response

(a) JMP = commercial software used in model fitting and evaluation (SAS institute).

Table 4.3. Goodness of Fit Measures for the T_L Models

Metric	Group	DWPFM	IPM	SPM w Cr&Ni	SPM w Ni&Fe	SLM	LMM
	1	0.709	0.863	0.253	0.154	0.885	0.902
R^2	2	0.668	0.844	0.243	0.218	0.890	0.888
(The bigger the better)	3	0.625	0.873	0.177	0.132	0.886	0.896
	4	0.633	0.867	0.181	0.134	0.886	0.894
	5	0.629	0.868	0.196	0.183	0.887	0.908
	Avg[(a)]	0.653	0.863	0.210	0.164	0.887	0.897
	1	0.307	0.833	0.006	0.186	0.775	0.789
R^2_{val}	2	0.510	0.903	0.047	-0.002	0.722	0.862
(The bigger the better)	3	0.705	0.797	0.285	0.231	0.826	0.845
	4	0.698	0.793	0.291	0.262	0.810	0.842
	5	0.734	0.809	0.245	0.021	0.804	0.785
	Avg	0.591	0.827	0.175	0.140	0.787	0.825
Avg Prediction	1	119	73	179	192	81	67
Uncertainty for Model	2	118	75	179	185	74	68
(The smaller the better)	3	130	68	181	187	79	66
	4	129	71	184	191	78	69
	5	132	71	190	185	80	64
	Avg	126	72	183	188	78	67
Avg Prediction	1	120	73	181	192	85	69
Uncertainty for	2	117	75	175	183	79	70
Validation	3	128	68	179	186	79	67
(The smaller the better)	4	129	72	185	191	80	69
	5	134	71	192	188	80	66
	Avg	126	72	183	188	80	68
% Successfully	1	92%	95%	93%	94%	96%	98%
Predicted for Model	2	95%	94%	92%	92%	96%	98%
(The bigger the better)	3	94%	95%	93%	93%	96%	97%
	4	95%	96%	94%	95%	97%	97%
	5	95%	96%	93%	94%	97%	97%
	Avg	94%	95%	93%	94%	96%	97%
% Successfully	1	91%	94%	90%	90%	97%	97%
Predicted for	2	88%	100%	90%	97%	88%	94%
(The bigger the better)	3	97%	91%	91%	97%	94%	94%
	4	97%	94%	89%	93%	90%	90%
	5	97%	94%	97%	88%	94%	94%
	Avg	94%	94%	91%	93%	92%	94%
UVESS	1	6.480	1.000	14.100	12.117	2.101	1.312
	2	7.924	1.000	17.711	19.310	4.105	1.447
(The smaller the better)	3	3.517	1.261	11.777	12.840	1.365	1.000
	4	2.973	1.301	11.184	11.437	1.294	1.000
	5	2.514	1.000	9.140	13.220	1.146	1.103
	Avg	4.682	1.112	12.782	13.785	2.002	1.172

(a) "Ave" values represent the numerical average of the values for the 5 individual data sets.

variables are T_L while other response variables are $1/T_L$. As another example, some T_L responses are expressed using degrees Celsius (°C), while others are expressed in Kelvin (K). Hence, care must be taken in comparing some of the JMP outputs for different models. The comparisons offered in this discussion are based on the results from the fitting process being converted over to T_L expressed in °C, for consistency. Also included in these exhibits are a table of "Parameter Estimates" (the estimated coefficients) for the fitted models and a table providing the statistical test for a significant LOF for the model. P-values are provided for each of the estimated parameters of the fitted model and for the F Ratio associated with the test for LOF. A p-value for the LOF test that is less than 0.05 indicates a LOF that is statistically significant at the 5% level. Note that there is a statistically significant (at a 5% level) LOF for most of the models for most of the data groupings. The exception is the Cr and Ni SPMs, which show no indication of a lack of fit for 4 of the data groupings. In assessing pure error, the statistical software uses each combination of levels of the independent variables that has multiple response measurements. Thus, for the Cr and Ni SPMs, if the Cr and Ni values are the same for several glasses, the scatter among their responses is assumed to represent the pure error of the process. This leads to the possibility of the software overestimating the pure error for such situations. A more representative test for LOF for this situation could have been conducted manually, but, due to time constraints, it was decided not to be necessary to support the conclusions of this study.

A comment is needed regarding the p-values for the estimated parameters of the fitted models provided as part of the JMP output. As a default, JMP provides the p-value associated with testing whether the estimated coefficient is statistically different from 0. For the ion potential and LMMs, such a test is not appropriate for their estimated coefficients. However, since reducing the models to their simplest form was not an objective of this task, no further exploration of these results for that purpose was pursued.

A plot of the residuals[(a)] versus predicted values for each model fit is also provided in these exhibits. Residual plots are useful for checking assumptions made about the errors of the model used for fitting the data. The assumptions on the errors include independence, zero mean, constant variance, and normal distribution. A leverage plot for each fitted parameter in the model is also provided. From Draper and Smith (1998), the "term leverage is used because a point exerts more influence on the fit if it is farther away from the middle of the plot in the horizontal direction." No problems are seen in these plots over this set of exhibits.

Tables C.1 through C.6 in Appendix C provide summary information for each of these fits for each of the six models, respectively. This information is presented in the units of the original response variables for the models, which are shown in these tables. The number of parameters associated with each model is also provided. The estimates for these parameters are shown for each data grouping and may be compared across the data groupings.

Also, note that no data are excluded in the analyses that follow (except for the three suspect data points discussed in Section 3.2). All of the data identified for use in model development and model validation are part of these calculations. The approach of looking for consensus among the models in identifying an outlying observation may have been unduly influenced by some of the models that fit the model data and predicted the validation data so poorly. Thus, while this approach made the task of including/excluding data in the fitting of the candidate models more manageable relative to the time available for this effort,

---

(a) A residual is the difference between the measured and predicted response values (i.e., $y_i - \hat{y}_i$).

there is the potential that some performance measures for the models with more terms (i.e., the SLM and LMM) may have been influenced by this approach.

Exhibits C.7 through C.11 in Appendix C provide plots of the residuals and prediction uncertainties (both model development, as open, green diamonds, and model validation, as closed, red circles) by glass-composition number for each of the fitted models for each of the five data groupings, respectively. Once again, the y-axis for each of these plots is in °C so that comparisons across all of the models can be readily made using these plots.

A review of these plots suggests that the IPM is the best performer relative to the behavior of the residuals and prediction uncertainties over the 5 data groups. The prediction performances of the LMM and SLM are closely following, although larger residuals and prediction uncertainties for a small number of points occur for these models. The LMM and SLM are expected to be more sensitive to outlying or influential data points (either in fitting or in validation) because of their larger number of fitted coefficients.

Tables C.7 through C.11 in Appendix C provide summaries of the six model fits for the five data groupings, respectively. The upper portion of each table provides information in the original unit of measure for the T_L response used by each of the models. The middle portion of each table provides this information with T_L being expressed in °C. Also, note that values for the goodness-of-fit measures that were discussed in Section 4.2.3 for the model-development data are presented in this middle section of each table. The lower portion of each table provides information on the validation-performance measures for each model. These values are also based upon T_L being expressed in °C.

Exhibit C.12 in Appendix C provides some plots of the goodness-of-fit measures across the five data groupings to facilitate comparisons of interest among the fitted models. Table 4.3 provides the details of the values in these plots along with values for additional goodness-of-fit measures. Different models appear to perform better relative to some of the metrics for some of the data groupings. The R^2 values for the IPM, SLM, and LMM are comparable, and the corresponding R^2_{val} values of the models are comparable to their R^2 counterparts.

The values for the UVESS statistic (from Equation 4.26) suggest that the IPM is best for 3 of the 5 data groupings and the most consistent performer across all 5 of the data groupings for this metric. Data grouping 2 appears to be the one for which the performance of the SLM weakens as compared to the performance of the IPM in particular.

4.6 $T_{0.01}$ Model Fitting and Comparisons

Each of the six model forms were fitted to each of the $T_{0.01}$ data groupings as described for T_L in Section 4.4. The summary statistics for the model fits and validation are tabulated in Table 4.4. JMP[(a)] Version 5.0 from SAS Institute, Inc. (2002) was used to fit all models. Appendix D provides additional details of the statistical analyses including tables of the fitting results and exhibits containing graphical results of the statistical analyses. Exhibits D.1 through D.6 provide the fits of each of the six models, respectively,

(a) JMP = commercial software used in model fitting and evaluation (SAS institute).

Table 4.4. Goodness of Fit Measures for the $T_{0.01}$ Models

Metric	Group	DWPFM	IPM	SPM w Cr&Ni	SPM w Ni&Fe	SLM	LMM
	1	0.614	0.697	0.154	0.270	0.899	0.907
R^2	2	0.642	0.611	0.254	0.402	0.897	0.881
(The bigger the better)	3	0.700	0.685	0.208	0.374	0.914	0.902
	4	0.714	0.596	0.132	0.359	0.877	0.861
	5	0.535	0.585	0.264	0.298	0.867	0.842
	Avg.[(a)]	0.641	0.635	0.202	0.341	0.891	0.879
	1	0.411	-1.090	-0.232	0.544	0.581	0.607
R^2_{val}	2	0.593	0.557	0.175	0.845	0.710	0.746
(The bigger the better)	3	0.088	-0.189	0.104	0.115	0.247	0.598
	4	-3.259	0.455	0.290	0.210	0.617	0.882
	5	0.832	0.538	-0.101	0.335	-21.166	0.908
	Avg.	-0.267	0.054	0.047	0.410	-3.802	0.748
Avg Prediction	1	224	180	329	317	195	123
Uncertainty for Model	2	226	203	310	271	192	129
(The smaller the better)	3	183	185	319	298	183	119
	4	196	209	329	301	239	140
	5	242	197	280	297	232	140
	Avg.	214	195	313	297	208	130
Avg Prediction	1	208	189	326	355	248	135
Uncertainty for Validation	2	230	203	291	247	543	139
(The smaller the better)	3	184	194	317	280	404	131
	4	274	207	327	300	382	158
	5	244	205	290	286	2293	179
	Avg.	228	200	310	294	774	148
% Successfully Predicted	1	97%	97%	97%	100%	100%	97%
for Model	2	97%	97%	97%	90%	100%	97%
(The bigger the better)	3	100%	100%	93%	90%	100%	100%
	4	97%	97%	93%	94%	100%	97%
	5	97%	97%	90%	94%	100%	97%
	Avg.	98%	98%	94%	94%	100%	98%
% Successfully Predicted	1	100%	86%	100%	100%	100%	100%
for Validation	2	100%	100%	86%	75%	100%	100%
(The bigger the better)	3	88%	88%	100%	100%	88%	88%
	4	75%	100%	88%	88%	100%	100%
	5	100%	89%	86%	88%	100%	100%
	Avg.	93%	92%	92%	90%	98%	98%
UVESS	1	2.306	8.605	4.367	1.564	1.340	1.000
	2	2.766	2.750	9.134	8.555	39.238	1.000
(The smaller the better)	3	3.174	4.962	5.802	4.194	5.417	1.000
	4	204.769	7.288	13.306	13.738	22.996	1.000
	5	2.904	6.162	13.854	7.723	3288.020	1.000
	Avg.	43.184	5.953	9.292	7.155	671.402	1.000

(a) "Ave." values represent the numerical average of the values for the 5 individual data sets.

to these data for each of the five data groupings. Included in the output generated by JMP are values for R^2, R^2_{adj}, s, and the PRESS statistic. In the graphical output from these fitting processes, an open, green diamond is used to represent a model-development data point and a closed, red circle is used to represent a model-validation data point. Note that the response variables for the models are not all the same. For example, some response variables are $T_{0.01}$ while other response variables are $1/T_{0.01}$. As another example, some $T_{0.01}$ responses are expressed using degrees Celsius (°C), while others are expressed in Kelvin (K). Hence, care must be taken in comparing some of the JMP outputs for different models. The comparisons offered in this discussion are based on the results from the fitting process being converted over to $T_{0.01}$ expressed in °C, for consistency.

As for the T_L case, included in the exhibits for the $T_{0.01}$ data are a table of "Parameter Estimates" (the estimated coefficients) for the fitted models and a table providing the statistical test for a significant LOF for the model. P-values are provided for each of the estimated parameters of the fitted model and for the F Ratio associated with the test for LOF. A p-value less than 0.05 indicates a LOF that is statistically significant at a significance level of 5%. Note that for each of the six models, there are one or more of the data groupings for which no statistically significant (at a 5% level) LOF is indicated. For the estimated coefficients, note that the p-values provided as a default by JMP for the IPM and LMM do not represent the appropriate statistical tests for these parameters.

Residual and leverage plots are provided for these model fits as part of the exhibits. In general, the plots for these model fits suggest problems that were not seen in the results for the T_L case. Specifically, more scatter is seen in the whole model plots (those plots in the exhibits showing both the model-development points [open, green diamonds] and the model validation points [closed, red circles] around the fitted model). More will be said on this topic in the discussion that follows.

Tables D.1 through D.6 in Appendix D provide summary information for each of the five split-data fits for each of the six models, respectively. This information is presented in the units of the original response variables for the models, which are shown in these tables. The number of parameters associated with each model is also provided. The estimates for these parameters are shown for each data grouping and may be compared across the data groupings. It is very apparent that there is less consistency in the values of the estimated parameters across the data groupings for the $T_{0.01}$ than in the estimated parameter values for the T_L models.

Note that there are substantially fewer data points for the $T_{0.01}$ data as compared to the T_L data. This leads to very few data being available for validation (~8 for each of the data groupings). Also, in general, there is more variation among the estimates of each of the model parameters across the five data groupings for the $T_{0.01}$ data as compared to the T_L data, and a model's root mean squared errors (the s values) for the $T_{0.01}$ data are larger than those for the T_L data. These aspects of the results from fitting models to the two sets of response variables suggest a more consistent performance of each model relative to the goodness-of-fit measures for the T_L models as compared to its performance relative to these measures for the $T_{0.01}$ models. This is explored in the next section.

Exhibits D.7 through D.11 in Appendix D provide plots of the residuals and prediction uncertainties (both model development, as open, green diamonds, and model validation, as closed, red circles) by glass-composition number for each of the fitted models for each of the five data groupings, respectively. The y-

axis for each of these plots is in °C so that comparisons across all of the models can be readily made using these plots.

In general, note the large residuals and prediction uncertainties that are indicated across all of these plots (i.e., for each of the models for each of the data groupings). As will be mentioned in a subsequent section, the inability for all models to reliably predict $T_{0.01}$ is based on either the model forms being ineffective for predicting $T_{0.01}$ or that the data set is insufficient to adequately fit the models. This significant issue resulted in a recommendation that WTP consider the benefits of using a T_L-based constraint or develop adequate data and models for prediction of $T_{0.01}$.

Tables D.7 through D.11 in Appendix D summarize the six models fitted to the five data groupings, respectively. The upper portion of each table provides information in the original unit of measure for the $T_{0.01}$ response used by each of the models. The middle portion of each table provides this information with $T_{0.01}$ being expressed in °C. Also, note that values for the goodness-of-fit measures that were discussed in Section 4.2.3 for the model-development data are presented in this middle section of each table. The lower portion of each table provides information on the validation-performance measures for each model. These values are also based upon $T_{0.01}$ being expressed in °C.

Exhibit D.12 in Appendix D provides some plots of the goodness-of-fit measures across the five data groupings to facilitate comparisons of interest among the fitted models. Table 4.4 provides the details of the values in these plots along with values for additional goodness-of-fit measures.

Different models appear to perform better relative to some of the metrics for some of the data groupings. The R^2 values for the LMM are slightly better than those for the SLM. However, the corresponding R^2_{val} values of these two models are much smaller than their R^2 counterparts across all of the data groupings. This suggests that the predictive capabilities of these fitted models may be less than adequate. (These capabilities over the $T_{0.01}$ data certainly are less appealing than those capabilities suggested for the fitted T_L models.)

With the current dataset, it appears as if the LMM most successfully predicts the $T_{0.01}$ for all five data groupings. However, the high prediction uncertainties are troubling. Note again that there are many fewer data points in this data set, with only about 8 data points for validation. More would be required to provide an adequate preliminary model for $T_{0.01}$.

5.0 Discussion and Recommendation

A database of T_L and $T_{0.01}$ values for glasses in the composition region of expected Hanford HLW glasses was developed. The T_L values of 25 glasses in the spinel primary phase field were measured and combined with T_L data from 135 glasses found in the literature. The T_L values ranged from 780°C to 1306°C for the new data set and from 811°C to 1350°C for the literature data set. The $T_{0.01}$ of 14 glasses in the spinel primary phase field were measured and combined with $T_{0.01}$ data from 31 glasses found in the literature. The $T_{0.01}$ values for the new glasses ranged from 740°C to 1180°C and from 633°C to 1158°C for the literature data set. The measured values are summarized in Table 5.1. These data, in conjunction with previous data reported in literature and data to be generated in future studies, will greatly assist in the development and validation of T_L or $T_{0.01}$ models by the WTP.

Table 5.1. Measured T_L and $T_{0.01}$ of Current Study Glasses in °C

Glass ID	T_L	$T_{0.01}$	Primary Phase	Glass ID	T_L	$T_{0.01}$	Primary Phase
WTP-TL-01	760	-[(a)]	crystobalite	WTP-TL-17	1,197	825	spinel
WTP-TL-02	771	-	albite	WTP-TL-18	852	-	spinel
WTP-TL-03	1,191	932	spinel	WTP-TL-19	1,070	876	spinel
WTP-TL-04	1,117	-	spinel	WTP-TL-20	1,259	1,068	spinel
WTP-TL-05	1,107	740	spinel	WTP-TL-21	1,181	764	spinel
WTP-TL-06	898	-	clinopyroxene	WTP-TL-22	1,249	-	zircon
WTP-TL-07	1,296	-	spinel	WTP-TL-23	1,219	947	spinel
WTP-TL-08	1,029	-	spinel	WTP-TL-24	1,071	891	spinel
WTP-TL-09	1,289	-	thorianite	WTP-TL-25	820	-	spinel
WTP-TL-10	1,194	-	spinel	WTP-TL-26	972	-	spinel
WTP-TL-11	1,070	-	spinel	WTP-TL-27	1,165	1,047	spinel
WTP-TL-12	1,306	-	spinel	WTP-TL-28	1,064	1,100	spinel
WTP-TL-13	1,006	-	spinel	WTP-TL-29	1,254	973	spinel
WTP-TL-14	1,195	-	spinel	WTP-TL-30	1,257	974	spinel
WTP-TL-15	780	-	spinel	WTP-TL-31	1,119	-	spinel
WTP-TL-16	-	1,180	spinel	-	-	-	-

(a) "-" signifies an empty data field.

Six different models (DWPFM, IPM, two variations of the SPM, SLM, and LMM) were fitted to the 5 model-fit data sets and used to predict responses of the 5 different validation data sets. The six model forms were fitted to both T_L and $T_{0.01}$. It was found that all six of the models had difficulty in predicting $T_{0.01}$ with good precision; those results are likely due to the small available data set or the fact that the model forms were not specifically developed for $T_{0.01}$. Of all the models, the LMM was found to predict the $T_{0.01}$ of validation glasses with the best precision.

The IPM and LMM models were found to most consistently predict the T_L of the model-development and validation data sets, with the smallest prediction uncertainties and the most favorable responses to other statistical measures for comparing models. Figure 5.1 shows the UVESS and R^2_{val} statistics as functions of T_L model-fit parameters. This relationship shows that generally, the higher the number of coefficients, the better the model tends to be at predicting the T_L of validation glasses. The small number of fit parameters and superior statistics make the IPM a good candidate for WTP use. However, the LMM has

similar statistical values and is of an easier form for the plant to implement (e.g., although there are 17 parameters, the concentrations of only those 17 components are used in the LMM model where the IPM uses all glass components in the model).

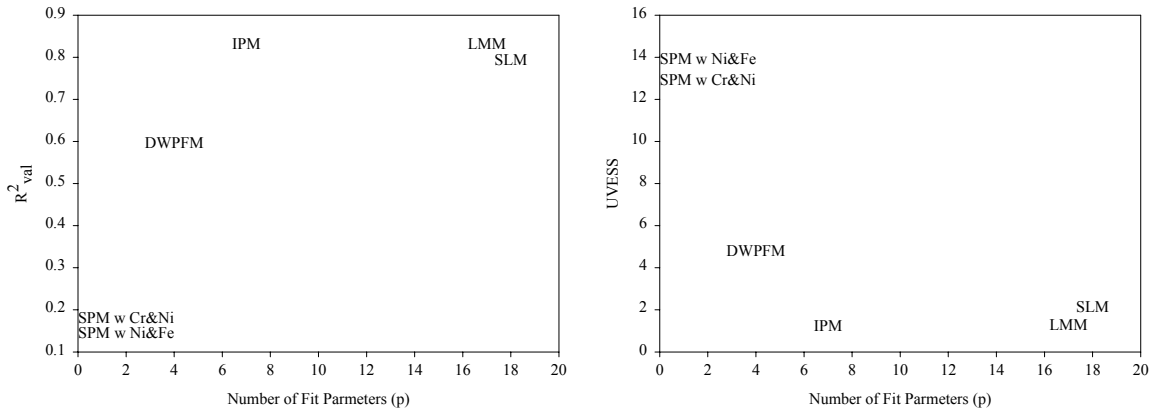

Figure 5.1. R^2_{val} and UVESS Statistics as Functions of the Number of T_L Model Parameters

It is recommended that the WTP evaluate the impacts of using a $T_{0.01}$ model with low precision or constraining glass composition based on T_L (using higher precision models). If the former is determined to be more beneficial, then we recommend further development of the $T_{0.01}$ database and, if necessary to obtain adequate prediction precision, further development of model forms specifically for $T_{0.01}$.

To support evaluations of the different crystal constraint strategies, we have fitted the LMM to the complete data sets for T_L and $T_{0.01}$ used in the model-development and validation in Sections 4.5 and 4.6. That is, the same LMMs reported earlier were fitted to the data without splitting a validation data set out. These preliminary models are summarized in Table 5.2. Interestingly, the coefficients for these preliminary models are relatively consistent as shown in Figure 5.2. These models represent good working models for the WTP HLW glasses in the spinel primary phase field. With the exception of the IPM fit to T_L data, these models give the best current prediction capability for glasses in this composition region of any investigated and thus, represent an improvement over previous models.

Table 5.2. Summary of Preliminary LMM for T_L and $T_{0.01}$

Component	T_L (°C)	$T_{0.01}$ (°C)
Al_2O_3	2831.3	3391.7
B_2O_3	755.7	378.1
CdO	6240.6	-[(a)]
Cr_2O_3	25944.9	27121.9
F	5337.4	-
Fe_2O_3	2759.1	3637.9
K_2O	-1211.1	-
Li_2O	-2019.2	-2655.9
MgO	2233.8	-
MnO	1862.0	2852.6
Na_2O	-827.1	-1786.5
NiO	9316.2	13169.6
P_2O_5	-3949.2	-
SiO_2	862.7	393.8
SrO	-	-479.8
ThO_2	1766.9	-
U_3O_8	2270.2	-
ZrO_2	2122.2	4056.8
# of Data	160	41[(b)]
p	17	11
R^2	0.892	0.869
R^2_{adj}	0.880	0.825
s	32.2	53.5
Mean	1062.1	920.9

(a) "-" signifies empty data field.
(b) Four of the 45 glasses had significant differences between T_L and T_0, and were excluded from modeling.

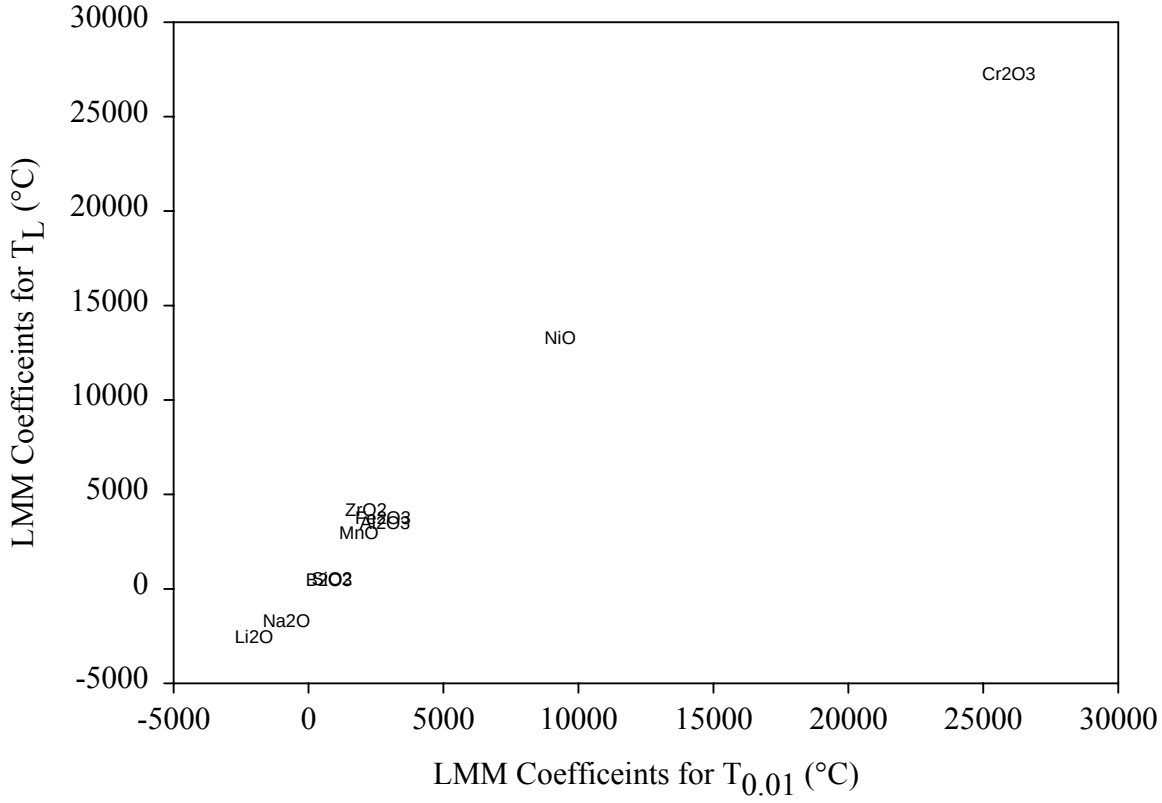

Figure 5.2. Comparison of LMM Coefficients for T_L and $T_{0.01}$

6.0 References

Arakali, A., J. M. Perez, R. A. Peterson, and C. A. Musick. 2003. *Research and Technology Plan*. 24590-WTP-PL-RT-01-002, Rev 2, Bechtel National Inc., Richland, WA.

Brown, K. G., C. M. Jantzen, and G. Ritzhaupt. 2001. *Relating Liquidus Temperature to Composition for Defense Waste Processing Facility (DWPF) Process Control (U)*. WSRC-TR-2001-00520, Westinghouse Savannah River Company, Aiken, SC.

Cornell, J. A. 2002. *Experiments with Mixtures.* 3rd ed., John Wiley & Sons, NY.

DOE. *See U. S. Department of Energy*.

Draper, N. R., and H. Smith. 1998. *Applied Regression Analysis*. Third Edition, John Wiley & Sons, New York, NY.

Gan, H., and I. L. Pegg. 2001. *Development of Property-Composition Models for RPP-WTP HLW Glasses*. VSL-01R3600-1, Vitreous State Laboratory, Washington, D.C.

Hrma, P. 1999. "Modeling of Spinel Settling in Waste Glass Melter." in *Science to Support DOE Site Cleanup*, PNNL-12208, Pacific Northwest National Laboratory, Richland, WA.

Hrma, P., G. F. Piepel, M. J. Schweiger, D. E. Smith, D.-S. Kim, P. E. Redgate, J. D. Vienna, C. A. LoPresti, D. B. Simpson, D. K. Peeler, and M. H. Langowski. 1994. *Property/Composition Relationships for Hanford High-Level Waste Glasses Melting at 1150°C*, PNL-10359, Vol. 1 and 2, Pacific Northwest Laboratory, Richland, WA.

Hrma, P., J. D. Vienna, and M. J. Schweiger. 1996. "Liquidus Temperature Limited Waste Loading Maximization for Vitrified HLW." In: *Ceramic Transactions 72*, pp. 449-456, American Ceramic Society, Westerville, OH.

Hrma, P., J. D. Vienna, M. Mika, J. V. Crum, and G. F. Piepel. 1999. *Liquidus Temperature Data for DWPF Glass*. PNNL-11790, Rev. 1, Pacific Northwest National Laboratory, Richland, WA.

Hrma, P., and J. D. Vienna. 2001. "Balancing Cost and Risk by Optimizing the High-Level Waste and Low-Activity Waste Vitrification." In: *Waste Management '00*, University of Arizona, Tucson, AZ.

Hrma, P., J. Alton, J. Klouzek, J. Matyas, M. Mika, L. Nemec, T. J. Plaisted, P. Schill, and M. Trochta. 2001. "Increasing High-Level Waste Loading in Glass without Changing the Baseline Melter Technology." *Waste Management '01*, University of Arizona, Tucson, AZ.

Izak, P., P. Hrma, B. K. Wilson, and J. D. Vienna. 2001. "The Effect of Oxygen Partial Pressure on Liquidus Temperature of a High-Level Waste Glass with Spinel as the Primary Phase," in *Ceramic Transactions, 119*, pp. 309-316, American Ceramic Society, Westerville, Ohio.

Jantzen, C. M. 1991. "First Principles Process-Product Models for Vitrification of Nuclear Waste: Relationship of Glass Composition to Glass Viscosity, Resistivity, Liquidus Temperature, and Durability." In: *Ceramic Transactions*, Vol. 23, American Ceramic Society, Westerville, OH.

Kot, W. K., and I. L. Pegg. 2001. *Glass Formulation and Testing With RPP-WTP HLW Simulants*. VSL-01R2540-2, Vitreous State Laboratory, Washington, D.C.

MDI. 2001a. *Jade Version 6.0 Users Manual.* MDI Inc., Livermore, CA.

MDI. 2001b. *RIQAS Version 4.0 Users Manual.* MDI Inc., Livermore, CA.

Mika, M., M. J. Schweiger, J. D. Vienna, and P. Hrma. 1997. "Liquidus Temperature of Spinel Precipitating High-Level Waste Glasses," in *Scientific Basis for Nuclear Waste Management XX*, pp. 71-78, Materials Research Society, Pittsburgh, Pennsylvania.

Mika, M., M. Patek, J. Maixner, S. Randakova, and P. Hrma. 2001. "The Effect of Temperature and Composition on Spinel Concentration and Crystal Size in High-Level Waste Glass," in *Proceedings of the 8th International Conference On Radioactive Waste Management and Environmental Remediation, ICEM'01*, Bruges, Belgium.

National Bureau of Standards (NBS). 1980. *Standard Reference Material 773 Soda-Lime-Silica Glass for Gradient Furnace Liquidus Temperature*. Washington, D.C.

Nelson, J. L. 2002. *Liquidus Temperature Testing and Modeling for HLW Glass Melts*. 24590-HLW-TSP-RT-02-002, Rev. 0, Test Specification, Bechtel National, Inc., Richland, WA.

Perez, J. M., D. F. Bickford, D. E. Day, D. S. Kim, S. L. Lambert, S. L. Marra, D. K. Peeler, D. M. Strachan, M. B. Triplett, J. D. Vienna, and R. S. Wittman. 2001. *High-Level Waste Melter Study Report.* PNNL-13582, Pacific Northwest National Laboratory, Richland, WA.

Piepel, G. F., C. M. Anderson, and P. E. Redgate. 1993. "Response Surface Designs for Irregularly-Shaped Regions." (Parts 1, 2, and 3, *1993 Proceedings of the Section on Physical and Engineering Sciences*, pp. 205-227, American Statistical Association, Alexandria, VA.

Piepel, G. F. and T. Redgate. 1997. "Mixture Experiment Techniques for Reducing the Number of Components Applied to Modeling Waste Glass Sodium Release." *J. Amer. Cer. Soc.* 80:3038-3044.

Piepel, G. F. 1999. *MIXSOFT–Software for the Design and Analysis of Mixture and Other Constrained Region Experiments, User's Guide Version 2.3.1*. MIXSOFT Mixture Experiment Software, Richland, WA.

Piepel, G. F., S. K. Cooley, D. K. Peeler, J. D. Vienna, and T. B. Edwards. 2002a. "Augmenting a Waste Glass Mixture Experiment Study with Additional Glass Components and Experimental Runs." *Quality Engineering* 15:91-111.

Piepel, G. F., J. M. Szychowski, and J. L. Loeppky. 2002b. "Augmenting Scheffé Linear Mixture Models with Squared and/or Crossproduct Terms." *J. Quality Tech.* 34:297-314.

Plaisted, T. J., J. Alton, B. K. Wilson, and P. Hrma. 2001. "Effect of Minor Component Addition on Spinel Crystallization in Simulated High-Level Waste Glass," in *Ceramic Transactions 119*, 291-299, American Ceramic Society, Westerville, OH.

Plodinec, M. J. 1999. "Solubility Approach for Modeling Waste Glass Liquidus." In: *Scientific Basis for Nuclear Waste Management XXII*, 223–230, Materials Research Society, Warrendale, Pennsylvania.

SAS Institute, Inc. 2002. *JMP Statistics and Graphics Guide Version 5*. Cary, NC.

Schill, P., M. Trochta, J. Matyas, L. Nemec, and P. Hrma. 2001. **"**Mathematical Model of Spinel Settling in a Real Waste Glass Melter." In: *Waste Management '01*, University of Arizona, Tucson, AZ.

Schweiger, M. J. 2002. *Glass Development Laboratory Technical Procedure: Glass Batching and Melting*. GDL-GBM, Pacific Northwest National Laboratory, Richland, WA.

Shannon, R. D. 1976. "Revised Effective Ionic Radii and Systematic Study of Interatomic Distances in Halides and Chalcogenides." *Acta Cryst.* A32:751–767.

Snee, R. D. 1977. "Validation of Regression Models: Methods and Examples." *Technometrics* 19(4):415-428.

U. S. Department of Energy. 2002. Quality Assurance Requirements Document (QARD), DOE/RW-0333P, Rev., 11, Office of Civilian Radioactive Waste Management, Washington, D.C.

U. S. Department of Energy. 2003. *Design, Construction, and Commissioning of the Hanford Tank Waste Treatment and Immobilization Plant*. Contract Number: DE-AC27-01RV14136, U. S. Department of Energy, Office of River Protection, Richland, WA.

Vienna, J. D., P. Hrma, and D. E. Smith. 1997. "Isothermal Crystallization Kinetics in Simulated High-Level Waste Glass." In: *Scientific Basis for Nuclear Waste Management XX*, pp. 17-24, Materials Research Society, Pittsburgh, PA.

Vienna, J. D. 2002. *Waste Treatment Plant Support Project Test Plan: Liquidus Temperature Studies for RPP-WTP HLW Glasses*. TP-RPP-WTP-182, Battelle—Pacific Northwest Division, Richland, WA.

Vienna, J. D., P. Hrma, J. V. Crum, and M. Mika. 2001. "Liquidus Temperature-Composition Model for Multi-component Glasses in the Fe, Cr, Ni, and Mn Spinel Primary Phase Field." *J. Non-cryst. Sol*. 292(1-3):1-24.

Vienna, J. D., D. S. Kim, and P. Hrma. 2002. *Database and Interim Glass Property Models for Hanford HLW and LAW Glasses*. PNNL-14060, Pacific Northwest National Laboratory, Richland, WA.

Welch, W. J. 1987. *ACED, Algorithms for the Construction of Experimental Designs, Users Guide Version 1.6.1*. University of Waterloo, Waterloo, Ontario, Canada.

Westsik, J. H. 2003. *Test Exception 24590- HLW-TEF-RT-03-001*. Bechtel National Inc., Richland, WA.

Wilson, B. K., P. Hrma, J. Alton, T. J. Plaisted, and J. D. Vienna. 2002. "The Effect of Composition on Spinel Equilibrium and Crystal Size in High-Level Waste Glass," in *J. Matl. Sci*., 37 [24], pp. 5327-5331.

Appendix A

Existing Glasses Augmented by Current Matrix

Appendix A: Existing Glasses Augmented by Current Matrix

Table A1. Glass Compositions (in mass fractions) and T_L Values

Glass ID	Reference	QA[(a)]	T_L,°C	Matrix	Ag_2O	Al_2O_3	As_2O_5	B_2O_3	BaO	Bi_2O_3	CaO	CdO	Ce_2O_3	Cl	CoO	Cr_2O_3
CVS1-19	Hrma et al. 1994	1	961	Y	0.0000	0.0636	0.0000	0.1142	0.0007	0.0000	0.0275	0.0055	0.0010	0.0000	0.0000	0.0009
CVS1-20	Hrma et al. 1994	1	966	Y	0.0000	0.0636	0.0000	0.1142	0.0007	0.0000	0.0275	0.0055	0.0010	0.0000	0.0000	0.0009
CVS1-23	Hrma et al. 1994	1	980	Y	0.0000	0.0456	0.0000	0.0956	0.0007	0.0000	0.0289	0.0053	0.0010	0.0000	0.0000	0.0009
CVS2-1	Hrma et al. 1994	1	1048	N	0.0000	0.0800	0.0000	0.0874	0.0014	0.0000	0.0000	0.0107	0.0021	0.0000	0.0000	0.0018
CVS2-15	Hrma et al. 1994	1	956	N	0.0000	0.0756	0.0000	0.0700	0.0014	0.0000	0.0601	0.0107	0.0021	0.0000	0.0000	0.0018
CVS2-17	Hrma et al. 1994	1	971	Y	0.0000	0.0636	0.0000	0.1142	0.0007	0.0000	0.0275	0.0055	0.0010	0.0000	0.0000	0.0009
CVS2-46	Hrma et al. 1994	1	1004	N	0.0000	0.0746	0.0000	0.1259	0.0012	0.0000	0.0200	0.0088	0.0017	0.0000	0.0000	0.0015
CVS2-49	Hrma et al. 1994	1	957	Y	0.0000	0.0785	0.0000	0.1357	0.0005	0.0000	0.0200	0.0040	0.0008	0.0000	0.0000	0.0007
CVS2-50	Hrma et al. 1994	1	1025	Y	0.0000	0.0636	0.0000	0.1142	0.0007	0.0000	0.0275	0.0055	0.0010	0.0000	0.0000	0.0009
CVS2-96	Hrma et al. 1994	1	1010	Y	0.0000	0.0636	0.0000	0.1142	0.0007	0.0000	0.0275	0.0055	0.0010	0.0000	0.0000	0.0009
CVS2-99	Hrma et al. 1994	1	988	Y	0.0010	0.0523	0.0000	0.0970	0.0005	0.0000	0.0097	0.0030	0.0013	0.0000	0.0009	0.0020
AH 131AV	Brown et al. 2001	1	1027	N	0.0000	0.0718	0.0000	0.1088	0.0000	0.0000	0.0074	0.0000	0.0000	0.0000	0.0000	0.0007
AH 168AV	Brown et al. 2001	1	1003	Y	0.0000	0.0531	0.0000	0.1265	0.0000	0.0000	0.0070	0.0000	0.0000	0.0000	0.0000	0.0000
AH 168AV	Brown et al. 2001	1	972	Y	0.0000	0.0531	0.0000	0.1265	0.0000	0.0000	0.0070	0.0000	0.0000	0.0000	0.0000	0.0000
AH 168AV	Brown et al. 2001	1	980	Y	0.0000	0.0558	0.0000	0.1060	0.0000	0.0000	0.0068	0.0000	0.0000	0.0000	0.0000	0.0000
AH 168AV	Brown et al. 2001	1	1015	Y	0.0000	0.0558	0.0000	0.1060	0.0000	0.0000	0.0068	0.0000	0.0000	0.0000	0.0000	0.0000
MS-3a	Hrma 1999	2	1185	N	0.0000	0.0800	0.0000	0.0700	0.0000	0.0000	0.0000	0.0000	0.0000	0.0000	0.0000	0.0050
MS-3b	Hrma 1999	2	1188	N	0.0000	0.0800	0.0000	0.0700	0.0000	0.0000	0.0000	0.0000	0.0000	0.0000	0.0000	0.0050
MS-4a	Hrma 1999	2	1139	N	0.0000	0.0800	0.0000	0.0700	0.0000	0.0000	0.0000	0.0000	0.0000	0.0000	0.0000	0.0050
MS-4b	Hrma 1999	2	1144	N	0.0000	0.0800	0.0000	0.0700	0.0000	0.0000	0.0000	0.0000	0.0000	0.0000	0.0000	0.0050
MS-5	Hrma 1999	2	1171	N	0.0000	0.0800	0.0000	0.0700	0.0000	0.0000	0.0000	0.0000	0.0000	0.0000	0.0000	0.0050
MS-6	Hrma 1999	2	1225	N	0.0000	0.0800	0.0000	0.0700	0.0000	0.0000	0.0000	0.0000	0.0000	0.0000	0.0000	0.0035
MS-7a	Hrma 1999	2	1078	N	0.0000	0.0800	0.0000	0.0700	0.0000	0.0000	0.0000	0.0000	0.0000	0.0000	0.0000	0.0030
MS-7b	Wilson et al. 2002	2	1078	N	0.0000	0.0800	0.0000	0.0700	0.0000	0.0000	0.0000	0.0000	0.0000	0.0000	0.0000	0.0030
MS-7c	Izak et al. 2001	2	1078	N	0.0000	0.0800	0.0000	0.0700	0.0000	0.0000	0.0000	0.0000	0.0000	0.0000	0.0000	0.0030
MS-7d	Hrma 1999	2	1114	N	0.0000	0.0800	0.0000	0.0700	0.0000	0.0000	0.0000	0.0000	0.0000	0.0000	0.0000	0.0030
MS-7e	Plaisted et al. 2001	2	1084	N	0.0000	0.0800	0.0000	0.0700	0.0000	0.0000	0.0000	0.0000	0.0000	0.0000	0.0000	0.0030
MS7-H-Al	Wilson et al. 2002	2	1150	Y	0.0000	0.1100	0.0000	0.0677	0.0000	0.0000	0.0000	0.0000	0.0000	0.0000	0.0000	0.0029
MS7-L-Al	Wilson et al. 2002	2	1000	N	0.0000	0.0500	0.0000	0.0723	0.0000	0.0000	0.0000	0.0000	0.0000	0.0000	0.0000	0.0031
MS7-H-Cr	Wilson et al. 2002	2	1095	N	0.0000	0.0790	0.0000	0.0700	0.0000	0.0000	0.0000	0.0000	0.0000	0.0000	0.0000	0.0050
MS7-L-Cr	Wilson et al. 2002	2	1021	N	0.0000	0.0802	0.0000	0.0701	0.0000	0.0000	0.0000	0.0000	0.0000	0.0000	0.0000	0.0010
MS7-L-Fe	Wilson et al. 2002	2	1015	N	0.0000	0.0832	0.0000	0.0728	0.0000	0.0000	0.0000	0.0000	0.0000	0.0000	0.0000	0.0031
MS7-H-Li	Wilson et al. 2002	2	1040	N	0.0000	0.0788	0.0000	0.0689	0.0000	0.0000	0.0000	0.0000	0.0000	0.0000	0.0000	0.0030
MS7-L-Li	Wilson et al. 2002	2	1110	N	0.0000	0.0813	0.0000	0.0711	0.0000	0.0000	0.0000	0.0000	0.0000	0.0000	0.0000	0.0030

Table A1. Glass Compositions (in mass fractions) and T_L Values, Cont.

Glass ID	Cs_2O	CuO	F	Fe_2O_3	K_2O	La_2O_3	Li_2O	MgO	MnO	MoO_3	Na_2O	Nd_2O_3	NiO	P_2O_5	PbO	PdO	Pr_2O_3	Rb_2O
CVS1-19	0.0011	0.0011	0.0022	0.0568	0.0000	0.0046	0.0376	0.0363	0.0009	0.0022	0.1003	0.0090	0.0042	0.0007	0.0000	0.0004	0.0007	0.0004
CVS1-20	0.0011	0.0011	0.0022	0.0568	0.0000	0.0046	0.0376	0.0363	0.0009	0.0022	0.1003	0.0090	0.0042	0.0007	0.0000	0.0004	0.0007	0.0004
CVS1-23	0.0011	0.0011	0.0021	0.1179	0.0000	0.0044	0.0375	0.0084	0.0009	0.0021	0.1052	0.0087	0.0040	0.0007	0.0000	0.0004	0.0007	0.0004
CVS2-1	0.0022	0.0022	0.0043	0.0400	0.0000	0.0090	0.0600	0.0500	0.0018	0.0043	0.0700	0.0177	0.0082	0.0014	0.0000	0.0007	0.0014	0.0007
CVS2-15	0.0022	0.0022	0.0043	0.0400	0.0000	0.0090	0.0214	0.0000	0.0018	0.0043	0.1701	0.0177	0.0082	0.0014	0.0000	0.0007	0.0014	0.0007
CVS2-17	0.0011	0.0011	0.0022	0.0568	0.0000	0.0046	0.0376	0.0363	0.0009	0.0022	0.1003	0.0090	0.0042	0.0007	0.0000	0.0004	0.0007	0.0004
CVS2-46	0.0018	0.0018	0.0035	0.0200	0.0000	0.0073	0.0700	0.0200	0.0014	0.0035	0.0577	0.0145	0.0067	0.0012	0.0000	0.0006	0.0012	0.0006
CVS2-49	0.0008	0.0008	0.0016	0.0515	0.0000	0.0034	0.0413	0.0200	0.0007	0.0016	0.0957	0.0066	0.0031	0.0005	0.0000	0.0003	0.0005	0.0003
CVS2-50	0.0011	0.0011	0.0022	0.0568	0.0000	0.0046	0.0376	0.0363	0.0009	0.0022	0.1003	0.0090	0.0042	0.0007	0.0000	0.0004	0.0007	0.0004
CVS2-96	0.0011	0.0011	0.0022	0.0568	0.0000	0.0046	0.0376	0.0363	0.0009	0.0022	0.1003	0.0090	0.0042	0.0007	0.0000	0.0004	0.0007	0.0004
CVS2-99	0.0000	0.0002	0.0000	0.1020	0.0212	0.0014	0.0356	0.0077	0.0039	0.0001	0.0981	0.0046	0.0029	0.0055	0.0020	0.0000	0.0000	0.0000
AH 131AV	0.0000	0.0000	0.0000	0.1170	0.0004	0.0000	0.0388	0.0128	0.0082	0.0000	0.1430	0.0000	0.0108	0.0000	0.0000	0.0000	0.0000	0.0000
AH 168AV	0.0000	0.0000	0.0000	0.1160	0.0005	0.0000	0.0428	0.0073	0.0272	0.0000	0.1030	0.0000	0.0098	0.0000	0.0000	0.0000	0.0000	0.0000
AH 168AV	0.0000	0.0000	0.0000	0.1160	0.0005	0.0000	0.0428	0.0073	0.0272	0.0000	0.1030	0.0000	0.0098	0.0000	0.0000	0.0000	0.0000	0.0000
AH 168AV	0.0000	0.0000	0.0000	0.1119	0.0000	0.0000	0.0424	0.0074	0.0264	0.0000	0.1010	0.0000	0.0102	0.0000	0.0000	0.0000	0.0000	0.0000
AH 168AV	0.0000	0.0000	0.0000	0.1119	0.0000	0.0000	0.0424	0.0074	0.0264	0.0000	0.1010	0.0000	0.0102	0.0000	0.0000	0.0000	0.0000	0.0000
MS-3a	0.0000	0.0000	0.0000	0.1150	0.0000	0.0000	0.0400	0.0060	0.0050	0.0000	0.1530	0.0000	0.0120	0.0000	0.0000	0.0000	0.0000	0.0000
MS-3b	0.0000	0.0000	0.0000	0.1150	0.0000	0.0000	0.0400	0.0060	0.0050	0.0000	0.1530	0.0000	0.0120	0.0000	0.0000	0.0000	0.0000	0.0000
MS-4a	0.0000	0.0000	0.0000	0.0889	0.0000	0.0000	0.0454	0.0060	0.0050	0.0000	0.1530	0.0000	0.0120	0.0000	0.0000	0.0000	0.0000	0.0000
MS-4b	0.0000	0.0000	0.0000	0.0889	0.0000	0.0000	0.0454	0.0060	0.0050	0.0000	0.1530	0.0000	0.0120	0.0000	0.0000	0.0000	0.0000	0.0000
MS-5	0.0000	0.0000	0.0000	0.1150	0.0000	0.0000	0.0410	0.0060	0.0050	0.0000	0.1530	0.0000	0.0074	0.0000	0.0000	0.0000	0.0000	0.0000
MS-6	0.0000	0.0000	0.0000	0.1250	0.0000	0.0000	0.0300	0.0060	0.0036	0.0000	0.1573	0.0000	0.0140	0.0000	0.0000	0.0000	0.0000	0.0000
MS-7a	0.0000	0.0000	0.0000	0.1150	0.0000	0.0000	0.0454	0.0060	0.0050	0.0000	0.1530	0.0000	0.0095	0.0000	0.0000	0.0000	0.0000	0.0000
MS-7b	0.0000	0.0000	0.0000	0.1150	0.0000	0.0000	0.0454	0.0060	0.0050	0.0000	0.1530	0.0000	0.0095	0.0000	0.0000	0.0000	0.0000	0.0000
MS-7c	0.0000	0.0000	0.0000	0.1150	0.0000	0.0000	0.0454	0.0060	0.0050	0.0000	0.1530	0.0000	0.0095	0.0000	0.0000	0.0000	0.0000	0.0000
MS-7d	0.0000	0.0000	0.0000	0.1150	0.0000	0.0000	0.0454	0.0060	0.0050	0.0000	0.1530	0.0000	0.0095	0.0000	0.0000	0.0000	0.0000	0.0000
MS-7e	0.0000	0.0000	0.0000	0.1150	0.0000	0.0000	0.0454	0.0060	0.0050	0.0000	0.1530	0.0000	0.0095	0.0000	0.0000	0.0000	0.0000	0.0000
MS7-H-Al	0.0000	0.0000	0.0000	0.1113	0.0000	0.0000	0.0439	0.0058	0.0048	0.0000	0.1480	0.0000	0.0092	0.0000	0.0000	0.0000	0.0000	0.0000
MS7-L-Al	0.0000	0.0000	0.0000	0.1181	0.0000	0.0000	0.0469	0.0062	0.0052	0.0000	0.1581	0.0000	0.0098	0.0000	0.0000	0.0000	0.0000	0.0000
MS7-H-Cr	0.0000	0.0000	0.0000	0.1149	0.0000	0.0000	0.0453	0.0060	0.0050	0.0000	0.1528	0.0000	0.0095	0.0000	0.0000	0.0000	0.0000	0.0000
MS7-L-Cr	0.0000	0.0000	0.0000	0.1152	0.0000	0.0000	0.0455	0.0060	0.0050	0.0000	0.1533	0.0000	0.0095	0.0000	0.0000	0.0000	0.0000	0.0000
MS7-L-Fe	0.0000	0.0000	0.0000	0.0800	0.0000	0.0000	0.0472	0.0062	0.0052	0.0000	0.1591	0.0000	0.0099	0.0000	0.0000	0.0000	0.0000	0.0000
MS7-H-Li	0.0000	0.0000	0.0000	0.1132	0.0000	0.0000	0.0600	0.0059	0.0049	0.0000	0.1507	0.0000	0.0094	0.0000	0.0000	0.0000	0.0000	0.0000
MS7-L-Li	0.0000	0.0000	0.0000	0.1169	0.0000	0.0000	0.0300	0.0061	0.0051	0.0000	0.1555	0.0000	0.0097	0.0000	0.0000	0.0000	0.0000	0.0000

Table A1. Glass Compositions (in mass fractions) and T_L Values, Cont.

Glass ID	Rh_2O_3	RuO_2	Sb_2O_5	SeO_2	SiO_2	Sm_2O_3	SO_3	SrO	TeO_2	ThO_2	TiO_2	Tl_2O	U_3O_8	V_2O_5	WO_3	Y_2O_3	ZnO	ZrO_2	Total
CVS1-19	0.0004	0.0011	0.0000	0.0000	0.4802	0.0004	0.0020	0.0007	0.0000	0.0000	0.0000	0.0000	0.0000	0.0000	0.0000	0.0004	0.0000	0.0429	1.0000
CVS1-20	0.0004	0.0011	0.0000	0.0000	0.4802	0.0004	0.0020	0.0007	0.0000	0.0000	0.0000	0.0000	0.0000	0.0000	0.0000	0.0004	0.0000	0.0429	1.0000
CVS1-23	0.0004	0.0011	0.0000	0.0000	0.5153	0.0004	0.0019	0.0007	0.0000	0.0000	0.0000	0.0000	0.0000	0.0000	0.0000	0.0004	0.0000	0.0063	1.0000
CVS2-1	0.0007	0.0022	0.0000	0.0000	0.5230	0.0007	0.0039	0.0014	0.0000	0.0000	0.0000	0.0000	0.0000	0.0000	0.0000	0.0007	0.0000	0.0100	1.0000
CVS2-15	0.0007	0.0022	0.0000	0.0000	0.4732	0.0007	0.0039	0.0014	0.0000	0.0000	0.0000	0.0000	0.0000	0.0000	0.0000	0.0007	0.0000	0.0100	1.0000
CVS2-17	0.0004	0.0011	0.0000	0.0000	0.4802	0.0004	0.0020	0.0007	0.0000	0.0000	0.0000	0.0000	0.0000	0.0000	0.0000	0.0004	0.0000	0.0429	1.0000
CVS2-46	0.0006	0.0018	0.0000	0.0000	0.5266	0.0006	0.0032	0.0012	0.0000	0.0000	0.0000	0.0000	0.0000	0.0000	0.0000	0.0006	0.0000	0.0200	1.0000
CVS2-49	0.0003	0.0008	0.0000	0.0000	0.5074	0.0003	0.0015	0.0005	0.0000	0.0000	0.0000	0.0000	0.0000	0.0000	0.0000	0.0003	0.0000	0.0200	1.0000
CVS2-50	0.0004	0.0011	0.0000	0.0000	0.4802	0.0004	0.0020	0.0007	0.0000	0.0000	0.0000	0.0000	0.0000	0.0000	0.0000	0.0004	0.0000	0.0429	1.0000
CVS2-96	0.0004	0.0011	0.0000	0.0000	0.4802	0.0004	0.0020	0.0007	0.0000	0.0000	0.0000	0.0000	0.0000	0.0000	0.0000	0.0004	0.0000	0.0429	1.0000
CVS2-99	0.0000	0.0000	0.0000	0.0000	0.5209	0.0000	0.0040	0.0004	0.0000	0.0000	0.0012	0.0000	0.0000	0.0000	0.0000	0.0000	0.0005	0.0199	1.0000
AH 131AV	0.0000	0.0000	0.0000	0.0000	0.4520	0.0000	0.0000	0.0000	0.0000	0.0000	0.0070	0.0000	0.0000	0.0000	0.0000	0.0000	0.0000	0.0000	0.9787
AH 168AV	0.0000	0.0000	0.0000	0.0000	0.5040	0.0000	0.0000	0.0000	0.0000	0.0000	0.0006	0.0000	0.0000	0.0000	0.0000	0.0000	0.0000	0.0000	0.9978
AH 168AV	0.0000	0.0000	0.0000	0.0000	0.5040	0.0000	0.0000	0.0000	0.0000	0.0000	0.0006	0.0000	0.0000	0.0000	0.0000	0.0000	0.0000	0.0000	0.9978
AH 168AV	0.0000	0.0000	0.0000	0.0000	0.5160	0.0000	0.0000	0.0000	0.0000	0.0000	0.0000	0.0000	0.0000	0.0000	0.0000	0.0000	0.0000	0.0000	0.9839
AH 168AV	0.0000	0.0000	0.0000	0.0000	0.5160	0.0000	0.0000	0.0000	0.0000	0.0000	0.0000	0.0000	0.0000	0.0000	0.0000	0.0000	0.0000	0.0000	0.9839
MS-3a	0.0000	0.0000	0.0000	0.0000	0.4540	0.0000	0.0000	0.0000	0.0000	0.0000	0.0000	0.0000	0.0000	0.0000	0.0000	0.0000	0.0000	0.0600	1.0000
MS-3b	0.0000	0.0000	0.0000	0.0000	0.4540	0.0000	0.0000	0.0000	0.0000	0.0000	0.0000	0.0000	0.0000	0.0000	0.0000	0.0000	0.0000	0.0600	1.0000
MS-4a	0.0000	0.0000	0.0000	0.0000	0.4746	0.0000	0.0000	0.0000	0.0000	0.0000	0.0000	0.0000	0.0000	0.0000	0.0000	0.0000	0.0000	0.0600	1.0000
MS-4b	0.0000	0.0000	0.0000	0.0000	0.4746	0.0000	0.0000	0.0000	0.0000	0.0000	0.0000	0.0000	0.0000	0.0000	0.0000	0.0000	0.0000	0.0600	1.0000
MS-5	0.0000	0.0000	0.0000	0.0000	0.4576	0.0000	0.0000	0.0000	0.0000	0.0000	0.0000	0.0000	0.0000	0.0000	0.0000	0.0000	0.0000	0.0600	1.0000
MS-6	0.0000	0.0000	0.0000	0.0000	0.4600	0.0000	0.0000	0.0000	0.0000	0.0000	0.0000	0.0000	0.0000	0.0000	0.0000	0.0000	0.0000	0.0506	1.0000
MS-7a	0.0000	0.0000	0.0000	0.0000	0.4531	0.0000	0.0000	0.0000	0.0000	0.0000	0.0000	0.0000	0.0000	0.0000	0.0000	0.0000	0.0000	0.0600	1.0000
MS-7b	0.0000	0.0000	0.0000	0.0000	0.4531	0.0000	0.0000	0.0000	0.0000	0.0000	0.0000	0.0000	0.0000	0.0000	0.0000	0.0000	0.0000	0.0600	1.0000
MS-7c	0.0000	0.0000	0.0000	0.0000	0.4531	0.0000	0.0000	0.0000	0.0000	0.0000	0.0000	0.0000	0.0000	0.0000	0.0000	0.0000	0.0000	0.0600	1.0000
MS-7d	0.0000	0.0000	0.0000	0.0000	0.4531	0.0000	0.0000	0.0000	0.0000	0.0000	0.0000	0.0000	0.0000	0.0000	0.0000	0.0000	0.0000	0.0600	1.0000
MS-7e	0.0000	0.0000	0.0000	0.0000	0.4531	0.0000	0.0000	0.0000	0.0000	0.0000	0.0000	0.0000	0.0000	0.0000	0.0000	0.0000	0.0000	0.0600	1.0000
MS7-H-Al	0.0000	0.0000	0.0000	0.0000	0.4383	0.0000	0.0000	0.0000	0.0000	0.0000	0.0000	0.0000	0.0000	0.0000	0.0000	0.0000	0.0000	0.0580	1.0000
MS7-L-Al	0.0000	0.0000	0.0000	0.0000	0.4682	0.0000	0.0000	0.0000	0.0000	0.0000	0.0000	0.0000	0.0000	0.0000	0.0000	0.0000	0.0000	0.0620	1.0000
MS7-H-Cr	0.0000	0.0000	0.0000	0.0000	0.4526	0.0000	0.0000	0.0000	0.0000	0.0000	0.0000	0.0000	0.0000	0.0000	0.0000	0.0000	0.0000	0.0599	1.0000
MS7-L-Cr	0.0000	0.0000	0.0000	0.0000	0.4540	0.0000	0.0000	0.0000	0.0000	0.0000	0.0000	0.0000	0.0000	0.0000	0.0000	0.0000	0.0000	0.0601	1.0000
MS7-L-Fe	0.0000	0.0000	0.0000	0.0000	0.4710	0.0000	0.0000	0.0000	0.0000	0.0000	0.0000	0.0000	0.0000	0.0000	0.0000	0.0000	0.0000	0.0624	1.0000
MS7-H-Li	0.0000	0.0000	0.0000	0.0000	0.4462	0.0000	0.0000	0.0000	0.0000	0.0000	0.0000	0.0000	0.0000	0.0000	0.0000	0.0000	0.0000	0.0591	1.0000
MS7-L-Li	0.0000	0.0000	0.0000	0.0000	0.4604	0.0000	0.0000	0.0000	0.0000	0.0000	0.0000	0.0000	0.0000	0.0000	0.0000	0.0000	0.0000	0.0610	1.0000

Table A1. Glass Compositions (in mass fractions) and T_L Values, Cont.

Glass ID	Reference	QA	T_L	Matrix	Ag_2O	Al_2O_3	As_2O_5	B_2O_3	BaO	Bi_2O_3	CaO	CdO	Ce_2O_3	Cl	CoO	Cr_2O_3	Cs_2O
MS7-H-Mg	Wilson et al. 2002	2	1145	Y	0.0000	0.0781	0.0000	0.0683	0.0000	0.0000	0.0000	0.0000	0.0000	0.0000	0.0000	0.0029	0.0000
MS7-L-Mg	Wilson et al. 2002	2	1060	N	0.0000	0.0805	0.0000	0.0704	0.0000	0.0000	0.0000	0.0000	0.0000	0.0000	0.0000	0.0030	0.0000
MS7-H-Na	Wilson et al. 2002	2	990	N	0.0000	0.0774	0.0000	0.0678	0.0000	0.0000	0.0000	0.0000	0.0000	0.0000	0.0000	0.0029	0.0000
MS7-L-Na	Wilson et al. 2002	2	1180	N	0.0000	0.0831	0.0000	0.0727	0.0000	0.0000	0.0000	0.0000	0.0000	0.0000	0.0000	0.0031	0.0000
MS7-H-Ni	Wilson et al. 2002	2	1143	N	0.0000	0.0793	0.0000	0.0694	0.0000	0.0000	0.0000	0.0000	0.0000	0.0000	0.0000	0.0030	0.0000
MS7-L-Ni	Wilson et al. 2002	2	1020	N	0.0000	0.0805	0.0000	0.0705	0.0000	0.0000	0.0000	0.0000	0.0000	0.0000	0.0000	0.0030	0.0000
MS7-Mn-0	Vienna et al. 2002	2	1082	N	0.0000	0.0804	0.0000	0.0704	0.0000	0.0000	0.0000	0.0000	0.0000	0.0000	0.0000	0.0030	0.0000
MS7-Mn-0.5	Vienna et al. 2002	2	1084	N	0.0000	0.0800	0.0000	0.0700	0.0000	0.0000	0.0000	0.0000	0.0000	0.0000	0.0000	0.0030	0.0000
MS7-Mn-1	Vienna et al. 2002	2	1086	N	0.0000	0.0796	0.0000	0.0696	0.0000	0.0000	0.0000	0.0000	0.0000	0.0000	0.0000	0.0030	0.0000
MS7-Mn-2	Vienna et al. 2002	2	1094	N	0.0000	0.0788	0.0000	0.0689	0.0000	0.0000	0.0000	0.0000	0.0000	0.0000	0.0000	0.0030	0.0000
MS7-Mn-3	Vienna et al. 2002	2	1110	Y	0.0000	0.0780	0.0000	0.0682	0.0000	0.0000	0.0000	0.0000	0.0000	0.0000	0.0000	0.0029	0.0000
MS7-Mn-4	Vienna et al. 2002	2	1121	Y	0.0000	0.0772	0.0000	0.0675	0.0000	0.0000	0.0000	0.0000	0.0000	0.0000	0.0000	0.0029	0.0000
MS7-Mn-5	Vienna et al. 2002	2	1133	Y	0.0000	0.0764	0.0000	0.0668	0.0000	0.0000	0.0000	0.0000	0.0000	0.0000	0.0000	0.0029	0.0000
MS7-Mn-6	Vienna et al. 2002	2	1144	Y	0.0000	0.0756	0.0000	0.0661	0.0000	0.0000	0.0000	0.0000	0.0000	0.0000	0.0000	0.0028	0.0000
MS-8	Hrma 1999	2	1125	N	0.0000	0.0800	0.0000	0.0700	0.0000	0.0000	0.0000	0.0000	0.0000	0.0000	0.0000	0.0035	0.0000
MS-7-m	Mika et al. 2001	2	1094	N	0.0000	0.0800	0.0000	0.0700	0.0000	0.0000	0.0000	0.0000	0.0000	0.0000	0.0000	0.0030	0.0000
GNi	Mika et al. 2001	3	1129	N	0.0000	0.0799	0.0000	0.0699	0.0000	0.0000	0.0000	0.0000	0.0000	0.0000	0.0000	0.0030	0.0000
GLi	Mika et al. 2001	3	1119	Y	0.0000	0.0777	0.0000	0.0680	0.0000	0.0000	0.0000	0.0000	0.0000	0.0000	0.0000	0.0029	0.0000
GNa	Mika et al. 2001	3	1148	Y	0.0000	0.0785	0.0000	0.0687	0.0000	0.0000	0.0000	0.0000	0.0000	0.0000	0.0000	0.0029	0.0000
GMg	Mika et al. 2001	3	1156	N	0.0000	0.0810	0.0000	0.0709	0.0000	0.0000	0.0000	0.0000	0.0000	0.0000	0.0000	0.0030	0.0000
AZB	Vienna et al. 2001	1	1043	Y	0.0005	0.0744	0.0000	0.1040	0.0004	0.0000	0.0023	0.0080	0.0010	0.0000	0.0009	0.0013	0.0000
C106	Vienna et al. 2001	1	910	N	0.0024	0.0664	0.0000	0.0844	0.0003	0.0003	0.0092	0.0000	0.0002	0.0000	0.0000	0.0008	0.0000
nom-2	Vienna et al. 2001	1	1009	N	0.0006	0.0687	0.0004	0.0991	0.0025	0.0000	0.0087	0.0058	0.0005	0.0000	0.0007	0.0018	0.0000
nom-3	Vienna et al. 2001	1	1047	N	0.0007	0.0817	0.0005	0.1105	0.0030	0.0000	0.0103	0.0069	0.0007	0.0000	0.0008	0.0022	0.0000
nomc-2	Vienna et al. 2001	1	998	Y	0.0007	0.0416	0.0005	0.0594	0.0029	0.0000	0.0101	0.0068	0.0006	0.0000	0.0008	0.0019	0.0000
c106a-4	Vienna et al. 2001	1	885	Y	0.0007	0.0945	0.0000	0.0836	0.0066	0.0000	0.0203	0.0005	0.0000	0.0000	0.0000	0.0017	0.0000
az-5	Vienna et al. 2001	1	953	N	0.0004	0.0561	0.0006	0.0986	0.0005	0.0000	0.0026	0.0086	0.0008	0.0000	0.0011	0.0018	0.0000
SG03	Hrma et al. 1999	2	1164	N	0.0000	0.0390	0.0000	0.0876	0.0000	0.0000	0.0158	0.0000	0.0000	0.0000	0.0000	0.0025	0.0000
SG05	Hrma et al. 1999	2	1084	N	0.0000	0.0530	0.0000	0.0752	0.0000	0.0000	0.0115	0.0000	0.0000	0.0000	0.0000	0.0020	0.0000
SG16	Hrma et al. 1999	2	995	N	0.0000	0.0664	0.0000	0.0626	0.0000	0.0000	0.0158	0.0000	0.0000	0.0000	0.0000	0.0015	0.0000
SG17	Hrma et al. 1999	2	1075	N	0.0000	0.0390	0.0000	0.0725	0.0000	0.0000	0.0158	0.0000	0.0000	0.0000	0.0000	0.0015	0.0000
SG19	Hrma et al. 1999	2	929	N	0.0000	0.0799	0.0000	0.0999	0.0000	0.0000	0.0030	0.0000	0.0000	0.0000	0.0000	0.0030	0.0000
SG22	Hrma et al. 1999	2	1145	N	0.0000	0.0664	0.0000	0.0626	0.0000	0.0000	0.0158	0.0000	0.0000	0.0000	0.0000	0.0025	0.0000
SG26	Hrma et al. 1999	2	1071	N	0.0000	0.0390	0.0000	0.0626	0.0000	0.0000	0.0073	0.0000	0.0000	0.0000	0.0000	0.0025	0.0000
SG27	Hrma et al. 1999	2	1086	N	0.0000	0.0664	0.0000	0.0876	0.0000	0.0000	0.0158	0.0000	0.0000	0.0000	0.0000	0.0025	0.0000

Table A1. Glass Compositions (in mass fractions) and T_L Values, Cont.

Glass ID	CuO	F	Fe_2O_3	K_2O	La_2O_3	Li_2O	MgO	MnO	MoO_3	Rb_2O	Rh_2O_3	RuO_2	Sb_2O_5	SeO_2	SiO_2	Sm_2O_3	SO_3
MS7-H-Mg	0.0000	0.0000	0.1122	0.0000	0.0000	0.0443	0.0300	0.0049	0.0000	0.0000	0.0000	0.0000	0.0000	0.0000	0.4422	0.0000	0.0000
MS7-L-Mg	0.0000	0.0000	0.1157	0.0000	0.0000	0.0457	0.0000	0.0050	0.0000	0.0000	0.0000	0.0000	0.0000	0.0000	0.4558	0.0000	0.0000
MS7-H-Na	0.0000	0.0000	0.1113	0.0000	0.0000	0.0440	0.0058	0.0048	0.0000	0.0000	0.0000	0.0000	0.0000	0.0000	0.4387	0.0000	0.0000
MS7-L-Na	0.0000	0.0000	0.1195	0.0000	0.0000	0.0472	0.0062	0.0052	0.0000	0.0000	0.0000	0.0000	0.0000	0.0000	0.4708	0.0000	0.0000
MS7-H-Ni	0.0000	0.0000	0.1140	0.0000	0.0000	0.0450	0.0059	0.0050	0.0000	0.0000	0.0000	0.0000	0.0000	0.0000	0.4492	0.0000	0.0000
MS7-L-Ni	0.0000	0.0000	0.1158	0.0000	0.0000	0.0457	0.0060	0.0050	0.0000	0.0000	0.0000	0.0000	0.0000	0.0000	0.4561	0.0000	0.0000
MS7-Mn-0	0.0000	0.0000	0.1156	0.0000	0.0000	0.0456	0.0060	0.0000	0.0000	0.0000	0.0000	0.0000	0.0000	0.0000	0.4554	0.0000	0.0000
MS7-Mn-0.5	0.0000	0.0000	0.1150	0.0000	0.0000	0.0454	0.0060	0.0050	0.0000	0.0000	0.0000	0.0000	0.0000	0.0000	0.4531	0.0000	0.0000
MS7-Mn-1	0.0000	0.0000	0.1144	0.0000	0.0000	0.0452	0.0060	0.0100	0.0000	0.0000	0.0000	0.0000	0.0000	0.0000	0.4508	0.0000	0.0000
MS7-Mn-2	0.0000	0.0000	0.1133	0.0000	0.0000	0.0447	0.0059	0.0200	0.0000	0.0000	0.0000	0.0000	0.0000	0.0000	0.4463	0.0000	0.0000
MS7-Mn-3	0.0000	0.0000	0.1121	0.0000	0.0000	0.0443	0.0058	0.0300	0.0000	0.0000	0.0000	0.0000	0.0000	0.0000	0.4417	0.0000	0.0000
MS7-Mn-4	0.0000	0.0000	0.1110	0.0000	0.0000	0.0438	0.0058	0.0400	0.0000	0.0000	0.0000	0.0000	0.0000	0.0000	0.4372	0.0000	0.0000
MS7-Mn-5	0.0000	0.0000	0.1098	0.0000	0.0000	0.0433	0.0057	0.0500	0.0000	0.0000	0.0000	0.0000	0.0000	0.0000	0.4326	0.0000	0.0000
MS7-Mn-6	0.0000	0.0000	0.1086	0.0000	0.0000	0.0429	0.0057	0.0600	0.0000	0.0000	0.0000	0.0000	0.0000	0.0000	0.4281	0.0000	0.0000
MS-8	0.0000	0.0000	0.1250	0.0000	0.0000	0.0300	0.0060	0.0036	0.0000	0.0000	0.0000	0.0000	0.0000	0.0000	0.4600	0.0000	0.0000
MS-7-m	0.0000	0.0000	0.1150	0.0000	0.0000	0.0454	0.0060	0.0050	0.0000	0.0000	0.0000	0.0000	0.0000	0.0000	0.4531	0.0000	0.0000
GNi	0.0000	0.0000	0.1148	0.0000	0.0000	0.0453	0.0060	0.0050	0.0000	0.0000	0.0000	0.0000	0.0000	0.0000	0.4460	0.0000	0.0000
GLi	0.0000	0.0000	0.1118	0.0000	0.0000	0.0348	0.0058	0.0049	0.0000	0.0000	0.0000	0.0000	0.0000	0.0000	0.4778	0.0000	0.0000
GNa	0.0000	0.0000	0.1129	0.0000	0.0000	0.0446	0.0059	0.0049	0.0000	0.0000	0.0000	0.0000	0.0000	0.0000	0.4827	0.0000	0.0000
GMg	0.0000	0.0000	0.1165	0.0000	0.0000	0.0460	0.0323	0.0051	0.0000	0.0000	0.0000	0.0000	0.0000	0.0000	0.4198	0.0000	0.0000
AZB	0.0003	0.0008	0.1003	0.0018	0.0029	0.0138	0.0008	0.0027	0.0000	0.0001	0.0000	0.0004	0.0024	0.0011	0.5051	0.0000	0.0031
C106	0.0000	0.0013	0.1390	0.0063	0.0001	0.0113	0.0014	0.0028	0.0000	0.0003	0.0000	0.0017	0.0000	0.0007	0.5066	0.0000	0.0000
nom-2	0.0003	0.0005	0.1086	0.0024	0.0023	0.0606	0.0051	0.0028	0.0001	0.0000	0.0002	0.0003	0.0007	0.0008	0.5057	0.0000	0.0016
nom-3	0.0003	0.0006	0.1292	0.0029	0.0027	0.0101	0.0061	0.0033	0.0001	0.0000	0.0003	0.0003	0.0008	0.0009	0.4159	0.0000	0.0019
nomc-2	0.0003	0.0005	0.1268	0.0028	0.0027	0.0527	0.0060	0.0033	0.0001	0.0000	0.0003	0.0003	0.0008	0.0009	0.5278	0.0000	0.0019
C106a-4	0.0002	0.0000	0.0911	0.0019	0.0000	0.0404	0.0133	0.0029	0.0000	0.0000	0.0000	0.0000	0.0000	0.0000	0.4833	0.0000	0.0000
az-5	0.0003	0.0006	0.1179	0.0027	0.0034	0.0151	0.0009	0.0026	0.0001	0.0000	0.0004	0.0004	0.0000	0.0000	0.4646	0.0000	0.0025
SG03	0.0000	0.0000	0.1202	0.0208	0.0000	0.0375	0.0200	0.0250	0.0000	0.0000	0.0000	0.0009	0.0000	0.0000	0.4741	0.0000	0.0000
SG05	0.0000	0.0000	0.1052	0.0266	0.0000	0.0450	0.0150	0.0200	0.0000	0.0000	0.0000	0.0009	0.0000	0.0000	0.5186	0.0000	0.0000
SG16	0.0000	0.0000	0.0825	0.0208	0.0000	0.0525	0.0200	0.0250	0.0000	0.0000	0.0000	0.0009	0.0000	0.0000	0.5026	0.0000	0.0000
SG17	0.0000	0.0000	0.1275	0.0323	0.0000	0.0525	0.0100	0.0150	0.0000	0.0000	0.0000	0.0009	0.0000	0.0000	0.4741	0.0000	0.0000
SG19	0.0000	0.0000	0.0599	0.0380	0.0000	0.0599	0.0050	0.0100	0.0000	0.0000	0.0000	0.0009	0.0000	0.0000	0.4541	0.0000	0.0000
SG22	0.0000	0.0000	0.1275	0.0208	0.0000	0.0525	0.0100	0.0150	0.0000	0.0000	0.0000	0.0009	0.0000	0.0000	0.4931	0.0000	0.0000
SG26	0.0000	0.0000	0.1275	0.0208	0.0000	0.0375	0.0100	0.0150	0.0000	0.0000	0.0000	0.0009	0.0000	0.0000	0.5276	0.0000	0.0000
SG27	0.0000	0.0000	0.1109	0.0323	0.0000	0.0525	0.0200	0.0150	0.0000	0.0000	0.0000	0.0009	0.0000	0.0000	0.4741	0.0000	0.0000

Table A1. Glass Compositions (in mass fractions) and T_L Values, Cont.

Glass ID	SrO	TeO_2	ThO_2	TiO_2	Tl_2O	U_3O_8	V_2O_5	WO_3	Y_2O_3	ZnO	ZrO_2	Total
MS7-H-Mg	0.0000	0.0000	0.0000	0.0000	0.0000	0.0000	0.0000	0.0000	0.0000	0.0000	0.0586	1.0000
MS7-L-Mg	0.0000	0.0000	0.0000	0.0000	0.0000	0.0000	0.0000	0.0000	0.0000	0.0000	0.0604	1.0000
MS7-H-Na	0.0000	0.0000	0.0000	0.0000	0.0000	0.0000	0.0000	0.0000	0.0000	0.0000	0.0581	1.0000
MS7-L-Na	0.0000	0.0000	0.0000	0.0000	0.0000	0.0000	0.0000	0.0000	0.0000	0.0000	0.0623	1.0000
MS7-H-Ni	0.0000	0.0000	0.0000	0.0000	0.0000	0.0000	0.0000	0.0000	0.0000	0.0000	0.0595	1.0000
MS7-L-Ni	0.0000	0.0000	0.0000	0.0000	0.0000	0.0000	0.0000	0.0000	0.0000	0.0000	0.0604	1.0000
MS7-Mn-0	0.0000	0.0000	0.0000	0.0000	0.0000	0.0000	0.0000	0.0000	0.0000	0.0000	0.0603	1.0000
MS7-Mn-0.5	0.0000	0.0000	0.0000	0.0000	0.0000	0.0000	0.0000	0.0000	0.0000	0.0000	0.0600	1.0000
MS7-Mn-1	0.0000	0.0000	0.0000	0.0000	0.0000	0.0000	0.0000	0.0000	0.0000	0.0000	0.0597	1.0000
MS7-Mn-2	0.0000	0.0000	0.0000	0.0000	0.0000	0.0000	0.0000	0.0000	0.0000	0.0000	0.0591	1.0000
MS7-Mn-3	0.0000	0.0000	0.0000	0.0000	0.0000	0.0000	0.0000	0.0000	0.0000	0.0000	0.0585	1.0000
MS7-Mn-4	0.0000	0.0000	0.0000	0.0000	0.0000	0.0000	0.0000	0.0000	0.0000	0.0000	0.0579	1.0000
MS7-Mn-5	0.0000	0.0000	0.0000	0.0000	0.0000	0.0000	0.0000	0.0000	0.0000	0.0000	0.0573	1.0000
MS7-Mn-6	0.0000	0.0000	0.0000	0.0000	0.0000	0.0000	0.0000	0.0000	0.0000	0.0000	0.0567	1.0000
MS-8	0.0000	0.0000	0.0000	0.0000	0.0000	0.0000	0.0000	0.0000	0.0000	0.0000	0.0571	1.0000
MS-7-m	0.0000	0.0000	0.0000	0.0000	0.0000	0.0000	0.0000	0.0000	0.0000	0.0000	0.0600	1.0000
GNi	0.0000	0.0000	0.0000	0.0000	0.0000	0.0000	0.0000	0.0000	0.0000	0.0000	0.0599	1.0000
GLi	0.0000	0.0000	0.0000	0.0000	0.0000	0.0000	0.0000	0.0000	0.0000	0.0000	0.0583	1.0000
GNa	0.0000	0.0000	0.0000	0.0000	0.0000	0.0000	0.0000	0.0000	0.0000	0.0000	0.0589	1.0000
GMg	0.0000	0.0000	0.0000	0.0000	0.0000	0.0000	0.0000	0.0000	0.0000	0.0000	0.0608	1.0000
AZB	0.0003	0.0002	0.0000	0.0003	0.0000	0.0000	0.0000	0.0000	0.0000	0.0002	0.0199	1.0000
C106	0.0000	0.0004	0.0000	0.0015	0.0000	0.0000	0.0000	0.0004	0.0000	0.0003	0.0010	1.0000
nom-2	0.0003	0.0006	0.0000	0.0002	0.0000	0.0000	0.0000	0.0000	0.0000	0.0002	0.0156	1.0000
nom-3	0.0003	0.0007	0.0000	0.0003	0.0000	0.0000	0.0000	0.0000	0.0000	0.0002	0.0186	1.0000
nomc-2	0.0003	0.0007	0.0000	0.0003	0.0000	0.0000	0.0000	0.0000	0.0000	0.0002	0.0183	1.0000
C106a-4	0.0001	0.0000	0.0000	0.0000	0.0000	0.0000	0.0000	0.0000	0.0000	0.0001	0.0034	1.0000
az-5	0.0003	0.0008	0.0000	0.0004	0.0000	0.0000	0.0000	0.0000	0.0000	0.0002	0.0223	1.0000
SG03	0.0000	0.0000	0.0000	0.0026	0.0000	0.0415	0.0000	0.0000	0.0000	0.0000	0.0000	1.0000
SG05	0.0000	0.0000	0.0000	0.0037	0.0000	0.0280	0.0000	0.0000	0.0000	0.0000	0.0000	1.0000
SG16	0.0000	0.0000	0.0000	0.0049	0.0000	0.0415	0.0000	0.0000	0.0000	0.0000	0.0000	1.0000
SG17	0.0000	0.0000	0.0000	0.0049	0.0000	0.0415	0.0000	0.0000	0.0000	0.0000	0.0000	1.0000
SG19	0.0000	0.0000	0.0000	0.0015	0.0000	0.0550	0.0000	0.0000	0.0000	0.0000	0.0000	1.0000
SG22	0.0000	0.0000	0.0000	0.0026	0.0000	0.0177	0.0000	0.0000	0.0000	0.0000	0.0000	1.0000
SG26	0.0000	0.0000	0.0000	0.0049	0.0000	0.0415	0.0000	0.0000	0.0000	0.0000	0.0000	1.0000
SG27	0.0000	0.0000	0.0000	0.0026	0.0000	0.0415	0.0000	0.0000	0.0000	0.0000	0.0000	1.0000

Table A1. Glass Compositions (in mass fractions) and T_L Values, Cont.

Glass ID	Reference	QA	T_L	Matrix	Ag_2O	Al_2O_3	As_2O_5	B_2O_3	BaO	Bi_2O_3	CaO	CdO	Ce_2O_3	Cl	CoO	Cr_2O_3	Cs_2O	CuO	F
SG29	Hrma et al. 1999	2	811	N	0.0000	0.0799	0.0000	0.0500	0.0000	0.0000	0.0030	0.0000	0.0000	0.0000	0.0000	0.0010	0.0000	0.0000	0.0000
SG30	Hrma et al. 1999	2	1031	N	0.0000	0.0799	0.0000	0.0500	0.0000	0.0000	0.0200	0.0000	0.0000	0.0000	0.0000	0.0010	0.0000	0.0000	0.0000
SG33	Hrma et al. 1999	2	943	N	0.0000	0.0799	0.0000	0.0999	0.0000	0.0000	0.0200	0.0000	0.0000	0.0000	0.0000	0.0030	0.0000	0.0000	0.0000
SG40	Hrma et al. 1999	2	1173	N	0.0000	0.0799	0.0000	0.0999	0.0000	0.0000	0.0030	0.0000	0.0000	0.0000	0.0000	0.0030	0.0000	0.0000	0.0000
SG42	Hrma et al. 1999	2	990	Y	0.0000	0.0449	0.0000	0.0876	0.0000	0.0000	0.0073	0.0000	0.0000	0.0000	0.0000	0.0025	0.0000	0.0000	0.0000
SG43	Hrma et al. 1999	2	924	Y	0.0000	0.0664	0.0000	0.0876	0.0000	0.0000	0.0073	0.0000	0.0000	0.0000	0.0000	0.0015	0.0000	0.0000	0.0000
SG44	Hrma et al. 1999	2	1244	N	0.0000	0.0664	0.0000	0.0876	0.0000	0.0000	0.0073	0.0000	0.0000	0.0000	0.0000	0.0015	0.0000	0.0000	0.0000
SG53	Hrma et al. 1999	2	1082	N	0.0000	0.0530	0.0000	0.0752	0.0000	0.0000	0.0115	0.0000	0.0000	0.0000	0.0000	0.0020	0.0000	0.0000	0.0000
SP-1a	Hrma et al. 1999	2	1048	N	0.0007	0.0800	0.0000	0.0700	0.0030	0.0000	0.0100	0.0070	0.0007	0.0001	0.0008	0.0022	0.0000	0.0003	0.0006
SP-1b	Hrma et al. 1999	2	1040	N	0.0007	0.0800	0.0000	0.0700	0.0030	0.0000	0.0100	0.0070	0.0007	0.0001	0.0008	0.0022	0.0000	0.0003	0.0006
SP-1c	Hrma et al. 1999	2	1039	N	0.0007	0.0800	0.0000	0.0700	0.0030	0.0000	0.0100	0.0070	0.0007	0.0001	0.0008	0.0022	0.0000	0.0003	0.0006
SP-1d	Hrma et al. 1999	2	1034	N	0.0007	0.0800	0.0000	0.0700	0.0030	0.0000	0.0100	0.0070	0.0007	0.0001	0.0008	0.0022	0.0000	0.0003	0.0006
SP-1e	Hrma et al. 1999	2	1036	N	0.0007	0.0800	0.0000	0.0700	0.0030	0.0000	0.0100	0.0070	0.0007	0.0001	0.0008	0.0022	0.0000	0.0003	0.0006
SP-1f	Hrma et al. 1999	2	1037	N	0.0007	0.0800	0.0000	0.0700	0.0030	0.0000	0.0100	0.0070	0.0007	0.0001	0.0008	0.0022	0.0000	0.0003	0.0006
SP-1g	Hrma et al. 1999	2	1041	N	0.0007	0.0800	0.0000	0.0700	0.0030	0.0000	0.0100	0.0070	0.0007	0.0001	0.0008	0.0022	0.0000	0.0003	0.0006
SP-1h	Hrma et al. 1999	2	1043	N	0.0007	0.0800	0.0000	0.0700	0.0030	0.0000	0.0100	0.0070	0.0007	0.0001	0.0008	0.0022	0.0000	0.0003	0.0006
SP-1i	Mika et al. 1997	2	1039	N	0.0007	0.0800	0.0000	0.0700	0.0030	0.0000	0.0100	0.0070	0.0007	0.0001	0.0008	0.0022	0.0000	0.0003	0.0006
SP-Al-1	Mika et al. 1997	2	1007	N	0.0007	0.0400	0.0000	0.0730	0.0032	0.0000	0.0104	0.0073	0.0007	0.0001	0.0009	0.0023	0.0000	0.0003	0.0006
SP-B-3	Mika et al. 1997	2	1058	N	0.0007	0.0826	0.0000	0.0400	0.0031	0.0000	0.0103	0.0072	0.0007	0.0001	0.0008	0.0023	0.0000	0.0003	0.0006
SP-B-4	Mika et al. 1997	2	1020	Y	0.0007	0.0757	0.0000	0.1200	0.0029	0.0000	0.0095	0.0066	0.0006	0.0001	0.0008	0.0021	0.0000	0.0003	0.0006
SP-Ca-1	Vienna et al. 2001	2	1039	N	0.0007	0.0784	0.0000	0.0686	0.0030	0.0000	0.0300	0.0068	0.0007	0.0001	0.0008	0.0022	0.0000	0.0003	0.0006
SP-Ca-2	Vienna et al. 2001	2	1035	N	0.0007	0.0768	0.0000	0.0672	0.0029	0.0000	0.0500	0.0067	0.0006	0.0001	0.0008	0.0021	0.0000	0.0003	0.0006
SP-Cr-1	Mika et al. 1997	2	1018	N	0.0007	0.0802	0.0000	0.0702	0.0030	0.0000	0.0100	0.0070	0.0007	0.0001	0.0008	0.0000	0.0000	0.0003	0.0006
SP-Cr-2	Mika et al. 1997	2	1058	N	0.0007	0.0798	0.0000	0.0698	0.0030	0.0000	0.0100	0.0069	0.0007	0.0001	0.0008	0.0050	0.0000	0.0003	0.0006
SP-Fe-1	Mika et al. 1997	2	948	N	0.0008	0.0859	0.0000	0.0752	0.0033	0.0000	0.0107	0.0075	0.0007	0.0001	0.0009	0.0024	0.0000	0.0003	0.0007
SP-Fe-2	Mika et al. 1997	2	966	N	0.0007	0.0832	0.0000	0.0728	0.0031	0.0000	0.0104	0.0072	0.0007	0.0001	0.0008	0.0023	0.0000	0.0003	0.0006
SP-K-1	Vienna et al. 2001	2	1021	N	0.0007	0.0786	0.0000	0.0688	0.0030	0.0000	0.0098	0.0068	0.0007	0.0001	0.0008	0.0022	0.0000	0.0003	0.0006
SP-K-2	Vienna et al. 2001	2	997	N	0.0007	0.0770	0.0000	0.0674	0.0029	0.0000	0.0096	0.0067	0.0006	0.0001	0.0008	0.0021	0.0000	0.0003	0.0006
SP-Li-1	Mika et al. 1997	2	1142	N	0.0007	0.0825	0.0000	0.0722	0.0031	0.0000	0.0103	0.0072	0.0007	0.0001	0.0008	0.0023	0.0000	0.0003	0.0006
SP-Li-2	Mika et al. 1997	2	1084	N	0.0007	0.0817	0.0000	0.0714	0.0031	0.0000	0.0102	0.0071	0.0007	0.0001	0.0008	0.0022	0.0000	0.0003	0.0006
SP-Li-3	Mika et al. 1997	2	1042	N	0.0007	0.0800	0.0000	0.0700	0.0030	0.0000	0.0100	0.0070	0.0007	0.0001	0.0008	0.0022	0.0000	0.0003	0.0006
SP-Li-5	Vienna et al. 2001	2	1035	N	0.0007	0.0788	0.0000	0.0689	0.0030	0.0000	0.0098	0.0068	0.0007	0.0001	0.0008	0.0022	0.0000	0.0003	0.0006
SP-Mg-1	Mika et al. 1997	2	1031	N	0.0007	0.0797	0.0000	0.0697	0.0030	0.0000	0.0100	0.0069	0.0007	0.0001	0.0008	0.0022	0.0000	0.0003	0.0006
SP-Mg-2	Mika et al. 1997	2	1075	N	0.0007	0.0789	0.0000	0.0690	0.0030	0.0000	0.0099	0.0069	0.0007	0.0001	0.0008	0.0022	0.0000	0.0003	0.0006
SP-Mn-1	Mika et al. 1997	2	1043	N	0.0007	0.0803	0.0000	0.0703	0.0030	0.0000	0.0100	0.0070	0.0007	0.0001	0.0008	0.0022	0.0000	0.0003	0.0006

Table A1. Glass Compositions (in mass fractions) and T_L Values, Cont.

Glass ID	Fe_2O_3	K_2O	La_2O_3	Li_2O	MgO	MnO	MoO_3	Na_2O	Nd_2O_3	NiO	P_2O_5	PbO	PdO	Pr_2O_3	Rb_2O	Rh_2O_3	RuO_2	Sb_2O_5
SG29	0.0599	0.0150	0.0000	0.0599	0.0050	0.0300	0.0000	0.1099	0.0000	0.0005	0.0000	0.0000	0.0000	0.0000	0.0000	0.0000	0.0009	0.0000
SG30	0.0599	0.0380	0.0000	0.0599	0.0250	0.0300	0.0000	0.1099	0.0000	0.0200	0.0000	0.0000	0.0000	0.0000	0.0000	0.0000	0.0009	0.0000
SG33	0.0599	0.0380	0.0000	0.0599	0.0050	0.0300	0.0000	0.1099	0.0000	0.0200	0.0000	0.0000	0.0000	0.0000	0.0000	0.0000	0.0009	0.0000
SG40	0.0599	0.0150	0.0000	0.0300	0.0250	0.0100	0.0000	0.1099	0.0000	0.0200	0.0000	0.0000	0.0000	0.0000	0.0000	0.0000	0.0009	0.0000
SG42	0.1275	0.0323	0.0000	0.0525	0.0200	0.0250	0.0000	0.0976	0.0000	0.0054	0.0000	0.0000	0.0000	0.0000	0.0000	0.0000	0.0009	0.0000
SG43	0.0825	0.0323	0.0000	0.0375	0.0100	0.0250	0.0000	0.0976	0.0000	0.0054	0.0000	0.0000	0.0000	0.0000	0.0000	0.0000	0.0009	0.0000
SG44	0.1275	0.0208	0.0000	0.0375	0.0200	0.0150	0.0000	0.0726	0.0000	0.0151	0.0000	0.0000	0.0000	0.0000	0.0000	0.0000	0.0009	0.0000
SG53	0.1052	0.0266	0.0000	0.0450	0.0150	0.0200	0.0000	0.0852	0.0000	0.0102	0.0000	0.0000	0.0000	0.0000	0.0000	0.0000	0.0009	0.0000
SP-1a	0.1250	0.0028	0.0027	0.0300	0.0060	0.0036	0.0001	0.1573	0.0018	0.0052	0.0046	0.0017	0.0000	0.0000	0.0000	0.0003	0.0003	0.0008
SP-1b	0.1250	0.0028	0.0027	0.0300	0.0060	0.0036	0.0001	0.1573	0.0018	0.0052	0.0046	0.0017	0.0000	0.0000	0.0000	0.0003	0.0003	0.0008
SP-1c	0.1250	0.0028	0.0027	0.0300	0.0060	0.0036	0.0001	0.1573	0.0018	0.0052	0.0046	0.0017	0.0000	0.0000	0.0000	0.0003	0.0003	0.0008
SP-1d	0.1250	0.0028	0.0027	0.0300	0.0060	0.0036	0.0001	0.1573	0.0018	0.0052	0.0046	0.0017	0.0000	0.0000	0.0000	0.0003	0.0003	0.0008
SP-1e	0.1250	0.0028	0.0027	0.0300	0.0060	0.0036	0.0001	0.1573	0.0018	0.0052	0.0046	0.0017	0.0000	0.0000	0.0000	0.0003	0.0003	0.0008
SP-1f	0.1250	0.0028	0.0027	0.0300	0.0060	0.0036	0.0001	0.1573	0.0018	0.0052	0.0046	0.0017	0.0000	0.0000	0.0000	0.0003	0.0003	0.0008
SP-1g	0.1250	0.0028	0.0027	0.0300	0.0060	0.0036	0.0001	0.1573	0.0018	0.0052	0.0046	0.0017	0.0000	0.0000	0.0000	0.0003	0.0003	0.0008
SP-1h	0.1250	0.0028	0.0027	0.0300	0.0060	0.0036	0.0001	0.1573	0.0018	0.0052	0.0046	0.0017	0.0000	0.0000	0.0000	0.0003	0.0003	0.0008
SP-1i	0.1250	0.0028	0.0027	0.0300	0.0060	0.0036	0.0001	0.1573	0.0018	0.0052	0.0046	0.0017	0.0000	0.0000	0.0000	0.0003	0.0003	0.0008
SP-Al-1	0.1304	0.0029	0.0028	0.0313	0.0063	0.0038	0.0001	0.1641	0.0019	0.0054	0.0048	0.0018	0.0000	0.0000	0.0000	0.0003	0.0003	0.0008
SP-B-3	0.1290	0.0029	0.0028	0.0310	0.0062	0.0037	0.0001	0.1624	0.0019	0.0054	0.0048	0.0018	0.0000	0.0000	0.0000	0.0003	0.0003	0.0008
SP-B-4	0.1183	0.0026	0.0026	0.0284	0.0057	0.0034	0.0001	0.1488	0.0017	0.0049	0.0044	0.0016	0.0000	0.0000	0.0000	0.0003	0.0003	0.0007
SP-Ca-1	0.1225	0.0027	0.0027	0.0294	0.0059	0.0036	0.0001	0.1541	0.0018	0.0051	0.0045	0.0017	0.0000	0.0000	0.0000	0.0003	0.0003	0.0008
SP-Ca-2	0.1200	0.0027	0.0026	0.0288	0.0058	0.0035	0.0001	0.1510	0.0017	0.0050	0.0044	0.0016	0.0000	0.0000	0.0000	0.0003	0.0003	0.0008
SP-Cr-1	0.1253	0.0028	0.0027	0.0301	0.0060	0.0036	0.0001	0.1577	0.0018	0.0052	0.0047	0.0017	0.0000	0.0000	0.0000	0.0003	0.0003	0.0008
SP-Cr-2	0.1247	0.0028	0.0027	0.0299	0.0060	0.0036	0.0001	0.1569	0.0018	0.0052	0.0046	0.0017	0.0000	0.0000	0.0000	0.0003	0.0003	0.0008
SP-Fe-1	0.0600	0.0030	0.0029	0.0322	0.0064	0.0039	0.0001	0.1690	0.0020	0.0056	0.0050	0.0018	0.0000	0.0000	0.0000	0.0003	0.0003	0.0008
SP-Fe-2	0.0900	0.0029	0.0028	0.0312	0.0062	0.0037	0.0001	0.1636	0.0019	0.0054	0.0048	0.0018	0.0000	0.0000	0.0000	0.0003	0.0003	0.0008
SP-K-1	0.1228	0.0200	0.0027	0.0295	0.0059	0.0036	0.0001	0.1546	0.0018	0.0051	0.0045	0.0017	0.0000	0.0000	0.0000	0.0003	0.0003	0.0008
SP-K-2	0.1203	0.0400	0.0026	0.0289	0.0058	0.0035	0.0001	0.1514	0.0017	0.0050	0.0045	0.0016	0.0000	0.0000	0.0000	0.0003	0.0003	0.0008
SP-Li-1	0.1289	0.0029	0.0028	0.0000	0.0062	0.0037	0.0001	0.1622	0.0019	0.0054	0.0048	0.0018	0.0000	0.0000	0.0000	0.0003	0.0003	0.0008
SP-Li-2	0.1276	0.0029	0.0028	0.0100	0.0061	0.0037	0.0001	0.1606	0.0019	0.0053	0.0047	0.0018	0.0000	0.0000	0.0000	0.0003	0.0003	0.0008
SP-Li-3	0.1250	0.0028	0.0027	0.0300	0.0060	0.0036	0.0001	0.1573	0.0018	0.0052	0.0046	0.0017	0.0000	0.0000	0.0000	0.0003	0.0003	0.0008
SP-Li-5	0.1231	0.0028	0.0027	0.0450	0.0059	0.0036	0.0001	0.1549	0.0018	0.0051	0.0046	0.0017	0.0000	0.0000	0.0000	0.0003	0.0003	0.0008
SP-Mg-1	0.1245	0.0028	0.0027	0.0299	0.0100	0.0036	0.0001	0.1567	0.0018	0.0052	0.0046	0.0017	0.0000	0.0000	0.0000	0.0003	0.0003	0.0008
SP-Mg-2	0.1232	0.0028	0.0027	0.0296	0.0200	0.0035	0.0001	0.1551	0.0018	0.0051	0.0046	0.0017	0.0000	0.0000	0.0000	0.0003	0.0003	0.0008
SP-Mn-1	0.1255	0.0028	0.0027	0.0301	0.0060	0.0000	0.0001	0.1579	0.0018	0.0052	0.0047	0.0017	0.0000	0.0000	0.0000	0.0003	0.0003	0.0008

Table A1. Glass Compositions (in mass fractions) and T_L Values, Cont.

Glass ID	SeO_2	SiO_2	Sm_2O_3	SO_3	SrO	TeO_2	ThO_2	TiO_2	Tl_2O	U_3O_8	V_2O_5	WO_3	Y_2O_3	ZnO	ZrO_2	Total
SG29	0.0000	0.5240	0.0000	0.0000	0.0000	0.0000	0.0000	0.0060	0.0000	0.0550	0.0000	0.0000	0.0000	0.0000	0.0000	1.0000
SG30	0.0000	0.4491	0.0000	0.0000	0.0000	0.0000	0.0000	0.0015	0.0000	0.0550	0.0000	0.0000	0.0000	0.0000	0.0000	1.0000
SG33	0.0000	0.4676	0.0000	0.0000	0.0000	0.0000	0.0000	0.0060	0.0000	0.0000	0.0000	0.0000	0.0000	0.0000	0.0000	1.0000
SG40	0.0000	0.4826	0.0000	0.0000	0.0000	0.0000	0.0000	0.0060	0.0000	0.0550	0.0000	0.0000	0.0000	0.0000	0.0000	1.0000
SG42	0.0000	0.4741	0.0000	0.0000	0.0000	0.0000	0.0000	0.0049	0.0000	0.0177	0.0000	0.0000	0.0000	0.0000	0.0000	1.0000
SG43	0.0000	0.5257	0.0000	0.0000	0.0000	0.0000	0.0000	0.0026	0.0000	0.0177	0.0000	0.0000	0.0000	0.0000	0.0000	1.0000
SG44	0.0000	0.5052	0.0000	0.0000	0.0000	0.0000	0.0000	0.0049	0.0000	0.0177	0.0000	0.0000	0.0000	0.0000	0.0000	1.0000
SG53	0.0000	0.5186	0.0000	0.0000	0.0000	0.0000	0.0000	0.0037	0.0000	0.0280	0.0000	0.0000	0.0000	0.0000	0.0000	1.0000
SP-1a	0.0009	0.4600	0.0000	0.0019	0.0003	0.0000	0.0000	0.0003	0.0000	0.0000	0.0000	0.0000	0.0000	0.0004	0.0185	1.0000
SP-1b	0.0009	0.4600	0.0000	0.0019	0.0003	0.0000	0.0000	0.0003	0.0000	0.0000	0.0000	0.0000	0.0000	0.0004	0.0185	1.0000
SP-1c	0.0009	0.4600	0.0000	0.0019	0.0003	0.0000	0.0000	0.0003	0.0000	0.0000	0.0000	0.0000	0.0000	0.0004	0.0185	1.0000
SP-1d	0.0009	0.4600	0.0000	0.0019	0.0003	0.0000	0.0000	0.0003	0.0000	0.0000	0.0000	0.0000	0.0000	0.0004	0.0185	1.0000
SP-1e	0.0009	0.4600	0.0000	0.0019	0.0003	0.0000	0.0000	0.0003	0.0000	0.0000	0.0000	0.0000	0.0000	0.0004	0.0185	1.0000
SP-1f	0.0009	0.4600	0.0000	0.0019	0.0003	0.0000	0.0000	0.0003	0.0000	0.0000	0.0000	0.0000	0.0000	0.0004	0.0185	1.0000
SP-1g	0.0009	0.4600	0.0000	0.0019	0.0003	0.0000	0.0000	0.0003	0.0000	0.0000	0.0000	0.0000	0.0000	0.0004	0.0185	1.0000
SP-1h	0.0009	0.4600	0.0000	0.0019	0.0003	0.0000	0.0000	0.0003	0.0000	0.0000	0.0000	0.0000	0.0000	0.0004	0.0185	1.0000
SP-1i	0.0009	0.4600	0.0000	0.0019	0.0003	0.0000	0.0000	0.0003	0.0000	0.0000	0.0000	0.0000	0.0000	0.0004	0.0185	1.0000
SP-Al-1	0.0009	0.4800	0.0000	0.0020	0.0003	0.0000	0.0000	0.0003	0.0000	0.0000	0.0000	0.0000	0.0000	0.0004	0.0193	1.0000
SP-B-3	0.0009	0.4749	0.0000	0.0020	0.0003	0.0000	0.0000	0.0003	0.0000	0.0000	0.0000	0.0000	0.0000	0.0004	0.0191	1.0000
SP-B-4	0.0009	0.4353	0.0000	0.0018	0.0003	0.0000	0.0000	0.0003	0.0000	0.0000	0.0000	0.0000	0.0000	0.0004	0.0175	1.0000
SP-Ca-1	0.0009	0.4507	0.0000	0.0019	0.0003	0.0000	0.0000	0.0003	0.0000	0.0000	0.0000	0.0000	0.0000	0.0004	0.0181	1.0000
SP-Ca-2	0.0009	0.4414	0.0000	0.0018	0.0003	0.0000	0.0000	0.0003	0.0000	0.0000	0.0000	0.0000	0.0000	0.0004	0.0178	1.0000
SP-Cr-1	0.0009	0.4610	0.0000	0.0019	0.0003	0.0000	0.0000	0.0003	0.0000	0.0000	0.0000	0.0000	0.0000	0.0004	0.0185	1.0000
SP-Cr-2	0.0009	0.4587	0.0000	0.0019	0.0003	0.0000	0.0000	0.0003	0.0000	0.0000	0.0000	0.0000	0.0000	0.0004	0.0184	1.0000
SP-Fe-1	0.0010	0.4942	0.0000	0.0021	0.0003	0.0000	0.0000	0.0003	0.0000	0.0000	0.0000	0.0000	0.0000	0.0004	0.0198	1.0000
SP-Fe-2	0.0009	0.4784	0.0000	0.0020	0.0003	0.0000	0.0000	0.0003	0.0000	0.0000	0.0000	0.0000	0.0000	0.0004	0.0192	1.0000
SP-K-1	0.0009	0.4521	0.0000	0.0019	0.0003	0.0000	0.0000	0.0003	0.0000	0.0000	0.0000	0.0000	0.0000	0.0004	0.0182	1.0000
SP-K-2	0.0009	0.4429	0.0000	0.0018	0.0003	0.0000	0.0000	0.0003	0.0000	0.0000	0.0000	0.0000	0.0000	0.0004	0.0178	1.0000
SP-Li-1	0.0009	0.4742	0.0000	0.0020	0.0003	0.0000	0.0000	0.0003	0.0000	0.0000	0.0000	0.0000	0.0000	0.0004	0.0190	1.0000
SP-Li-2	0.0009	0.4695	0.0000	0.0020	0.0003	0.0000	0.0000	0.0003	0.0000	0.0000	0.0000	0.0000	0.0000	0.0004	0.0188	1.0000
SP-Li-3	0.0009	0.4600	0.0000	0.0019	0.0003	0.0000	0.0000	0.0003	0.0000	0.0000	0.0000	0.0000	0.0000	0.0004	0.0185	1.0000
SP-Li-5	0.0009	0.4529	0.0000	0.0019	0.0003	0.0000	0.0000	0.0003	0.0000	0.0000	0.0000	0.0000	0.0000	0.0004	0.0182	1.0000
SP-Mg-1	0.0009	0.4582	0.0000	0.0019	0.0003	0.0000	0.0000	0.0003	0.0000	0.0000	0.0000	0.0000	0.0000	0.0004	0.0184	1.0000
SP-Mg-2	0.0009	0.4535	0.0000	0.0019	0.0003	0.0000	0.0000	0.0003	0.0000	0.0000	0.0000	0.0000	0.0000	0.0004	0.0182	1.0000
SP-Mn-1	0.0009	0.4617	0.0000	0.0019	0.0003	0.0000	0.0000	0.0003	0.0000	0.0000	0.0000	0.0000	0.0000	0.0004	0.0185	1.0000

Table A1. Glass Compositions (in mass fractions) and T_L Values, Cont.

Glass ID	Reference	QA	T_L	Matrix	Ag_2O	Al_2O_3	As_2O_5	B_2O_3	BaO	Bi_2O_3	CaO	CdO	Ce_2O_3	Cl	CoO	Cr_2O_3	Cs_2O	CuO
SP-Mn-2	Mika et al. 1997	2	1060	N	0.0007	0.0795	0.0000	0.0696	0.0030	0.0000	0.0099	0.0069	0.0007	0.0001	0.0008	0.0022	0.0000	0.0003
SP-Mn-3	Mika et al. 1997	2	1080	N	0.0007	0.0771	0.0000	0.0674	0.0029	0.0000	0.0096	0.0067	0.0006	0.0001	0.0008	0.0021	0.0000	0.0003
SP-Na-1	Mika et al. 1997	2	1350	N	0.0008	0.0873	0.0000	0.0764	0.0033	0.0000	0.0109	0.0076	0.0007	0.0001	0.0009	0.0024	0.0000	0.0003
SP-Na-2	Mika et al. 1997	2	1147	N	0.0007	0.0835	0.0000	0.0731	0.0032	0.0000	0.0104	0.0073	0.0007	0.0001	0.0009	0.0023	0.0000	0.0003
SP-Na-3	Mika et al. 1997	2	941	N	0.0007	0.0759	0.0000	0.0665	0.0029	0.0000	0.0095	0.0066	0.0006	0.0001	0.0008	0.0021	0.0000	0.0003
SP-Ni-1	Mika et al. 1997	2	970	N	0.0007	0.0804	0.0000	0.0704	0.0030	0.0000	0.0101	0.0070	0.0007	0.0001	0.0008	0.0022	0.0000	0.0003
SP-Ni-2	Mika et al. 1997	2	1078	N	0.0007	0.0796	0.0000	0.0697	0.0030	0.0000	0.0100	0.0069	0.0007	0.0001	0.0008	0.0022	0.0000	0.0003
SP-Ni-3	Mika et al. 1997	2	1222	N	0.0007	0.0780	0.0000	0.0683	0.0030	0.0000	0.0098	0.0068	0.0007	0.0001	0.0008	0.0021	0.0000	0.0003
SP-Si-2	Mika et al. 1997	2	1007	Y	0.0006	0.0711	0.0000	0.0622	0.0027	0.0000	0.0089	0.0062	0.0006	0.0001	0.0007	0.0020	0.0000	0.0003
SP-Zr-1	Vienna et al. 2001	2	1070	N	0.0007	0.0783	0.0000	0.0685	0.0030	0.0000	0.0098	0.0068	0.0007	0.0001	0.0008	0.0022	0.0000	0.0003
Sp-Ru-1	Mika et al. 1997	2	1065	N	0.0009	0.0800	0.0000	0.0700	0.0038	0.0000	0.0000	0.0088	0.0009	0.0001	0.0010	0.0022	0.0000	0.0004
Sp-Ru-2	Mika et al. 1997	2	1076	N	0.0009	0.0799	0.0000	0.0699	0.0038	0.0000	0.0000	0.0088	0.0009	0.0001	0.0010	0.0022	0.0000	0.0004
SP-Others-1	Vienna et al. 2001	2	1090	N	0.0013	0.0777	0.0000	0.0680	0.0055	0.0000	0.0097	0.0127	0.0012	0.0002	0.0015	0.0021	0.0000	0.0006
Sp-LHLL	Vienna et al. 2001	2	893	N	0.0009	0.0500	0.0000	0.0706	0.0039	0.0000	0.0000	0.0089	0.0009	0.0001	0.0010	0.0005	0.0000	0.0004
Sp-LHLH	Vienna et al. 2001	2	1063	N	0.0009	0.0500	0.0000	0.0688	0.0038	0.0000	0.0000	0.0087	0.0008	0.0001	0.0010	0.0005	0.0000	0.0004
Sp-LHMM	Vienna et al. 2001	2	935	N	0.0009	0.0500	0.0000	0.0700	0.0038	0.0000	0.0000	0.0088	0.0009	0.0001	0.0010	0.0022	0.0000	0.0004
Sp-MMLL	Vienna et al. 2001	2	1036	N	0.0009	0.0800	0.0000	0.0706	0.0039	0.0000	0.0000	0.0089	0.0009	0.0001	0.0010	0.0005	0.0000	0.0004
Sp-MMLH	Vienna et al. 2001	2	1129	N	0.0009	0.0800	0.0000	0.0688	0.0038	0.0000	0.0000	0.0087	0.0008	0.0001	0.0010	0.0005	0.0000	0.0004
Sp-MMMM	Vienna et al. 2001	2	1038	N	0.0009	0.0800	0.0000	0.0700	0.0038	0.0000	0.0000	0.0088	0.0009	0.0001	0.0010	0.0022	0.0000	0.0004
Sp-HLLL	Vienna et al. 2001	2	1068	Y	0.0009	0.1100	0.0000	0.0706	0.0039	0.0000	0.0000	0.0089	0.0009	0.0001	0.0010	0.0005	0.0000	0.0004
Sp-HLLH	Vienna et al. 2001	2	1232	N	0.0009	0.1100	0.0000	0.0688	0.0038	0.0000	0.0000	0.0087	0.0008	0.0001	0.0010	0.0005	0.0000	0.0004
Sp-HLMM	Vienna et al. 2001	2	1228	Y	0.0009	0.1100	0.0000	0.0700	0.0038	0.0000	0.0000	0.0088	0.0009	0.0001	0.0010	0.0022	0.0000	0.0004
Sp-LHLH(b)	Vienna et al. 2001	2	1102	N	0.0009	0.0500	0.0000	0.0688	0.0038	0.0000	0.0000	0.0087	0.0008	0.0001	0.0010	0.0005	0.0000	0.0004
Sp-MMLL(b)	Vienna et al. 2001	2	1033	N	0.0009	0.0800	0.0000	0.0706	0.0039	0.0000	0.0000	0.0089	0.0009	0.0001	0.0010	0.0005	0.0000	0.0004
Sp-HLLL(b)	Vienna et al. 2001	2	1089	Y	0.0009	0.1100	0.0000	0.0706	0.0039	0.0000	0.0000	0.0089	0.0009	0.0001	0.0010	0.0005	0.0000	0.0004
SG1-01 = SP-1	Vienna et al. 2002	2	1070	N	0.0007	0.0800	0.0000	0.0700	0.0030	0.0000	0.0100	0.0070	0.0007	0.0001	0.0008	0.0022	0.0000	0.0003
SG1-22 = SP-1	Vienna et al. 2002	2	1069	N	0.0007	0.0800	0.0000	0.0700	0.0030	0.0000	0.0100	0.0070	0.0007	0.0001	0.0008	0.0022	0.0000	0.0003
SG1-24 = SG33	Vienna et al. 2002	2	937	N	0.0000	0.0799	0.0000	0.0999	0.0000	0.0000	0.0200	0.0000	0.0000	0.0000	0.0000	0.0030	0.0000	0.0000
SG1-25 = SG37	Vienna et al. 2002	2	956	N	0.0000	0.0800	0.0000	0.1000	0.0000	0.0000	0.0200	0.0000	0.0000	0.0000	0.0000	0.0030	0.0000	0.0000
SG1-26 = SP1	Vienna et al. 2002	2	1049	N	0.0007	0.0800	0.0000	0.0700	0.0030	0.0000	0.0100	0.0070	0.0007	0.0001	0.0008	0.0022	0.0000	0.0003
SG1-27 = SP1	Vienna et al. 2002	2	1054	N	0.0007	0.0800	0.0000	0.0700	0.0030	0.0000	0.0100	0.0070	0.0007	0.0001	0.0008	0.0022	0.0000	0.0003
SPA-18	Vienna et al. 2002	1	983	N	0.0004	0.0600	0.0006	0.0818	0.0007	0.0000	0.0200	0.0000	0.0044	0.0001	0.0001	0.0030	0.0000	0.0002
SPA-32	Vienna et al. 2002	1	866	N	0.0004	0.0605	0.0006	0.1009	0.0007	0.0000	0.0000	0.0000	0.0044	0.0001	0.0001	0.0030	0.0000	0.0002
SPA-38	Vienna et al. 2002	1	1048	N	0.0007	0.0800	0.0000	0.0700	0.0030	0.0000	0.0100	0.0070	0.0007	0.0001	0.0008	0.0022	0.0000	0.0003
minimum			811		0.0000	0.0390	0.0000	0.0400	0.0000	0.0000	0.0000	0.0000	0.0000	0.0000	0.0000	0.0000	0.0000	0.0000
maximum			1350		0.0024	0.1100	0.0006	0.1357	0.0066	0.0003	0.0601	0.0127	0.0044	0.0002	0.0015	0.0050	0.0022	0.0022

Table A1. Glass Compositions (in mass fractions) and T_L Values, Cont.

Glass ID	F	Fe_2O_3	K_2O	La_2O_3	Li_2O	MgO	MnO	MoO_3	Na_2O	Nd_2O_3	NiO	P_2O_5	PbO	PdO	Pr_2O_3	Rb_2O	Rh_2O_3
SP-Mn-2	0.0006	0.1242	0.0028	0.0027	0.0298	0.0060	0.0100	0.0001	0.1563	0.0018	0.0052	0.0046	0.0017	0.0000	0.0000	0.0000	0.0003
SP-Mn-3	0.0006	0.1204	0.0027	0.0026	0.0289	0.0058	0.0400	0.0001	0.1516	0.0018	0.0050	0.0045	0.0017	0.0000	0.0000	0.0000	0.0003
SP-Na-1	0.0007	0.1365	0.0031	0.0030	0.0328	0.0066	0.0039	0.0001	0.0800	0.0020	0.0057	0.0051	0.0019	0.0000	0.0000	0.0000	0.0003
SP-Na-2	0.0006	0.1305	0.0029	0.0028	0.0313	0.0063	0.0038	0.0001	0.1200	0.0019	0.0054	0.0049	0.0018	0.0000	0.0000	0.0000	0.0003
SP-Na-3	0.0006	0.1187	0.0027	0.0026	0.0285	0.0057	0.0034	0.0001	0.2000	0.0017	0.0049	0.0044	0.0016	0.0000	0.0000	0.0000	0.0003
SP-Ni-1	0.0006	0.1257	0.0028	0.0027	0.0302	0.0060	0.0036	0.0001	0.1581	0.0018	0.0000	0.0047	0.0017	0.0000	0.0000	0.0000	0.0003
SP-Ni-2	0.0006	0.1244	0.0028	0.0027	0.0299	0.0060	0.0036	0.0001	0.1565	0.0018	0.0100	0.0046	0.0017	0.0000	0.0000	0.0000	0.0003
SP-Ni-3	0.0006	0.1219	0.0027	0.0027	0.0293	0.0059	0.0035	0.0001	0.1534	0.0018	0.0300	0.0045	0.0017	0.0000	0.0000	0.0000	0.0003
SP-Si-2	0.0005	0.1111	0.0025	0.0024	0.0267	0.0053	0.0032	0.0001	0.1398	0.0016	0.0046	0.0041	0.0015	0.0000	0.0000	0.0000	0.0003
SP-Zr-1	0.0006	0.1223	0.0027	0.0027	0.0293	0.0059	0.0036	0.0001	0.1539	0.0018	0.0051	0.0045	0.0017	0.0000	0.0000	0.0000	0.0003
Sp-Ru-1	0.0008	0.1249	0.0000	0.0035	0.0300	0.0060	0.0036	0.0001	0.1572	0.0023	0.0052	0.0059	0.0022	0.0000	0.0000	0.0000	0.0004
Sp-Ru-2	0.0008	0.1249	0.0000	0.0034	0.0300	0.0060	0.0036	0.0001	0.1572	0.0023	0.0052	0.0059	0.0022	0.0000	0.0000	0.0000	0.0004
SP-Others-1	0.0011	0.1215	0.0027	0.0050	0.0292	0.0058	0.0067	0.0002	0.1529	0.0033	0.0051	0.0085	0.0031	0.0000	0.0000	0.0000	0.0006
Sp-LHLL	0.0008	0.1260	0.0000	0.0035	0.0302	0.0061	0.0036	0.0001	0.1873	0.0023	0.0010	0.0059	0.0022	0.0000	0.0000	0.0000	0.0004
Sp-LHLH	0.0008	0.1228	0.0000	0.0034	0.0295	0.0059	0.0035	0.0001	0.1873	0.0023	0.0200	0.0058	0.0021	0.0000	0.0000	0.0000	0.0004
Sp-LHMM	0.0008	0.1250	0.0000	0.0035	0.0300	0.0060	0.0036	0.0001	0.1873	0.0023	0.0052	0.0059	0.0022	0.0000	0.0000	0.0000	0.0004
Sp-MMLL	0.0008	0.1260	0.0000	0.0035	0.0302	0.0061	0.0036	0.0001	0.1573	0.0023	0.0010	0.0059	0.0022	0.0000	0.0000	0.0000	0.0004
Sp-MMLH	0.0008	0.1228	0.0000	0.0034	0.0295	0.0059	0.0035	0.0001	0.1573	0.0023	0.0200	0.0058	0.0021	0.0000	0.0000	0.0000	0.0004
Sp-MMMM	0.0008	0.1250	0.0000	0.0035	0.0300	0.0060	0.0036	0.0001	0.1573	0.0023	0.0052	0.0059	0.0022	0.0000	0.0000	0.0000	0.0004
Sp-HLLL	0.0008	0.1260	0.0000	0.0035	0.0302	0.0061	0.0036	0.0001	0.1273	0.0023	0.0010	0.0059	0.0022	0.0000	0.0000	0.0000	0.0004
Sp-HLLH	0.0008	0.1228	0.0000	0.0034	0.0295	0.0059	0.0035	0.0001	0.1273	0.0023	0.0200	0.0058	0.0021	0.0000	0.0000	0.0000	0.0004
Sp-HLMM	0.0008	0.1250	0.0000	0.0035	0.0300	0.0060	0.0036	0.0001	0.1273	0.0023	0.0052	0.0059	0.0022	0.0000	0.0000	0.0000	0.0004
Sp-LHLH(b)	0.0008	0.1228	0.0000	0.0034	0.0295	0.0059	0.0035	0.0001	0.1873	0.0023	0.0200	0.0058	0.0021	0.0000	0.0000	0.0000	0.0004
Sp-MMLL(b)	0.0008	0.1260	0.0000	0.0035	0.0302	0.0061	0.0036	0.0001	0.1573	0.0023	0.0010	0.0059	0.0022	0.0000	0.0000	0.0000	0.0004
Sp-HLLL(b)	0.0008	0.1260	0.0000	0.0035	0.0302	0.0061	0.0036	0.0001	0.1273	0.0023	0.0010	0.0059	0.0022	0.0000	0.0000	0.0000	0.0004
SG1-01 = SP-1	0.0006	0.1250	0.0028	0.0027	0.0300	0.0060	0.0036	0.0001	0.1573	0.0018	0.0052	0.0046	0.0017	0.0000	0.0000	0.0000	0.0003
SG1-22 = SP-1	0.0006	0.1250	0.0028	0.0027	0.0300	0.0060	0.0036	0.0001	0.1573	0.0018	0.0052	0.0046	0.0017	0.0000	0.0000	0.0000	0.0003
SG1-24 = SG33	0.0000	0.0599	0.0380	0.0000	0.0599	0.0050	0.0300	0.0000	0.1099	0.0000	0.0200	0.0000	0.0000	0.0000	0.0000	0.0000	0.0000
SG1-25 = SG37	0.0000	0.0600	0.0380	0.0000	0.0600	0.0050	0.0300	0.0000	0.1100	0.0000	0.0200	0.0000	0.0000	0.0000	0.0000	0.0000	0.0000
SG1-26 = SP1	0.0006	0.1250	0.0028	0.0027	0.0300	0.0060	0.0036	0.0001	0.1573	0.0018	0.0052	0.0046	0.0017	0.0000	0.0000	0.0000	0.0003
SG1-27 = SP1	0.0006	0.1250	0.0028	0.0027	0.0300	0.0060	0.0036	0.0001	0.1573	0.0018	0.0052	0.0046	0.0017	0.0000	0.0000	0.0000	0.0003
SPA-18	0.0150	0.1400	0.0389	0.0026	0.0379	0.0000	0.0100	0.0001	0.1589	0.0008	0.0050	0.0050	0.0029	0.0000	0.0000	0.0000	0.0000
SPA-32	0.0150	0.0700	0.0450	0.0026	0.0150	0.0000	0.0300	0.0001	0.1750	0.0008	0.0050	0.0125	0.0029	0.0000	0.0000	0.0000	0.0000
SPA-38	0.0006	0.1250	0.0028	0.0027	0.0300	0.0060	0.0036	0.0001	0.1573	0.0018	0.0052	0.0046	0.0017	0.0000	0.0000	0.0000	0.0003
minimum	0.0000	0.0200	0.0000	0.0000	0.0000	0.0000	0.0000	0.0000	0.0577	0.0000	0.0000	0.0000	0.0000	0.0000	0.0000	0.0000	0.0000
maximum	0.0150	0.1400	0.0450	0.0090	0.0700	0.0500	0.0600	0.0043	0.2000	0.0177	0.0300	0.0125	0.0031	0.0007	0.0014	0.0007	0.0007

Table A1. Glass Compositions (in mass fractions) and T_L Values, Cont.

Glass ID	RuO_2	Sb_2O_5	SeO_2	SiO_2	Sm_2O_3	SO_3	SrO	TeO_2	ThO_2	TiO_2	Tl_2O	U_3O_8	V_2O_5	WO_3	Y_2O_3	ZnO	ZrO_2	Total
SP-Mn-2	0.0003	0.0008	0.0009	0.4571	0.0000	0.0019	0.0003	0.0000	0.0000	0.0003	0.0000	0.0000	0.0000	0.0000	0.0000	0.0004	0.0183	1.0000
SP-Mn-3	0.0003	0.0008	0.0009	0.4432	0.0000	0.0018	0.0003	0.0000	0.0000	0.0003	0.0000	0.0000	0.0000	0.0000	0.0000	0.0004	0.0178	1.0000
SP-Na-1	0.0003	0.0009	0.0010	0.5022	0.0000	0.0021	0.0003	0.0000	0.0000	0.0003	0.0000	0.0000	0.0000	0.0000	0.0000	0.0004	0.0202	1.0000
SP-Na-2	0.0003	0.0008	0.0009	0.4804	0.0000	0.0020	0.0003	0.0000	0.0000	0.0003	0.0000	0.0000	0.0000	0.0000	0.0000	0.0004	0.0193	1.0000
SP-Na-3	0.0003	0.0007	0.0009	0.4367	0.0000	0.0018	0.0003	0.0000	0.0000	0.0003	0.0000	0.0000	0.0000	0.0000	0.0000	0.0004	0.0175	1.0000
SP-Ni-1	0.0003	0.0008	0.0009	0.4624	0.0000	0.0019	0.0003	0.0000	0.0000	0.0003	0.0000	0.0000	0.0000	0.0000	0.0000	0.0004	0.0186	1.0000
SP-Ni-2	0.0003	0.0008	0.0009	0.4578	0.0000	0.0019	0.0003	0.0000	0.0000	0.0003	0.0000	0.0000	0.0000	0.0000	0.0000	0.0004	0.0184	1.0000
SP-Ni-3	0.0003	0.0008	0.0009	0.4486	0.0000	0.0019	0.0003	0.0000	0.0000	0.0003	0.0000	0.0000	0.0000	0.0000	0.0000	0.0004	0.0180	1.0000
SP-Si-2	0.0003	0.0007	0.0008	0.5200	0.0000	0.0017	0.0003	0.0000	0.0000	0.0003	0.0000	0.0000	0.0000	0.0000	0.0000	0.0004	0.0164	1.0000
SP-Zr-1	0.0003	0.0008	0.0009	0.4499	0.0000	0.0019	0.0003	0.0000	0.0000	0.0003	0.0000	0.0000	0.0000	0.0000	0.0000	0.0004	0.0400	1.0000
Sp-Ru-1	0.0009	0.0010	0.0011	0.4597	0.0000	0.0024	0.0004	0.0000	0.0000	0.0003	0.0000	0.0000	0.0000	0.0000	0.0000	0.0005	0.0234	1.0000
Sp-Ru-2	0.0012	0.0010	0.0011	0.4596	0.0000	0.0024	0.0004	0.0000	0.0000	0.0003	0.0000	0.0000	0.0000	0.0000	0.0000	0.0005	0.0234	1.0000
SP-Others-1	0.0005	0.0014	0.0017	0.4471	0.0000	0.0035	0.0006	0.0000	0.0000	0.0003	0.0000	0.0000	0.0000	0.0000	0.0000	0.0007	0.0180	1.0000
Sp-LHLL	0.0003	0.0010	0.0012	0.4636	0.0000	0.0025	0.0004	0.0000	0.0000	0.0003	0.0000	0.0000	0.0000	0.0000	0.0000	0.0005	0.0236	1.0000
Sp-LHLH	0.0003	0.0010	0.0011	0.4520	0.0000	0.0024	0.0004	0.0000	0.0000	0.0003	0.0000	0.0000	0.0000	0.0000	0.0000	0.0005	0.0231	1.0000
Sp-LHMM	0.0003	0.0010	0.0011	0.4600	0.0000	0.0024	0.0004	0.0000	0.0000	0.0003	0.0000	0.0000	0.0000	0.0000	0.0000	0.0005	0.0234	1.0000
Sp-MMLL	0.0003	0.0010	0.0012	0.4636	0.0000	0.0025	0.0004	0.0000	0.0000	0.0003	0.0000	0.0000	0.0000	0.0000	0.0000	0.0005	0.0236	1.0000
Sp-MMLH	0.0003	0.0010	0.0011	0.4520	0.0000	0.0024	0.0004	0.0000	0.0000	0.0003	0.0000	0.0000	0.0000	0.0000	0.0000	0.0005	0.0231	1.0000
Sp-MMMM	0.0003	0.0010	0.0011	0.4600	0.0000	0.0024	0.0004	0.0000	0.0000	0.0003	0.0000	0.0000	0.0000	0.0000	0.0000	0.0005	0.0234	1.0000
Sp-HLLL	0.0003	0.0010	0.0012	0.4636	0.0000	0.0025	0.0004	0.0000	0.0000	0.0003	0.0000	0.0000	0.0000	0.0000	0.0000	0.0005	0.0236	1.0000
Sp-HLLH	0.0003	0.0010	0.0011	0.4520	0.0000	0.0024	0.0004	0.0000	0.0000	0.0003	0.0000	0.0000	0.0000	0.0000	0.0000	0.0005	0.0231	1.0000
Sp-HLMM	0.0003	0.0010	0.0011	0.4600	0.0000	0.0024	0.0004	0.0000	0.0000	0.0003	0.0000	0.0000	0.0000	0.0000	0.0000	0.0005	0.0234	1.0000
Sp-LHLH(b)	0.0003	0.0010	0.0011	0.4520	0.0000	0.0024	0.0004	0.0000	0.0000	0.0003	0.0000	0.0000	0.0000	0.0000	0.0000	0.0005	0.0231	1.0000
Sp-MMLL(b)	0.0003	0.0010	0.0012	0.4636	0.0000	0.0025	0.0004	0.0000	0.0000	0.0003	0.0000	0.0000	0.0000	0.0000	0.0000	0.0005	0.0236	1.0000
Sp-HLLL(b)	0.0003	0.0010	0.0012	0.4636	0.0000	0.0025	0.0004	0.0000	0.0000	0.0003	0.0000	0.0000	0.0000	0.0000	0.0000	0.0005	0.0236	1.0000
SG1-01 = SP-1	0.0003	0.0008	0.0009	0.4600	0.0000	0.0019	0.0003	0.0000	0.0000	0.0003	0.0000	0.0000	0.0000	0.0000	0.0000	0.0004	0.0185	1.0000
SG1-22 = SP-1	0.0003	0.0008	0.0009	0.4600	0.0000	0.0019	0.0003	0.0000	0.0000	0.0003	0.0000	0.0000	0.0000	0.0000	0.0000	0.0004	0.0185	1.0000
SG1-24 = SG33	0.0009	0.0000	0.0000	0.4676	0.0000	0.0000	0.0000	0.0000	0.0000	0.0060	0.0000	0.0000	0.0000	0.0000	0.0000	0.0000	0.0000	1.0000
SG1-25 = SG37	0.0003	0.0000	0.0000	0.4679	0.0000	0.0000	0.0000	0.0000	0.0000	0.0060	0.0000	0.0000	0.0000	0.0000	0.0000	0.0000	0.0000	1.0000
SG1-26 = SP1	0.0003	0.0008	0.0009	0.4600	0.0000	0.0019	0.0003	0.0000	0.0000	0.0003	0.0000	0.0000	0.0000	0.0000	0.0000	0.0004	0.0185	1.0000
SG1-27 = SP1	0.0003	0.0008	0.0009	0.4600	0.0000	0.0019	0.0003	0.0000	0.0000	0.0003	0.0000	0.0000	0.0000	0.0000	0.0000	0.0004	0.0185	1.0000
SPA-18	0.0000	0.0003	0.0006	0.3554	0.0000	0.0009	0.0142	0.0001	0.0000	0.0000	0.0000	0.0000	0.0003	0.0000	0.0000	0.0099	0.0300	1.0000
SPA-32	0.0000	0.0003	0.0006	0.4227	0.0000	0.0009	0.0000	0.0001	0.0000	0.0000	0.0000	0.0000	0.0003	0.0000	0.0000	0.0200	0.0104	1.0000
SPA-38	0.0003	0.0007	0.0009	0.4601	0.0000	0.0019	0.0003	0.0000	0.0000	0.0003	0.0000	0.0000	0.0000	0.0000	0.0000	0.0004	0.0185	1.0000
minimum	0.0000	0.0000	0.0000	0.3554	0.0000	0.0000	0.0000	0.0000	0.0000	0.0000	0.0000	0.0000	0.0000	0.0000	0.0000	0.0000	0.0000	0.9787
maximum	0.0022	0.0024	0.0017	0.5278	0.0007	0.0040	0.0142	0.0008	0.0000	0.0070	0.0000	0.0550	0.0003	0.0004	0.0007	0.0200	0.0624	1.0000

Table A2. Measured Crystal Fraction in Literature Glasses (mass%)

Glass[(a)]	T (°C)	c (wt%)	Glass	T (°C)	c (wt%)	Glass	T (°C)	c (wt%)	Glass	T (°C)	c (wt%)
MS-7d	959	1.43	MS7-H-Cr	1047	1.08	MS7-L-Na	949	4.05	SP-Li-3-r	701	2.62
MS-7d	1000	1.01	MS7-H-Cr	1096	0.37	MS7-L-Na	1019	3.24	SP-Mg-1	1028	0.13
MS-7d	1045	0.65	MS7-L-Cr	730	5.17	MS7-H-Ni	808	7.58	SP-Mg-1	952	1.11
MS-7d	1011	0.99	MS7-L-Cr	860	3.44	MS7-H-Ni	812	7.56	SP-Mg-1	898	1.87
MS-7d	985	1.21	MS7-L-Cr	905	2.52	MS7-H-Ni	840	7.30	SP-Mg-1	854	2.69
MS-7d	919	1.57	MS7-L-Cr	925	2.13	MS7-H-Ni	870	7.30	SP-Mg-1	808	3.48
MS-7a	864	2.30	MS7-L-Cr	969	1.15	MS7-H-Ni	915	6.61	SP-Mg-1	717	2.91
MS-7a	893	2.19	MS7-L-Cr	1006	0.43	MS7-H-Ni	930	6.84	SP-Mn-1	1028	0.92
MS-7a	934	1.80	MS7-L-Fe	808	3.40	MS7-H-Ni	1000	5.25	SP-Mn-1	952	2.17
MS-7a	971	1.37	MS7-L-Fe	840	2.95	MS7-H-Ni	1041	4.83	SP-Mn-1	943	1.51
MS-7a	1014	0.98	MS7-L-Fe	919	1.47	MS7-H-Ni	1047	2.85	SP-Mn-1	852	2.64
MS-7a	1062	0.22	MS7-L-Fe	946	0.77	MS7-H-Ni	1060	3.25	SP-Mn-1	808	3.20
MS-7e	734	3.52	MS7-L-Fe	960	0.77	MS7-H-Ni	1133	1.07	SP-Mn-1	717	3.00
MS-7e	734	3.52	MS7-L-Fe	1000	0.32	MS7-H-Ni	1000	3.91	SP-Mn-3	1028	0.82
MS-7e	750	3.67	MS7-H-Li	705	5.63	MS7-H-Ni	915	5.29	SP-Mn-3	952	1.98
MS-7e	750	3.46	MS7-H-Li	839	3.31	MS7-H-Ni	808	6.48	SP-Mn-3	900	2.50
MS-7e	801	3.37	MS7-H-Li	905	2.47	MS7-L-Ni	750	2.55	SP-Mn-3	898	3.25
MS-7e	801	3.12	MS7-H-Li	925	1.66	MS7-L-Ni	860	1.60	SP-Mn-3	854	4.17
MS-7e	801	3.02	MS7-H-Li	942	1.89	MS7-L-Ni	919	0.84	SP-Mn-3	808	4.93
MS-7e	801	2.81	MS7-H-Li	987	1.10	MS7-L-Ni	949	0.31	SP-Mn-3	736	5.42
MS-7e	801	2.74	MS7-H-Li	1047	0.22	MS7-L-Ni	964	0.38	SP-Na-1	1125	2.31
MS-7e	801	3.36	MS7-L-Li	750	5.02	MS7-L-Ni	1006	0.24	SP-Na-1	1028	3.34
MS-7e	853	2.68	MS7-L-Li	875	3.73	MS7-Mn-0	950	1.54	SP-Na-1	952	5.41
MS-7e	853	2.15	MS7-L-Li	919	3.18	MS7-Mn-0.5	950	1.71	SP-Na-1	898	7.07
MS-7e	853	2.27	MS7-L-Li	949	3.41	MS7-Mn-1	950	1.81	SP-Na-1	808	8.57
MS-7e	853	2.90	MS7-L-Li	964	2.60	MS7-Mn-2	950	2.23	SP-Na-3	898	1.36
MS-7e	853	2.87	MS7-L-Li	1000	2.12	MS7-Mn-3	950	3.25	SP-Na-3	852	1.72
MS-7e	928	2.37	MS7-L-Li	1096	0.47	MS7-Mn-4	950	3.77	SP-Na-3	808	1.99
MS-7e	950	1.66	MS7-H-Mg	808	5.51	MS7-Mn-5	950	3.91	SP-Na-3	717	2.54
MS-7e	950	1.82	MS7-H-Mg	924	4.28	MS7-Mn-6	950	4.31	SP-Ni-3-o	1123	4.90
MS-7e	977	1.32	MS7-H-Mg	946	3.69	SP-Al-1	952	0.19	SP-Ni-3-o	1023	6.30
MS-7e	1005	0.89	MS7-H-Mg	1000	3.02	SP-Al-1	898	0.37	SP-Ni-3-o	923	6.80
MS-7e	1039	0.24	MS7-H-Mg	1060	1.70	SP-Al-1	854	0.64	SP-Ni-3-o	822	7.40
MS-7e	1052	0.42	MS7-H-Mg	1133	0.40	SP-Al-1	808	1.17	SP-Ni-3-r	1097	3.36
MS7-H-Al	730	6.15	MS7-L-Mg	808	4.10	SP-Al-1	717	1.60	SP-Ni-3-r	999	5.73
MS7-H-Al	839	5.11	MS7-L-Mg	854	3.76	SP-Cr-1-o	897	0.36	SP-Ni-3-r	949	8.01
MS7-H-Al	946	4.59	MS7-L-Mg	924	2.95	SP-Cr-1-o	848	0.75	SP-Ni-3-r	845	9.48
MS7-H-Al	987	3.13	MS7-L-Mg	997	1.99	SP-Cr-1-o	797	1.15	SP-Ni-3-r	796	9.74
MS7-H-Al	997	2.77	MS7-L-Mg	1046	0.41	SP-Cr-1-o	744	1.79	SP-Ni-3-r	745	8.31
MS7-H-Al	1040	2.20	MS7-H-Na	750	4.54	SP-Cr-1-o	701	1.61	SPA-18	875	1.93
MS7-H-Al	1092	1.14	MS7-H-Na	860	2.63	SP-Cr-1-r	897	0.56	SPA-18	900	1.34
MS7-H-Al	1118	0.71	MS7-H-Na	905	1.78	SP-Cr-1-r	848	1.18	SPA-18	926	1.15
MS7-L-Al	798	3.32	MS7-H-Na	969	0.62	SP-Cr-1-r	797	1.84	SPA-18	951	0.46
MS7-L-Al	875	1.94	MS7-L-Na	728	7.00	SP-Cr-1-r	744	2.89	SPA-32	750	1.08
MS7-L-Al	919	1.91	MS7-L-Na	860	6.40	SP-Cr-1-r	701	2.59	SPA-32	702	1.44
MS7-L-Al	964	0.76	MS7-L-Na	905	5.60	SP-Li-3-o	938	1.40	SPA-32	654	1.78
MS7-L-Al	1000	0.34	MS7-L-Na	919	5.25	SP-Li-3-o	892	1.50	SPA-32	824	0.09
MS7-H-Cr	730	5.40	MS7-L-Na	969	3.72	SP-Li-3-o	793	2.10	SPA-38	851	2.03
MS7-H-Cr	875	3.86	MS7-L-Na	1006	2.61	SP-Li-3-o	740	3.30	SPA-38	901	1.27
MS7-H-Cr	905	3.35	MS7-L-Na	1092	1.61	SP-Li-3-r	951	0.52	SPA-38	951	0.63
MS7-H-Cr	949	2.87	MS7-L-Na	1118	1.54	SP-Li-3-r	897	0.92	SPA-38	975	0.41
MS7-H-Cr	1000	2.07	MS7-L-Na	1155	0.85	SP-Li-3-r	737	2.68	SPA-38	1003	0.29

[(a)] A "-o" after the glass name represents original measurement and a "-r" represents a remeasurement.

Appendix B

Heat-treatments and Observations of Samples Tested in this Study

Appendix B: Heat-Treatments and Observations of Samples Tested in this Study

Table B1. Summary Crystallinity Data for WTP-TL-×× Glasses.

Sample ID	T,°C	t, h	c_{spinel}, wt%	c_{zircon}, wt%	$c_{hematite}$, wt%	$c_{thorianite}$, wt%	spinel cell constant, Å	optical observations
WTP-TL-01	901	24						undissolved material no crystals
WTP-TL-01	1001	24						undissolved material no crystals
WTP-TL-01	1101	24						undissolved material no crystals
WTP-TL-01	1200	24						undissolved material no crystals
WTP-TL-01	801	48						lots of undissolved material
WTP-TL-01	953	24						undissolved material no crystals
WTP-TL-01	725	72						lots of crystals (not spinel)
WTP-TL-01	1050	24						undissolved material
WTP-TL-01	1150	24						amorphous
WTP-TL-01	1129	24						amorphous
WTP-TL-01	851	48						undissolved material no crystals
WTP-TL-01	822	48						undissolved material no crystals
WTP-TL-01	765	72						undissolved material no crystals
WTP-TL-01	746	72						crystals maybe crystobalite
WTP-TL-01	755	72						crystals maybe crystobalite
WTP-TL-02	901	24						undissolved material
WTP-TL-02	1001	24						undissolved material on surface
WTP-TL-02	1101	24						undissolved material on surface
WTP-TL-02	1200	24						undissolved material
WTP-TL-02	801	48						undissolved material and surface covered
WTP-TL-02	953	24						undissolved material
WTP-TL-02	725	72						lots of crystals (not spinel)
WTP-TL-02	1050	24						undissolved material
WTP-TL-02	1150	24						undissolved material
WTP-TL-02	1156	24						amorphous
WTP-TL-02	851	48						amorphous
WTP-TL-02	822	48						undissolved material
WTP-TL-02	765	72						crystals (albite?) in glass
WTP-TL-02	783	72						amorphous
WTP-TL-02	776	72						amorphous

Sample ID	T,°C	t, h	c_{spinel}, wt%	c_{zircon}, wt%	$c_{hematite}$, wt%	$c_{thorianite}$, wt%	spinel cell constant, Å	optical observations
WTP-TL-03	901	24	2.2					crystals on surface
WTP-TL-03	1001	24	1.2					crystals on surface
WTP-TL-03	1100	24	0.6					crystals on surface
WTP-TL-03	1200	24	0					amorphous
WTP-TL-03	1150	24	0					crystals in sample
WTP-TL-03	1126	24						crystals in sample
WTP-TL-03	1140	24						few crystals
WTP-TL-03	1176	24						few crystals
WTP-TL-03	1187	24						few crystals
WTP-TL-03	1194	24						amorphous
WTP-TL-04	901	24	1.6					lots of spinel
WTP-TL-04	1001	24						crystals
WTP-TL-04	1099	24						crystals
WTP-TL-04	1196	24						amorphous
WTP-TL-04	1151	24						amorphous
WTP-TL-04	1175	24						amorphous
WTP-TL-04	1123	24						amorphous
WTP-TL-04	1111	24						few spinels
WTP-TL-05	901	24	1.2					crystals on surface
WTP-TL-05	1001	24						crystals on surface
WTP-TL-05	1101	24						crystals on surface
WTP-TL-05	1200	24						amorphous
WTP-TL-05	802	48	1.6					lots of crystals on the surface and in bulk
WTP-TL-05	1050	24	0.3					lots of crystals in sample
WTP-TL-05	1025	24	0.5					crystals in sample
WTP-TL-05	1037	24						crystals in sample
WTP-TL-05	1075	24						lots of crystals in sample
WTP-TL-05	1150	24						amorphous
WTP-TL-05	1125	24						amorphous
WTP-TL-05	1112	24						amorphous
WTP-TL-06	901	24						amorphous
WTP-TL-06	1001	24						amorphous

Sample ID	T,°C	t, h	c_{spinel}, wt%	c_{zircon}, wt%	$c_{hematite}$, wt%	$c_{thorianite}$, wt%	spinel cell constant, Å	optical observations
WTP-TL-06	800	95						crystals
WTP-TL-06	849	48						crystals
WTP-TL-06	875	72						crystals
WTP-TL-06	885	72						crystals
WTP-TL-06	896	72						crystals spinel and clinopyroxene
WTP-TL-07	901	24						crystals
WTP-TL-07	1001	24	1.1			0.2		crystals
WTP-TL-07	1099	24						crystals
WTP-TL-07	1198	24						crystals
WTP-TL-07	1300	24						amorphous
WTP-TL-07	1250	24						crystals
WTP-TL-07	1275	24						crystals
WTP-TL-07	1285	24						crystals
WTP-TL-07	1292	24						crystals
WTP-TL-08	901	24	3.3			1.8		crystals
WTP-TL-08	1000	24						crystals
WTP-TL-08	1099	24						sample lost due to leaking or pumping
WTP-TL-08	799	95						crystals
WTP-TL-08	849	48						crystals
WTP-TL-08	1100	24						amorphous
WTP-TL-08	1053	24						amorphous
WTP-TL-08	1030	24						amorphous
WTP-TL-08	1015	24						crystals
WTP-TL-08	1027	24						few spinels
WTP-TL-09	901	24						crystals (surface covered with crystals)
WTP-TL-09	1001	24	0.5			0.7		crystals
WTP-TL-09	1099	24						sample lost due to leaking or pumping
WTP-TL-09	1100	24						crystals
WTP-TL-09	1198	24						crystals
WTP-TL-09	1300	24						amorphous
WTP-TL-09	1250	24						clear cubic crystals
WTP-TL-09	1275	24						lots of clear cubic crystals settled along bottom region

Sample ID	T,°C	t, h	c_{spinel}, wt%	c_{zircon}, wt%	$c_{hematite}$, wt%	$c_{thorianite}$, wt%	spinel cell constant, Å	optical observations
WTP-TL-09	1285	24						lots of clear cubic crystals settled along bottom region
WTP-TL-09	1292	24						amorphous
WTP-TL-10	901	24						crystals
WTP-TL-10	1000	24						crystals
WTP-TL-10	1100	24						lots of spinel
WTP-TL-10	1100	24						no analysis
WTP-TL-10	1198	24						amorphous
WTP-TL-10	1151	24						lots of spinel
WTP-TL-10	1175	24						spinels
WTP-TL-10	1186	24						spinels in TS
WTP-TL-11	901	24						lots of crystals
WTP-TL-11	1000	24						lots of crystals
WTP-TL-11	1100	24						amorphous
WTP-TL-11	799	95						crystals
WTP-TL-11	849	48						crystals
WTP-TL-11	875	72						lots of spinel in TS
WTP-TL-11	885	72						crystals in TS
WTP-TL-11	1051	24						crystals in TS
WTP-TL-11	1073	24						amorphous in TS
WTP-TL-11	1067	24						crystals in TS
WTP-TL-12	901	24						crystals
WTP-TL-12	1000	24						no analysis
WTP-TL-12	1100	24						crystals
WTP-TL-12	799	95						crystals
WTP-TL-12	849	48						crystals
WTP-TL-12	1198	24						crystals
WTP-TL-12	1300	24						crystals
WTP-TL-12	1350	24						amorphous in TS
WTP-TL-12	1324	24						amorphous in TS
WTP-TL-12	1313	24						amorphous in TS
WTP-TL-13	901	24						lots of spinel in TS
WTP-TL-13	1000	24						spinel in TS

Sample ID	T,°C	t, h	c_{spinel}, wt%	c_{zircon}, wt%	$c_{hematite}$, wt%	$c_{thorianite}$, wt%	spinel cell constant, Å	optical observations
WTP-TL-13	1100	24						amorphous in TS
WTP-TL-13	799	95						crystals
WTP-TL-13	849	48						crystals
WTP-TL-13	875	72						spinel in TS
WTP-TL-13	885	72						spinel in TS
WTP-TL-13	1051	24						amorphous in TS
WTP-TL-13	1027	24						amorphous in TS
WTP-TL-13	1013	24						amorphous in TS
WTP-TL-14	901	24						crystals
WTP-TL-14	1000	24						spinel in TS
WTP-TL-14	1100	24						amorphous
WTP-TL-14	1100	24						no analysis
WTP-TL-14	1053	24						spinel and clear crystals in TS
WTP-TL-14	1075	24						spinel in TS
WTP-TL-14	1090	24						spinel in TS
WTP-TL-15	901	24						amorphous
WTP-TL-15	801	48						few crystals
WTP-TL-15	750	72						some foaming occurred, crystals in sample
WTP-TL-15	725	72						sample lost due to foaming
WTP-TL-15	776	72						few crystals
WTP-TL-15	785	72						some foaming occurred, amorphous
WTP-TL-16	894	24	8.10				8.434	crystals on surface
WTP-TL-16	1001	24	4.50				8.433	lots of surface crystals and bubbles
WTP-TL-16	1100	24	3.00				8.426	lots of surface crystals and bubbles
WTP-TL-16	1200	24	1.80					lots of surface crystals and bubbles
WTP-TL-16	1301	24	3.30				8.417	lots of surface crystals and bubbles
WTP-TL-16	1251	24	0.90				8.416	foaming occurred and lots of spinel in sample
WTP-TL-16	1275	24	0.70				8.414	foaming occurred and lots of spinel in sample
WTP-TL-16	1288	24						lots of crystals
WTP-TL-16	1295	24						lots of spinel crystals in sample
WTP-TL-16	1325	24						lots of spinel crystals in sample
WTP-TL-16	1376	24						lots of spinel crystals in sample

Sample ID	T,°C	t, h	c_{spinel}, wt%	c_{zircon}, wt%	$c_{hematite}$, wt%	$c_{thorianite}$, wt%	spinel cell constant, Å	optical observations
WTP-TL-16	1426	24						lots of spinel crystals in sample
WTP-TL-16	1450	24						foaming occurred and lots of spinel in sample
WTP-TL-17	894	24	1.1					lots of crystals
WTP-TL-17	1002	24	0.6					surface crystals
WTP-TL-17	1100	24	0.2					surface crystals, air bubbles
WTP-TL-17	1199	24	0					amorphous, air bubbles, some foaming
WTP-TL-17	802	48	2.1					crystals throughout sample
WTP-TL-17	1150	24	0					lots of crystals, some foaming
WTP-TL-17	1126	24						crystals in sample, some foaming
WTP-TL-17	1140	24	0.1					lots of crystals
WTP-TL-17	1176	24						crystals in sample
WTP-TL-17	1186	24						sample lost due to excessive foaming
WTP-TL-17	1185	24						few spinels in glass
WTP-TL-17	1194	24						amorphous
WTP-TL-18	894	24						sample lost due to foaming
WTP-TL-18	1001	24						phase separated, sample yellow-green in color
WTP-TL-18	1101	24	0.0					phase separated, pea-green color
WTP-TL-18	1200	24	0.0					phase separated, pea-green color
WTP-TL-18	802	48	0.0					crystals throughout sample
WTP-TL-18	750	72	0.2					crystals in sample, some foaming
WTP-TL-18	847	72						few spinel crystals
WTP-TL-18	856	48						amorphous
WTP-TL-18	879	48						amorphous
WTP-TL-19	894	24	1.7					surface crystals
WTP-TL-19	1002	24	0.5					surface crystals
WTP-TL-19	1100	24						surface crystals, air bubbles
WTP-TL-19	1199	24						amorphous, some foaming
WTP-TL-19	802	48						lots of surface crystals and bubbles
WTP-TL-19	1050	24	0					crystals in sample
WTP-TL-19	1150	24						few crystals
WTP-TL-19	1025	24	0.4					crystals in sample
WTP-TL-19	750	72						spinel & zircon crystals in sample

Sample ID	T,°C	t, h	c_{spinel}, wt%	c_{zircon}, wt%	$c_{hematite}$, wt%	$c_{thorianite}$, wt%	spinel cell constant, Å	optical observations
WTP-TL-19	1037	24						crystals in sample
WTP-TL-19	1065	24						one spinel in sample
WTP-TL-19	1075	24						few crystals in sample
WTP-TL-19	1176	24						amorphous
WTP-TL-19	1089	24						amorphous
WTP-TL-19	1081	24						couple of tiny spinels
WTP-TL-20	894	24	3.4	4.2				lots of crystals
WTP-TL-20	1002	24	2.2	1.8				lots of surface crystals and bubbles
WTP-TL-20	1100	24	1.4					surface crystals, air bubbles
WTP-TL-20	1199	24	0.5					crystals in sample, some foaming
WTP-TL-20	1301	24						few rounded particles, foaming occurred
WTP-TL-20	1226	24						spinel crystals
WTP-TL-20	1275	24						amorphous, some foaming
WTP-TL-20	1250	24						spinel crystals
WTP-TL-20	1262	24						amorphous
WTP-TL-20	1256	24						spinel crystals
WTP-TL-21	901	24	1.2				8.430	crystals and undissolved material on surface, bubbles throughout sample
WTP-TL-21	1002	24	0.7				8.410	lots of crystals and undissolved material on surface
WTP-TL-21	1100	24	0.4				8.407	surface crystals, air bubbles
WTP-TL-21	1199	24						amorphous, some foaming
WTP-TL-21	802	48	1.7					crystals
WTP-TL-21	1150	24	0					lots of crystals
WTP-TL-21	1126	24						crystals
WTP-TL-21	1140	24						lots of crystals
WTP-TL-21	1176	24						few crystals
WTP-TL-21	1162	24						lots of crystals
WTP-TL-21	1185	24						amorphous, some foaming
WTP-TL-22	901	24		7.3	8.3			rectangular crystals and tiny crystals
WTP-TL-22	1000	24		4.7	3.9			surface crystals, air bubbles
WTP-TL-22	1100	24		4.5	2.3			lots of crystals and bubbles
WTP-TL-22	1199	24		2.8	0			crystals and undissolved material
WTP-TL-22	1251	24						lots of crystals, zircon

Sample ID	T,°C	t, h	c_{spinel}, wt%	c_{zircon}, wt%	$c_{hematite}$, wt%	$c_{thorianite}$, wt%	spinel cell constant, Å	optical observations
WTP-TL-22	1225	24						lots of crystals (hematite?)
WTP-TL-22	1238	24						few crystals, some foaming
WTP-TL-22	1246	24						crystals (zircon, hematite?)
WTP-TL-23	901	24	2.7				8.381	crystals and bubbles
WTP-TL-23	1000	24	1				8.371	lots of crystals and bubbles
WTP-TL-23	1100	24	0.4				8.367	lots of crystals and bubbles
WTP-TL-23	1199	24	0					crystals
WTP-TL-23	1150	24						lots of crystals
WTP-TL-23	1126	24	0.3				8.367	crystals
WTP-TL-23	1140	24	0.2				8.367	lots of crystals
WTP-TL-23	1176	24	0.1					lots of crystals
WTP-TL-23	1301	24						amorphous
WTP-TL-23	1251	24						amorphous
WTP-TL-23	1225	24						amorphous
WTP-TL-23	1213	24						few spinels
WTP-TL-24	901	24	1.7					tiny crystals, air bubbles
WTP-TL-24	1000	24	0.4					lots of crystals, air bubbles
WTP-TL-24	1100	24	0					surface crystals
WTP-TL-24	1199	24	0					amorphous
WTP-TL-24	1050	24	0					few crystals
WTP-TL-24	1025	24	0.2					crystals
WTP-TL-24	1037	24						crystals
WTP-TL-24	1075	24						amorphous
WTP-TL-24	1061	24						few crystals
WTP-TL-24	1067	24						few crystals
WTP-TL-25	901	24						crystals and air bubbles
WTP-TL-25	1000	24						surface crystals, air bubbles
WTP-TL-25	1100	24	0					surface crystals
WTP-TL-25	1199	24						lost sample do to foaming
WTP-TL-25	801	48	0					foaming occurred, tiny spinel in sample
WTP-TL-25	750	72						crystals, some foaming
WTP-TL-25	951	24						amorphous

Sample ID	T,°C	t, h	c_{spinel}, wt%	c_{zircon}, wt%	$c_{hematite}$, wt%	$c_{thorianite}$, wt%	spinel cell constant, Å	optical observations
WTP-TL-25	928	48						amorphous
WTP-TL-25	914	24						amorphous
WTP-TL-25	853	48						amorphous
WTP-TL-25	825	48						amorphous
WTP-TL-25	814	48						few spinels
WTP-TL-26	899	24	0.2					crystals, some foaming
WTP-TL-26	1000	24						surface crystals, air bubbles
WTP-TL-26	1100	24	0					surface crystals
WTP-TL-26	1199	24						lost sample do to foaming
WTP-TL-26	801	48	0.3					tiny crystals, air bubbles
WTP-TL-26	953	24						amorphous
WTP-TL-26	750	72	0.4					crystals, some foaming
WTP-TL-26	951	24						amorphous
WTP-TL-26	928	48	0					amorphous
WTP-TL-26	914	24	0.1					lots of crystals
WTP-TL-26	929	24						spinel
WTP-TL-26	975	24						amorphous
WTP-TL-26	967	24						spinel
WTP-TL-27	899	24	5.3	0.6				crystals, air bubbles
WTP-TL-27	1001	24	2.1	0.4				crystals, air bubbles
WTP-TL-27	1101	24	0.7	0				crystals on surface
WTP-TL-27	1200	24						lost sample do to foaming
WTP-TL-27	1251	24						amorphous
WTP-TL-27	1150	24						amorphous
WTP-TL-27	1125	24						lots of spinel
WTP-TL-27	1139	24						spinel
WTP-TL-28	899	24	1.6	1.7				crystals, air bubbles
WTP-TL-28	1001	24	1.3	0				crystals, air bubbles
WTP-TL-28	1101	24						crystals, air bubbles
WTP-TL-28	1200	24	0					amorphous
WTP-TL-28	1050	24	0					few crystals
WTP-TL-28	1150	24						few crystals, some foaming

Sample ID	T,°C	t, h	c_{spinel}, wt%	c_{zircon}, wt%	$c_{hematite}$, wt%	$c_{thorianite}$, wt%	spinel cell constant, Å	optical observations
WTP-TL-28	1025	24						crystals
WTP-TL-28	1037	24						few crystals
WTP-TL-28	1075	24						amorphous
WTP-TL-28	1061	24						few crystals
WTP-TL-28	1067	24						amorphous
WTP-TL-29	899	24	2.7	0.2				surface crystals, air bubbles
WTP-TL-29	1001	24	1.5					surface crystals, air bubbles
WTP-TL-29	1101	24	0.9					crystals, air bubbles
WTP-TL-29	1200	24	0.6					crystals
WTP-TL-29	1251	24						few crystals
WTP-TL-29	1275	24						amorphous
WTP-TL-29	1262	24						amorphous
WTP-TL-29	1256	24						amorphous
WTP-TL-30	899	24	1.8	2				crystals, air bubbles
WTP-TL-30	1001	24	1.2	0.7				crystals, air bubbles
WTP-TL-30	1101	24	0.8					crystals, air bubbles
WTP-TL-30	1200	24	0.3					crystals
WTP-TL-30	1251	24						crystals
WTP-TL-30	1225	24						crystals
WTP-TL-30	1238	24						few crystals
WTP-TL-30	1249	24						lots of tiny spinel
WTP-TL-30	1275	24						amorphous
WTP-TL-30	1263	24						amorphous
WTP-TL-31	899	24						surface crystals, air bubbles
WTP-TL-31	1002	24	0.7					surface crystals, air bubbles
WTP-TL-31	1100	24	0					surface crystals, air bubbles
WTP-TL-31	1199	24	0					amorphous
WTP-TL-31	1150	24						amorphous
WTP-TL-31	1125	24						amorphous
WTP-TL-31	1112	24						few spinel

Appendix C

Model Fitting Results for TL Data

Appendix C: Model Fitting Results TL Data

Table C.1: Summary of Fitting Results for DWPFM

	Data Grouping				
DWPFM (1/T(K))	1	2	3	4	5
n	128	128	127	129	128
R2	0.694621	0.668112	0.614229	0.636914	0.626722
R2 Adj	0.687233	0.660083	0.60482	0.6282	0.617692
RMSE	0.000031	0.00003	0.000033	0.000033	0.000034
SSEPRESS	1.36E-07	1.29E-07	1.56E-07	1.54E-07	1.62E-07
Corrected TSS	3.79E-07	3.42E-07	3.49E-07	3.73E-07	3.76E-07
R2 PRESS	0.642616	0.6233964	0.553024	0.587747	0.569897
Sig. Lack of Fit (p-value)	0.0001	0.0001	0.0001	0.0001	0.0001
Number of Parameters	4				
Intercept	-0.00076	0.000645	-0.00069	-0.00071	-0.0008
ln(SM2/(SM2+SM1+SMT+Ne1+NeT)	-0.00018	-0.000151	-0.00017	-0.00016	-0.00018
ln(SM1/(SM2+SM1+SMT+Ne1+NeT)	-0.00036	-0.000368	-0.00036	-0.00037	-0.00038
ln(SMT/(SM2+SM1+SMT+Ne1+NeT)	-0.00016	-0.000083	-0.00012	-0.00012	-0.00014

Table C.2: Summary of Fitting Results for IPM

	Data Grouping				
IPM (T°C)	1	2	3	4	5
n	128	128	127	129	128
R2	0.862782	0.844152	0.872663	0.866791	0.867595
R2 Adj	0.855978	0.836424	0.866296	0.86024	0.861029
RMSE	35.83183	36.69189	33.3455	35.09126	35.11738
SSEPRESS	186189.6	198341.2	159815.1	175101.2	180256.9
Corrected TSS	1132174	1045260	1047855	1127779	1127000
R2 PRESS	0.835547	0.810247	0.847484	0.844738	0.840056
Sig. Lack of Fit (p-value)	0.0001	0.0001	0.0004	0.0001	0.0001
Number of Parameters	7				
IPM (Cr moles)	45752.42	46236.33	37323.67	42830.89	40952.8
IPM (Mn moles)	1812.102	1835.027	2190.883	1347.005	2218.839
IPM (Ni moles)	13608.58	13591.32	12649.57	13957.52	13367.96
IPM (alkali moles) int	-1665.18	-1519.31	-1424.57	-1362.59	-1487.68
IPM (alkali moles) slp	1591.221	1481.791	1439.688	1224.457	1371.164
IPM (nonalkali moles) int	5203.741	5072.646	5237.886	5020.14	5183.371
IPM (nonalkali moles) slp	-403.407	-391.577	-410.499	-378.753	-398.364

Table C.3: Summary of Fitting Results for SPM w Cr and Ni

	Data Grouping				
SPM w Cr and Ni (1000/T(K))	1	2	3	4	5
n	121	122	119	124	122
R2	0.256402	0.243088	0.169083	0.182425	0.199013
R2 Adj	0.250153	0.23678	0.161981	0.175723	0.192338
RMSE	0.044325	0.044412	0.044604	0.045534	0.046734
SSEPRESS	2.45E-01	2.50E-01	2.43E-01	2.64E-01	2.74E-01
Corrected TSS	3.14E-01	3.13E-01	2.80E-01	3.09E-01	3.27E-01
R2 PRESS	0.219293	0.200345	0.131551	0.146074	0.162492
Sig. Lack of Fit (p-value)	0.3275	0.4696	0.864	0.0015	0.69
Number of Parameters	2				
Intercept	0.703963	0.70106	0.71038	0.71223	0.709768
ln(Cr2O3 * NiO in wt%'s)	-0.02146	-0.02489	-0.01921	-0.01813	-0.01927

Table C.4: Summary of Fitting Results for SPM w Ni and Fe

	Data Grouping				
SPM w Ni and Fe (1000/T(K))	1	2	3	4	5
n	126	126	124	127	125
R2	0.179056	0.217828	0.141014	0.155083	0.218268
R2 Adj	0.172435	0.21152	0.133974	0.148324	0.211912
RMSE	0.047281	0.045964	0.046215	0.047208	0.045815
SSEPRESS	2.89E-01	2.73E-01	2.43E-01	2.90E-01	2.69E-01
Corrected TSS	3.38E-01	3.35E-01	3.03E-01	3.30E-01	3.30E-01
R2 PRESS	0.144926	0.18612	0.197998	0.121856	0.186006
Sig. Lack of Fit (p-value)	0.0069	0.0007	0.077	0.0002	0.69
Number of Parameters	2				
Intercept	0.803947	0.815715	0.799836	0.801032	0.808331
ln(NiO * Fe2O3 in wt%'s)	-0.02834	-0.03384	-0.02601	-0.02674	-0.03154

Table C.5: Summary of Fitting Results for SLM

	Data Grouping				
SLM (1/T(K))	1	2	3	4	5
n	128	128	127	129	128
R2	0.882076	0.889933	0.878898	0.887127	0.882776
R2 Adj	0.863851	0.872922	0.86001	0.86984	0.864659
RMSE	0.00002	0.000018	0.00002	0.000019	0.00002
SSEPRESS	9.23E-08	6.70E-08	7.57E-08	8.68E-08	8.47E-08
Corrected TSS	3.79E-07	3.42E-07	3.49E-07	3.73E-07	3.76E-07
R2 PRESS	0.7566431	0.8039869	0.7833372	0.7671487	0.7749269
Sig. Lack of Fit (p-value)	0.0001	0.0001	0.0005	0.0001	0.0002
Number of Parameters	18				
Intercept	5.39E-04	5.09E-04	6.93E-04	6.34E-04	5.76E-04
SPL	-1.22E-02	-1.09E-02	-8.47E-03	-3.55E-03	-1.22E-02
Al2O3 wt%	-8.00E-06	-7.00E-06	-1.00E-05	-9.00E-06	-9.00E-06
B2O3wt%	6.10E-06	4.90E-06	5.60E-06	4.30E-06	6.40E-06
CaO wt%	1.30E-06	1.20E-06	2.51E-07	3.45E-07	-2.56E-07
Cr2O3 wt%	-9.90E-05	-1.70E-04	-9.90E-05	-1.25E-04	-1.12E-04
Fe2O3 wt%	-8.00E-06	-9.00E-06	-9.00E-06	-9.00E-06	-9.00E-06
K2O wt%	1.35E-05	1.82E-05	1.43E-05	1.42E-05	1.41E-05
Li2O wt%	2.11E-05	1.86E-05	1.78E-05	2.29E-05	2.39E-05
MgO wt%	-8.00E-06	-1.00E-05	-9.00E-06	-9.00E-06	-1.00E-05
MnO2 wt%	-2.00E-06	-3.00E-06	-5.00E-06	-3.00E-06	-5.00E-06
Na2O wt%	1.38E-05	1.32E-05	1.11E-05	1.26E-05	1.36E-05
NiO wt%	-4.60E-05	-4.40E-05	-3.90E-05	-4.90E-05	-4.20E-05
SiO2 wt%	2.80E-06	4.00E-06	1.10E-06	1.70E-06	2.20E-06
TiO2 wt%	2.43E-05	2.13E-05	1.50E-06	7.20E-06	6.10E-06
UO2 wt%	-6.00E-06	-3.00E-06	-6.00E-06	-4.00E-06	-4.00E-06
ZnO wt%	-4.00E-06	2.30E-06	-9.00E-06	-4.00E-06	4.50E-06
ZrO2 wt%	-6.00E-06	-9.26E-07	-6.00E-06	-5.00E-06	-6.00E-06

Table C.6: Summary of Fitting Results for LMM

	Data Grouping				
LMM (T_L °C)	1	2	3	4	5
N	128	128	127	129	128
R2	0.902005	0.887993	0.89597	0.893795	0.907659
R2 Adj	0.88788	0.871848	0.880838	0.878623	0.894348
RMSE	31.61525	32.4768	31.47994	32.70204	30.61951
SSEPRESS	204958.3	215186	179970.6	200828.6	183033.4
Corrected TSS	1132174	1045260	1047855	1127779	1127000
R2 PRESS	0.818969	0.794132	0.828249	0.821926	0.837592
Sig. Lack of Fit (p-value)	0.0001	0.0001	0.001	0.0001	0.0007
Number of Parameters	17	17	17	17	17
Al2O2 n	2932.86	2677.97	2870.61	2687.24	2997.92
B2O3 n	817.11	775.23	644.07	840.54	662.70
CdO n	7840.80	5497.21	6680.19	5124.10	5913.10
Cr2O3 n	25829.58	30968.54	24870.14	25591.05	26246.94
F n	4882.64	5477.21	5342.19	3726.33	7155.36
Fe2O3 n	2818.90	2748.15	2684.89	2814.91	2827.79
K2O n	-1233.54	-1646.16	-1189.62	-997.05	-1102.70
Li2O n	-1846.95	-1733.49	-1758.15	-2318.60	-2317.73
MgO n	2243.98	2402.66	1991.44	2248.83	2363.91
MnO n	1538.35	1811.44	2068.60	1723.92	1999.77
Na2O n	-911.09	-754.36	-814.81	-858.72	-871.77
NiO n	9721.27	9522.29	8690.03	9732.16	8710.27
P2O5 n	-6203.04	-3443.08	-3781.53	-2308.18	-4710.89
SiO2 n	821.57	845.80	878.78	894.02	874.05
ThO2 n	1638.68	2443.08	658.58	2262.80	1870.63
U3O8 n	2541.06	2105.10	2283.11	1947.82	2352.97
ZrO2 n	2241.06	1800.35	2113.57	2140.79	2120.53

Table C.7: Summary of Fitting Results Generated for Data Grouping 1

	DWPFM	IPM	SPM w Cr&Ni	SPM w Ni&Fe	SLM	LMM
Model Response (Y)	1/T°K	T°C	1000/T°K	1000/T°K	1/T°K	T°C
Total Number of Obs	160	160	160	160	160	160
n + m	160	160	152	157	160	160
Obs for which model not defined	0	0	8	3	0	0
p	4	7	2	2	18	19
n	128	128	121	126	128	128
R2	0.695	0.863	0.256	0.179	0.882	0.902
R2 Adj	0.687	0.856	0.250	0.172	0.864	0.888
RMSE	3.100E-05	3.583E+01	4.433E-02	4.728E-02	2.000E-05	3.162E+01
SSEPRESS	1.356E-07	1.862E+05	2.455E-01	2.887E-01	9.233E-08	2.050E+05
Corrected TSS	3.794E-07	1.132E+06	3.144E-01	3.377E-01	3.794E-07	1.132E+06
R2 PRESS	0.643	0.836	0.219	0.145	0.757	0.819
Sig. Lack of Fit (p-value)	0.0001	0.0001	0.3275	0.0069	0.0001	0.0001
Based Upon °C and Model Data						
R2	0.709	0.863	0.253	0.154	0.885	0.902
RMSE	51.5	35.8	78.6	84.4	34.5	31.9
SSE	329032	155354	734362	883219	130728	110947
Corrected TSS	1132174	1132174	983570	1043447	1132174	1132174
Avg Prediction Uncertainty at 95%	119.2	72.8	179.5	191.7	80.9	66.6
# Successfully Predicted by Model	118	122	113	119	123	125
% Successfully Predicted	92.2%	95.3%	93.4%	94.4%	96.1%	97.7%
Based Upon °C and Valid. Data						
m	32	32	31	31	32	32
R2 val	0.307	0.833	0.006	0.186	0.775	0.789
ROOT Avg Prediction Error Sum of Squares val	71.7	35.2	84.7	76.7	40.9	39.6
Prediction Error Sum of Squares val	164693	39655	222403	182193	53471	50214
Corrected Total Sum of Squares	237666	237666	223769	223769	237666	237666
Avg Prediction Uncertainty at 95%	119.8	72.9	180.9	191.8	85.4	69.0
# Successfully Predicted by Model	29	30	28	28	31	31
% Successfully Predicted	90.6%	93.8%	90.3%	90.3%	96.9%	96.9%
Uncertainty Weighted, Prediction Error Sum of Squares						
Total Raw Score	19165719	2957891	40403648	34720459	6213633	3881479
Avg Raw Score	598929	92434	1303343	1120015	194176	121296
Scaled Score	6.480	1.000	14.100	12.117	2.101	1.312

Table C.8: Summary of Fitting Results Generated for Data Grouping 2

	DWPFM	IPM	SPM w Cr&Ni	SPM w Ni&Fe	SLM	LMM
Model Response (Y)	1/T°K	T°C	1000/T°K	1000/T°K	1/T°K	T°C
Total Number of Obs	160	160	160	160	160	160
n + m	160	160	152	157	160	160
Obs for which model not defined	0	0	8	3	0	0
p	4	7	2	2	18	19
n	128	128	122	126	128	128
R2	0.668	0.844	0.243	0.218	0.890	0.888
R2 Adj	0.660	0.836	0.237	0.212	0.873	0.872
RMSE	3.000E-05	3.669E+01	4.441E-02	4.596E-02	1.800E-05	3.248E+01
SSEPRESS	1.287E-07	1.983E+05	2.501E-01	2.726E-01	6.699E-08	2.152E+05
Corrected TSS	3.418E-07	1.045E+06	3.127E-01	3.349E-01	3.418E-07	1.045E+06
R2 PRESS	0.623	0.810	0.200	0.186	0.804	0.794
Sig. Lack of Fit (p-value)	0.0001	0.0001	0.4696	0.0007	0.0001	0.0001
Based Upon °C and Model Data						
R2	0.664	0.844	0.232	0.186	0.887	0.888
RMSE	53.2	36.7	78.7	81.9	32.7	32.8
SSE	351252	162902	742679	832142	117667	117176
Corrected TSS	1045260	1045260	966633	1022810	1045260	1045260
Avg Prediction Uncertainty at 95%	118.1	74.6	179.2	185.3	73.9	68.4
# Successfully Predicted by Model	121	120	112	116	123	125
% Successfully Predicted	94.5%	93.8%	91.8%	92.1%	96.1%	97.7%
Based Upon °C and Valid. Data						
m	32	32	30	31	32	32
R2 val	0.510	0.903	0.047	-0.002	0.722	0.862
ROOT Avg Prediction Error Sum of Squares val	70.4	31.4	87.7	89.3	53.1	37.3
Prediction Error Sum of Squares val	158740	31531	230494	247309	90115	44579
Corrected Total Sum of Squares	324167	324167	241838	246822	324167	324167
Avg Prediction Uncertainty at 95%	117.1	75.1	175.3	182.9	78.6	69.7
# Successfully Predicted by Model	28	32	27	30	28	30
% Successfully Predicted	87.5%	100.0%	90.0%	96.8%	87.5%	93.8%
Uncertainty Weighted, Prediction Error Sum of Squares						
Total Raw Score	18833941	2376824	39464674	44462485	9757205	3438489
Avg Raw Score	588561	74276	1315489	1434274	304913	107453
Scaled Score	7.924	1.000	17.711	19.310	4.105	1.447

Table C.9: Summary of Fitting Results Generated for Data Grouping 3

	DWPFM	IPM	SPM w Cr&Ni	SPM w Ni&Fe	SLM	LMM
Model Response (Y)	1/T°K	T°C	1000/T°K	1000/T°K	1/T°K	T°C
Total Number of Obs	160	160	160	160	160	160
n + m	160	160	152	157	160	160
Obs for which model not defined	0	0	8	3	0	0
p	4	7	2	2	18	19
n	127	127	119	124	127	127
R2	0.614	0.873	0.169	0.141	0.879	0.896
R2 Adj	0.605	0.866	0.162	0.134	0.860	0.881
RMSE	3.300E-05	3.335E+01	4.460E-02	4.622E-02	2.000E-05	3.148E+01
SSEPRESS	1.561E-07	1.598E+05	2.433E-01	2.433E-01	7.567E-08	1.800E+05
Corrected TSS	3.492E-07	1.048E+06	2.801E-01	3.033E-01	3.492E-07	1.048E+06
R2 PRESS	0.553	0.847	0.132	0.198	0.783	0.828
Sig. Lack of Fit (p-value)	0.0001	0.0004	0.864	0.077	0.0005	0.001
Based Upon °C and Model Data						
R2	0.625	0.873	0.177	0.132	0.886	0.896
RMSE	56.5	33.3	79.1	82.0	33.2	31.8
SSE	392530	133431	732501	821010	119783	109009
Corrected TSS	1047855	1047855	889902	945433	1047855	1047855
Avg Prediction Uncertainty at 95%	130.0	67.8	180.5	186.7	78.9	66.3
# Successfully Predicted by Model	119	121	111	115	122	123
% Successfully Predicted	93.7%	95.3%	93.3%	92.7%	96.1%	96.9%
Based Upon °C and Valid. Data						
m	33	33	33	33	33	33
R2 val	0.705	0.797	0.285	0.231	0.826	0.845
ROOT Avg Prediction Error Sum of Squares val	53.6	44.5	83.6	86.6	41.2	38.9
Prediction Error Sum of Squares val	94871	65437	230379	247699	56116	49954
Corrected Total Sum of Squares	322129	322129	322129	322129	322129	322129
Avg Prediction Uncertainty at 95%	128.3	67.6	179.4	185.8	78.6	66.5
# Successfully Predicted by Model	32	30	30	32	31	31
% Successfully Predicted	97.0%	90.9%	90.9%	97.0%	93.9%	93.9%
Uncertainty Weighted, Prediction Error Sum of Squares						
Total Raw Score	12487638	4476822	41813350	45589068	4846861	3550543
Avg Raw Score	378413	135661	1267071	1381487	146875	107592
Scaled Score	3.517	1.261	11.777	12.840	1.365	1.000

Table C.10: Summary of Fitting Results Generated for Data Grouping 4

	DWPFM	IPM	SPM w Cr&Ni	SPM w Ni&Fe	SLM	LMM
Model Response (Y)	1/T°K	T°C	1000/T°K	1000/T°K	1/T°K	T°C
Total Number of Obs	160	160	160	160	160	160
n + m	160	160	152	157	160	160
Obs for which model not defined	0	0	8	3	0	0
p	4	7	2	2	18	19
n	129	129	124	127	129	129
R2	0.637	0.867	0.182	0.155	0.887	0.894
R2 Adj	0.628	0.860	0.176	0.148	0.870	0.879
RMSE	3.300E-05	3.509E+01	4.553E-02	4.721E-02	1.900E-05	3.270E+01
SSEPRESS	1.537E-07	1.751E+05	2.642E-01	2.895E-01	8.680E-08	2.008E+05
Corrected TSS	3.728E-07	1.128E+06	3.094E-01	3.297E-01	3.728E-07	1.128E+06
R2 PRESS	0.588	0.845	0.146	0.122	0.767	0.822
Sig. Lack of Fit (p-value)	0.0001	0.0001	0.0015	0.0002	0.0001	0.0001
Based Upon °C and Model Data						
R2	0.633	0.867	0.181	0.134	0.886	0.894
RMSE	57.5	35.1	81.3	84.6	34.0	33.0
SSE	413996	150230	805979	895305	128232	119775
Corrected TSS	1127779	1127779	983966	1033986	1127779	1127779
Avg Prediction Uncertainty at 95%	129.2	71.3	184.1	190.9	77.9	68.8
# Successfully Predicted by Model	122	124	117	121	125	125
% Successfully Predicted	94.6%	96.1%	94.4%	95.3%	96.9%	96.9%
Based Upon °C and Valid. Data						
m	31	31	28	30	31	31
R2 val	0.698	0.793	0.291	0.262	0.810	0.842
ROOT Avg Prediction Error Sum of Squares val	48.6	40.2	75.4	75.8	38.6	35.2
Prediction Error Sum of Squares val	73112	50084	159141	172216	46116	38350
Corrected Total Sum of Squares	242283	242283	224328	233476	242283	242283
Avg Prediction Uncertainty at 95%	128.8	71.7	185.4	191.2	80.0	69.2
# Successfully Predicted by Model	30	29	25	28	28	28
% Successfully Predicted	96.8%	93.5%	89.3%	93.3%	90.3%	90.3%
Uncertainty Weighted, Prediction Error Sum of Squares						
Total Raw Score	8621089	3771318	29291287	32094659	3751198	2899657
Avg Raw Score	278100	121655	1046117	1069822	121006	93537
Scaled Score	2.973	1.301	11.184	11.437	1.294	1.000

Table C.11: Summary of Fitting Results Generated for Data Grouping 5

	DWPFM	IPM	SPM w Cr&Ni	SPM w Ni&Fe	SLM	LMM
Model Response (Y)	1/T°K	T°C	1000/T°K	1000/T°K	1/T°K	T°C
Total Number of Obs	160	160	160	160	160	160
n + m	160	160	152	157	160	160
Obs for which model not defined	0	0	8	3	0	0
p	4	7	2	2	18	19
n	128	128	122	125	128	128
R2	0.627	0.868	0.199	0.218	0.883	0.908
R2 Adj	0.618	0.861	0.192	0.212	0.865	0.894
RMSE	3.400E-05	3.512E+01	4.673E-02	4.582E-02	2.000E-05	3.062E+01
SSEPRESS	1.618E-07	1.803E+05	2.740E-01	2.688E-01	8.466E-08	1.830E+05
Corrected TSS	3.762E-07	1.127E+06	3.272E-01	3.303E-01	3.762E-07	1.127E+06
R2 PRESS	0.570	0.840	0.162	0.186	0.775	0.838
Sig. Lack of Fit (p-value)	0.0001	0.0001	0.69	0.69	0.0002	0.0007
Based Upon °C and Model Data						
R2	0.629	0.868	0.196	0.183	0.887	0.908
RMSE	58.1	35.1	82.4	82.1	34.0	30.9
SSE	418584	149221	814841	828770	127446	104069
Corrected TSS	1127000	1127000	1013720	1013945	1127000	1127000
Avg Prediction Uncertainty at 95%	132.5	71.4	189.6	185.0	80.4	64.5
# Successfully Predicted by Model	121	123	113	117	124	124
% Successfully Predicted	94.5%	96.1%	92.6%	93.6%	96.9%	96.9%
Based Upon °C and Valid. Data						
m	32	32	30	32	32	32
R2 val	0.734	0.809	0.245	0.021	0.804	0.785
ROOT Avg Prediction Error Sum of Squares val	44.9	38.1	69.9	86.2	38.6	40.4
Prediction Error Sum of Squares val	64603	46406	146608	237849	47663	52318
Corrected Total Sum of Squares	243064	243064	194287	243064	243064	243064
Avg Prediction Uncertainty at 95%	134.3	71.3	191.9	188.0	79.6	66.1
# Successfully Predicted by Model	31	30	29	28	30	30
% Successfully Predicted	96.9%	93.8%	96.7%	87.5%	93.8%	93.8%
Uncertainty Weighted, Prediction Error Sum of Squares						
Total Raw Score	8423936	3350304	28709301	44292165	3839368	3694798
Avg Raw Score	263248	104697	956977	1384130	119980	115462
Scaled Score	2.514	1.000	9.140	13.220	1.146	1.103

Appendix C. Model Fitting Results for TL Data

Exhibit C.1: Statistical Results from the Fitting of the DWPFM to Each Data Grouping

Groupings=1

Response 1/TL (K)
Whole Model
Actual by Predicted Plot

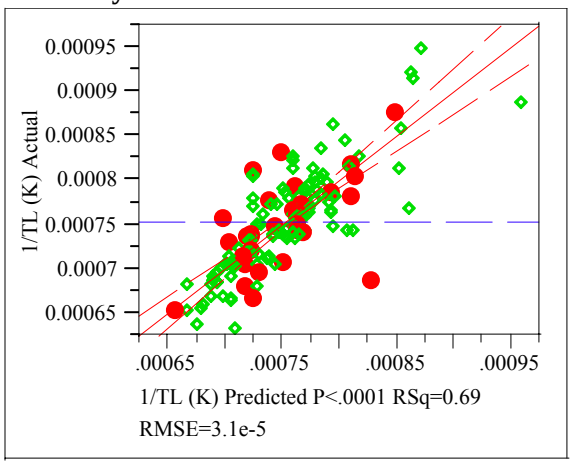

Summary of Fit

RSquare	0.694621
RSquare Adj	0.687233
Root Mean Square Error	0.000031
Mean of Response	0.000753
Observations (or Sum Wgts)	128

Analysis of Variance

Source	DF	Sum of Squares	Mean Square	F Ratio
Model	3	2.63532e-7	8.7844e-8	94.0178
Error	124	1.15858e-7	9.343e-10	Prob > F
C. Total	127	3.7939e-7		<.0001

Lack Of Fit

Source	DF	Sum of Squares	Mean Square	F Ratio
Lack Of Fit	102	1.14045e-7	1.1181e-9	13.5715
Pure Error	22	1.81247e-9	8.239e-11	Prob > F
Total Error	124	1.15858e-7		<.0001
				Max RSq
				0.9952

Parameter Estimates

Term	Estimate	Std Error	t Ratio	Prob>|t|
Intercept	-0.00076	0.000099	-7.68	<.0001
log(SM2/ (SM2+SM1+SMT+Ne1+NeT))	-0.000178	0.000019	-9.55	<.0001
log(SM1/ (SM2+SM1+SMT+Ne1+NeT))	-0.000361	0.000026	-14.03	<.0001
log(SMT/ (SM2+SM1+SMT+Ne1+NeT))	-0.000159	0.000017	-9.14	<.0001

Effect Tests

Source	Nparm	DF	Sum of Squares	F Ratio	Prob > F
log(SM2/ (SM2+SM1+SMT+Ne1+NeT))	1	1	8.52729e-8	91.2659	<.0001
log(SM1/ (SM2+SM1+SMT+Ne1+NeT))	1	1	1.83797e-7	196.7146	<.0001
log(SMT/ (SM2+SM1+SMT+Ne1+NeT))	1	1	7.80338e-8	83.5181	<.0001

Appendix C. Model Fitting Results for TL Data

Exhibit C.1: Statistical Results from the Fitting of the DWPFM to Each Data Grouping

Residual by Predicted Plot

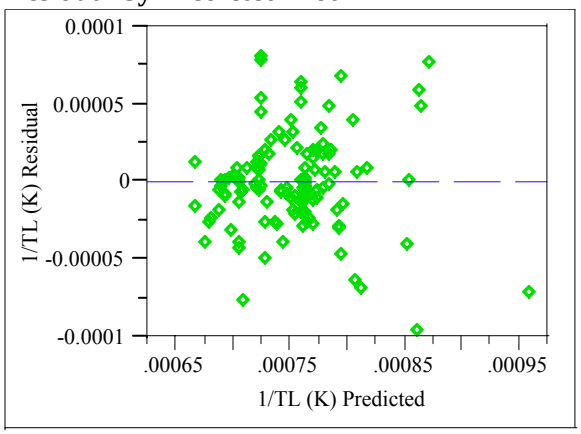

Press
1.3448805e-7

log(SM1/ (SM2+SM1+SMT+Ne1+NeT)) Leverage Plot

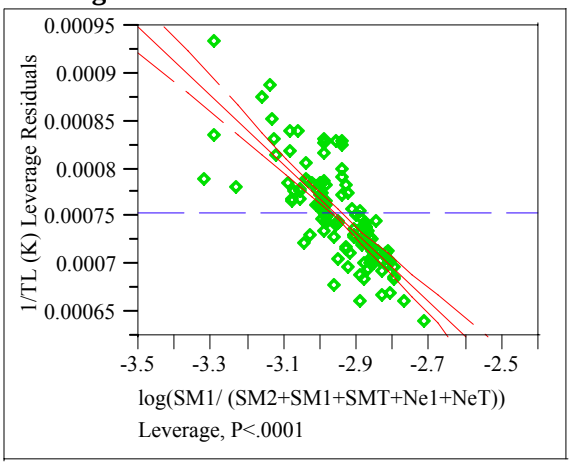

log(SM2/ (SM2+SM1+SMT+Ne1+NeT)) Leverage Plot

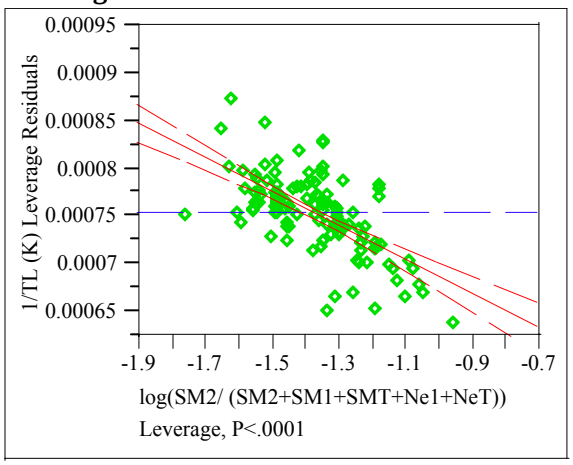

log(SMT/ (SM2+SM1+SMT+Ne1+NeT)) Leverage Plot

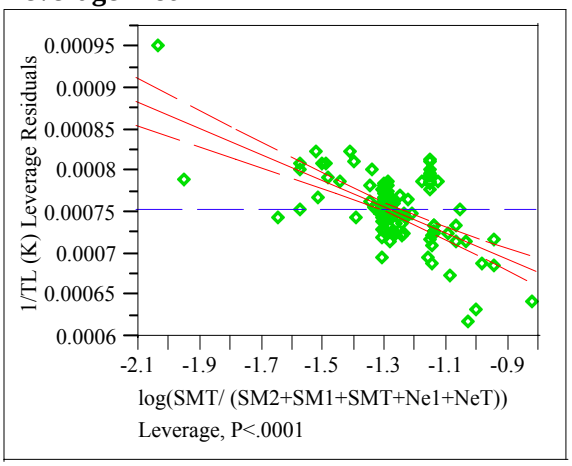

Appendix C. Model Fitting Results for TL Data

Exhibit C.1: Statistical Results from the Fitting of the DWPFM to Each Data Grouping

Groupings=2
Response 1/TL (K)
Whole Model
Actual by Predicted Plot

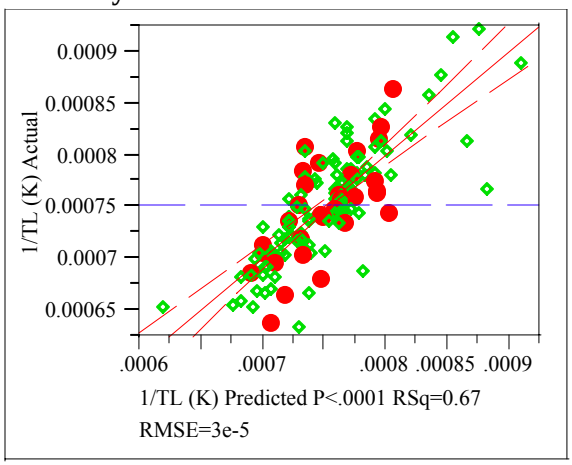

Summary of Fit

RSquare	0.668112
RSquare Adj	0.660083
Root Mean Square Error	0.00003
Mean of Response	0.000752
Observations (or Sum Wgts)	128

Analysis of Variance

Source	DF	Sum of Squares	Mean Square	F Ratio
Model	3	2.28345e-7	7.6115e-8	83.2068
Error	124	1.13431e-7	9.148e-10	Prob > F
C. Total	127	3.41777e-7		<.0001

Lack Of Fit

Source	DF	Sum of Squares	Mean Square	F Ratio
Lack Of Fit	101	1.11809e-7	1.107e-9	15.6890
Pure Error	23	1.62288e-9	7.056e-11	Prob > F
Total Error	124	1.13431e-7		<.0001
				Max RSq
				0.9953

Parameter Estimates

Term	Estimate	Std Error	t Ratio	Prob>|t|
Intercept	-0.000645	0.0001	-6.45	<.0001
log(SM2/ (SM2+SM1+SMT+Ne1+NeT))	-0.000151	0.00002	-7.58	<.0001
log(SM1/ (SM2+SM1+SMT+Ne1+NeT))	-0.000368	0.000024	-15.28	<.0001
log(SMT/ (SM2+SM1+SMT+Ne1+NeT))	-0.000083	0.000018	-4.63	<.0001

Effect Tests

Source	Nparm	DF	Sum of Squares	F Ratio	Prob > F
log(SM2/ (SM2+SM1+SMT+Ne1+NeT))	1	1	5.26216e-8	57.5244	<.0001
log(SM1/ (SM2+SM1+SMT+Ne1+NeT))	1	1	2.13702e-7	233.6123	<.0001
log(SMT/ (SM2+SM1+SMT+Ne1+NeT))	1	1	1.96191e-8	21.4470	<.0001

Appendix C. Model Fitting Results for TL Data

Exhibit C.1: Statistical Results from the Fitting of the DWPFM to Each Data Grouping

Residual by Predicted Plot

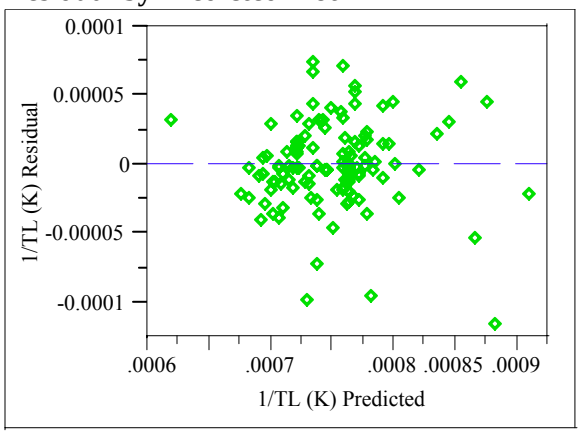

Press
1.2871444e-7

log(SM1/ (SM2+SM1+SMT+Ne1+NeT)) Leverage Plot

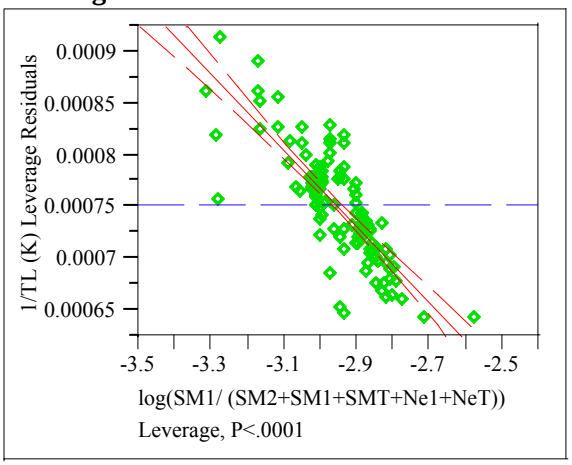

log(SM2/ (SM2+SM1+SMT+Ne1+NeT)) Leverage Plot

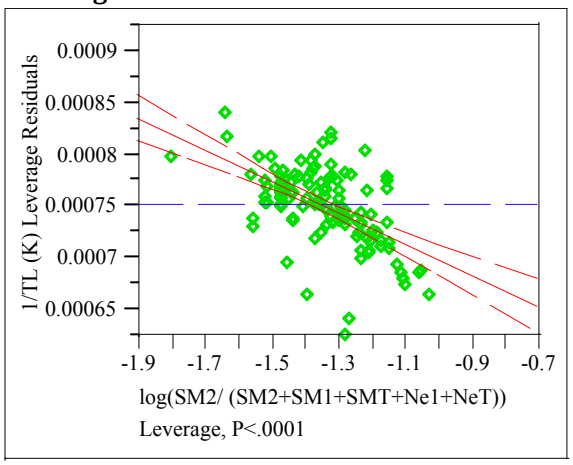

log(SMT/ (SM2+SM1+SMT+Ne1+NeT)) Leverage Plot

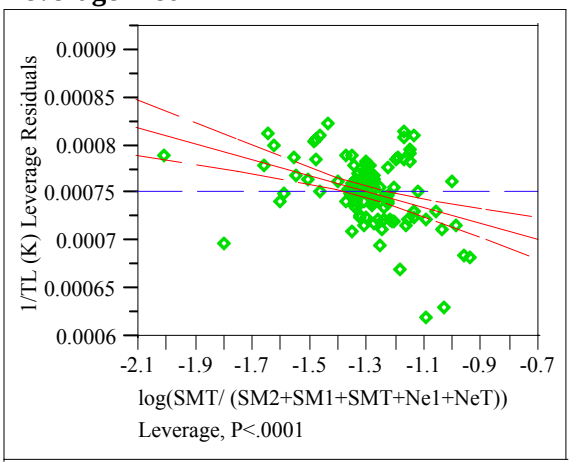

Appendix C. Model Fitting Results for TL Data

Exhibit C.1: Statistical Results from the Fitting of the DWPFM to Each Data Grouping

Groupings=3
Response 1/TL (K)
Whole Model
Actual by Predicted Plot

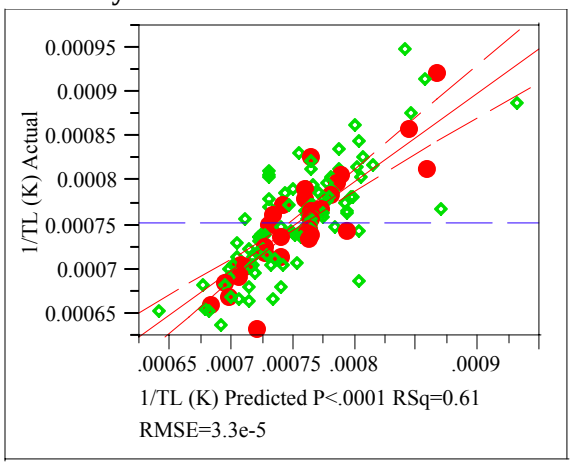

Summary of Fit

RSquare	0.614229
RSquare Adj	0.60482
Root Mean Square Error	0.000033
Mean of Response	0.000753
Observations (or Sum Wgts)	127

Analysis of Variance

Source	DF	Sum of Squares	Mean Square	F Ratio
Model	3	2.14515e-7	7.1505e-8	65.2806
Error	123	1.34728e-7	1.0953e-9	Prob > F
C. Total	126	3.49243e-7		<.0001

Lack Of Fit

Source	DF	Sum of Squares	Mean Square	F Ratio
Lack Of Fit	103	1.32451e-7	1.2859e-9	11.2937
Pure Error	20	2.27726e-9	1.139e-10	Prob > F
Total Error	123	1.34728e-7		<.0001
				Max RSq
				0.9935

Parameter Estimates

Term	Estimate	Std Error	t Ratio	Prob>|t|
Intercept	-0.000685	0.00011	-6.21	<.0001
log(SM2/ (SM2+SM1+SMT+Ne1+NeT))	-0.000166	0.000021	-7.97	<.0001
log(SM1/ (SM2+SM1+SMT+Ne1+NeT))	-0.000359	0.000028	-12.88	<.0001
log(SMT/ (SM2+SM1+SMT+Ne1+NeT))	-0.000119	0.000018	-6.70	<.0001

Effect Tests

Source	Nparm	DF	Sum of Squares	F Ratio	Prob > F
log(SM2/ (SM2+SM1+SMT+Ne1+NeT))	1	1	6.96434e-8	63.5810	<.0001
log(SM1/ (SM2+SM1+SMT+Ne1+NeT))	1	1	1.81617e-7	165.8072	<.0001
log(SMT/ (SM2+SM1+SMT+Ne1+NeT))	1	1	4.91431e-8	44.8652	<.0001

Appendix C. Model Fitting Results for TL Data

Exhibit C.1: Statistical Results from the Fitting of the DWPFM to Each Data Grouping

Residual by Predicted Plot

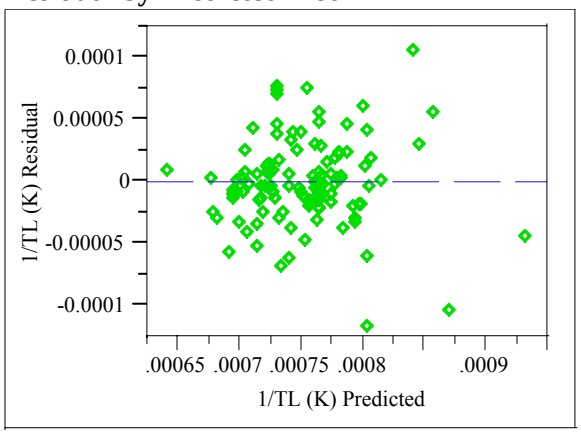

Press
1.5610312e-7

log(SM1/ (SM2+SM1+SMT+Ne1+NeT)) Leverage Plot

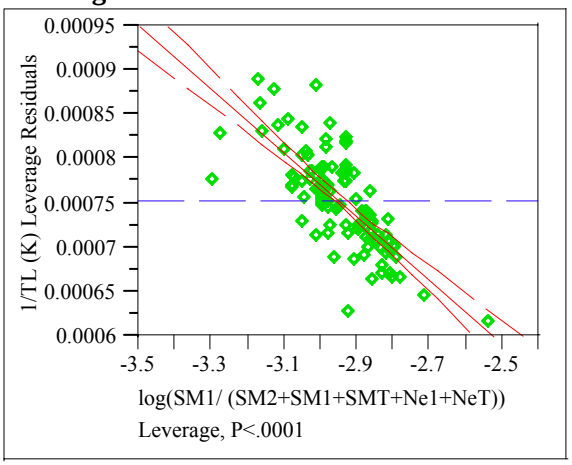

log(SM2/ (SM2+SM1+SMT+Ne1+NeT)) Leverage Plot

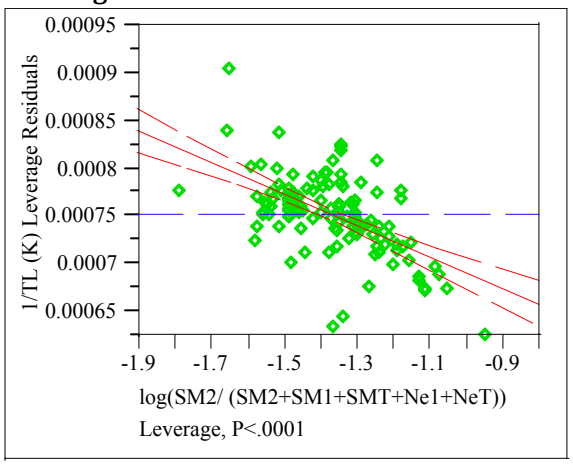

log(SMT/ (SM2+SM1+SMT+Ne1+NeT)) Leverage Plot

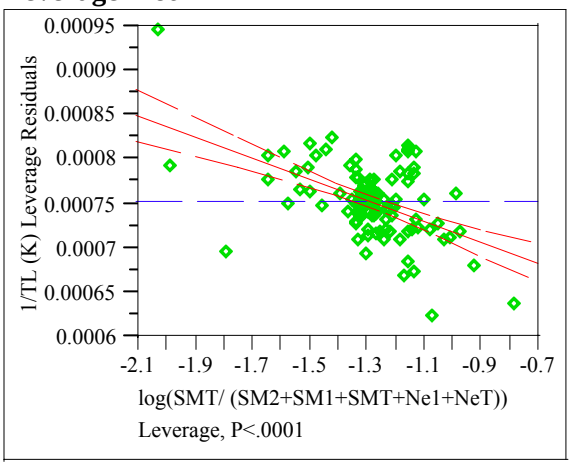

Appendix C. Model Fitting Results for TL Data

Exhibit C.1: Statistical Results from the Fitting of the DWPFM to Each Data Grouping

Groupings=4
Response 1/TL (K)
Whole Model
Actual by Predicted Plot

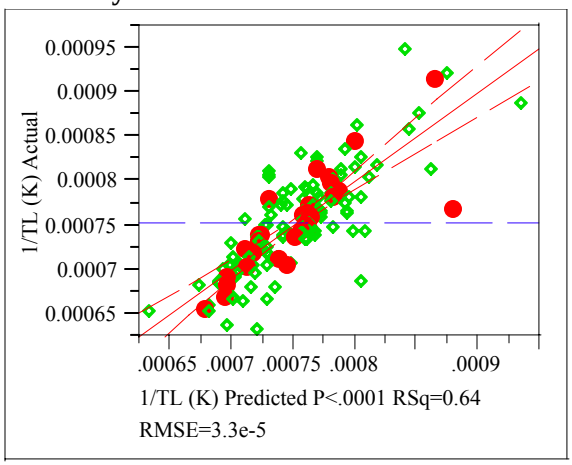

Summary of Fit

RSquare	0.636914
RSquare Adj	0.6282
Root Mean Square Error	0.000033
Mean of Response	0.000753
Observations (or Sum Wgts)	129

Analysis of Variance

Source	DF	Sum of Squares	Mean Square	F Ratio
Model	3	2.37428e-7	7.9143e-8	73.0905
Error	125	1.3535e-7	1.0828e-9	Prob > F
C. Total	128	3.72778e-7		<.0001

Lack Of Fit

Source	DF	Sum of Squares	Mean Square	F Ratio
Lack Of Fit	101	1.33429e-7	1.3211e-9	16.5013
Pure Error	24	1.92142e-9	8.006e-11	Prob > F
Total Error	125	1.3535e-7		<.0001
				Max RSq
				0.9948

Parameter Estimates

Term	Estimate	Std Error	t Ratio	Prob>|t|
Intercept	-0.000708	0.000107	-6.60	<.0001
log(SM2/ (SM2+SM1+SMT+Ne1+NeT))	-0.000157	0.000021	-7.55	<.0001
log(SM1/ (SM2+SM1+SMT+Ne1+NeT))	-0.000372	0.000027	-13.56	<.0001
log(SMT/ (SM2+SM1+SMT+Ne1+NeT))	-0.000116	0.000017	-6.70	<.0001

Effect Tests

Source	Nparm	DF	Sum of Squares	F Ratio	Prob > F
log(SM2/ (SM2+SM1+SMT+Ne1+NeT))	1	1	6.17131e-8	56.9939	<.0001
log(SM1/ (SM2+SM1+SMT+Ne1+NeT))	1	1	1.99122e-7	183.8948	<.0001
log(SMT/ (SM2+SM1+SMT+Ne1+NeT))	1	1	4.86682e-8	44.9465	<.0001

Appendix C. Model Fitting Results for TL Data

Exhibit C.1: Statistical Results from the Fitting of the DWPFM to Each Data Grouping

Residual by Predicted Plot

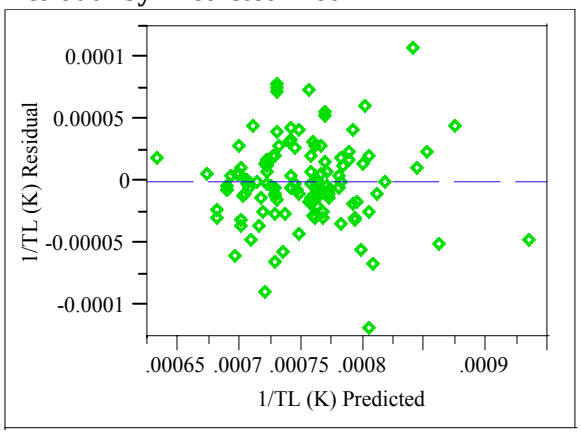

Press
1.5367886e-7

log(SM1/ (SM2+SM1+SMT+Ne1+NeT)) Leverage Plot

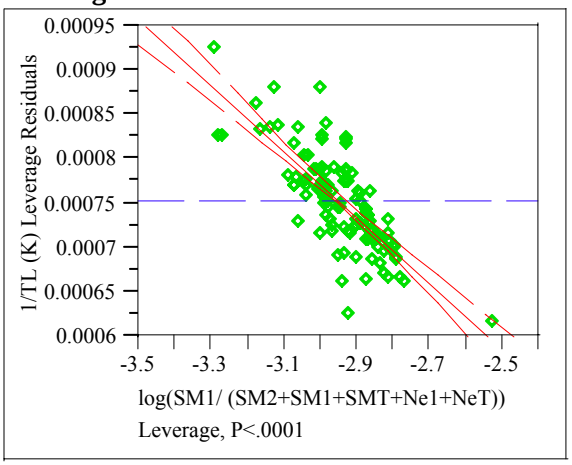

log(SM2/ (SM2+SM1+SMT+Ne1+NeT)) Leverage Plot

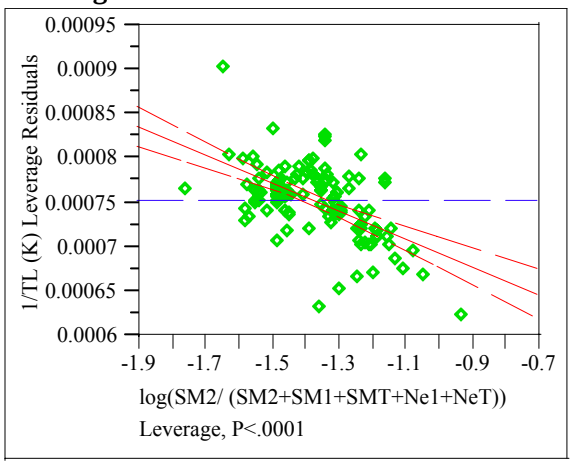

log(SMT/ (SM2+SM1+SMT+Ne1+NeT)) Leverage Plot

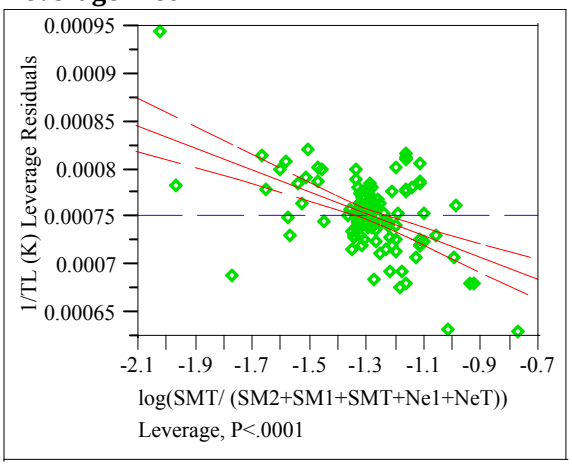

Appendix C. Model Fitting Results for TL Data

Exhibit C.1: Statistical Results from the Fitting of the DWPFM to Each Data Grouping

Groupings=5
Response 1/TL (K)
Whole Model
Actual by Predicted Plot

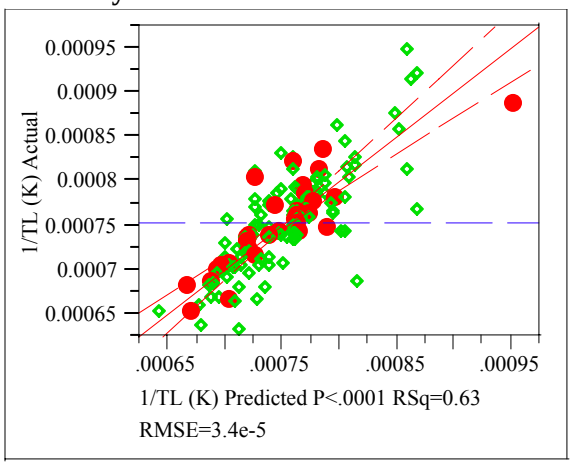

Summary of Fit

RSquare	0.626722
RSquare Adj	0.617692
Root Mean Square Error	0.000034
Mean of Response	0.000753
Observations (or Sum Wgts)	128

Analysis of Variance

Source	DF	Sum of Squares	Mean Square	F Ratio
Model	3	2.35743e-7	7.8581e-8	69.3975
Error	124	1.40409e-7	1.1323e-9	Prob > F
C. Total	127	3.76151e-7		<.0001

Lack Of Fit

Source	DF	Sum of Squares	Mean Square	F Ratio
Lack Of Fit	103	1.38186e-7	1.3416e-9	12.6738
Pure Error	21	2.22299e-9	1.059e-10	Prob > F
Total Error	124	1.40409e-7		<.0001
				Max RSq
				0.9941

Parameter Estimates

Term	Estimate	Std Error	t Ratio	Prob>|t|
Intercept	-0.000796	0.000114	-6.99	<.0001
log(SM2/ (SM2+SM1+SMT+Ne1+NeT))	-0.000183	0.000021	-8.55	<.0001
log(SM1/ (SM2+SM1+SMT+Ne1+NeT))	-0.000377	0.000028	-13.58	<.0001
log(SMT/ (SM2+SM1+SMT+Ne1+NeT))	-0.000144	0.000019	-7.51	<.0001

Effect Tests

Source	Nparm	DF	Sum of Squares	F Ratio	Prob > F
log(SM2/ (SM2+SM1+SMT+Ne1+NeT))	1	1	8.28117e-8	73.1339	<.0001
log(SM1/ (SM2+SM1+SMT+Ne1+NeT))	1	1	2.08755e-7	184.3592	<.0001
log(SMT/ (SM2+SM1+SMT+Ne1+NeT))	1	1	6.38452e-8	56.3839	<.0001

Appendix C. Model Fitting Results for TL Data

Exhibit C.1: Statistical Results from the Fitting of the DWPFM to Each Data Grouping

Residual by Predicted Plot

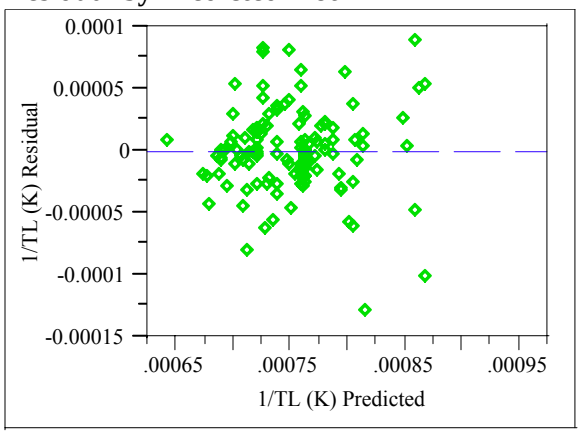

Press
1.6178359e-7

log(SM1/ (SM2+SM1+SMT+Ne1+NeT)) Leverage Plot

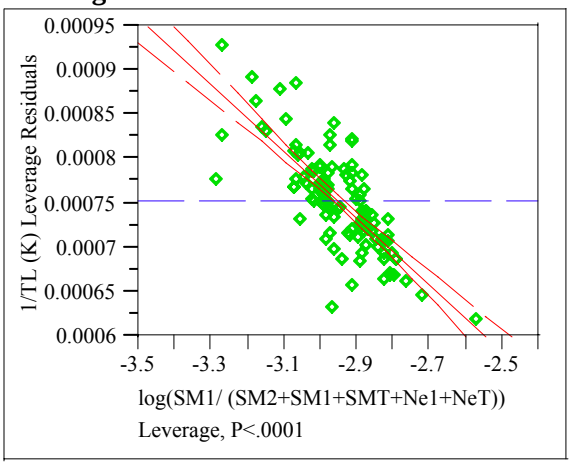

log(SM2/ (SM2+SM1+SMT+Ne1+NeT)) Leverage Plot

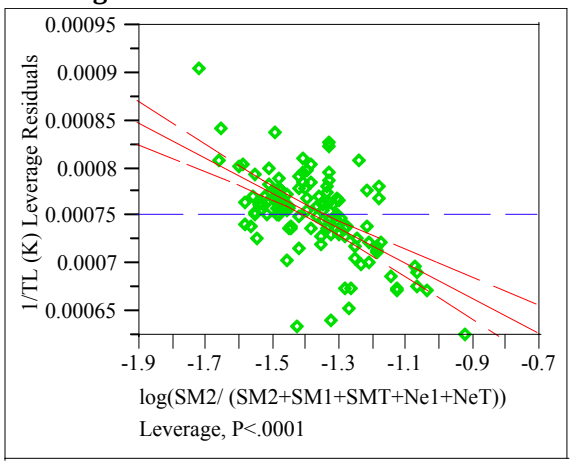

log(SMT/ (SM2+SM1+SMT+Ne1+NeT)) Leverage Plot

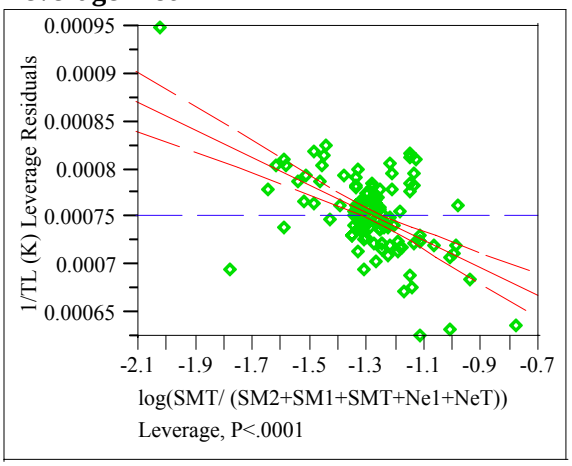

Appendix C. Model Fitting Results for TL Data

Exhibit C.2: Statistical Results from the Fitting of the IPM to Each Data Grouping

Groupings=1
Response TL (°C)
Singularity Details: Intercept = 0
Whole Model
Actual by Predicted Plot

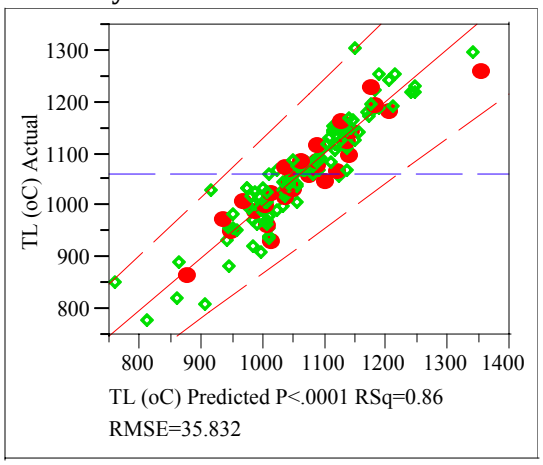

Summary of Fit

RSquare	0.862782
RSquare Adj	0.855978
Root Mean Square Error	35.83183
Mean of Response	1061.511
Observations (or Sum Wgts)	128

Analysis of Variance

Source	DF	Sum of Squares	Mean Square	F Ratio
Model	6	976819.7	162803	126.8017
Error	121	155354.4	1284	Prob > F
C. Total	127	1132174.1		<.0001

Tested against reduced model: Y=mean

Lack Of Fit

Source	DF	Sum of Squares	Mean Square	F Ratio
Lack Of Fit	99	150454.96	1519.75	6.8242
Pure Error	22	4899.40	222.70	Prob > F
Total Error	121	155354.36		<.0001
				Max RSq
				0.9957

Parameter Estimates

Term	Estimate	Std Error	t Ratio	Prob>|t|
IPM (Cr moles)	45752.422	4157.804	11.00	<.0001
IPM (Mn moles)	1812.1022	349.8156	5.18	<.0001
IPM (Ni moles)	13608.577	1026.932	13.25	<.0001
IPM (alkali moles) int	-1665.177	209.9956	-7.93	<.0001
IPM (alkali moles) slp	1591.2206	196.9564	8.08	<.0001
IPM (nonalkali moles) int	5203.7406	232.2671	22.40	<.0001
IPM (nonalkali moles) slp	-403.4072	23.80029	-16.95	<.0001

Effect Tests

Source	DF	Sum of Squares	F Ratio	Prob > F
IPM (Cr moles)	1	155467.03	121.0878	<.0001
IPM (Mn moles)	1	34452.85	26.8341	<.0001
IPM (Ni moles)	1	225465.61	175.6072	<.0001
IPM (alkali moles) int	1	80730.73	62.8783	<.0001
IPM (alkali moles) slp	1	83802.85	65.2711	<.0001
IPM (nonalkali moles) int	1	644457.21	501.9449	<.0001
IPM (nonalkali moles) slp	1	368859.19	287.2913	<.0001

Residual by Predicted Plot

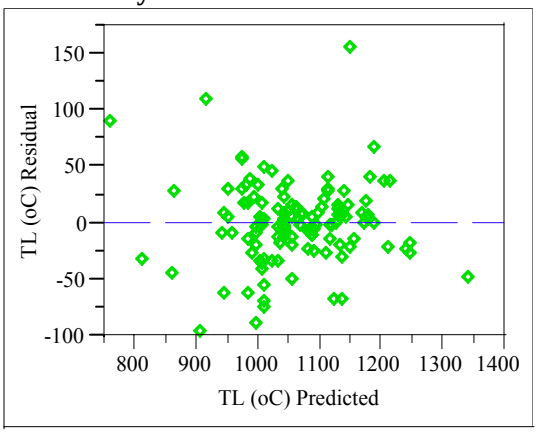

Press
186189.59068

IPM (Cr moles)
Leverage Plot

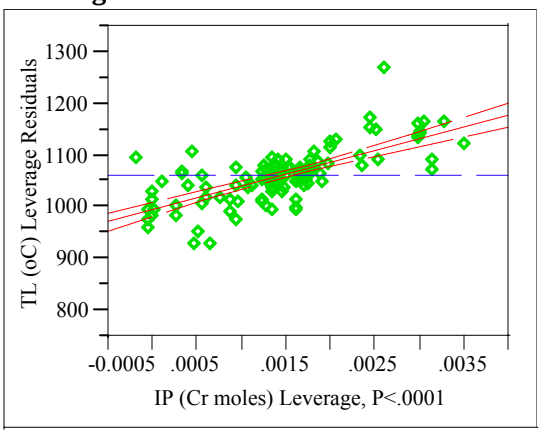

Appendix C. Model Fitting Results for TL Data

Exhibit C.2: Statistical Results from the Fitting of the IPM to Each Data Grouping

IPM (Mn moles)
Leverage Plot

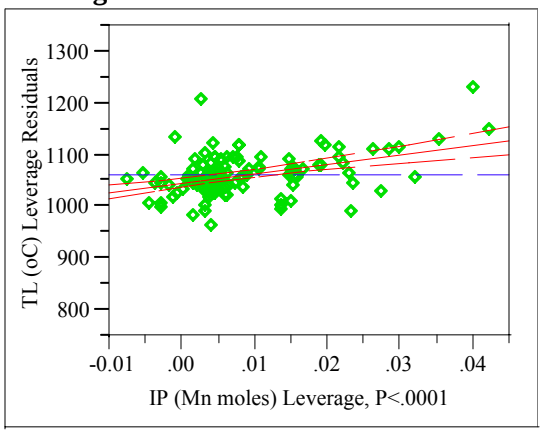

IPM (alkali moles) slp
Leverage Plot

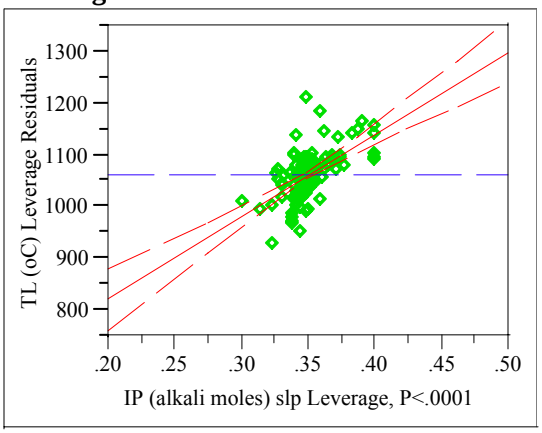

IPM (Ni moles)
Leverage Plot

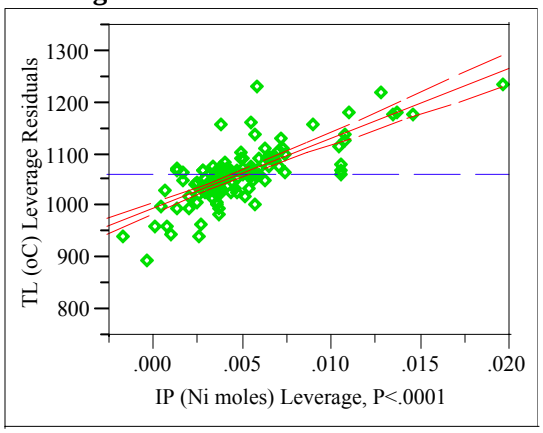

IPM (nonalkali moles) int
Leverage Plot

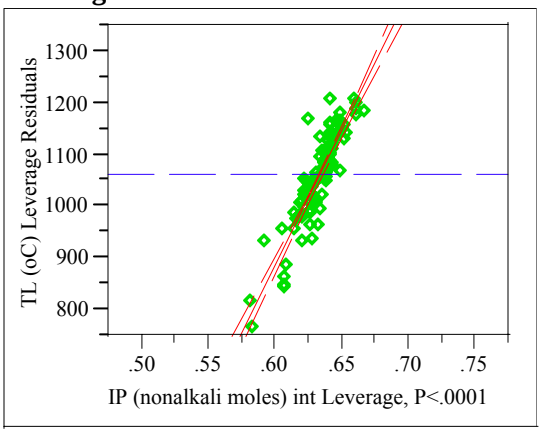

IPM (alkali moles) int
Leverage Plot

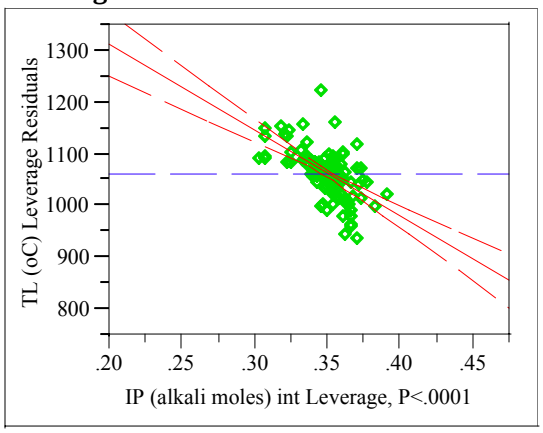

IPM (nonalkali moles) slp
Leverage Plot

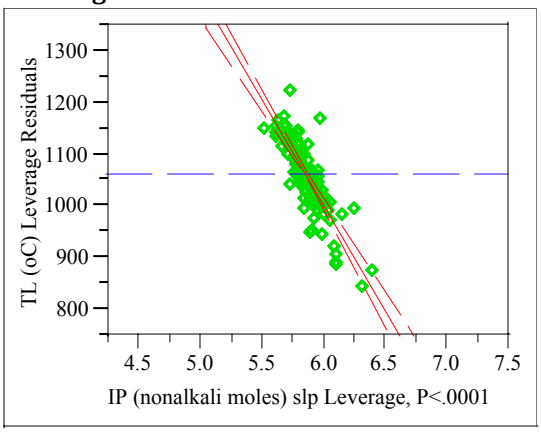

Appendix C. Model Fitting Results for TL Data

Exhibit C.2: Statistical Results from the Fitting of the IPM to Each Data Grouping

Groupings=2
Response TL (°C)
Singularity Details: Intercept = 0
Whole Model
Actual by Predicted Plot

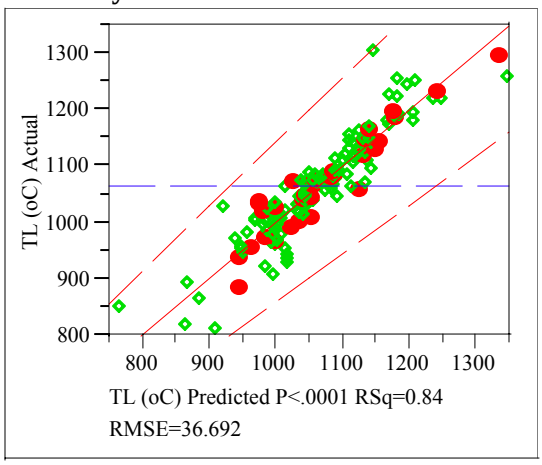

Summary of Fit

RSquare	0.844152
RSquare Adj	0.836424
Root Mean Square Error	36.69189
Mean of Response	1063.101
Observations (or Sum Wgts)	128

Analysis of Variance

Source	DF	Sum of Squares	Mean Square	F Ratio
Model	6	882358.2	147060	109.2329
Error	121	162901.7	1346	Prob > F
C. Total	127	1045259.8		<.0001

Tested against reduced model: Y=mean

Lack Of Fit

Source	DF	Sum of Squares	Mean Square	F Ratio
Lack Of Fit	98	158179.75	1614.08	7.8620
Pure Error	23	4721.94	205.30	Prob > F
Total Error	121	162901.69		<.0001
				Max RSq
				0.9955

Parameter Estimates

Term	Estimate	Std Error	t Ratio	Prob>|t|
IPM (Cr moles)	46236.325	4855.928	9.52	<.0001
IPM (Mn moles)	1835.0274	352.5853	5.20	<.0001
IPM (Ni moles)	13591.315	1113.11	12.21	<.0001
IPM (alkali moles) int	-1519.311	195.3499	-7.78	<.0001
IPM (alkali moles) slp	1481.7911	186.3251	7.95	<.0001
IPM (nonalkali moles) int	5072.6456	245.198	20.69	<.0001
IPM (nonalkali moles) slp	-391.5769	25.12418	-15.59	<.0001

Effect Tests

Source	DF	Sum of Squares	F Ratio	Prob > F
IPM (Cr moles)	1	122056.91	90.6613	<.0001
IPM (Mn moles)	1	36466.75	27.0867	<.0001
IPM (Ni moles)	1	200718.23	149.0893	<.0001
IPM (alkali moles) int	1	81434.34	60.4877	<.0001
IPM (alkali moles) slp	1	85147.46	63.2458	<.0001
IPM (nonalkali moles) int	1	576203.07	427.9917	<.0001
IPM (nonalkali moles) slp	1	327032.36	242.9129	<.0001

Residual by Predicted Plot

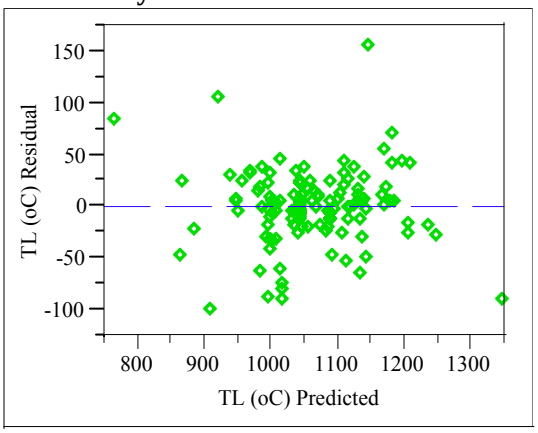

Press
198341.24792

IPM (Cr moles)
Leverage Plot

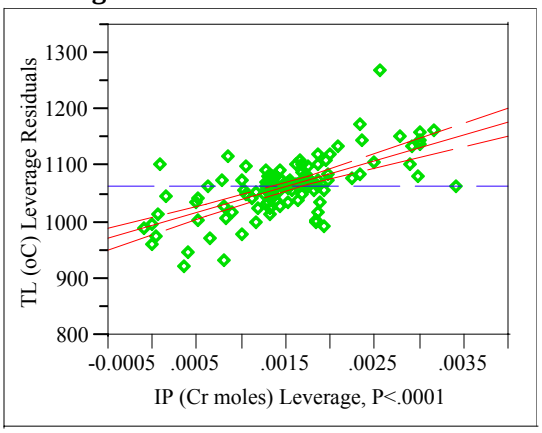

Appendix C. Model Fitting Results for TL Data

Exhibit C.2: Statistical Results from the Fitting of the IPM to Each Data Grouping

IPM (Mn moles)
Leverage Plot

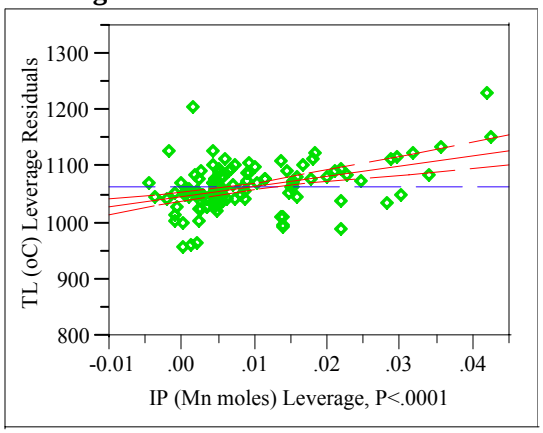

IPM (alkali moles) slp
Leverage Plot

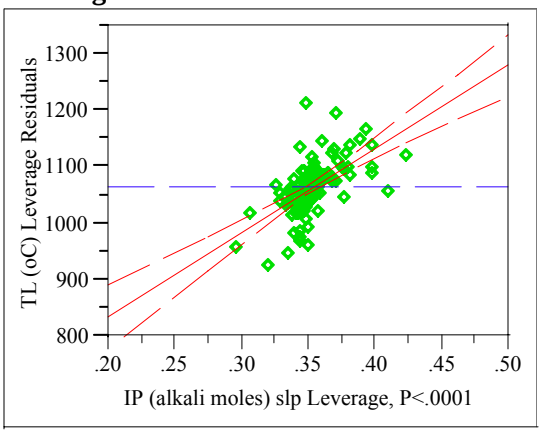

IPM (Ni moles)
Leverage Plot

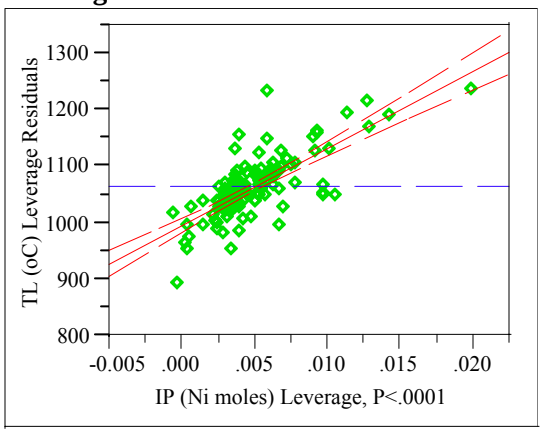

IPM (nonalkali moles) int
Leverage Plot

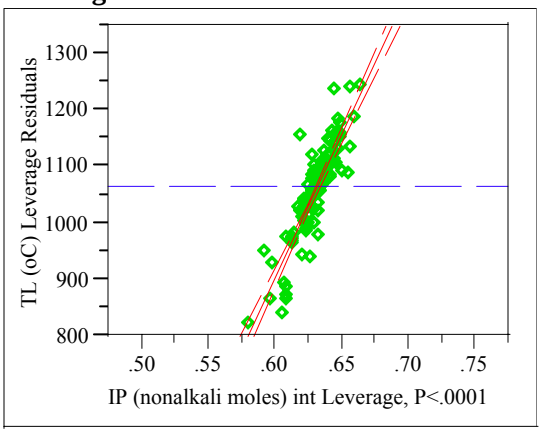

IPM (alkali moles) int
Leverage Plot

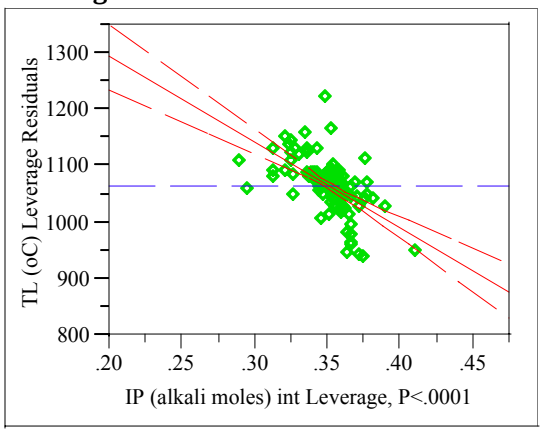

IPM (nonalkali moles) slp
Leverage Plot

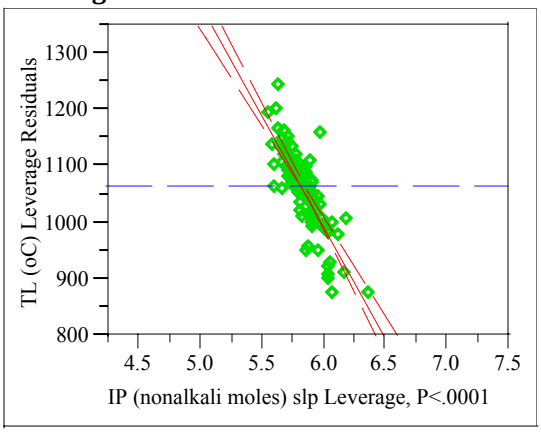

Appendix C. Model Fitting Results for TL Data

Exhibit C.2: Statistical Results from the Fitting of the IPM to Each Data Grouping

Groupings=3
Response TL (°C)
Singularity Details: Intercept = 0
Whole Model
Actual by Predicted Plot

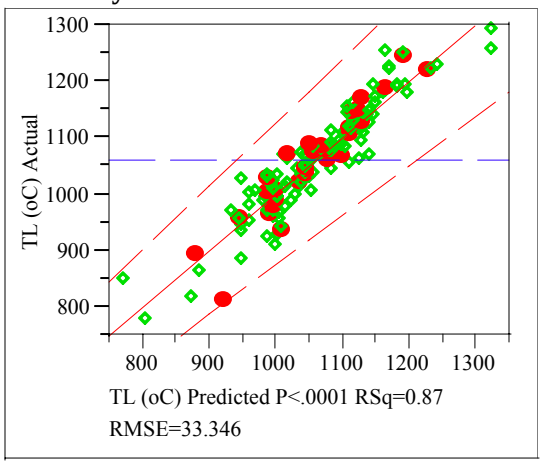

Summary of Fit

RSquare	0.872663
RSquare Adj	0.866296
Root Mean Square Error	33.3455
Mean of Response	1061.743
Observations (or Sum Wgts)	127

Analysis of Variance

Source	DF	Sum of Squares	Mean Square	F Ratio
Model	6	914424.7	152404	137.0636
Error	120	133430.7	1112	Prob > F
C. Total	126	1047855.4		<.0001

Tested against reduced model: Y=mean

Lack Of Fit

Source	DF	Sum of Squares	Mean Square	F Ratio
Lack Of Fit	100	127072.38	1270.72	3.9970
Pure Error	20	6358.31	317.92	Prob > F
Total Error	120	133430.69		0.0004
				Max RSq
				0.9939

Parameter Estimates

Term	Estimate	Std Error	t Ratio	Prob>|t|
IPM (Cr moles)	37323.674	4104.766	9.09	<.0001
IPM (Mn moles)	2190.8831	313.07	7.00	<.0001
IPM (Ni moles)	12649.571	983.6044	12.86	<.0001
IPM (alkali moles) int	-1424.565	167.0143	-8.53	<.0001
IPM (alkali moles) slp	1439.6876	156.5942	9.19	<.0001
IPM (nonalkali moles) int	5237.8862	211.6171	24.75	<.0001
IPM (nonalkali moles) slp	-410.499	21.98802	-18.67	<.0001

Effect Tests

Source	DF	Sum of Squares	F Ratio	Prob > F
IPM (Cr moles)	1	91931.93	82.6784	<.0001
IPM (Mn moles)	1	54454.02	48.9729	<.0001
IPM (Ni moles)	1	183901.44	165.3905	<.0001
IPM (alkali moles) int	1	80896.95	72.7541	<.0001
IPM (alkali moles) slp	1	93985.30	84.5251	<.0001
IPM (nonalkali moles) int	1	681216.63	612.6476	<.0001
IPM (nonalkali moles) slp	1	387549.02	348.5396	<.0001

Residual by Predicted Plot

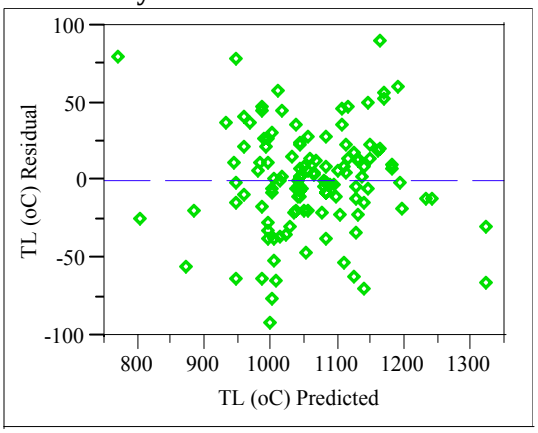

Press
159815.06594

IPM (Cr moles)
Leverage Plot

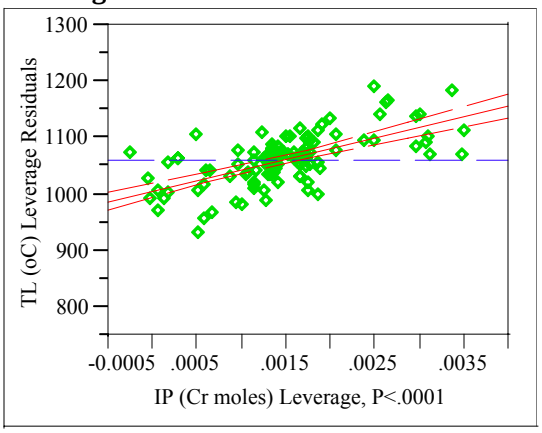

Appendix C. Model Fitting Results for TL Data

Exhibit C.2: Statistical Results from the Fitting of the IPM to Each Data Grouping

IPM (Mn moles)
Leverage Plot

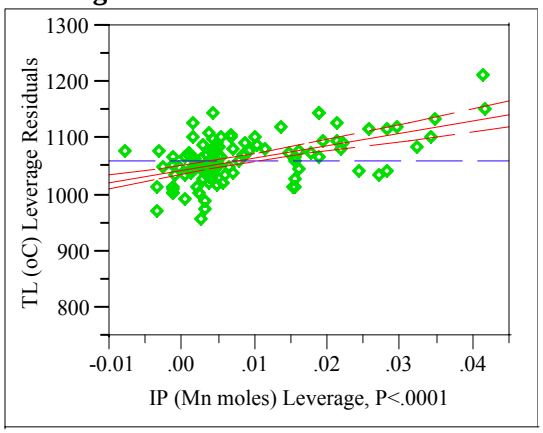

IPM (alkali moles) slp
Leverage Plot

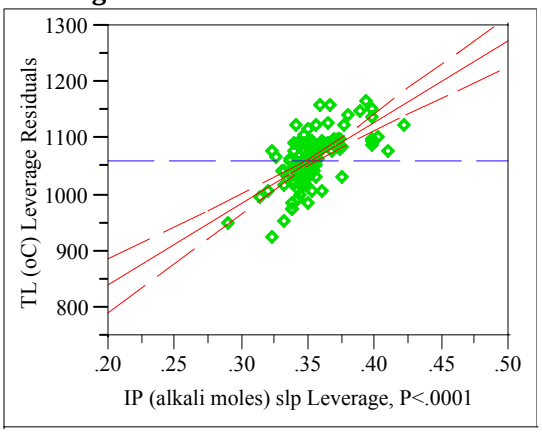

IPM (Ni moles)
Leverage Plot

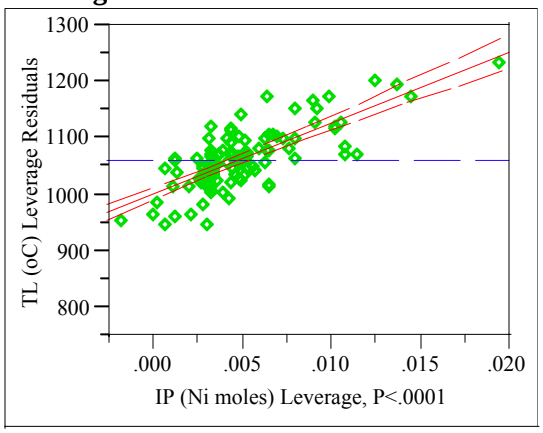

IPM (nonalkali moles) int
Leverage Plot

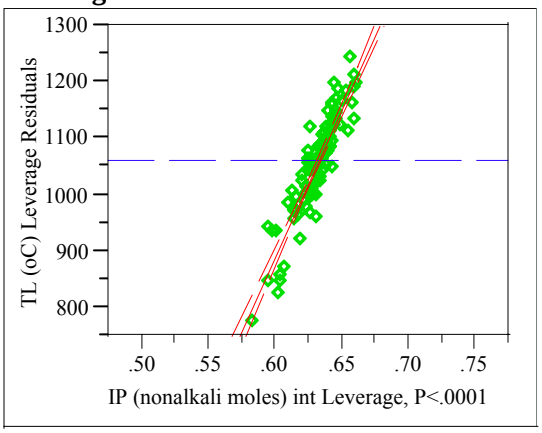

IPM (alkali moles) int
Leverage Plot

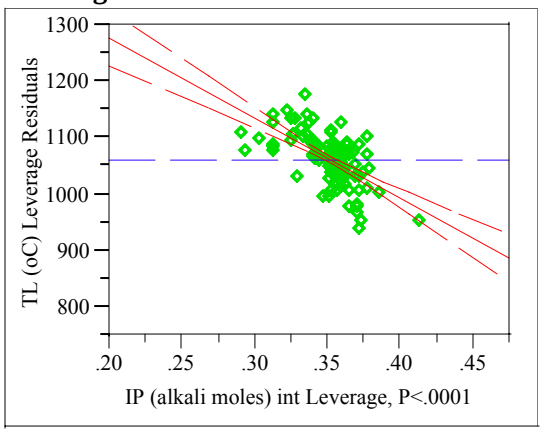

IPM (nonalkali moles) slp
Leverage Plot

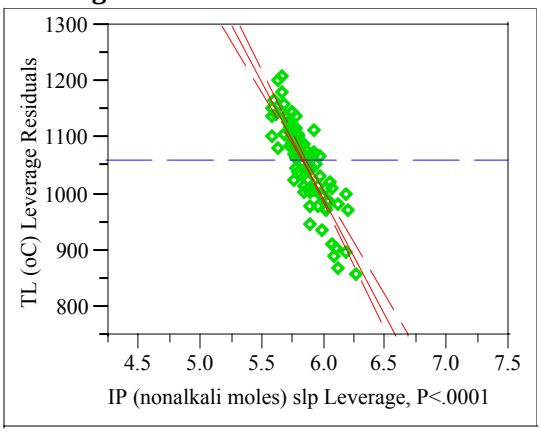

Appendix C. Model Fitting Results for TL Data

Exhibit C.2: Statistical Results from the Fitting of the IPM to Each Data Grouping

Groupings=4
Response TL (°C)
Singularity Details: Intercept = 0
Whole Model
Actual by Predicted Plot

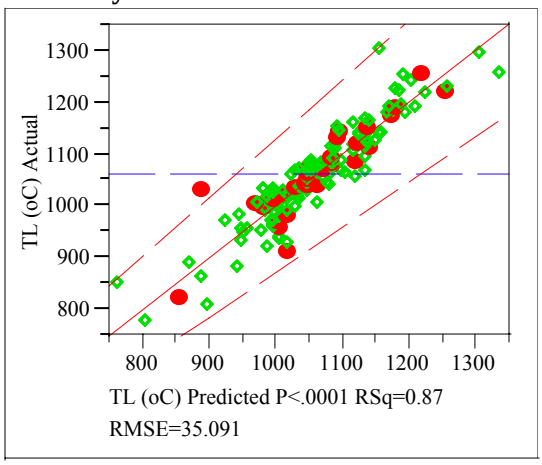

Summary of Fit

RSquare	0.866791
RSquare Adj	0.86024
Root Mean Square Error	35.09126
Mean of Response	1062.05
Observations (or Sum Wgts)	129

Analysis of Variance

Source	DF	Sum of Squares	Mean Square	F Ratio
Model	6	977549.0	162925	132.3090
Error	122	150230.4	1231	Prob > F
C. Total	128	1127779.4		<.0001

Tested against reduced model: Y=mean

Lack Of Fit

Source	DF	Sum of Squares	Mean Square	F Ratio
Lack Of Fit	98	144795.22	1477.50	6.5242
Pure Error	24	5435.16	226.46	Prob > F
Total Error	122	150230.38		<.0001
				Max RSq
				0.9952

Parameter Estimates

Term	Estimate	Std Error	t Ratio	Prob>|t|
IPM (Cr moles)	42830.892	3989.468	10.74	<.0001
IPM (Mn moles)	1347.0046	381.5371	3.53	0.0006
IPM (Ni moles)	13957.516	1101.836	12.67	<.0001
IPM (alkali moles) int	-1362.593	175.8238	-7.75	<.0001
IPM (alkali moles) slp	1224.4567	166.7897	7.34	<.0001
IPM (nonalkali moles) int	5020.1398	212.1302	23.67	<.0001
IPM (nonalkali moles) slp	-378.7527	22.18141	-17.08	<.0001

Effect Tests

Source	DF	Sum of Squares	F Ratio	Prob > F
IPM (Cr moles)	1	141932.63	115.2615	<.0001
IPM (Mn moles)	1	15348.38	12.4642	0.0006
IPM (Ni moles)	1	197596.83	160.4656	<.0001
IPM (alkali moles) int	1	73956.28	60.0589	<.0001
IPM (alkali moles) slp	1	66366.14	53.8950	<.0001
IPM (nonalkali moles) int	1	689643.58	560.0500	<.0001
IPM (nonalkali moles) slp	1	359030.28	291.5635	<.0001

Residual by Predicted Plot

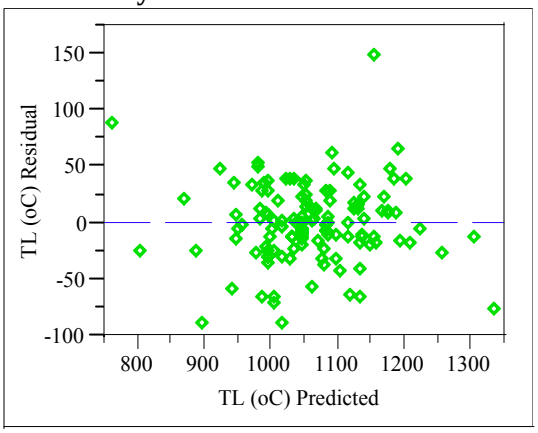

Press
175101.16425

IPM (Cr moles)
Leverage Plot

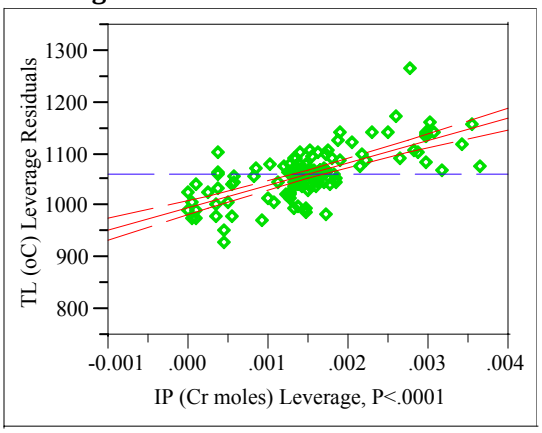

Appendix C. Model Fitting Results for TL Data

Exhibit C.2: Statistical Results from the Fitting of the IPM to Each Data Grouping

IPM (Mn moles)
Leverage Plot

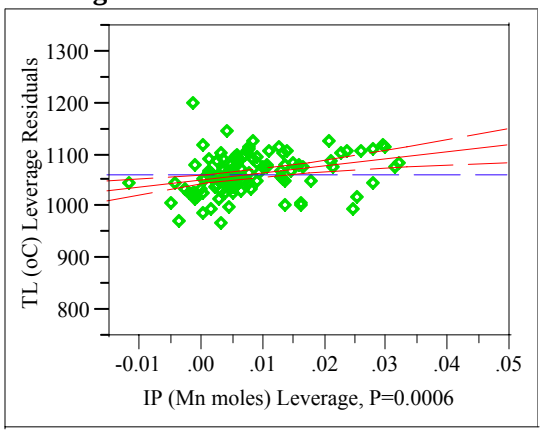

IPM (alkali moles) slp
Leverage Plot

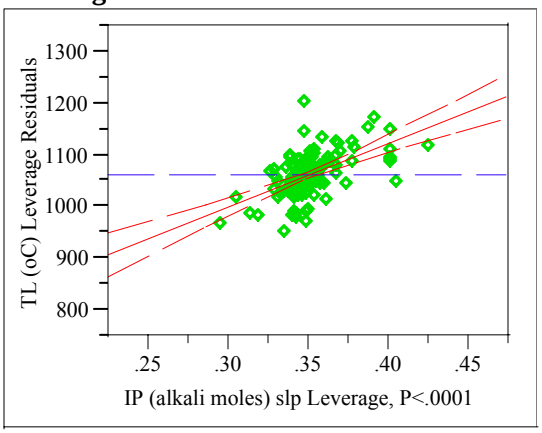

IPM (Ni moles)
Leverage Plot

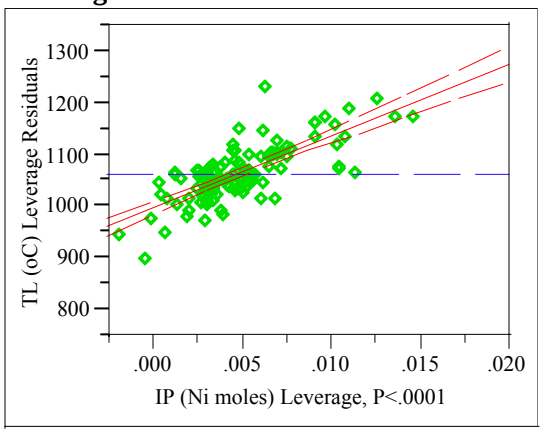

IPM (nonalkali moles) int
Leverage Plot

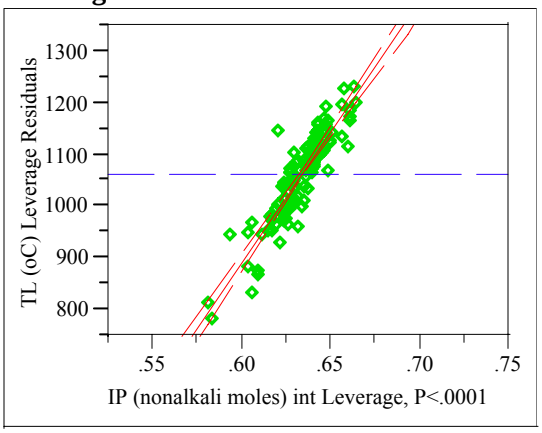

IPM (alkali moles) int
Leverage Plot

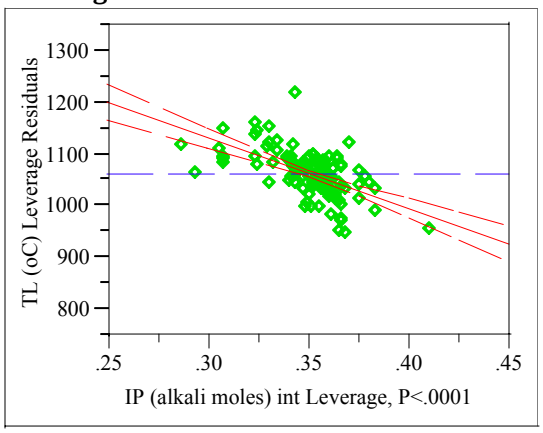

IPM (nonalkali moles) slp
Leverage Plot

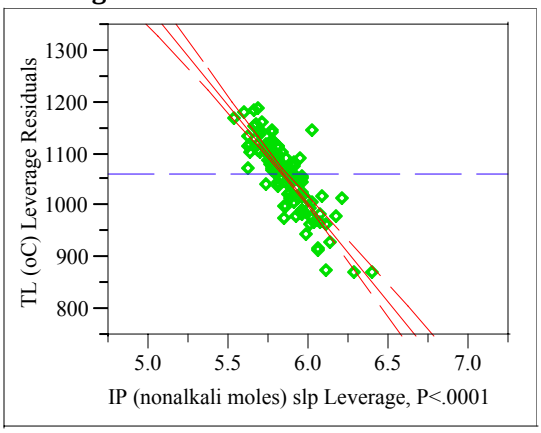

Appendix C. Model Fitting Results for TL Data

Exhibit C.2: Statistical Results from the Fitting of the IPM to Each Data Grouping

Groupings=5
Response TL (°C)
Singularity Details: Intercept = 0
Whole Model
Actual by Predicted Plot

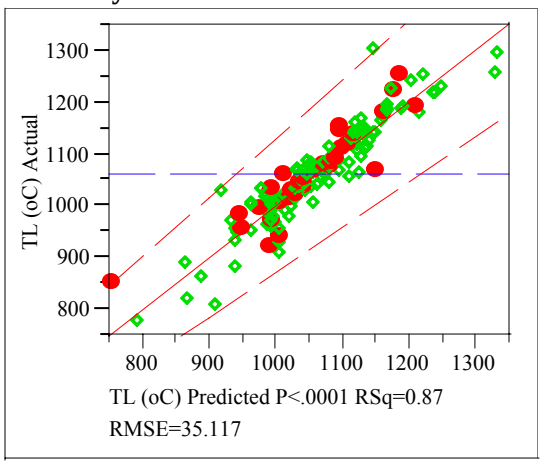

Summary of Fit

RSquare	0.867595
RSquare Adj	0.861029
Root Mean Square Error	35.11738
Mean of Response	1062.106
Observations (or Sum Wgts)	128

Analysis of Variance

Source	DF	Sum of Squares	Mean Square	F Ratio
Model	6	977779.4	162963	132.1434
Error	121	149220.8	1233	Prob > F
C. Total	127	1127000.2		<.0001

Tested against reduced model: Y=mean

Lack Of Fit

Source	DF	Sum of Squares	Mean Square	F Ratio
Lack Of Fit	100	142953.93	1429.54	4.7903
Pure Error	21	6266.91	298.42	Prob > F
Total Error	121	149220.83		<.0001
				Max RSq
				0.9944

Parameter Estimates

Term	Estimate	Std Error	t Ratio	Prob>|t|
IPM (Cr moles)	40952.795	4136.705	9.90	<.0001
IPM (Mn moles)	2218.8385	335.19	6.62	<.0001
IPM (Ni moles)	13367.961	1015.218	13.17	<.0001
IPM (alkali moles) int	-1487.677	182.2523	-8.16	<.0001
IPM (alkali moles) slp	1371.1643	171.1534	8.01	<.0001
IPM (nonalkali moles) int	5183.3713	216.4532	23.95	<.0001
IPM (nonalkali moles) slp	-398.3644	22.403	-17.78	<.0001

Effect Tests

Source	DF	Sum of Squares	F Ratio	Prob > F
IPM (Cr moles)	1	120865.44	98.0072	<.0001
IPM (Mn moles)	1	54039.76	43.8197	<.0001
IPM (Ni moles)	1	213823.85	173.3852	<.0001
IPM (alkali moles) int	1	82170.33	66.6302	<.0001
IPM (alkali moles) slp	1	79150.18	64.1812	<.0001
IPM (nonalkali moles) int	1	707197.80	573.4516	<.0001
IPM (nonalkali moles) slp	1	389935.40	316.1903	<.0001

Residual by Predicted Plot

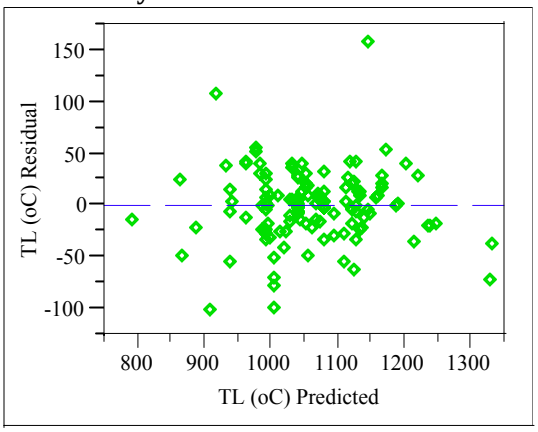

Press
180256.9233

IPM (Cr moles)
Leverage Plot

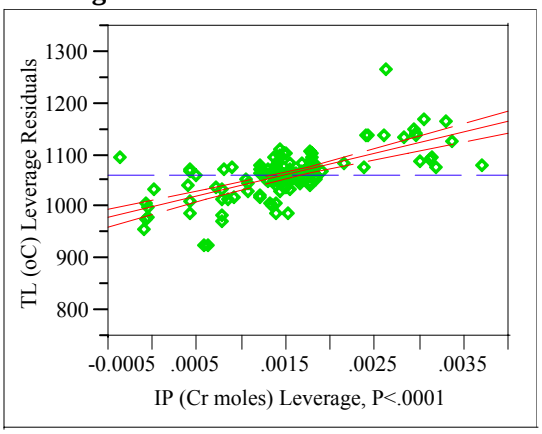

Appendix C. Model Fitting Results for TL Data

Exhibit C.2: Statistical Results from the Fitting of the IPM to Each Data Grouping

IPM (Mn moles)
Leverage Plot

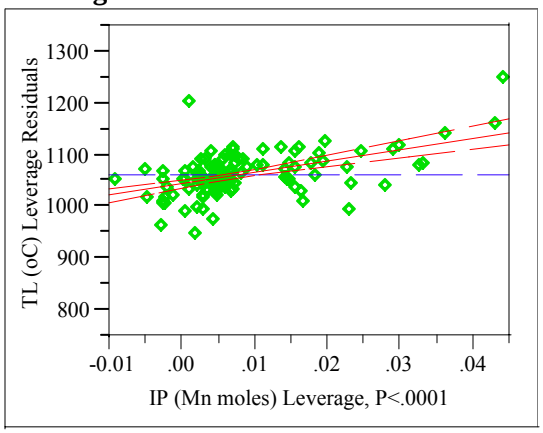

IPM (alkali moles) slp
Leverage Plot

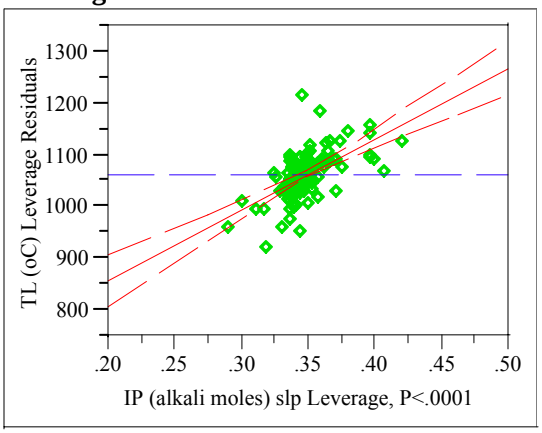

IPM (Ni moles)
Leverage Plot

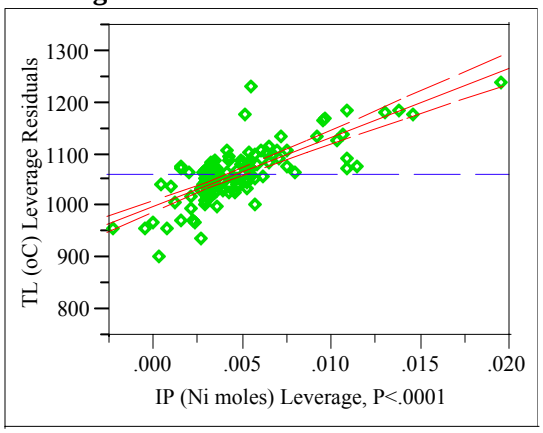

IPM (nonalkali moles) int
Leverage Plot

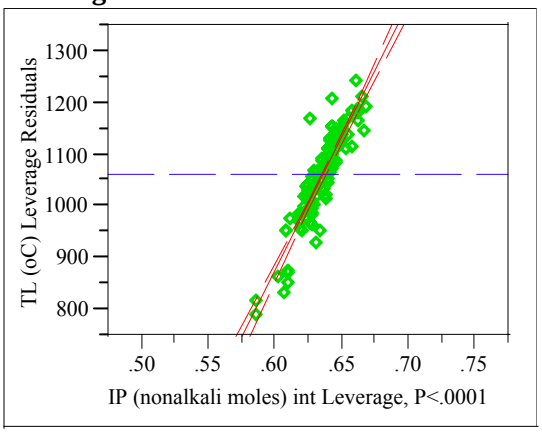

IPM (alkali moles) int
Leverage Plot

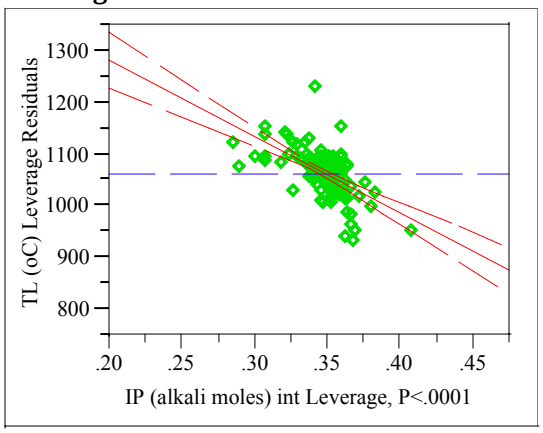

IPM (nonalkali moles) slp
Leverage Plot

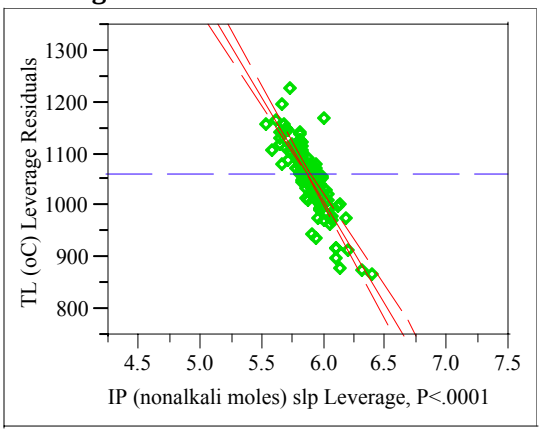

Appendix C. Model Fitting Results for TL Data

Exhibit C.3: Statistical Results from the Fitting of the SPM w Cr and Fe to Each Data Grouping

Groupings=1
Response 1000/TL (K)
Whole Model
Actual by Predicted Plot

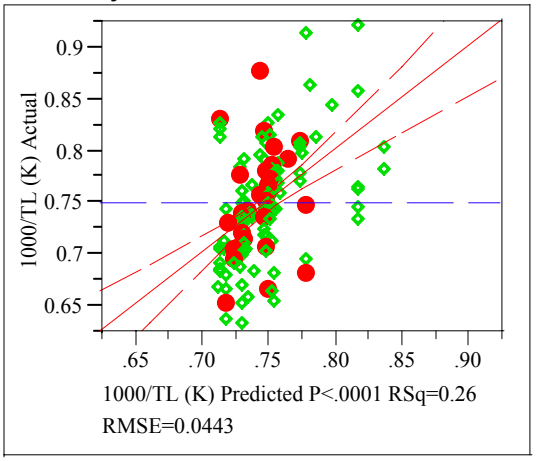

Summary of Fit

RSquare	0.256402
RSquare Adj	0.250153
Root Mean Square Error	0.044325
Mean of Response	0.749027
Observations (or Sum Wgts)	121

Analysis of Variance

Source	DF	Sum of Squares	Mean Square	F Ratio
Model	1	0.08061721	0.080617	41.0326
Error	119	0.23380059	0.001965	Prob > F
C. Total	120	0.31441780		<.0001

Lack Of Fit

Source	DF	Sum of Squares	Mean Square	F Ratio
Lack Of Fit	82	0.16777906	0.002046	1.1467
Pure Error	37	0.06602154	0.001784	Prob > F
Total Error	119	0.23380059		0.3275
				Max RSq
				0.7900

Parameter Estimates

Term	Estimate	Std Error	t Ratio	Prob>|t|
Intercept	0.7039633	0.008107	86.83	<.0001
SPMw Cr & Ni	-0.021456	0.003349	-6.41	<.0001

Effect Tests

Source	DF	Sum of Squares	F Ratio	Prob > F
SPMw Cr & Ni	1	0.08061721	41.0326	<.0001

Residual by Predicted Plot

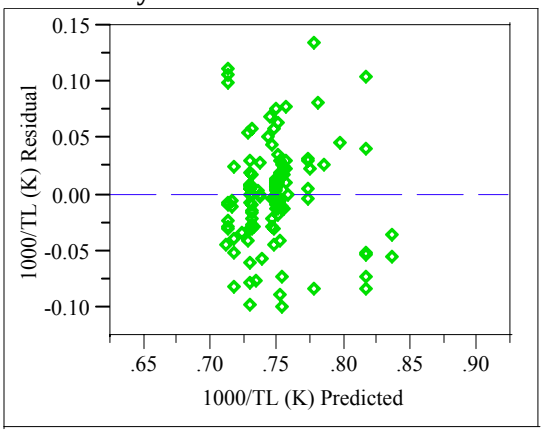

Press
0.2454680772

SPM w Cr & Ni
Leverage Plot

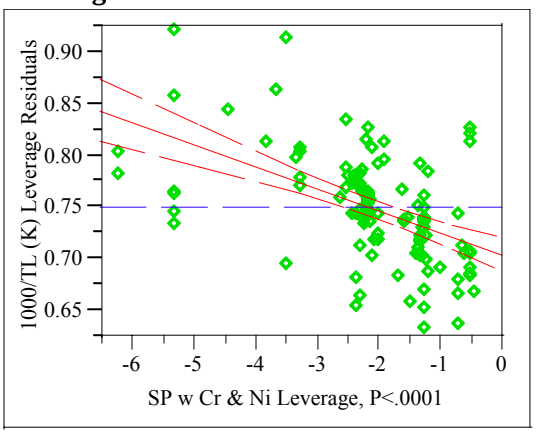

Appendix C. Model Fitting Results for TL Data

Exhibit C.3: Statistical Results from the Fitting of the SPM w Cr and Fe to Each Data Grouping

Groupings=2
Response 1000/TL (K)
Whole Model
Actual by Predicted Plot

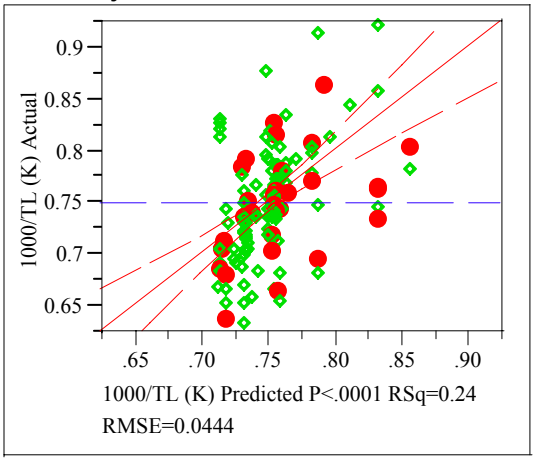

Summary of Fit

RSquare	0.243088
RSquare Adj	0.23678
Root Mean Square Error	0.044412
Mean of Response	0.750093
Observations (or Sum Wgts)	122

Analysis of Variance

Source	DF	Sum of Squares	Mean Square	F Ratio
Model	1	0.07601570	0.076016	38.5388
Error	120	0.23669349	0.001972	Prob > F
C. Total	121	0.31270919		<.0001

Lack Of Fit

Source	DF	Sum of Squares	Mean Square	F Ratio
Lack Of Fit	82	0.16330958	0.001992	1.0313
Pure Error	38	0.07338391	0.001931	Prob > F
Total Error	120	0.23669349		0.4696
				Max RSq
				0.7653

Parameter Estimates

Term	Estimate	Std Error	t Ratio	Prob>|t|
Intercept	0.7010599	0.008863	79.10	<.0001
SPMw Cr & Ni	-0.024887	0.004009	-6.21	<.0001

Effect Tests

Source	DF	Sum of Squares	F Ratio	Prob > F
SPMw Cr & Ni	1	0.07601570	38.5388	<.0001

Residual by Predicted Plot

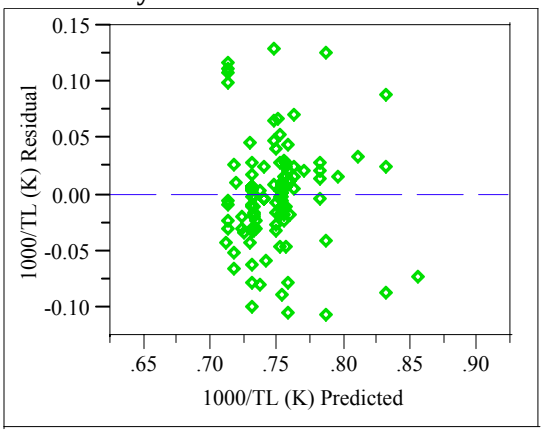

Press
0.2500595338

SPM w Cr & Ni
Leverage Plot

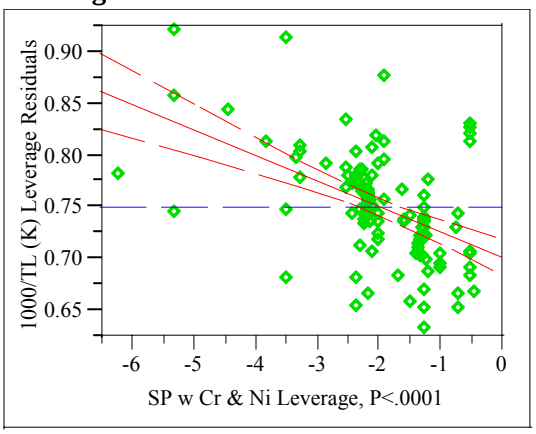

Appendix C. Model Fitting Results for TL Data

Exhibit C.3: Statistical Results from the Fitting of the SPM w Cr and Fe to Each Data Grouping

Groupings=3
Response 1000/TL (K)
Whole Model
Actual by Predicted Plot

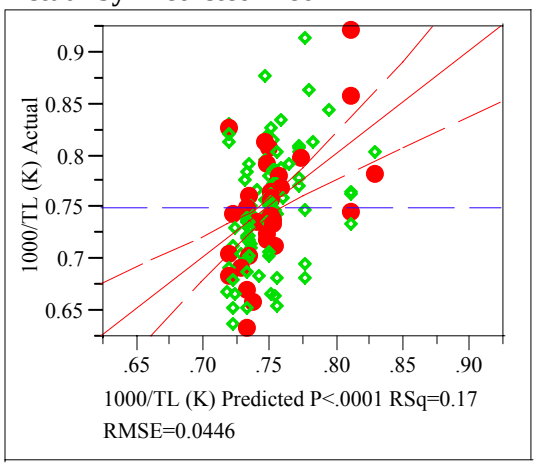

Summary of Fit

RSquare	0.169083
RSquare Adj	0.161981
Root Mean Square Error	0.044604
Mean of Response	0.749086
Observations (or Sum Wgts)	119

Analysis of Variance

Source	DF	Sum of Squares	Mean Square	F Ratio
Model	1	0.04736630	0.047366	23.8082
Error	117	0.23277079	0.001989	Prob > F
C. Total	118	0.28013708		<.0001

Lack Of Fit

Source	DF	Sum of Squares	Mean Square	F Ratio
Lack Of Fit	81	0.14565009	0.001798	0.7430
Pure Error	36	0.08712069	0.002420	Prob > F
Total Error	117	0.23277079		0.8640
				Max RSq
				0.6890

Parameter Estimates

Term	Estimate	Std Error	t Ratio	Prob>|t|
Intercept	0.7103796	0.008924	79.60	<.0001
SPMw Cr & Ni	-0.019206	0.003936	-4.88	<.0001

Effect Tests

Source	DF	Sum of Squares	F Ratio	Prob > F
SPMw Cr & Ni	1	0.04736630	23.8082	<.0001

Residual by Predicted Plot

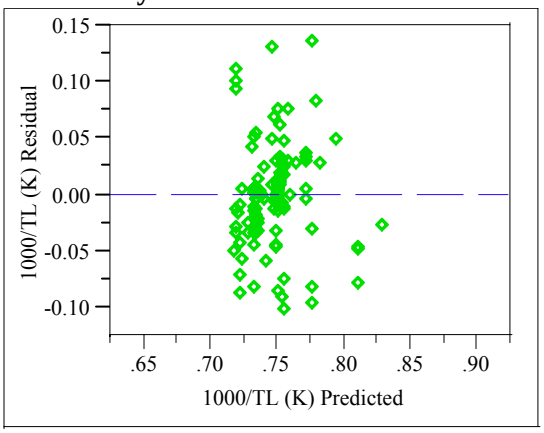

Press
0.2432847973

SPM w Cr & Ni
Leverage Plot

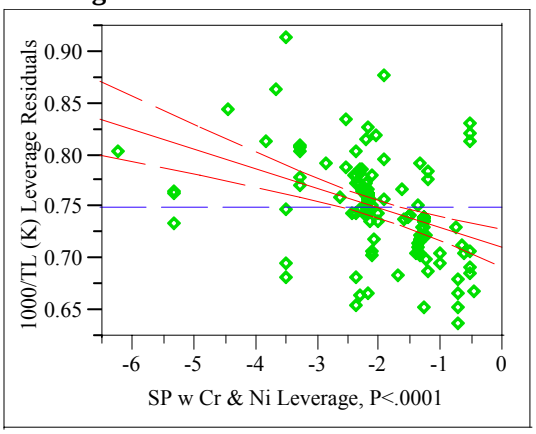

Appendix C. Model Fitting Results for TL Data

Exhibit C.3: Statistical Results from the Fitting of the SPM w Cr and Fe to Each Data Grouping

Groupings=4
Response 1000/TL (K)
Whole Model
Actual by Predicted Plot

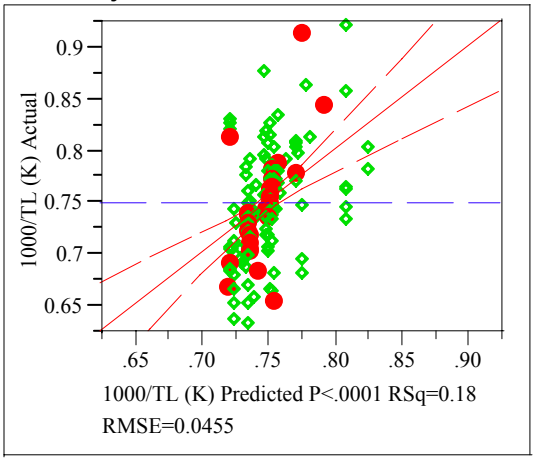

Summary of Fit

RSquare	0.182425
RSquare Adj	0.175723
Root Mean Square Error	0.045534
Mean of Response	0.750159
Observations (or Sum Wgts)	124

Analysis of Variance

Source	DF	Sum of Squares	Mean Square	F Ratio
Model	1	0.05643907	0.056439	27.2217
Error	122	0.25294384	0.002073	Prob > F
C. Total	123	0.30938291		<.0001

Lack Of Fit

Source	DF	Sum of Squares	Mean Square	F Ratio
Lack Of Fit	79	0.20525523	0.002598	2.3427
Pure Error	43	0.04768861	0.001109	Prob > F
Total Error	122	0.25294384		0.0015
				Max RSq
				0.8459

Parameter Estimates

Term	Estimate	Std Error	t Ratio	Prob>|t|
Intercept	0.7122303	0.008341	85.39	<.0001
SPMw Cr & Ni	-0.018129	0.003475	-5.22	<.0001

Effect Tests

Source	DF	Sum of Squares	F Ratio	Prob > F
SPMw Cr & Ni	1	0.05643907	27.2217	<.0001

Residual by Predicted Plot

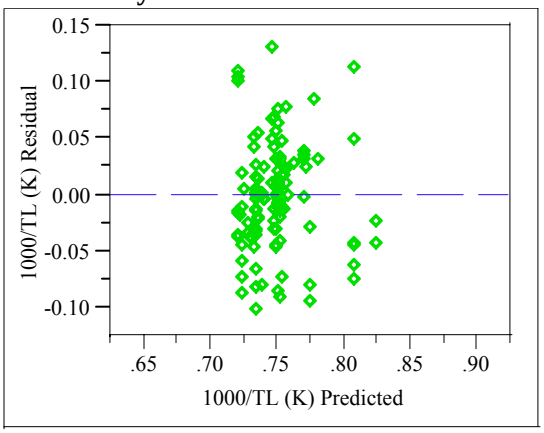

Press
0.2641902116

SPM w Cr & Ni
Leverage Plot

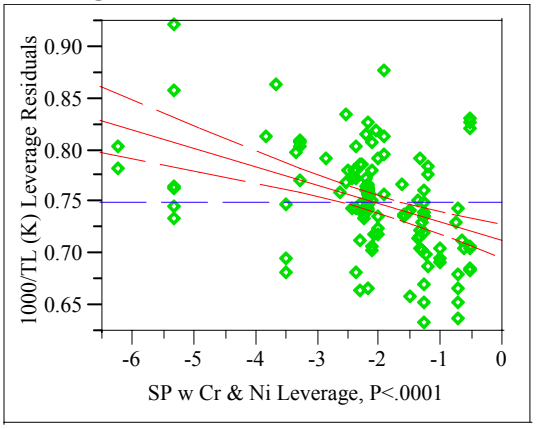

Appendix C. Model Fitting Results for TL Data

Exhibit C.3: Statistical Results from the Fitting of the SPM w Cr and Fe to Each Data Grouping

Groupings=5
Response 1000/TL (K)
Whole Model
Actual by Predicted Plot

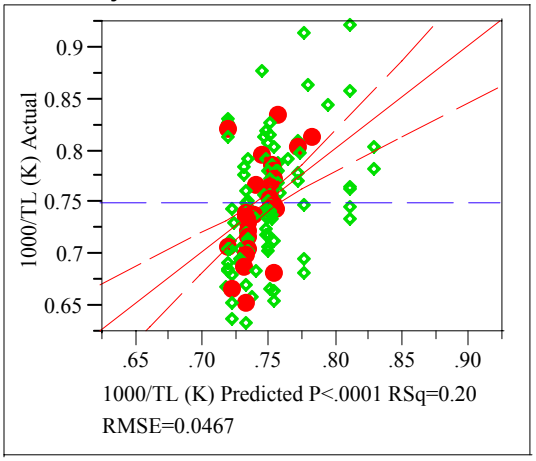

Summary of Fit

RSquare	0.199013
RSquare Adj	0.192338
Root Mean Square Error	0.046734
Mean of Response	0.750522
Observations (or Sum Wgts)	122

Analysis of Variance

Source	DF	Sum of Squares	Mean Square	F Ratio
Model	1	0.06511718	0.065117	29.8152
Error	120	0.26208317	0.002184	Prob > F
C. Total	121	0.32720035		<.0001

Lack Of Fit

Source	DF	Sum of Squares	Mean Square	F Ratio
Lack Of Fit	81	0.16942012	0.002092	0.8803
Pure Error	39	0.09266305	0.002376	Prob > F
Total Error	120	0.26208317		0.6900
				Max RSq
				0.7168

Parameter Estimates

Term	Estimate	Std Error	t Ratio	Prob>|t|
Intercept	0.7097676	0.008579	82.73	<.0001
SPMw Cr & Ni	-0.01927	0.003529	-5.46	<.0001

Effect Tests

Source	DF	Sum of Squares	F Ratio	Prob > F
SPMw Cr & Ni	1	0.06511718	29.8152	<.0001

Residual by Predicted Plot

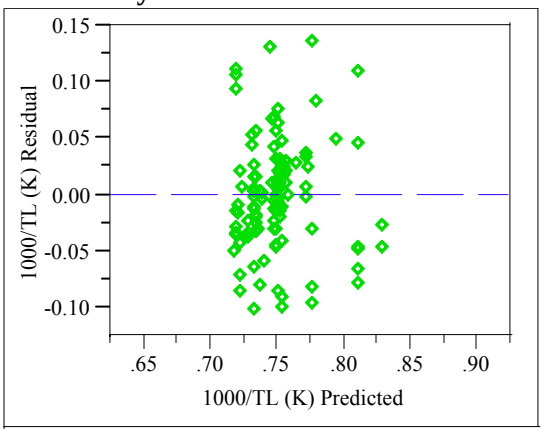

Press
0.2740330417

SPM w Cr & Ni
Leverage Plot

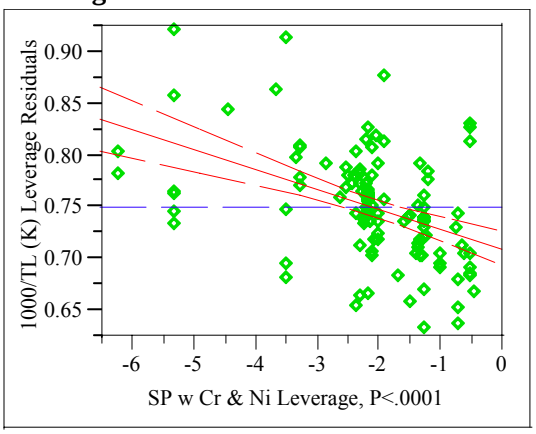

Appendix C. Model Fitting Results for TL Data

Exhibit C.4: Statistical Results from the Fitting of the SPM w Ni and Fe to Each Data Grouping

Groupings=1
Response 1000/TL (K)
Whole Model
Actual by Predicted Plot

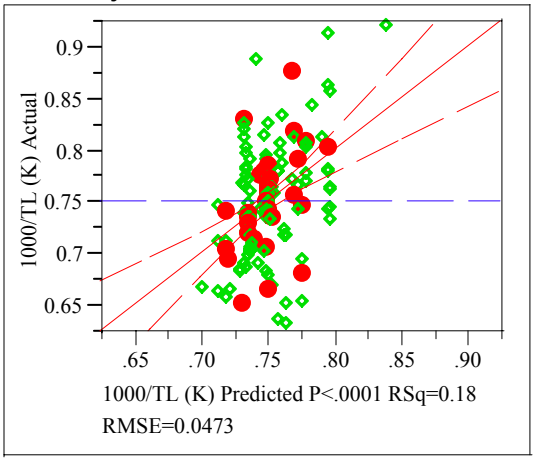

Summary of Fit

RSquare	0.179056
RSquare Adj	0.172435
Root Mean Square Error	0.047281
Mean of Response	0.751096
Observations (or Sum Wgts)	126

Analysis of Variance

Source	DF	Sum of Squares	Mean Square	F Ratio
Model	1	0.06046102	0.060461	27.0456
Error	124	0.27720497	0.002236	Prob > F
C. Total	125	0.33766599		<.0001

Lack Of Fit

Source	DF	Sum of Squares	Mean Square	F Ratio
Lack Of Fit	90	0.23569490	0.002619	2.1450
Pure Error	34	0.04151007	0.001221	Prob > F
Total Error	124	0.27720497		0.0069
				Max RSq
				0.8771

Parameter Estimates

Term	Estimate	Std Error	t Ratio	Prob>|t|
Intercept	0.8039467	0.011001	73.08	<.0001
SPMw Ni & Fe	-0.028636	0.005506	-5.20	<.0001

Effect Tests

Source	DF	Sum of Squares	F Ratio	Prob > F
SPMw Ni & Fe	1	0.06046102	27.0456	<.0001

Residual by Predicted Plot

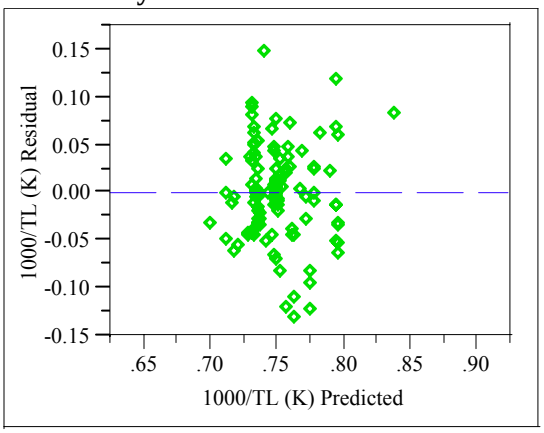

Press
0.288729412

SPM w Ni & Fe
Leverage Plot

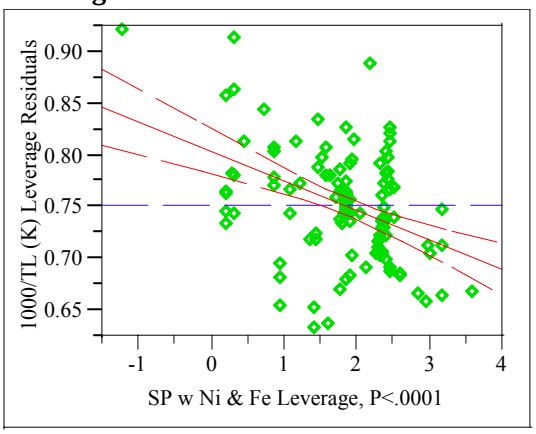

Appendix C. Model Fitting Results for TL Data

Exhibit C.4: Statistical Results from the Fitting of the SPM w Ni and Fe to Each Data Grouping

Groupings=2
Response 1000/TL (K)
Whole Model
Actual by Predicted Plot

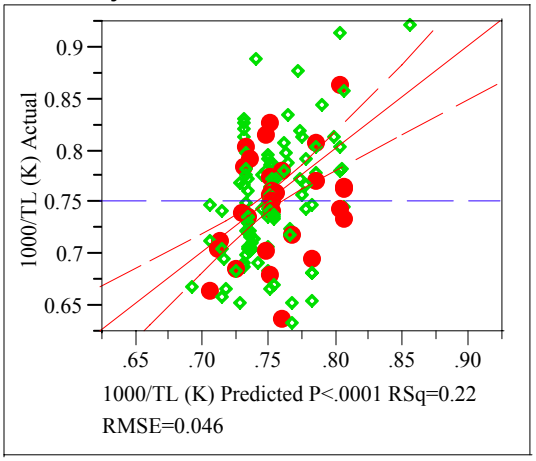

Summary of Fit

RSquare	0.217828
RSquare Adj	0.21152
Root Mean Square Error	0.045964
Mean of Response	0.751927
Observations (or Sum Wgts)	126

Analysis of Variance

Source	DF	Sum of Squares	Mean Square	F Ratio
Model	1	0.07295639	0.072956	34.5328
Error	124	0.26197074	0.002113	Prob > F
C. Total	125	0.33492713		<.0001

Lack Of Fit

Source	DF	Sum of Squares	Mean Square	F Ratio
Lack Of Fit	90	0.23034405	0.002559	2.7514
Pure Error	34	0.03162669	0.000930	Prob > F
Total Error	124	0.26197074		0.0007
				Max RSq
				0.9056

Parameter Estimates

Term	Estimate	Std Error	t Ratio	Prob>|t|
Intercept	0.8157148	0.011601	70.31	<.0001
SPMw Ni & Fe	-0.033843	0.005759	-5.88	<.0001

Effect Tests

Source	DF	Sum of Squares	F Ratio	Prob > F
SPMw Ni & Fe	1	0.07295639	34.5328	<.0001

Residual by Predicted Plot

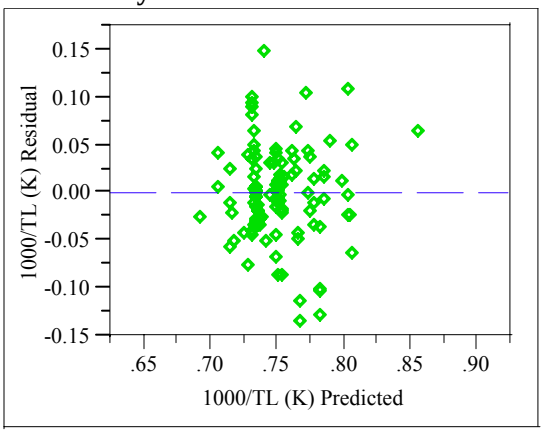

Press
0.272590517

SPM w Ni & Fe
Leverage Plot

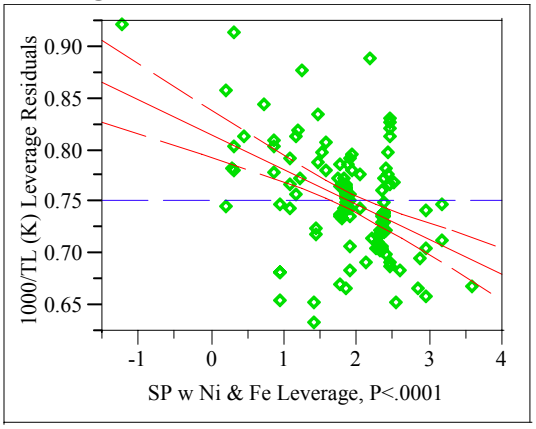

Appendix C. Model Fitting Results for TL Data

Exhibit C.4: Statistical Results from the Fitting of the SPM w Ni and Fe to Each Data Grouping

Groupings=3
Response 1000/TL (K)
Whole Model
Actual by Predicted Plot

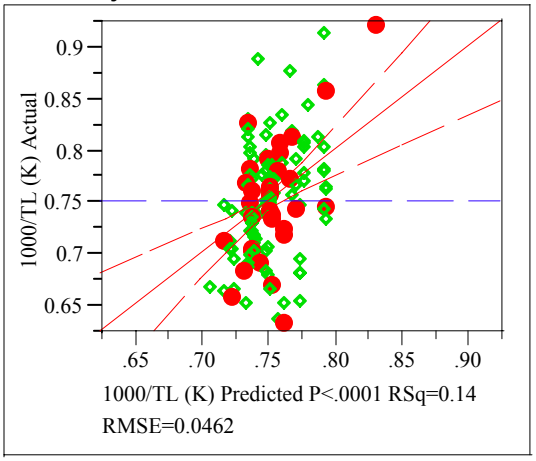

Summary of Fit

RSquare	0.141014
RSquare Adj	0.133974
Root Mean Square Error	0.046215
Mean of Response	0.751187
Observations (or Sum Wgts)	124

Analysis of Variance

Source	DF	Sum of Squares	Mean Square	F Ratio
Model	1	0.04277630	0.042776	20.0280
Error	122	0.26057055	0.002136	Prob > F
C. Total	123	0.30334685		<.0001

Lack Of Fit

Source	DF	Sum of Squares	Mean Square	F Ratio
Lack Of Fit	90	0.21228903	0.002359	1.5633
Pure Error	32	0.04828151	0.001509	Prob > F
Total Error	122	0.26057055		0.0770
				Max RSq
				0.8408

Parameter Estimates

Term	Estimate	Std Error	t Ratio	Prob>|t|
Intercept	0.7998356	0.011636	68.74	<.0001
SPM w Ni & Fe	-0.026011	0.005812	-4.48	<.0001

Effect Tests

Source	DF	Sum of Squares	F Ratio	Prob > F
SPM w Ni & Fe	1	0.04277630	20.0280	<.0001

Residual by Predicted Plot

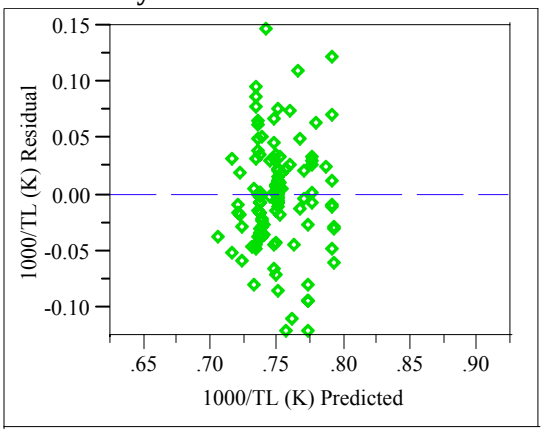

Press
0.2702745085

SPM w Ni & Fe
Leverage Plot

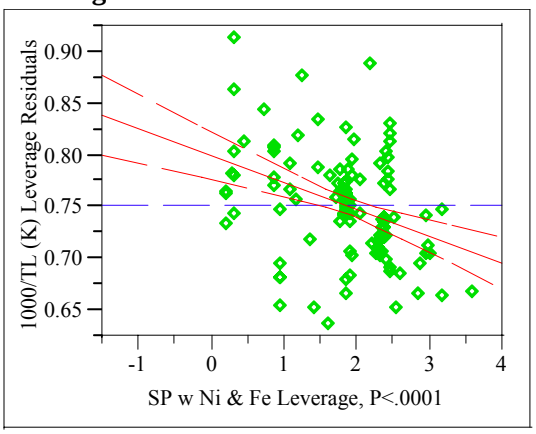

Appendix C. Model Fitting Results for TL Data

Exhibit C.4: Statistical Results from the Fitting of the SPM w Ni and Fe to Each Data Grouping

Groupings=4
Response 1000/TL (K)
Whole Model
Actual by Predicted Plot

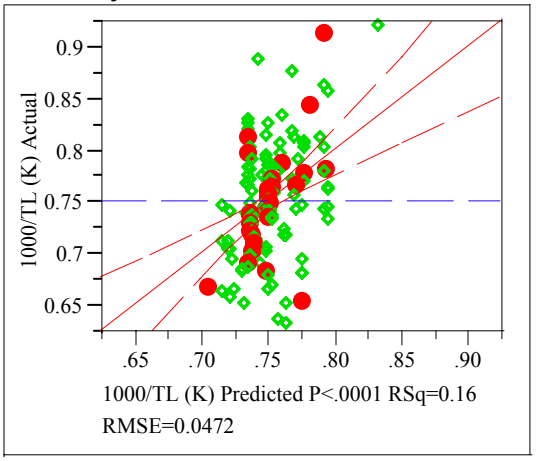

Summary of Fit

RSquare	0.155083
RSquare Adj	0.148324
Root Mean Square Error	0.047208
Mean of Response	0.751651
Observations (or Sum Wgts)	127

Analysis of Variance

Source	DF	Sum of Squares	Mean Square	F Ratio
Model	1	0.05113078	0.051131	22.9435
Error	125	0.27856859	0.002229	Prob > F
C. Total	126	0.32969938		<.0001

Lack Of Fit

Source	DF	Sum of Squares	Mean Square	F Ratio
Lack Of Fit	89	0.24600930	0.002764	3.0563
Pure Error	36	0.03255930	0.000904	Prob > F
Total Error	125	0.27856859		0.0002
				Max RSq
				0.9012

Parameter Estimates

Term	Estimate	Std Error	t Ratio	Prob>|t|
Intercept	0.8010324	0.011128	71.98	<.0001
SPM w Ni & Fe	-0.026741	0.005583	-4.79	<.0001

Effect Tests

Source	DF	Sum of Squares	F Ratio	Prob > F
SPM w Ni & Fe	1	0.05113078	22.9435	<.0001

Residual by Predicted Plot

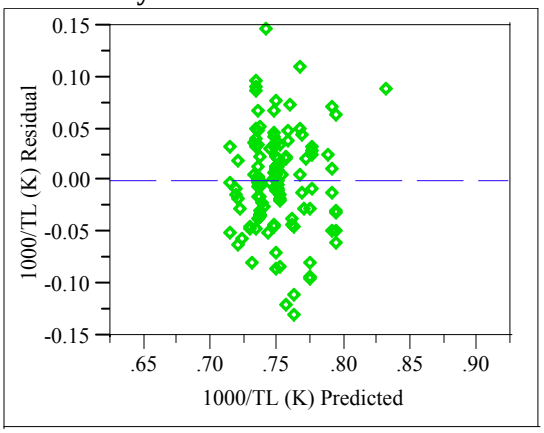

Press
0.2895233891

SPM w Ni & Fe
Leverage Plot

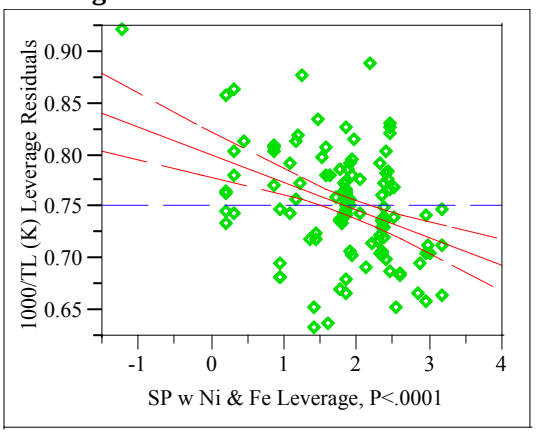

Appendix C. Model Fitting Results for TL Data

Exhibit C.4: Statistical Results from the Fitting of the SPM w Ni and Fe to Each Data Grouping

Groupings=5
Response 1000/TL (K)
Whole Model
Actual by Predicted Plot

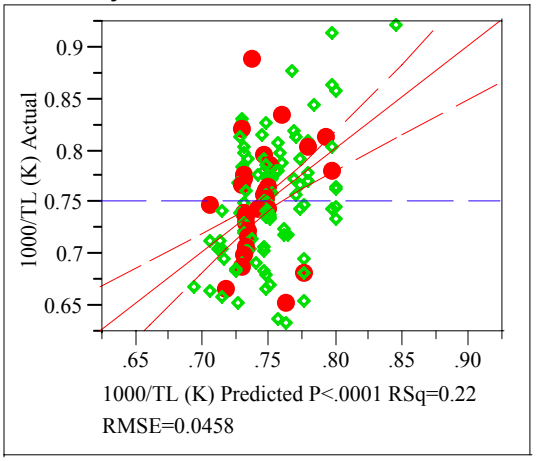

Summary of Fit

RSquare	0.218268
RSquare Adj	0.211912
Root Mean Square Error	0.045815
Mean of Response	0.751233
Observations (or Sum Wgts)	125

Analysis of Variance

Source	DF	Sum of Squares	Mean Square	F Ratio
Model	1	0.07208721	0.072087	34.3429
Error	123	0.25818234	0.002099	Prob > F
C. Total	124	0.33026956		<.0001

Lack Of Fit

Source	DF	Sum of Squares	Mean Square	F Ratio
Lack Of Fit	90	0.20386486	0.002265	1.3762
Pure Error	33	0.05431748	0.001646	Prob > F
Total Error	123	0.25818234		0.1511
				Max RSq
				0.8355

Parameter Estimates

Term	Estimate	Std Error	t Ratio	Prob>|t|
Intercept	0.8083309	0.01057	76.47	<.0001
SPM w Ni & Fe	-0.031536	0.005381	-5.86	<.0001

Effect Tests

Source	DF	Sum of Squares	F Ratio	Prob > F
SPM w Ni & Fe	1	0.07208721	34.3429	<.0001

Residual by Predicted Plot

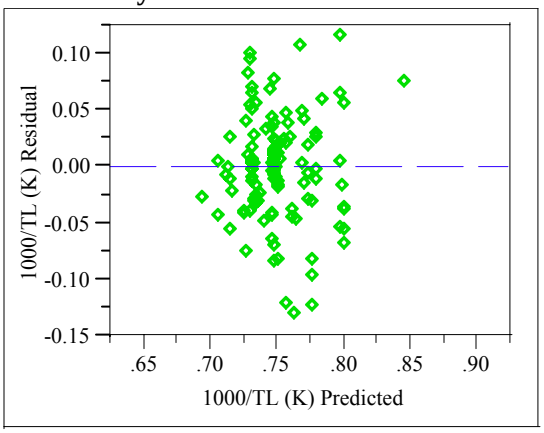

Press
0.2688375257

SPM w Ni & Fe
Leverage Plot

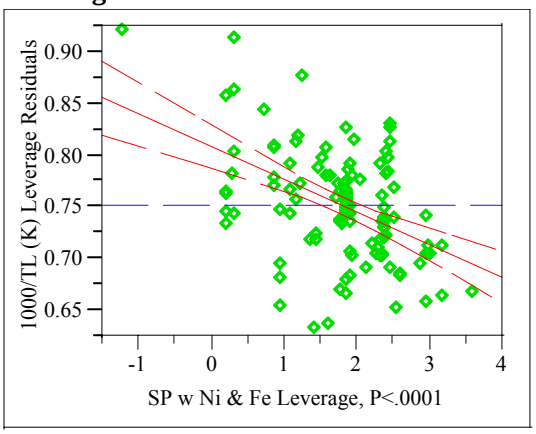

Appendix C. Model Fitting Results for TL Data

Exhibit C.5: Statistical Results from the Fitting of the SLM to Each Data Grouping

Groupings=1
Response 1/TL (K)
Whole Model
Actual by Predicted Plot

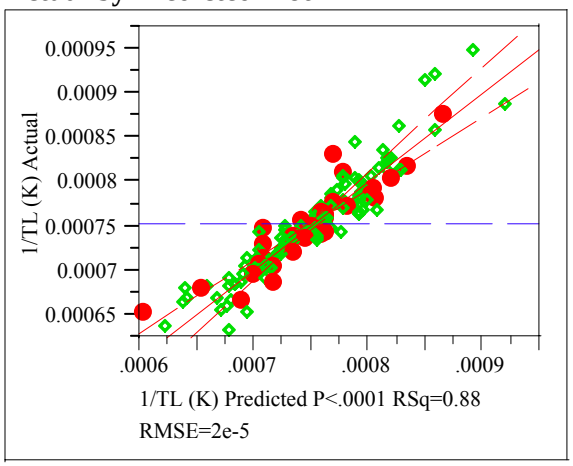

Summary of Fit

RSquare	0.882076
RSquare Adj	0.863851
Root Mean Square Error	0.00002
Mean of Response	0.000753
Observations (or Sum Wgts)	128

Analysis of Variance

Source	DF	Sum of Squares	Mean Square	F Ratio
Model	17	3.34651e-7	1.9685e-8	48.4002
Error	110	4.47392e-8	4.067e-10	Prob > F
C. Total	127	3.7939e-7		<.0001

Lack Of Fit

Source	DF	Sum of Squares	Mean Square	F Ratio
Lack Of Fit	88	4.29267e-8	4.878e-10	5.9210
Pure Error	22	1.81247e-9	8.239e-11	Prob > F
Total Error	110	4.47392e-8		<.0001
				Max RSq
				0.9952

Parameter Estimates

Term	Estimate	Std Error	t Ratio	Prob>|t|
Intercept	0.0005391	0.000097	5.56	<.0001
SL SPL	-0.012235	0.004562	-2.68	0.0085
Al2O3 wt%	-0.000008	0.000002	-4.75	<.0001
B2O3 wt%	0.0000061	0.000001	4.19	<.0001
CaO wt%	0.0000013	0.000003	0.48	0.6353
Cr2O3 wt%	-0.000099	0.000021	-4.77	<.0001
Fe2O3 wt%	-0.000008	0.000001	-6.27	<.0001
K2O wt%	0.0000135	0.000003	4.73	<.0001
Li2O wt%	0.0000211	0.000002	10.80	<.0001
MgO wt%	-0.000008	0.000003	-2.50	0.0139
MnO2 wt%	-0.000002	0.000002	-1.25	0.2154
Na2O wt%	0.0000138	0.000001	10.03	<.0001
NiO wt%	-0.000046	0.000004	-10.94	<.0001
SiO2 wt%	0.0000028	0.000001	2.52	0.0130
TiO2 wt%	0.0000243	0.000019	1.26	0.2109
UO2 wt%	-0.000006	0.000002	-2.37	0.0197
ZnO wt%	-0.000004	0.000006	-0.65	0.5156
ZrO2 wt%	-0.000006	0.000001	-4.36	<.0001

Appendix C. Model Fitting Results for TL Data

Exhibit C.5: Statistical Results from the Fitting of the SLM to Each Data Grouping

Effect Tests

Source	DF	Sum of Squares	F Ratio	Prob > F
SL SPL	1	2.92477e-9	7.1911	0.0085
Al2O3 wt%	1	9.17981e-9	22.5703	<.0001
B2O3 wt%	1	7.12925e-9	17.5287	<.0001
CaO wt%	1	9.2007e-11	0.2262	0.6353
Cr2O3 wt%	1	9.24605e-9	22.7332	<.0001
Fe2O3 wt%	1	1.59923e-8	39.3201	<.0001
K2O wt%	1	9.09341e-9	22.3579	<.0001
Li2O wt%	1	4.74307e-8	116.6175	<.0001
MgO wt%	1	2.54187e-9	6.2497	0.0139
MnO2 wt%	1	6.3157e-10	1.5528	0.2154
Na2O wt%	1	4.09061e-8	100.5756	<.0001
NiO wt%	1	4.86607e-8	119.6417	<.0001
SiO2 wt%	1	2.59205e-9	6.3731	0.0130
TiO2 wt%	1	6.4408e-10	1.5836	0.2109
UO2 wt%	1	2.27935e-9	5.6042	0.0197
ZnO wt%	1	1.7302e-10	0.4254	0.5156
ZrO2 wt%	1	7.74135e-9	19.0336	<.0001

Residual by Predicted Plot

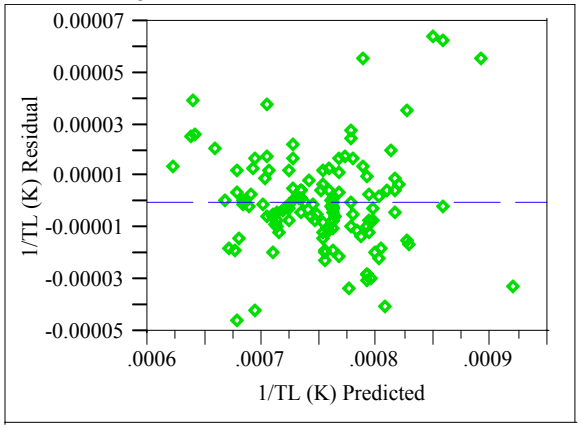

Press
9.2327158e-8

SL SPL
Leverage Plot

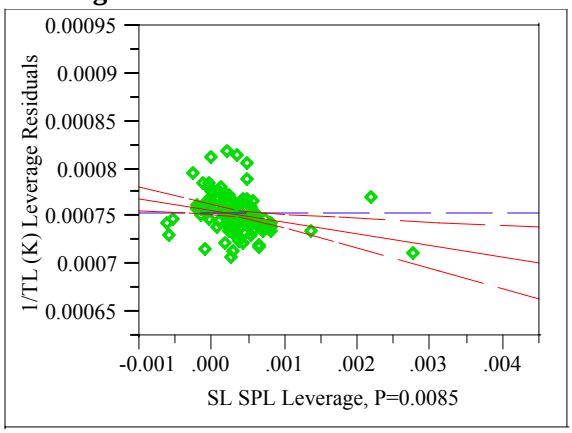

Al2O3 wt%
Leverage Plot

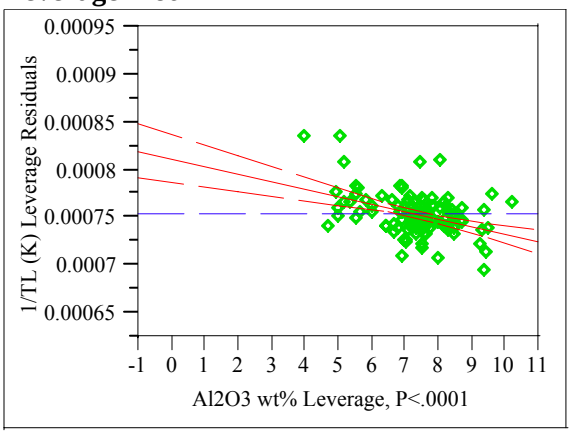

B2O3 wt%
Leverage Plot

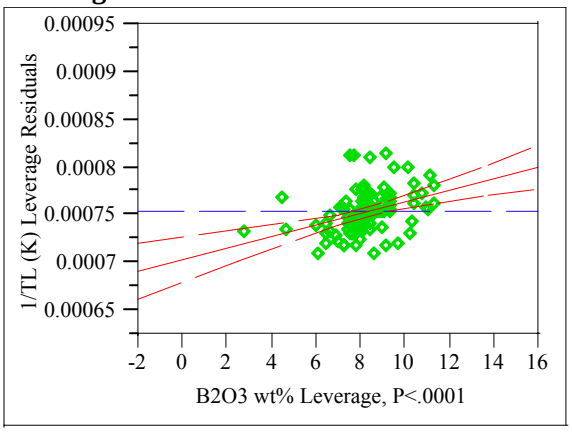

CaO wt%
Leverage Plot

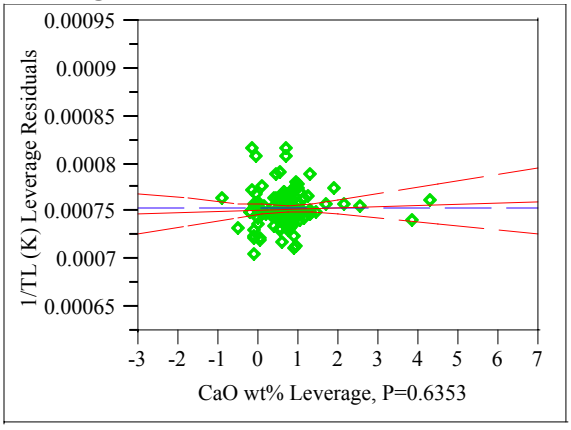

Appendix C. Model Fitting Results for TL Data

Exhibit C.5: Statistical Results from the Fitting of the SLM to Each Data Grouping

Cr2O3 wt%
Leverage Plot

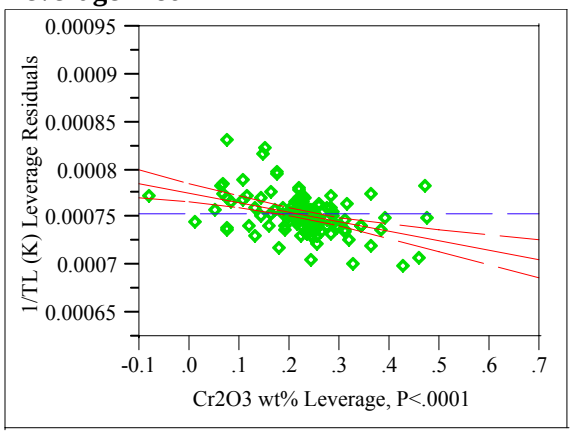

Li2O wt%
Leverage Plot

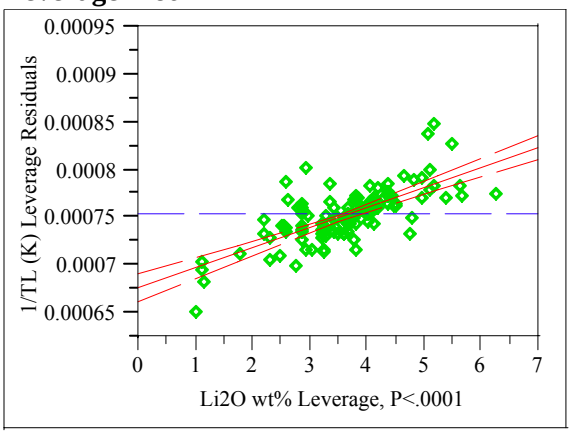

Fe2O3 wt%
Leverage Plot

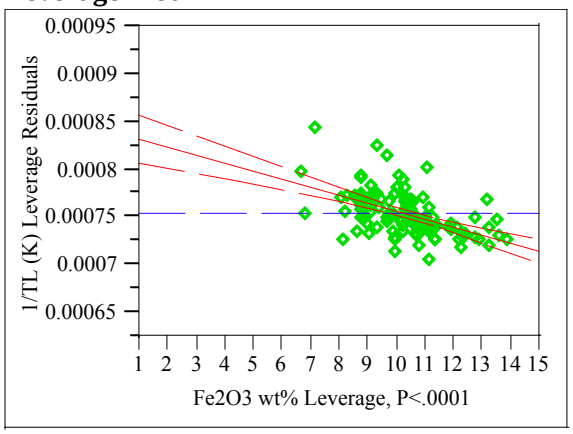

MgO wt%
Leverage Plot

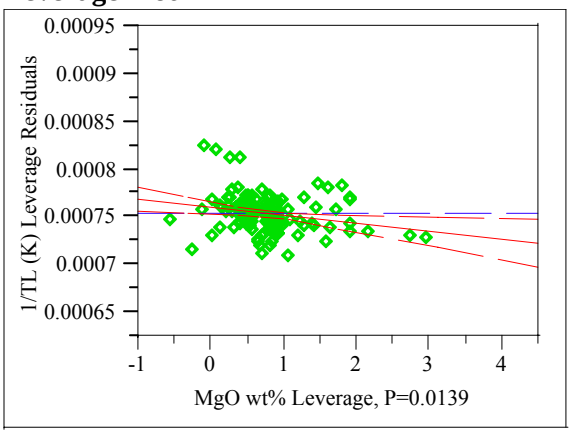

K2O wt%
Leverage Plot

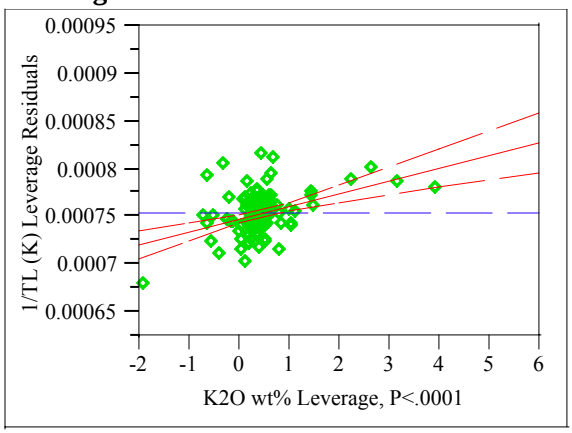

MnO2 wt%
Leverage Plot

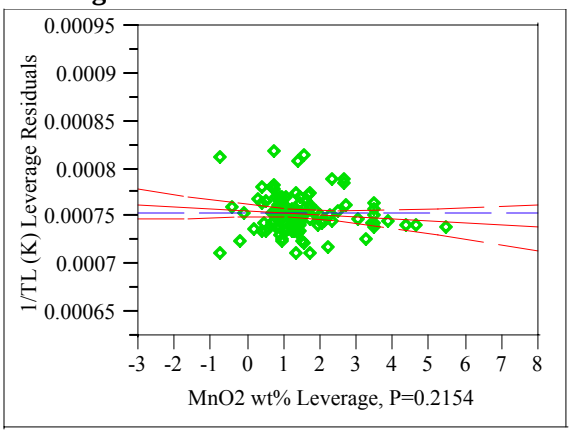

Appendix C. Model Fitting Results for TL Data

Exhibit C.5: Statistical Results from the Fitting of the SLM to Each Data Grouping

Na2O wt%
Leverage Plot

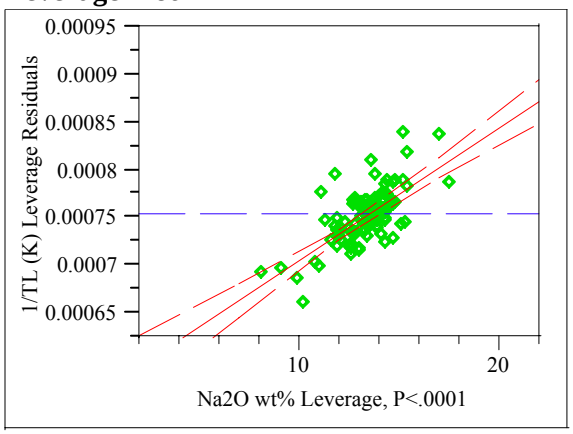

TiO2 wt%
Leverage Plot

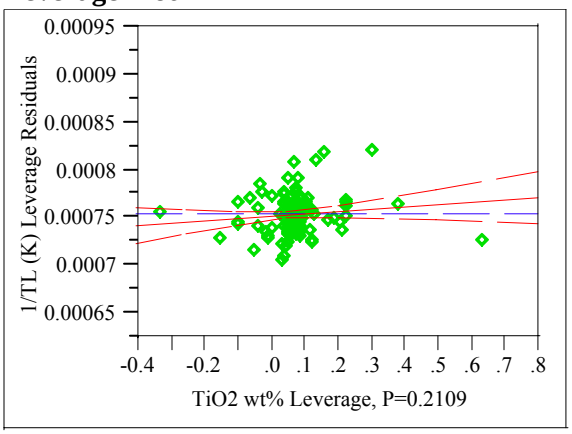

NiO wt%
Leverage Plot

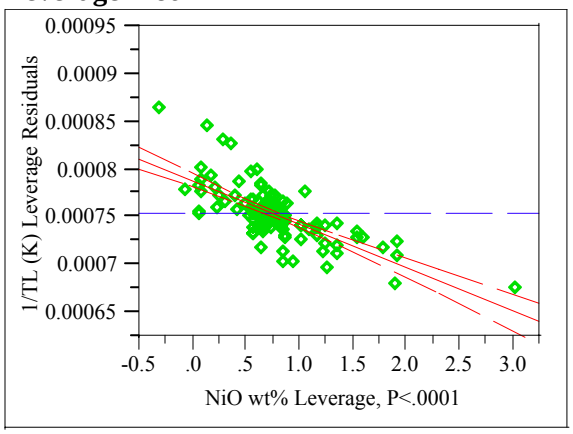

UO2 wt%
Leverage Plot

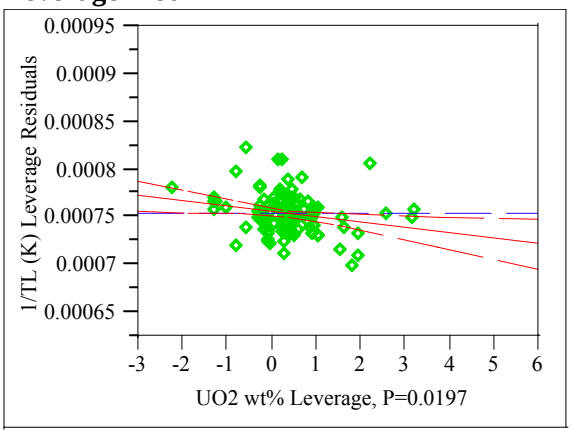

SiO2 wt%
Leverage Plot

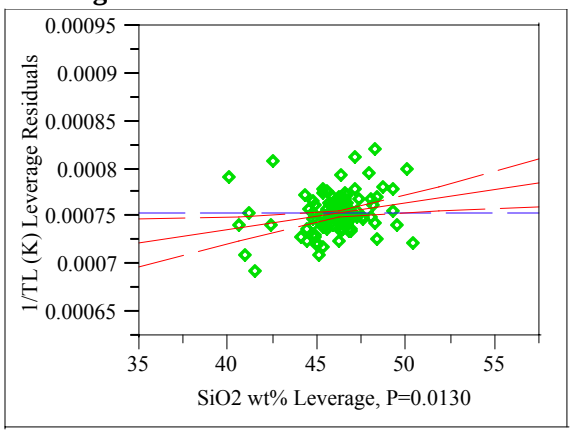

ZnO wt%
Leverage Plot

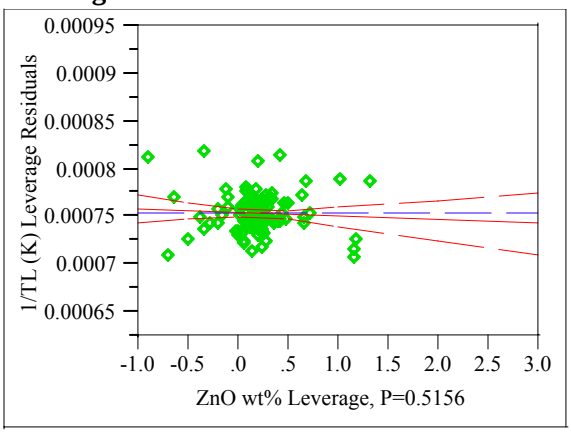

Appendix C. Model Fitting Results for TL Data

Exhibit C.5: Statistical Results from the Fitting of the SLM to Each Data Grouping

ZrO2 wt%
Leverage Plot

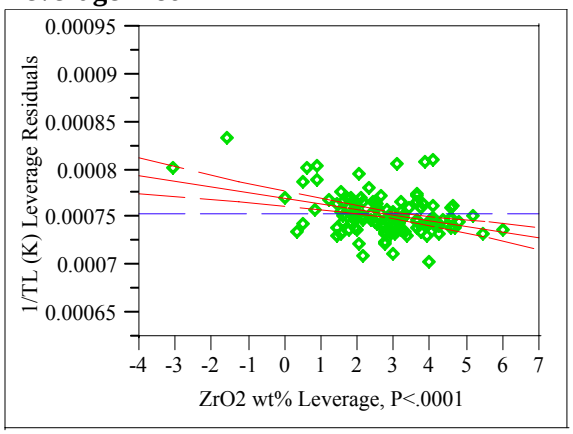

Appendix C. Model Fitting Results for TL Data

Exhibit C.5: Statistical Results from the Fitting of the SLM to Each Data Grouping

Groupings=2
Response 1/TL (K)
Whole Model
Actual by Predicted Plot

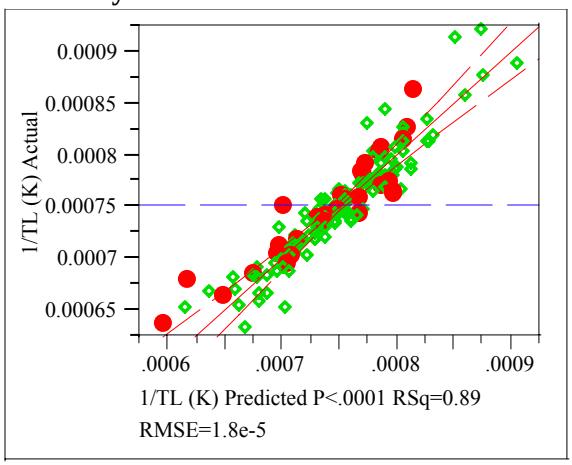

Summary of Fit

RSquare	0.889933
RSquare Adj	0.872922
Root Mean Square Error	0.000018
Mean of Response	0.000752
Observations (or Sum Wgts)	128

Analysis of Variance

Source	DF	Sum of Squares	Mean Square	F Ratio
Model	17	3.04158e-7	1.7892e-8	52.3170
Error	110	3.76185e-8	3.42e-10	Prob > F
C. Total	127	3.41777e-7		<.0001

Lack Of Fit

Source	DF	Sum of Squares	Mean Square	F Ratio
Lack Of Fit	87	3.59956e-8	4.137e-10	5.8637
Pure Error	23	1.62288e-9	7.056e-11	Prob > F
Total Error	110	3.76185e-8		<.0001
				Max RSq
				0.9953

Parameter Estimates

Term	Estimate	Std Error	t Ratio	Prob>|t|
Intercept	0.0005092	0.00009	5.68	<.0001
SL SPL	-0.010905	0.005285	-2.06	0.0414
Al2O3 wt%	-0.000007	0.000002	-4.69	<.0001
B2O3 wt%	0.0000049	0.000001	3.82	0.0002
CaO wt%	0.0000012	0.000003	0.48	0.6328
Cr2O3 wt%	-0.00017	0.000023	-7.29	<.0001
Fe2O3 wt%	-0.000009	0.000001	-6.71	<.0001
K2O wt%	0.0000182	0.000002	8.35	<.0001
Li2O wt%	0.0000186	0.000002	10.38	<.0001
MgO wt%	-0.00001	0.000003	-3.72	0.0003
MnO2 wt%	-0.000003	0.000002	-1.61	0.1093
Na2O wt%	0.0000132	0.000001	11.52	<.0001
NiO wt%	-0.000044	0.000004	-10.84	<.0001
SiO2 wt%	0.000004	0.000001	3.94	0.0001
TiO2 wt%	0.0000213	0.000016	1.32	0.1884
UO2 wt%	-0.000003	0.000002	-1.58	0.1171
ZnO wt%	0.0000023	0.000005	0.44	0.6591
ZrO2 wt%	-9.262e-7	0.000001	-0.62	0.5357

Appendix C. Model Fitting Results for TL Data

Exhibit C.5: Statistical Results from the Fitting of the SLM to Each Data Grouping

Effect Tests

Source	DF	Sum of Squares	F Ratio	Prob > F
SL SPL	1	1.45626e-9	4.2582	0.0414
Al2O3 wt%	1	7.50712e-9	21.9516	<.0001
B2O3 wt%	1	4.99458e-9	14.6046	0.0002
CaO wt%	1	7.8496e-11	0.2295	0.6328
Cr2O3 wt%	1	1.81711e-8	53.1339	<.0001
Fe2O3 wt%	1	1.54038e-8	45.0423	<.0001
K2O wt%	1	2.38222e-8	69.6583	<.0001
Li2O wt%	1	3.68467e-8	107.7433	<.0001
MgO wt%	1	4.72505e-9	13.8165	0.0003
MnO2 wt%	1	8.9125e-10	2.6061	0.1093
Na2O wt%	1	4.54082e-8	132.7779	<.0001
NiO wt%	1	4.0151e-8	117.4053	<.0001
SiO2 wt%	1	5.29774e-9	15.4911	0.0001
TiO2 wt%	1	5.9913e-10	1.7519	0.1884
UO2 wt%	1	8.531e-10	2.4946	0.1171
ZnO wt%	1	6.694e-11	0.1957	0.6591
ZrO2 wt%	1	1.3201e-10	0.3860	0.5357

Residual by Predicted Plot

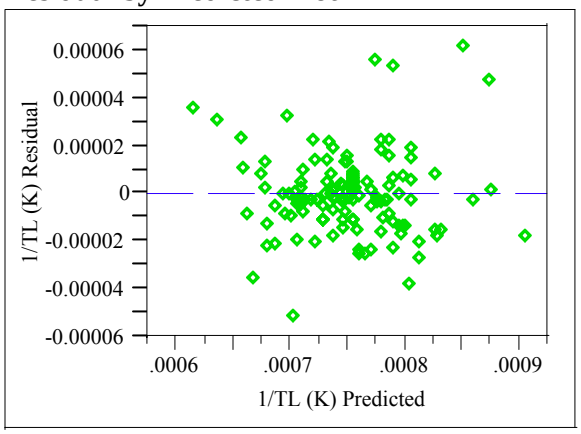

Press
6.6992765e-8

SL SPL
Leverage Plot

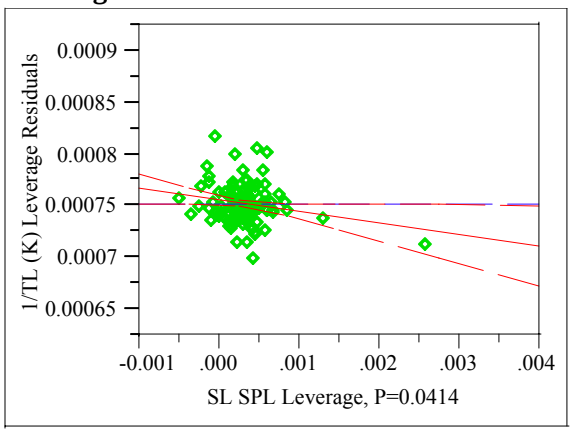

Al2O3 wt%
Leverage Plot

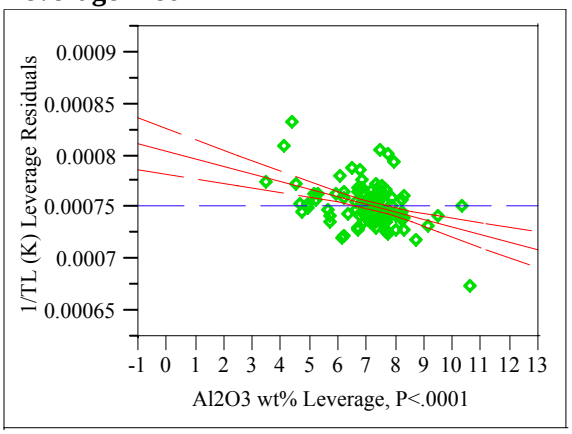

B2O3 wt%
Leverage Plot

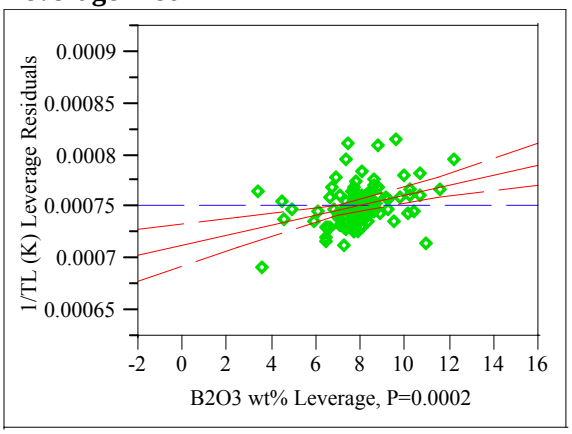

CaO wt%
Leverage Plot

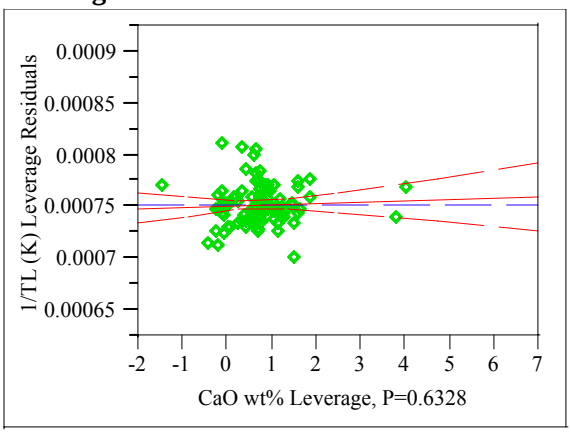

Appendix C. Model Fitting Results for TL Data

Exhibit C.5: Statistical Results from the Fitting of the SLM to Each Data Grouping

Cr2O3 wt%
Leverage Plot

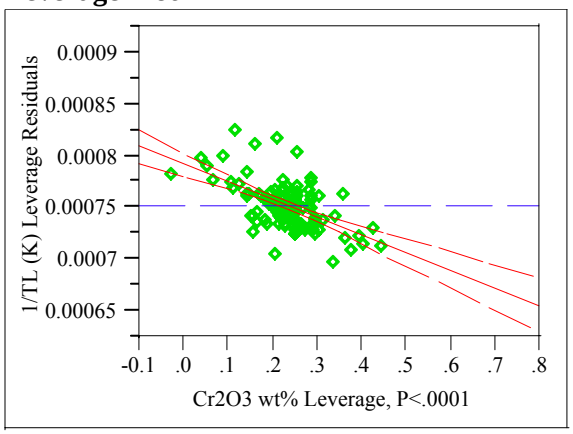

Li2O wt%
Leverage Plot

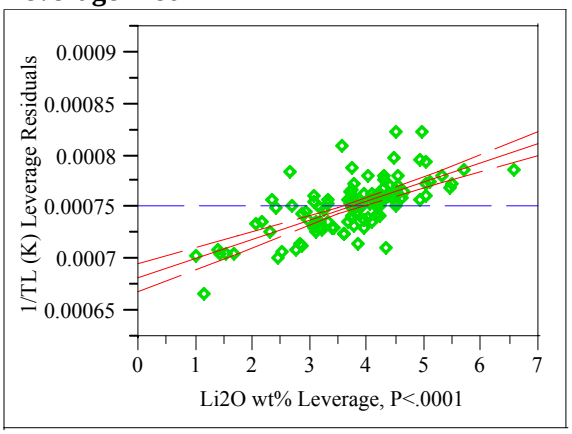

Fe2O3 wt%
Leverage Plot

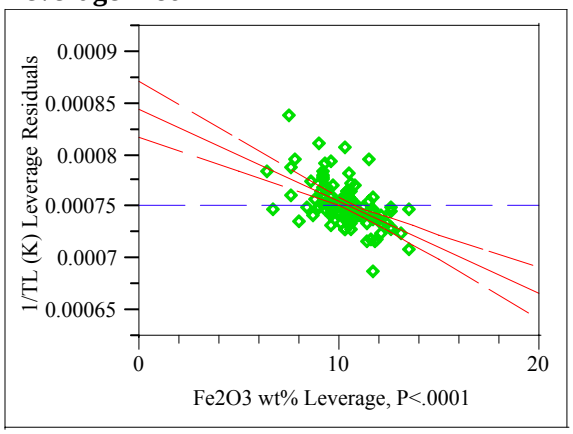

MgO wt%
Leverage Plot

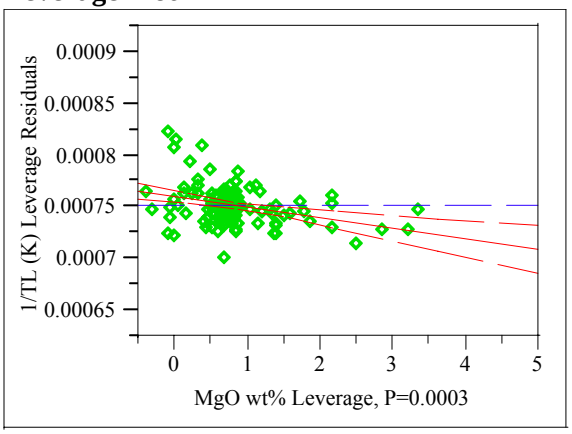

K2O wt%
Leverage Plot

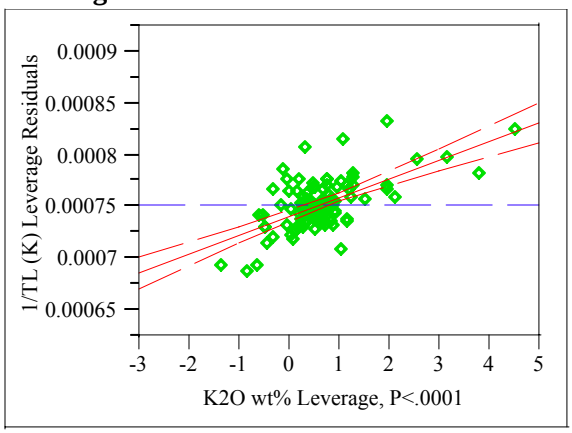

MnO2 wt%
Leverage Plot

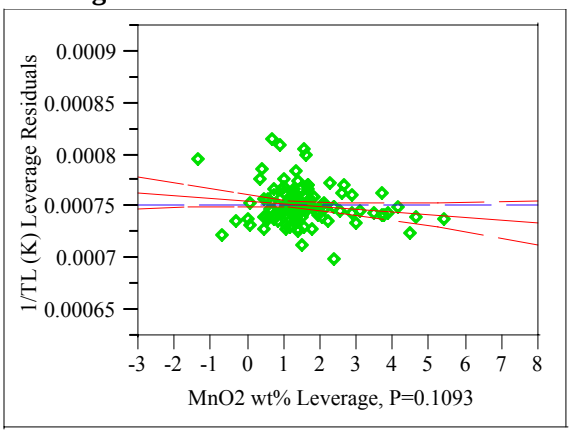

Appendix C. Model Fitting Results for TL Data

Exhibit C.5: Statistical Results from the Fitting of the SLM to Each Data Grouping

Na2O wt%
Leverage Plot

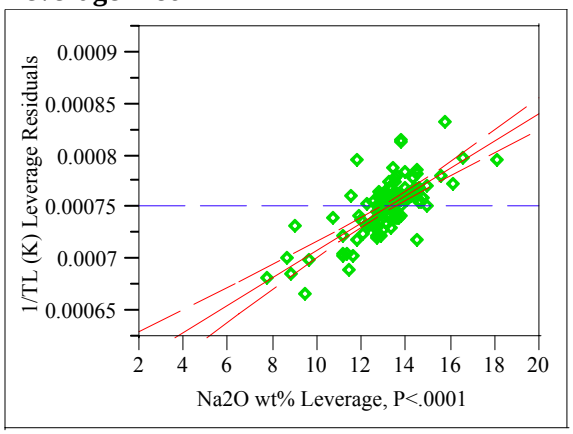

TiO2 wt%
Leverage Plot

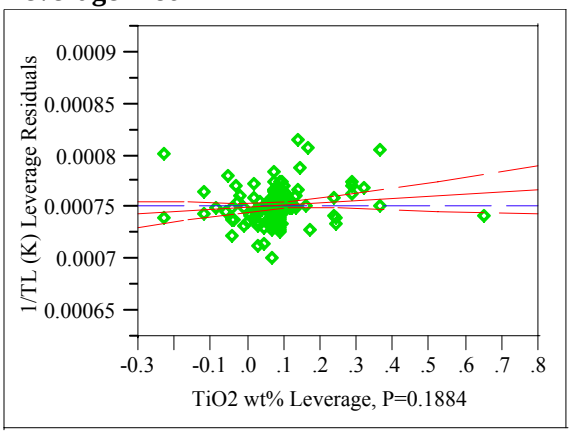

NiO wt%
Leverage Plot

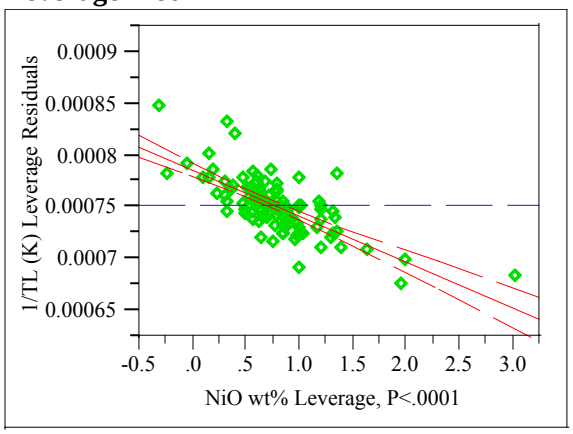

UO2 wt%
Leverage Plot

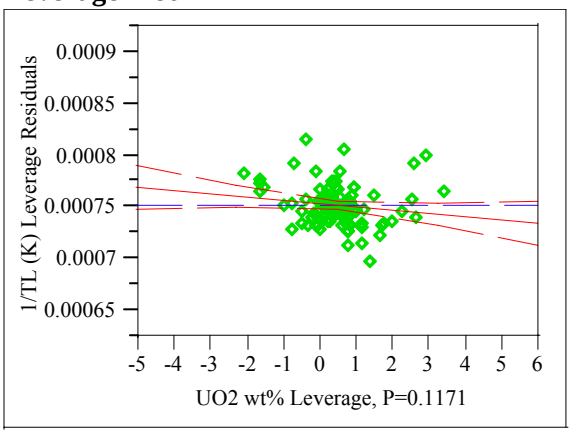

SiO2 wt%
Leverage Plot

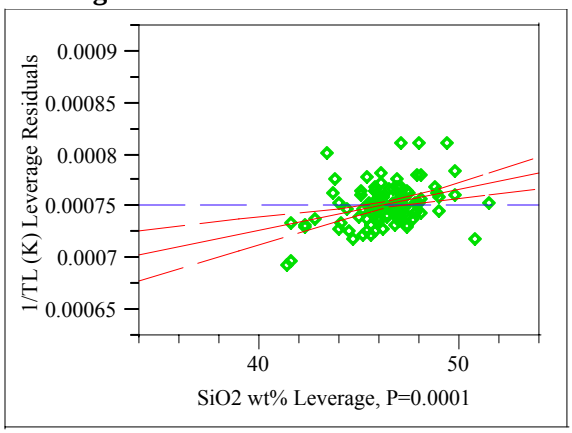

ZnO wt%
Leverage Plot

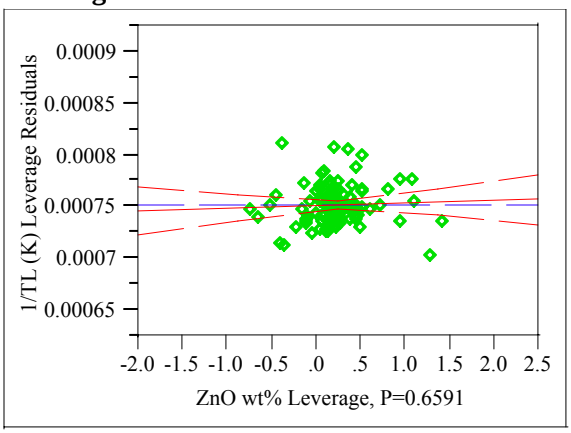

Appendix C. Model Fitting Results for TL Data

Exhibit C.5: Statistical Results from the Fitting of the SLM to Each Data Grouping

ZrO2 wt%
Leverage Plot

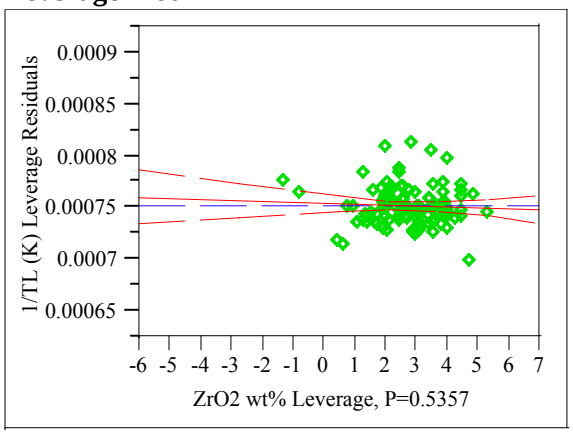

Appendix C. Model Fitting Results for TL Data

Exhibit C.5: Statistical Results from the Fitting of the SLM to Each Data Grouping

Groupings=3
Response 1/TL (K)
Whole Model
Actual by Predicted Plot

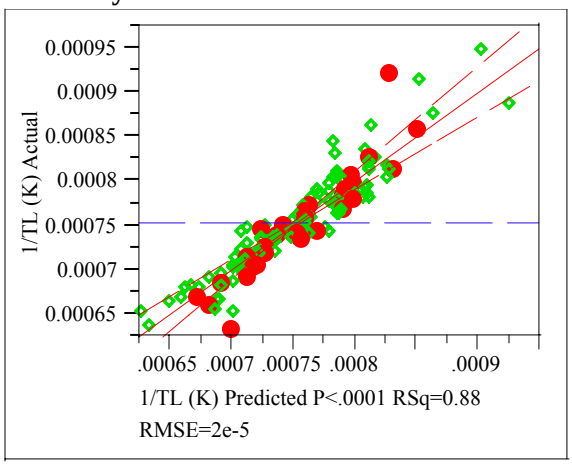

Summary of Fit

RSquare	0.878898
RSquare Adj	0.86001
Root Mean Square Error	0.00002
Mean of Response	0.000753
Observations (or Sum Wgts)	127

Analysis of Variance

Source	DF	Sum of Squares	Mean Square	F Ratio
Model	17	3.06949e-7	1.8056e-8	46.5333
Error	109	4.22942e-8	3.88e-10	Prob > F
C. Total	126	3.49243e-7		<.0001

Lack Of Fit

Source	DF	Sum of Squares	Mean Square	F Ratio
Lack Of Fit	89	4.00169e-8	4.496e-10	3.9489
Pure Error	20	2.27726e-9	1.139e-10	Prob > F
Total Error	109	4.22942e-8		0.0005
				Max RSq
				0.9935

Parameter Estimates

Term	Estimate	Std Error	t Ratio	Prob>|t|
Intercept	0.0006925	0.000084	8.21	<.0001
SL SPL	-0.008473	0.004698	-1.80	0.0741
Al2O3 wt%	-0.00001	0.000001	-7.10	<.0001
B2O3 wt%	0.0000056	0.000001	4.59	<.0001
CaO wt%	2.5072e-7	0.000003	0.09	0.9322
Cr2O3 wt%	-0.000099	0.00002	-4.98	<.0001
Fe2O3 wt%	-0.000009	0.000001	-7.01	<.0001
K2O wt%	0.0000143	0.000002	5.97	<.0001
Li2O wt%	0.0000178	0.000002	8.86	<.0001
MgO wt%	-0.000009	0.000003	-3.20	0.0018
MnO2 wt%	-0.000005	0.000002	-2.63	0.0097
Na2O wt%	0.0000111	0.000001	9.88	<.0001
NiO wt%	-0.000039	0.000004	-8.83	<.0001
SiO2 wt%	0.0000011	9.673e-7	1.13	0.2614
TiO2 wt%	0.0000015	0.000023	0.07	0.9483
UO2 wt%	-0.000006	0.000002	-2.93	0.0041
ZnO wt%	-0.000009	0.000005	-1.89	0.0608
ZrO2 wt%	-0.000006	0.000001	-4.48	<.0001

Effect Tests

Source	DF	Sum of Squares	F Ratio	Prob > F
SL SPL	1	1.26218e-9	3.2529	0.0741
Al2O3 wt%	1	1.95872e-8	50.4799	<.0001
B2O3 wt%	1	8.17533e-9	21.0694	<.0001
CaO wt%	1	2.8224e-12	0.0073	0.9322
Cr2O3 wt%	1	9.60677e-9	24.7585	<.0001
Fe2O3 wt%	1	1.90667e-8	49.1386	<.0001
K2O wt%	1	1.38279e-8	35.6371	<.0001
Li2O wt%	1	3.04269e-8	78.4159	<.0001
MgO wt%	1	3.98442e-9	10.2686	0.0018
MnO2 wt%	1	2.68959e-9	6.9316	0.0097
Na2O wt%	1	3.7864e-8	97.5826	<.0001
NiO wt%	1	3.02205e-8	77.8838	<.0001
SiO2 wt%	1	4.9462e-10	1.2747	0.2614
TiO2 wt%	1	1.6401e-12	0.0042	0.9483
UO2 wt%	1	3.34182e-9	8.6125	0.0041
ZnO wt%	1	1.39296e-9	3.5899	0.0608
ZrO2 wt%	1	7.79283e-9	20.0836	<.0001

Residual by Predicted Plot

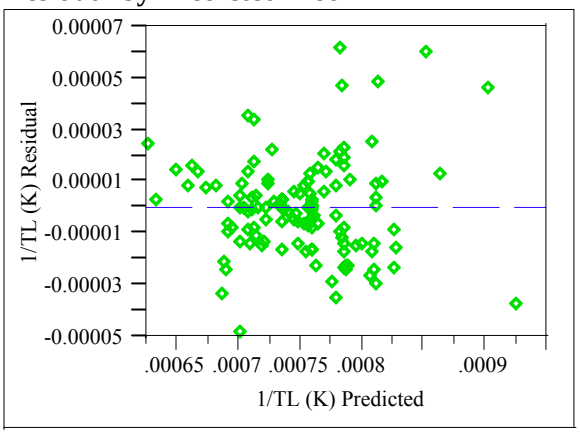

Press
7.5667986e-8

Appendix C. Model Fitting Results for TL Data

Exhibit C.5: Statistical Results from the Fitting of the SLM to Each Data Grouping

SL SPL
Leverage Plot

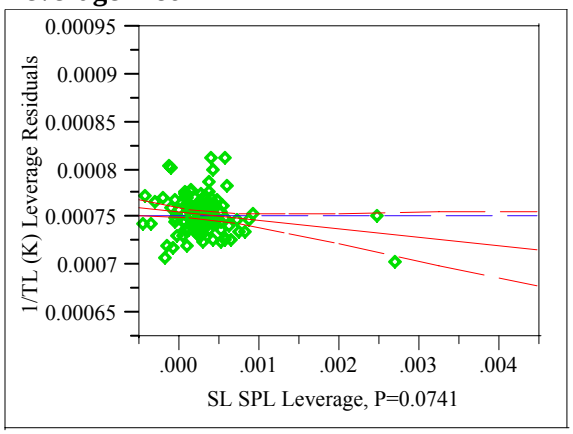

CaO wt%
Leverage Plot

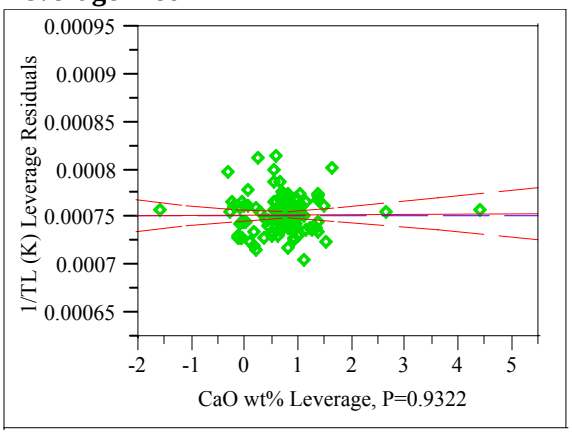

Al2O3 wt%
Leverage Plot

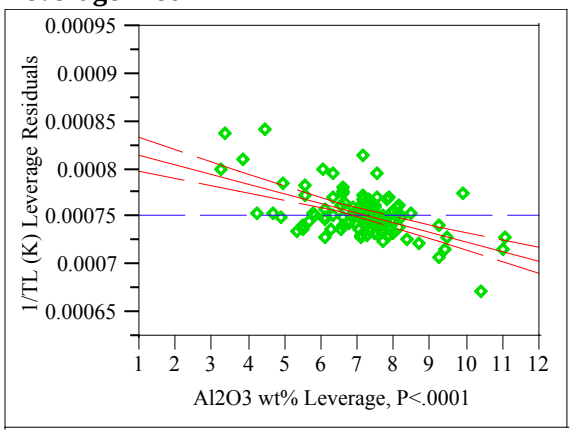

Cr2O3 wt%
Leverage Plot

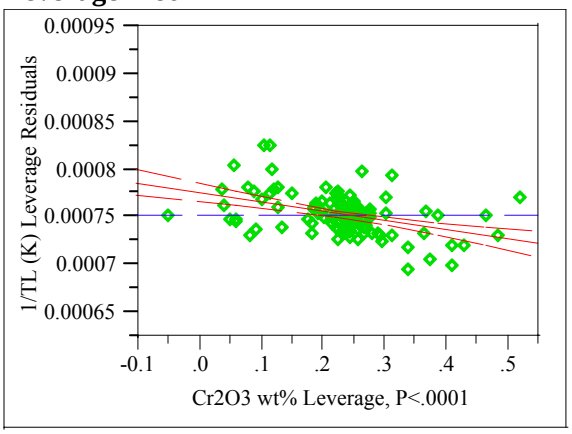

B2O3 wt%
Leverage Plot

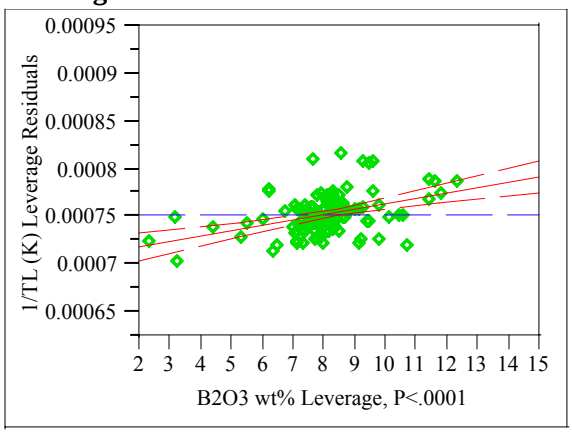

Fe2O3 wt%
Leverage Plot

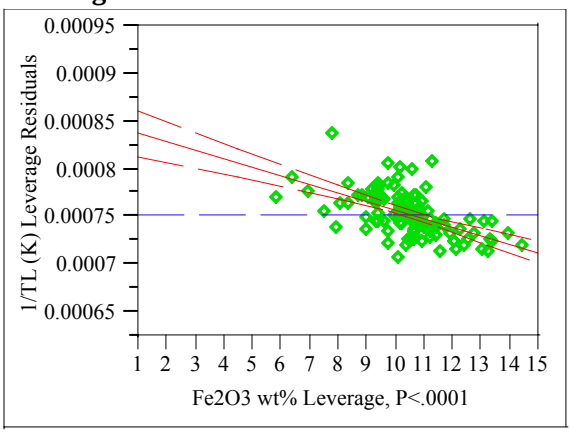

Appendix C. Model Fitting Results for TL Data

Exhibit C.5: Statistical Results from the Fitting of the SLM to Each Data Grouping

K2O wt%
Leverage Plot

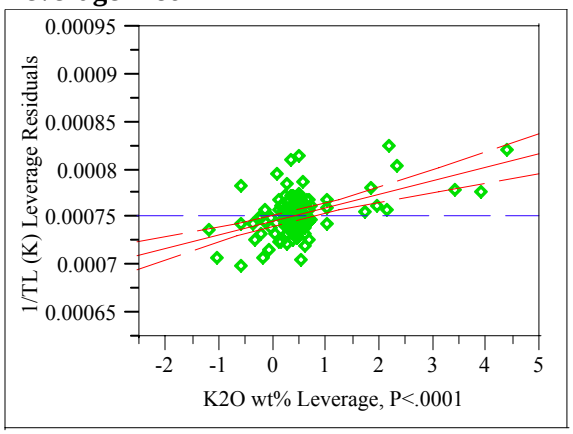

MnO2 wt%
Leverage Plot

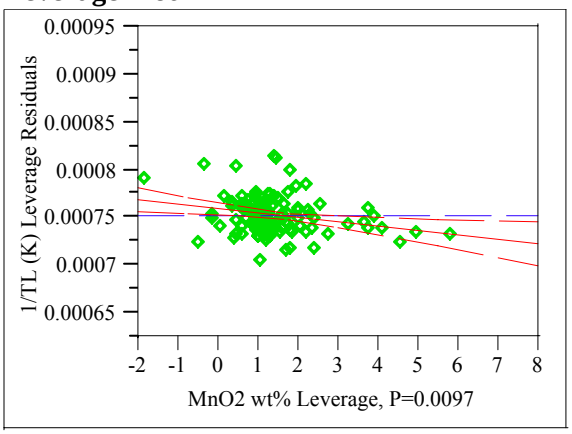

Li2O wt%
Leverage Plot

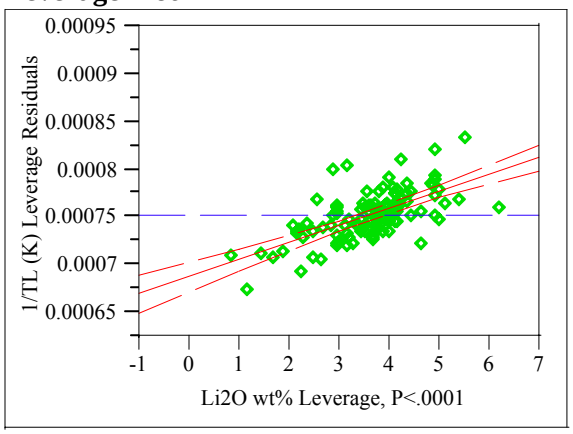

Na2O wt%
Leverage Plot

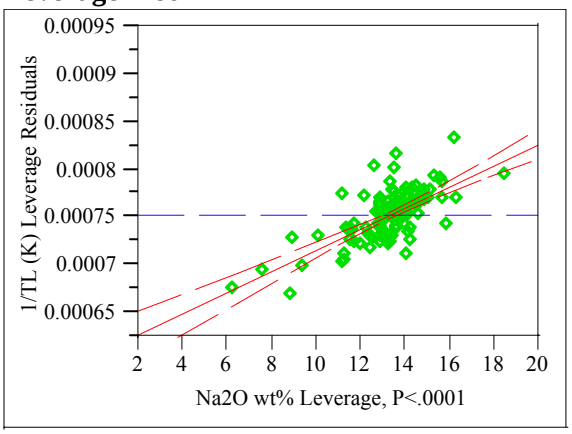

MgO wt%
Leverage Plot

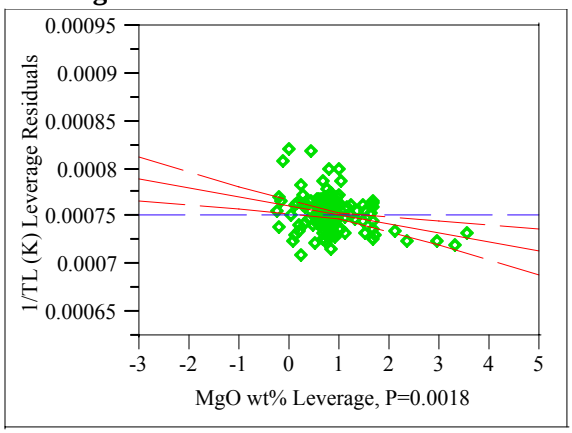

NiO wt%
Leverage Plot

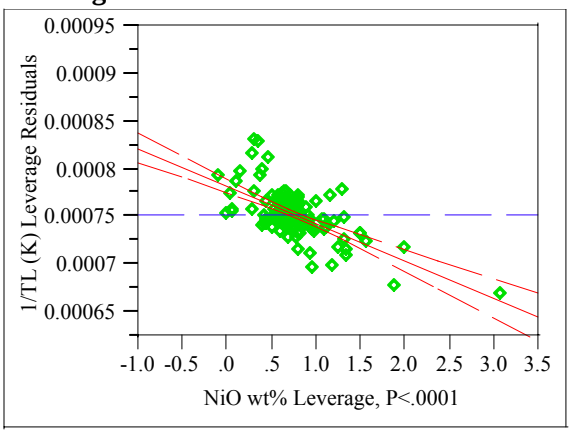

Appendix C. Model Fitting Results for TL Data

Exhibit C.5: Statistical Results from the Fitting of the SLM to Each Data Grouping

SiO2 wt%
Leverage Plot

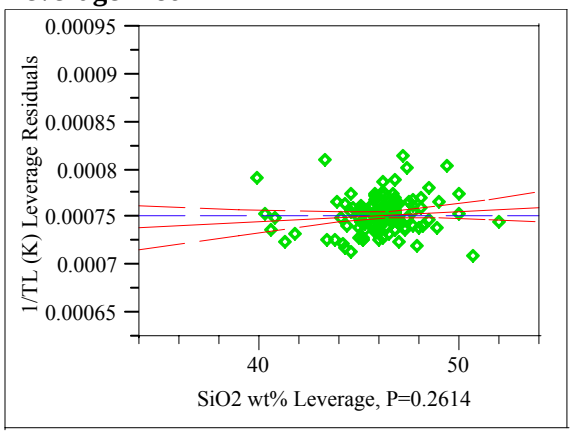

ZnO wt%
Leverage Plot

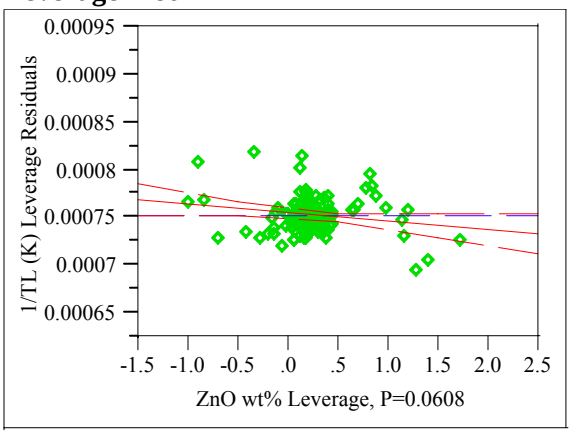

TiO2 wt%
Leverage Plot

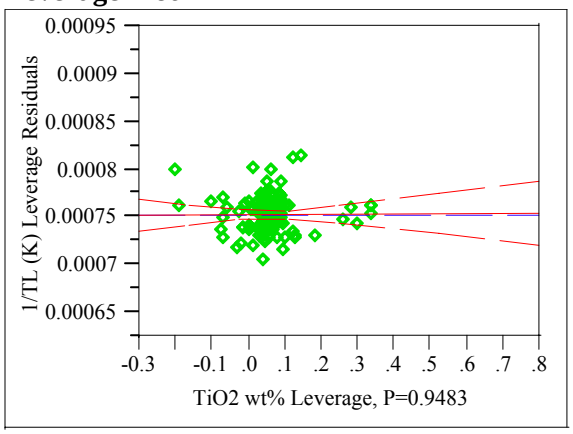

ZrO2 wt%
Leverage Plot

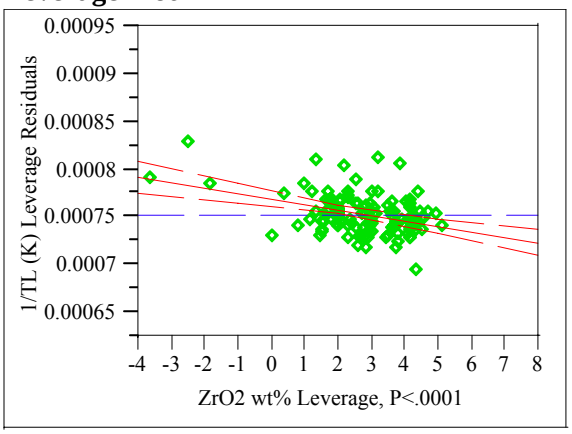

UO2 wt%
Leverage Plot

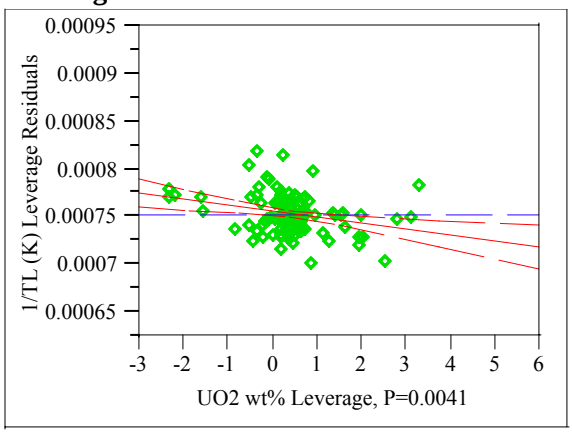

Appendix C. Model Fitting Results for TL Data

Exhibit C.5: Statistical Results from the Fitting of the SLM to Each Data Grouping

Groupings=4
Response 1/TL (K)
Whole Model
Actual by Predicted Plot

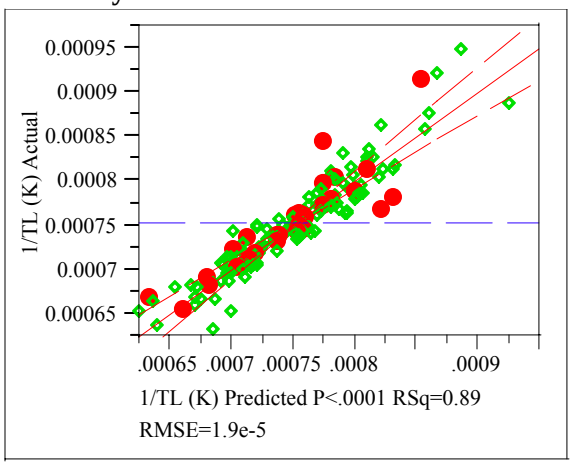

Summary of Fit

RSquare	0.887127
RSquare Adj	0.86984
Root Mean Square Error	0.000019
Mean of Response	0.000753
Observations (or Sum Wgts)	129

Analysis of Variance

Source	DF	Sum of Squares	Mean Square	F Ratio
Model	17	3.30701e-7	1.9453e-8	51.3179
Error	111	4.20767e-8	3.791e-10	Prob > F
C. Total	128	3.72778e-7		<.0001

Lack Of Fit

Source	DF	Sum of Squares	Mean Square	F Ratio
Lack Of Fit	87	4.01553e-8	4.616e-10	5.7652
Pure Error	24	1.92142e-9	8.006e-11	Prob > F
Total Error	111	4.20767e-8		<.0001
				Max RSq
				0.9948

Parameter Estimates

Term	Estimate	Std Error	t Ratio	Prob>|t|
Intercept	0.0006337	0.000088	7.17	<.0001
SL SPL	-0.003548	0.005242	-0.68	0.4999
Al2O3 wt%	-0.000009	0.000001	-6.36	<.0001
B2O3 wt%	0.0000043	0.000001	3.43	0.0008
CaO wt%	3.445e-7	0.000003	0.13	0.9005
Cr2O3 wt%	-0.000125	0.000021	-6.05	<.0001
Fe2O3 wt%	-0.000009	0.000001	-6.98	<.0001
K2O wt%	0.0000142	0.000002	6.23	<.0001
Li2O wt%	0.0000229	0.000002	11.40	<.0001
MgO wt%	-0.000009	0.000003	-3.13	0.0022
MnO2 wt%	-0.000003	0.000002	-1.74	0.0851
Na2O wt%	0.0000126	0.000001	11.45	<.0001
NiO wt%	-0.000049	0.000005	-10.30	<.0001
SiO2 wt%	0.0000017	0.000001	1.64	0.1046
TiO2 wt%	0.0000072	0.000019	0.38	0.7083
UO2 wt%	-0.000004	0.000002	-1.81	0.0722
ZnO wt%	-0.000004	0.000004	-0.87	0.3840
ZrO2 wt%	-0.000005	0.000001	-4.44	<.0001

Effect Tests

Source	DF	Sum of Squares	F Ratio	Prob > F
SL SPL	1	1.7364e-10	0.4581	0.4999
Al2O3 wt%	1	1.53481e-8	40.4889	<.0001
B2O3 wt%	1	4.46461e-9	11.7778	0.0008
CaO wt%	1	5.9497e-12	0.0157	0.9005
Cr2O3 wt%	1	1.38567e-8	36.5544	<.0001
Fe2O3 wt%	1	1.84708e-8	48.7268	<.0001
K2O wt%	1	1.47238e-8	38.8421	<.0001
Li2O wt%	1	4.92844e-8	130.0143	<.0001
MgO wt%	1	3.71547e-9	9.8016	0.0022
MnO2 wt%	1	1.14448e-9	3.0192	0.0851
Na2O wt%	1	4.96848e-8	131.0706	<.0001
NiO wt%	1	4.02201e-8	106.1023	<.0001
SiO2 wt%	1	1.0151e-9	2.6779	0.1046
TiO2 wt%	1	5.3348e-11	0.1407	0.7083
UO2 wt%	1	1.24862e-9	3.2939	0.0722
ZnO wt%	1	2.8957e-10	0.7639	0.3840
ZrO2 wt%	1	7.48382e-9	19.7426	<.0001

Residual by Predicted Plot

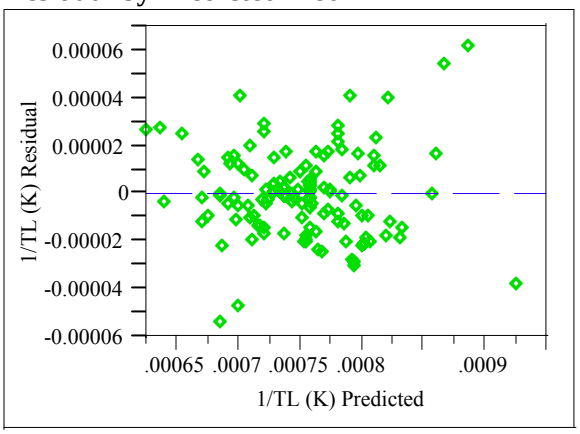

Press
8.6801834e-8

Appendix C. Model Fitting Results for TL Data

Exhibit C.5: Statistical Results from the Fitting of the SLM to Each Data Grouping

SL SPL
Leverage Plot

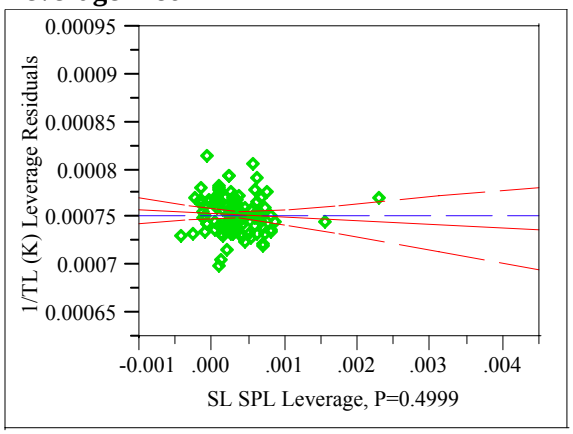

CaO wt%
Leverage Plot

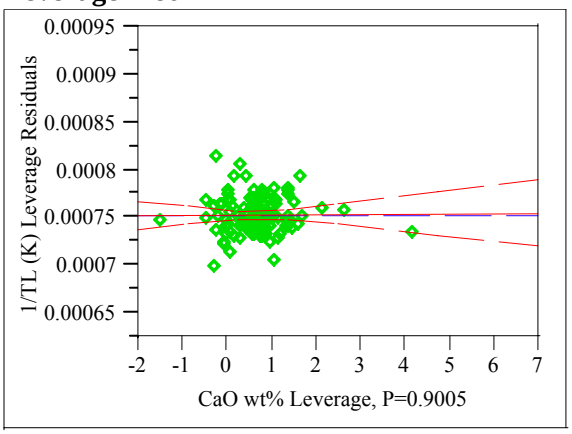

Al2O3 wt%
Leverage Plot

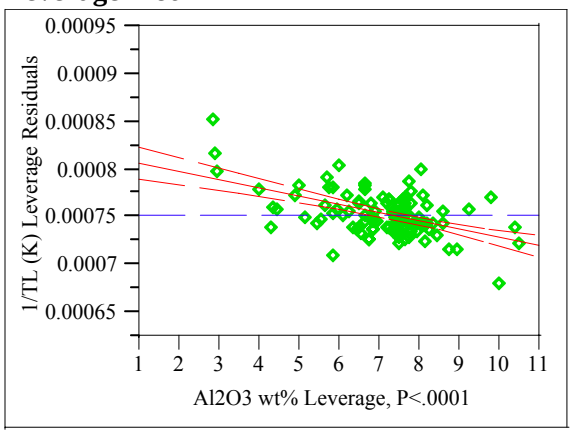

Cr2O3 wt%
Leverage Plot

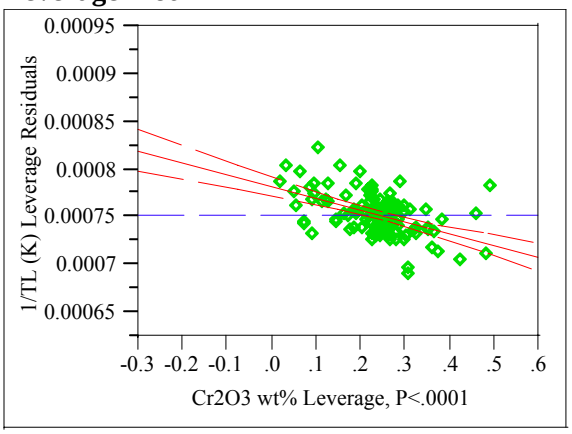

B2O3 wt%
Leverage Plot

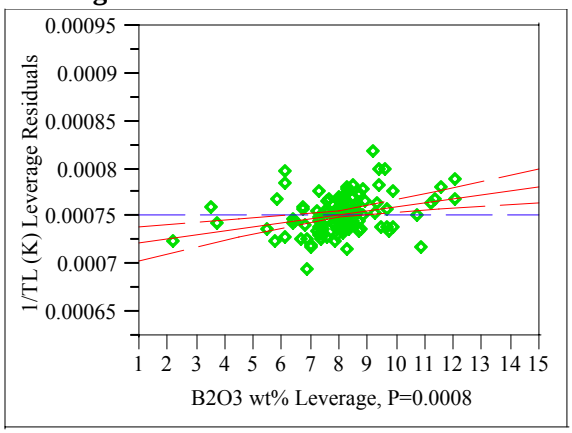

Fe2O3 wt%
Leverage Plot

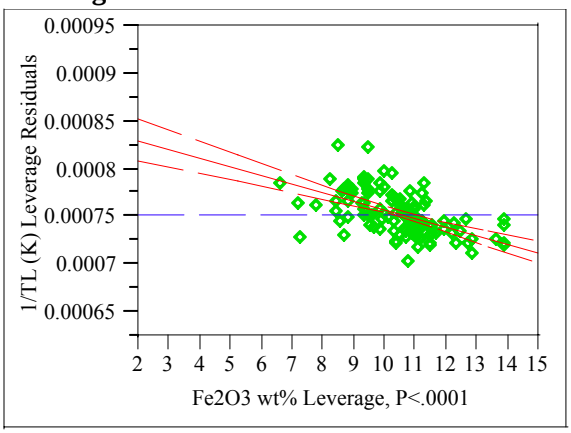

Appendix C. Model Fitting Results for TL Data

Exhibit C.5: Statistical Results from the Fitting of the SLM to Each Data Grouping

K2O wt%
Leverage Plot

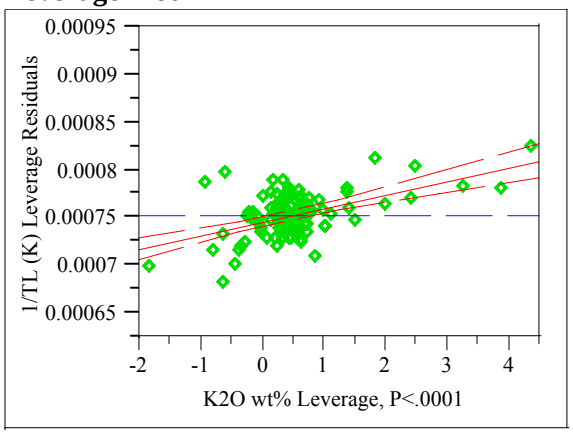

MnO2 wt%
Leverage Plot

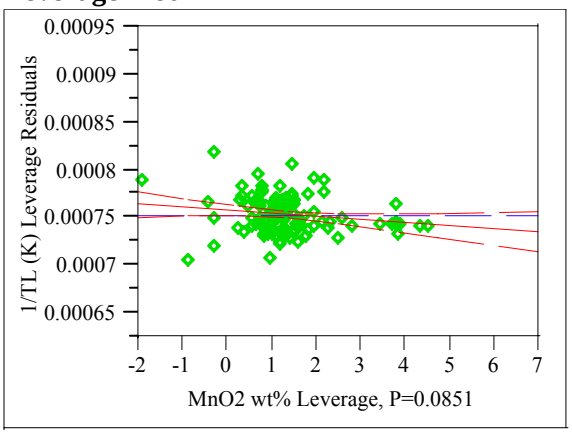

Li2O wt%
Leverage Plot

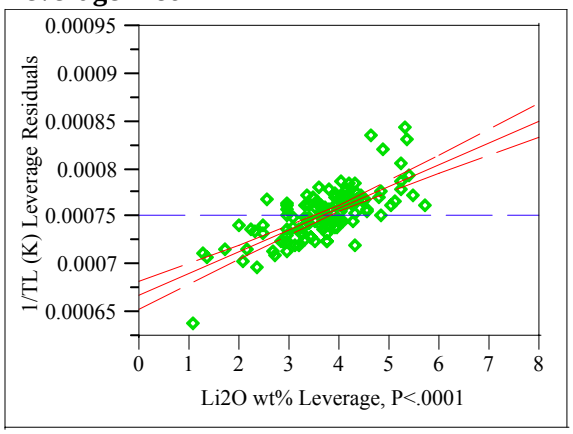

Na2O wt%
Leverage Plot

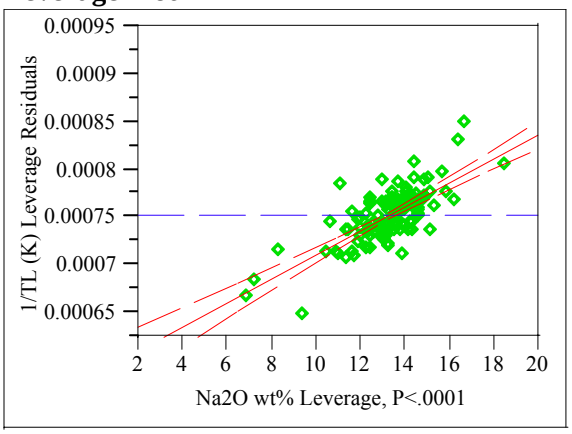

MgO wt%
Leverage Plot

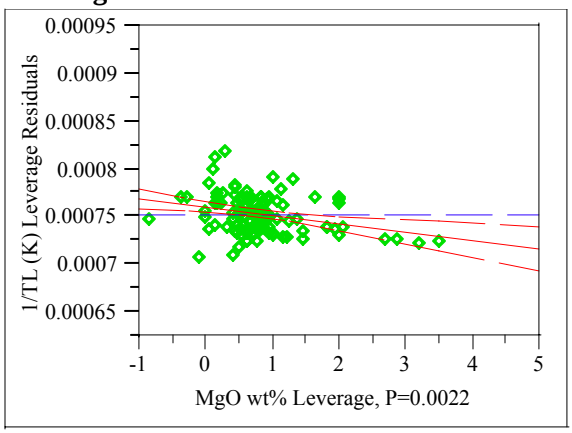

NiO wt%
Leverage Plot

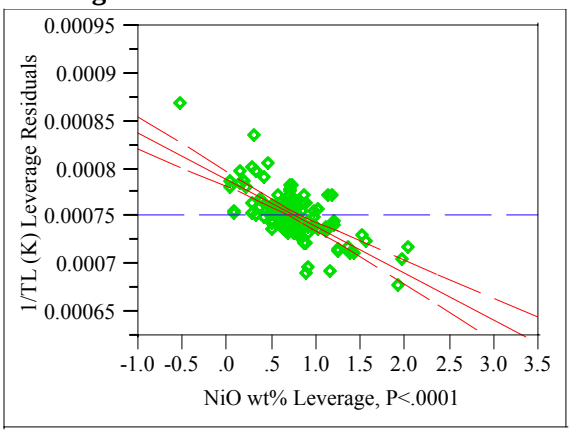

Appendix C. Model Fitting Results for TL Data

Exhibit C.5: Statistical Results from the Fitting of the SLM to Each Data Grouping

SiO2 wt%
Leverage Plot

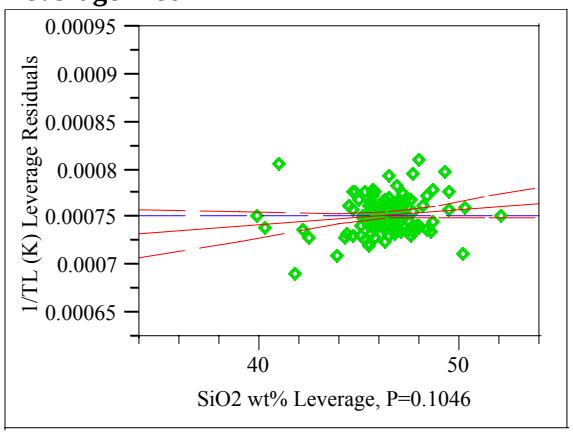

ZnO wt%
Leverage Plot

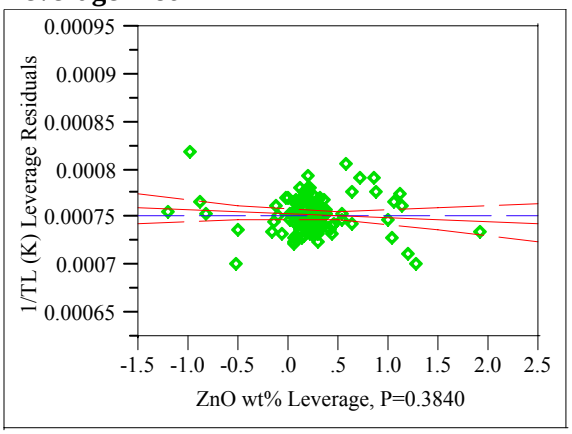

TiO2 wt%
Leverage Plot

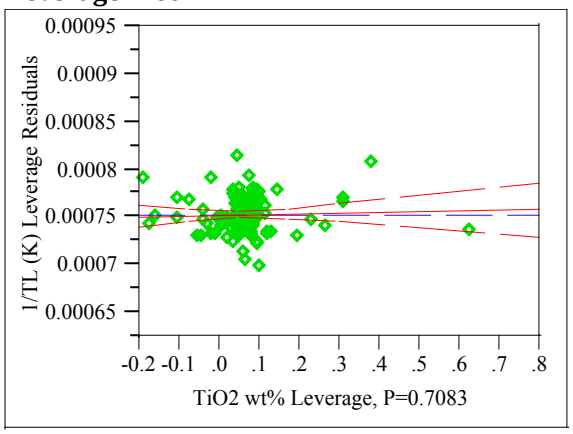

ZrO2 wt%
Leverage Plot

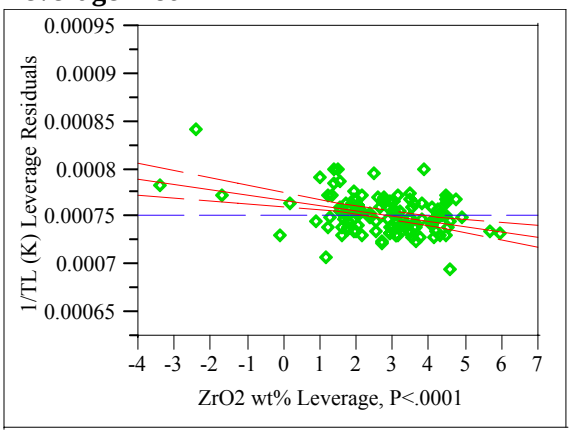

UO2 wt%
Leverage Plot

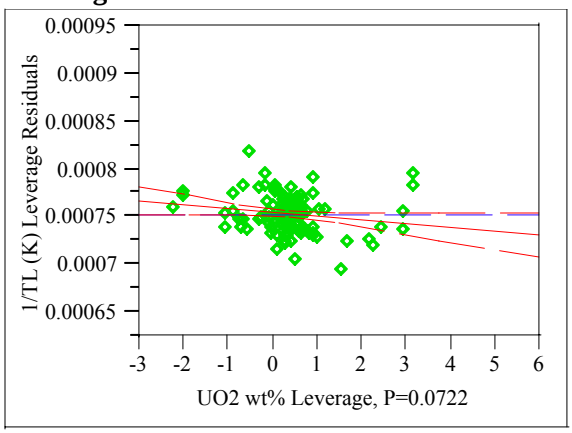

Appendix C. Model Fitting Results for TL Data

Exhibit C.5: Statistical Results from the Fitting of the SLM to Each Data Grouping

Groupings=5
Response 1/TL (K)
Whole Model
Actual by Predicted Plot

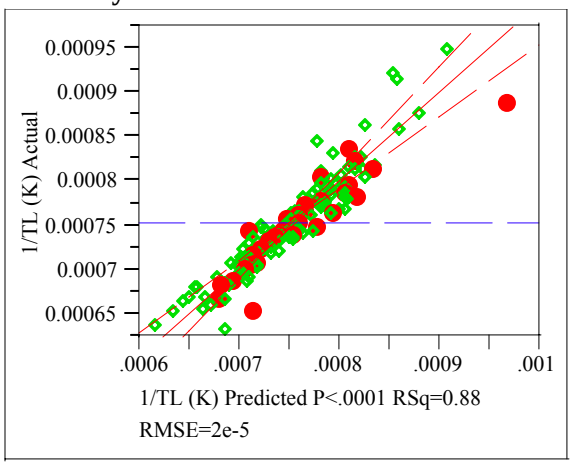

Summary of Fit

RSquare	0.882776
RSquare Adj	0.864659
Root Mean Square Error	0.00002
Mean of Response	0.000753
Observations (or Sum Wgts)	128

Analysis of Variance

Source	DF	Sum of Squares	Mean Square	F Ratio
Model	17	3.32057e-7	1.9533e-8	48.7278
Error	110	4.40941e-8	4.009e-10	Prob > F
C. Total	127	3.76151e-7		<.0001

Lack Of Fit

Source	DF	Sum of Squares	Mean Square	F Ratio
Lack Of Fit	89	4.18711e-8	4.705e-10	4.4443
Pure Error	21	2.22299e-9	1.059e-10	Prob > F
Total Error	110	4.40941e-8		0.0002
				Max RSq
				0.9941

Parameter Estimates

Term	Estimate	Std Error	t Ratio	Prob>|t|
Intercept	0.0005756	0.000091	6.35	<.0001
SL SPL	-0.012176	0.00455	-2.68	0.0086
Al2O3 wt%	-0.000009	0.000002	-5.67	<.0001
B2O3 wt%	0.0000064	0.000001	4.70	<.0001
CaO wt%	-2.564e-7	0.000003	-0.10	0.9214
Cr2O3 wt%	-0.000112	0.00002	-5.48	<.0001
Fe2O3 wt%	-0.000009	0.000001	-7.35	<.0001
K2O wt%	0.0000141	0.000003	4.88	<.0001
Li2O wt%	0.0000239	0.000002	11.66	<.0001
MgO wt%	-0.00001	0.000003	-3.16	0.0020
MnO2 wt%	-0.000005	0.000002	-2.87	0.0050
Na2O wt%	0.0000136	0.000001	12.01	<.0001
NiO wt%	-0.000042	0.000004	-9.56	<.0001
SiO2 wt%	0.0000022	0.000001	2.13	0.0351
TiO2 wt%	0.0000061	0.000019	0.32	0.7496
UO2 wt%	-0.000004	0.000002	-1.99	0.0489
ZnO wt%	0.0000045	0.000005	0.83	0.4107
ZrO2 wt%	-0.000006	0.000001	-4.61	<.0001

Effect Tests

Source	DF	Sum of Squares	F Ratio	Prob > F
SL SPL	1	2.87054e-9	7.1610	0.0086
Al2O3 wt%	1	1.28732e-8	32.1143	<.0001
B2O3 wt%	1	8.8608e-9	22.1047	<.0001
CaO wt%	1	3.9186e-12	0.0098	0.9214
Cr2O3 wt%	1	1.20486e-8	30.0573	<.0001
Fe2O3 wt%	1	2.16457e-8	53.9989	<.0001
K2O wt%	1	9.52767e-9	23.7684	<.0001
Li2O wt%	1	5.45089e-8	135.9815	<.0001
MgO wt%	1	3.99837e-9	9.9746	0.0020
MnO2 wt%	1	3.29685e-9	8.2245	0.0050
Na2O wt%	1	5.78439e-8	144.3013	<.0001
NiO wt%	1	3.6617e-8	91.3473	<.0001
SiO2 wt%	1	1.82441e-9	4.5513	0.0351
TiO2 wt%	1	4.1039e-11	0.1024	0.7496
UO2 wt%	1	1.58998e-9	3.9665	0.0489
ZnO wt%	1	2.7334e-10	0.6819	0.4107
ZrO2 wt%	1	8.50116e-9	21.2076	<.0001

Residual by Predicted Plot

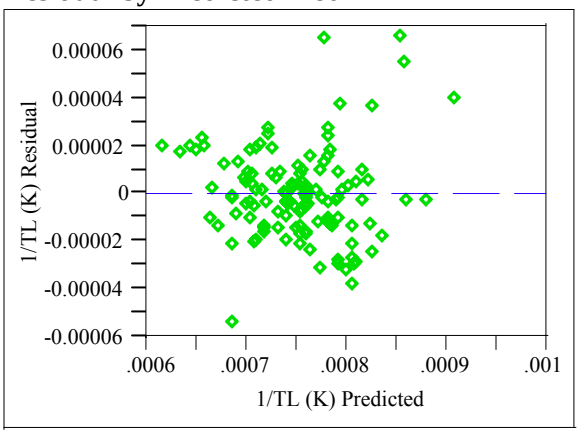

Press
8.4661476e-8

Appendix C. Model Fitting Results for TL Data

Exhibit C.5: Statistical Results from the Fitting of the SLM to Each Data Grouping

SL SPL
Leverage Plot

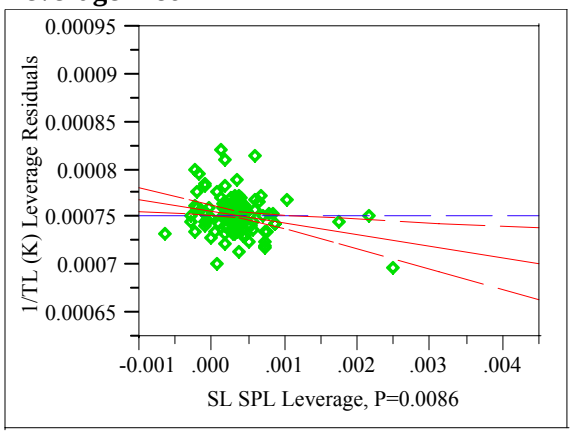

CaO wt%
Leverage Plot

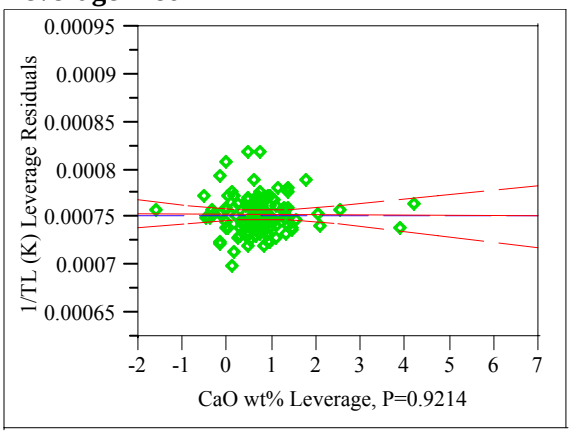

Al2O3 wt%
Leverage Plot

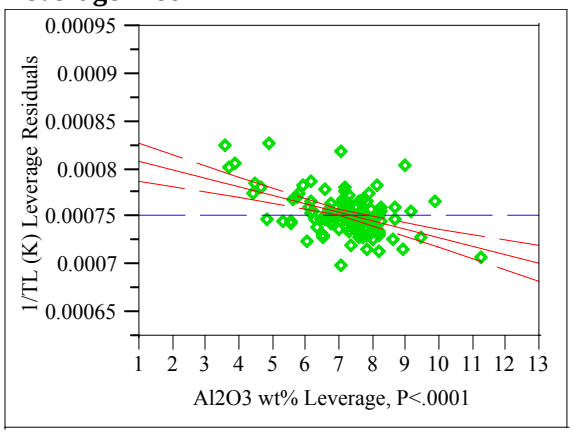

Cr2O3 wt%
Leverage Plot

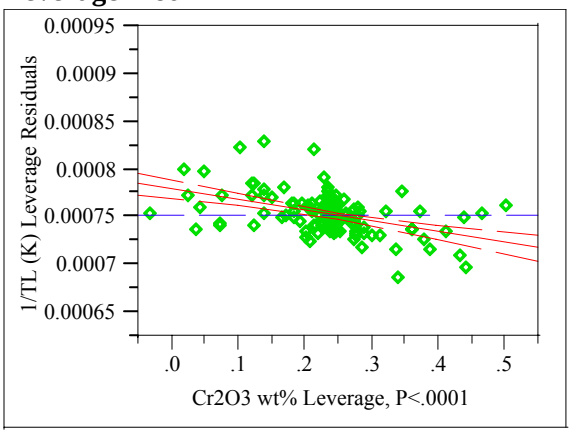

B2O3 wt%
Leverage Plot

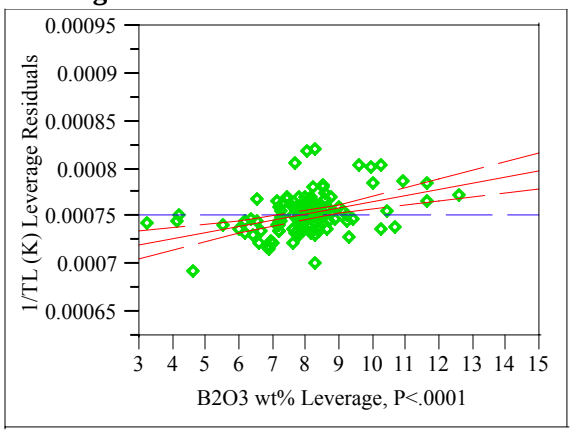

Fe2O3 wt%
Leverage Plot

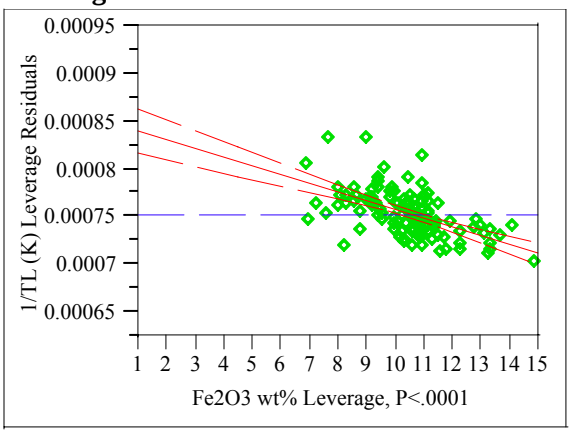

Appendix C. Model Fitting Results for TL Data

Exhibit C.5: Statistical Results from the Fitting of the SLM to Each Data Grouping

K2O wt%
Leverage Plot

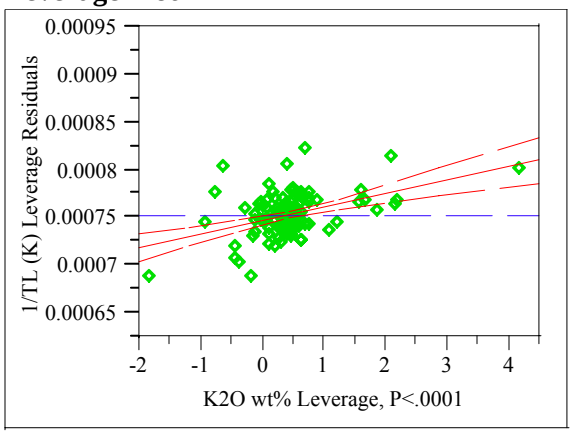

MnO2 wt%
Leverage Plot

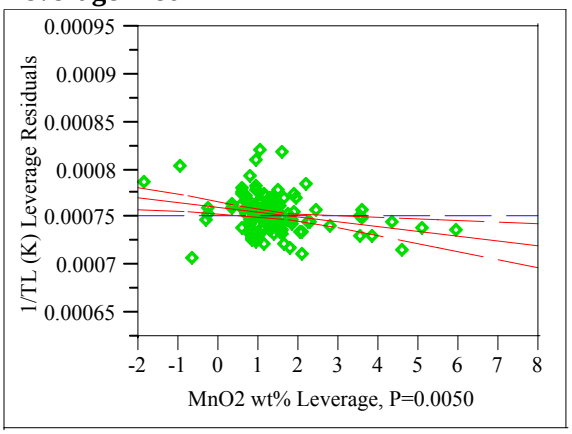

Li2O wt%
Leverage Plot

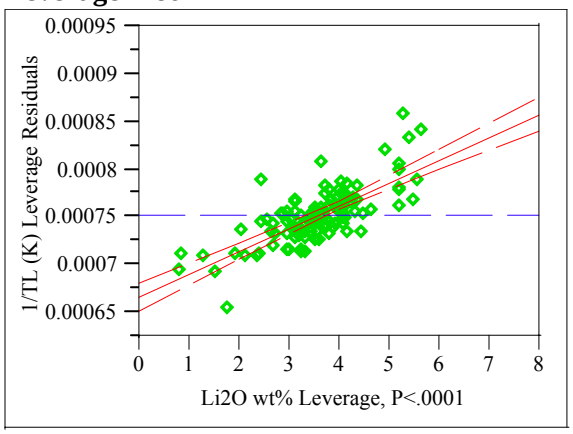

Na2O wt%
Leverage Plot

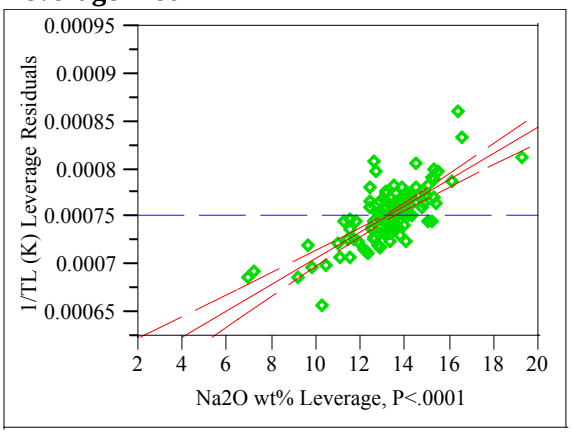

MgO wt%
Leverage Plot

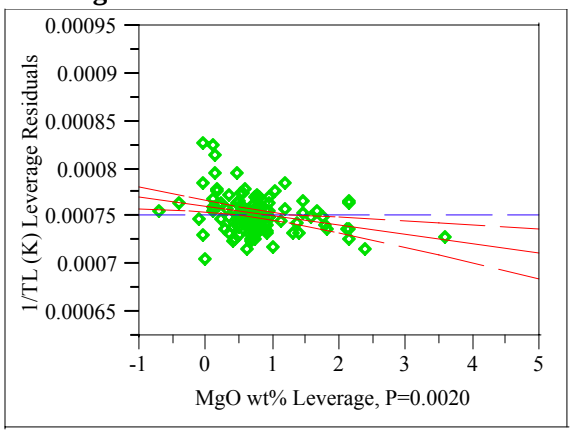

NiO wt%
Leverage Plot

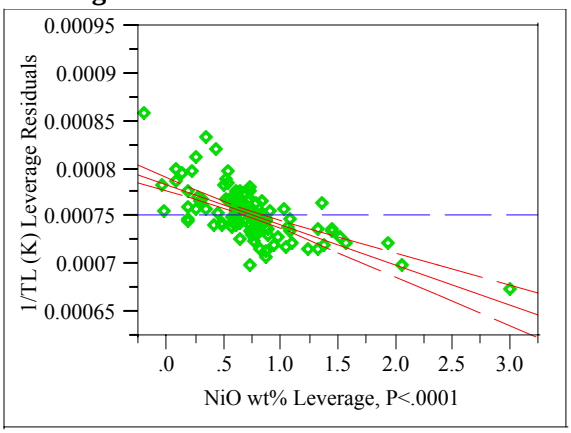

Appendix C. Model Fitting Results for TL Data

Exhibit C.5: Statistical Results from the Fitting of the SLM to Each Data Grouping

SiO2 wt%
Leverage Plot

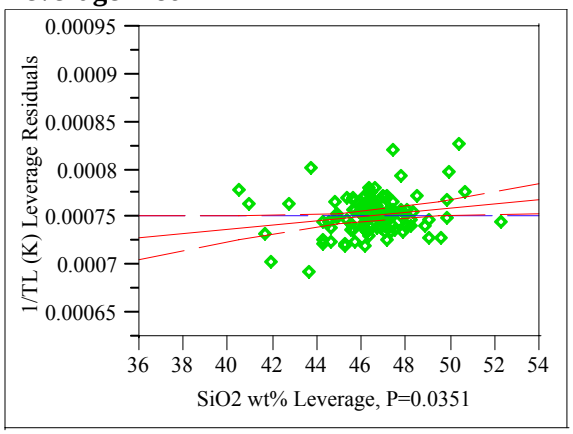

ZnO wt%
Leverage Plot

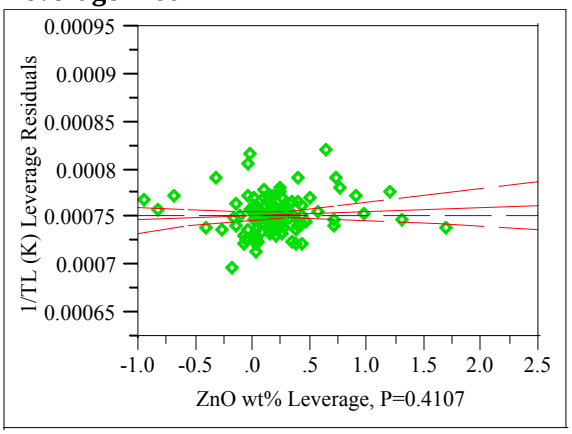

TiO2 wt%
Leverage Plot

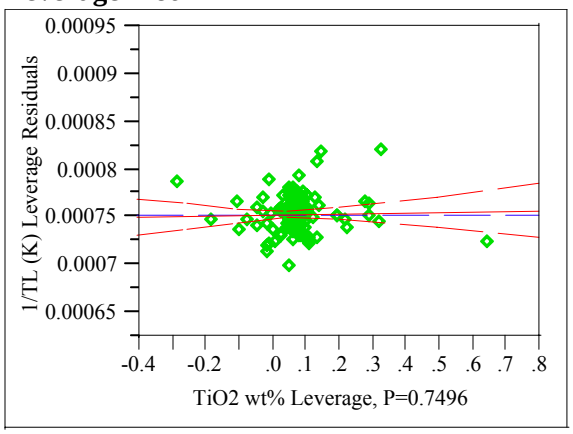

ZrO2 wt%
Leverage Plot

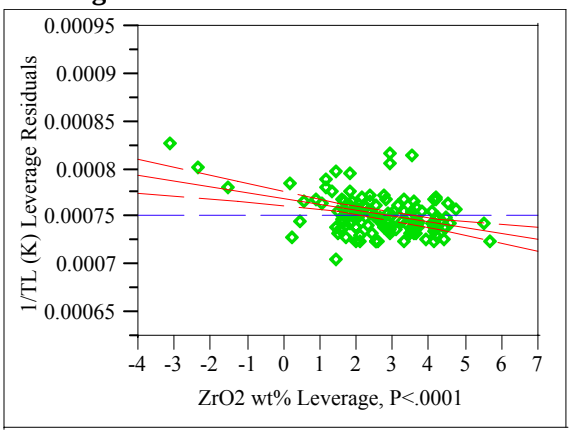

UO2 wt%
Leverage Plot

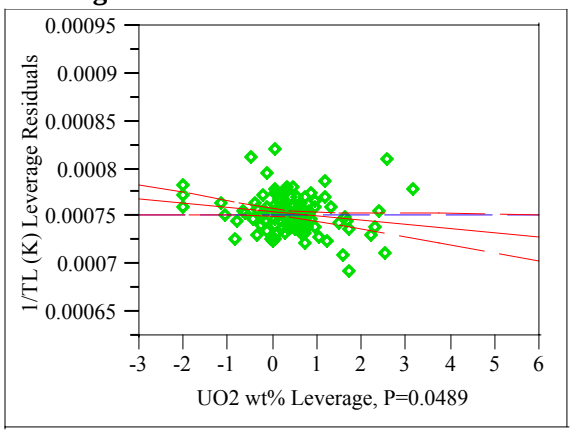

Appendix C. Model Fitting Results for TL Data

Exhibit C.6: Statistical Results from the Fitting of the LMM to Each Data Grouping

Groupings=1
Response TL (°C)
Singularity Detail
Intercept = 0
Whole Model
Actual by Predicted Plot

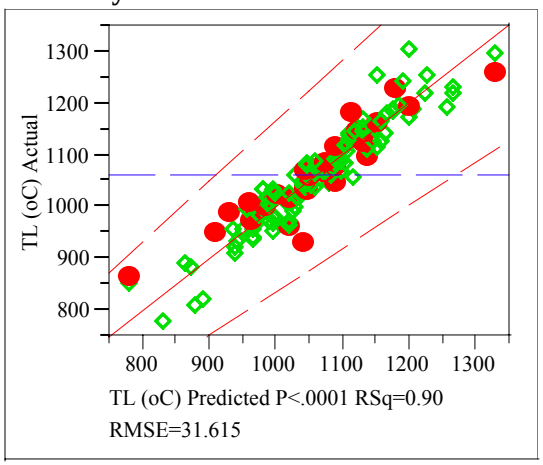

Summary of Fit

RSquare	0.902005
RSquare Adj	0.88788
Root Mean Square Error	31.61525
Mean of Response	1061.511
Observations (or Sum Wgts)	128

Analysis of Variance

Source	DF	Sum of Squares	Mean Square	F Ratio
Model	16	1021226.9	63826.7	63.8571
Error	111	110947.2	999.5	Prob > F
C. Total	127	1132174.1		<.0001

Tested against reduced model: Y=mean

Lack Of Fit

Source	DF	Sum of Squares	Mean Square	F Ratio
Lack Of Fit	89	106047.78	1191.55	5.3505
Pure Error	22	4899.40	222.70	Prob > F
Total Error	111	110947.18		<.0001
				Max RSq
				0.9957

Parameter Estimates

Term		Estimate	Std Error	t Ratio	Prob>|t|
Intercept	Zeroed	0	0	.	.
Al2O2 n		2932.8632	187.091	15.68	<.0001
B2O3 n		817.11485	128.6517	6.35	<.0001
CdO n		7840.7991	1341.977	5.84	<.0001
Cr2O3 n		25829.579	2796.233	9.24	<.0001
F n		4882.6425	2121.705	2.30	0.0232
Fe2O3 n		2818.902	150.9225	18.68	<.0001
K2O n		-1233.544	433.7682	-2.84	0.0053
Li2O n		-1846.952	250.0692	-7.39	<.0001
MgO n		2243.9843	454.5602	4.94	<.0001
MnO n		1538.3463	253.3092	6.07	<.0001
Na2O n		-911.0931	116.0937	-7.85	<.0001

Appendix C. Model Fitting Results for TL Data

Exhibit C.6: Statistical Results from the Fitting of the LMM to Each Data Grouping

Term	Estimate	Std Error	t Ratio	Prob>|t|
NiO n	9721.2736	629.6947	15.44	<.0001
P2O5 n	-6203.041	2943.121	-2.11	0.0373
SiO2 n	821.5697	58.4473	14.06	<.0001
ThO2 n	1638.6765	601.3613	2.72	0.0075
U3O8 n	2541.0642	306.1032	8.30	<.0001
ZrO2 n	2241.0646	215.3444	10.41	<.0001

Residual by Predicted Plot

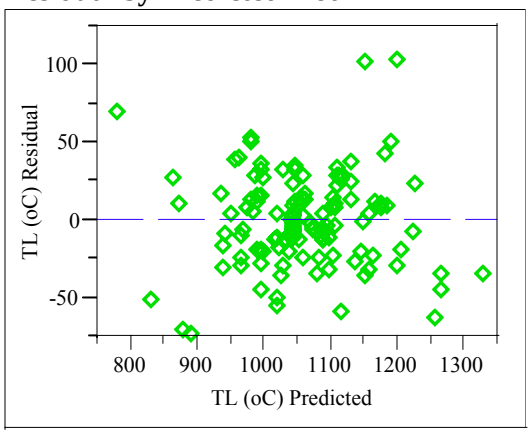

Press
204958.29123

B2O3 n
Leverage Plot

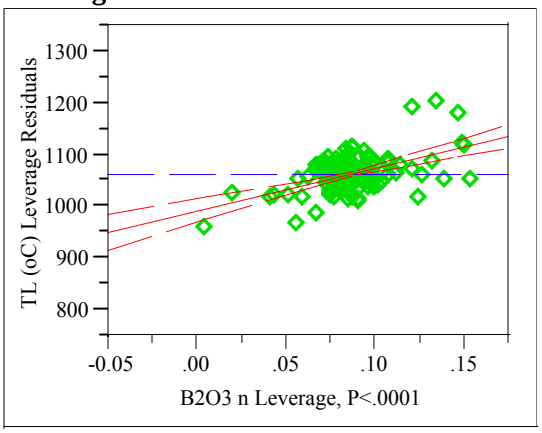

Al2O2 n
Leverage Plot

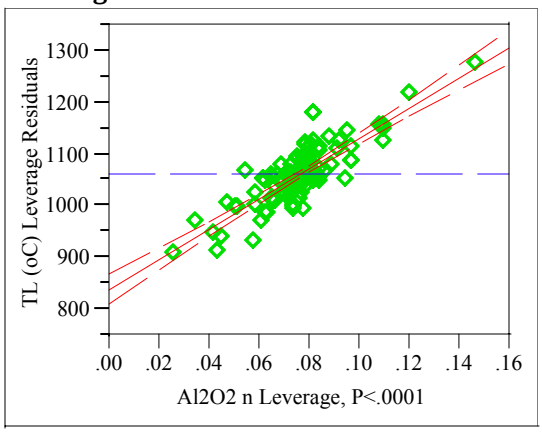

CdO n
Leverage Plot

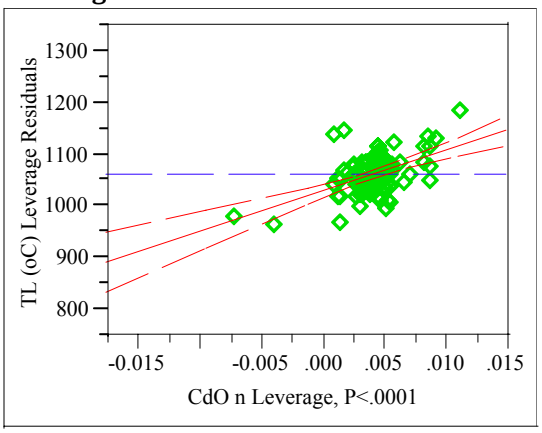

Appendix C. Model Fitting Results for TL Data

Exhibit C.6: Statistical Results from the Fitting of the LMM to Each Data Grouping

Cr2O3 n
Leverage Plot

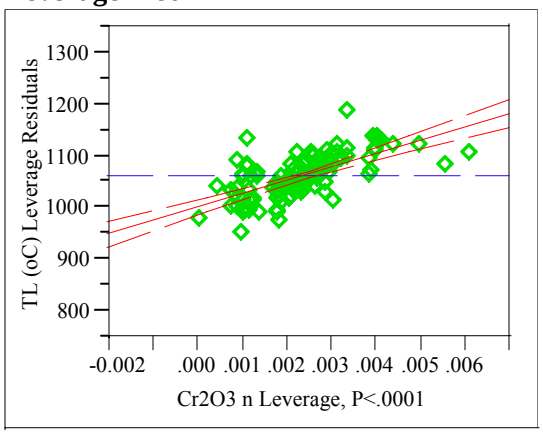

K2O n
Leverage Plot

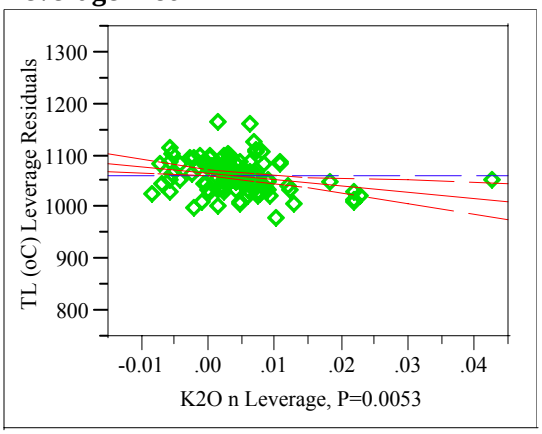

F n
Leverage Plot

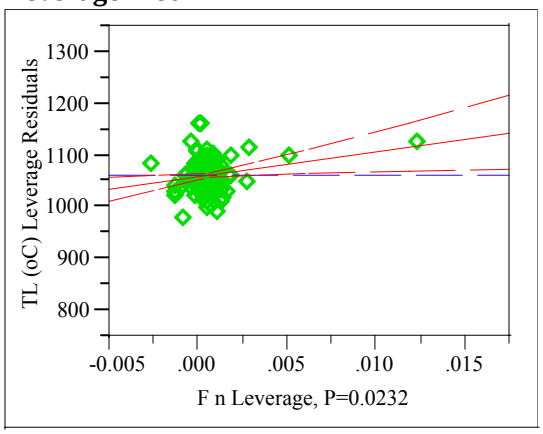

Li2O n
Leverage Plot

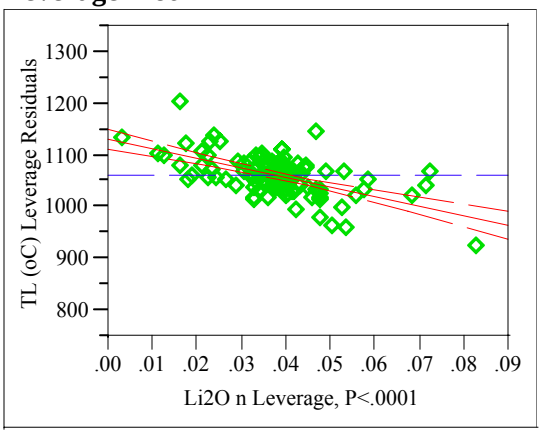

Fe2O3 n
Leverage Plot

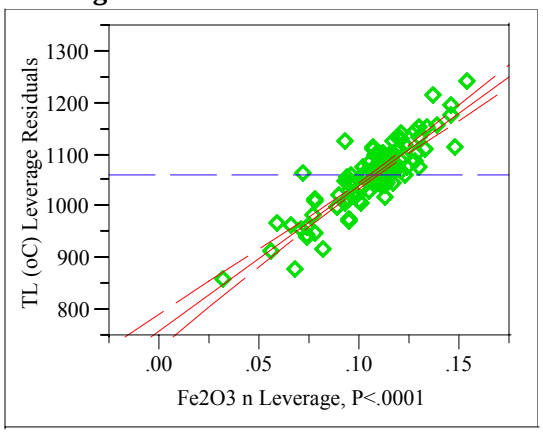

MgO n
Leverage Plot

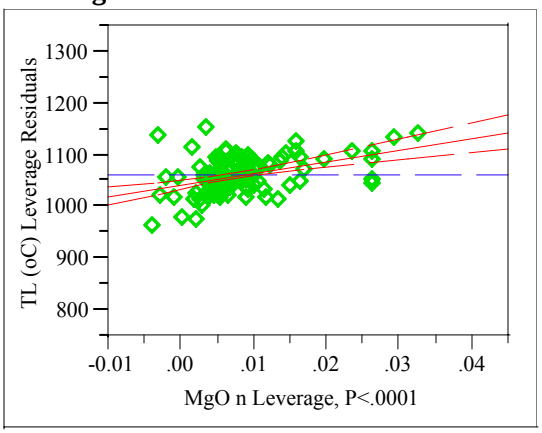

Appendix C. Model Fitting Results for TL Data

Exhibit C.6: Statistical Results from the Fitting of the LMM to Each Data Grouping

MnO n
Leverage Plot

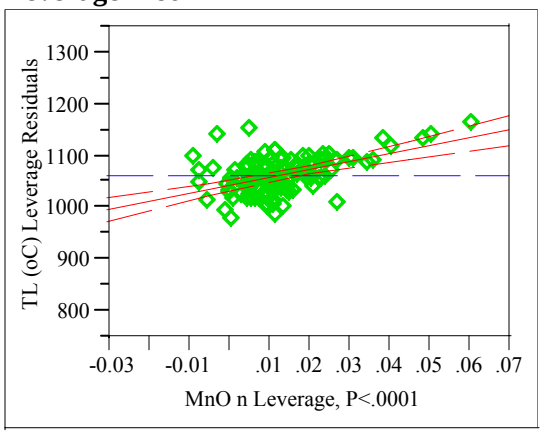

P2O5 n
Leverage Plot

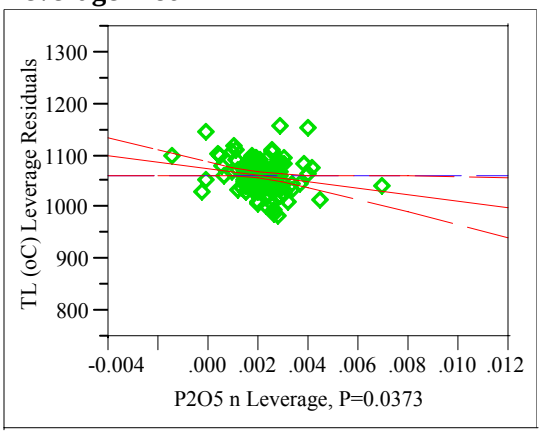

Na2O n
Leverage Plot

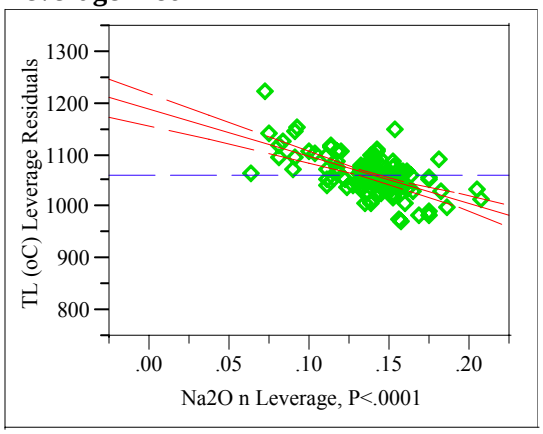

SiO2 n
Leverage Plot

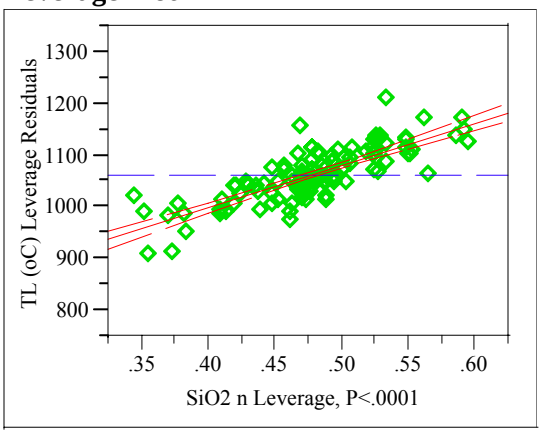

NiO n
Leverage Plot

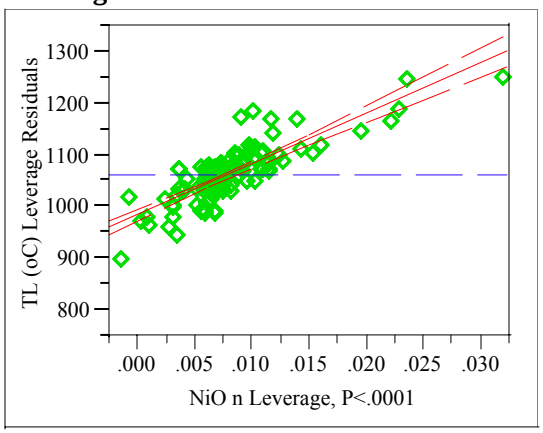

ThO2 n
Leverage Plot

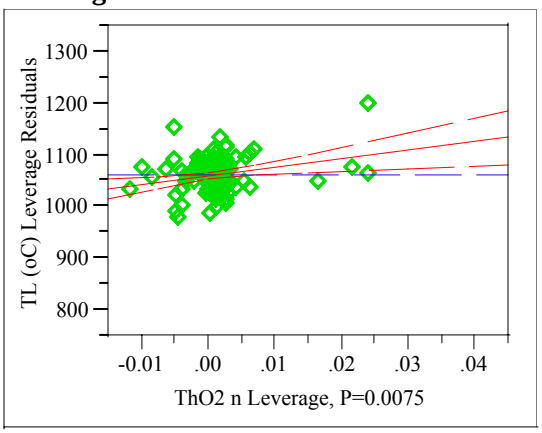

Appendix C. Model Fitting Results for TL Data

Exhibit C.6: Statistical Results from the Fitting of the LMM to Each Data Grouping

U3O8 n
Leverage Plot

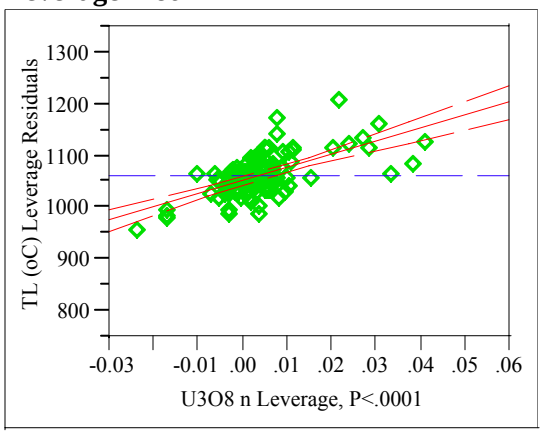

ZrO2 n
Leverage Plot

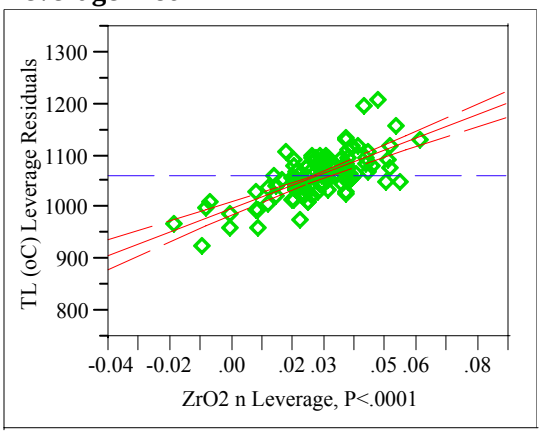

Appendix C. Model Fitting Results for TL Data

Exhibit C.6: Statistical Results from the Fitting of the LMM to Each Data Grouping

Groupings=2
Response TL (°C)
Singularity Details
Intercept = 0
Whole Model
Actual by Predicted Plot

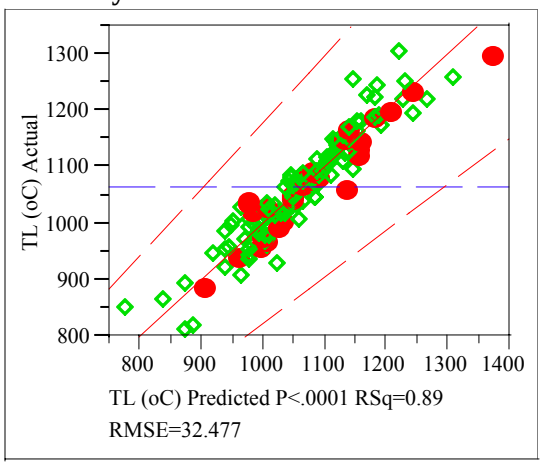

Summary of Fit

RSquare	0.887993
RSquare Adj	0.871848
Root Mean Square Error	32.4768
Mean of Response	1063.101
Observations (or Sum Wgts)	128

Analysis of Variance

Source	DF	Sum of Squares	Mean Square	F Ratio
Model	16	928183.4	58011.5	55.0006
Error	111	117076.4	1054.7	Prob > F
C. Total	127	1045259.8		<.0001

Tested against reduced model: Y=mean

Lack Of Fit

Source	DF	Sum of Squares	Mean Square	F Ratio
Lack Of Fit	88	112354.48	1276.76	6.2189
Pure Error	23	4721.94	205.30	Prob > F
Total Error	111	117076.42		<.0001
				Max RSq
				0.9955

Parameter Estimates

Term		Estimate	Std Error	t Ratio	Prob>|t|
Intercept	Zeroed	0	0	.	.
Al2O2 n		2677.9715	191.6624	13.97	<.0001
B2O3 n		775.23163	142.8087	5.43	<.0001
CdO n		5497.2086	1229.31	4.47	<.0001
Cr2O3 n		30968.545	3263.024	9.49	<.0001
F n		5477.2112	1883.904	2.91	0.0044
Fe2O3 n		2748.1509	136.2151	20.18	<.0001
K2O n		-1646.163	449.986	-3.66	0.0004
Li2O n		-1733.486	282.4707	-6.14	<.0001
MgO n		2402.6566	438.7462	5.48	<.0001
MnO n		1811.4398	239.4692	7.56	<.0001
Na2O n		-754.3637	115.1393	-6.55	<.0001

Appendix C. Model Fitting Results for TL Data

Exhibit C.6: Statistical Results from the Fitting of the LMM to Each Data Grouping

Term	Estimate	Std Error	t Ratio	Prob>|t|
NiO n	9522.2881	678.3015	14.04	<.0001
P2O5 n	-3443.079	2588.191	-1.33	0.1861
SiO2 n	845.80286	59.93345	14.11	<.0001
ThO2 n	2443.0825	685.1296	3.57	0.0005
U3O8 n	2105.1001	303.4084	6.94	<.0001
ZrO2 n	1800.3461	227.213	7.92	<.0001

Residual by Predicted Plot

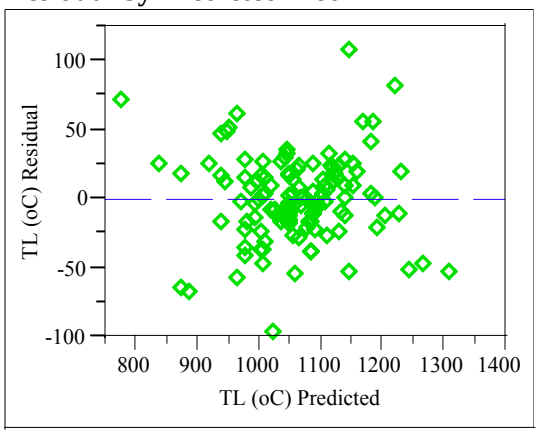

Press
215186.00174

B2O3 n
Leverage Plot

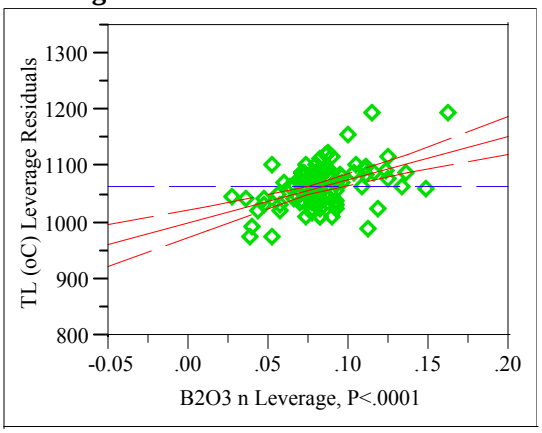

Al2O2 n
Leverage Plot

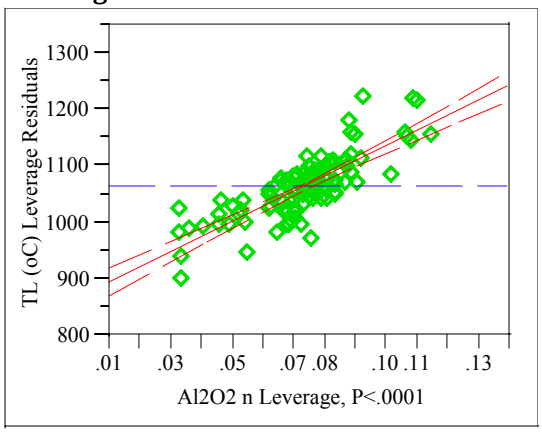

CdO n
Leverage Plot

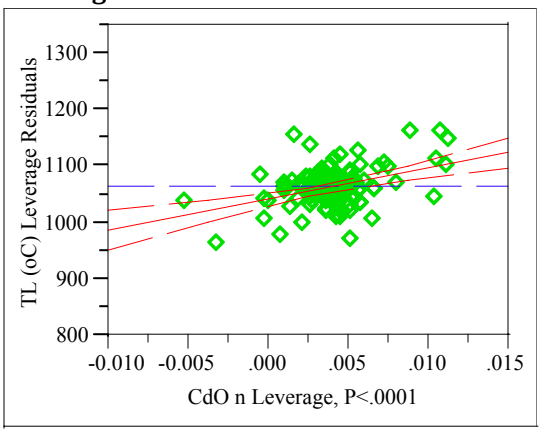

Appendix C. Model Fitting Results for TL Data

Exhibit C.6: Statistical Results from the Fitting of the LMM to Each Data Grouping

Cr2O3 n
Leverage Plot

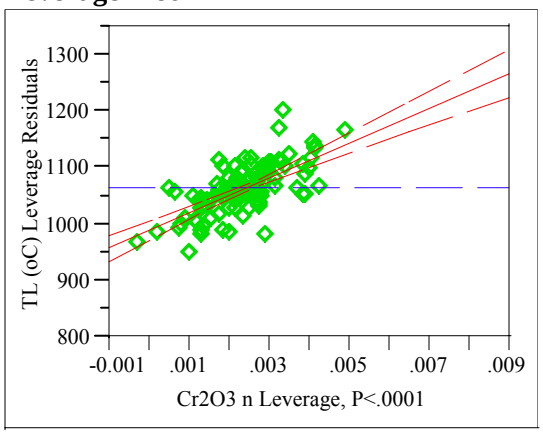

K2O n
Leverage Plot

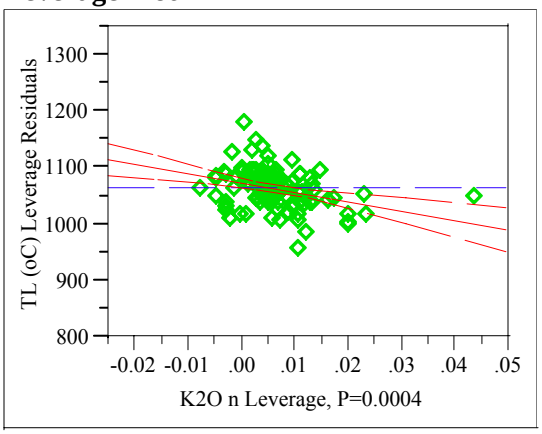

F n
Leverage Plot

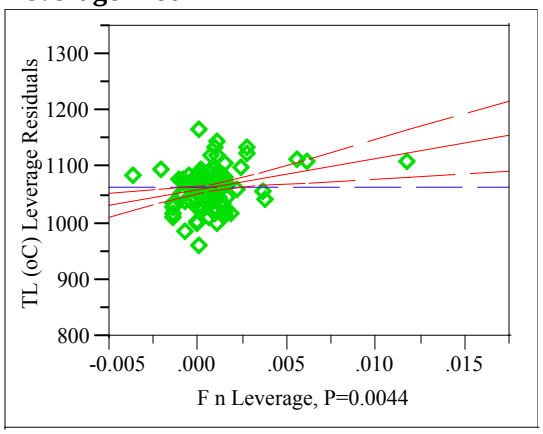

Li2O n
Leverage Plot

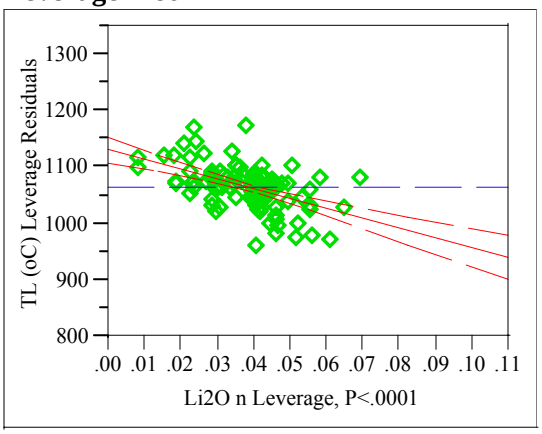

Fe2O3 n
Leverage Plot

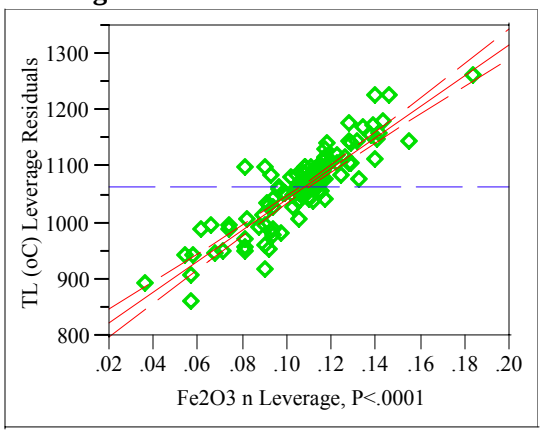

MgO n
Leverage Plot

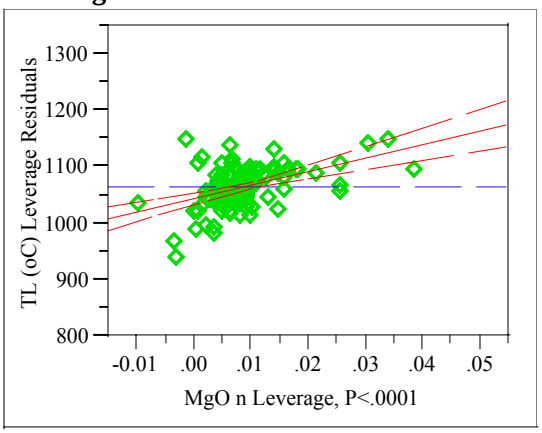

Appendix C. Model Fitting Results for TL Data

Exhibit C.6: Statistical Results from the Fitting of the LMM to Each Data Grouping

MnO n
Leverage Plot

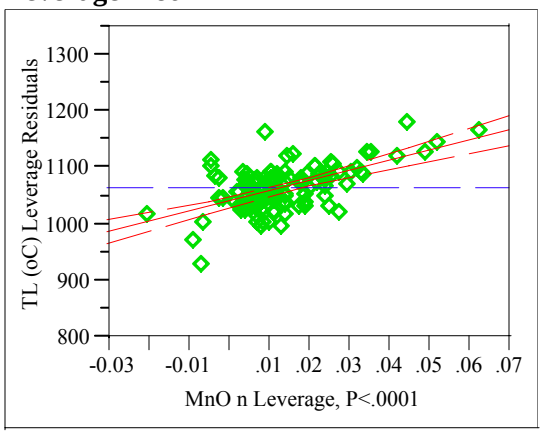

P2O5 n
Leverage Plot

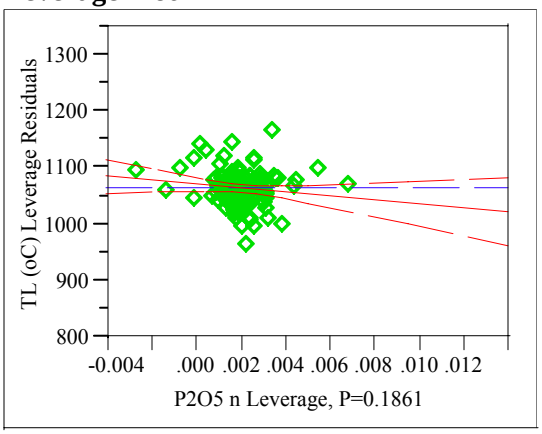

Na2O n
Leverage Plot

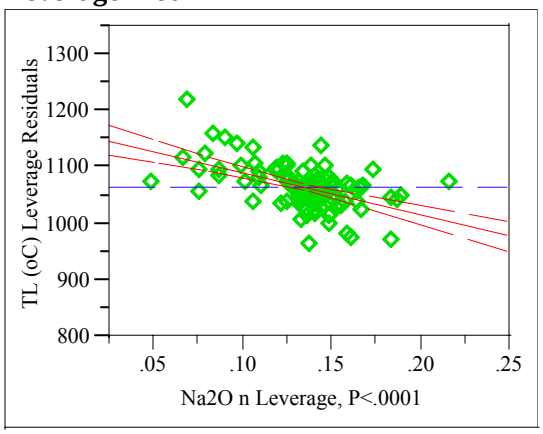

SiO2 n
Leverage Plot

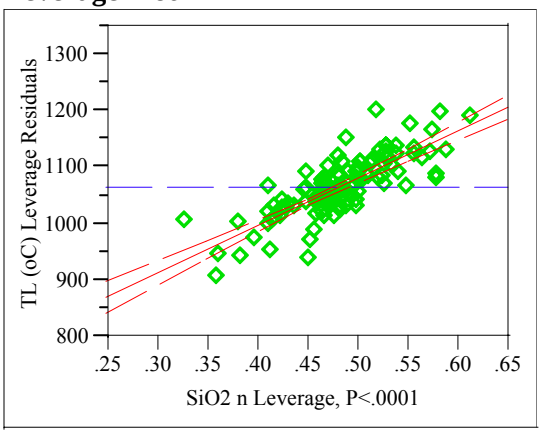

NiO n
Leverage Plot

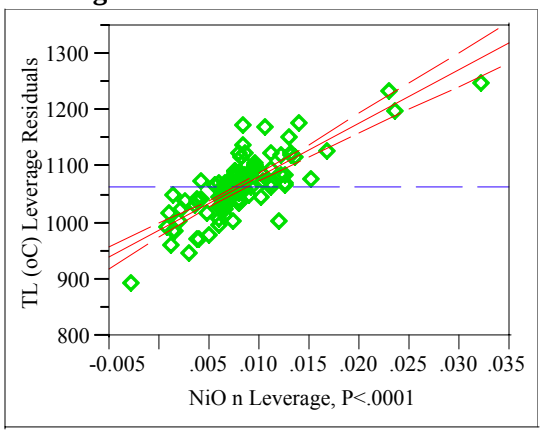

ThO2 n
Leverage Plot

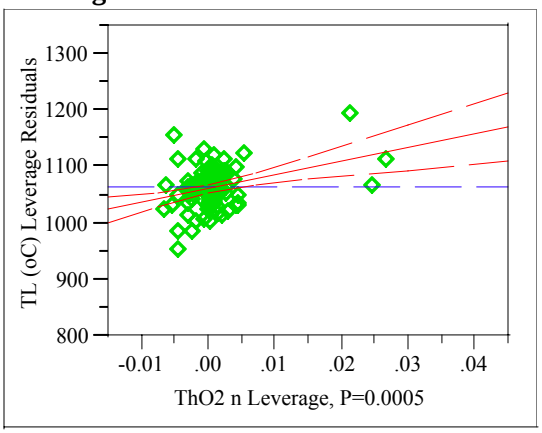

Appendix C. Model Fitting Results for TL Data

Exhibit C.6: Statistical Results from the Fitting of the LMM to Each Data Grouping

U3O8 n
Leverage Plot

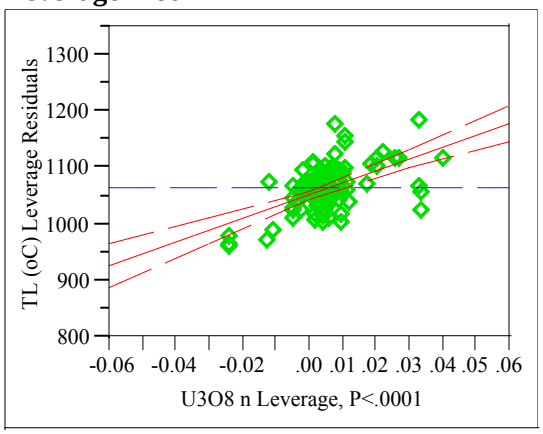

ZrO2 n
Leverage Plot

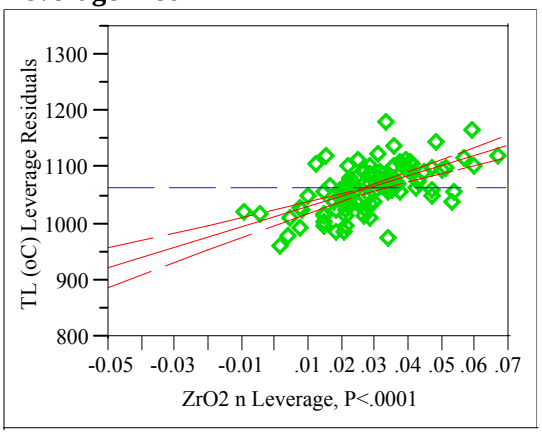

Appendix C. Model Fitting Results for TL Data

Exhibit C.6: Statistical Results from the Fitting of the LMM to Each Data Grouping

Groupings=3
Response TL (°C)
Singularity Details
Intercept = 0
Whole Model
Actual by Predicted Plot

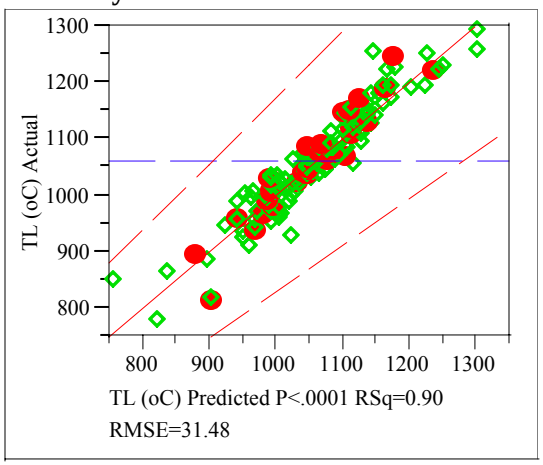

Summary of Fit

RSquare	0.89597
RSquare Adj	0.880838
Root Mean Square Error	31.47994
Mean of Response	1061.743
Observations (or Sum Wgts)	127

Analysis of Variance

Source	DF	Sum of Squares	Mean Square	F Ratio
Model	16	938846.8	58677.9	59.2116
Error	110	109008.5	991.0	Prob > F
C. Total	126	1047855.4		<.0001

Tested against reduced model: Y=mean

Lack Of Fit

Source	DF	Sum of Squares	Mean Square	F Ratio
Lack Of Fit	90	102650.23	1140.56	3.5876
Pure Error	20	6358.31	317.92	Prob > F
Total Error	110	109008.54		0.0010
				Max RSq
				0.9939

Parameter Estimates

Term		Estimate	Std Error	t Ratio	Prob>|t|
Intercept	Zeroed	0	0	.	.
Al2O2 n		2870.608	169.0862	16.98	<.0001
B2O3 n		644.06717	121.8768	5.28	<.0001
CdO n		6680.186	1107.851	6.03	<.0001
Cr2O3 n		24870.142	2642.83	9.41	<.0001
F n		5342.1888	2031.149	2.63	0.0098
Fe2O3 n		2684.8892	143.0674	18.77	<.0001
K2O n		-1189.616	437.7838	-2.72	0.0076
Li2O n		-1758.146	252.2639	-6.97	<.0001
MgO n		1991.4357	436.9113	4.56	<.0001
MnO n		2068.6032	253.0031	8.18	<.0001
Na2O n		-814.8105	109.63	-7.43	<.0001

Appendix C. Model Fitting Results for TL Data

Exhibit C.6: Statistical Results from the Fitting of the LMM to Each Data Grouping

Term	Estimate	Std Error	t Ratio	Prob>|t|
NiO n	8690.0273	669.0073	12.99	<.0001
P2O5 n	-3781.527	2611.15	-1.45	0.1504
SiO2 n	878.78414	58.46798	15.03	<.0001
ThO2 n	658.57925	587.3949	1.12	0.2647
U3O8 n	2283.1096	297.4859	7.67	<.0001
ZrO2 n	2113.5703	201.0399	10.51	<.0001

Residual by Predicted Plot

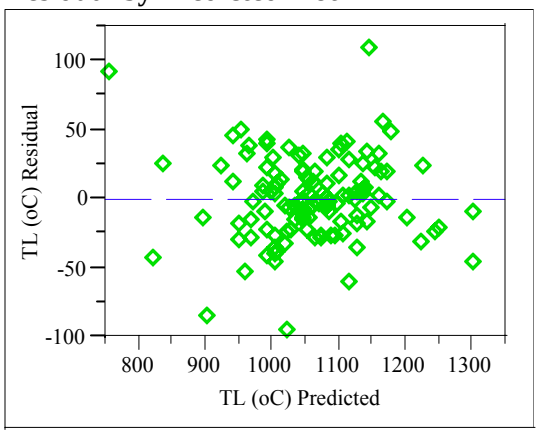

Press
179970.57226

B2O3 n
Leverage Plot

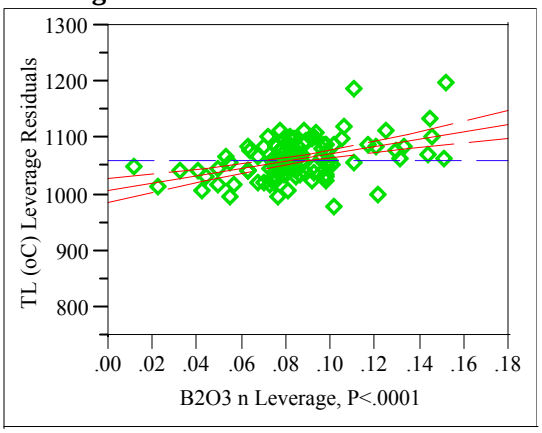

Al2O2 n
Leverage Plot

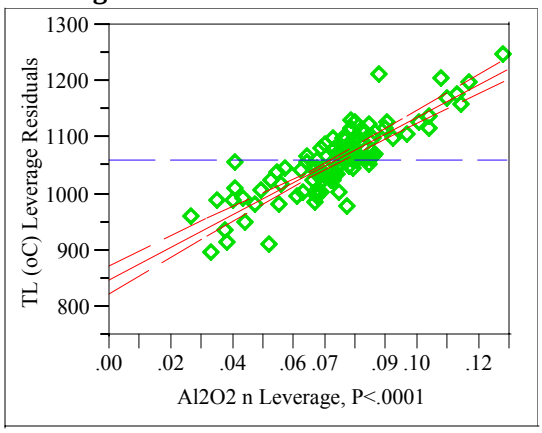

CdO n
Leverage Plot

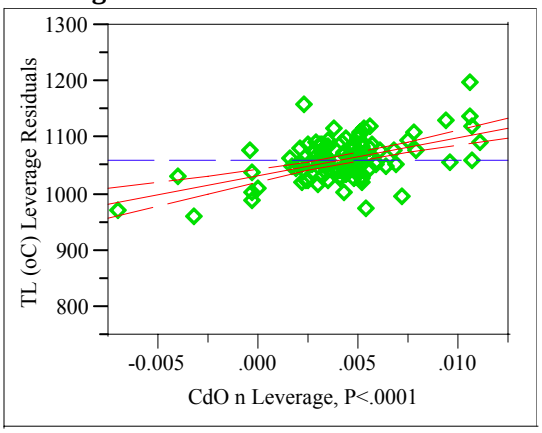

Appendix C. Model Fitting Results for TL Data

Exhibit C.6: Statistical Results from the Fitting of the LMM to Each Data Grouping

Cr2O3 n
Leverage Plot

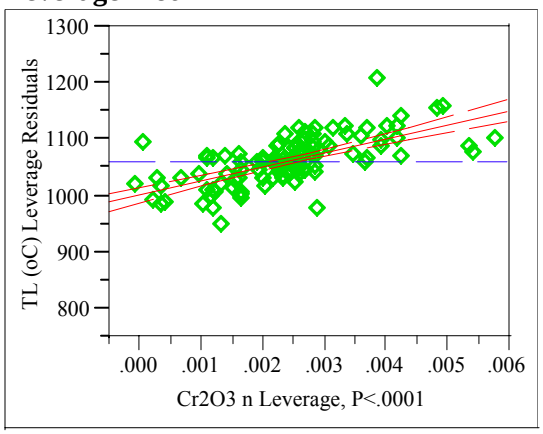

K2O n
Leverage Plot

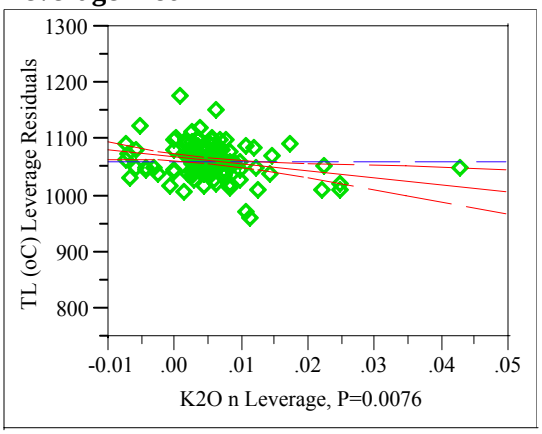

F n
Leverage Plot

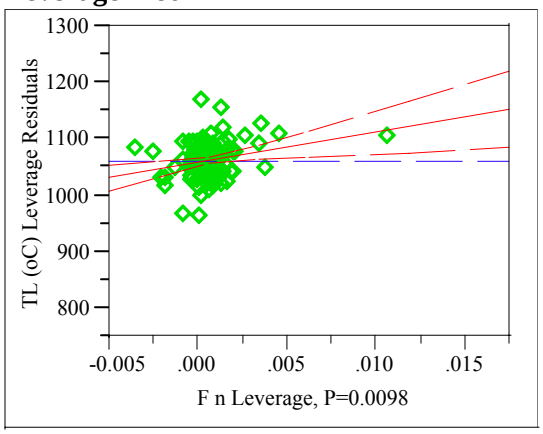

Li2O n
Leverage Plot

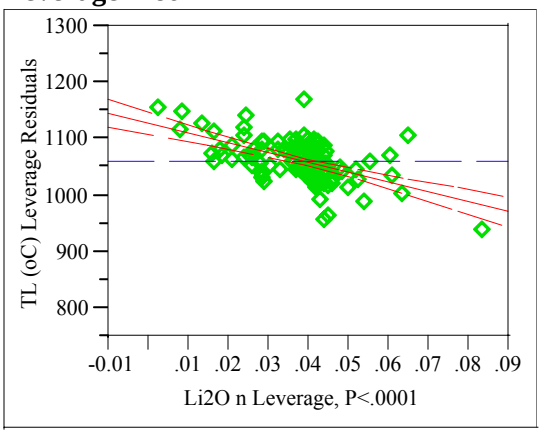

Fe2O3 n
Leverage Plot

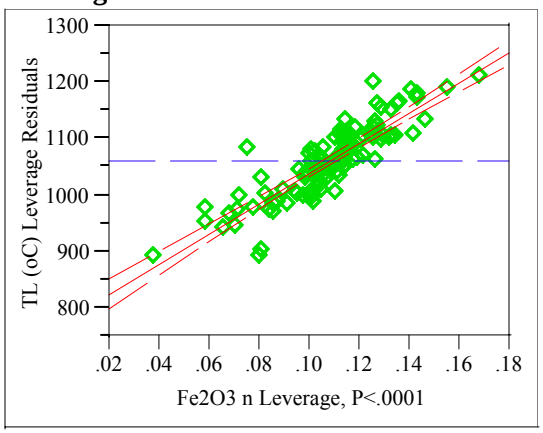

MgO n
Leverage Plot

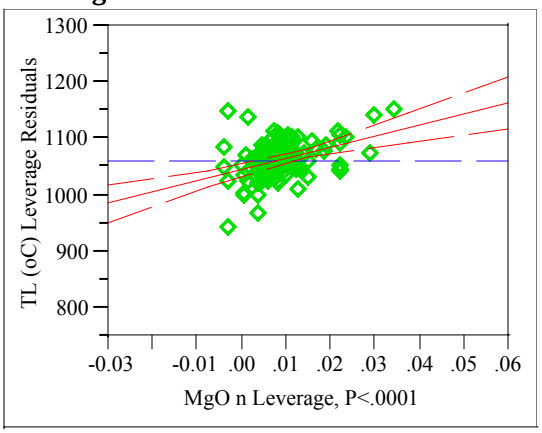

Appendix C. Model Fitting Results for TL Data

Exhibit C.6: Statistical Results from the Fitting of the LMM to Each Data Grouping

MnO n
Leverage Plot

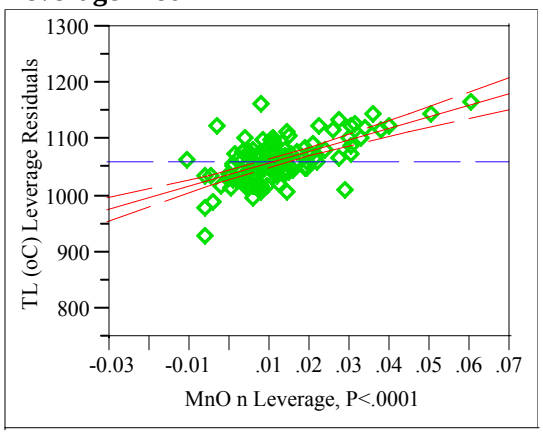

P2O5 n
Leverage Plot

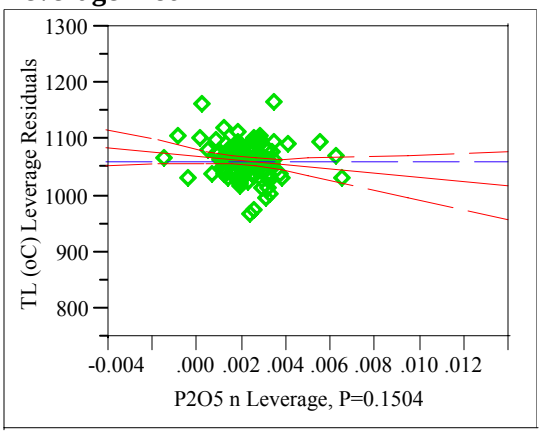

Na2O n
Leverage Plot

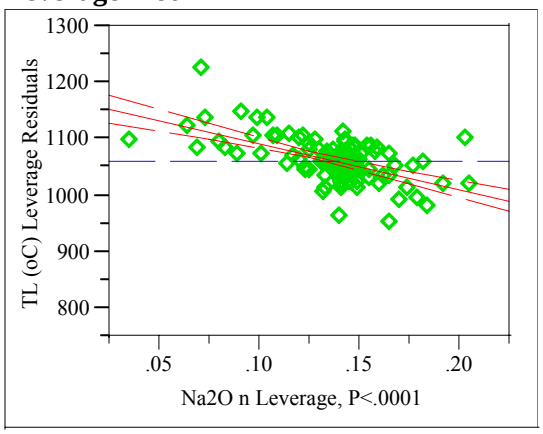

SiO2 n
Leverage Plot

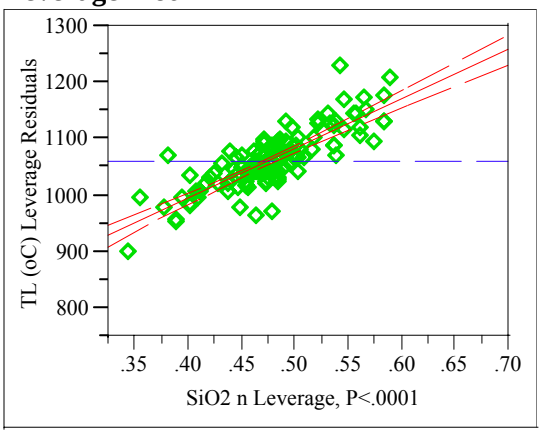

NiO n
Leverage Plot

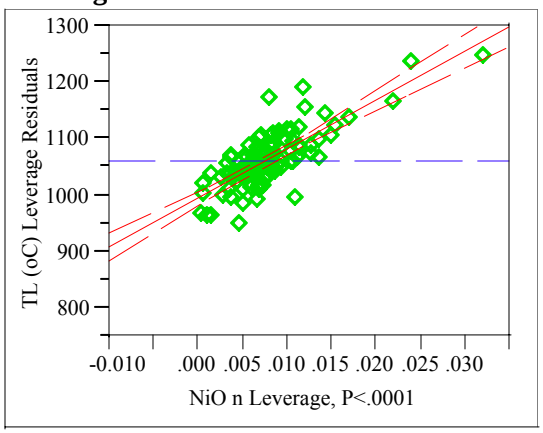

ThO2 n
Leverage Plot

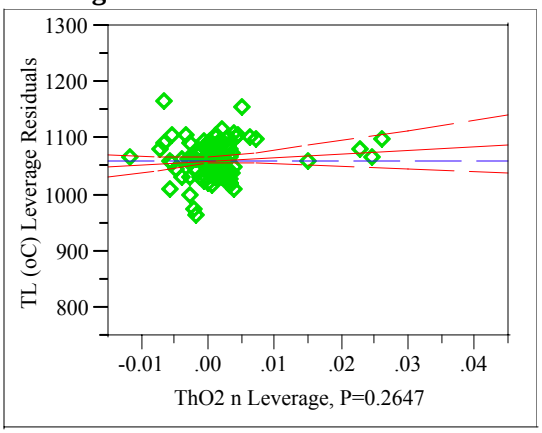

Appendix C. Model Fitting Results for TL Data

Exhibit C.6: Statistical Results from the Fitting of the LMM to Each Data Grouping

U3O8 n
Leverage Plot

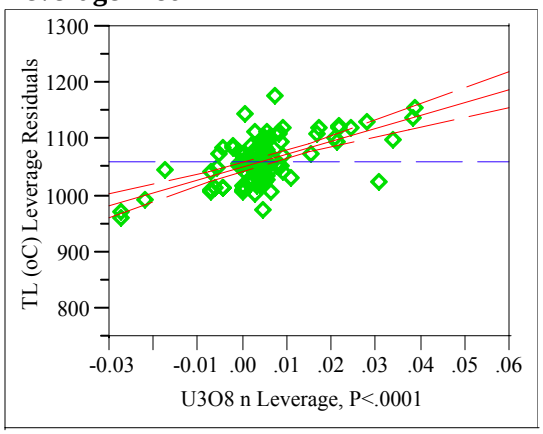

ZrO2 n
Leverage Plot

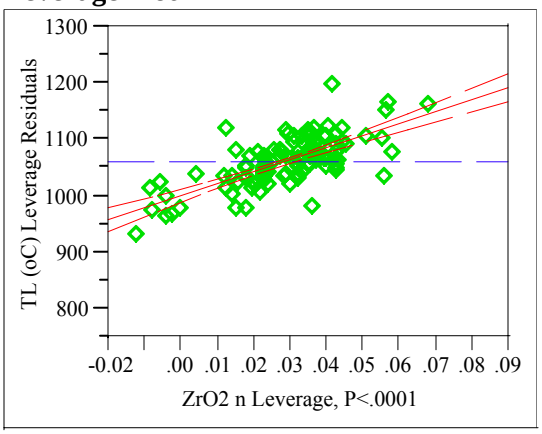

Appendix C. Model Fitting Results for TL Data

Exhibit C.6: Statistical Results from the Fitting of the LMM to Each Data Grouping

Groupings=4
Response TL (°C)
Singularity Details
Intercept = 0
Whole Model
Actual by Predicted Plot

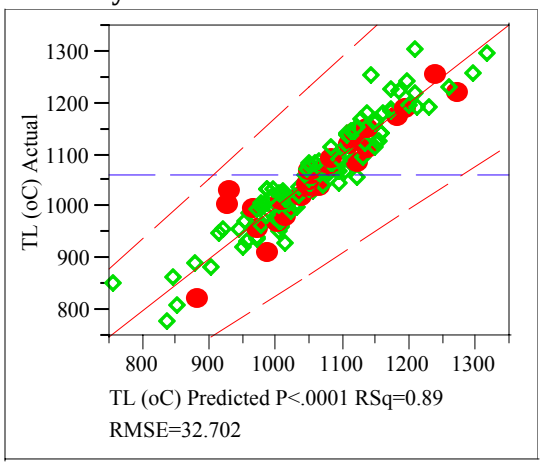

Summary of Fit

RSquare	0.893795
RSquare Adj	0.878623
Root Mean Square Error	32.70204
Mean of Response	1062.05
Observations (or Sum Wgts)	129

Analysis of Variance

Source	DF	Sum of Squares	Mean Square	F Ratio
Model	16	1008003.9	63000.2	58.9105
Error	112	119775.5	1069.4	Prob > F
C. Total	128	1127779.4		<.0001

Tested against reduced model: Y=mean

Lack Of Fit

Source	DF	Sum of Squares	Mean Square	F Ratio
Lack Of Fit	88	114340.29	1299.32	5.7374
Pure Error	24	5435.16	226.46	Prob > F
Total Error	112	119775.45		<.0001
				Max RSq
				0.9952

Parameter Estimates

Term		Estimate	Std Error	t Ratio	Prob>|t|
Intercept	Zeroed	0	0	.	.
Al2O2 n		2687.2437	171.773	15.64	<.0001
B2O3 n		840.53532	123.4323	6.81	<.0001
CdO n		5124.1007	1244.536	4.12	<.0001
Cr2O3 n		25591.049	2626.946	9.74	<.0001
F n		3726.3338	1926.481	1.93	0.0556
Fe2O3 n		2814.9059	135.4752	20.78	<.0001
K2O n		-997.049	459.0004	-2.17	0.0319
Li2O n		-2318.604	262.3583	-8.84	<.0001
MgO n		2248.8328	421.0819	5.34	<.0001
MnO n		1723.9199	290.2494	5.94	<.0001
Na2O n		-858.7209	113.309	-7.58	<.0001

Appendix C. Model Fitting Results for TL Data

Exhibit C.6: Statistical Results from the Fitting of the LMM to Each Data Grouping

Term	Estimate	Std Error	t Ratio	Prob>|t|
NiO n	9732.1603	731.7381	13.30	<.0001
P2O5 n	-2308.178	2414.849	-0.96	0.3412
SiO2 n	894.01736	61.62212	14.51	<.0001
ThO2 n	2262.8046	578.3329	3.91	0.0002
U3O8 n	1947.8208	337.4448	5.77	<.0001
ZrO2 n	2140.789	195.8221	10.93	<.0001

Residual by Predicted Plot

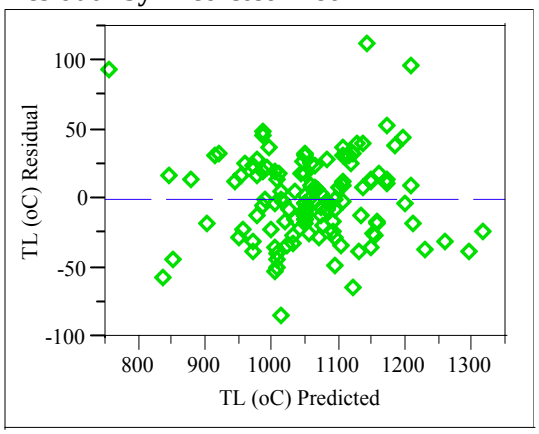

Press
200828.60263

B2O3 n
Leverage Plot

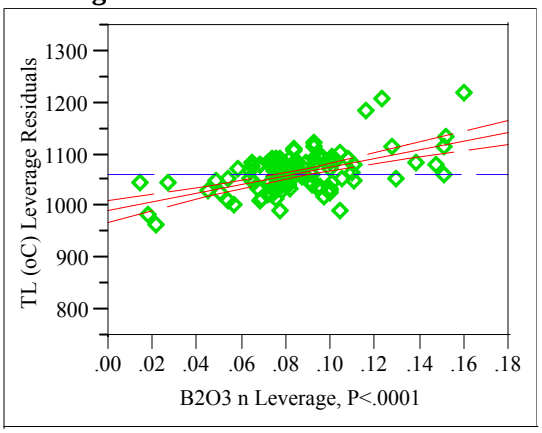

Al2O2 n
Leverage Plot

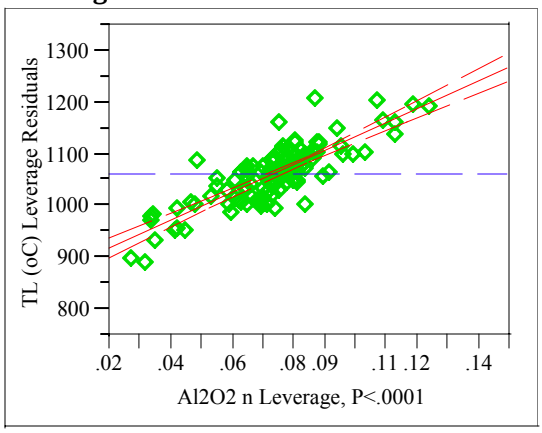

CdO n
Leverage Plot

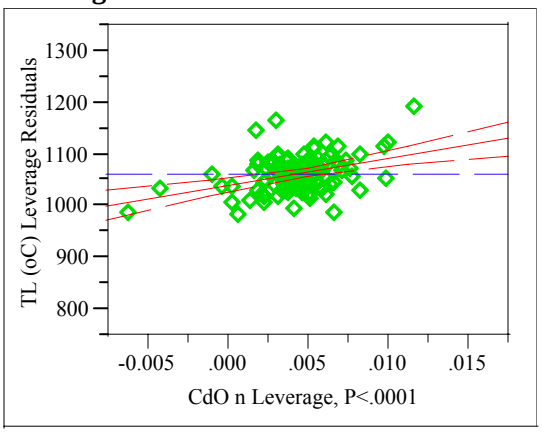

Appendix C. Model Fitting Results for TL Data

Exhibit C.6: Statistical Results from the Fitting of the LMM to Each Data Grouping

Cr2O3 n
Leverage Plot

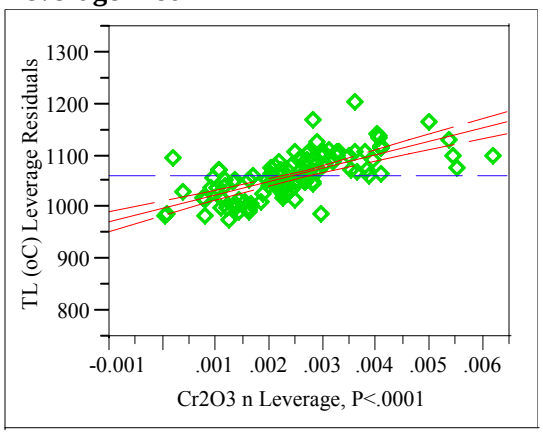

K2O n
Leverage Plot

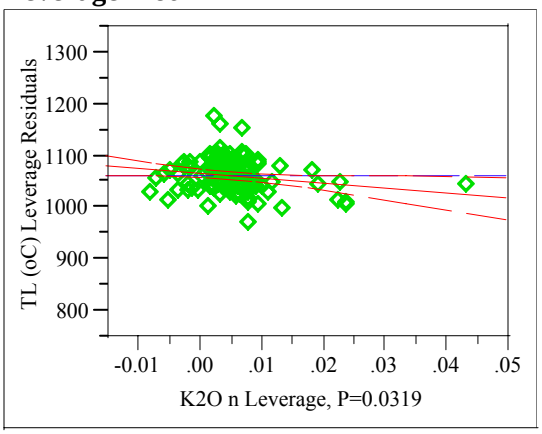

F n
Leverage Plot

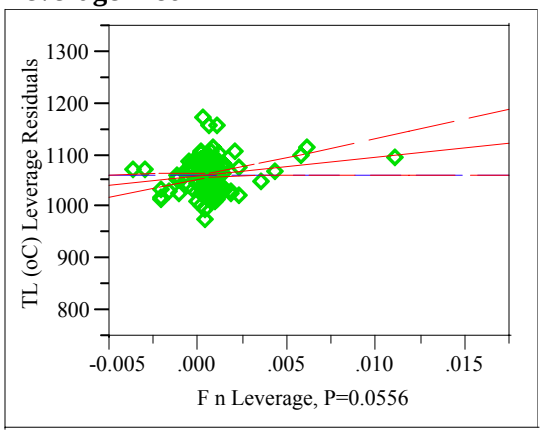

Li2O n
Leverage Plot

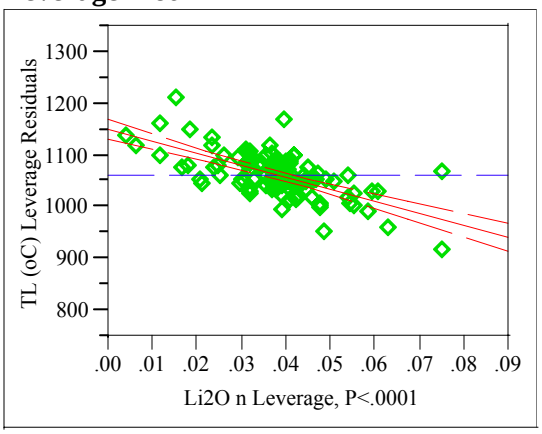

Fe2O3 n
Leverage Plot

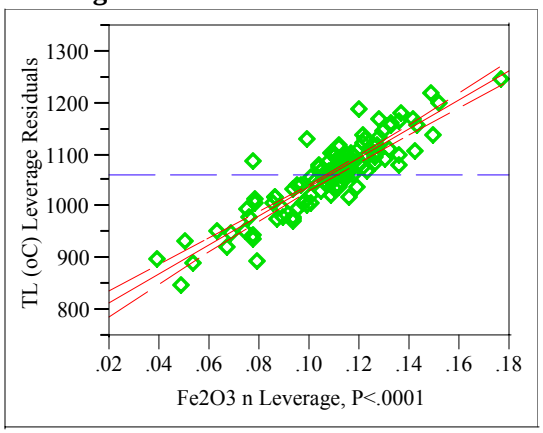

MgO n
Leverage Plot

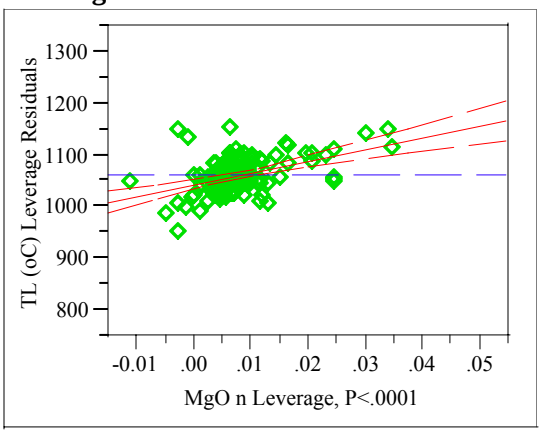

Appendix C. Model Fitting Results for TL Data

Exhibit C.6: Statistical Results from the Fitting of the LMM to Each Data Grouping

MnO n
Leverage Plot

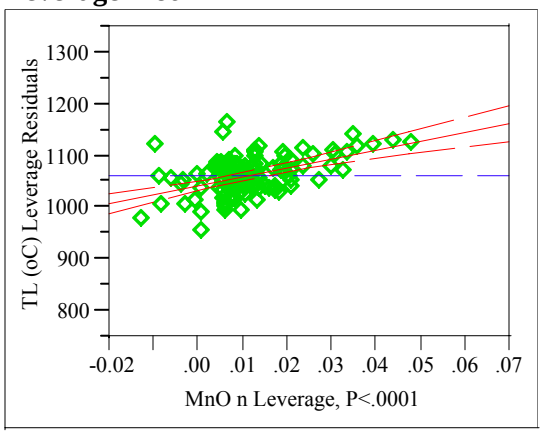

P2O5 n
Leverage Plot

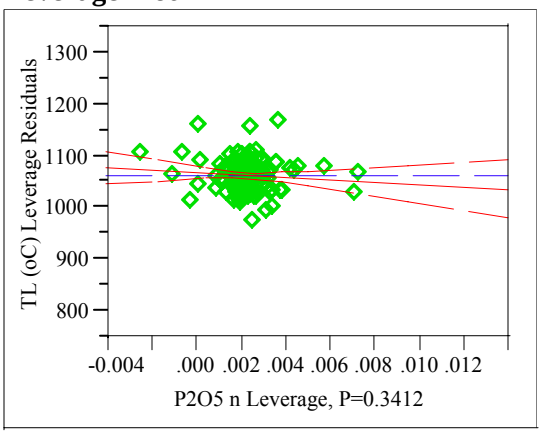

Na2O n
Leverage Plot

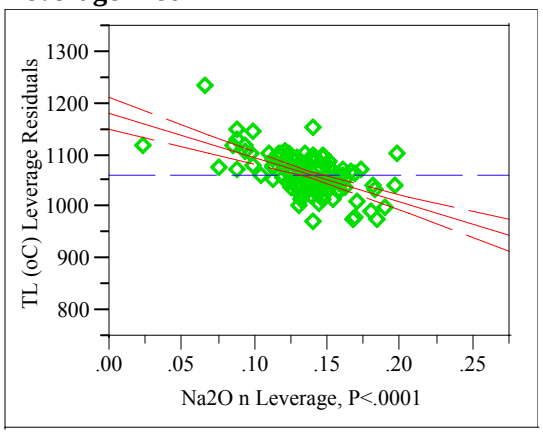

SiO2 n
Leverage Plot

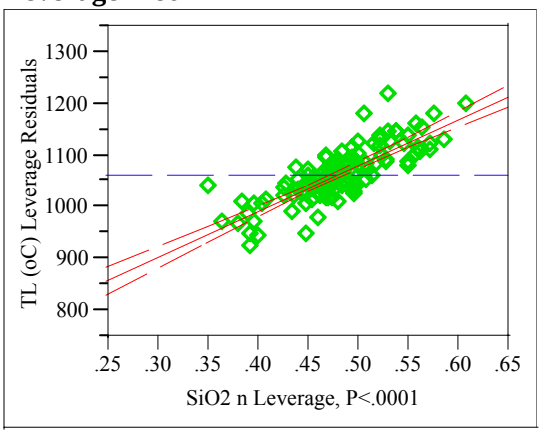

NiO n
Leverage Plot

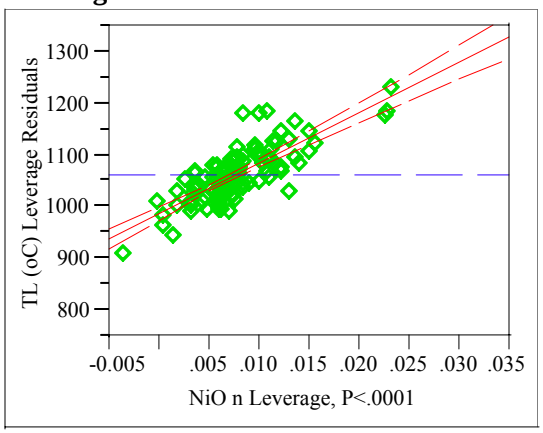

ThO2 n
Leverage Plot

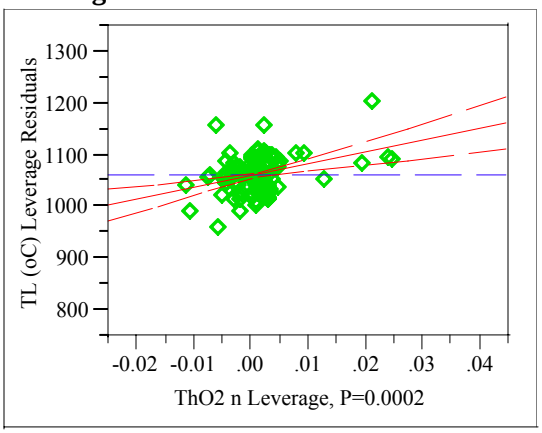

Appendix C. Model Fitting Results for TL Data

Exhibit C.6: Statistical Results from the Fitting of the LMM to Each Data Grouping

U3O8 n
Leverage Plot

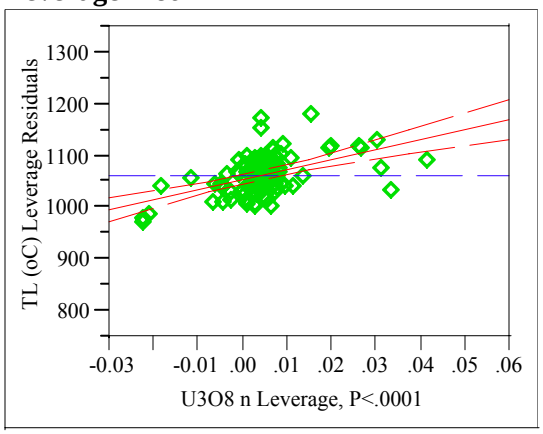

ZrO2 n
Leverage Plot

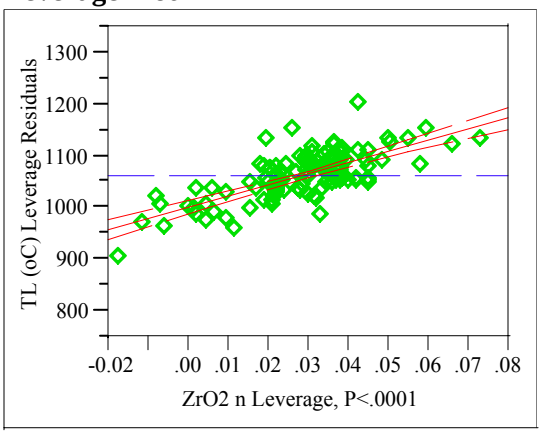

Appendix C. Model Fitting Results for TL Data

Exhibit C.6: Statistical Results from the Fitting of the LMM to Each Data Grouping

Groupings=5
Response TL (°C)
Singularity Details
Intercept = 0
Whole Model
Actual by Predicted Plot

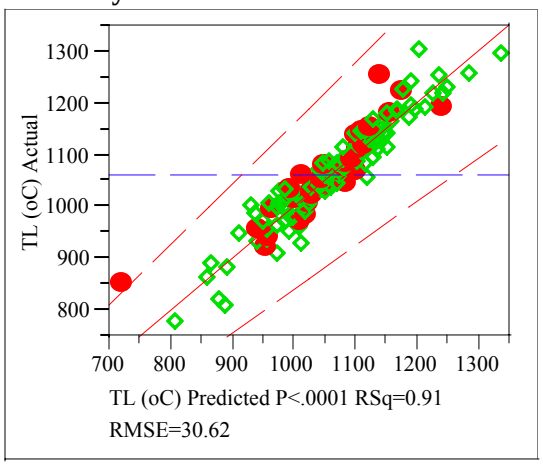

Summary of Fit

RSquare	0.907659
RSquare Adj	0.894348
Root Mean Square Error	30.61951
Mean of Response	1062.106
Observations (or Sum Wgts)	128

Analysis of Variance

Source	DF	Sum of Squares	Mean Square	F Ratio
Model	16	1022931.7	63933.2	68.1915
Error	111	104068.5	937.6	Prob > F
C. Total	127	1127000.2		<.0001

Tested against reduced model: Y=mean

Lack Of Fit

Source	DF	Sum of Squares	Mean Square	F Ratio
Lack Of Fit	90	97801.63	1086.68	3.6414
Pure Error	21	6266.91	298.42	Prob > F
Total Error	111	104068.54		0.0007
				Max RSq
				0.9944

Parameter Estimates

Term		Estimate	Std Error	t Ratio	Prob>|t|
Intercept	Zeroed	0	0	.	.
Al2O2 n		2997.9237	164.4884	18.23	<.0001
B2O3 n		662.70301	124.5907	5.32	<.0001
CdO n		5913.1	1160.006	5.10	<.0001
Cr2O3 n		26246.939	2592.413	10.12	<.0001
F n		7155.3622	2547.834	2.81	0.0059
Fe2O3 n		2827.7899	142.5136	19.84	<.0001
K2O n		-1102.702	510.5114	-2.16	0.0329
Li2O n		-2317.727	243.8708	-9.50	<.0001
MgO n		2363.9121	447.3588	5.28	<.0001
MnO n		1999.7735	236.337	8.46	<.0001
Na2O n		-871.7687	111.9424	-7.79	<.0001

Appendix C. Model Fitting Results for TL Data

Exhibit C.6: Statistical Results from the Fitting of the LMM to Each Data Grouping

Term	Estimate	Std Error	t Ratio	Prob>|t|
NiO n	8710.2743	643.5559	13.53	<.0001
P2O5 n	-4710.889	2491.155	-1.89	0.0612
SiO2 n	874.04977	63.42843	13.78	<.0001
ThO2 n	1870.6322	564.4447	3.31	0.0012
U3O8 n	2352.9709	299.9155	7.85	<.0001
ZrO2 n	2120.5328	184.1703	11.51	<.0001

Appendix C. Model Fitting Results for TL Data

Exhibit C.6: Statistical Results from the Fitting of a LMM to Each Data Grouping

Residual by Predicted Plot

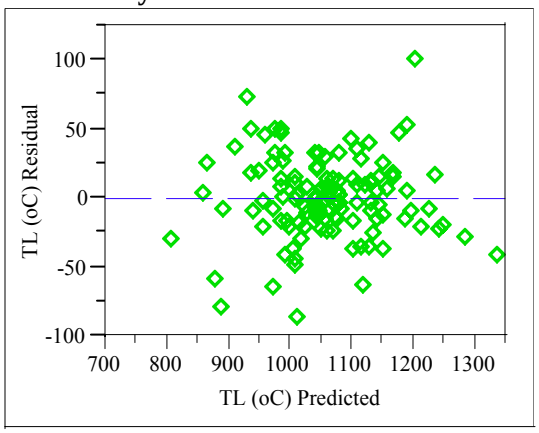

Press
183033.38726

CdO n
Leverage Plot

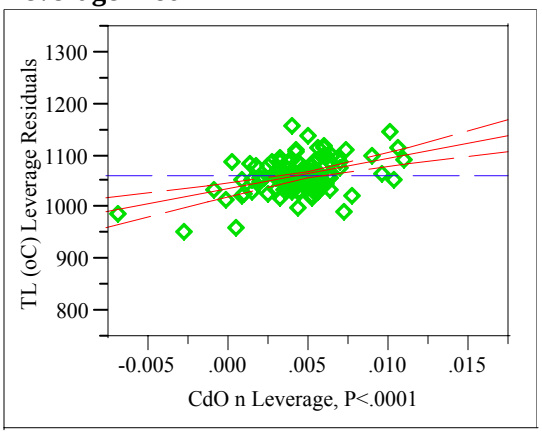

Al2O2 n
Leverage Plot

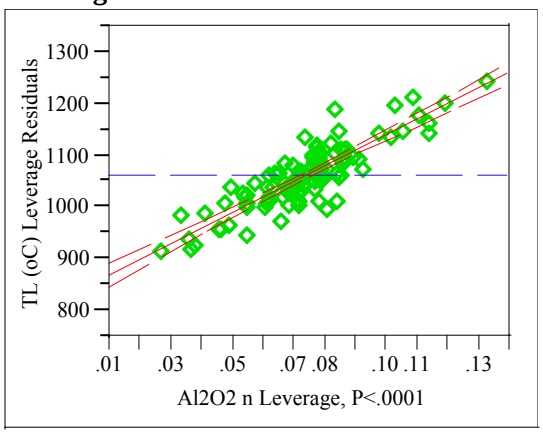

Cr2O3 n
Leverage Plot

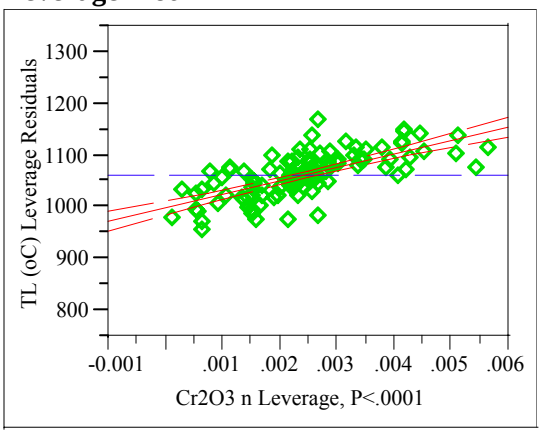

B2O3 n
Leverage Plot

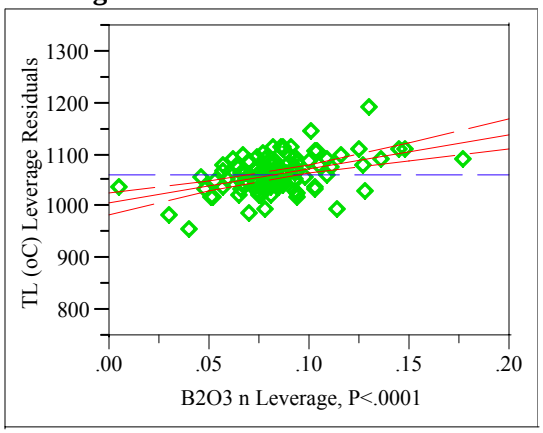

F n
Leverage Plot

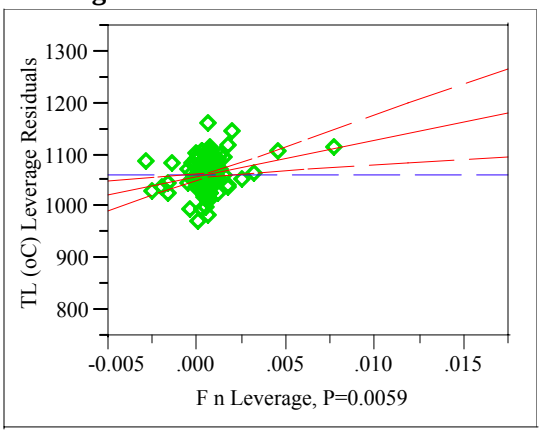

Appendix C. Model Fitting Results for TL Data

Exhibit C.6: Statistical Results from the Fitting of a LMM to Each Data Grouping

Fe2O3 n
Leverage Plot

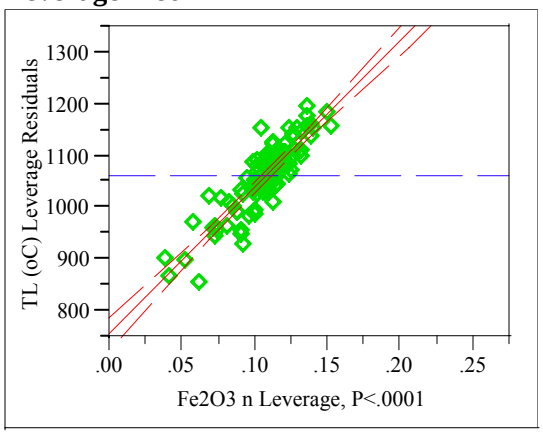

MgO n
Leverage Plot

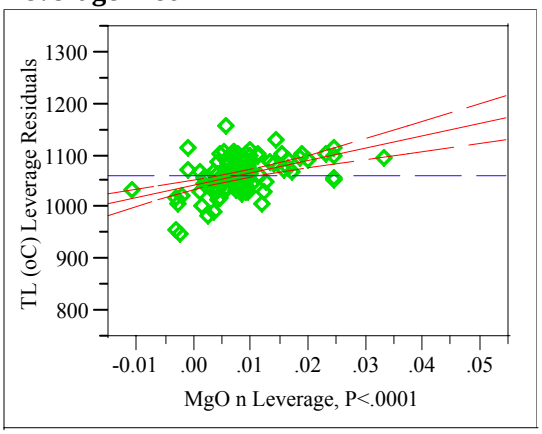

K2O n
Leverage Plot

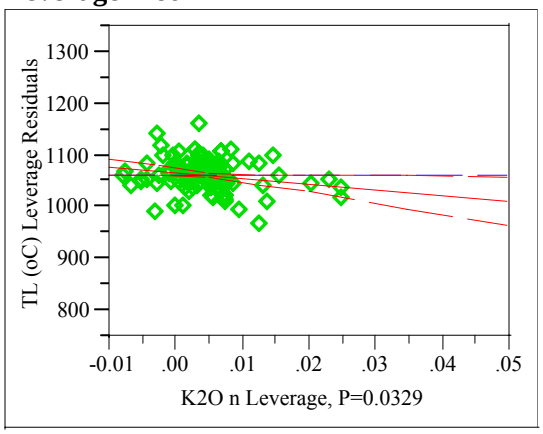

MnO n
Leverage Plot

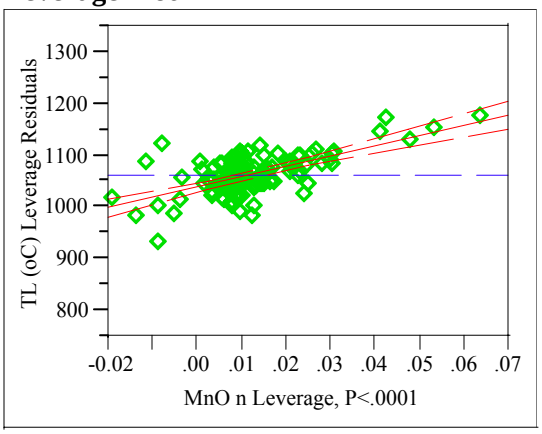

Li2O n
Leverage Plot

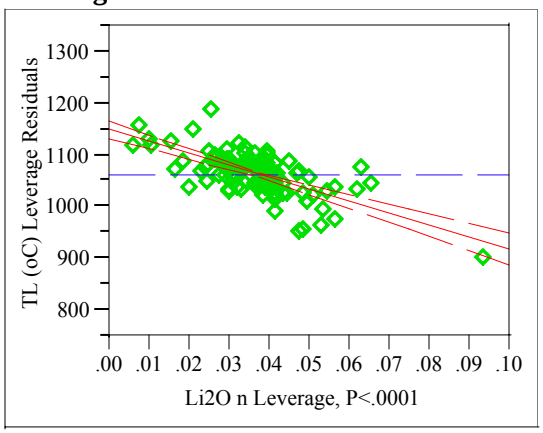

Na2O n
Leverage Plot

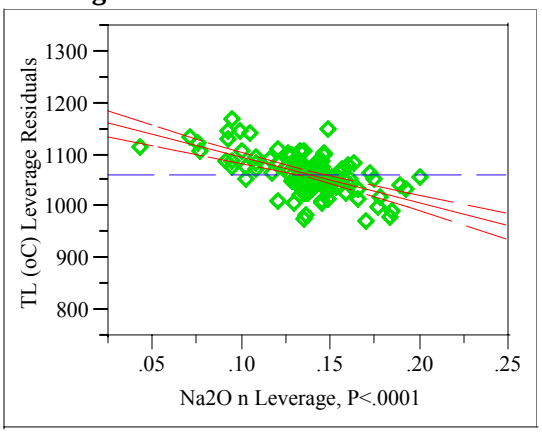

Appendix C. Model Fitting Results for TL Data

Exhibit C.6: Statistical Results from the Fitting of a LMM to Each Data Grouping

NiO n
Leverage Plot

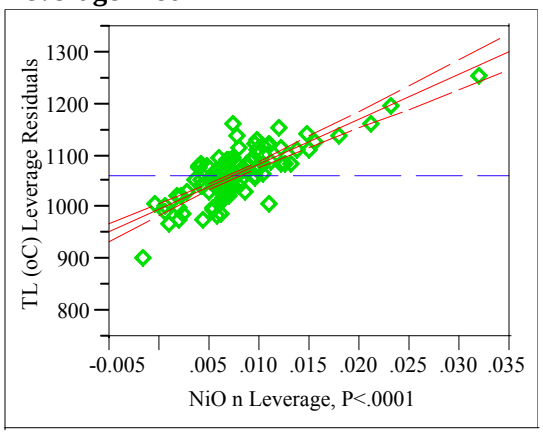

ThO2 n
Leverage Plot

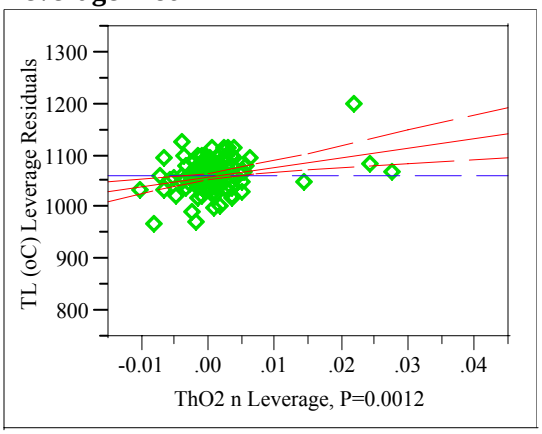

P2O5 n
Leverage Plot

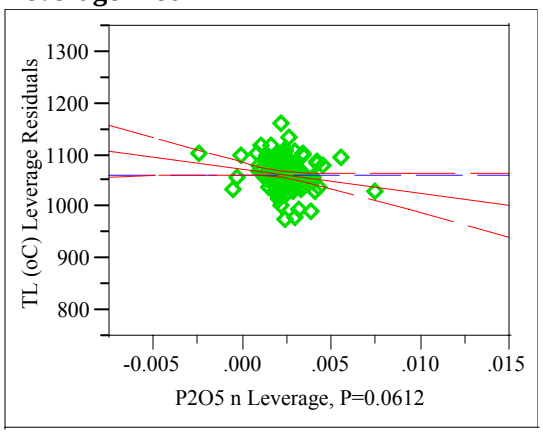

U3O8 n
Leverage Plot

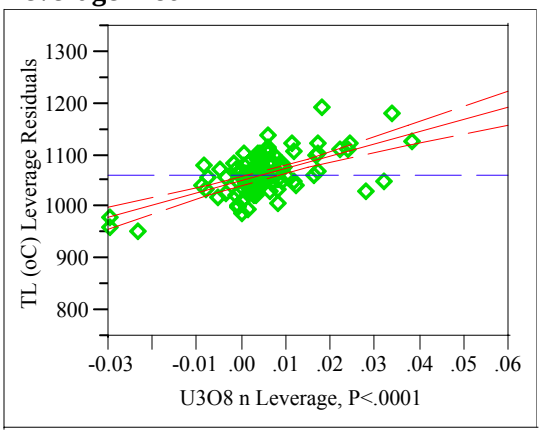

SiO2 n
Leverage Plot

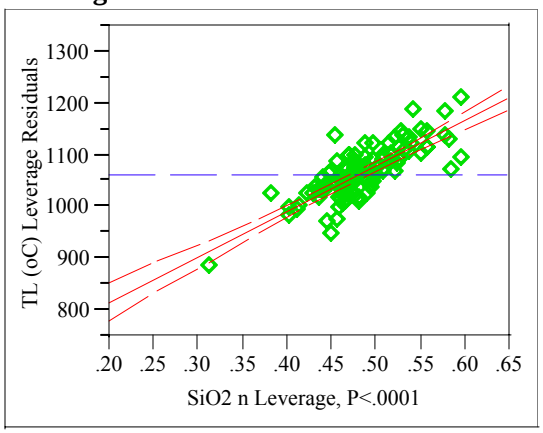

ZrO2 n
Leverage Plot

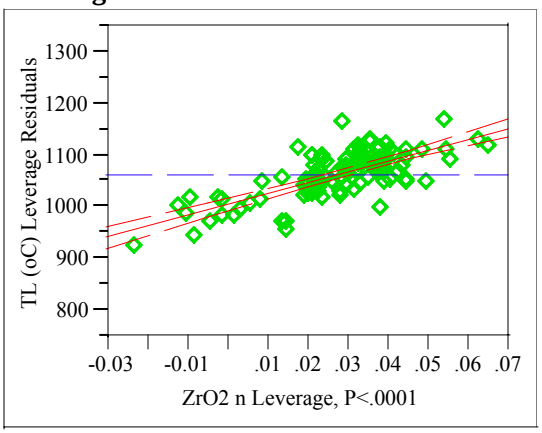

Appendix C. Model Fitting Results for TL Data

Exhibit C.7: Residual and Uncertainty Plots for Data Grouping 1

DWPFM Residuals in °C By #

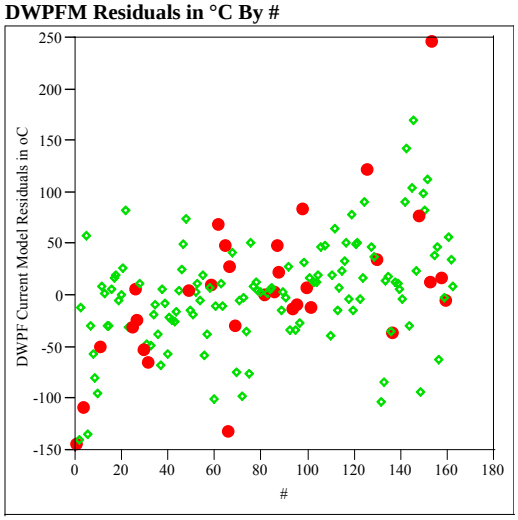

Prediction Uncertainty in °C for IPM By #

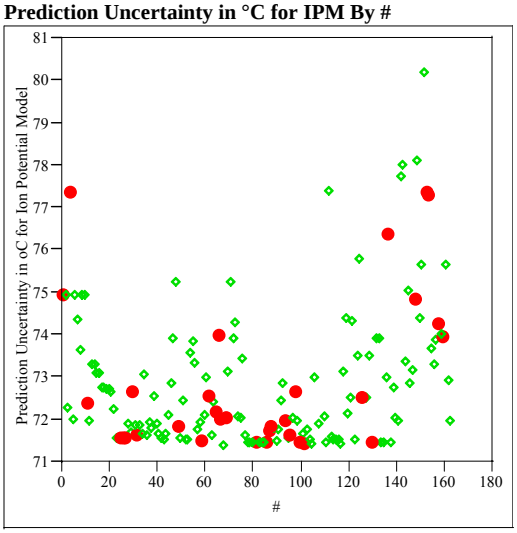

Prediction Uncertainty at 95% in °C for DWPFM By #

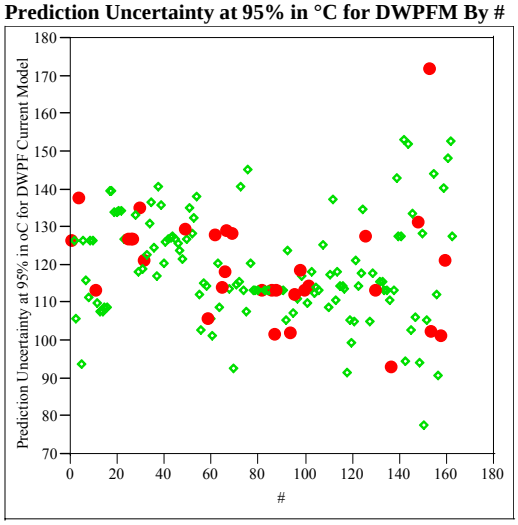

SPM w Cr and Ni Residual in °C By #

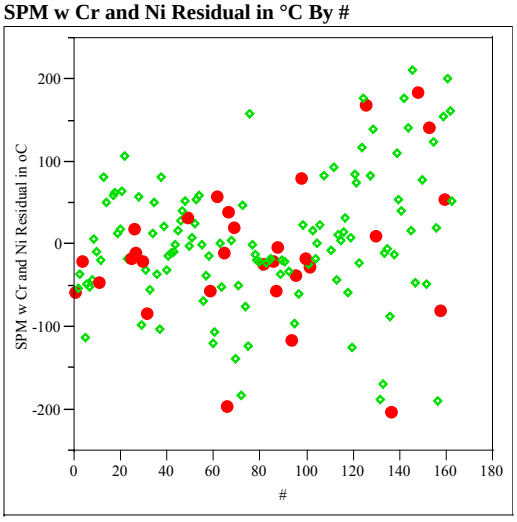

IPM Residual in °C By #

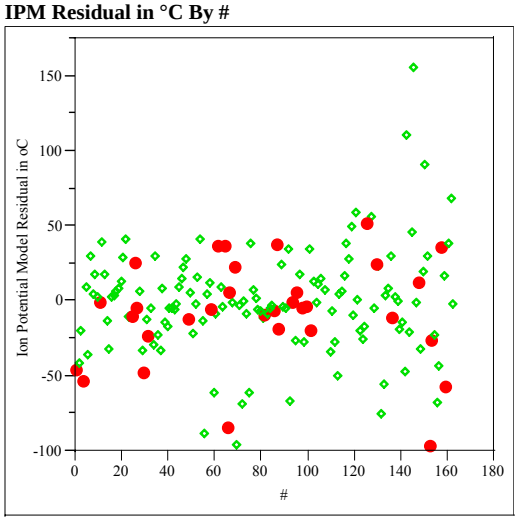

Prediction Uncertainty for SPM w Cr and Ni By #

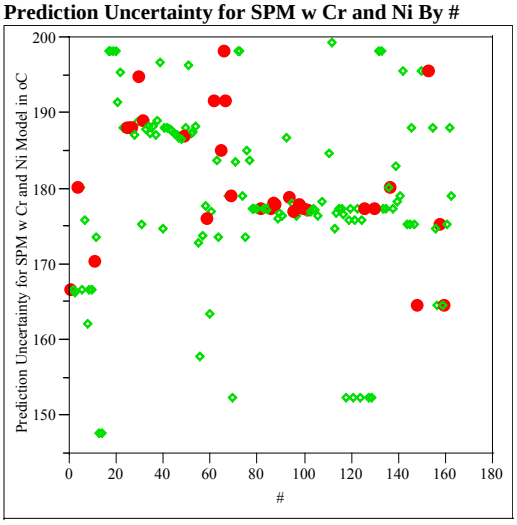

Appendix C. Model Fitting Results for TL Data

Exhibit C.7: Residual and Uncertainty Plots for Data Grouping 1

SPM w Ni and Fe Residual in °C By #

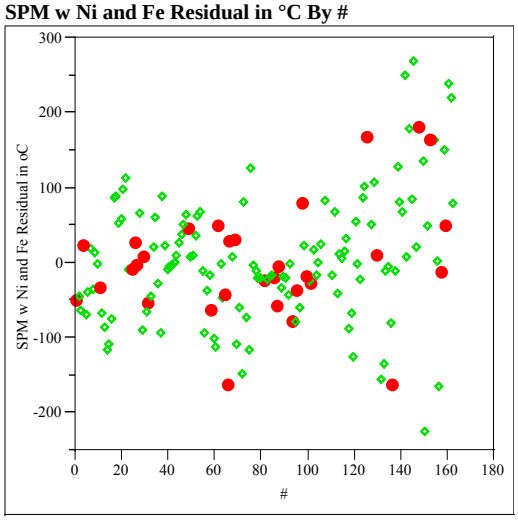

Prediction Uncertainty for SLM in °C By #

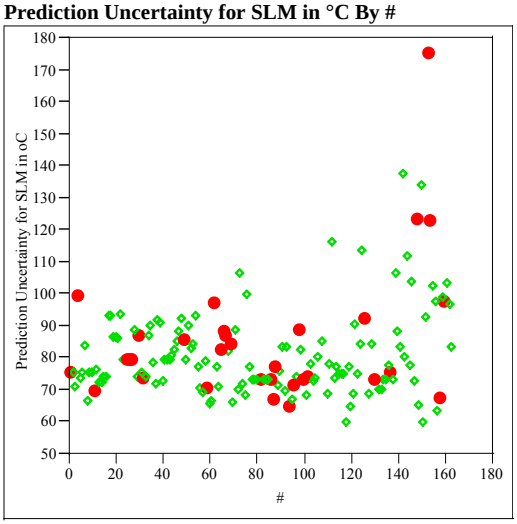

Prediction Uncertainty in °C for SPM w Ni and Fe By #

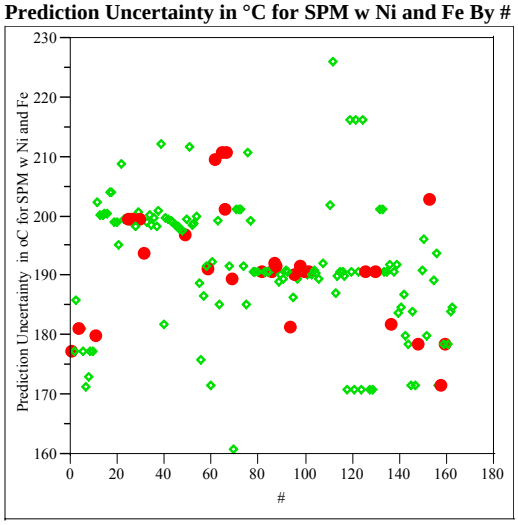

Prediction Uncertainty at 95% in °C for LMM Fit By #

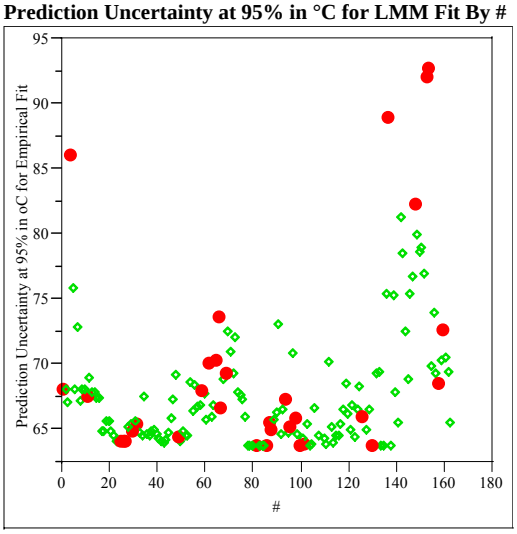

SLM Residual in °C By #

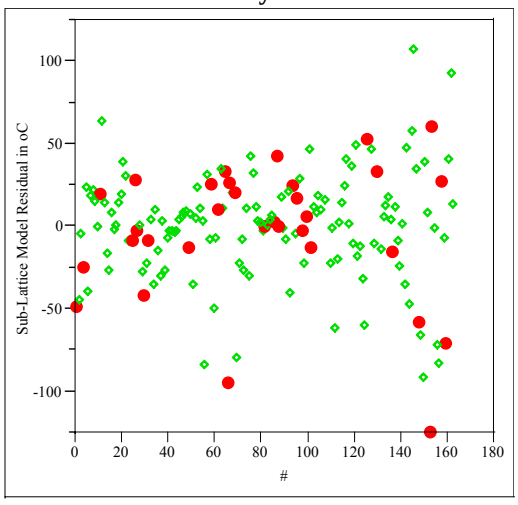

LMM Fit Residual °C By #

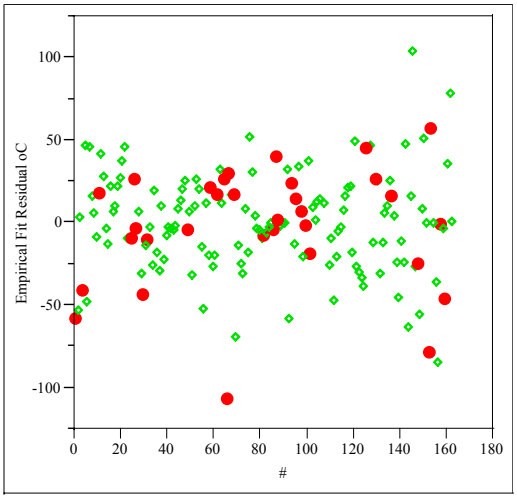

Appendix C. Model Fitting Results for TL Data

Exhibit C.8: Residual and Uncertainty Plots for Data Grouping 2

Prediction Uncertainty °C for DWPFM By #

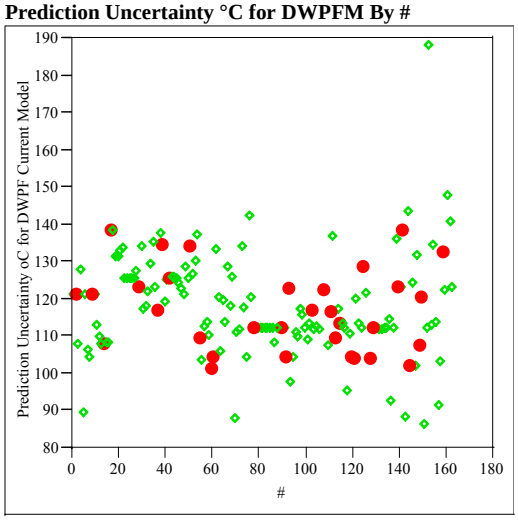

Residual °C for IPM By #

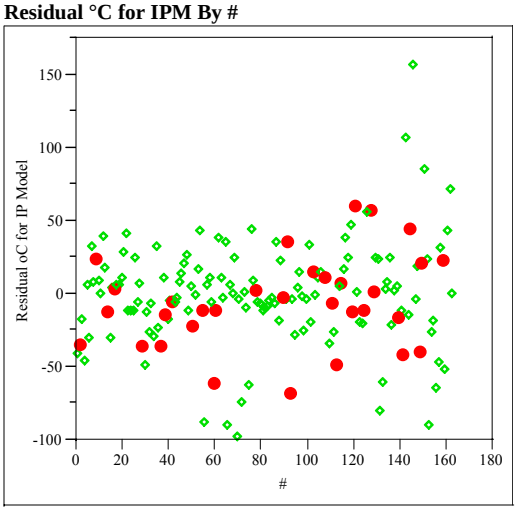

Residual °C for DWPFM By #

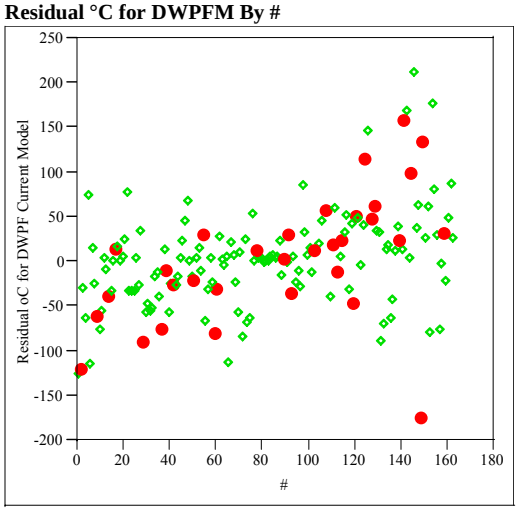

Prediction Uncertainty °C for SPM w Cr and Ni By #

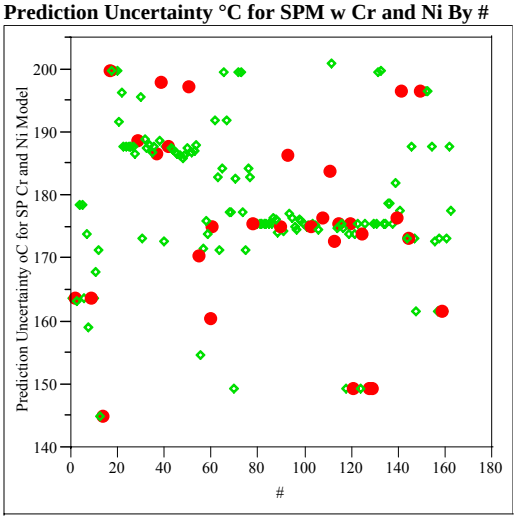

Prediction Uncertainty °C for IPM By #

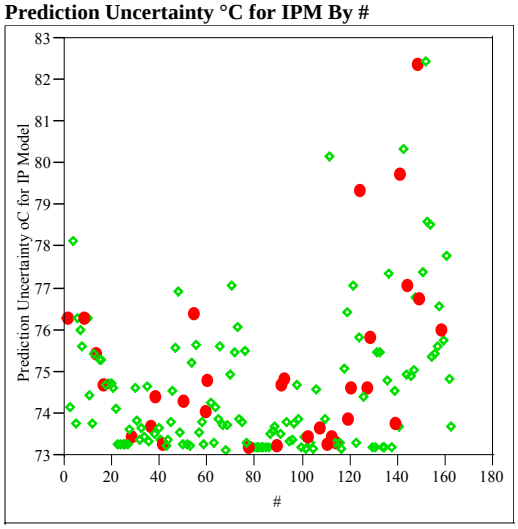

Residual °C for SPM w Cr and Ni By #

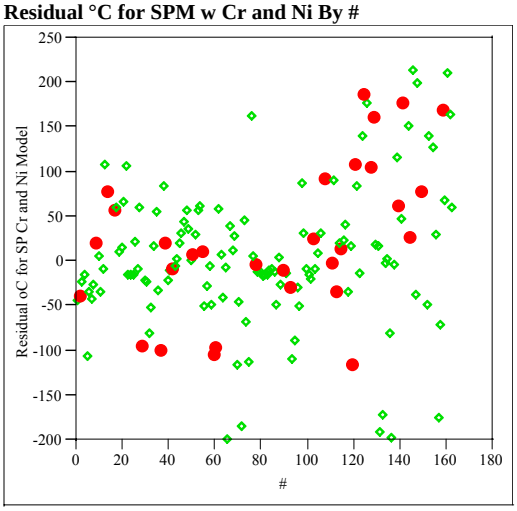

Appendix C. Model Fitting Results for TL Data

Exhibit C.8: Residual and Uncertainty Plots for Data Grouping 2

Prediction Uncertainty °C for SPM w Ni and Fe By #

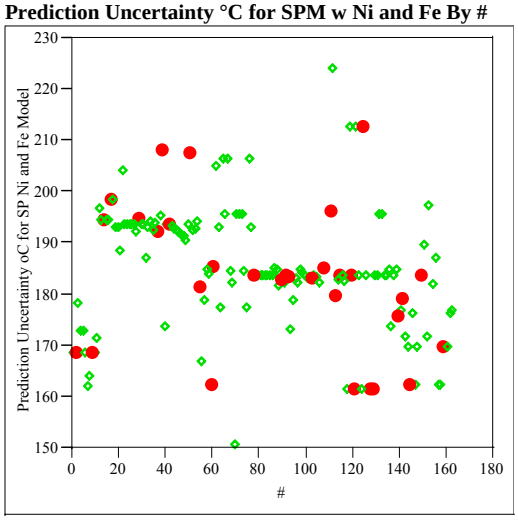

Residual °C for SLM By #

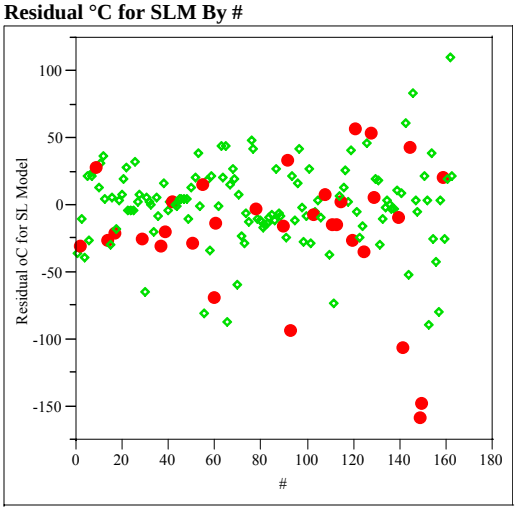

Residual °C for SPM w Ni and Fe By #

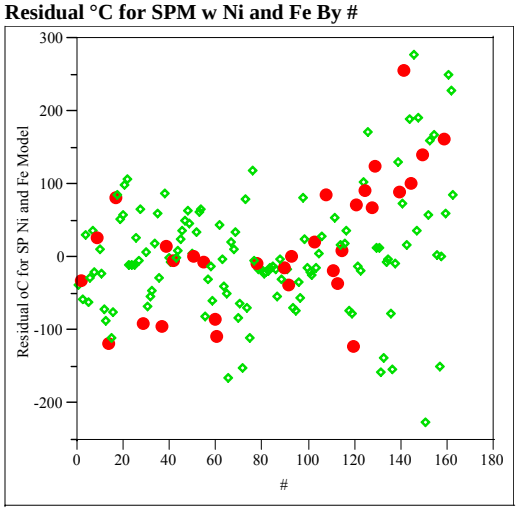

Prediction Uncertainty °C for LMM By #

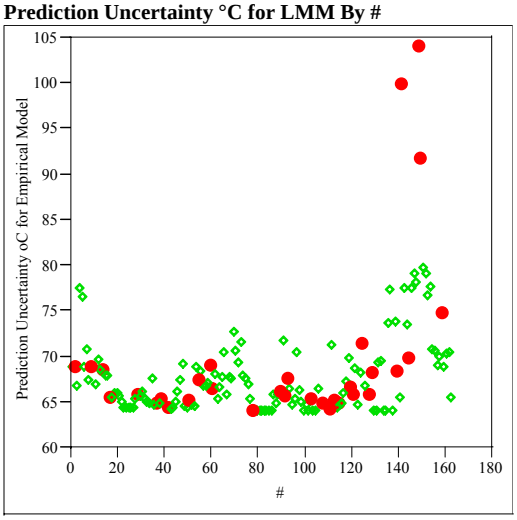

Prediction Uncertainty °C for SLM By #

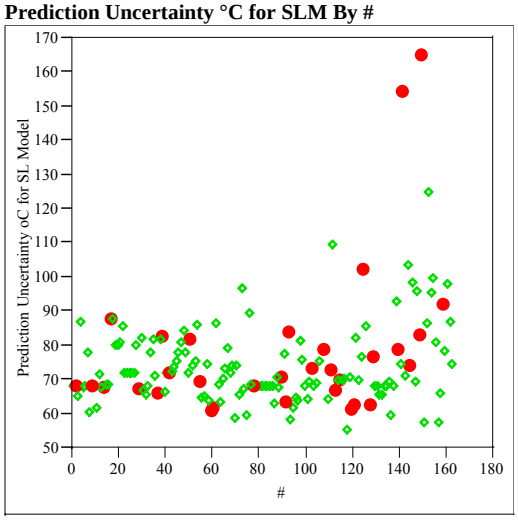

Residual °C for LMM By #

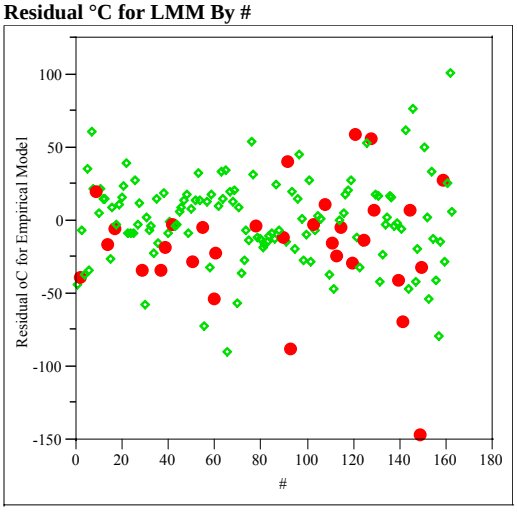

Prediction Uncertainty °C for DWPFM By #

Appendix C. Model Fitting Results for TL Data

Exhibit C.9: Residual and Uncertainty Plots for Data Grouping 3

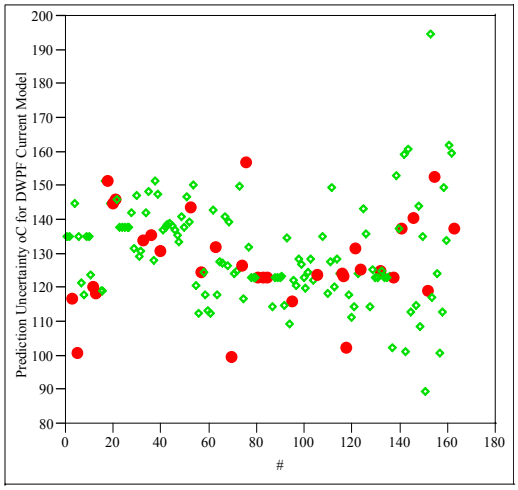

Residual °C for DWPFM By #

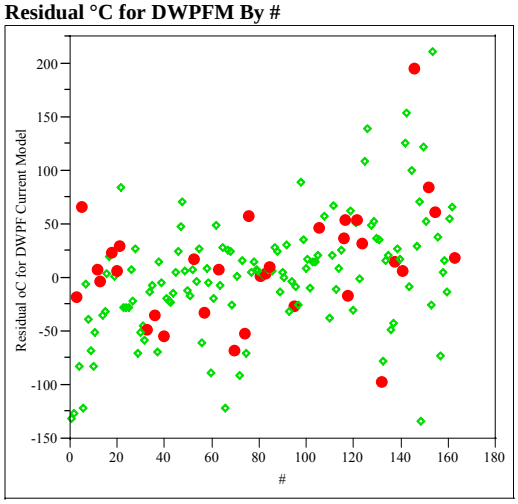

Prediction Uncertainty °C for IPM By #

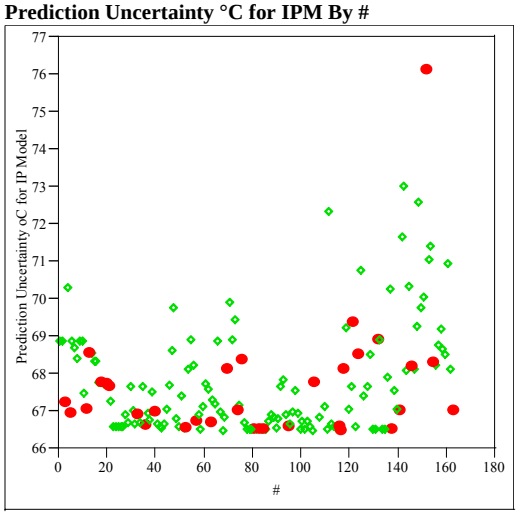

Residual °C for IPM By #

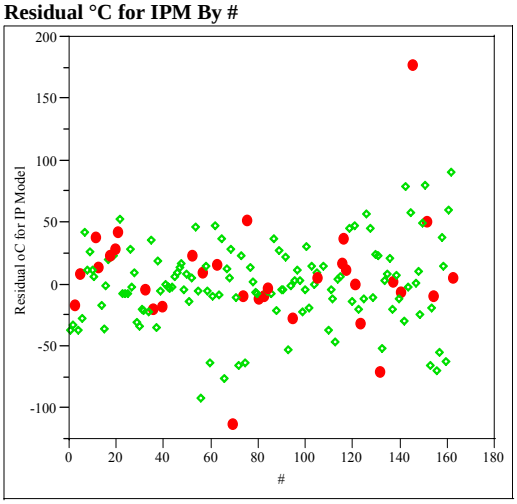

Prediction Uncertainty °C for SPM w Cr and Ni By #

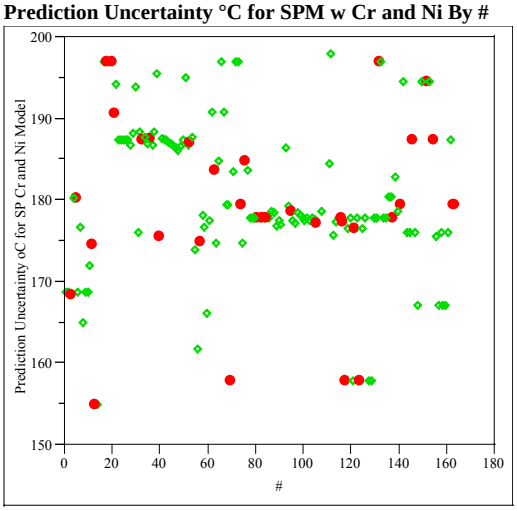

Residual °C for SPM w Cr and Ni By #

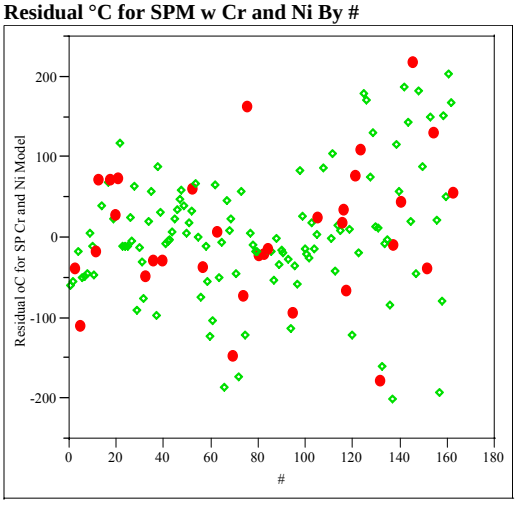

Appendix C. Model Fitting Results for TL Data

Exhibit C.9: Residual and Uncertainty Plots for Data Grouping 3

Prediction Uncertainty °C for SPM w Ni and Fe By #

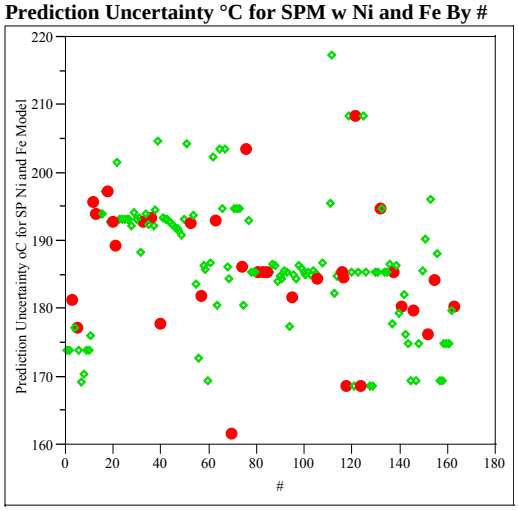

Residual °C for SLM By #

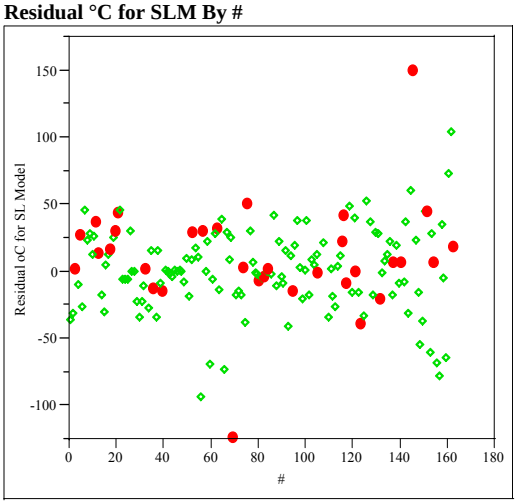

Residual °C for SPM w Ni and Fe By #

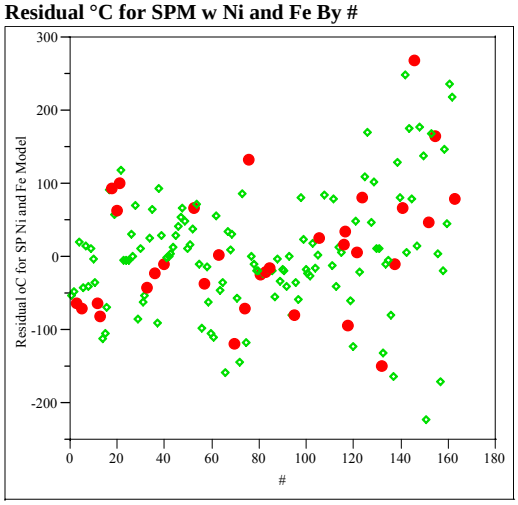

Prediction Uncertainty °C for LMM By #

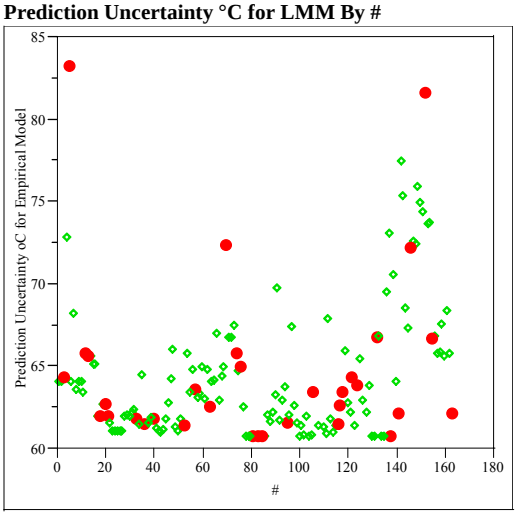

Prediction Uncertainty for SLM By #

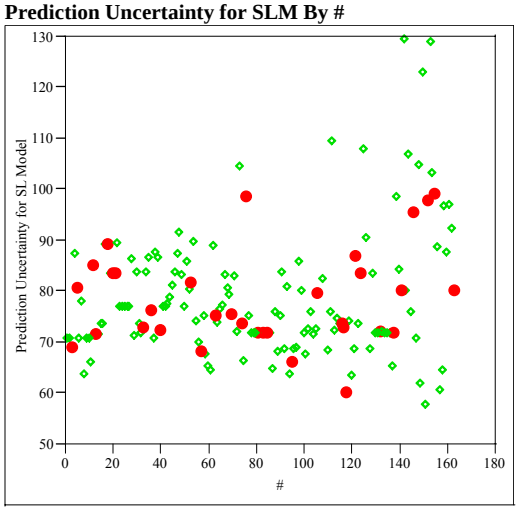

Residual °C for LMM By #

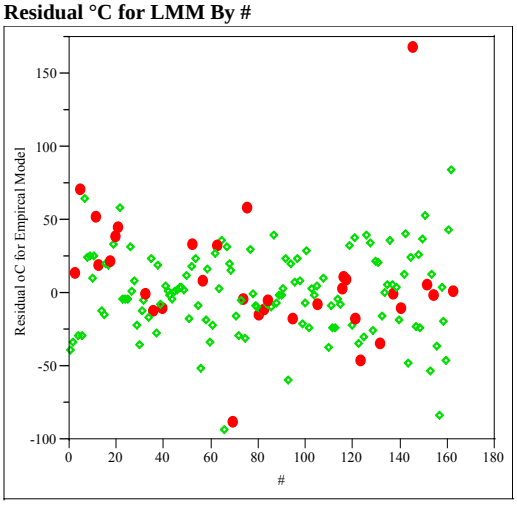

Appendix C. Model Fitting Results for TL Data

Exhibit C.10: Residual and Uncertainty Plots for Data Grouping 4

Prediction Uncertainty °C for DWPFM By #

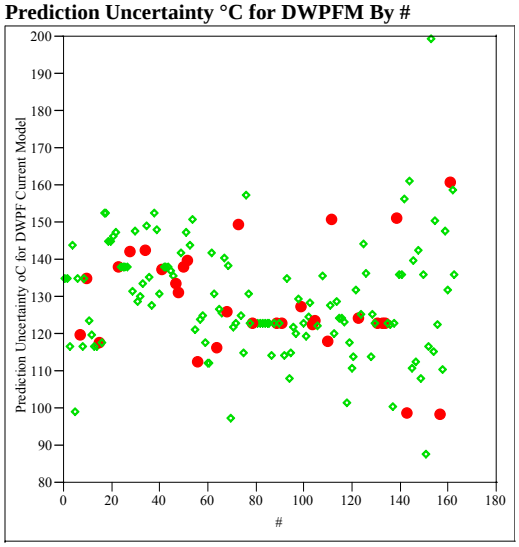

Residual °C for IPM By #

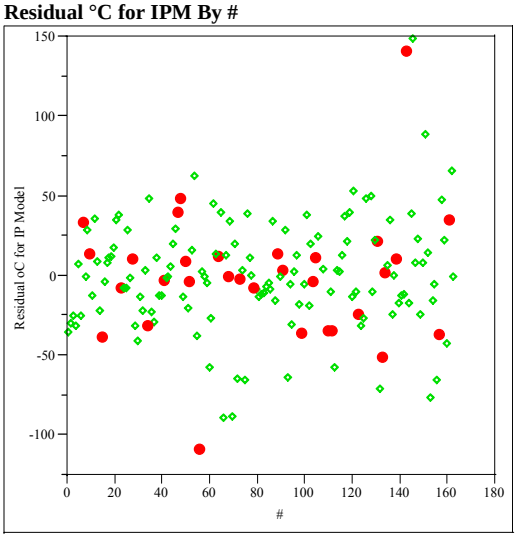

Residual °C for DWPFM By #

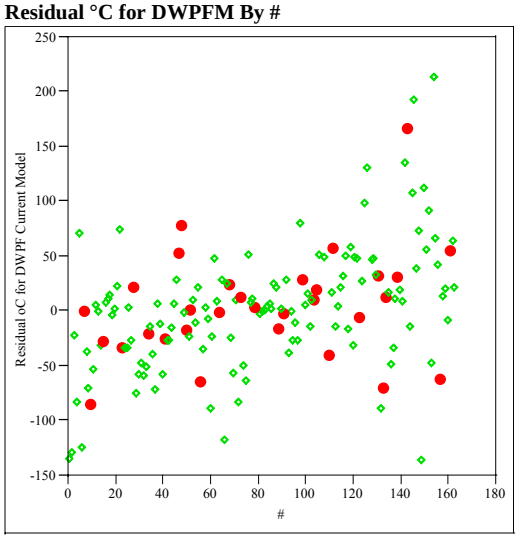

Prediction Uncertainty °C for SPM w Cr and Ni By #

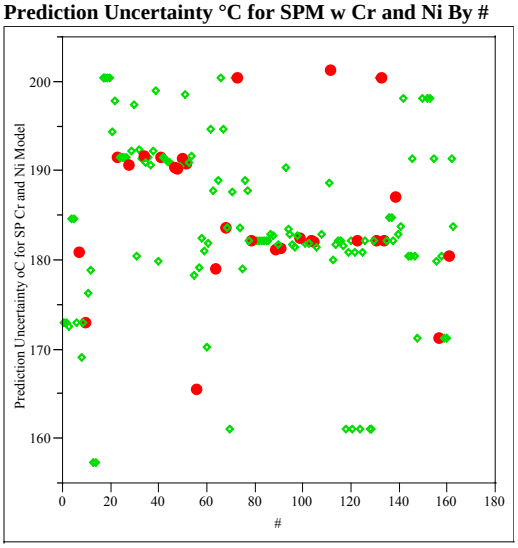

Prediction Uncertainty °C for IPM By #

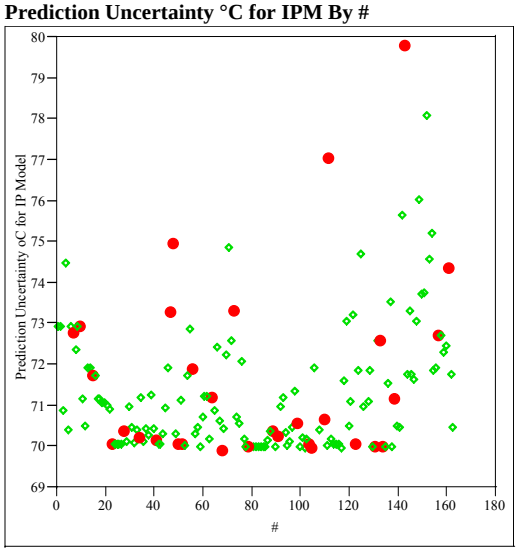

Residual °C for SPM w Cr and Ni By #

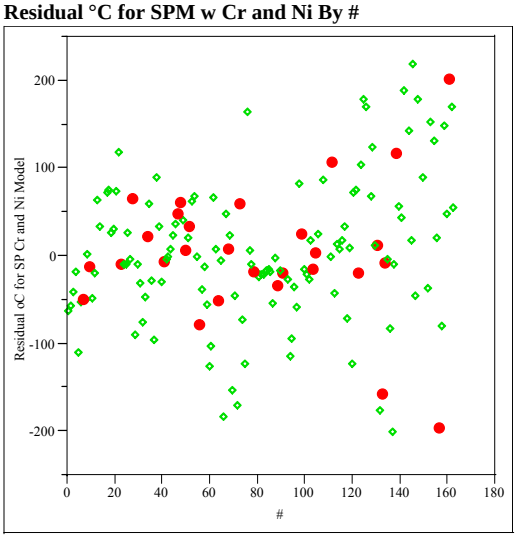

Appendix C. Model Fitting Results for TL Data

Exhibit C.10: Residual and Uncertainty Plots for Data Grouping 4

Prediction Uncertainty °C for SPM w Ni and Fe By #

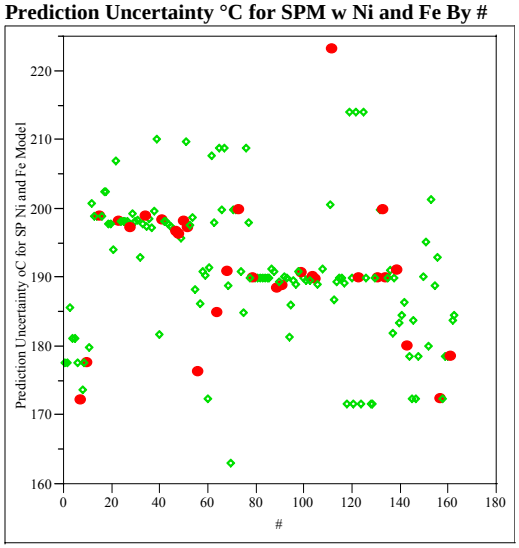

Residual °C for SLM By #

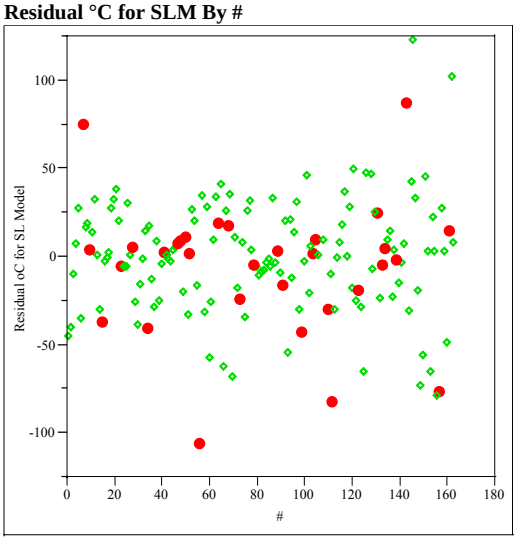

Residual °C for SPM w Ni and Fe By #

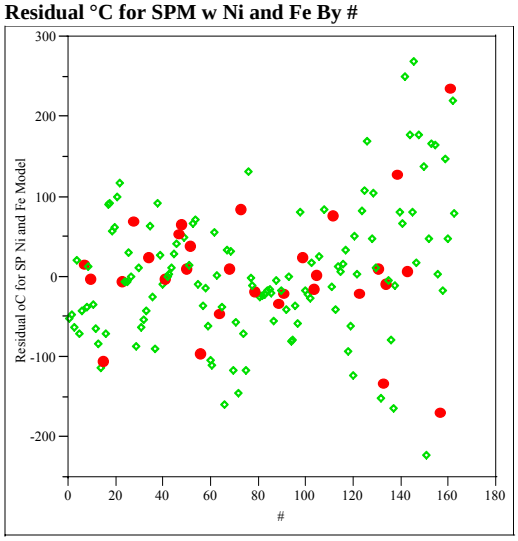

Prediction Uncertainty °C for LMM By #

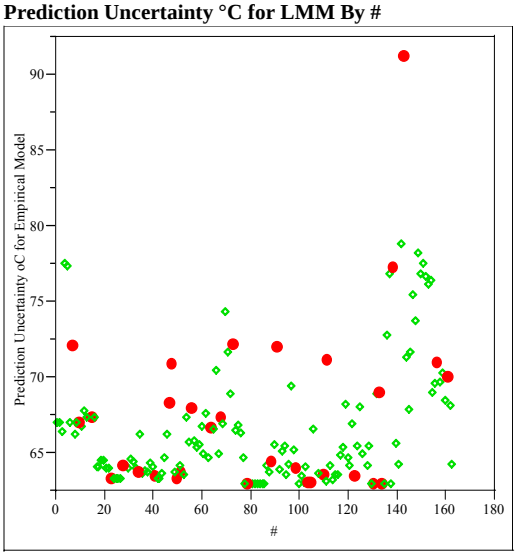

Prediction Uncertainty °C for SLM By #

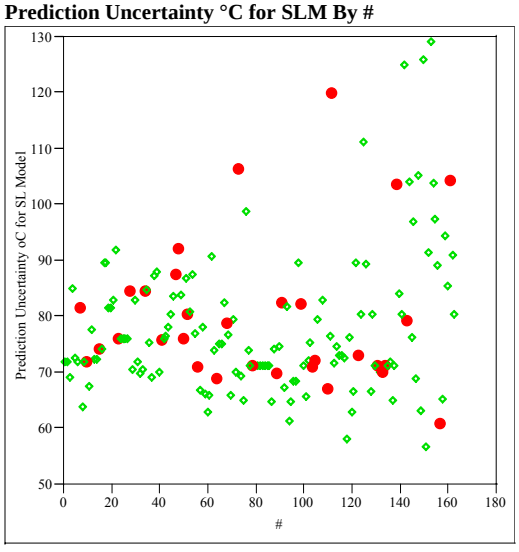

Residual °C for LMM By #

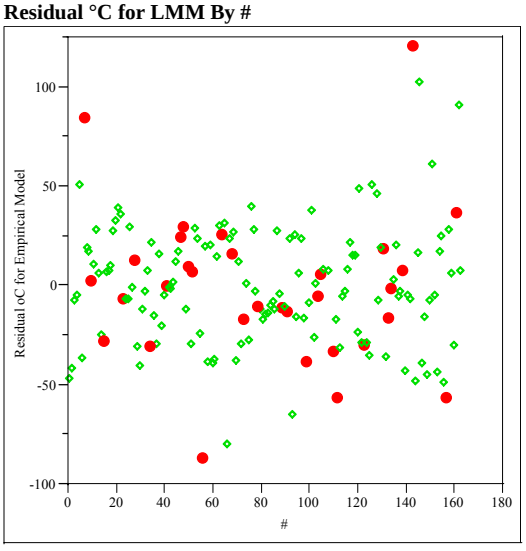

Appendix C. Model Fitting Results for TL Data

Exhibit C.11: Residual and Uncertainty Plots for Data Grouping 5

Prediction Uncertainty °C for DWPFM By #

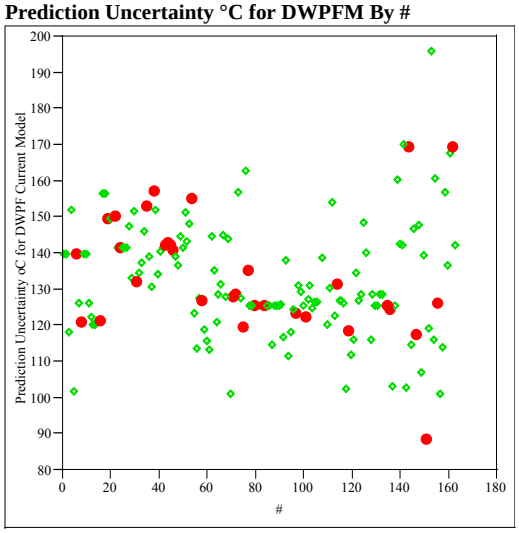

Residual °C for IPM By #

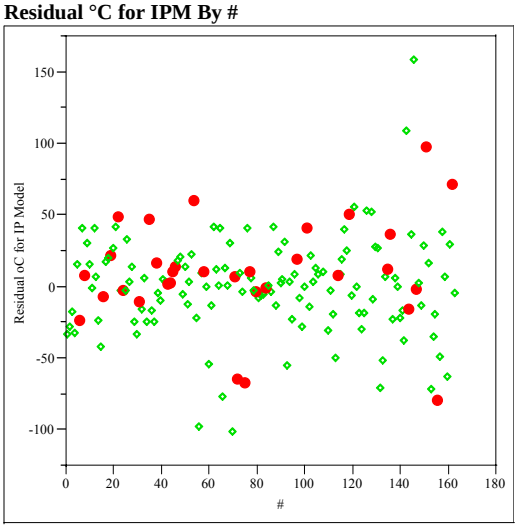

Residual °C for DWPFM By #

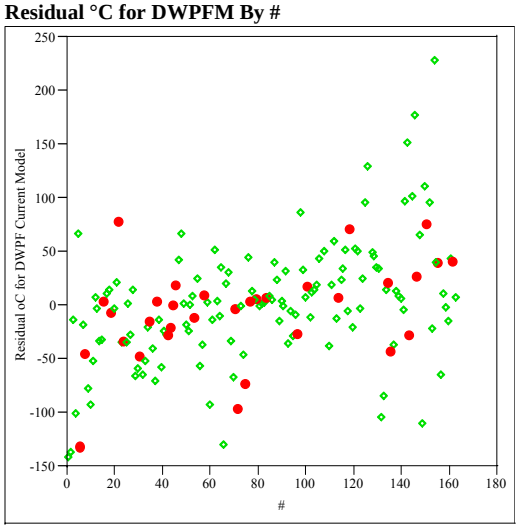

Prediction Uncertainty °C for SPM w Cr and Ni By #

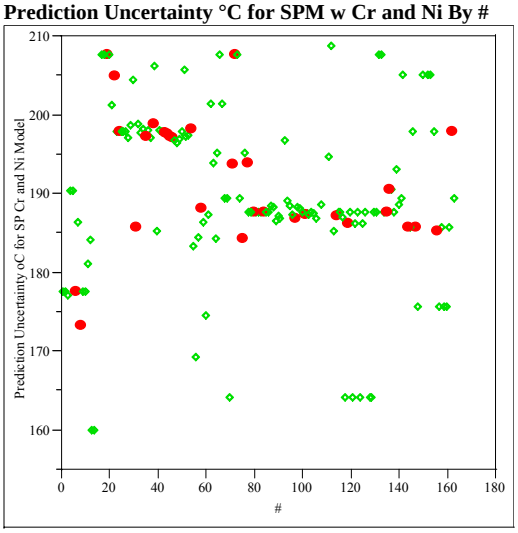

Prediction Uncertainty for IPM By #

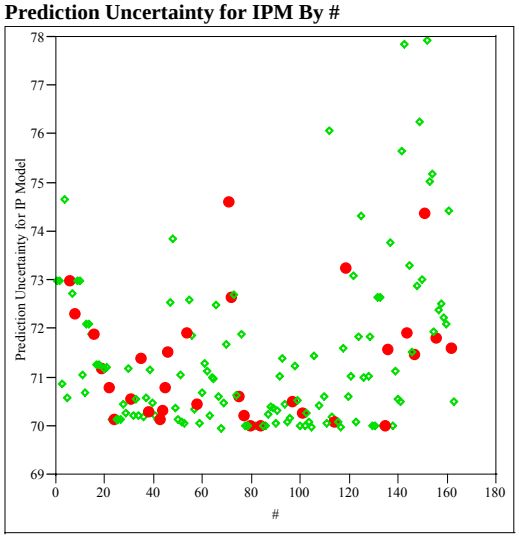

Residual °C for SPM w Cr and Ni By #

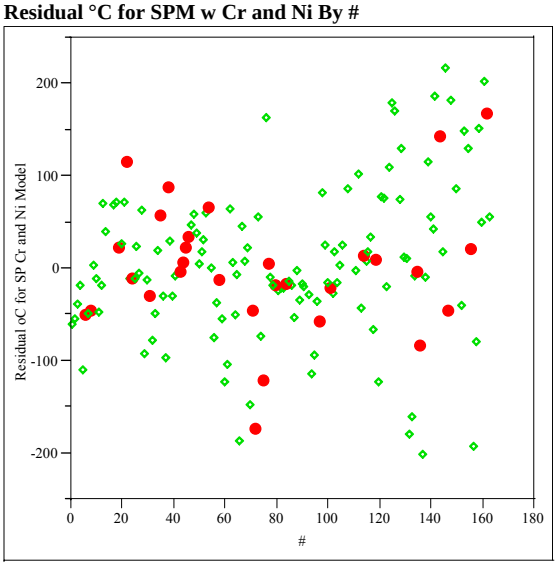

Appendix C. Model Fitting Results for TL Data

Exhibit C.11: Residual and Uncertainty Plots for Data Grouping 5

Prediction Uncertainty °C for SPM w Ni and Fe By #

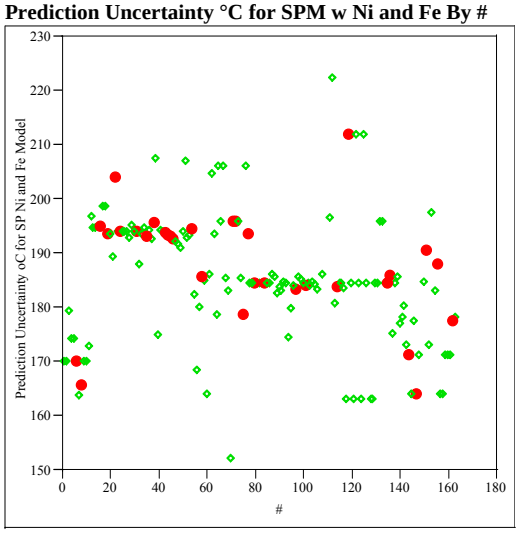

Residual °C for SLM By #

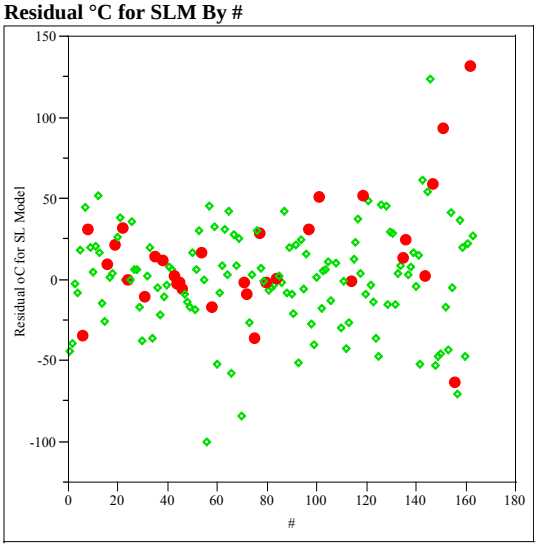

Residual °C for SPM w Ni and Fe By #

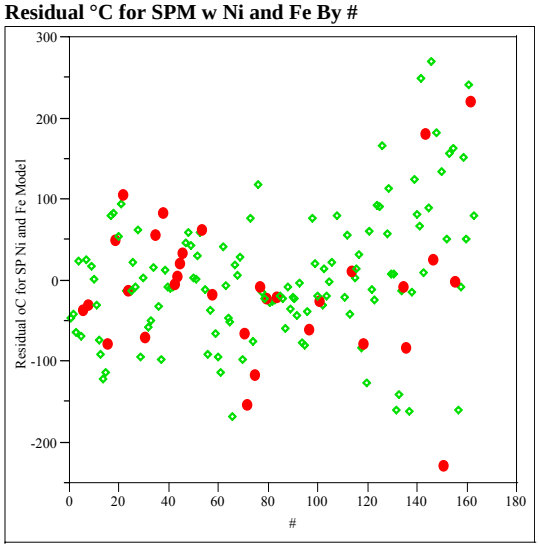

Prediction Uncertainty °C for LMM By #

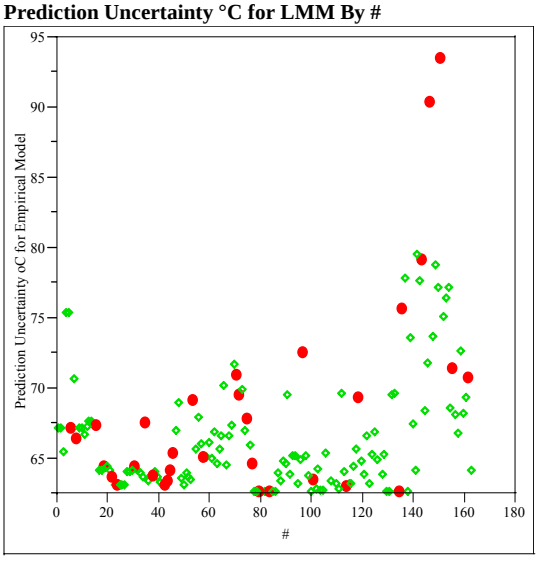

Prediction Uncertainty °C for SLM By #

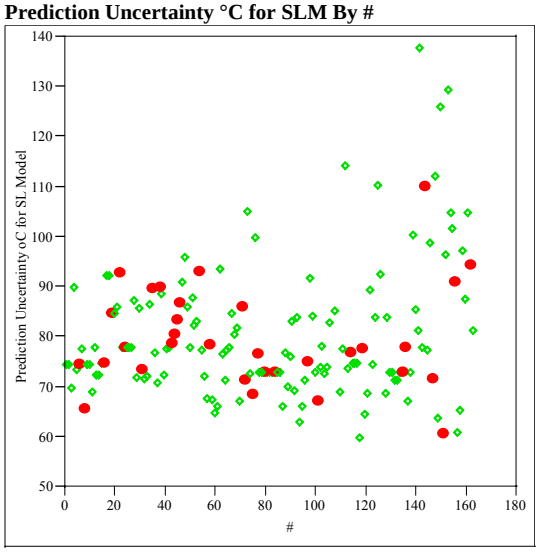

Residual °C for LMM By #

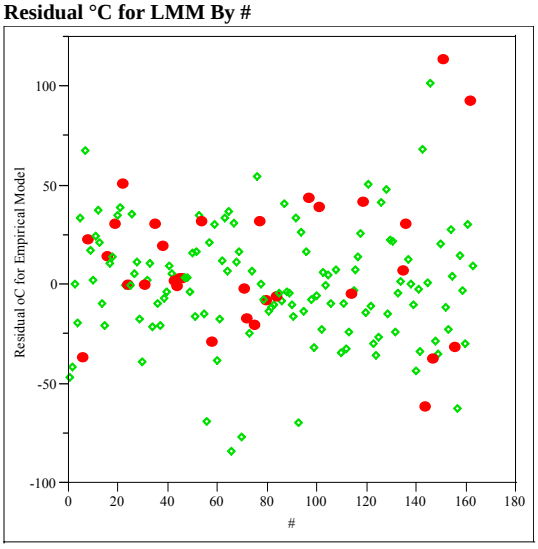

Appendix C. Model Fitting Results for TL Data

Exhibit C.12: Comparisons of Performance Metrics

R2 by Data Grouping

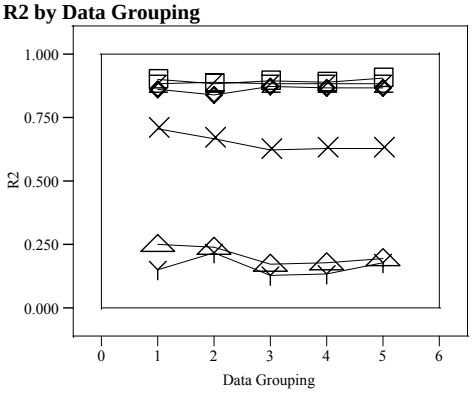

% Successfully Predicted (Model) by Data Grouping

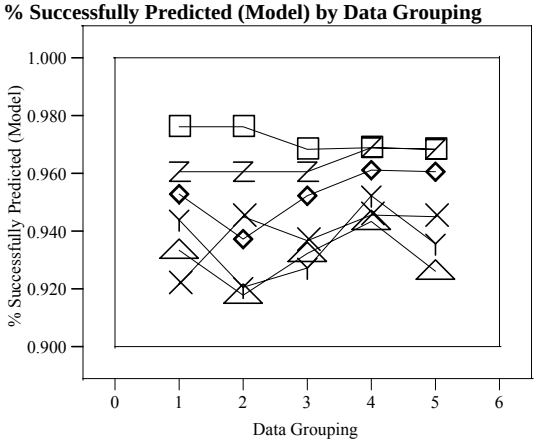

R2 val by Data Grouping

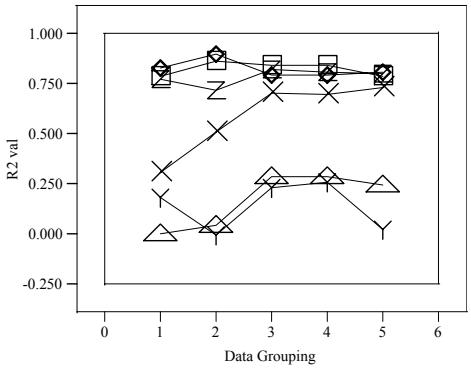

% Successfully Predicted (Valid) by Data Grouping

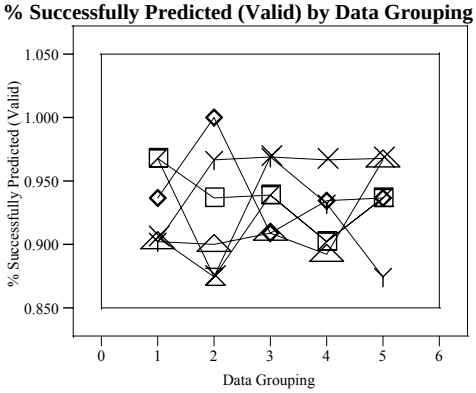

Avg Pred Uncertainty (Model) by Data Grouping

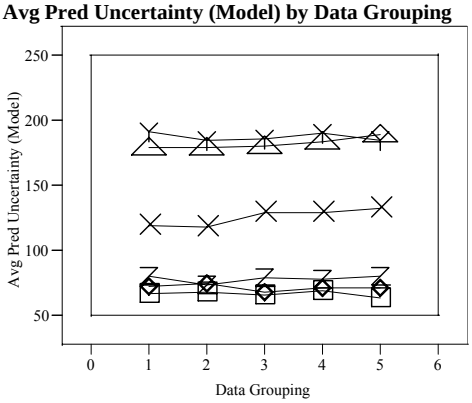

Relative, Uncertainty Weighted, Prediction Error Sum of Squares

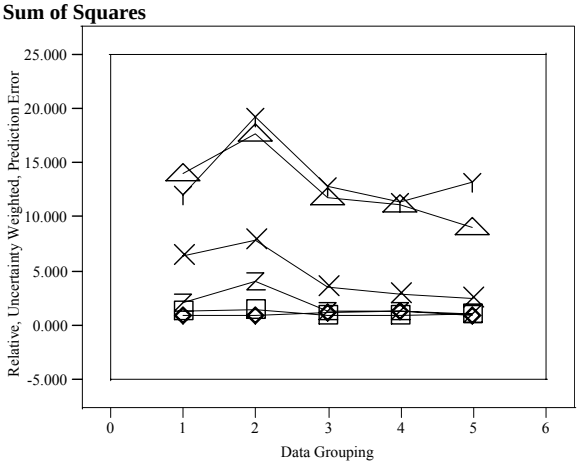

Avg Pred Uncertainty (Valid) by Data Grouping

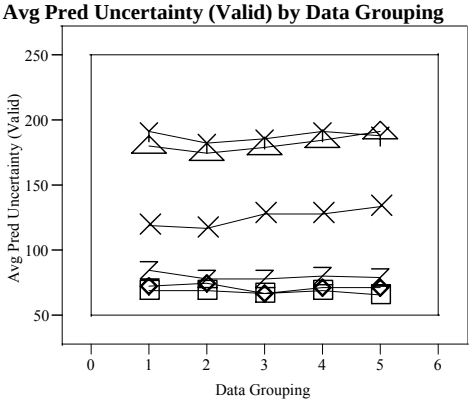

Y
- DWPF Current Model
- Empirical Linear Mixture Model
- Ion Potential Model
- Solubility Product (Cr & Ni) Model
- Solubility Product (Ni & Fe) Model
- Sub-Lattice Model

Appendix D

Model Fitting Results for T0.01 Data

Appendix D: Model Fitting Results for T0.01 Data

Table D.1: Summary of Fitting Results for DWPFM

	Data Grouping				
DWPFM (1/T(K))	1	2	3	4	5
n	34	33	33	33	32
R2	0.648873	0.641697	0.755494	0.719875	0.530825
R2 Adj	0.61497	0.604631	0.7302	0.690897	0.480556
RMSE	0.000062	0.000061	0.000051	0.000054	0.000065
SSEPRESS	1.72E-07	1.62E-07	1.19E-07	1.14E-07	1.80E-07
Corrected TSS	3.25E-07	3.02E-07	3.06E-07	3.03E-07	2.49E-07
R2 PRESS	0.468916	0.4647563	0.611416	0.6225329	0.278176
Sig. Lack of Fit (p-value)	0.4011	0.0458	0.4236	0.3716	0.0065
Number of Parameters	4				
Intercept	-0.00179	-0.00172	-0.00195	-0.002117	-0.00148
ln(SM2/(SM2+SM1+SMT+Ne1+NeT)	-0.00031	-0.000291	-0.00033	-0.000251	-0.00025
ln(SM1/(SM2+SM1+SMT+Ne1+NeT)	-0.00068	-0.000654	-0.0007	-0.000866	-0.0006
ln(SMT/(SM2+SM1+SMT+Ne1+NeT)	-0.00019	-0.00021	-0.00024	-0.000079	-0.00018

Appendix D. Model Fitting Results for T0.01 Data

Table D.2: Summary of Fitting Results for IPM

	Data Grouping				
IPM (T°C)	1	2	3	4	5
n	34	33	33	33	32
R2	0.697145	0.611305	0.684638	0.595972	0.585366
R2 Adj	0.629844	0.521607	0.611862	0.502734	0.485854
RMSE	79.90688	89.89458	81.89737	92.4829	86.72204
SSEPRESS	326326.9	486707.5	376751.7	515172.3	540115.7
Corrected TSS	569242.8	540545.1	1047855	548806.6	453455
R2 PRESS	0.426735	0.099599	0.640455	0.061286	-0.19111
Sig. Lack of Fit (p-value)	0.271	0.0476	0.199	0.1466	0.0111
Number of Parameters	7				
IPM (Cr moles)	58150.17	31615.01	23966.33	47258.12	33436.54
IPM (Mn moles)	6112.782	2764.728	3058.042	1423.303	1462.321
IPM (Ni moles)	20073.04	18919.39	17733.84	18116.64	20017.86
IPM (alkali moles) int	-560.877	-1961.61	-2263.59	-2628.63	-1046.85
IPM (alkali moles) slp	594.7945	2399.273	2703.604	3028.45	1348.807
IPM (nonalkali moles) int	7237.206	4513.683	6033.492	4418.599	3988.593
IPM (nonalkali moles) slp	-679.779	-391.946	-555.494	-378.969	-326.381

Appendix D. Model Fitting Results for T0.01 Data

Table D.3: Summary of Fitting Results for SPM w Cr and Ni

	Data Grouping				
SPM w Cr and Ni (1000/T(K))	1	2	3	4	5
n	31	30	29	29	30
R2	0.133039	0.254172	0.161676	0.106306	0.213916
R2 Adj	0.103144	0.227535	0.130627	0.073206	0.185841
RMSE	0.087515	0.082255	0.082677	0.084544	0.074204
SSEPRESS	2.84E-01	2.19E-01	2.34E-01	2.41E-01	1.94E-01
Corrected TSS	2.56E-01	2.54E-01	2.20E-01	2.16E-01	1.96E-01
R2 PRESS	-0.10755	0.139519	-0.06161	-0.11557	0.008825
Sig. Lack of Fit (p-value)	0.4907	0.0969	0.5821	0.4392	0.1726
Number of Parameters	2				
Intercept	0.773101	0.732393	0.760414	0.77189	0.750647
ln(Cr2O3 * NiO in wt%'s)	-0.04925	-0.07687	-0.04896	-0.04041	-0.05168

Appendix D. Model Fitting Results for T0.01 Data

Table D.4: Summary of Fitting Results for SPM w Ni and Fe

	Data Grouping				
SPM w Ni and Fe (1000/T(K))	1	2	3	4	5
n	33	31	31	31	31
R2	0.221239	0.401863	0.311191	0.295744	0.230343
R2 Adj	0.196118	0.381238	0.287439	0.271459	0.203803
RMSE	0.086363	0.073697	0.079656	0.080108	0.078877
SSEPRESS	2.69E-01	1.91E-01	2.19E-01	2.18E-01	2.08E-01
Corrected TSS	2.97E-01	2.63E-01	2.67E-01	2.64E-01	2.34E-01
R2 PRESS	0.093005	0.274969	0.179684	0.174568	0.112161
Sig. Lack of Fit (p-value)	0.0394	0.0089	0.0646	0.0764	0.0115
Number of Parameters	2				
Intercept	1.016201	1.072497	1.039044	1.006801	0.980589
ln(NiO * Fe2O3 in wt%'s)	-0.07937	-0.1045	-0.09064	-0.07925	-0.06683

Appendix D. Model Fitting Results for T0.01 Data

Table D.5: Summary of Fitting Results for SLM

	Data Grouping				
SLM (1/T(K))	1	2	3	4	5
n	34	33	33	33	32
R2	0.892779	0.897375	0.907452	0.85384	0.843348
R2 Adj	0.791865	0.79475	0.814905	0.70768	0.676253
RMSE	0.000045	0.000044	0.000042	0.000053	0.000051
SSEPRESS	8.31E-07	2.06E-06	4.88E-07	1.02E-06	2.02E-04
Corrected TSS	3.25E-07	3.02E-07	3.06E-07	3.03E-07	2.49E-07
R2 PRESS	-1.559361	-5.813627	-0.594145	-2.35615	-809.7196
Sig. Lack of Fit (p-value)	0.6079	0.1027	0.584	0.3741	0.0097
Number of Parameters	17				
Intercept	2.40E-03	1.52E-03	1.76E-04	2.08E-03	1.39E-03
SPL	-4.83E-02	-7.20E-02	5.77E-02	-5.40E-02	-1.20E-01
Al2O3 wt%	-3.58E-05	-2.20E-05	-1.50E-05	-2.40E-05	-2.65E-05
B2O3wt%	-4.90E-06	2.30E-06	8.00E-06	-4.00E-06	-3.60E-06
CaO wt%	-5.06E-05	-4.70E-05	-6.20E-05	-2.70E-05	1.22E-04
Cr2O3 wt%	-1.98E-04	7.70E-06	-2.71E-04	-1.18E-04	-4.15E-05
Fe2O3 wt%	-3.93E-05	-3.80E-05	-1.46E-08	-3.80E-05	-4.19E-05
K2O wt%	-3.11E-05	-1.00E-05	5.14E-05	-2.50E-05	-7.59E-05
Li2O wt%	7.49E-06	1.29E-05	2.48E-05	2.80E-06	1.04E-05
MgO wt%	-3.97E-05	-2.40E-05	-1.70E-05	-3.40E-05	-2.04E-04
MnO2 wt%	-3.57E-05	-3.60E-05	-5.00E-06	-2.80E-05	-2.58E-05
Na2O wt%	1.06E-05	1.89E-05	1.56E-05	1.28E-05	1.82E-05
NiO wt%	-1.01E-04	-8.50E-05	-7.90E-05	-9.40E-05	-8.69E-05
SiO2 wt%	-1.26E-05	-4.00E-06	4.14E-05	-1.00E-05	2.09E-06
TiO2 wt%	-1.97E-04	2.14E-03	8.28E-04	-2.14E-04	-4.14E-04
ZnO wt%	4.57E-06	2.09E-05	-1.70E-05	4.00E-06	4.81E-06
ZrO2 wt%	-3.72E-05	-2.30E-05	-2.30E-05	-3.10E-05	1.09E-07

Appendix D. Model Fitting Results for T0.01 Data

Table D.6: Summary of Fitting Results for LMM

	Data Grouping				
LMM (TL °C)	1	2	3	4	5
n	34	33	33	33	32
R2	0.890357	0.880718	0.901772	0.861097	0.842477
R2 Adj	0.842686	0.826499	0.857123	0.797958	0.767466
RMSE	52.09255	54.13677	49.68872	58.86469	58.32162
SSEPRESS	165014.5	186047.211	125983.6	160718.2	207781.96
Corrected TSS	569242.8	540545.12	552972.4	548806.6	453454.98
R2 PRESS	0.710116	0.65581558	0.77217	0.70715	0.5417804
Sig. Lack of Fit (p-value)	0.5278	0.1828	0.5768	0.4181	0.0239
Number of Parameters	11	11	11	11	11
Al2O3 n	3482.48	3296.49	3705.31	3155.44	3112.86
B2O3 n	177.47	546.12	134.97	532.70	440.22
Cr2O3 n	37400.52	19937.95	23518.88	28570.39	24798.63
Fe2O3 n	3734.58	3975.02	3573.51	3603.80	3778.70
Li2O n	-3028.20	-2458.44	-2315.93	-2510.31	-2642.67
MnO n	3016.40	3447.72	2679.50	2300.46	2992.40
Na2O n	-1902.76	-1519.36	-1821.94	-1813.82	-1858.23
NiO n	13835.50	12877.71	12502.12	12988.92	13354.07
SiO2 n	385.03	200.03	443.23	433.06	413.45
SrO n	-850.92	-9.82	-164.22	-569.39	-723.00
ZrO2 n	3969.51	4419.71	3779.37	3983.77	4105.90

Appendix D. Model Fitting Results for T0.01 Data

Table D.7: Summary of Fitting Results Generated for Data Grouping 1

	DWPFM	IPM	SPM w Cr&Ni	SPM w Ni&Fe	SLM	LMM
Model Response (Y)	1/ToK	ToC	1000/ToK	1000/ToK	1/ToK	ToC
Total Number of Obs	41	41	41	41	41	41
n + m	41	41	37	37	41	41
Obs for which model not defined	0	0	4	4	0	0
p	4	7	2	2	17	17
n	34	34	31	31	34	34
R2	0.649	0.697	0.133	0.221	0.893	0.890
R2 Adj	0.615	0.630	0.103	0.196	0.792	0.843
RMSE	6.200E-05	7.991E+01	8.752E-02	8.636E-02	4.500E-05	5.209E+01
SSEPRESS	1.724E-07	3.263E+05	2.837E-01	2.693E-01	8.306E-07	1.650E+05
Corrected TSS	3.245E-07	5.692E+05	2.562E-01	2.969E-01	3.245E-07	5.692E+05
R2 PRESS	0.469	0.427	-0.108	0.093	-1.559	0.710
Sig. Lack of Fit (p-value)	0.4011	0.271	0.4907	0.0394	0.6079	0.5278
Based Upon °C and Model Data						
R2	0.614	0.697	0.154	0.270	0.899	0.907
RMSE	85.6	79.9	112.5	111.8	58.0	55.9
SSE	219753	172398	367321	362796	57279	53198
Corrected TSS	569243	569243	434021	497137	569243	569243
Avg Prediction Uncertainty at 95%	224.2	179.7	329.3	317.1	194.7	123.5
# Successfully Predicted by Model	33	33	30	31	34	33
% Successfully Predicted	97.1%	97.1%	96.8%	100.0%	100.0%	97.1%
Based Upon °C and Valid. Data						
m	7	7	6	6	7	7
R2 val	0.411	-1.090	-0.232	0.544	0.581	0.607
ROOT Avg Prediction Error Sum of Squares val	81.7	153.9	89.6	54.5	68.9	66.8
Prediction Error Sum of Squares val	46751	165830	48125	17826	33274	31203
Corrected Total Sum of Squares	79350	79350	39066	39066	79350	79350
Avg Prediction Uncertainty at 95%	208.2	189.5	325.8	354.8	248.2	134.5
# Successfully Predicted by Model	7	6	6	6	7	7
% Successfully Predicted	100.0%	85.7%	100.0%	100.0%	100.0%	100.0%
Uncertainty Weighted, Predicted Error Sum of Squares						
Total Raw Score	10288830	38398941	16703091	5982985	5978903	4462500
Avg Raw Score	1469833	5485563	2783848	997164	854129	637500
Scaled Score	2.306	8.605	4.367	1.564	1.340	1.000

Appendix D. Model Fitting Results for T0.01 Data

Table D.8: Summary of Fitting Results Generated for Data Grouping 2

	DWPFM	IPM	SPM w Cr&Ni	SPM w Ni&Fe	SLM	LMM
Model Response (Y)	1/TK	T°C	1000/TK	1000/TK	1/TK	T°C
Total Number of Obs	41	41	41	41	41	41
n + m	41	41	37	39	41	41
Obs for which model not defined	0	0	4	2	0	0
p	4	7	2	2	17	17
n	33	33	30	31	33	33
R2	0.642	0.611	0.254	0.402	0.897	0.881
R2 Adj	0.605	0.522	0.228	0.381	0.795	0.826
RMSE	6.100E-05	8.989E+01	8.226E-02	7.370E-02	4.400E-05	5.414E+01
SSEPRESS	1.618E-07	4.867E+05	2.186E-01	1.909E-01	2.060E-06	1.860E+05
Corrected TSS	3.024E-07	5.405E+05	2.540E-01	2.633E-01	3.024E-07	5.405E+05
R2 PRESS	0.465	0.100	0.140	0.275	-5.814	0.656
Sig. Lack of Fit (p-value)	0.0458	0.0476	0.0969	0.0089	0.1027	0.1828
Based Upon °C and Model Data						
R2	0.628	0.611	0.291	0.458	0.904	0.881
RMSE	83.3	89.9	104.4	91.6	57.0	63.5
SSE	201135	210107	305398	243364	51904	64477
Corrected TSS	540545	540545	430866	448780	540545	540545
Avg Prediction Uncertainty at 95%	225.8	203.0	310.4	270.5	191.8	129.1
# Successfully Predicted by Model	32	32	29	28	33	32
% Successfully Predicted	97.0%	97.0%	96.7%	90.3%	100.0%	97.0%
Based Upon °C and Valid. Data						
m	8	8	7	8	8	8
R2 val	0.593	0.557	0.175	0.845	0.710	0.746
ROOT Avg Prediction Error Sum of Squares val	76.4	79.7	82.9	47.2	64.5	60.3
Prediction Error Sum of Squares val	46751	50790	48125	17826	33274	29120
Corrected Total Sum of Squares	114749	114749	58306	114749	114749	114749
Avg Prediction Uncertainty at 95%	230.1	203.0	291.3	246.8	542.6	138.7
# Successfully Predicted by Model	8	8	6	6	8	8
% Successfully Predicted	100.0%	100.0%	85.7%	75.0%	100.0%	100.0%
Uncertainty Weighted, Predicted Error Sum of Squares						
Total Raw Score	10653629	10594443	30786218	32953453	151149171	3852124
Avg Raw Score	1331704	1324305	4398031	4119182	18893646	481516
Scaled Score	2.766	2.750	9.134	8.555	39.238	1.000

Appendix D. Model Fitting Results for T0.01 Data

Table D.9: Summary of Fitting Results Generated for Data Grouping 3

	DWPFM	IPM	SPM w Cr&Ni	SPM w Ni&Fe	SLM	LMM
Model Response (Y)	1/TK	T°C	1000/TK	1000/TK	1/TK	T°C
Total Number of Obs	41	41	41	41	41	41
n + m	41	41	36	39	41	41
Obs for which model not defined	0	0	5	2	0	0
p	4	7	2	2	17	17
n	33	33	29	31	33	33
R2	0.755	0.685	0.162	0.311	0.907	0.902
R2 Adj	0.730	0.612	0.131	0.287	0.815	0.857
RMSE	5.100E-05	8.190E+01	8.268E-02	7.966E-02	4.200E-05	4.969E+01
SSEPRESS	1.189E-07	3.768E+05	2.337E-01	2.191E-01	4.879E-07	1.260E+05
Corrected TSS	3.060E-07	1.048E+06	2.201E-01	2.671E-01	3.060E-07	5.530E+05
R2 PRESS	0.611	0.640	-0.062	0.180	-0.594	0.772
Sig. Lack of Fit (p-value)	0.4236	0.199	0.5821	0.0646	0.584	0.5768
Based Upon °C and Model Data						
R2	0.700	0.685	0.208	0.374	0.914	0.902
RMSE	75.6	81.9	106.6	99.9	54.4	58.3
SSE	165843	174387	307076	289165	47315	54317
Corrected TSS	552972	552972	387781	461702	552972	552972
Avg Prediction Uncertainty at 95%	183.5	185.0	318.7	298.1	183.2	118.5
# Successfully Predicted by Model	33	33	27	28	33	33
% Successfully Predicted	100.0%	100.0%	93.1%	90.3%	100.0%	100.0%
Based Upon °C and Valid. Data						
m	8	8	7	8	8	8
R2 val	0.088	-0.189	0.104	0.115	0.247	0.598
ROOT Avg Prediction Error Sum of Squares val	107.1	122.2	113.4	105.4	97.3	71.0
Prediction Error Sum of Squares val	91727	119523	90065	88953	75694	40378
Corrected Total Sum of Squares	100534	100534	100534	100534	100534	100534
Avg Prediction Uncertainty at 95%	183.9	194.4	316.7	279.7	403.8	130.7
# Successfully Predicted by Model	7	7	7	8	7	7
% Successfully Predicted	87.5%	87.5%	100.0%	100.0%	87.5%	87.5%
Uncertainty Weighted, Predicted Error Sum of Squares	17467974.1	27306286.1	27940014.9	23080326.2	29812641.3	5503113.9
Avg Raw Score	2183497	3413286	3991431	2885041	3726580	687889
Scaled Score	3.174	4.962	5.802	4.194	5.417	1.000

Appendix D. Model Fitting Results for T0.01 Data

Table D.10: Summary of Fitting Results Generated for Data Grouping 4

	DWPFM	IPM	SPM w Cr&Ni	SPM w Ni&Fe	SLM	LMM
Model Response (Y)	1/TK	T°C	1000/TK	1000/TK	1/TK	T°C
Total Number of Obs	41	41	41	41	41	41
n + m	41	41	37	39	41	41
Obs for which model not defined	0	0	4	2	0	0
p	4	7	2	2	17	17
n	33	33	29	31	33	33
R2	0.720	0.596	0.106	0.296	0.854	0.861
R2 Adj	0.691	0.503	0.073	0.271	0.708	0.798
RMSE	5.400E-05	9.248E+01	8.454E-02	8.011E-02	5.300E-05	5.886E+01
SSEPRESS	1.144E-07	5.152E+05	2.409E-01	2.181E-01	1.017E-06	1.607E+05
Corrected TSS	3.030E-07	5.488E+05	2.159E-01	2.643E-01	3.030E-07	5.488E+05
R2 PRESS	0.623	0.061	-0.116	0.175	-2.356	0.707
Sig. Lack of Fit (p-value)	0.3716	0.1466	0.4392	0.0764	0.3741	0.4181
Based Upon °C and Model Data						
R2	0.714	0.596	0.132	0.359	0.877	0.861
RMSE	73.6	92.3	110.8	100.6	64.9	69.0
SSE	156946	221733	331482	293534	67318	76231
Corrected TSS	548807	548807	381864	458077	548807	548807
Avg Prediction Uncertainty at 95%	196.4	208.6	329.2	301.3	238.8	140.5
# Successfully Predicted by Model	32	32	27	29	33	32
% Successfully Predicted	97.0%	97.0%	93.1%	93.5%	100.0%	97.0%
Based Upon °C and Valid. Data						
m	8	8	8	8	8	8
R2 val	-3.259	0.455	0.290	0.210	0.617	0.882
ROOT Avg Prediction Error Sum of Squares val	231.0	82.6	94.3	99.5	69.3	38.4
Prediction Error Sum of Squares val	426796	54581	71183	79193	38366	11793
Corrected Total Sum of Squares	100218	100218	100218	100218	100218	100218
Avg Prediction Uncertainty at 95%	273.9	207.0	327.3	300.2	382.1	157.5
# Successfully Predicted by Model	6	8	7	7	8	8
% Successfully Predicted	75.0%	100.0%	87.5%	87.5%	100.0%	100.0%
Uncertainty Weighted, Predicted Error Sum of Squares						
Total Raw Score	345590111.0	12299453.4	22456184.1	23185062.1	38809741.7	1687704.7
Avg Raw Score	43198764	1537432	2807023	2898133	4851218	210963
Scaled Score	204.769	7.288	13.306	13.738	22.996	1.000

Appendix D. Model Fitting Results for T0.01 Data

Table D.11: Summary of Fitting Results Generated for Data Grouping 5

	DWPFM	IPM	SPM w Cr&Ni	SPM w Ni&Fe	SLM	LMM
Model Response (Y)	1/ToK	ToC	1000/ToK	1000/ToK	1/ToK	ToC
Total Number of Obs	41	41	41	41	41	41
n + m	41	41	37	39	41	41
Obs for which model not defined	0	0	4	2	0	0
p	4	7	2	2	17	17
n	32	32	30	31	32	32
R2	0.531	0.585	0.214	0.230	0.843	0.842
R2 Adj	0.481	0.486	0.186	0.204	0.676	0.767
RMSE	6.500E-05	8.672E+01	7.420E-02	7.888E-02	5.100E-05	5.832E+01
SSEPRESS	1.799E-07	5.401E+05	1.944E-01	2.081E-01	2.021E-04	2.078E+05
Corrected TSS	2.492E-07	4.535E+05	1.961E-01	2.344E-01	2.492E-07	4.535E+05
R2 PRESS	0.278	-0.191	0.009	0.112	-809.720	0.542
Sig. Lack of Fit (p-value)	0.0065	0.0111	0.1726	0.0115	0.0097	0.0239
Based Upon °C and Model Data						
R2	0.535	0.585	0.264	0.298	0.867	0.842
RMSE	86.8	86.7	98.8	101.7	63.3	69.0
SSE	211053	188018	273113	299977	60146	71430
Corrected TSS	453455	453455	370878	427253	453455	453455
Avg Prediction Uncertainty at 95%	242.1	196.7	279.7	296.8	231.7	140.2
# Successfully Predicted by Model	31	31	27	29	32	31
% Successfully Predicted	96.9%	96.9%	90.0%	93.5%	100.0%	96.9%
Based Upon °C and Valid. Data						
m	9	9	7	8	9	9
R2 val	0.832	0.538	-0.101	0.335	-21.166	0.908
ROOT Avg Prediction Error Sum of Squares val	61.3	101.7	132.6	100.7	704.3	45.5
Prediction Error Sum of Squares val	33818	93064	123160	81046	4464417	18616
Corrected Total Sum of Squares	201405	201405	111886	121850	201405	201405
Avg Prediction Uncertainty at 95%	243.6	204.8	289.5	286.0	2293.2	179.0
# Successfully Predicted by Model	9	8	6	7	9	9
% Successfully Predicted	100.0%	88.9%	85.7%	87.5%	100.0%	100.0%
Uncertainty Weighted, Predicted Error Sum of Squares						
Total Raw Score	9325779.1	19790218.0	34606932.9	22049519.4	10560400000.0	3211781.2
Avg Raw Score	1036198	2198913	4943848	2756190	1173377778	356865
Scaled Score	2.904	6.162	13.854	7.723	3288.020	1.000

Appendix D. Model Fitting Results for T0.01 Data

Appendix D. Model Fitting Results for T0.01 Data

Exhibit D.1: Statistical Results from the Fitting of the DWPFM to Each Data Grouping

Groupings=1
Response 1/T0.01 (K)
Whole Model
Actual by Predicted Plot

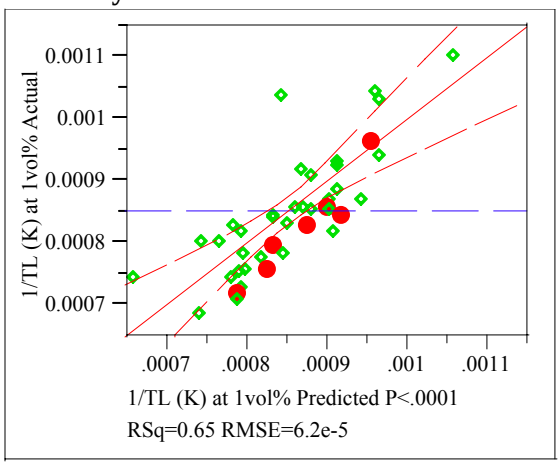

Summary of Fit

RSquare	0.649973
RSquare Adj	0.61497
Root Mean Square Error	0.000062
Mean of Response	0.000852
Observations (or Sum Wgts)	34

Analysis of Variance

Source	DF	Sum of Squares	Mean Square	F Ratio
Model	3	2.10945e-7	7.0315e-8	18.5692
Error	30	1.136e-7	3.7867e-9	Prob > F
C. Total	33	3.24545e-7		<.0001

Lack Of Fit

Source	DF	Sum of Squares	Mean Square	F Ratio
Lack Of Fit	28	1.09515e-7	3.9113e-9	1.9153
Pure Error	2	4.08415e-9	2.0421e-9	Prob > F
Total Error	30	1.136e-7		0.4011
				Max RSq
				0.9874

Parameter Estimates

Term	Estimate	Std Error	t Ratio	Prob>|t|
Intercept	-0.001786	0.000362	-4.93	<.0001
log(SM2/ (SM2+SM1+SMT+Ne1+NeT))	-0.00031	0.000069	-4.51	<.0001
log(SM1/ (SM2+SM1+SMT+Ne1+NeT))	-0.000682	0.000094	-7.25	<.0001
log(SMT/ (SM2+SM1+SMT+Ne1+NeT))	-0.000187	0.000061	-3.09	0.0043

Effect Tests

Source	Nparm	DF	Sum of Squares	F Ratio	Prob > F
log(SM2/ (SM2+SM1+SMT+Ne1+NeT))	1	1	7.69723e-8	20.3273	<.0001
log(SM1/ (SM2+SM1+SMT+Ne1+NeT))	1	1	1.99089e-7	52.5765	<.0001
log(SMT/ (SM2+SM1+SMT+Ne1+NeT))	1	1	3.61193e-8	9.5386	0.0043

Appendix D. Model Fitting Results for T0.01 Data

Exhibit D.1: Statistical Results from the Fitting of the DWPFM to Each Data Grouping

Residual by Predicted Plot

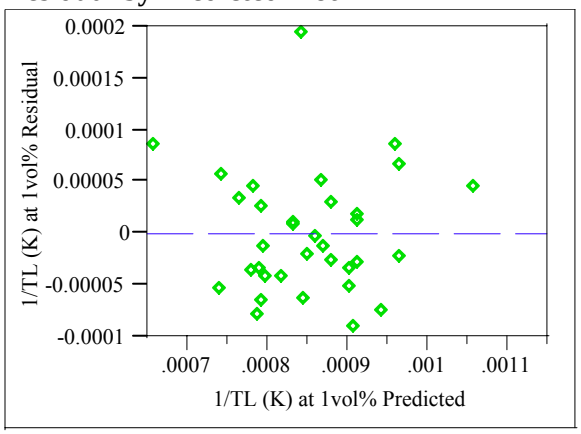

Press
1.7236075e-7

log(SM1/ (SM2+SM1+SMT+Ne1+NeT)) Leverage Plot

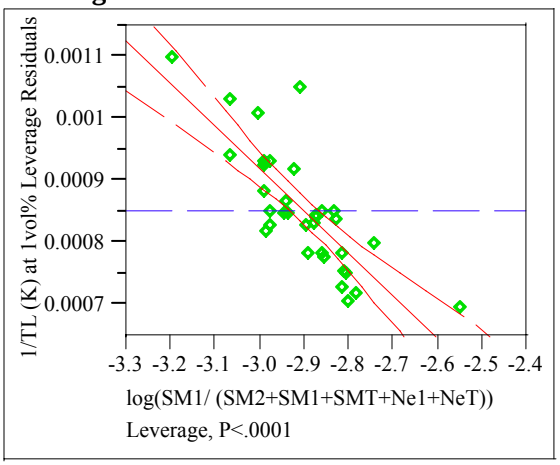

log(SM2/ (SM2+SM1+SMT+Ne1+NeT)) Leverage Plot

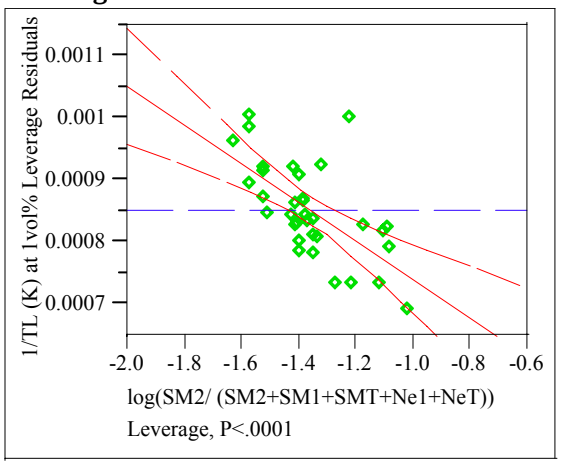

log(SMT/ (SM2+SM1+SMT+Ne1+NeT)) Leverage Plot

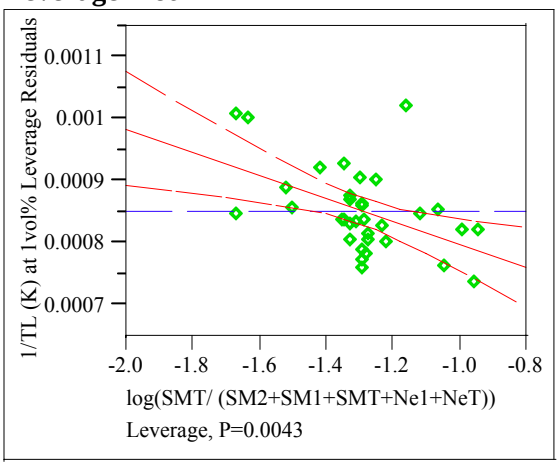

Appendix D. Model Fitting Results for T0.01 Data

Exhibit D.1: Statistical Results from the Fitting of the DWPFM to Each Data Grouping

Groupings=2
Response 1/T0.01 (K)
Whole Model
Actual by Predicted Plot

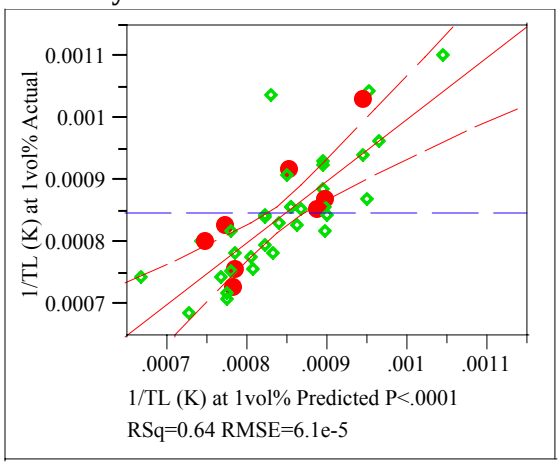

Summary of Fit

RSquare	0.641697
RSquare Adj	0.604631
Root Mean Square Error	0.000061
Mean of Response	0.000847
Observations (or Sum Wgts)	33

Analysis of Variance

Source	DF	Sum of Squares	Mean Square	F Ratio
Model	3	1.94017e-7	6.4672e-8	17.3124
Error	29	1.08333e-7	3.7356e-9	Prob > F
C. Total	32	3.0235e-7		<.0001

Lack Of Fit

Source	DF	Sum of Squares	Mean Square	F Ratio
Lack Of Fit	26	1.06991e-7	4.115e-9	9.1990
Pure Error	3	1.34201e-9	4.473e-10	Prob > F
Total Error	29	1.08333e-7		0.0458
				Max RSq
				0.9956

Parameter Estimates

Term	Estimate	Std Error	t Ratio	Prob>|t|
Intercept	-0.00172	0.000395	-4.35	0.0002
log(SM2/ (SM2+SM1+SMT+Ne1+NeT))	-0.000291	0.000078	-3.71	0.0009
log(SM1/ (SM2+SM1+SMT+Ne1+NeT))	-0.000654	0.000097	-6.72	<.0001
log(SMT/ (SM2+SM1+SMT+Ne1+NeT))	-0.00021	0.000062	-3.36	0.0022

Effect Tests

Source	Nparm	DF	Sum of Squares	F Ratio	Prob > F
log(SM2/ (SM2+SM1+SMT+Ne1+NeT))	1	1	5.1519e-8	13.7913	0.0009
log(SM1/ (SM2+SM1+SMT+Ne1+NeT))	1	1	1.68768e-7	45.1782	<.0001
log(SMT/ (SM2+SM1+SMT+Ne1+NeT))	1	1	4.21105e-8	11.2727	0.0022

Appendix D. Model Fitting Results for T0.01 Data

Exhibit D.1: Statistical Results from the Fitting of the DWPFM to Each Data Grouping

Residual by Predicted Plot

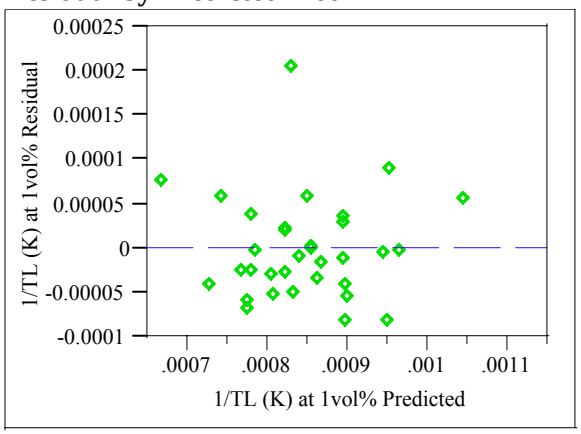

Press
1.6183093e-7

log(SM1/ (SM2+SM1+SMT+Ne1+NeT)) Leverage Plot

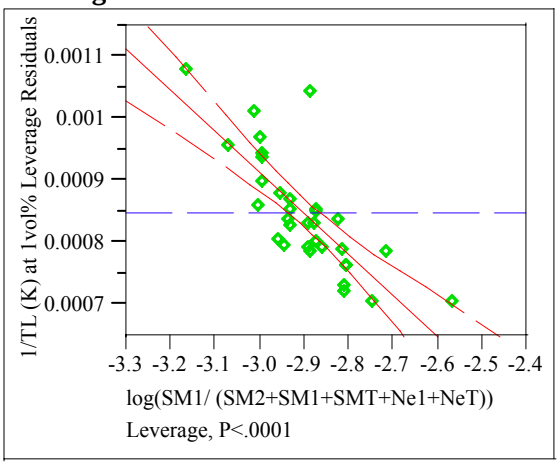

log(SM2/ (SM2+SM1+SMT+Ne1+NeT)) Leverage Plot

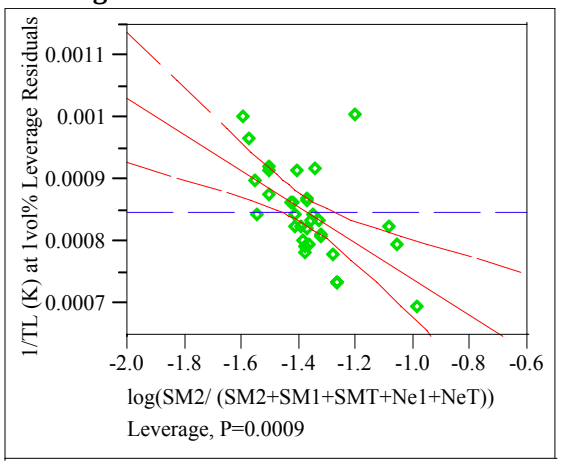

log(SMT/ (SM2+SM1+SMT+Ne1+NeT)) Leverage Plot

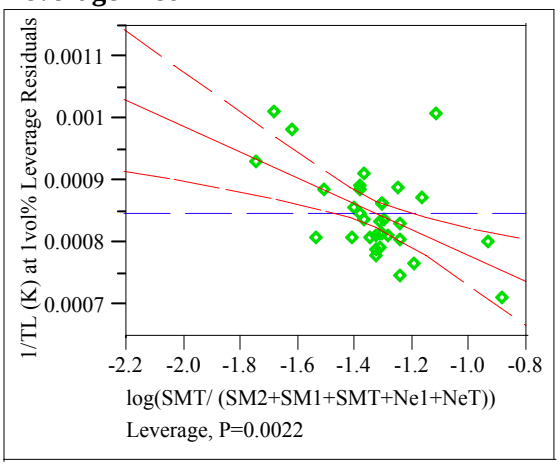

Appendix D. Model Fitting Results for T0.01 Data

Exhibit D.1: Statistical Results from the Fitting of the DWPFM to Each Data Grouping

Groupings=3
Response 1/T0.01 (K)
Whole Model
Actual by Predicted Plot

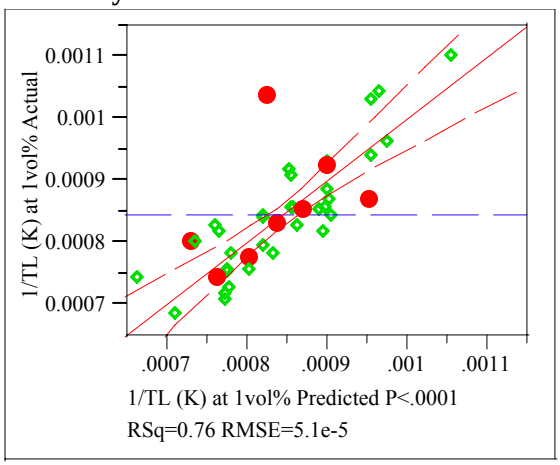

Summary of Fit

RSquare	0.755494
RSquare Adj	0.7302
Root Mean Square Error	0.000051
Mean of Response	0.000845
Observations (or Sum Wgts)	33

Analysis of Variance

Source	DF	Sum of Squares	Mean Square	F Ratio
Model	3	2.31205e-7	7.7068e-8	29.8688
Error	29	7.48266e-8	2.5802e-9	Prob > F
C. Total	32	3.06032e-7		<.0001

Lack Of Fit

Source	DF	Sum of Squares	Mean Square	F Ratio
Lack Of Fit	26	6.94348e-8	2.6706e-9	1.4859
Pure Error	3	5.39179e-9	1.7973e-9	Prob > F
Total Error	29	7.48266e-8		0.4236
				Max RSq
				0.9824

Parameter Estimates

Term	Estimate	Std Error	t Ratio	Prob>|t|
Intercept	-0.001954	0.00031	-6.30	<.0001
log(SM2/ (SM2+SM1+SMT+Ne1+NeT))	-0.000334	0.000061	-5.51	<.0001
log(SM1/ (SM2+SM1+SMT+Ne1+NeT))	-0.000701	0.00008	-8.75	<.0001
log(SMT/ (SM2+SM1+SMT+Ne1+NeT))	-0.00024	0.000047	-5.15	<.0001

Effect Tests

Source	Nparm	DF	Sum of Squares	F Ratio	Prob > F
log(SM2/ (SM2+SM1+SMT+Ne1+NeT))	1	1	7.81983e-8	30.3067	<.0001
log(SM1/ (SM2+SM1+SMT+Ne1+NeT))	1	1	1.97523e-7	76.5524	<.0001
log(SMT/ (SM2+SM1+SMT+Ne1+NeT))	1	1	6.83792e-8	26.5012	<.0001

Appendix D. Model Fitting Results for T0.01 Data

Exhibit D.1: Statistical Results from the Fitting of the DWPFM to Each Data Grouping

Residual by Predicted Plot

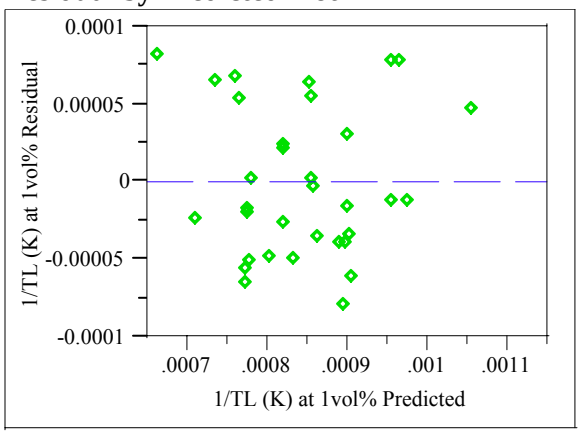

Press
1.1891909e-7

log(SM1/ (SM2+SM1+SMT+Ne1+NeT)) Leverage Plot

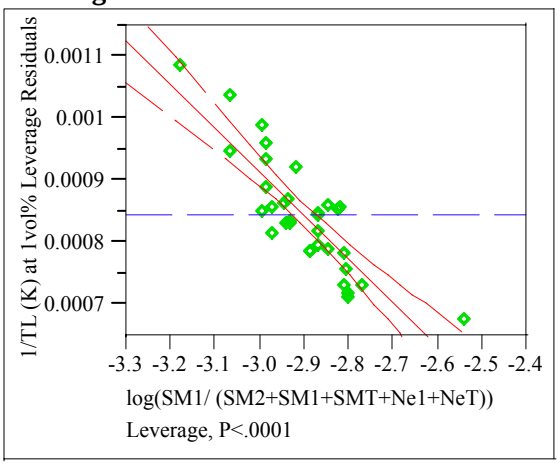

log(SM2/ (SM2+SM1+SMT+Ne1+NeT)) Leverage Plot

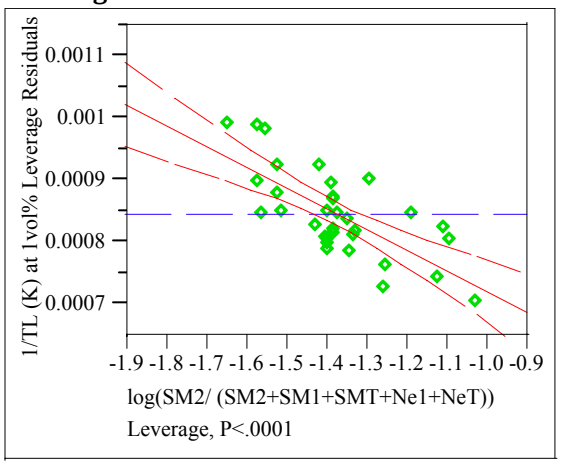

log(SMT/ (SM2+SM1+SMT+Ne1+NeT)) Leverage Plot

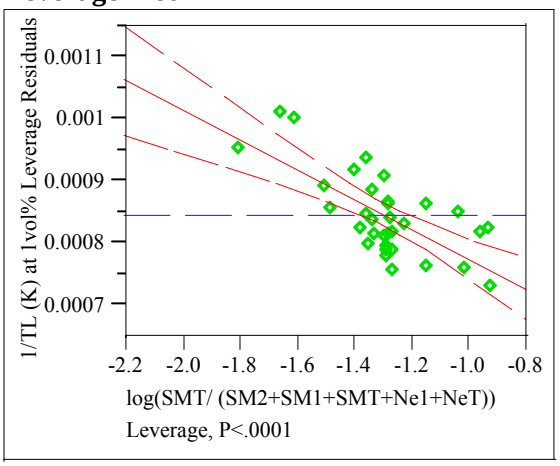

Appendix D. Model Fitting Results for T0.01 Data

Exhibit D.1: Statistical Results from the Fitting of the DWPFM to Each Data Grouping

Groupings=4
Response 1/T0.01 (K)
Whole Model
Actual by Predicted Plot

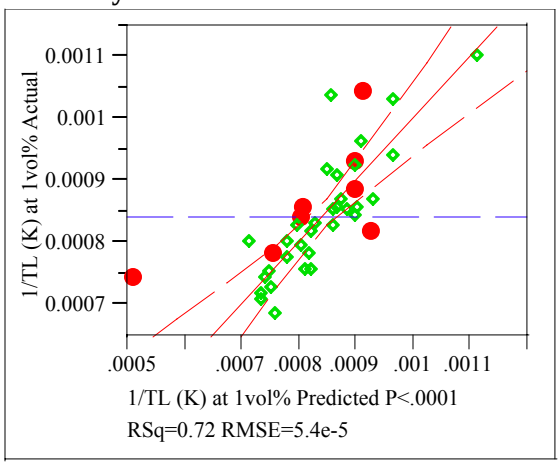

Summary of Fit

RSquare	0.719875
RSquare Adj	0.690897
Root Mean Square Error	0.000054
Mean of Response	0.000843
Observations (or Sum Wgts)	33

Analysis of Variance

Source	DF	Sum of Squares	Mean Square	F Ratio
Model	3	2.18119e-7	7.2706e-8	24.8418
Error	29	8.48767e-8	2.9268e-9	Prob > F
C. Total	32	3.02996e-7		<.0001

Lack Of Fit

Source	DF	Sum of Squares	Mean Square	F Ratio
Lack Of Fit	26	7.94849e-8	3.0571e-9	1.7010
Pure Error	3	5.39179e-9	1.7973e-9	Prob > F
Total Error	29	8.48767e-8		0.3716
				Max RSq
				0.9822

Parameter Estimates

Term	Estimate	Std Error	t Ratio	Prob>|t|
Intercept	-0.002117	0.000366	-5.79	<.0001
log(SM2/ (SM2+SM1+SMT+Ne1+NeT))	-0.000251	0.000063	-3.99	0.0004
log(SM1/ (SM2+SM1+SMT+Ne1+NeT))	-0.000866	0.000107	-8.07	<.0001
log(SMT/ (SM2+SM1+SMT+Ne1+NeT))	-0.000079	0.000057	-1.40	0.1731

Effect Tests

Source	Nparm	DF	Sum of Squares	F Ratio	Prob > F
log(SM2/ (SM2+SM1+SMT+Ne1+NeT))	1	1	4.66667e-8	15.9447	0.0004
log(SM1/ (SM2+SM1+SMT+Ne1+NeT))	1	1	1.90557e-7	65.1081	<.0001
log(SMT/ (SM2+SM1+SMT+Ne1+NeT))	1	1	5.70988e-9	1.9509	0.1731

Appendix D. Model Fitting Results for T0.01 Data

Exhibit D.1: Statistical Results from the Fitting of the DWPFM to Each Data Grouping

Residual by Predicted Plot

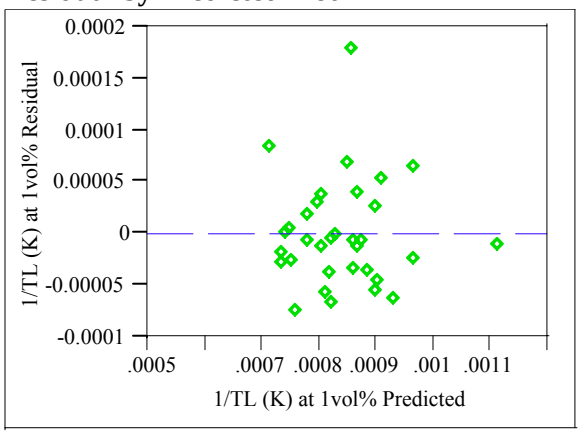

Press
1.1437103e-7

log(SM1/ (SM2+SM1+SMT+Ne1+NeT)) Leverage Plot

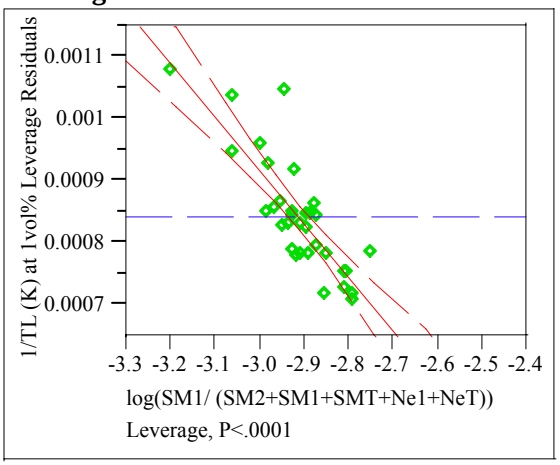

log(SM2/ (SM2+SM1+SMT+Ne1+NeT)) Leverage Plot

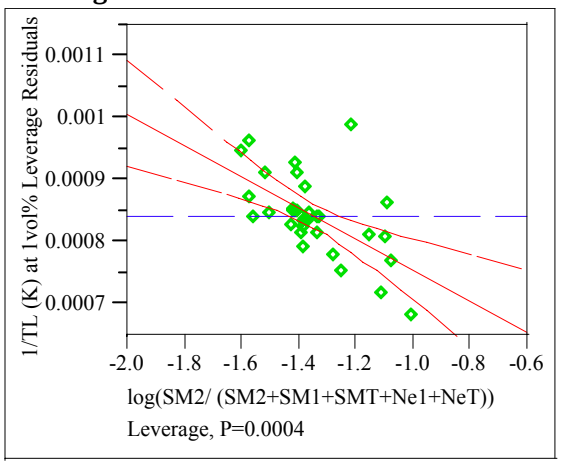

log(SMT/ (SM2+SM1+SMT+Ne1+NeT)) Leverage Plot

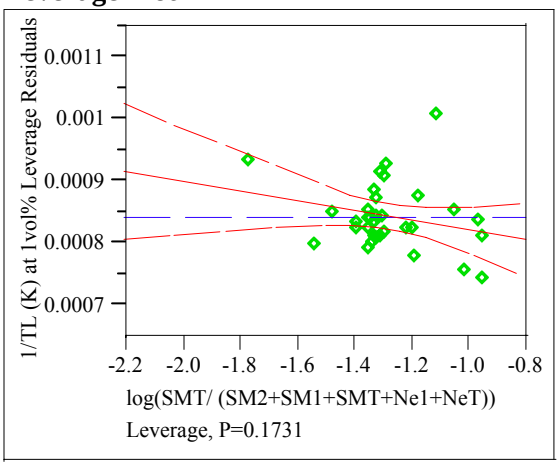

Appendix D. Model Fitting Results for T0.01 Data

Exhibit D.1: Statistical Results from the Fitting of the DWPFM to Each Data Grouping

Groupings=5
Response 1/T0.01 (K)
Whole Model
Actual by Predicted Plot

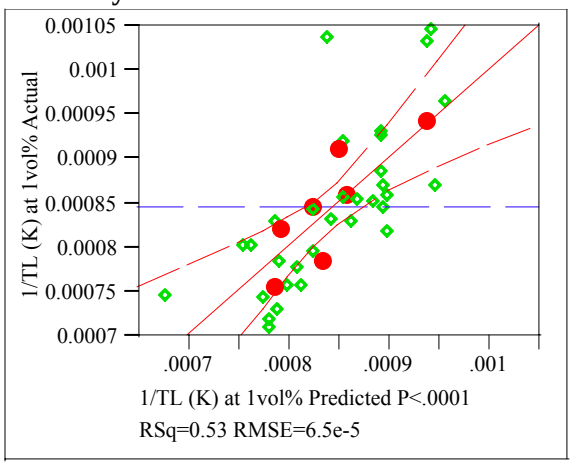

Summary of Fit

RSquare	0.530825
RSquare Adj	0.480556
Root Mean Square Error	0.000065
Mean of Response	0.000845
Observations (or Sum Wgts)	32

Analysis of Variance

Source	DF	Sum of Squares	Mean Square	F Ratio
Model	3	1.32296e-7	4.4099e-8	10.5597
Error	28	1.16931e-7	4.1761e-9	Prob > F
C. Total	31	2.49226e-7		<.0001

Lack Of Fit

Source	DF	Sum of Squares	Mean Square	F Ratio
Lack Of Fit	26	1.16872e-7	4.4951e-9	153.5749
Pure Error	2	5.8539e-11	2.927e-11	Prob > F
Total Error	28	1.16931e-7		0.0065
				Max RSq
				0.9998

Parameter Estimates

Term	Estimate	Std Error	t Ratio	Prob>|t|
Intercept	-0.001484	0.000453	-3.28	0.0028
log(SM2/ (SM2+SM1+SMT+Ne1+NeT))	-0.000252	0.000088	-2.88	0.0075
log(SM1/ (SM2+SM1+SMT+Ne1+NeT))	-0.000604	0.000116	-5.19	<.0001
log(SMT/ (SM2+SM1+SMT+Ne1+NeT))	-0.000182	0.000065	-2.79	0.0093

Effect Tests

Source	Nparm	DF	Sum of Squares	F Ratio	Prob > F
log(SM2/ (SM2+SM1+SMT+Ne1+NeT))	1	1	3.46629e-8	8.3003	0.0075
log(SM1/ (SM2+SM1+SMT+Ne1+NeT))	1	1	1.1234e-7	26.9007	<.0001
log(SMT/ (SM2+SM1+SMT+Ne1+NeT))	1	1	3.25401e-8	7.7920	0.0093

Appendix D. Model Fitting Results for T0.01 Data

Exhibit D.1: Statistical Results from the Fitting of the DWPFM to Each Data Grouping

Residual by Predicted Plot

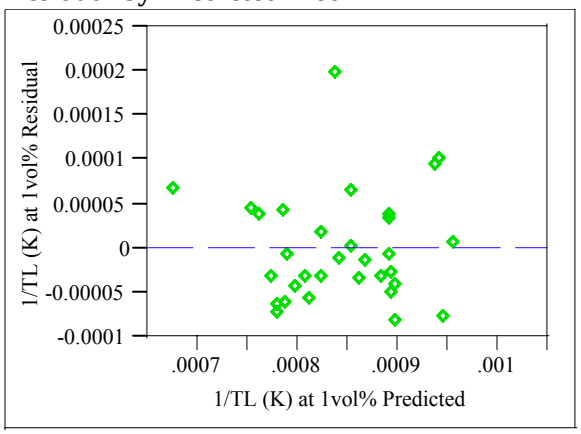

Press
1.7989741e-7

log(SM1/ (SM2+SM1+SMT+Ne1+NeT)) Leverage Plot

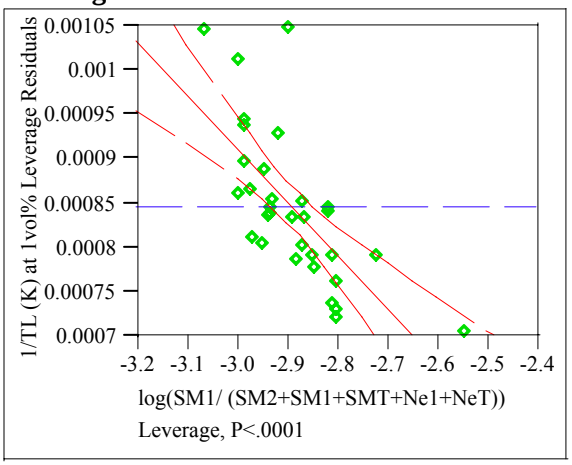

log(SM2/ (SM2+SM1+SMT+Ne1+NeT)) Leverage Plot

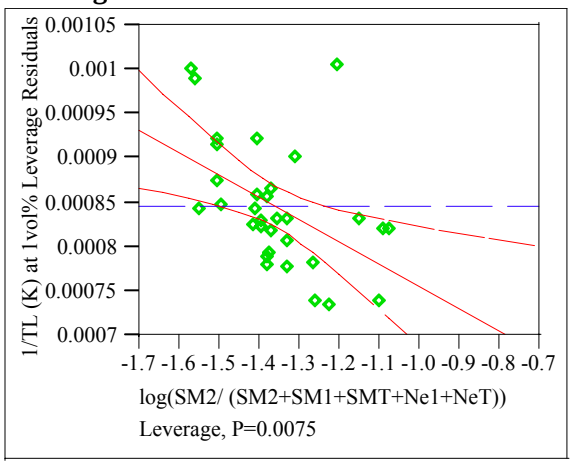

log(SMT/ (SM2+SM1+SMT+Ne1+NeT)) Leverage Plot

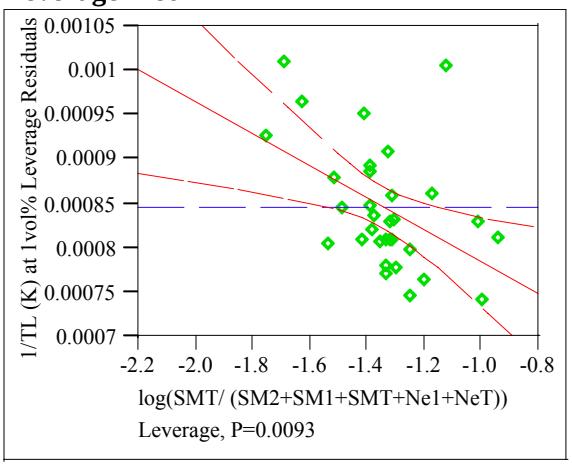

Appendix D. Model Fitting Results for T0.01 Data

Exhibit D.2: Statistical Results from the Fitting of the IPM to Each Data Grouping

Groupings=1
Response T0.01 (°C)
Singularity Details: Intercept = 0
Whole Model
Actual by Predicted Plot

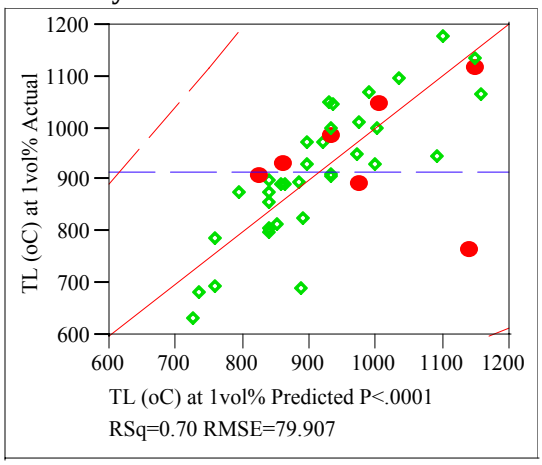

Summary of Fit

RSquare	0.697145
RSquare Adj	0.629844
Root Mean Square Error	79.90688
Mean of Response	915.0585
Observations (or Sum Wgts)	34

Analysis of Variance

Source	DF	Sum of Squares	Mean Square	F Ratio
Model	6	396844.87	66140.8	10.3586
Error	27	172397.97	6385.1	Prob > F
C. Total	33	569242.84		<.0001

Tested against reduced model: Y=mean

Lack Of Fit

Source	DF	Sum of Squares	Mean Square	F Ratio
Lack Of Fit	25	168093.98	6723.76	3.1244
Pure Error	2	4303.99	2151.99	Prob > F
Total Error	27	172397.97		0.2710
				Max RSq
				0.9924

Parameter Estimates

Term	Estimate	Std Error	t Ratio	Prob>|t|
IPM (Cr moles)	58150.172	19737.87	2.95	0.0066
IPM (Mn moles)	6112.782	1908.807	3.20	0.0035
IPM (Ni moles)	20073.041	4514.078	4.45	0.0001
IPM (alkali moles) int	-560.8767	985.7782	-0.57	0.5741
IPM (alkali moles) slp	594.79448	1189.434	0.50	0.6211
IPM (nonalkali moles) int	7237.2055	1607.374	4.50	0.0001
IPM (nonalkali moles) slp	-679.7787	163.0395	-4.17	0.0003

Effect Tests

Source	DF	Sum of Squares	F Ratio	Prob > F
IPM (Cr moles)	1	55420.41	8.6796	0.0066
IPM (Mn moles)	1	65482.01	10.2554	0.0035
IPM (Ni moles)	1	126257.34	19.7737	0.0001
IPM (alkali moles) int	1	2067.02	0.3237	0.5741
IPM (alkali moles) slp	1	1596.69	0.2501	0.6211
IPM (nonalkali moles) int	1	129442.37	20.2725	0.0001
IPM (nonalkali moles) slp	1	110998.65	17.3840	0.0003

Residual by Predicted Plot

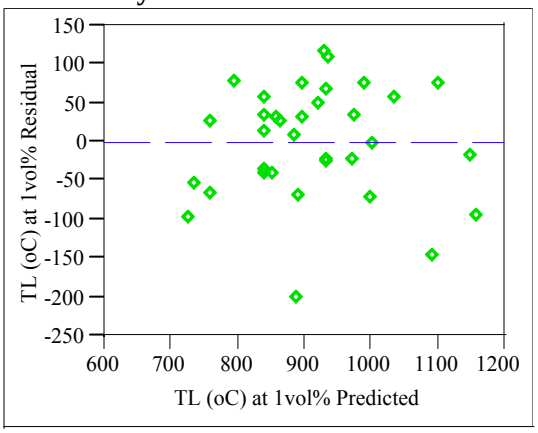

Press
326326.90389

IPM (Cr moles)
Leverage Plot

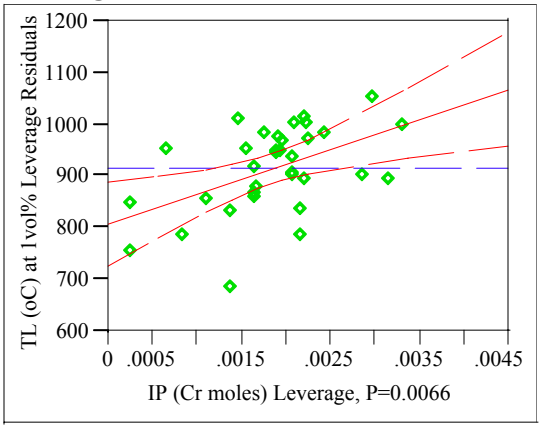

Appendix D. Model Fitting Results for T0.01 Data

Exhibit D.2: Statistical Results from the Fitting of the IPM to Each Data Grouping

IPM (Mn moles)
Leverage Plot

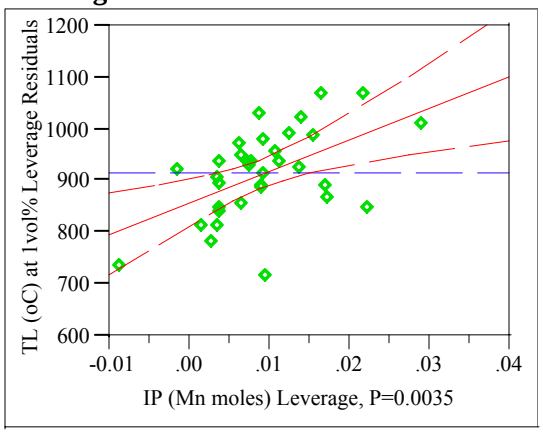

IPM (alkali moles) slp
Leverage Plot

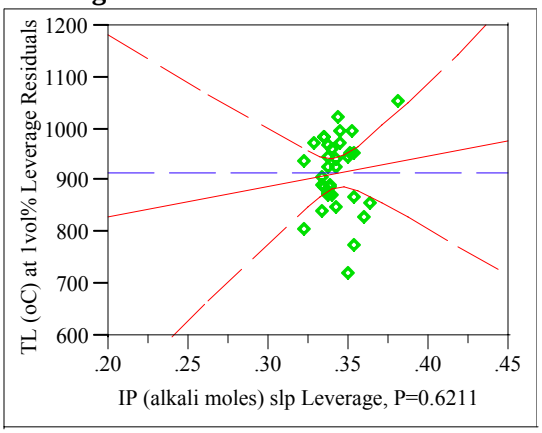

IPM (Ni moles)
Leverage Plot

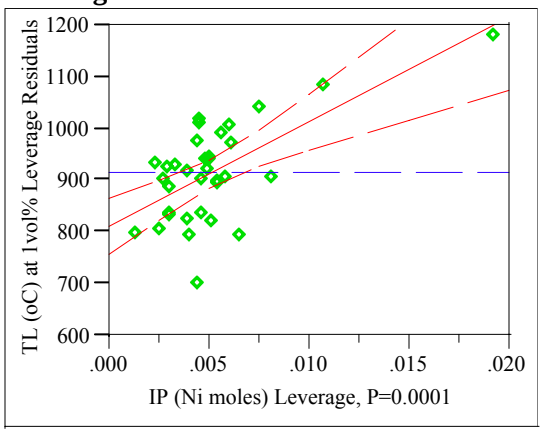

IPM (nonalkali moles) int
Leverage Plot

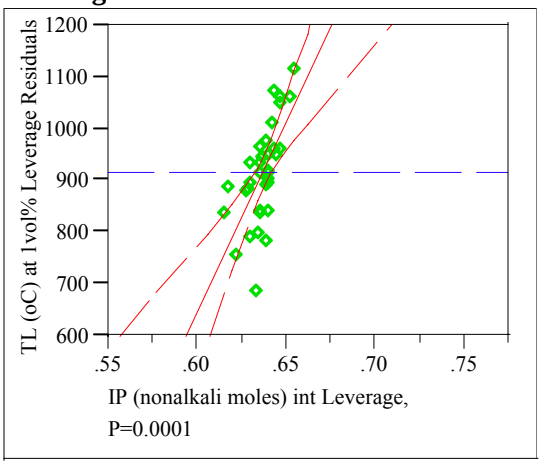

IPM (alkali moles) int
Leverage Plot

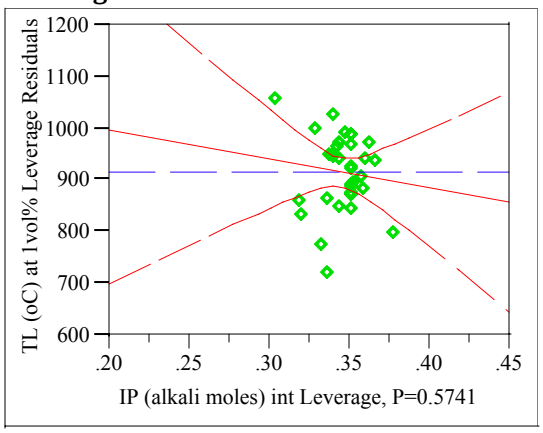

IPM (nonalkali moles) slp
Leverage Plot

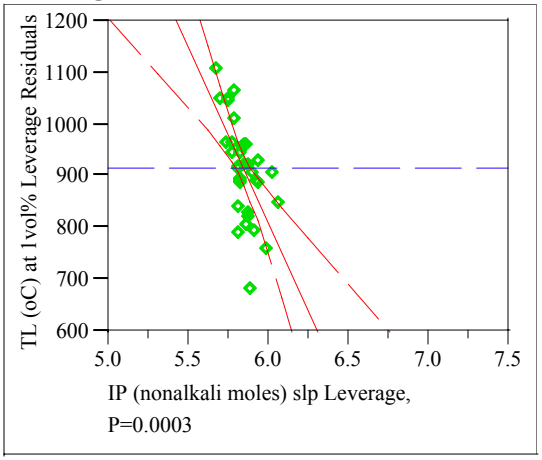

Appendix D. Model Fitting Results for T0.01 Data

Exhibit D.2: Statistical Results from the Fitting of the IPM to Each Data Grouping

Groupings=2
Response T0.01 (°C)
Singularity Details: Intercept = 0
Whole Model
Actual by Predicted Plot

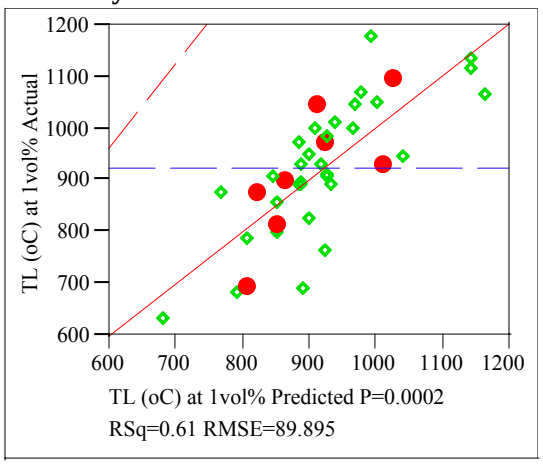

Summary of Fit

RSquare	0.611305
RSquare Adj	0.521607
Root Mean Square Error	89.89458
Mean of Response	921.9422
Observations (or Sum Wgts)	33

Analysis of Variance

Source	DF	Sum of Squares	Mean Square	F Ratio
Model	6	330438.19	55073.0	6.8151
Error	26	210106.93	8081.0	Prob > F
C. Total	32	540545.12		0.0002

Tested against reduced model: Y=mean

Lack Of Fit

Source	DF	Sum of Squares	Mean Square	F Ratio
Lack Of Fit	23	207089.22	9003.88	8.9510
Pure Error	3	3017.71	1005.90	Prob > F
Total Error	26	210106.93		0.0476
				Max RSq
				0.9944

Parameter Estimates

Term	Estimate	Std Error	t Ratio	Prob>|t|
IPM (Cr moles)	31915.011	22407.98	1.42	0.1663
IPM (Mn moles)	2764.7275	2045.11	1.35	0.1881
IPM (Ni moles)	18919.388	4282.439	4.42	0.0002
IPM (alkali moles) int	-1961.614	1068.514	-1.84	0.0778
IPM (alkali moles) slp	2399.2729	1215.792	1.97	0.0592
IPM (nonalkali moles) int	4513.6828	1485.546	3.04	0.0054
IPM (nonalkali moles) slp	-391.9457	148.9715	-2.63	0.0141

Effect Tests

Source	DF	Sum of Squares	F Ratio	Prob > F
IPM (Cr moles)	1	16392.74	2.0285	0.1663
IPM (Mn moles)	1	14768.57	1.8276	0.1881
IPM (Ni moles)	1	157724.36	19.5178	0.0002
IPM (alkali moles) int	1	27235.40	3.3703	0.0778
IPM (alkali moles) slp	1	31470.81	3.8944	0.0592
IPM (nonalkali moles) int	1	74603.09	9.2319	0.0054
IPM (nonalkali moles) slp	1	55938.68	6.9222	0.0141

Residual by Predicted Plot

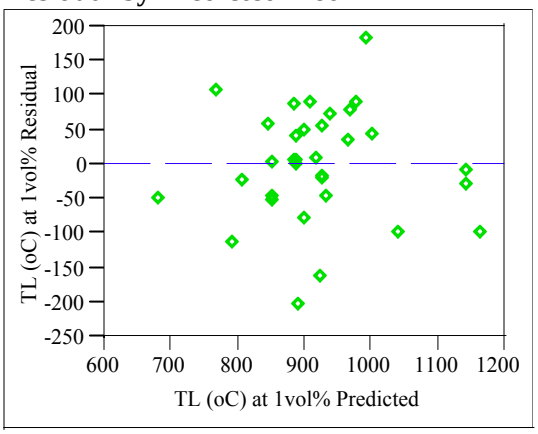

Press
486707.47266

IPM (Cr moles)
Leverage Plot

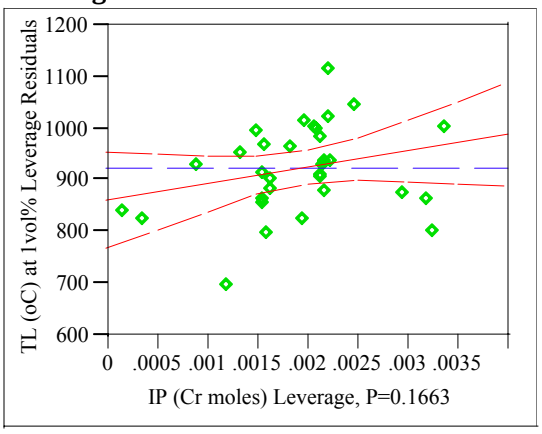

Appendix D. Model Fitting Results for T0.01 Data

Exhibit D.2: Statistical Results from the Fitting of the IPM to Each Data Grouping

IPM (Mn moles)
Leverage Plot

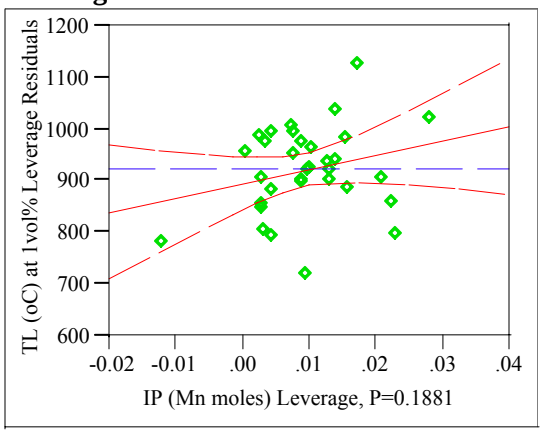

IPM (alkali moles) slp
Leverage Plot

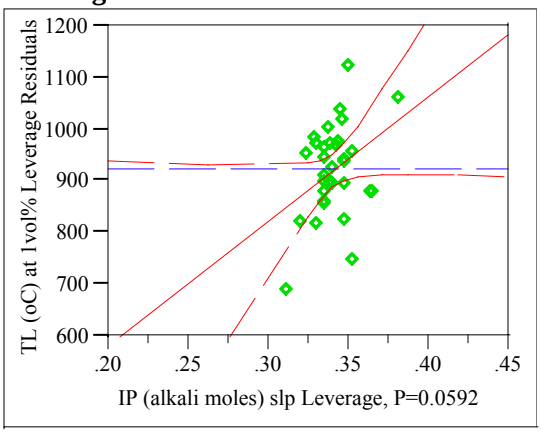

IPM (Ni moles)
Leverage Plot

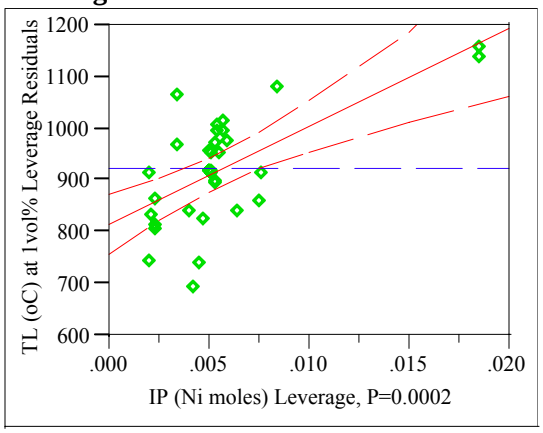

IPM (nonalkali moles) int
Leverage Plot

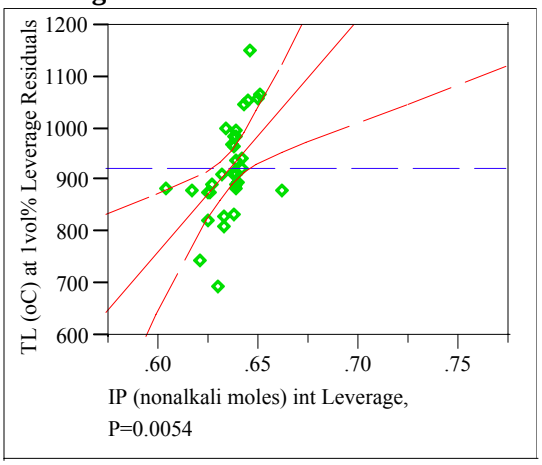

IPM (alkali moles) int
Leverage Plot

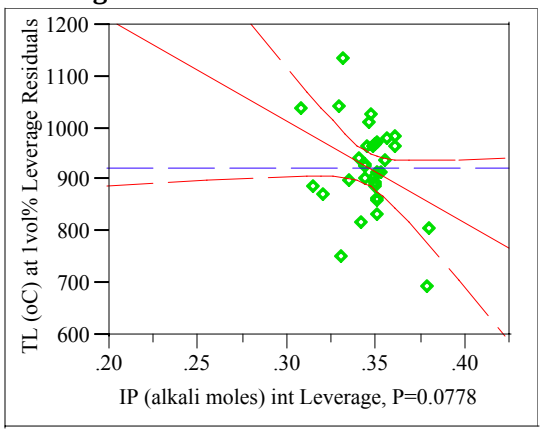

IPM (nonalkali moles) slp
Leverage Plot

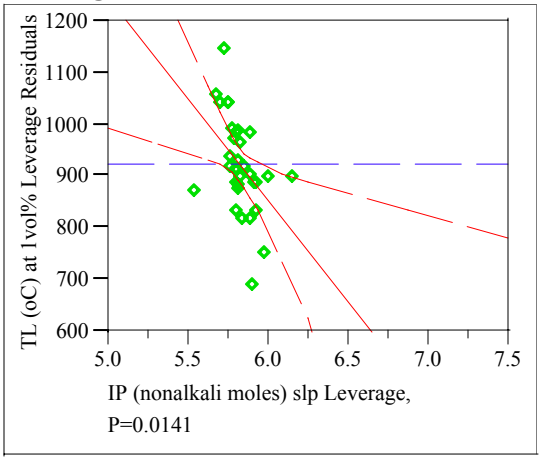

Appendix D. Model Fitting Results for T0.01 Data

Exhibit D.2: Statistical Results from the Fitting of the IPM to Each Data Grouping

Groupings=3
Response T0.01 (°C)
Singularity Details: Intercept = 0
Whole Model
Actual by Predicted Plot

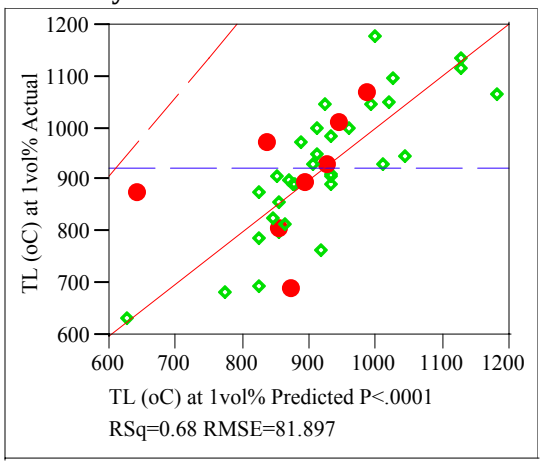

Summary of Fit

RSquare	0.684638
RSquare Adj	0.611862
Root Mean Square Error	81.89737
Mean of Response	924.3378
Observations (or Sum Wgts)	33

Analysis of Variance

Source	DF	Sum of Squares	Mean Square	F Ratio
Model	6	378585.77	63097.6	9.4075
Error	26	174386.64	6707.2	Prob > F
C. Total	32	552972.42		<.0001

Tested against reduced model: Y=mean

Lack Of Fit

Source	DF	Sum of Squares	Mean Square	F Ratio
Lack Of Fit	23	167111.12	7265.70	2.9959
Pure Error	3	7275.53	2425.18	Prob > F
Total Error	26	174386.64		0.1990
				Max RSq
				0.9868

Parameter Estimates

Term	Estimate	Std Error	t Ratio	Prob>|t|
IPM (Cr moles)	23966.327	17497.72	1.37	0.1825
IPM (Mn moles)	3058.0417	1804.82	1.69	0.1021
IPM (Ni moles)	17733.835	3689.778	4.81	<.0001
IPM (alkali moles) int	-2263.593	902.7624	-2.51	0.0187
IPM (alkali moles) slp	2703.6036	1086.848	2.49	0.0196
IPM (nonalkali moles) int	6033.4923	1848.933	3.26	0.0031
IPM (nonalkali moles) slp	-555.4941	187.3891	-2.96	0.0064

Effect Tests

Source	DF	Sum of Squares	F Ratio	Prob > F
IPM (Cr moles)	1	12582.87	1.8760	0.1825
IPM (Mn moles)	1	19255.68	2.8709	0.1021
IPM (Ni moles)	1	154933.28	23.0996	<.0001
IPM (alkali moles) int	1	42168.65	6.2871	0.0187
IPM (alkali moles) slp	1	41503.87	6.1880	0.0196
IPM (nonalkali moles) int	1	71422.54	10.6487	0.0031
IPM (nonalkali moles) slp	1	58940.01	8.7876	0.0064

Residual by Predicted Plot

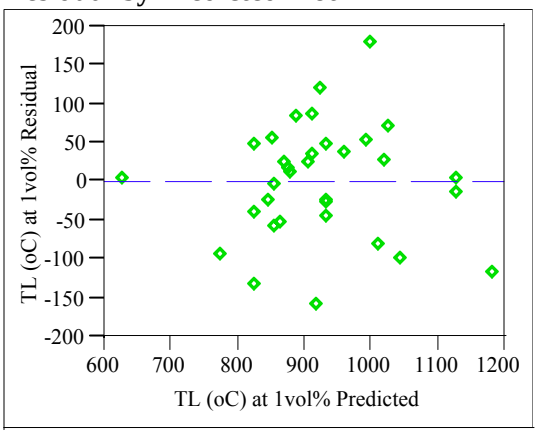

Press
376751.69178

IPM (Cr moles)
Leverage Plot

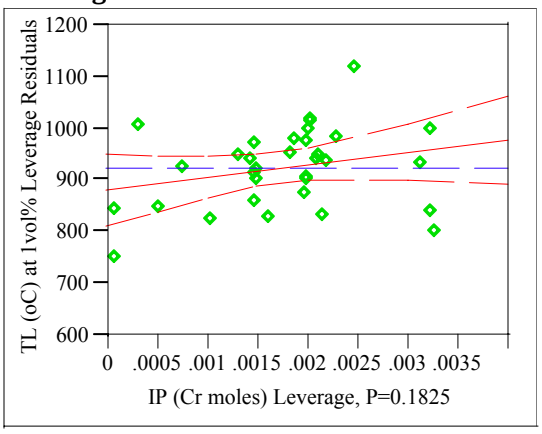

Appendix D. Model Fitting Results for T0.01 Data

Exhibit D.2: Statistical Results from the Fitting of the IPM to Each Data Grouping

IPM (Mn moles)
Leverage Plot

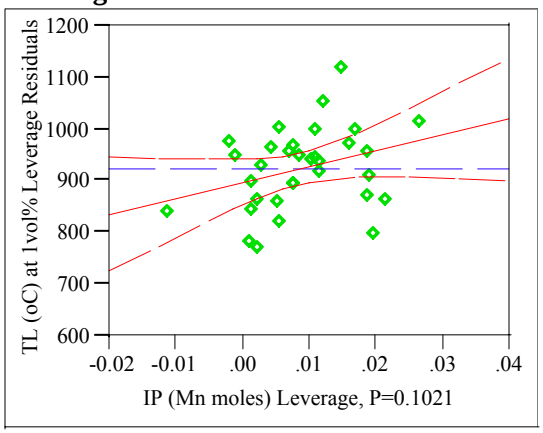

IPM (alkali moles) slp
Leverage Plot

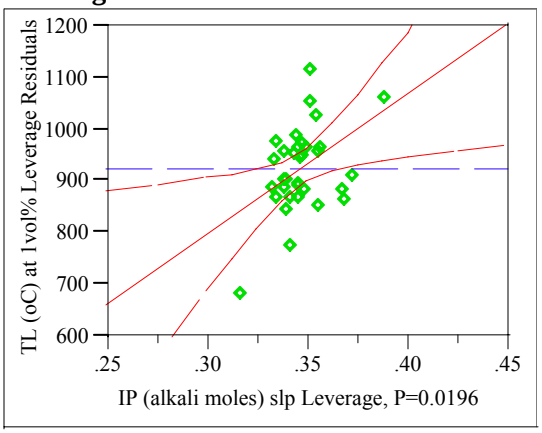

IPM (Ni moles)
Leverage Plot

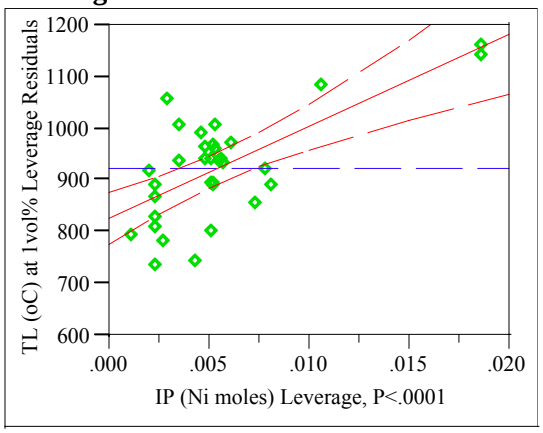

IPM (nonalkali moles) int
Leverage Plot

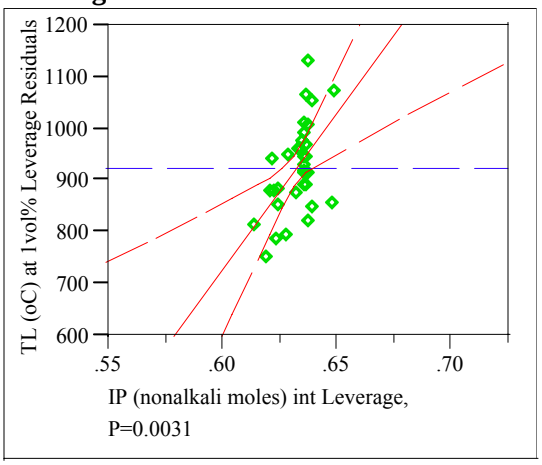

IPM (alkali moles) int
Leverage Plot

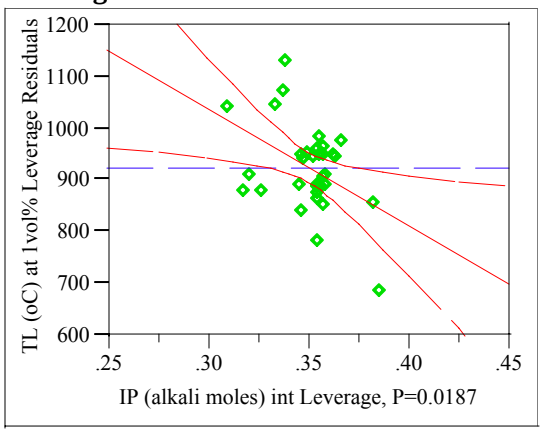

IPM (nonalkali moles) slp
Leverage Plot

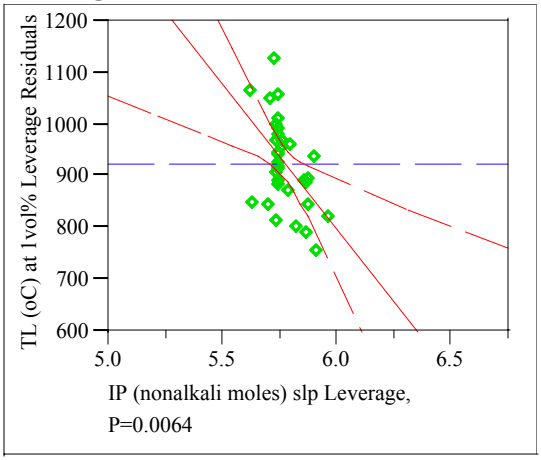

Appendix D. Model Fitting Results for T0.01 Data

Exhibit D.2: Statistical Results from the Fitting of the IPM to Each Data Grouping

Groupings=4
Response T0.01 (°C)
Singularity Details: Intercept = 0
Whole Model
Actual by Predicted Plot

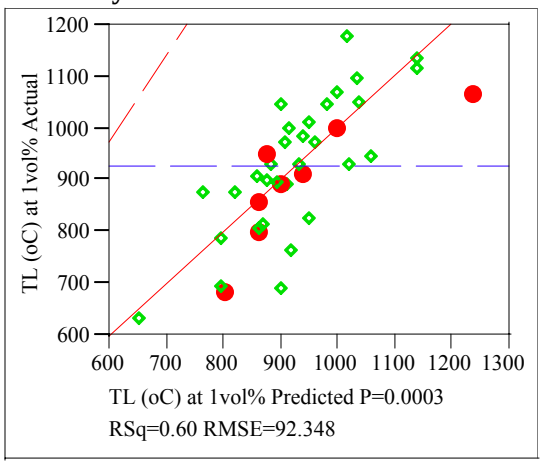

Summary of Fit

RSquare	0.595972
RSquare Adj	0.502734
Root Mean Square Error	92.34829
Mean of Response	927.1052
Observations (or Sum Wgts)	33

Analysis of Variance

Source	DF	Sum of Squares	Mean Square	F Ratio
Model	6	327073.25	54512.2	6.3920
Error	26	221733.38	8528.2	Prob > F
C. Total	32	548806.63		0.0003

Tested against reduced model: Y=mean

Lack Of Fit

Source	DF	Sum of Squares	Mean Square	F Ratio
Lack Of Fit	23	214457.85	9324.25	3.8448
Pure Error	3	7275.53	2425.18	Prob > F
Total Error	26	221733.38		0.1466
				Max RSq
				0.9867

Parameter Estimates

Term	Estimate	Std Error	t Ratio	Prob>|t|
IPM (Cr moles)	47258.119	22810.36	2.07	0.0483
IPM (Mn moles)	1423.3029	2193.735	0.65	0.5222
IPM (Ni moles)	18116.637	4172.77	4.34	0.0002
IPM (alkali moles) int	-2628.628	1093.087	-2.40	0.0236
IPM (alkali moles) slp	3028.4504	1261.655	2.40	0.0238
IPM (nonalkali moles) int	4418.5991	1570.112	2.81	0.0092
IPM (nonalkali moles) slp	-378.9691	157.7501	-2.40	0.0237

Effect Tests

Source	DF	Sum of Squares	F Ratio	Prob > F
IPM (Cr moles)	1	36605.51	4.2923	0.0483
IPM (Mn moles)	1	3589.91	0.4209	0.5222
IPM (Ni moles)	1	160754.84	18.8498	0.0002
IPM (alkali moles) int	1	49318.17	5.7829	0.0236
IPM (alkali moles) slp	1	49138.01	5.7618	0.0238
IPM (nonalkali moles) int	1	67540.74	7.9197	0.0092
IPM (nonalkali moles) slp	1	49218.26	5.7712	0.0237

Residual by Predicted Plot

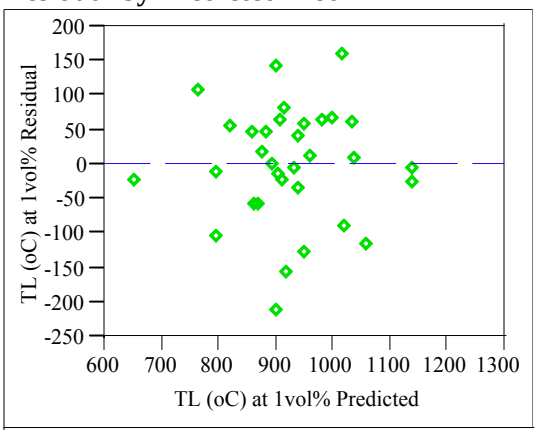

Press
515172.34026

IPM (Cr moles)
Leverage Plot

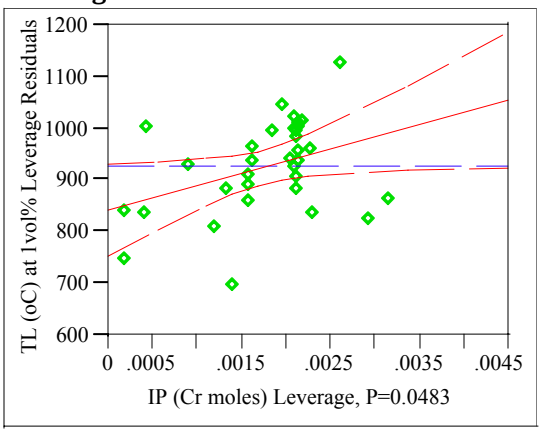

Appendix D. Model Fitting Results for T0.01 Data

Exhibit D.2: Statistical Results from the Fitting of the IPM to Each Data Grouping

IPM (Mn moles)
Leverage Plot

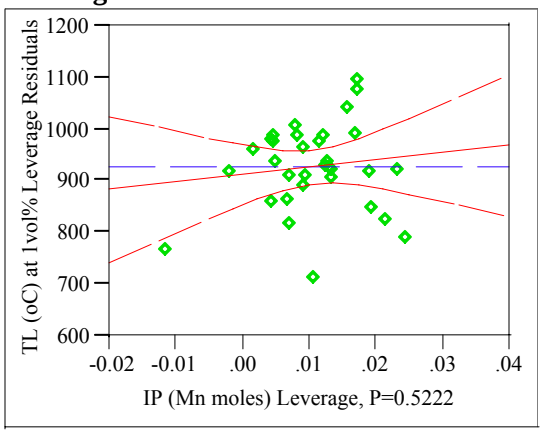

IPM (alkali moles) slp
Leverage Plot

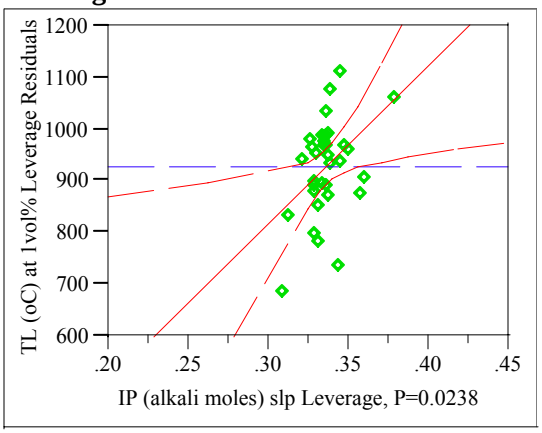

IPM (Ni moles)
Leverage Plot

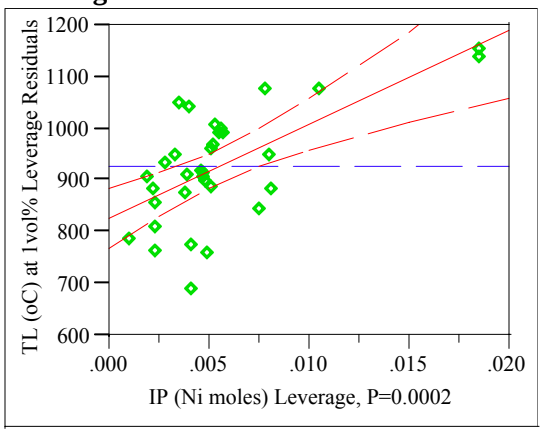

IPM (nonalkali moles) int
Leverage Plot

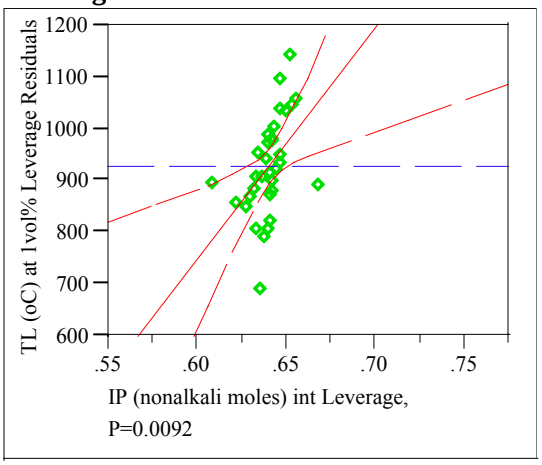

IPM (alkali moles) int
Leverage Plot

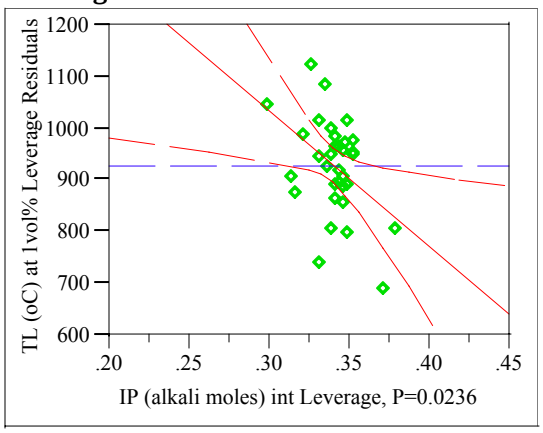

IPM (nonalkali moles) slp
Leverage Plot

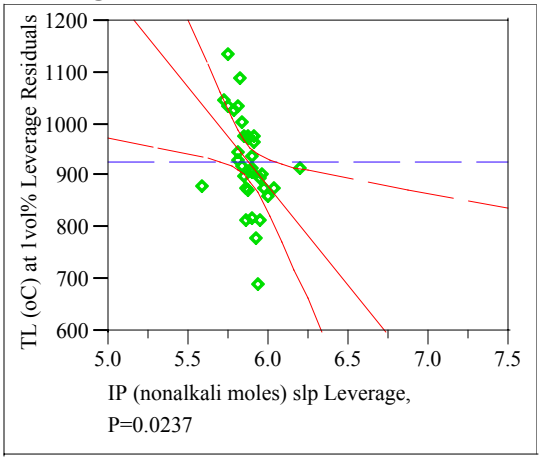

Appendix D. Model Fitting Results for T0.01 Data

Exhibit D.2: Statistical Results from the Fitting of the IPM to Each Data Grouping

Groupings=5
Response T0.01 (°C)
Singularity Details: Intercept = 0
Whole Model
Actual by Predicted Plot

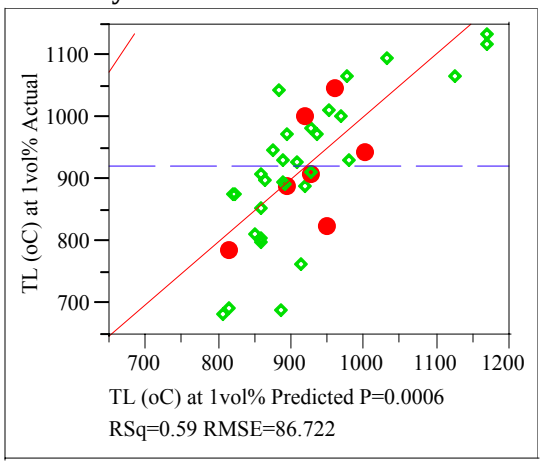

Summary of Fit

RSquare	0.585366
RSquare Adj	0.485854
Root Mean Square Error	86.72204
Mean of Response	922.9736
Observations (or Sum Wgts)	32

Analysis of Variance

Source	DF	Sum of Squares	Mean Square	F Ratio
Model	6	265437.16	44239.5	5.8824
Error	25	188017.82	7520.7	Prob > F
C. Total	31	453454.98		0.0006

Tested against reduced model: Y=mean

Lack Of Fit

Source	DF	Sum of Squares	Mean Square	F Ratio
Lack Of Fit	23	187835.90	8166.78	89.7864
Pure Error	2	181.92	90.96	Prob > F
Total Error	25	188017.82		0.0111
				Max RSq
				0.9996

Parameter Estimates

Term	Estimate	Std Error	t Ratio	Prob>|t|
IPM (Cr moles)	33436.539	20662.93	1.62	0.1182
IPM (Mn moles)	1462.3211	2287.767	0.64	0.5285
IPM (Ni moles)	20017.857	3874.548	5.17	<.0001
IPM (alkali moles) int	-1046.847	1280.15	-0.82	0.4212
IPM (alkali moles) slp	1348.8068	1533.393	0.88	0.3874
IPM (nonalkali moles) int	3988.5928	1577.415	2.53	0.0181
IPM (nonalkali moles) slp	-326.3808	155.7672	-2.10	0.0464

Effect Tests

Source	DF	Sum of Squares	F Ratio	Prob > F
IPM (Cr moles)	1	19693.27	2.6185	0.1182
IPM (Mn moles)	1	3072.70	0.4086	0.5285
IPM (Ni moles)	1	200748.35	26.6927	<.0001
IPM (alkali moles) int	1	5029.25	0.6687	0.4212
IPM (alkali moles) slp	1	5819.05	0.7737	0.3874
IPM (nonalkali moles) int	1	48084.65	6.3936	0.0181
IPM (nonalkali moles) slp	1	33018.43	4.3903	0.0464

Residual by Predicted Plot

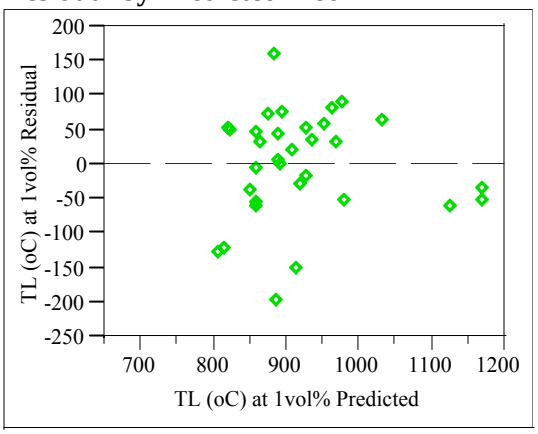

Press
540115.69009

IPM (Cr moles)
Leverage Plot

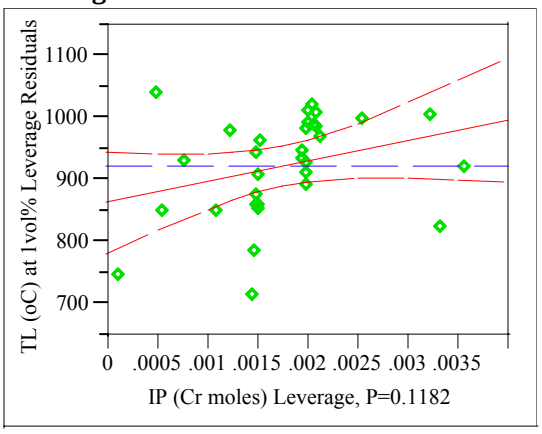

Appendix D. Model Fitting Results for T0.01 Data

Exhibit D.2: Statistical Results from the Fitting of the IPM to Each Data Grouping

IPM (Mn moles)
Leverage Plot

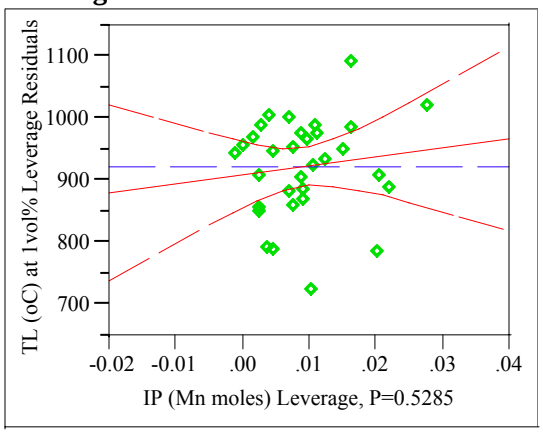

IPM (alkali moles) slp
Leverage Plot

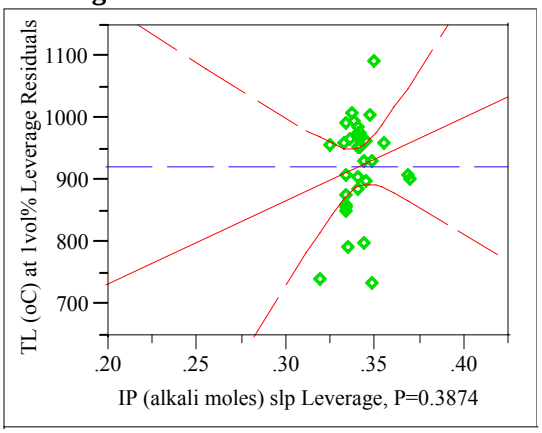

IPM (Ni moles)
Leverage Plot

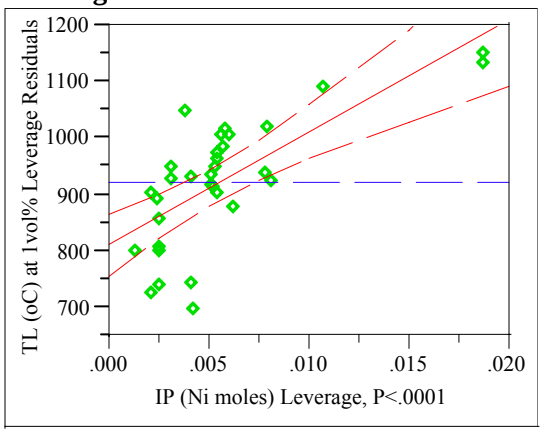

IPM (nonalkali moles) int
Leverage Plot

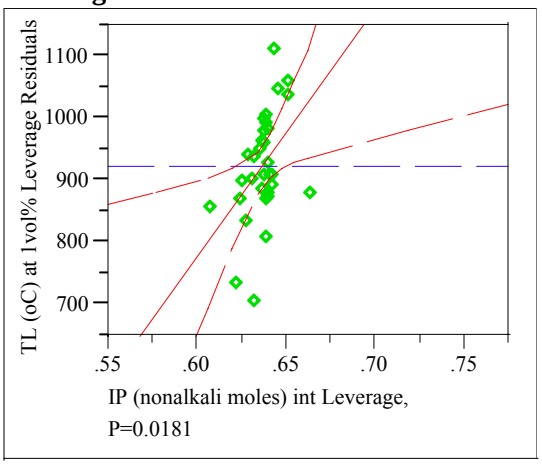

IPM (alkali moles) int
Leverage Plot

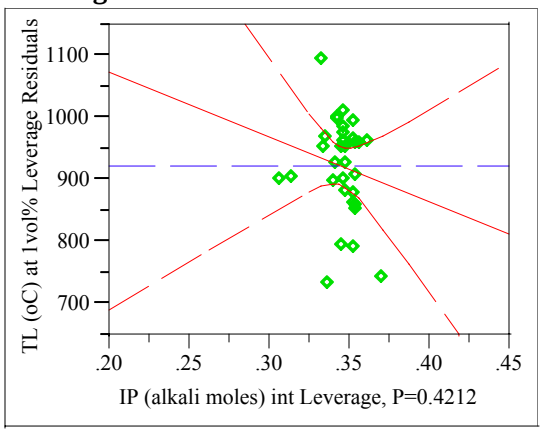

IPM (nonalkali moles) slp
Leverage Plot

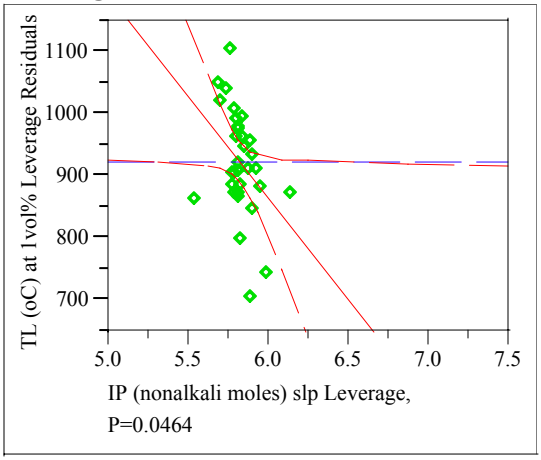

Appendix D. Model Fitting Results for T0.01 Data

Exhibit D.2: Statistical Results from the Fitting of the IPM to Each Data Grouping

Appendix D. Model Fitting Results for T0.01 Data

Exhibit D.3: Statistical Results from the Fitting of the SPM w Cr and Ni to Each Data Grouping

Groupings=1
Response 1000/T0.01 (K)
Whole Model
Actual by Predicted Plot

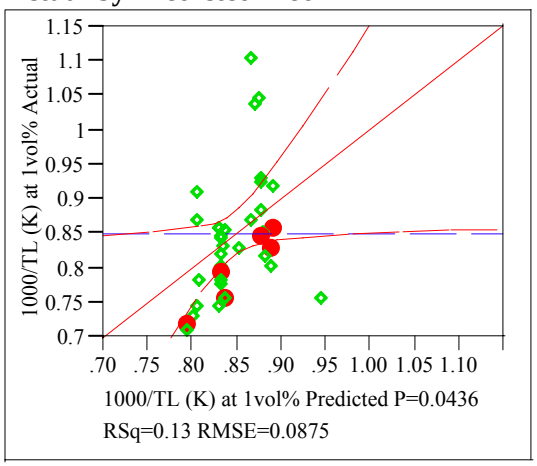

Residual by Predicted Plot

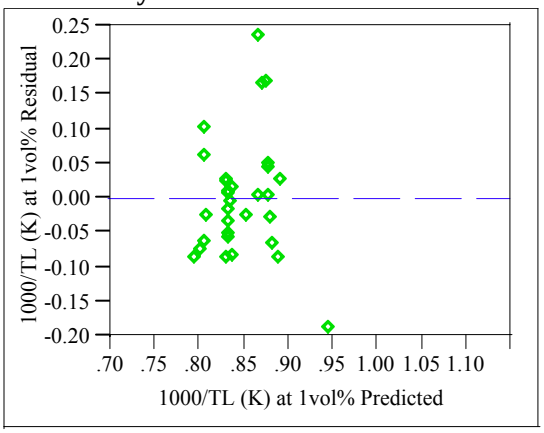

Press
0.2837468385

SPM w Cr & Ni
Leverage Plot

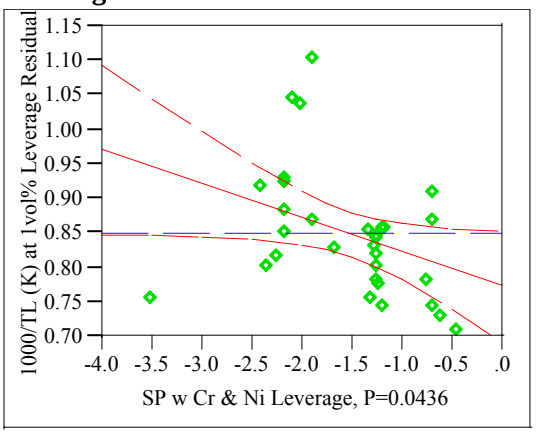

Summary of Fit

RSquare	0.133039
RSquare Adj	0.103144
Root Mean Square Error	0.087515
Mean of Response	0.848635
Observations (or Sum Wgts)	31

Analysis of Variance

Source	DF	Sum of Squares	Mean Square	F Ratio
Model	1	0.03408367	0.034084	4.4502
Error	29	0.22210935	0.007659	Prob > F
C. Total	30	0.25619302		0.0436

Lack Of Fit

Source	DF	Sum of Squares	Mean Square	F Ratio
Lack Of Fit	23	0.17973875	0.007815	1.1066
Pure Error	6	0.04237060	0.007062	Prob > F
Total Error	29	0.22210935		0.4907
				Max RSq
				0.8346

Parameter Estimates

Term	Estimate	Std Error	t Ratio	Prob>|t|
Intercept	0.7731007	0.039104	19.77	<.0001
SP w Cr & Ni	-0.049245	0.023344	-2.11	0.0436

Effect Tests

Source	DF	Sum of Squares	F Ratio	Prob > F
SP w Cr & Ni	1	0.03408367	4.4502	0.0436

Appendix D. Model Fitting Results for T0.01 Data

Exhibit D.3: Statistical Results from the Fitting of the SPM w Cr and Ni to Each Data Grouping

Groupings=2
Response 1000/T0.01 (K)
Whole Model
Actual by Predicted Plot

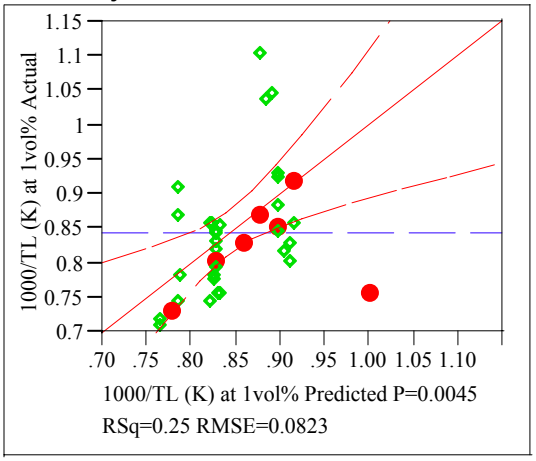

Residual by Predicted Plot

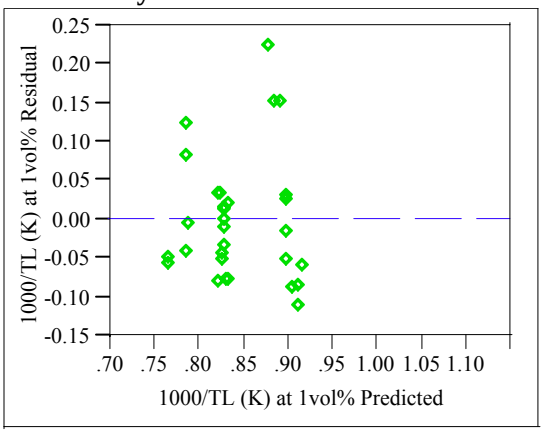

Press
0.2185656293

SPM w Cr & Ni
Leverage Plot

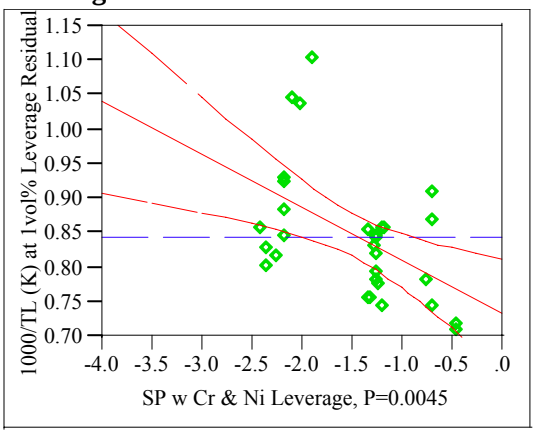

Summary of Fit

RSquare	0.254172
RSquare Adj	0.227535
Root Mean Square Error	0.082255
Mean of Response	0.845055
Observations (or Sum Wgts)	30

Analysis of Variance

Source	DF	Sum of Squares	Mean Square	F Ratio
Model	1	0.06456066	0.064561	9.5422
Error	28	0.18944331	0.006766	Prob > F
C. Total	29	0.25400397		0.0045

Lack Of Fit

Source	DF	Sum of Squares	Mean Square	F Ratio
Lack Of Fit	22	0.17299731	0.007864	2.8688
Pure Error	6	0.01644600	0.002741	Prob > F
Total Error	28	0.18944331		0.0969
				Max RSq
				0.9353

Parameter Estimates

Term	Estimate	Std Error	t Ratio	Prob>|t|
Intercept	0.7323932	0.039442	18.57	<.0001
SP w Cr & Ni	-0.07687	0.024885	-3.09	0.0045

Effect Tests

Source	DF	Sum of Squares	F Ratio	Prob > F
SP w Cr & Ni	1	0.06456066	9.5422	0.0045

Appendix D. Model Fitting Results for T0.01 Data

Exhibit D.3: Statistical Results from the Fitting of the SPM w Cr and Ni to Each Data Grouping

Groupings=3
Response 1000/T0.01 (K)
Whole Model
Actual by Predicted Plot

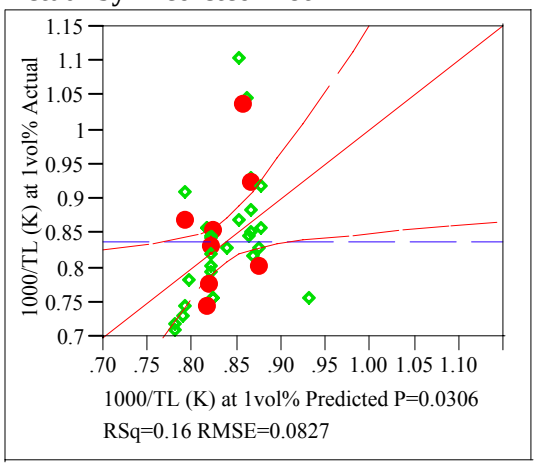

Residual by Predicted Plot

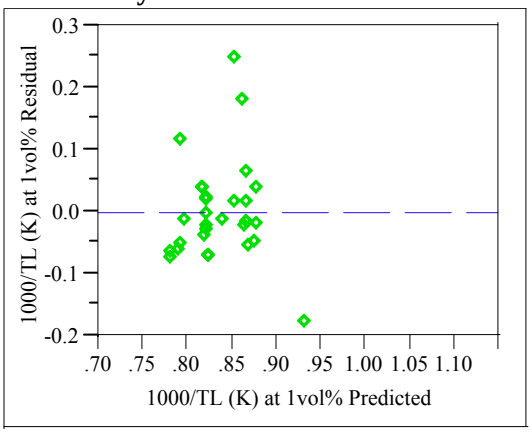

Press
0.2337110512

SPM w Cr & Ni
Leverage Plot

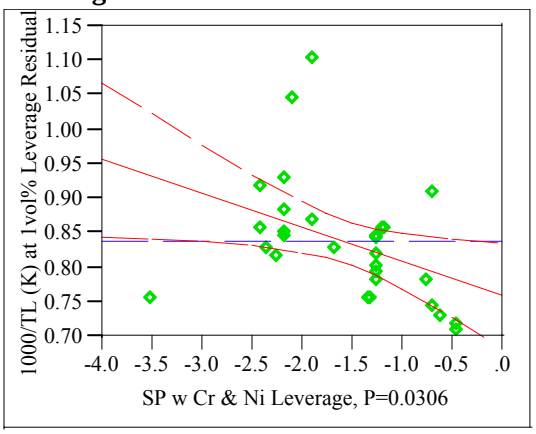

Summary of Fit

RSquare	0.161676
RSquare Adj	0.130627
Root Mean Square Error	0.082677
Mean of Response	0.836836
Observations (or Sum Wgts)	29

Analysis of Variance

Source	DF	Sum of Squares	Mean Square	F Ratio
Model	1	0.03559265	0.035593	5.2071
Error	27	0.18455592	0.006835	Prob > F
C. Total	28	0.22014857		0.0306

Lack Of Fit

Source	DF	Sum of Squares	Mean Square	F Ratio
Lack Of Fit	21	0.14171908	0.006749	0.9452
Pure Error	6	0.04283684	0.007139	Prob > F
Total Error	27	0.18455592		0.5821
				Max RSq
				0.8054

Parameter Estimates

Term	Estimate	Std Error	t Ratio	Prob>|t|
Intercept	0.760414	0.036842	20.64	<.0001
SP w Cr & Ni	-0.048957	0.021454	-2.28	0.0306

Effect Tests

Source	DF	Sum of Squares	F Ratio	Prob > F
SP w Cr & Ni	1	0.03559265	5.2071	0.0306

Appendix D. Model Fitting Results for T0.01 Data

Exhibit D.3: Statistical Results from the Fitting of the SPM w Cr and Ni to Each Data Grouping

Groupings=4
Response 1000/T0.01 (K)
Whole Model
Actual by Predicted Plot

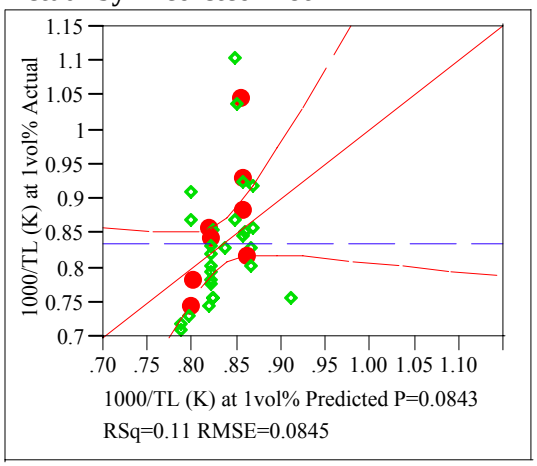

Residual by Predicted Plot

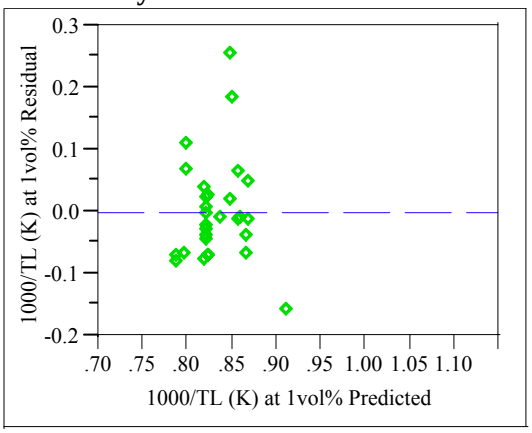

Press
0.2409007966

SPM w Cr & Ni
Leverage Plot

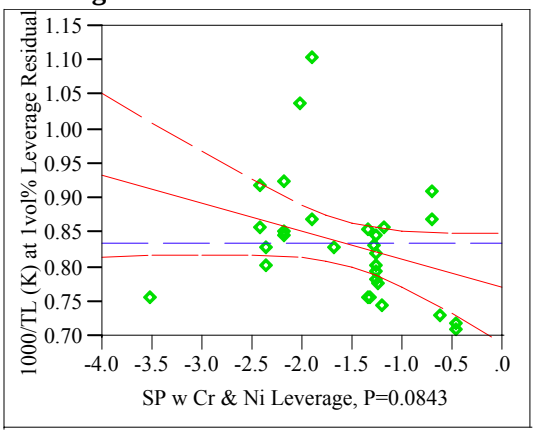

Summary of Fit

RSquare	0.106306
RSquare Adj	0.073206
Root Mean Square Error	0.084544
Mean of Response	0.834517
Observations (or Sum Wgts)	29

Analysis of Variance

Source	DF	Sum of Squares	Mean Square	F Ratio
Model	1	0.02295610	0.022956	3.2117
Error	27	0.19298846	0.007148	Prob > F
C. Total	28	0.21594457		0.0843

Lack Of Fit

Source	DF	Sum of Squares	Mean Square	F Ratio
Lack Of Fit	22	0.16326204	0.007421	1.2482
Pure Error	5	0.02972642	0.005945	Prob > F
Total Error	27	0.19298846		0.4392
				Max RSq
				0.8623

Parameter Estimates

Term	Estimate	Std Error	t Ratio	Prob>|t|
Intercept	0.7718902	0.038311	20.15	<.0001
SP w Cr & Ni	-0.040408	0.022548	-1.79	0.0843

Effect Tests

Source	DF	Sum of Squares	F Ratio	Prob > F
SP w Cr & Ni	1	0.02295610	3.2117	0.0843

Appendix D. Model Fitting Results for T0.01 Data

Exhibit D.3: Statistical Results from the Fitting of the SPM w Cr and Ni to Each Data Grouping

Groupings=5
Response 1000/T0.01 (K)
Whole Model
Actual by Predicted Plot

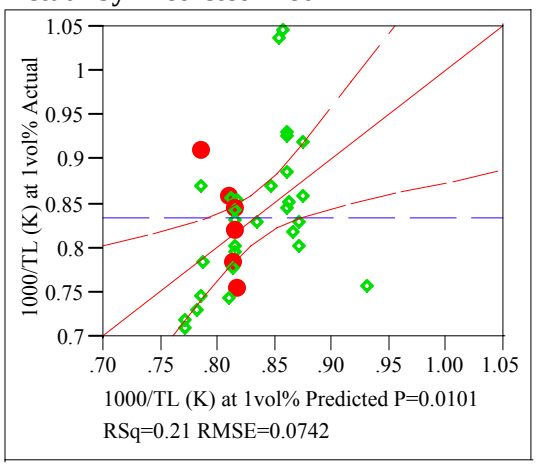

Summary of Fit

RSquare	0.213916
RSquare Adj	0.185841
Root Mean Square Error	0.074204
Mean of Response	0.83447
Observations (or Sum Wgts)	30

Analysis of Variance

Source	DF	Sum of Squares	Mean Square	F Ratio
Model	1	0.04195547	0.041955	7.6196
Error	28	0.15417519	0.005506	Prob > F
C. Total	29	0.19613065		0.0101

Lack Of Fit

Source	DF	Sum of Squares	Mean Square	F Ratio
Lack Of Fit	24	0.14521210	0.006051	2.7002
Pure Error	4	0.00896308	0.002241	Prob > F
Total Error	28	0.15417519		0.1726
				Max RSq
				0.9543

Parameter Estimates

Term	Estimate	Std Error	t Ratio	Prob>|t|
Intercept	0.7506465	0.033252	22.57	<.0001
SP w Cr & Ni	-0.051677	0.018721	-2.76	0.0101

Effect Tests

Source	DF	Sum of Squares	F Ratio	Prob > F
SP w Cr & Ni	1	0.04195547	7.6196	0.0101

Residual by Predicted Plot

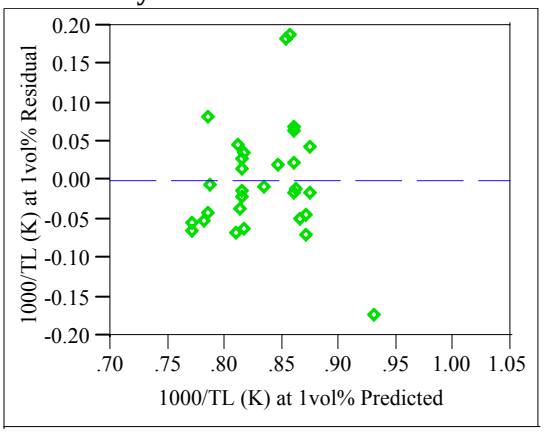

Press
0.1943997324

SPM w Cr & Ni
Leverage Plot

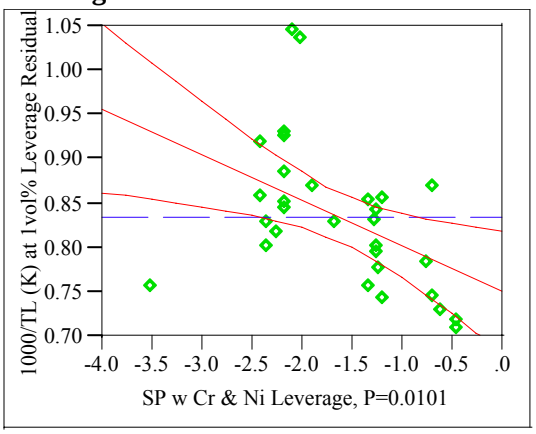

Appendix D. Model Fitting Results for T0.01 Data

Exhibit D.4: Statistical Results from the Fitting of the SPM w Ni and Fe to Each Data Grouping

Groupings=1
Response 1000/T0.01 (K)
Whole Model
Actual by Predicted Plot

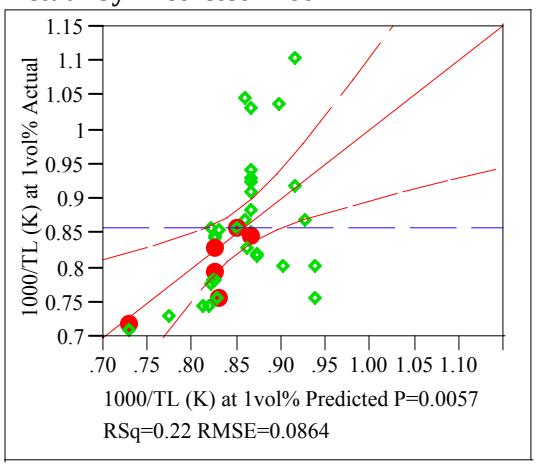

Residual by Predicted Plot

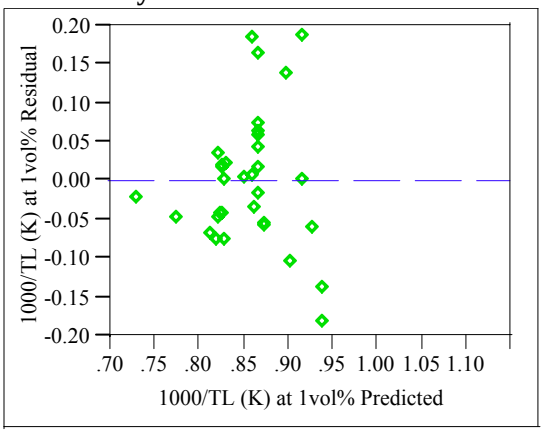

SPM w Ni & Fe
Leverage Plot

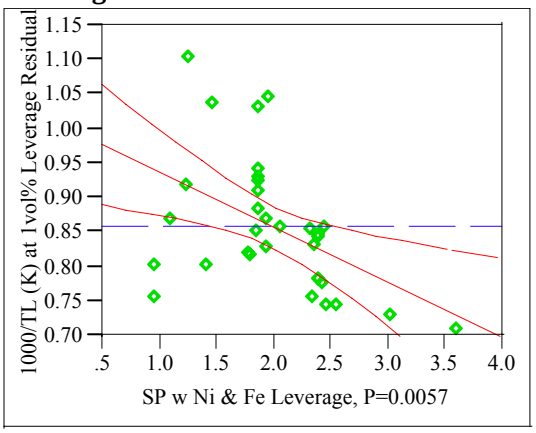

Summary of Fit

RSquare	0.221239
RSquare Adj	0.196118
Root Mean Square Error	0.086363
Mean of Response	0.8571
Observations (or Sum Wgts)	33

Analysis of Variance

Source	DF	Sum of Squares	Mean Square	F Ratio
Model	1	0.06568699	0.065687	8.8068
Error	31	0.23121815	0.007459	Prob > F
C. Total	32	0.29690514		0.0057

Lack Of Fit

Source	DF	Sum of Squares	Mean Square	F Ratio
Lack Of Fit	27	0.22613831	0.008375	6.5951
Pure Error	4	0.00507984	0.001270	Prob > F
Total Error	31	0.23121815		0.0394
				Max RSq
				0.9829

Parameter Estimates

Term	Estimate	Std Error	t Ratio	Prob>|t|
Intercept	1.0162013	0.05568	18.25	<.0001
SP w Ni & Fe	-0.079371	0.026745	-2.97	0.0057

Effect Tests

Source	DF	Sum of Squares	F Ratio	Prob > F
SP w Ni & Fe	1	0.06568699	8.8068	0.0057

Appendix D. Model Fitting Results for T0.01 Data

Exhibit D.4: Statistical Results from the Fitting of the SPM w Ni and Fe to Each Data Grouping

Groupings=2
Response 1000/T0.01 (K)
Whole Model
Actual by Predicted Plot

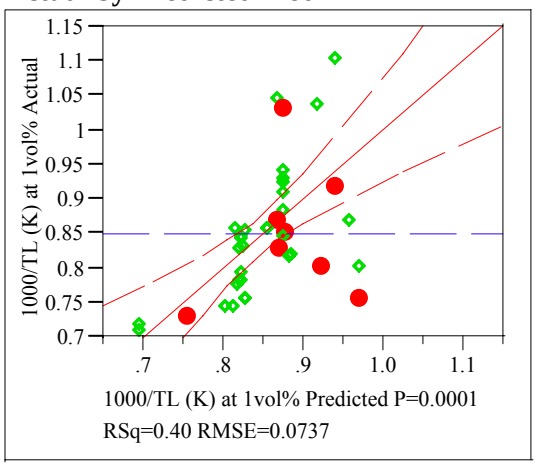

Residual by Predicted Plot

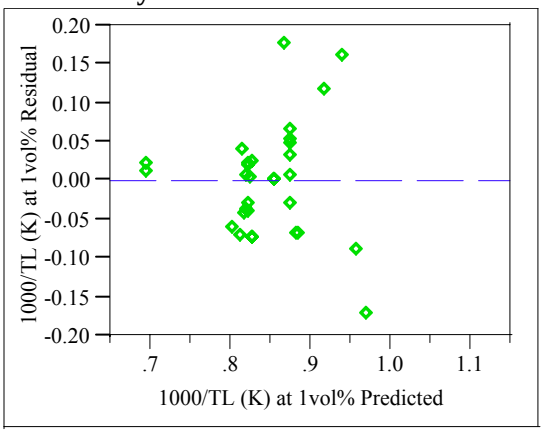

SPM w Ni & Fe
Leverage Plot

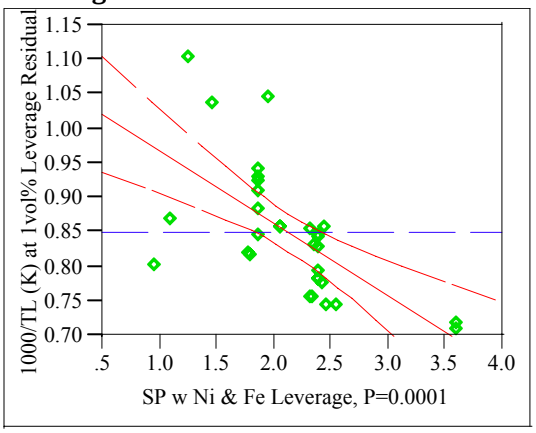

Summary of Fit

RSquare	0.401863
RSquare Adj	0.381238
Root Mean Square Error	0.073697
Mean of Response	0.848221
Observations (or Sum Wgts)	31

Analysis of Variance

Source	DF	Sum of Squares	Mean Square	F Ratio
Model	1	0.10582084	0.105821	19.4839
Error	29	0.15750487	0.005431	Prob > F
C. Total	30	0.26332571		0.0001

Lack Of Fit

Source	DF	Sum of Squares	Mean Square	F Ratio
Lack Of Fit	25	0.15581890	0.006233	14.7874
Pure Error	4	0.00168597	0.000421	Prob > F
Total Error	29	0.15750487		0.0089
				Max RSq
				0.9936

Parameter Estimates

Term	Estimate	Std Error	t Ratio	Prob>|t|
Intercept	1.0724968	0.052505	20.43	<.0001
SP w Ni & Fe	-0.104501	0.023675	-4.41	0.0001

Effect Tests

Source	DF	Sum of Squares	F Ratio	Prob > F
SP w Ni & Fe	1	0.10582084	19.4839	0.0001

Appendix D. Model Fitting Results for T0.01 Data

Exhibit D.4: Statistical Results from the Fitting of the SPM w Ni and Fe to Each Data Grouping

Groupings=3
Response 1000/T0.01 (K)
Whole Model
Actual by Predicted Plot

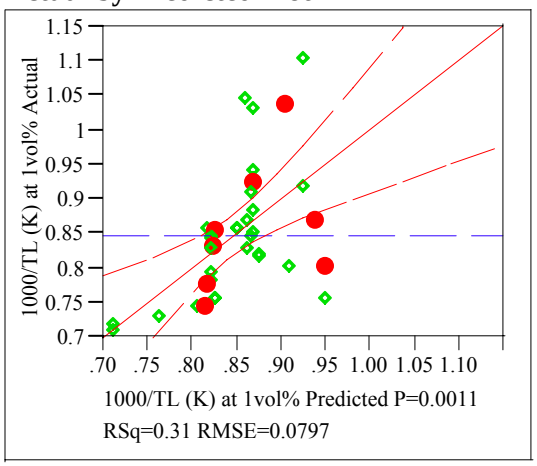

Residual by Predicted Plot

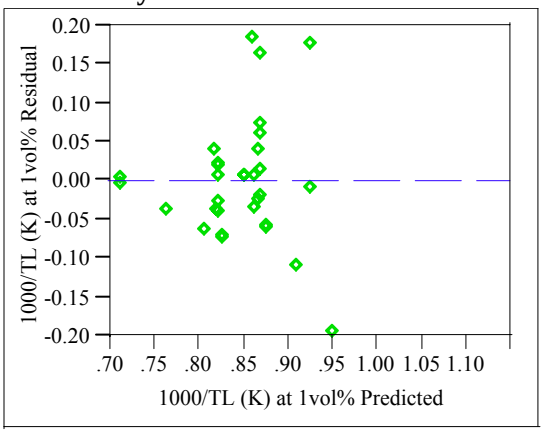

SPM w Ni & Fe
Leverage Plot

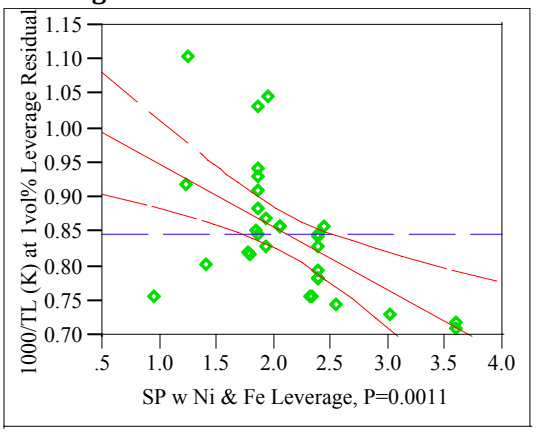

Summary of Fit

RSquare	0.311191
RSquare Adj	0.287439
Root Mean Square Error	0.079656
Mean of Response	0.846607
Observations (or Sum Wgts)	31

Analysis of Variance

Source	DF	Sum of Squares	Mean Square	F Ratio
Model	1	0.08312998	0.083130	13.1016
Error	29	0.18400505	0.006345	Prob > F
C. Total	30	0.26713503		0.0011

Lack Of Fit

Source	DF	Sum of Squares	Mean Square	F Ratio
Lack Of Fit	25	0.17826930	0.007131	4.9729
Pure Error	4	0.00573575	0.001434	Prob > F
Total Error	29	0.18400505		0.0646
				Max RSq
				0.9785

Parameter Estimates

Term	Estimate	Std Error	t Ratio	Prob>|t|
Intercept	1.0390435	0.055056	18.87	<.0001
SP w Ni & Fe	-0.090644	0.025042	-3.62	0.0011

Effect Tests

Source	DF	Sum of Squares	F Ratio	Prob > F
SP w Ni & Fe	1	0.08312998	13.1016	0.0011

Appendix D. Model Fitting Results for T0.01 Data

Exhibit D.4: Statistical Results from the Fitting of the SPM w Ni and Fe to Each Data Grouping

Groupings=4
Response 1000/T0.01 (K)
Whole Model
Actual by Predicted Plot

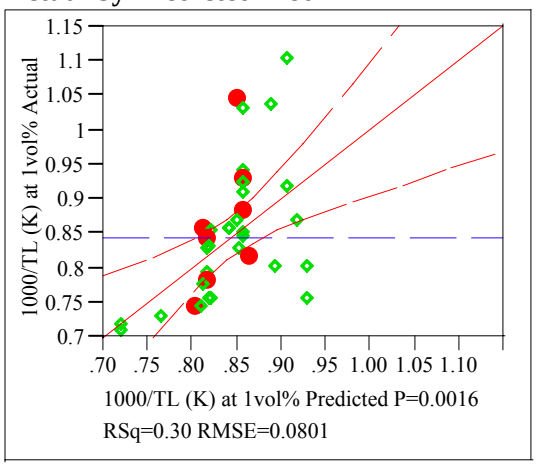

Residual by Predicted Plot

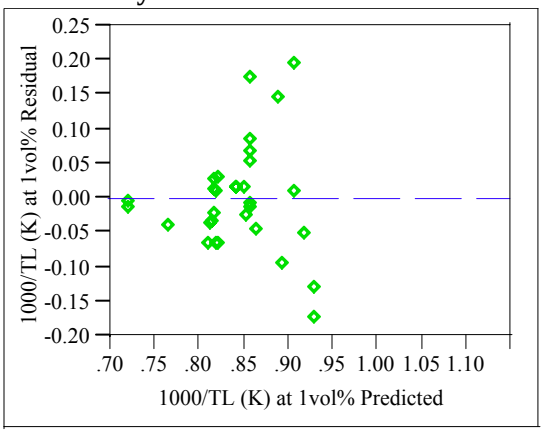

Summary of Fit

RSquare	0.295744
RSquare Adj	0.271459
Root Mean Square Error	0.080108
Mean of Response	0.844438
Observations (or Sum Wgts)	31

Analysis of Variance

Source	DF	Sum of Squares	Mean Square	F Ratio
Model	1	0.07815180	0.078152	12.1782
Error	29	0.18610335	0.006417	Prob > F
C. Total	30	0.26425516		0.0016

Lack Of Fit

Source	DF	Sum of Squares	Mean Square	F Ratio
Lack Of Fit	25	0.17971931	0.007189	4.5042
Pure Error	4	0.00638405	0.001596	Prob > F
Total Error	29	0.18610335		0.0764
				Max RSq
				0.9758

Parameter Estimates

Term	Estimate	Std Error	t Ratio	Prob>|t|
Intercept	1.006801	0.0487	20.67	<.0001
SP w Ni & Fe	-0.079254	0.022711	-3.49	0.0016

Effect Tests

Source	DF	Sum of Squares	F Ratio	Prob > F
SP w Ni & Fe	1	0.07815180	12.1782	0.0016

SPM w Ni & Fe
Leverage Plot

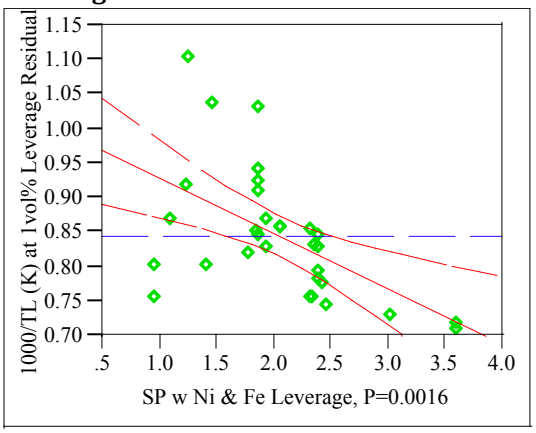

Appendix D. Model Fitting Results for T0.01 Data

Exhibit D.4: Statistical Results from the Fitting of the SPM w Ni and Fe to Each Data Grouping

Groupings=5
Response 1000/T0.01 (K)
Whole Model
Actual by Predicted Plot

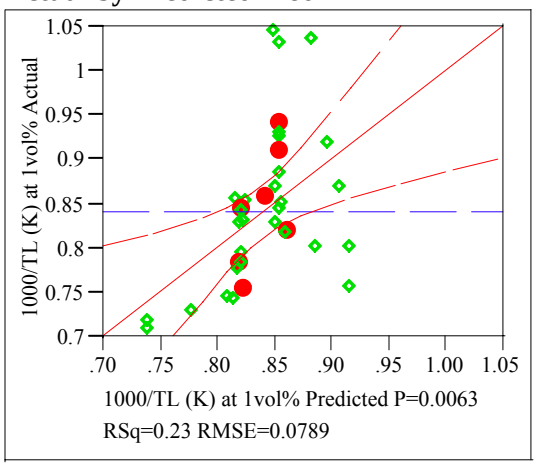

Summary of Fit

RSquare	0.230343
RSquare Adj	0.203803
Root Mean Square Error	0.078877
Mean of Response	0.840887
Observations (or Sum Wgts)	31

Analysis of Variance

Source	DF	Sum of Squares	Mean Square	F Ratio
Model	1	0.05399754	0.053998	8.6791
Error	29	0.18042521	0.006222	Prob > F
C. Total	30	0.23442275		0.0063

Lack Of Fit

Source	DF	Sum of Squares	Mean Square	F Ratio
Lack Of Fit	25	0.17822017	0.007129	12.9318
Pure Error	4	0.00220505	0.000551	Prob > F
Total Error	29	0.18042521		0.0115
				Max RSq
				0.9906

Parameter Estimates

Term	Estimate	Std Error	t Ratio	Prob>|t|
Intercept	0.9805887	0.049491	19.81	<.0001
SP w Ni & Fe	-0.066826	0.022683	-2.95	0.0063

Effect Tests

Source	DF	Sum of Squares	F Ratio	Prob > F
SP w Ni & Fe	1	0.05399754	8.6791	0.0063

Residual by Predicted Plot

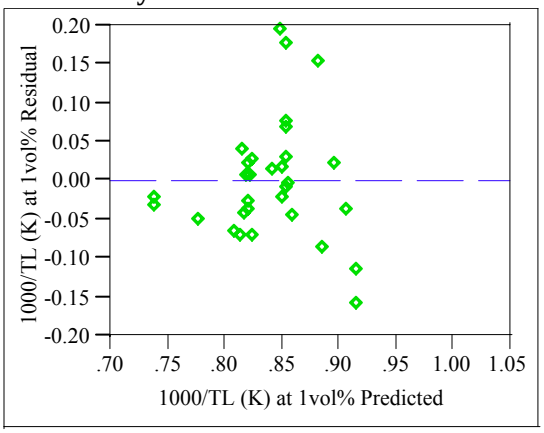

SP w Ni & Fe
Leverage Plot

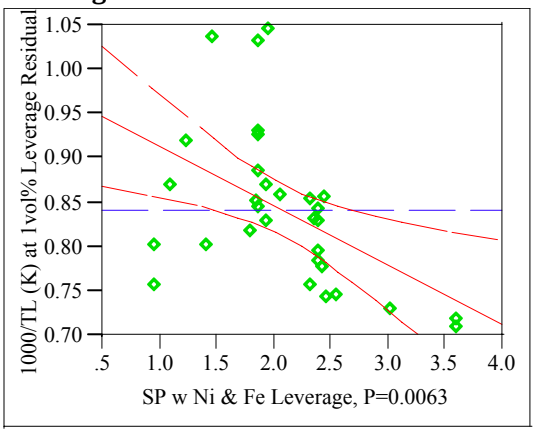

Appendix D. Model Fitting Results for T0.01 Data

Exhibit D.5: Statistical Results from the Fitting of the SLM to Each Data Grouping

Groupings=1
Response 1/T0.01 (K)
Whole Model
Actual by Predicted Plot

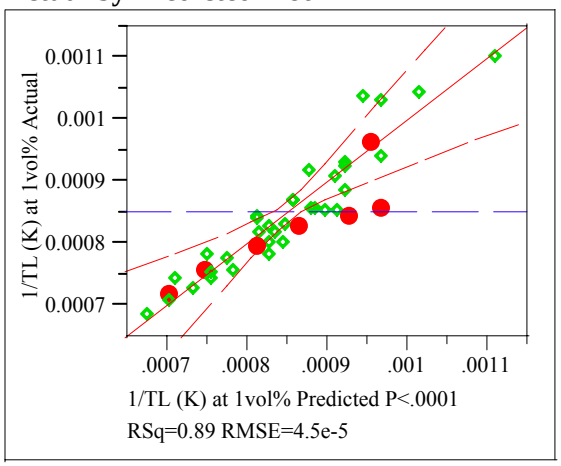

Summary of Fit

RSquare	0.892779
RSquare Adj	0.791865
Root Mean Square Error	0.000045
Mean of Response	0.000852
Observations (or Sum Wgts)	34

Analysis of Variance

Source	DF	Sum of Squares	Mean Square	F Ratio
Model	16	2.89747e-7	1.8109e-8	8.8469
Error	17	3.47981e-8	2.0469e-9	Prob > F
C. Total	33	3.24545e-7		<.0001

Lack Of Fit

Source	DF	Sum of Squares	Mean Square	F Ratio
Lack Of Fit	15	3.07139e-8	2.0476e-9	1.0027
Pure Error	2	4.08415e-9	2.0421e-9	Prob > F
Total Error	17	3.47981e-8		0.6079
				Max RSq
				0.9874

Parameter Estimates

Term	Estimate	Std Error	t Ratio	Prob>|t|
Intercept	0.0024029	0.000877	2.74	0.0140
SL SPL	-0.048304	0.03415	-1.41	0.1753
Al2O3 wt%	-0.000036	0.000011	-3.18	0.0054
B2O3 wt%	-0.000005	0.000007	-0.66	0.5184
CaO wt%	-0.000051	0.00004	-1.27	0.2223
Cr2O3 wt%	-0.000198	0.000132	-1.50	0.1516
Fe2O3 wt%	-0.000039	0.000013	-3.07	0.0069
K2O wt%	-0.000031	0.000027	-1.15	0.2657
Li2O wt%	0.0000075	0.000014	0.53	0.6049
MgO wt%	-0.00004	0.00002	-1.99	0.0629
MnO2 wt%	-0.000036	0.000013	-2.81	0.0120
Na2O wt%	0.0000106	0.000008	1.34	0.1968
NiO wt%	-0.000101	0.000019	-5.24	<.0001
SiO2 wt%	-0.000013	0.000011	-1.16	0.2630
TiO2 wt%	-0.000197	0.000403	-0.49	0.6308
ZnO wt%	0.0000046	0.000037	0.12	0.9028
ZrO2 wt%	-0.000037	0.000011	-3.50	0.0028

Appendix D. Model Fitting Results for T0.01 Data

Exhibit D.5: Statistical Results from the Fitting of the SLM to Each Data Grouping

Effect Tests

Source	DF	Sum of Squares	F Ratio	Prob > F
SL SPL	1	4.09542e-9	2.0007	0.1753
Al2O3 wt%	1	2.07493e-8	10.1367	0.0054
B2O3 wt%	1	8.902e-10	0.4349	0.5184
CaO wt%	1	3.28521e-9	1.6049	0.2223
Cr2O3 wt%	1	4.61352e-9	2.2539	0.1516
Fe2O3 wt%	1	1.93167e-8	9.4368	0.0069
K2O wt%	1	2.71099e-9	1.3244	0.2657
Li2O wt%	1	5.6885e-10	0.2779	0.6049
MgO wt%	1	8.10712e-9	3.9606	0.0629
MnO2 wt%	1	1.61662e-8	7.8977	0.0120
Na2O wt%	1	3.69372e-9	1.8045	0.1968
NiO wt%	1	5.62547e-8	27.4823	<.0001
SiO2 wt%	1	2.74302e-9	1.3401	0.2630
TiO2 wt%	1	4.9026e-10	0.2395	0.6308
ZnO wt%	1	3.143e-11	0.0154	0.9028
ZrO2 wt%	1	2.50194e-8	12.2228	0.0028

Residual by Predicted Plot

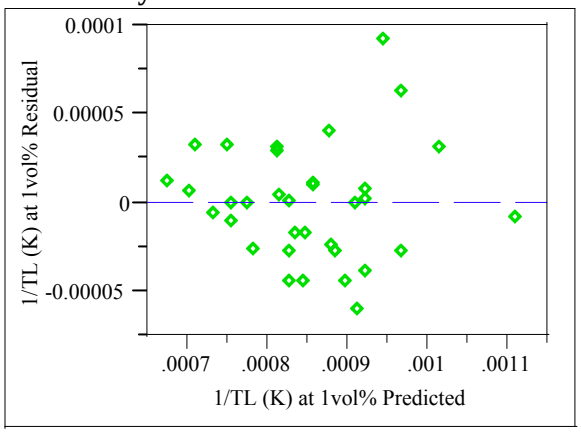

Press
8.3062788e-7

SL SPL
Leverage Plot

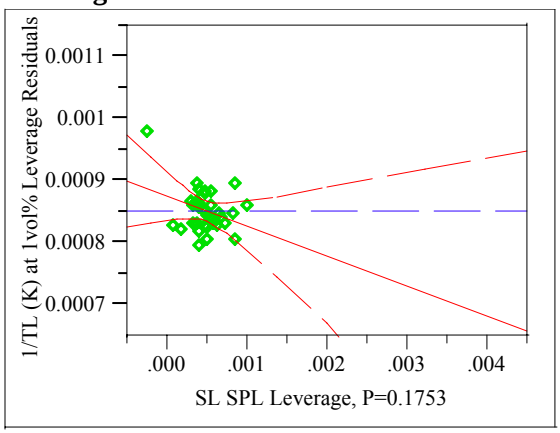

Al2O3 wt%
Leverage Plot

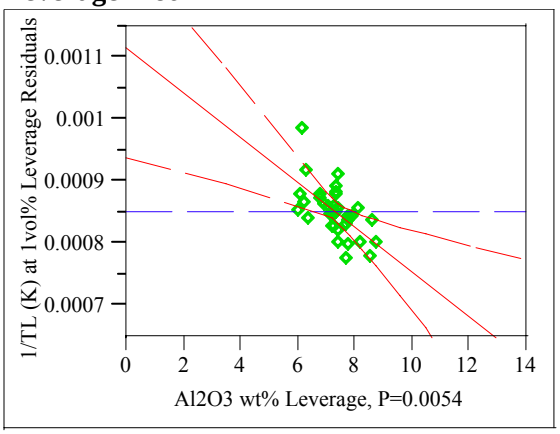

B2O3 wt%
Leverage Plot

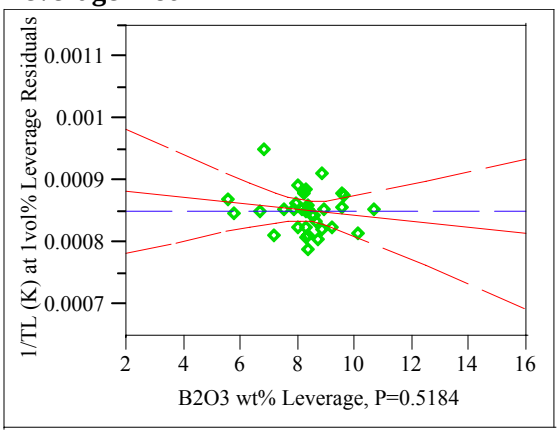

CaO wt%
Leverage Plot

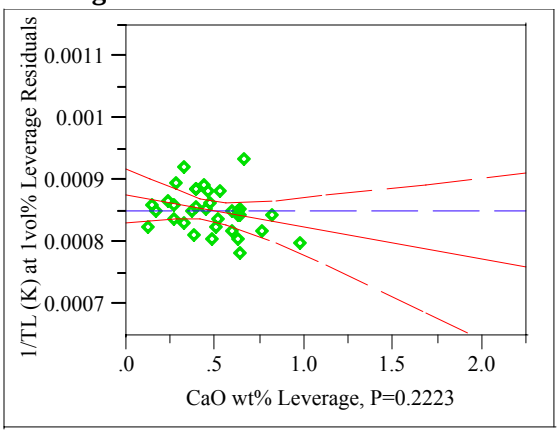

Appendix D. Model Fitting Results for T0.01 Data

Exhibit D.5: Statistical Results from the Fitting of the SLM to Each Data Grouping

Cr2O3 wt%
Leverage Plot

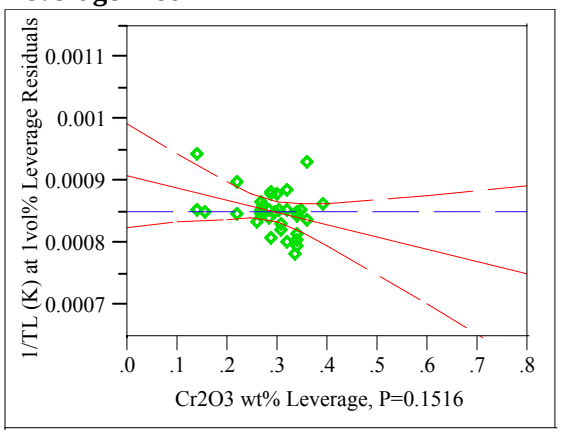

Li2O wt%
Leverage Plot

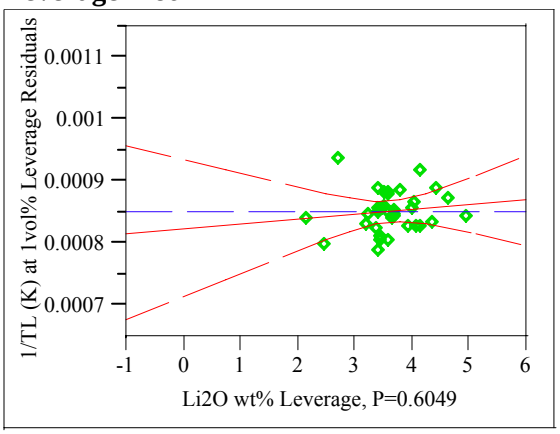

Fe2O3 wt%
Leverage Plot

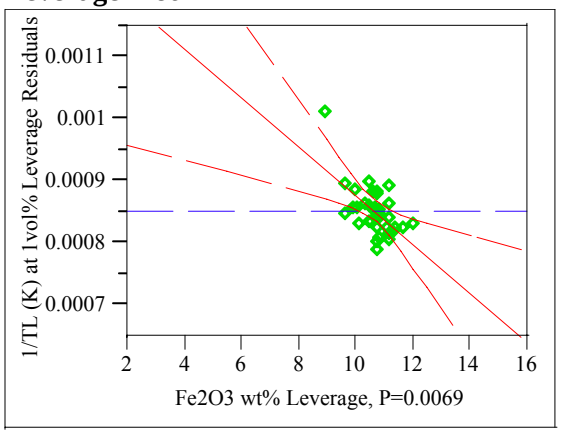

MgO wt%
Leverage Plot

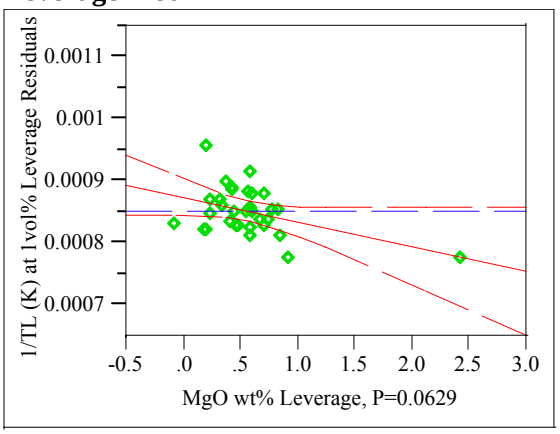

K2O wt%
Leverage Plot

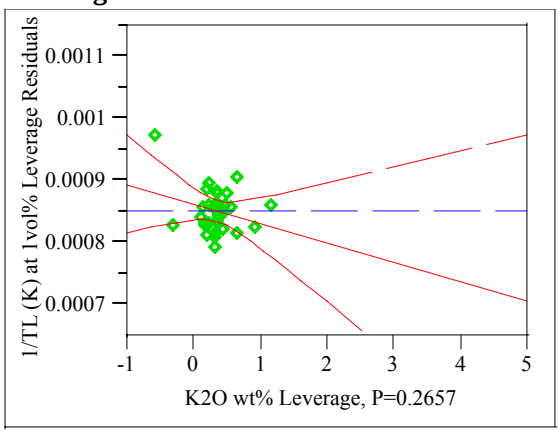

MnO2 wt%
Leverage Plot

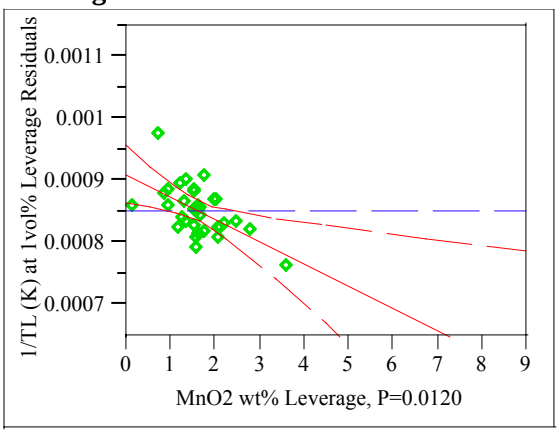

Appendix D. Model Fitting Results for T0.01 Data

Exhibit D.5: Statistical Results from the Fitting of the SLM to Each Data Grouping

Na2O wt%
Leverage Plot

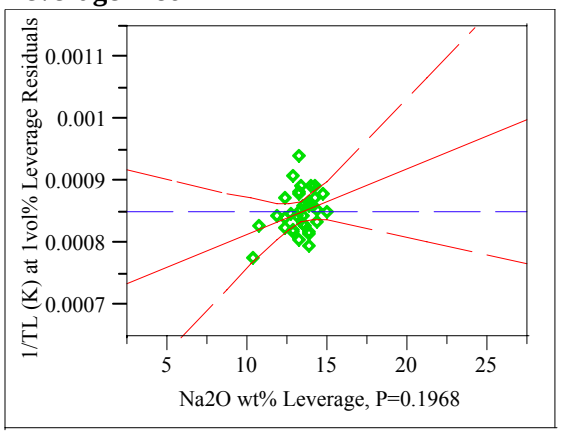

TiO2 wt%
Leverage Plot

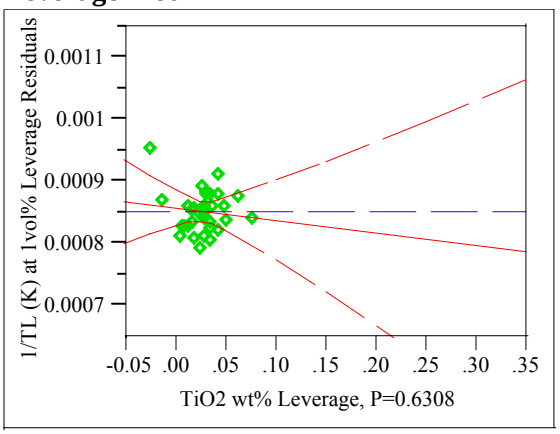

NiO wt%
Leverage Plot

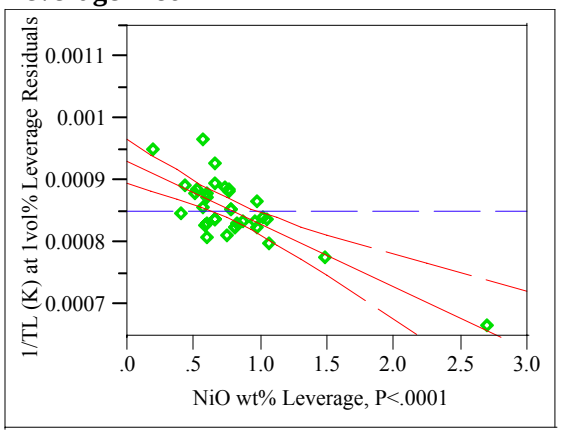

ZnO wt%
Leverage Plot

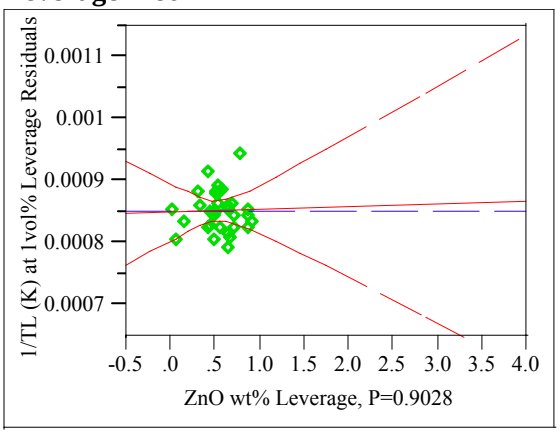

SiO2 wt%
Leverage Plot

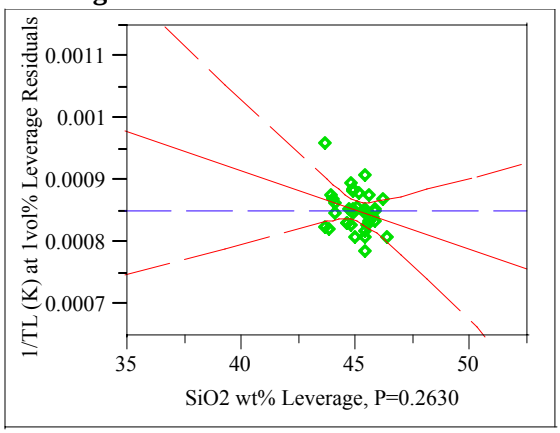

ZrO2 wt%
Leverage Plot

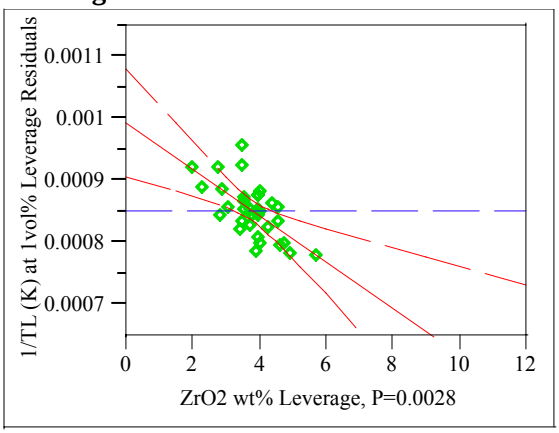

Appendix D. Model Fitting Results for T0.01 Data

Exhibit D.5: Statistical Results from the Fitting of the SLM to Each Data Grouping

Groupings=2
Response 1/T0.01 (K)
Whole Model
Actual by Predicted Plot

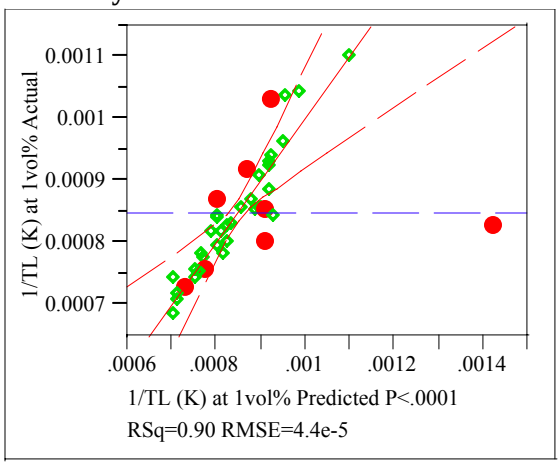

Summary of Fit

RSquare	0.897375
RSquare Adj	0.79475
Root Mean Square Error	0.000044
Mean of Response	0.000847
Observations (or Sum Wgts)	33

Analysis of Variance

Source	DF	Sum of Squares	Mean Square	F Ratio
Model	16	2.71321e-7	1.6958e-8	8.7442
Error	16	3.10287e-8	1.9393e-9	Prob > F
C. Total	32	3.0235e-7		<.0001

Lack Of Fit

Source	DF	Sum of Squares	Mean Square	F Ratio
Lack Of Fit	13	2.96867e-8	2.2836e-9	5.1049
Pure Error	3	1.34201e-9	4.473e-10	Prob > F
Total Error	16	3.10287e-8		0.1027
				Max RSq
				0.9956

Parameter Estimates

Term	Estimate	Std Error	t Ratio	Prob>|t|
Intercept	0.0015204	0.001138	1.34	0.2001
SL SPL	-0.071999	0.039375	-1.83	0.0862
Al2O3 wt%	-0.000022	0.000014	-1.57	0.1369
B2O3 wt%	0.0000023	0.000009	0.27	0.7884
CaO wt%	-0.000047	0.000172	-0.27	0.7881
Cr2O3 wt%	0.0000077	0.000137	0.06	0.9562
Fe2O3 wt%	-0.000038	0.00002	-1.88	0.0784
K2O wt%	-0.00001	0.000051	-0.20	0.8427
Li2O wt%	0.0000129	0.000017	0.76	0.4566
MgO wt%	-0.000024	0.000021	-1.13	0.2733
MnO2 wt%	-0.000036	0.000011	-3.39	0.0037
Na2O wt%	0.0000189	0.000011	1.70	0.1081
NiO wt%	-0.000085	0.000018	-4.86	0.0002
SiO2 wt%	-0.000004	0.000013	-0.31	0.7581
TiO2 wt%	0.0021376	0.005919	0.36	0.7227
ZnO wt%	0.0000209	0.00004	0.52	0.6104
ZrO2 wt%	-0.000023	0.000016	-1.41	0.1782

Appendix D. Model Fitting Results for T0.01 Data

Exhibit D.5: Statistical Results from the Fitting of the SLM to Each Data Grouping

Effect Tests

Source	DF	Sum of Squares	F Ratio	Prob > F
SL SPL	1	6.48419e-9	3.3436	0.0862
Al2O3 wt%	1	4.75642e-9	2.4527	0.1369
B2O3 wt%	1	1.4442e-10	0.0745	0.7884
CaO wt%	1	1.4486e-10	0.0747	0.7881
Cr2O3 wt%	1	6.0475e-12	0.0031	0.9562
Fe2O3 wt%	1	6.85496e-9	3.5348	0.0784
K2O wt%	1	7.8844e-11	0.0407	0.8427
Li2O wt%	1	1.12889e-9	0.5821	0.4566
MgO wt%	1	2.49612e-9	1.2871	0.2733
MnO2 wt%	1	2.233e-8	11.5145	0.0037
Na2O wt%	1	5.61808e-9	2.8970	0.1081
NiO wt%	1	4.57386e-8	23.5852	0.0002
SiO2 wt%	1	1.9028e-10	0.0981	0.7581
TiO2 wt%	1	2.5295e-10	0.1304	0.7227
ZnO wt%	1	5.2386e-10	0.2701	0.6104
ZrO2 wt%	1	3.8453e-9	1.9828	0.1782

Residual by Predicted Plot

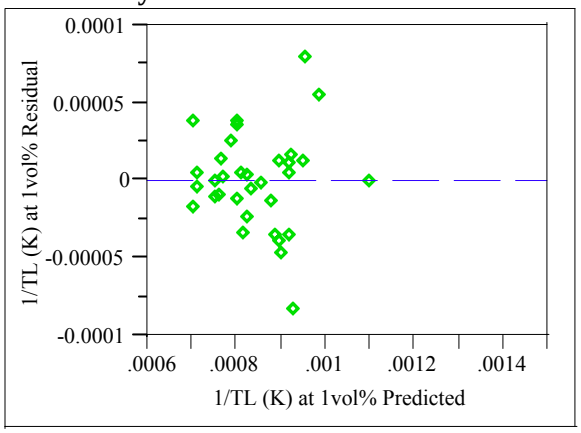

Press
0.0000020601

SL SPL
Leverage Plot

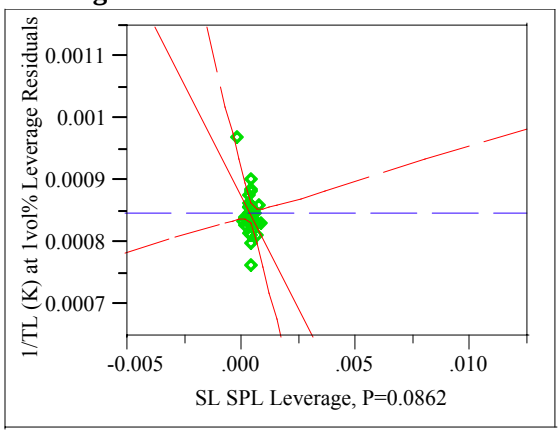

Al2O3 wt%
Leverage Plot

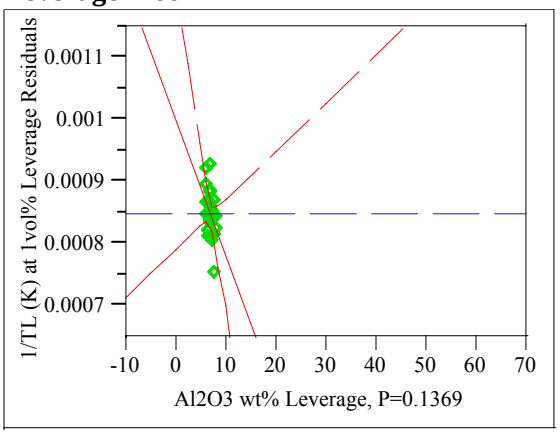

B2O3 wt%
Leverage Plot

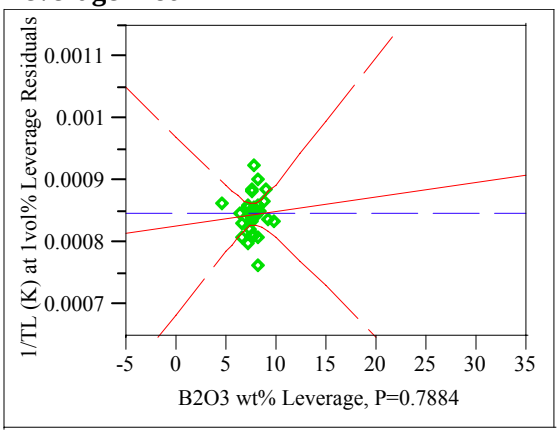

CaO wt%
Leverage Plot

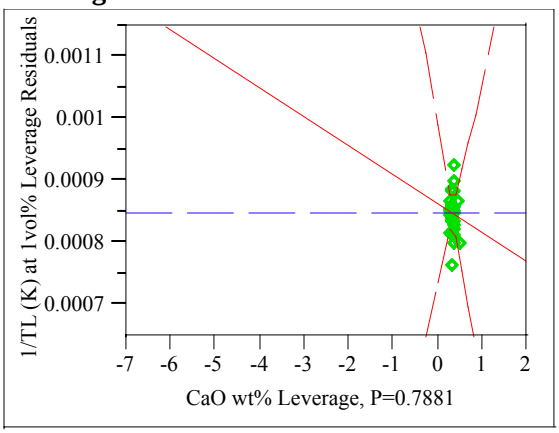

Appendix D. Model Fitting Results for T0.01 Data

Exhibit D.5: Statistical Results from the Fitting of the SLM to Each Data Grouping

Cr2O3 wt%
Leverage Plot

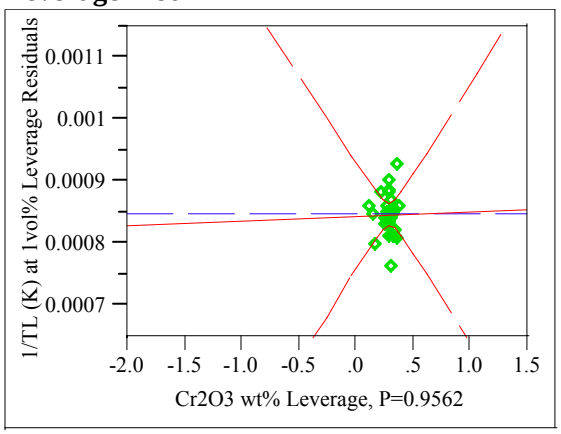

Li2O wt%
Leverage Plot

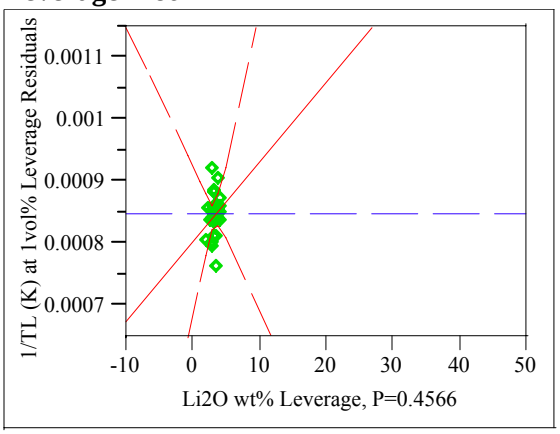

Fe2O3 wt%
Leverage Plot

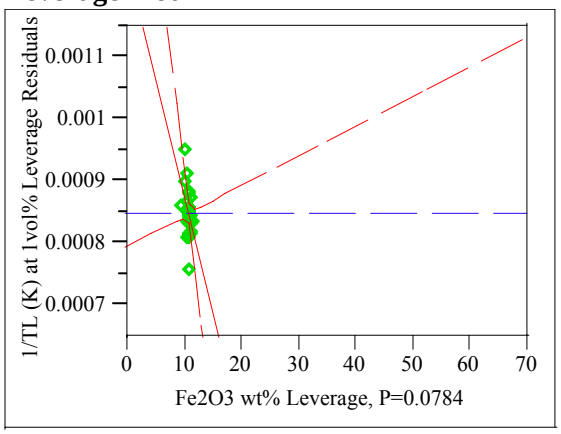

MgO wt%
Leverage Plot

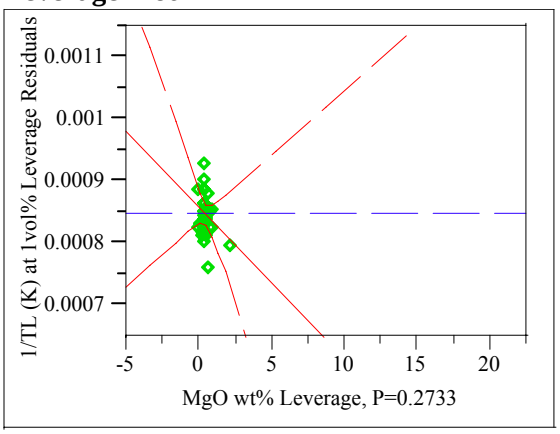

K2O wt%
Leverage Plot

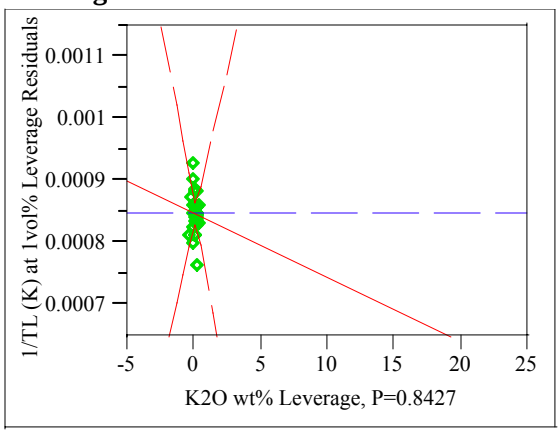

MnO2 wt%
Leverage Plot

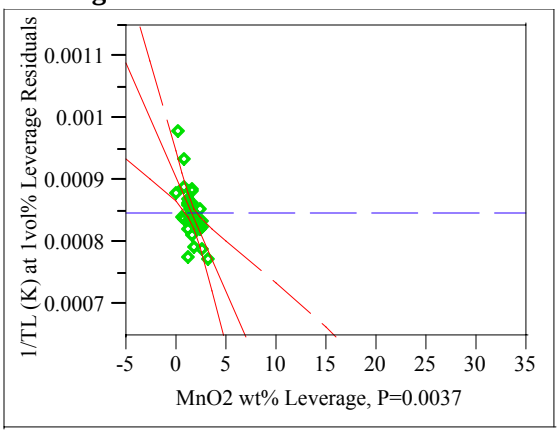

Appendix D. Model Fitting Results for T0.01 Data

Exhibit D.5: Statistical Results from the Fitting of the SLM to Each Data Grouping

Na2O wt%
Leverage Plot

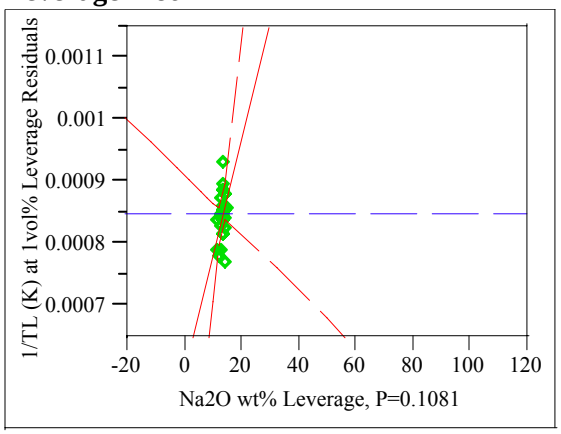

TiO2 wt%
Leverage Plot

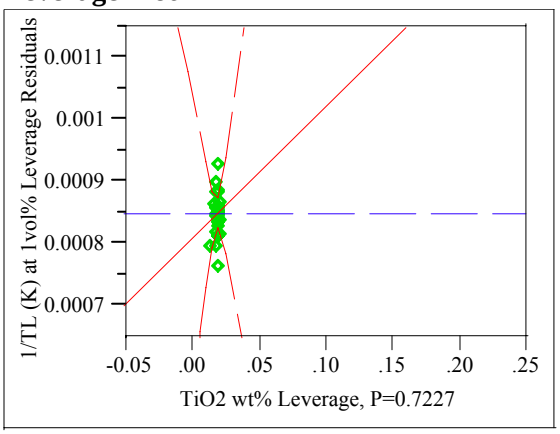

NiO wt%
Leverage Plot

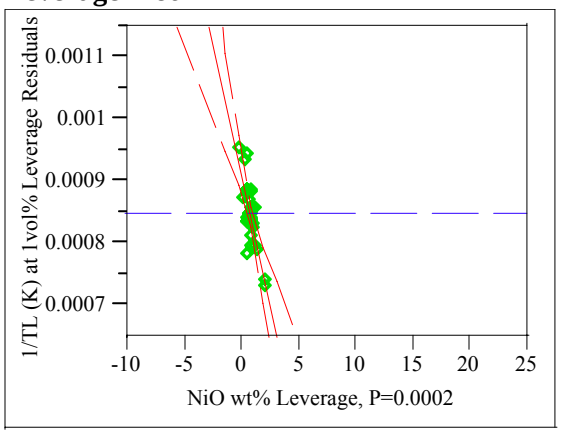

ZnO wt%
Leverage Plot

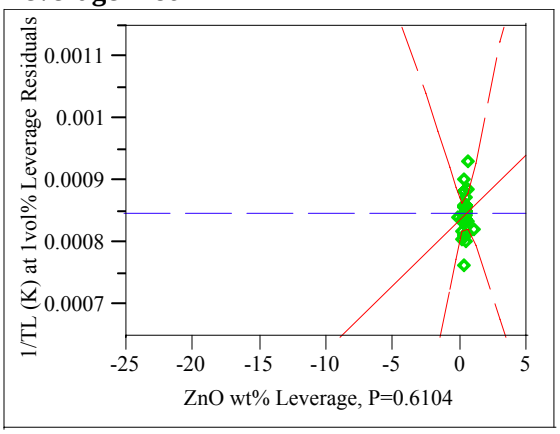

SiO2 wt%
Leverage Plot

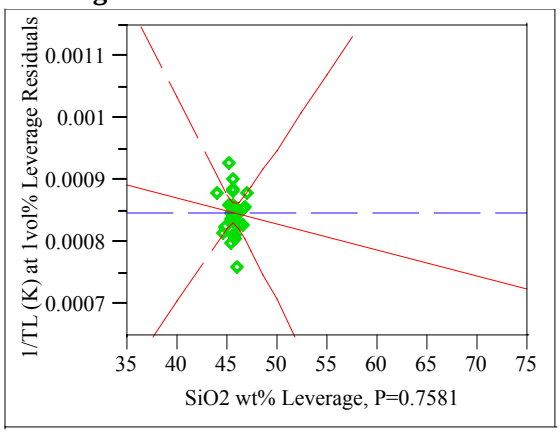

ZrO2 wt%
Leverage Plot

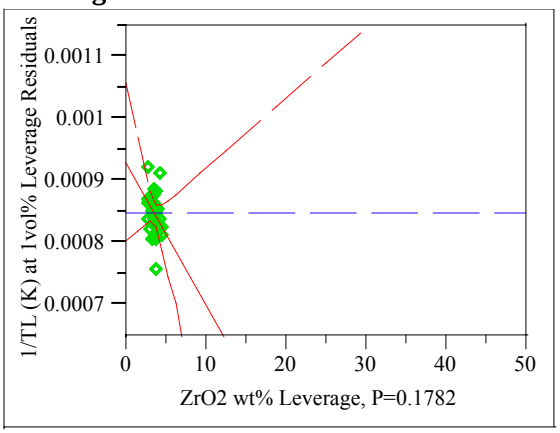

Appendix D. Model Fitting Results for T0.01 Data

Exhibit D.5: Statistical Results from the Fitting of the SLM to Each Data Grouping

Groupings=3
Response 1/T0.01 (K)
Whole Model
Actual by Predicted Plot

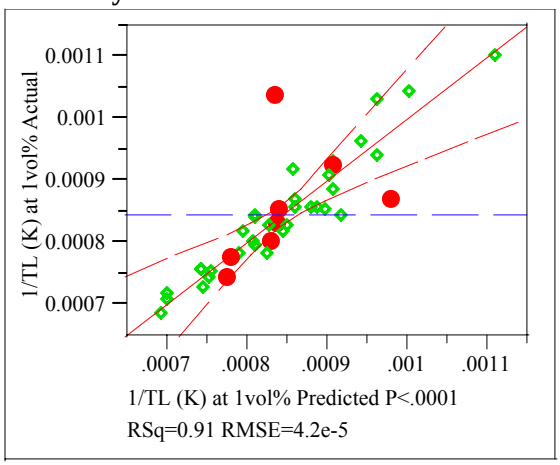

Summary of Fit

RSquare	0.907452
RSquare Adj	0.814905
Root Mean Square Error	0.000042
Mean of Response	0.000845
Observations (or Sum Wgts)	33

Analysis of Variance

Source	DF	Sum of Squares	Mean Square	F Ratio
Model	16	2.77709e-7	1.7357e-8	9.8053
Error	16	2.83225e-8	1.7702e-9	Prob > F
C. Total	32	3.06032e-7		<.0001

Lack Of Fit

Source	DF	Sum of Squares	Mean Square	F Ratio
Lack Of Fit	13	2.29307e-8	1.7639e-9	0.9814
Pure Error	3	5.39179e-9	1.7973e-9	Prob > F
Total Error	16	2.83225e-8		0.5840
				Max RSq
				0.9824

Parameter Estimates

Term	Estimate	Std Error	t Ratio	Prob>|t|
Intercept	0.000176	0.001462	0.12	0.9057
SL SPL	0.0576749	0.070983	0.81	0.4284
Al2O3 wt%	-0.000015	0.000016	-0.94	0.3595
B2O3 wt%	0.000008	0.000013	0.63	0.5344
CaO wt%	-0.000062	0.000039	-1.61	0.1271
Cr2O3 wt%	-0.000271	0.000144	-1.88	0.0788
Fe2O3 wt%	-1.462e-8	0.000026	-0.00	0.9996
K2O wt%	0.0000514	0.000056	0.91	0.3762
Li2O wt%	0.0000248	0.00003	0.82	0.4235
MgO wt%	-0.000017	0.000023	-0.73	0.4732
MnO2 wt%	-0.000005	0.000021	-0.25	0.8050
Na2O wt%	0.0000156	0.000012	1.35	0.1951
NiO wt%	-0.000079	0.000018	-4.30	0.0005
SiO2 wt%	0.0000141	0.000019	0.74	0.4703
TiO2 wt%	0.0008284	0.000614	1.35	0.1962
ZnO wt%	-0.000017	0.000046	-0.38	0.7061
ZrO2 wt%	-0.000023	0.000016	-1.46	0.1644

Appendix D. Model Fitting Results for T0.01 Data

Exhibit D.5: Statistical Results from the Fitting of the SLM to Each Data Grouping

Effect Tests

Source	DF	Sum of Squares	F Ratio	Prob > F
SL SPL	1	1.16864e-9	0.6602	0.4284
Al2O3 wt%	1	1.57567e-9	0.8901	0.3595
B2O3 wt%	1	7.1374e-10	0.4032	0.5344
CaO wt%	1	4.58414e-9	2.5897	0.1271
Cr2O3 wt%	1	6.24127e-9	3.5258	0.0788
Fe2O3 wt%	1	5.5477e-16	0.0000	0.9996
K2O wt%	1	1.46681e-9	0.8286	0.3762
Li2O wt%	1	1.19416e-9	0.6746	0.4235
MgO wt%	1	9.5519e-10	0.5396	0.4732
MnO2 wt%	1	1.1154e-10	0.0630	0.8050
Na2O wt%	1	3.23641e-9	1.8283	0.1951
NiO wt%	1	3.28062e-8	18.5329	0.0005
SiO2 wt%	1	9.683e-10	0.5470	0.4703
TiO2 wt%	1	3.22085e-9	1.8195	0.1962
ZnO wt%	1	2.608e-10	0.1473	0.7061
ZrO2 wt%	1	3.75805e-9	2.1230	0.1644

Residual by Predicted Plot

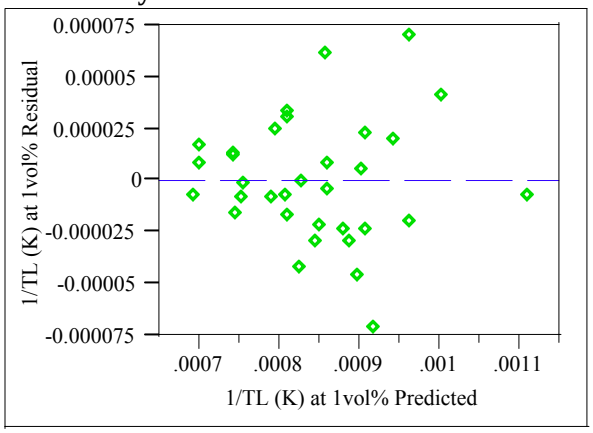

Press
4.8785924e-7

SL SPL
Leverage Plot

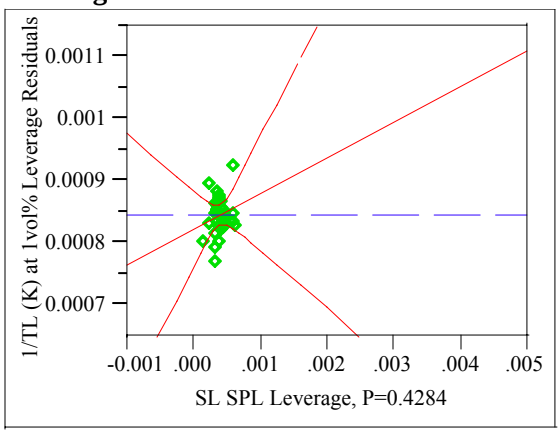

Al2O3 wt%
Leverage Plot

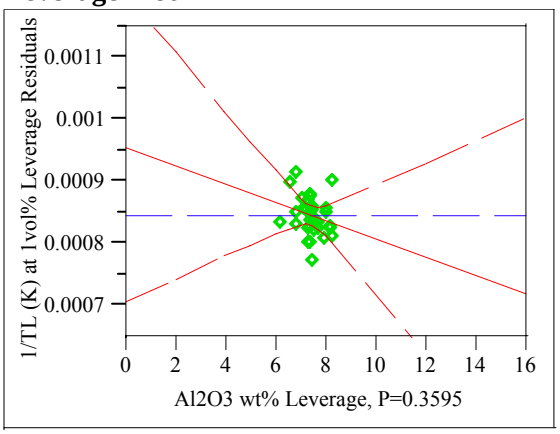

B2O3 wt%
Leverage Plot

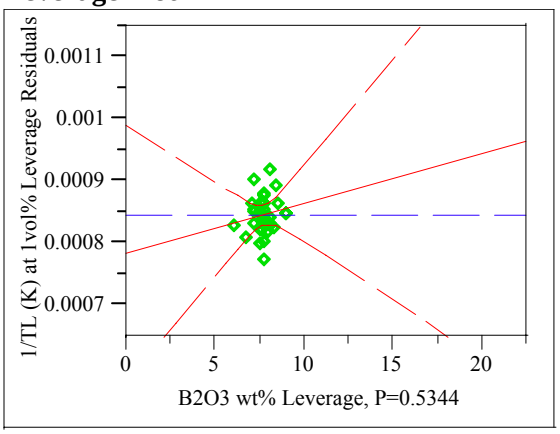

CaO wt%
Leverage Plot

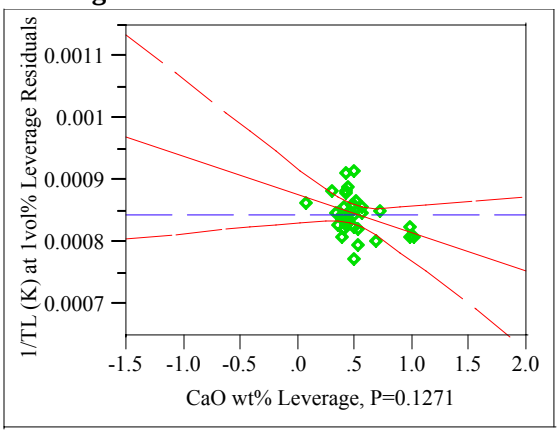

Appendix D. Model Fitting Results for T0.01 Data

Exhibit D.5: Statistical Results from the Fitting of the SLM to Each Data Grouping

Cr2O3 wt%
Leverage Plot

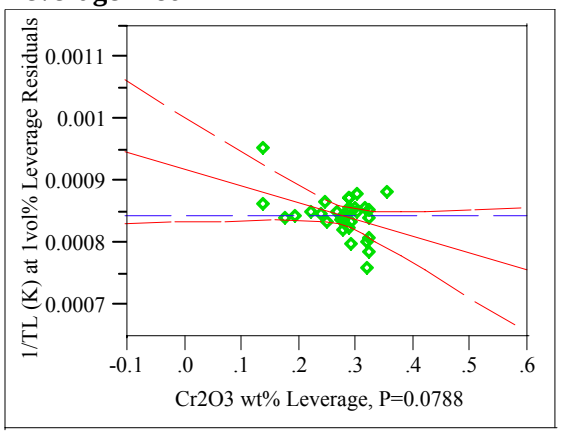

Li2O wt%
Leverage Plot

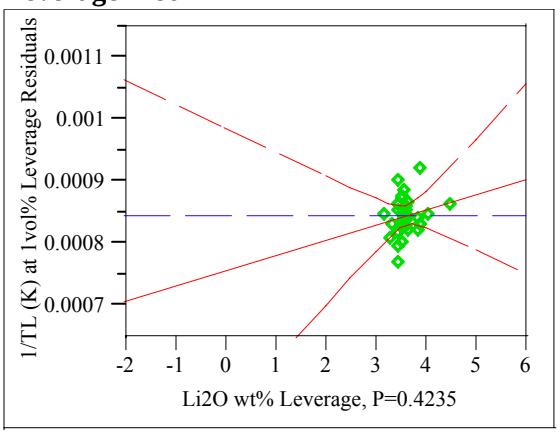

Fe2O3 wt%
Leverage Plot

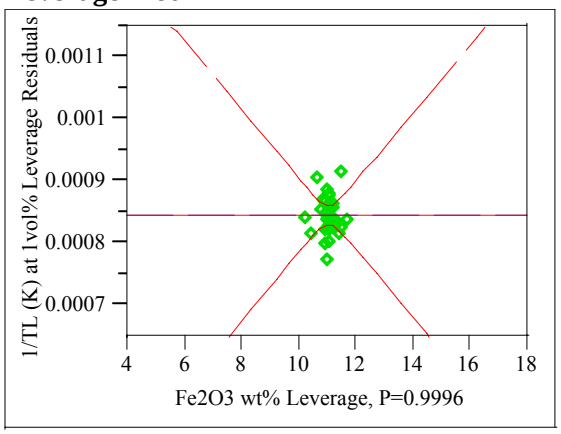

MgO wt%
Leverage Plot

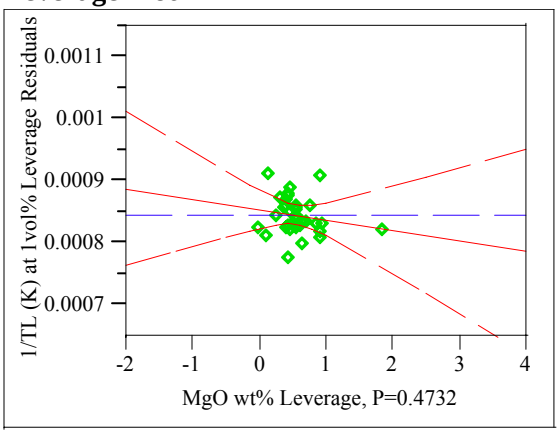

K2O wt%
Leverage Plot

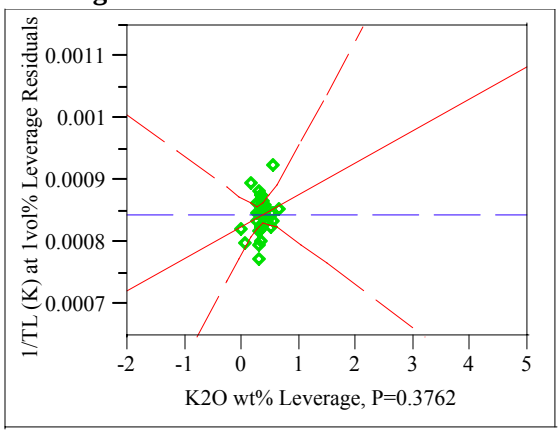

MnO2 wt%
Leverage Plot

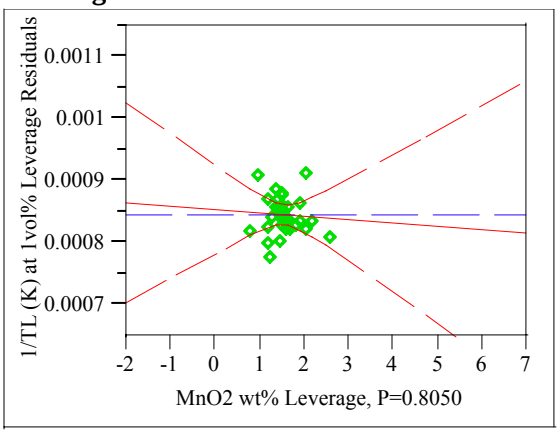

Appendix D. Model Fitting Results for T0.01 Data

Exhibit D.5: Statistical Results from the Fitting of the SLM to Each Data Grouping

Na2O wt%
Leverage Plot

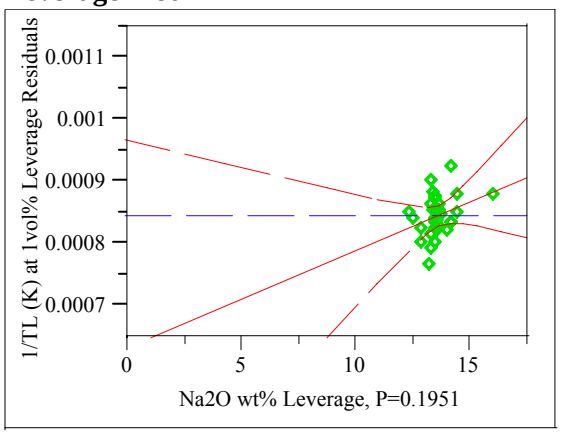

TiO2 wt%
Leverage Plot

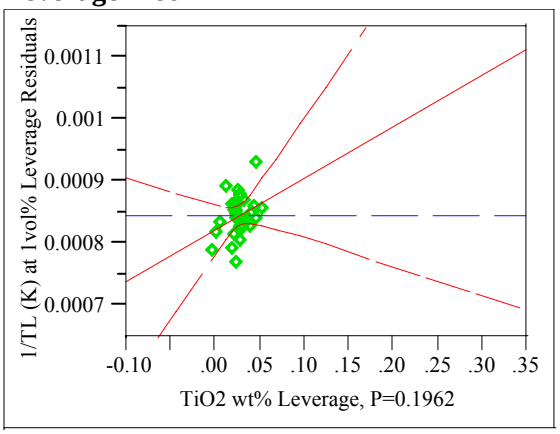

NiO wt%
Leverage Plot

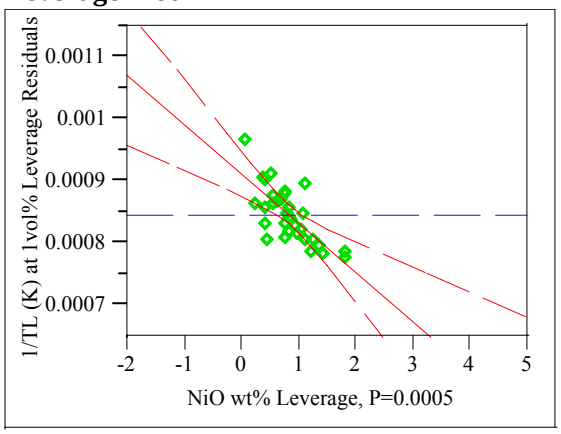

ZnO wt%
Leverage Plot

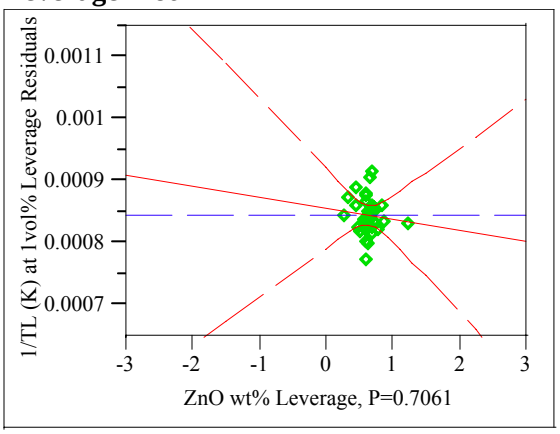

SiO2 wt%
Leverage Plot

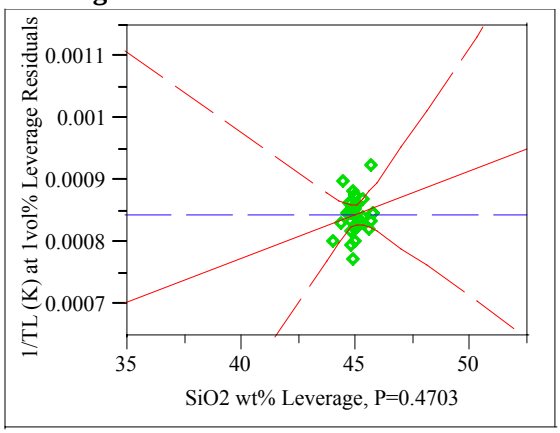

ZrO2 wt%
Leverage Plot

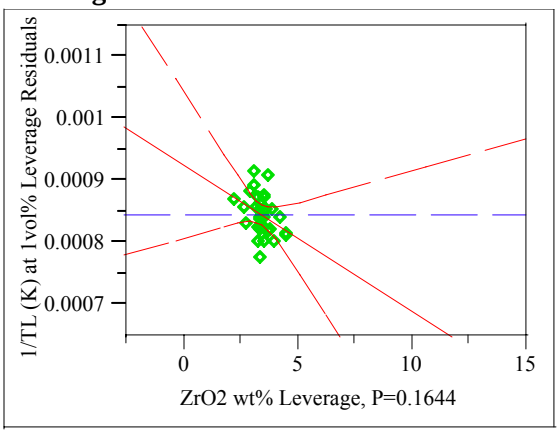

Appendix D. Model Fitting Results for T0.01 Data

Exhibit D.5: Statistical Results from the Fitting of the SLM to Each Data Grouping

Groupings=4
Response 1/T0.01 (K)
Whole Model
Actual by Predicted Plot

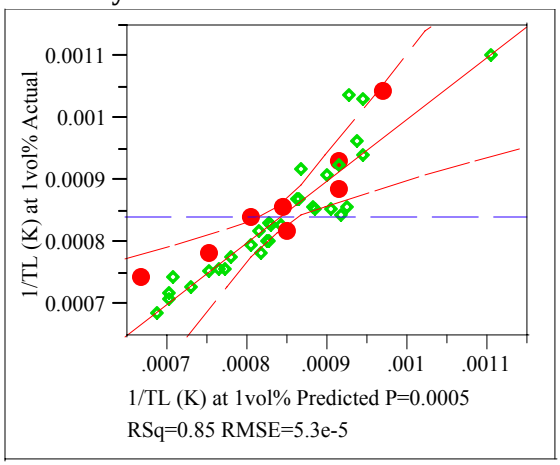

Summary of Fit

RSquare	0.85384
RSquare Adj	0.70768
Root Mean Square Error	0.000053
Mean of Response	0.000843
Observations (or Sum Wgts)	33

Analysis of Variance

Source	DF	Sum of Squares	Mean Square	F Ratio
Model	16	2.5871e-7	1.6169e-8	5.8418
Error	16	4.42858e-8	2.7679e-9	Prob > F
C. Total	32	3.02996e-7		0.0005

Lack Of Fit

Source	DF	Sum of Squares	Mean Square	F Ratio
Lack Of Fit	13	3.88941e-8	2.9919e-9	1.6647
Pure Error	3	5.39179e-9	1.7973e-9	Prob > F
Total Error	16	4.42858e-8		0.3741
				Max RSq
				0.9822

Parameter Estimates

Term	Estimate	Std Error	t Ratio	Prob>|t|
Intercept	0.0020803	0.000872	2.39	0.0297
SL SPL	-0.054048	0.046017	-1.17	0.2574
Al2O3 wt%	-0.000024	0.000015	-1.65	0.1192
B2O3 wt%	-0.000004	0.000009	-0.38	0.7065
CaO wt%	-0.000027	0.000045	-0.60	0.5554
Cr2O3 wt%	-0.000118	0.000132	-0.89	0.3842
Fe2O3 wt%	-0.000038	0.000015	-2.60	0.0194
K2O wt%	-0.000025	0.000032	-0.78	0.4486
Li2O wt%	0.0000028	0.000018	0.15	0.8814
MgO wt%	-0.000034	0.000023	-1.49	0.1551
MnO2 wt%	-0.000028	0.000015	-1.86	0.0808
Na2O wt%	0.0000128	0.000007	1.71	0.1062
NiO wt%	-0.000094	0.000018	-5.18	<.0001
SiO2 wt%	-0.00001	0.000011	-0.90	0.3828
TiO2 wt%	-0.000214	0.000481	-0.45	0.6619
ZnO wt%	0.000004	0.000024	0.17	0.8698
ZrO2 wt%	-0.000031	0.000011	-2.72	0.0153

Appendix D. Model Fitting Results for T0.01 Data

Exhibit D.5: Statistical Results from the Fitting of the SLM to Each Data Grouping

Effect Tests

Source	DF	Sum of Squares	F Ratio	Prob > F
SL SPL	1	3.81832e-9	1.3795	0.2574
Al2O3 wt%	1	7.50256e-9	2.7106	0.1192
B2O3 wt%	1	4.0692e-10	0.1470	0.7065
CaO wt%	1	1.00408e-9	0.3628	0.5554
Cr2O3 wt%	1	2.21597e-9	0.8006	0.3842
Fe2O3 wt%	1	1.8696e-8	6.7547	0.0194
K2O wt%	1	1.66988e-9	0.6033	0.4486
Li2O wt%	1	6.361e-11	0.0230	0.8814
MgO wt%	1	6.16301e-9	2.2266	0.1551
MnO2 wt%	1	9.61738e-9	3.4747	0.0808
Na2O wt%	1	8.11372e-9	2.9314	0.1062
NiO wt%	1	7.42024e-8	26.8085	<.0001
SiO2 wt%	1	2.22885e-9	0.8053	0.3828
TiO2 wt%	1	5.494e-10	0.1985	0.6619
ZnO wt%	1	7.6827e-11	0.0278	0.8698
ZrO2 wt%	1	2.04041e-8	7.3718	0.0153

Residual by Predicted Plot

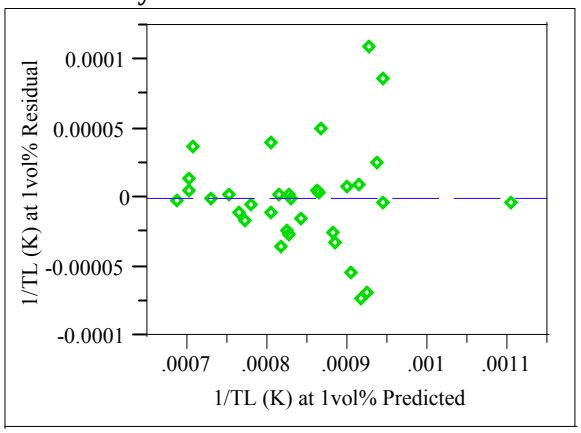

Press
0.0000010169

SL SPL
Leverage Plot

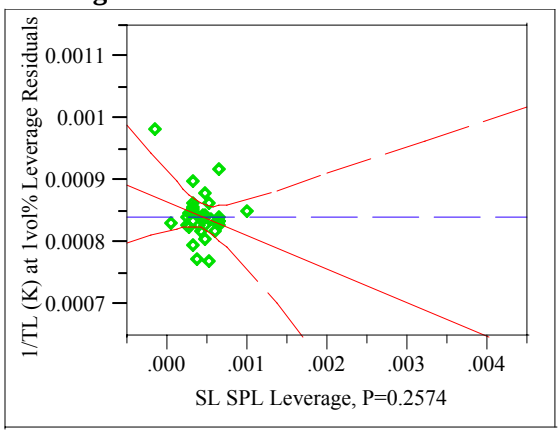

Al2O3 wt%
Leverage Plot

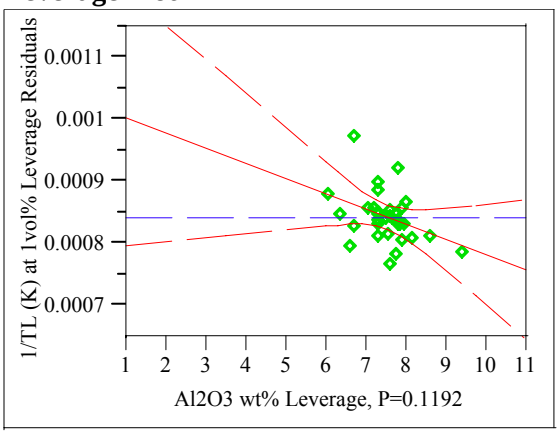

B2O3 wt%
Leverage Plot

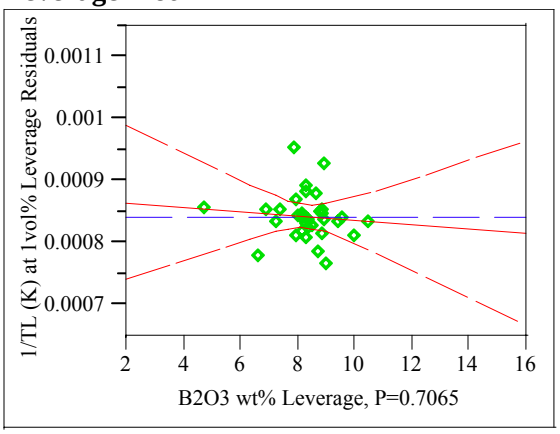

CaO wt%
Leverage Plot

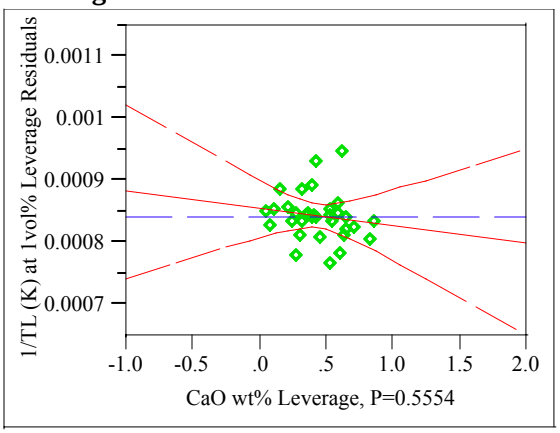

Appendix D. Model Fitting Results for T0.01 Data

Exhibit D.5: Statistical Results from the Fitting of the SLM to Each Data Grouping

Cr2O3 wt%
Leverage Plot

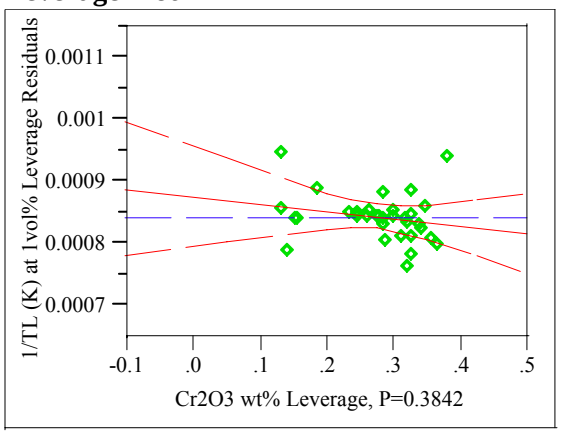

Li2O wt%
Leverage Plot

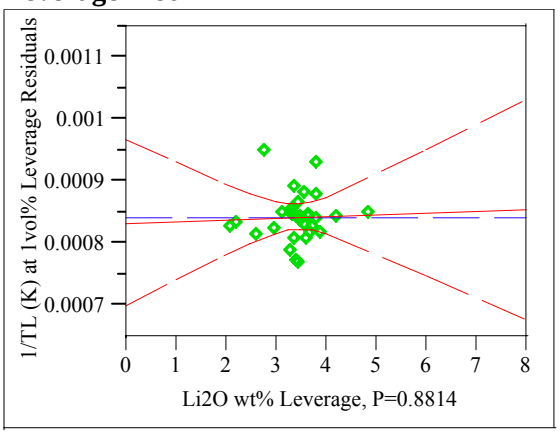

Fe2O3 wt%
Leverage Plot

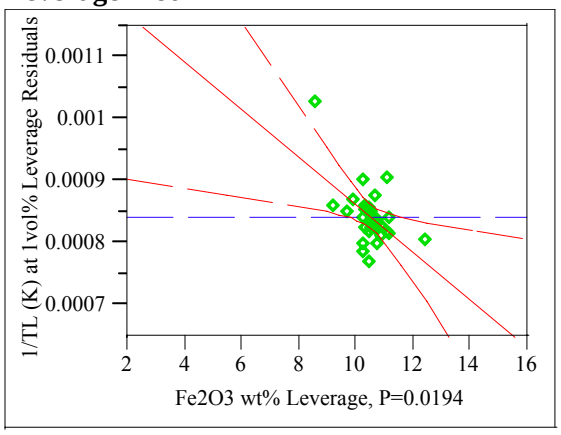

MgO wt%
Leverage Plot

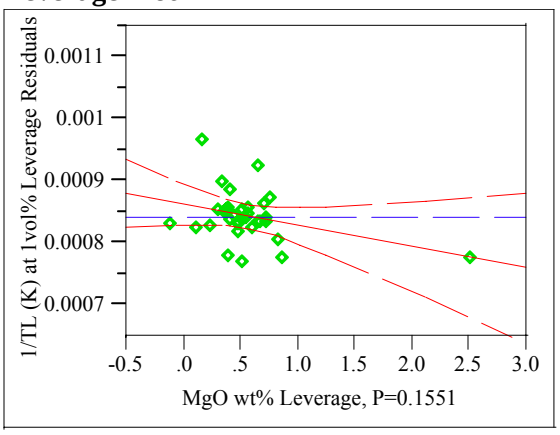

K2O wt%
Leverage Plot

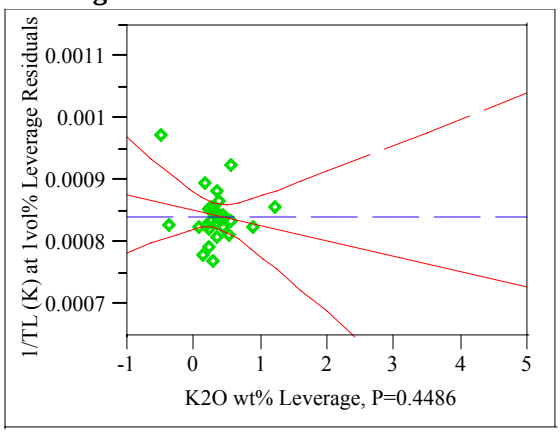

MnO2 wt%
Leverage Plot

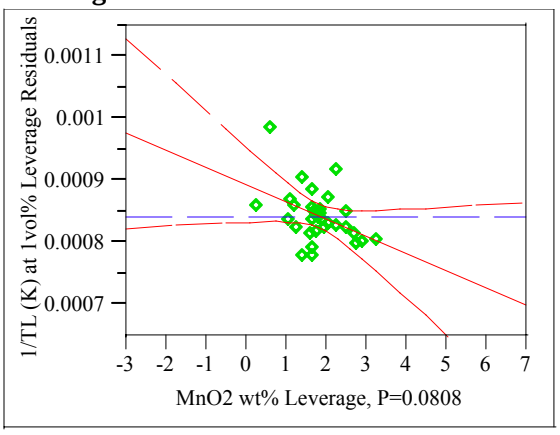

Appendix D. Model Fitting Results for T0.01 Data

Exhibit D.5: Statistical Results from the Fitting of the SLM to Each Data Grouping

Na2O wt%
Leverage Plot

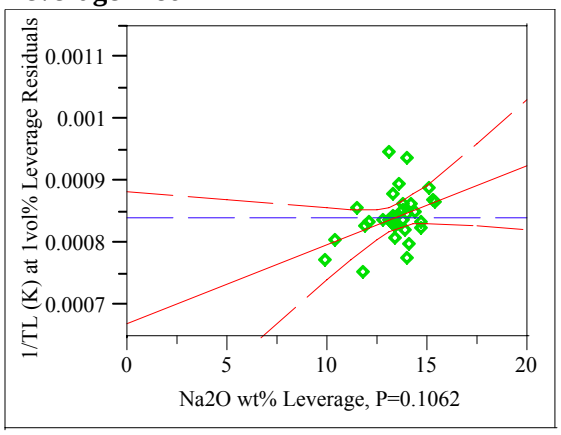

TiO2 wt%
Leverage Plot

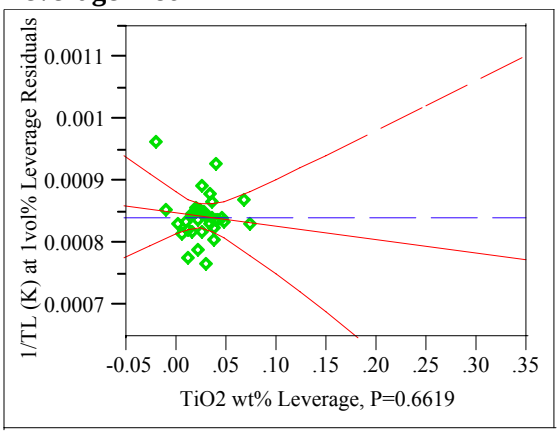

NiO wt%
Leverage Plot

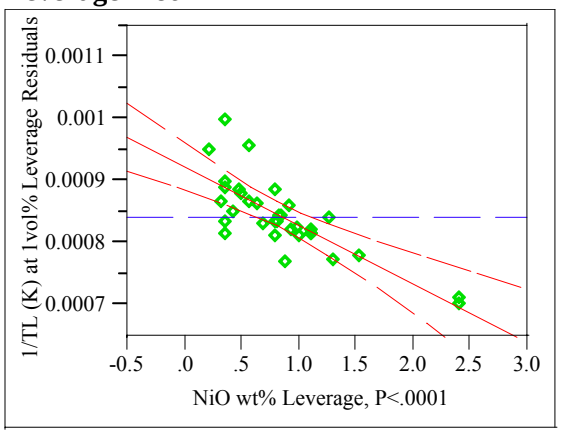

ZnO wt%
Leverage Plot

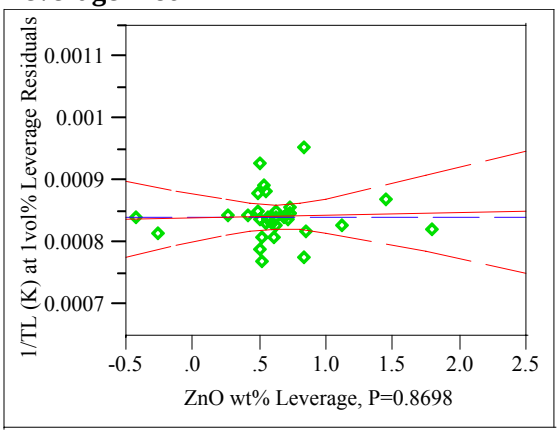

SiO2 wt%
Leverage Plot

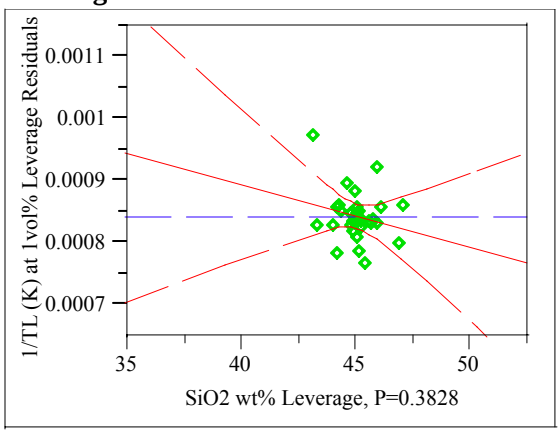

ZrO2 wt%
Leverage Plot

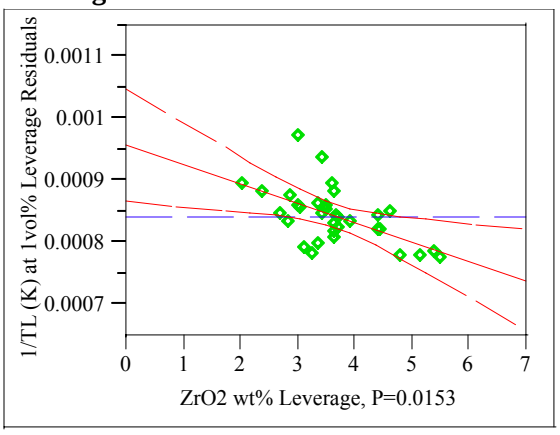

Appendix D. Model Fitting Results for T0.01 Data

Exhibit D.5: Statistical Results from the Fitting of the SLM to Each Data Grouping

Groupings=5
Response 1/T0.01 (K)
Whole Model
Actual by Predicted Plot

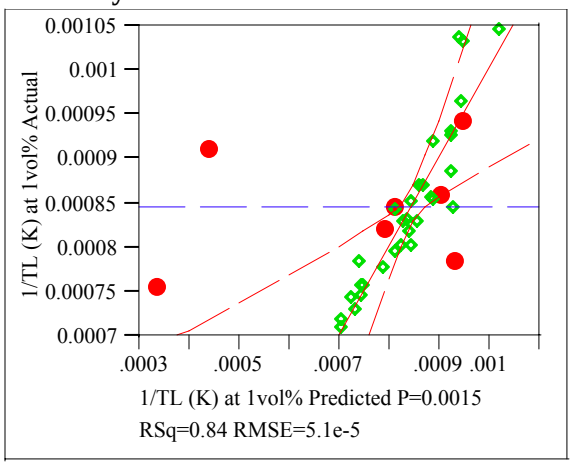

Summary of Fit

RSquare	0.843348
RSquare Adj	0.676253
Root Mean Square Error	0.000051
Mean of Response	0.000845
Observations (or Sum Wgts)	32

Analysis of Variance

Source	DF	Sum of Squares	Mean Square	F Ratio
Model	16	2.10185e-7	1.3137e-8	5.0471
Error	15	3.90418e-8	2.6028e-9	Prob > F
C. Total	31	2.49226e-7		0.0015

Lack Of Fit

Source	DF	Sum of Squares	Mean Square	F Ratio
Lack Of Fit	13	3.89833e-8	2.9987e-9	102.4512
Pure Error	2	5.8539e-11	2.927e-11	Prob > F
Total Error	15	3.90418e-8		0.0097
				Max RSq
				0.9998

Parameter Estimates

Term	Estimate	Std Error	t Ratio	Prob>|t|
Intercept	0.001388	0.001164	1.19	0.2514
SL SPL	-0.119793	0.079465	-1.51	0.1525
Al2O3 wt%	-0.000027	0.000012	-2.25	0.0398
B2O3 wt%	-0.000004	0.000014	-0.26	0.7983
CaO wt%	0.0001219	0.000158	0.77	0.4536
Cr2O3 wt%	-0.000041	0.000166	-0.25	0.8065
Fe2O3 wt%	-0.000042	0.000021	-2.03	0.0604
K2O wt%	-0.000076	0.000075	-1.01	0.3273
Li2O wt%	0.0000104	0.000023	0.44	0.6656
MgO wt%	-0.000204	0.000134	-1.52	0.1502
MnO2 wt%	-0.000026	0.000016	-1.59	0.1323
Na2O wt%	0.0000182	0.000008	2.14	0.0488
NiO wt%	-0.000087	0.000021	-4.20	0.0008
SiO2 wt%	0.0000021	0.000016	0.13	0.8953
TiO2 wt%	-0.000414	0.000908	-0.46	0.6549
ZnO wt%	0.0000048	0.000036	0.13	0.8958
ZrO2 wt%	1.0948e-7	0.000033	0.00	0.9974

Appendix D. Model Fitting Results for T0.01 Data

Exhibit D.5: Statistical Results from the Fitting of the SLM to Each Data Grouping

Effect Tests

Source	DF	Sum of Squares	F Ratio	Prob > F
SL SPL	1	5.91497e-9	2.2726	0.1525
Al2O3 wt%	1	1.31859e-8	5.0661	0.0398
B2O3 wt%	1	1.7619e-10	0.0677	0.7983
CaO wt%	1	1.54082e-9	0.5920	0.4536
Cr2O3 wt%	1	1.6173e-10	0.0621	0.8065
Fe2O3 wt%	1	1.07297e-8	4.1224	0.0604
K2O wt%	1	2.66909e-9	1.0255	0.3273
Li2O wt%	1	5.0595e-10	0.1944	0.6656
MgO wt%	1	5.98444e-9	2.2992	0.1502
MnO2 wt%	1	6.59313e-9	2.5331	0.1323
Na2O wt%	1	1.19643e-8	4.5967	0.0488
NiO wt%	1	4.58296e-8	17.6079	0.0008
SiO2 wt%	1	4.6594e-11	0.0179	0.8953
TiO2 wt%	1	5.4126e-10	0.2080	0.6549
ZnO wt%	1	4.6216e-11	0.0178	0.8958
ZrO2 wt%	1	2.8309e-14	0.0000	0.9974

Residual by Predicted Plot

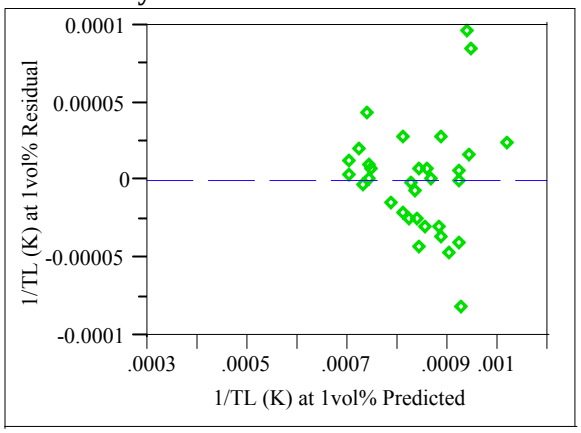

Press
0.0002020524

SL SPL
Leverage Plot

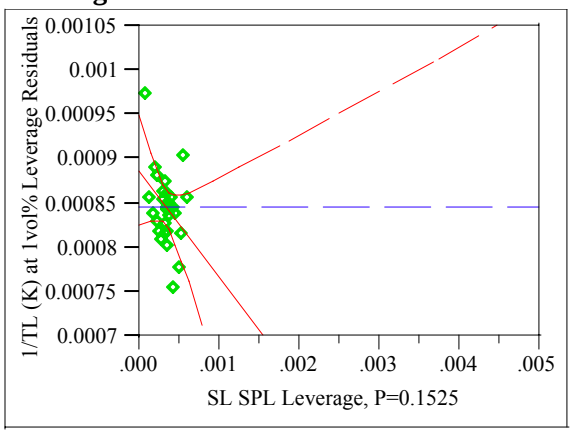

Al2O3 wt%
Leverage Plot

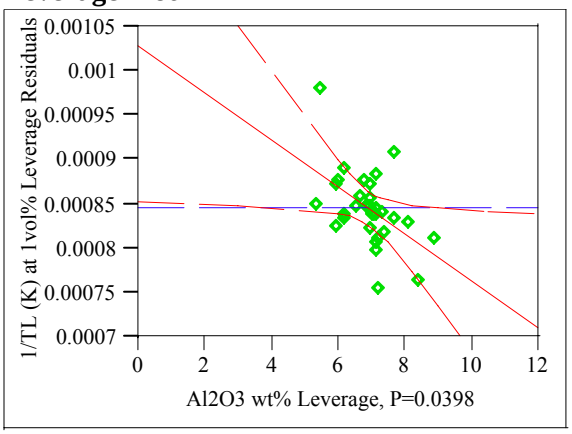

B2O3 wt%
Leverage Plot

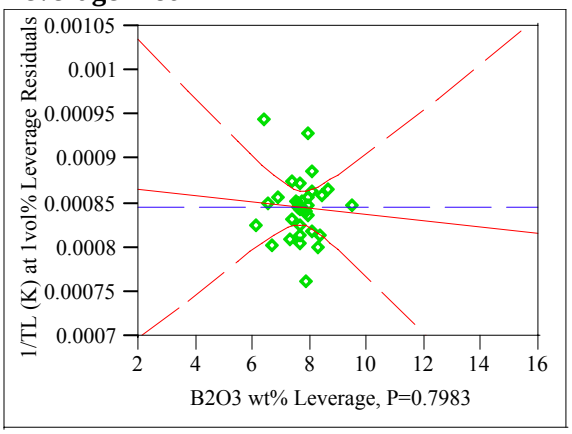

CaO wt%
Leverage Plot

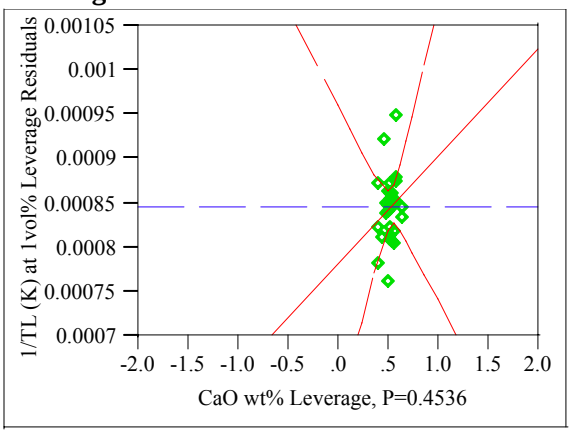

Appendix D. Model Fitting Results for T0.01 Data

Exhibit D.5: Statistical Results from the Fitting of the SLM to Each Data Grouping

Cr2O3 wt%
Leverage Plot

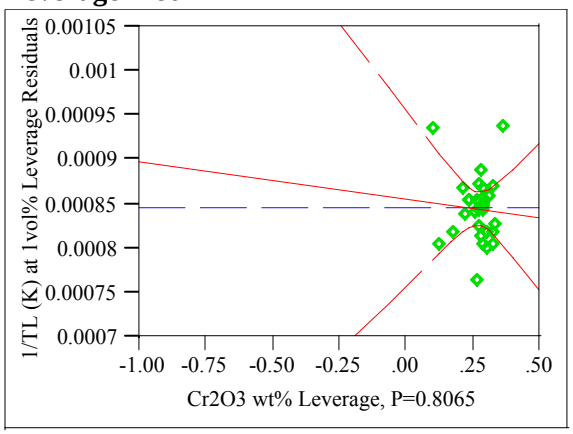

Li2O wt%
Leverage Plot

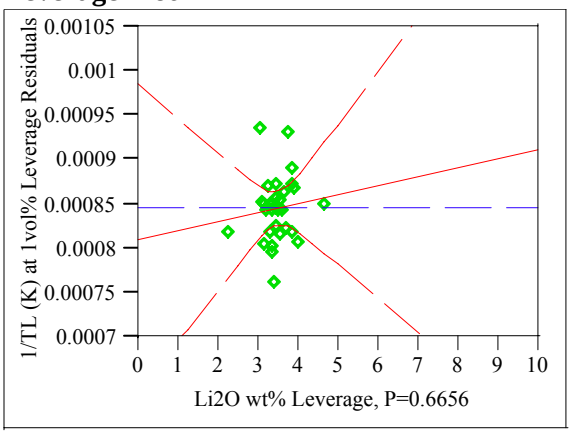

Fe2O3 wt%
Leverage Plot

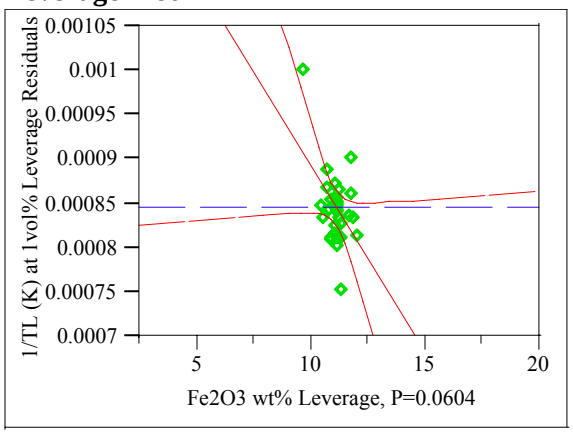

MgO wt%
Leverage Plot

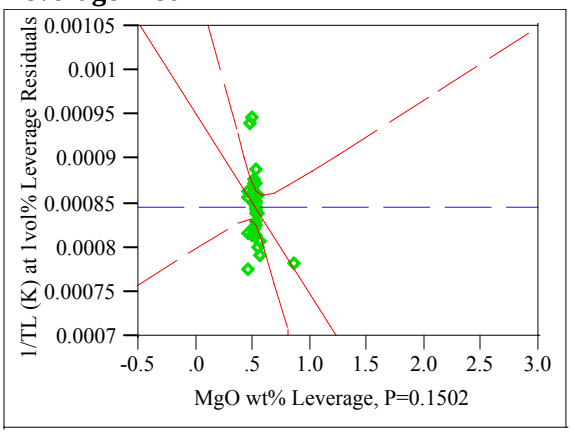

K2O wt%
Leverage Plot

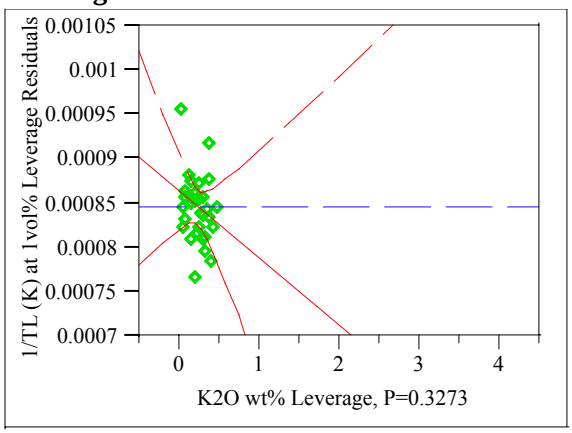

MnO2 wt%
Leverage Plot

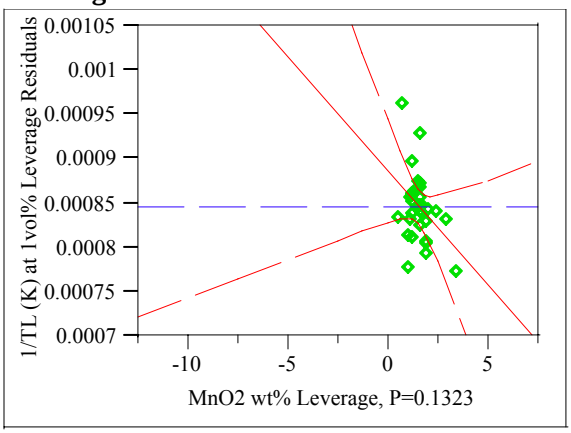

Appendix D. Model Fitting Results for T0.01 Data

Exhibit D.5: Statistical Results from the Fitting of the SLM to Each Data Grouping

Na2O wt%
Leverage Plot

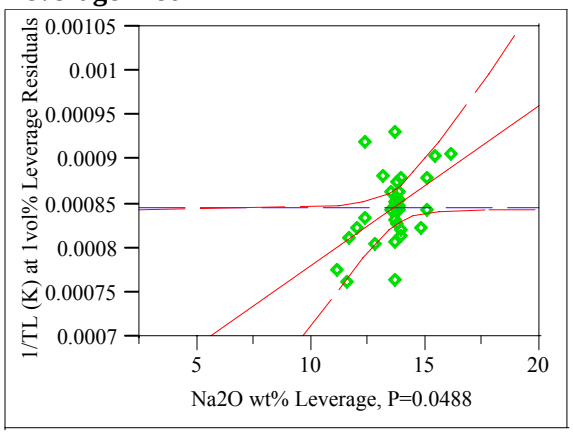

TiO2 wt%
Leverage Plot

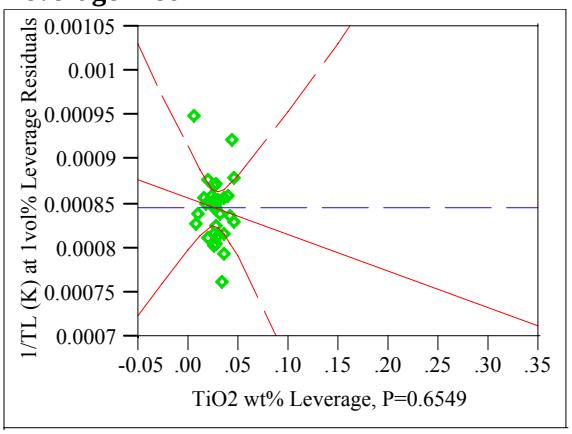

NiO wt%
Leverage Plot

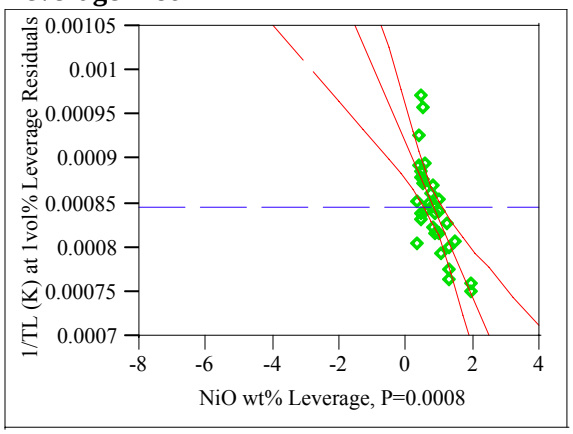

ZnO wt%
Leverage Plot

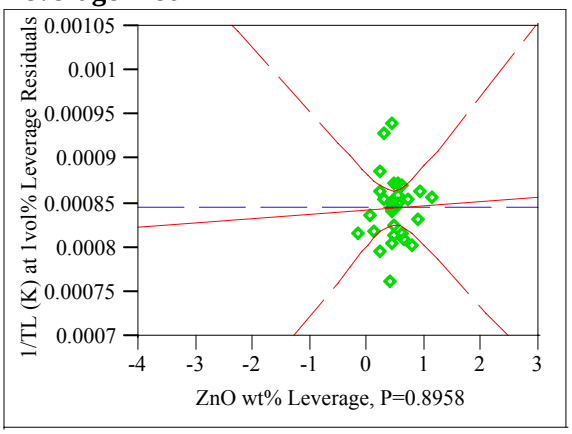

SiO2 wt%
Leverage Plot

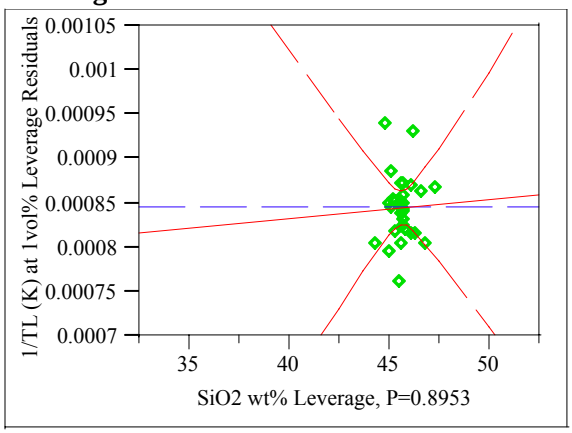

ZrO2 wt%
Leverage Plot

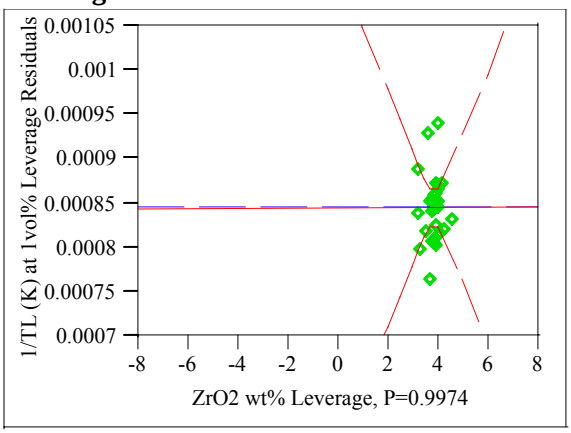

Appendix D. Model Fitting Results for T0.01 Data

Exhibit D.6: Statistical Results from the Fitting of the LMM to Each Data Grouping

Groupings=1
Response T0.01 (°C)
Singularity Details
Intercept = 0
Whole Model
Actual by Predicted Plot

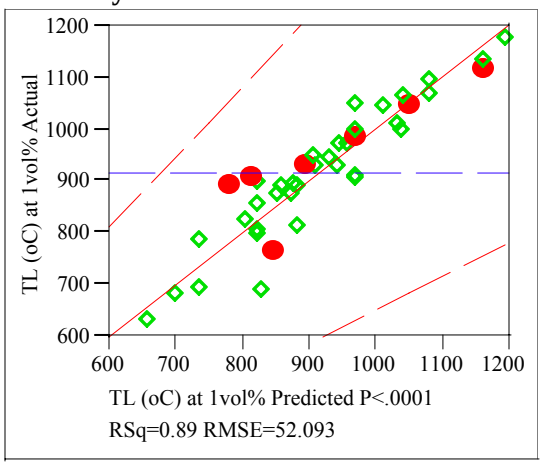

Summary of Fit

RSquare	0.890357
RSquare Adj	0.842686
Root Mean Square Error	52.09255
Mean of Response	915.0585
Observations (or Sum Wgts)	34

Analysis of Variance

Source	DF	Sum of Squares	Mean Square	F Ratio
Model	10	506829.28	50682.9	18.6771
Error	23	62413.57	2713.6	Prob > F
C. Total	33	569242.84		<.0001

Tested against reduced model: Y=mean

Lack Of Fit

Source	DF	Sum of Squares	Mean Square	F Ratio
Lack Of Fit	21	58109.580	2767.12	1.2858
Pure Error	2	4303.986	2151.99	Prob > F
Total Error	23	62413.566		0.5278
				Max RSq
				0.9924

Parameter Estimates

Term		Estimate	Std Error	t Ratio	Prob>|t|
Intercept	Zeroed	0	0	.	.
Al2O3 n		3482.4764	600.4207	5.80	<.0001
B2O3 n		177.46649	541.6785	0.33	0.7462
Cr2O3 n		37400.516	9429.496	3.97	0.0006
Fe2O3 n		3734.5827	501.4485	7.45	<.0001
Li2O n		-3028.204	1322.422	-2.29	0.0315
MnO n		3016.3954	921.3025	3.27	0.0033
Na2O n		-1902.764	388.6419	-4.90	<.0001
NiO n		13835.503	1903.177	7.27	<.0001
SiO2 n		385.03352	184.5586	2.09	0.0482
SrO n		-850.9212	510.7436	-1.67	0.1093
ZrO2 n		3969.5109	670.1202	5.92	<.0001

Appendix D. Model Fitting Results for T0.01 Data

Exhibit D.6: Statistical Results from the Fitting of the LMM to Each Data Grouping

Residual by Predicted Plot

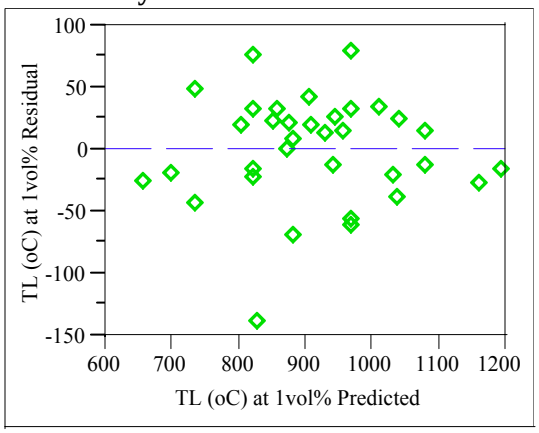

Press
165014.47067

Cr2O3 n
Leverage Plot

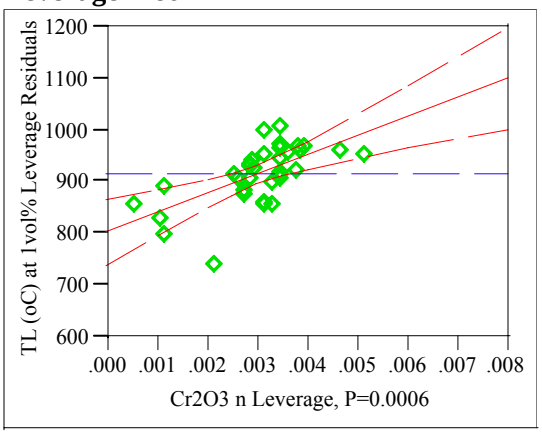

Al2O3 n
Leverage Plot

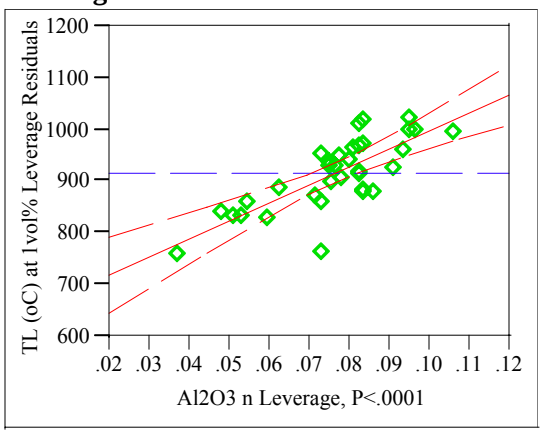

Fe2O3 n
Leverage Plot

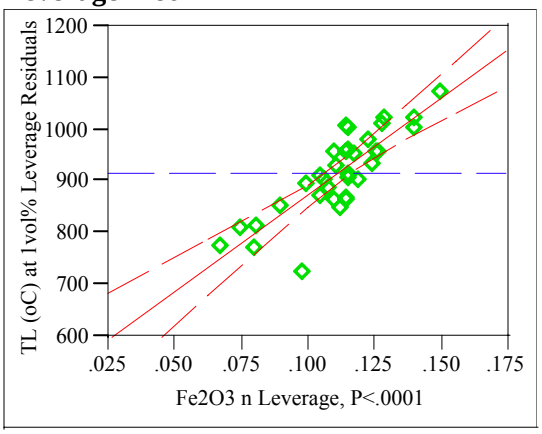

B2O3 n
Leverage Plot

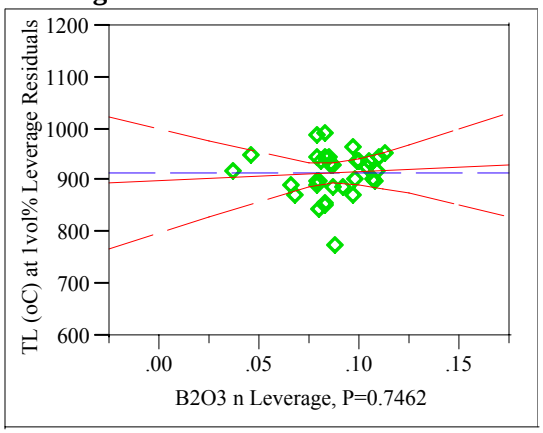

Li2O n
Leverage Plot

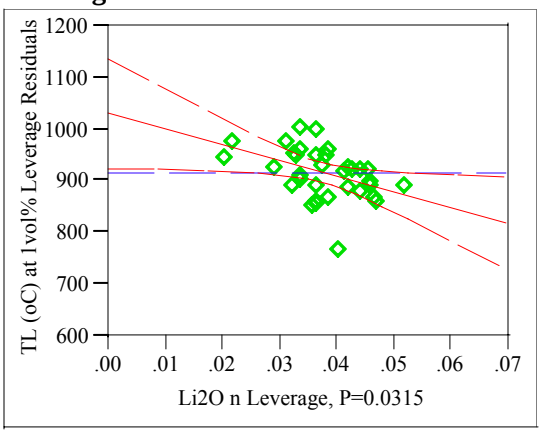

Appendix D. Model Fitting Results for T0.01 Data

Exhibit D.6: Statistical Results from the Fitting of the LMM to Each Data Grouping

MnO n
Leverage Plot

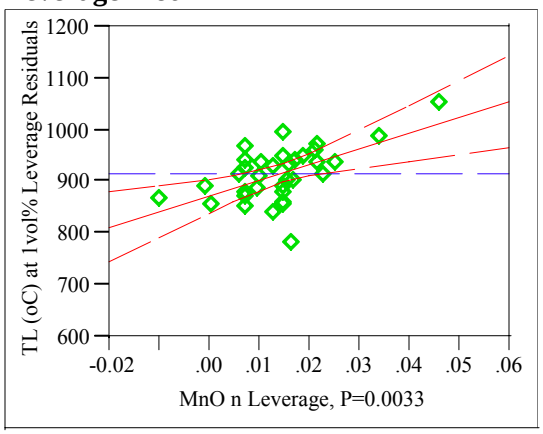

SiO2 n
Leverage Plot

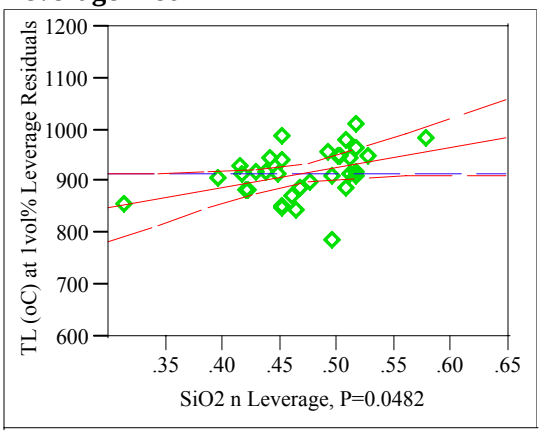

Na2O n
Leverage Plot

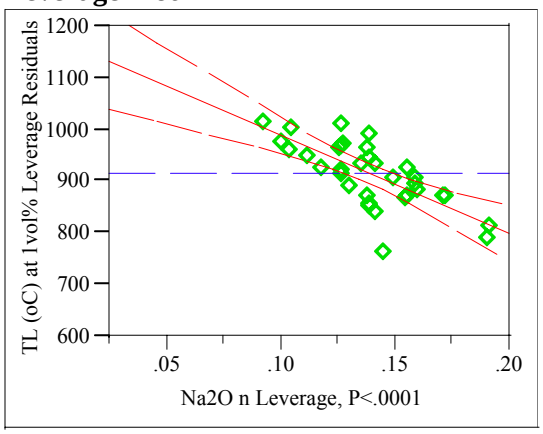

SrO n
Leverage Plot

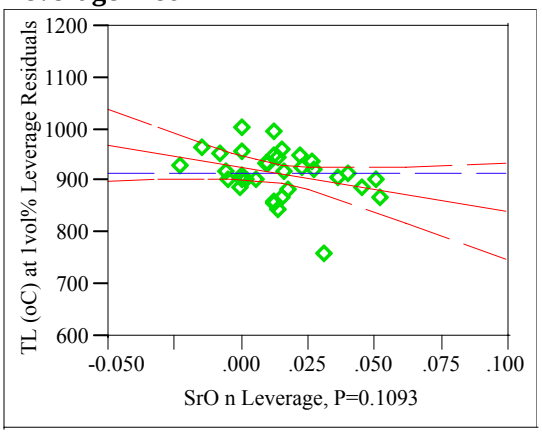

NiO n
Leverage Plot

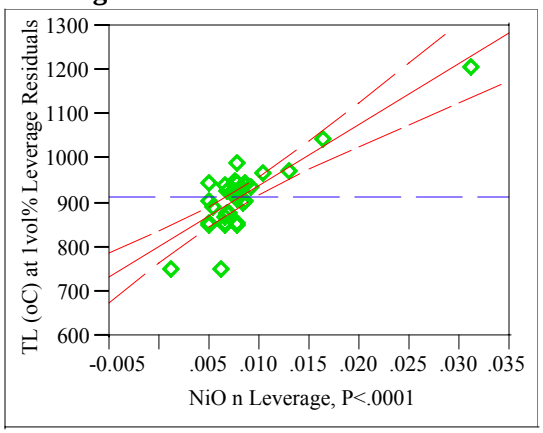

ZrO2 n
Leverage Plot

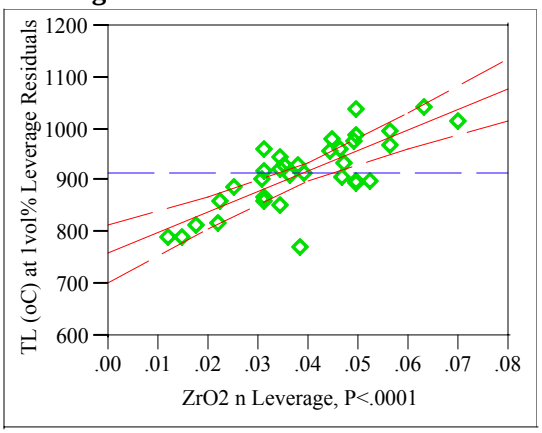

Appendix D. Model Fitting Results for T0.01 Data

Exhibit D.6: Statistical Results from the Fitting of the LMM to Each Data Grouping

Groupings=2
Response T0.01 (°C)
Singularity Details
Intercept = 0
Whole Model
Actual by Predicted Plot

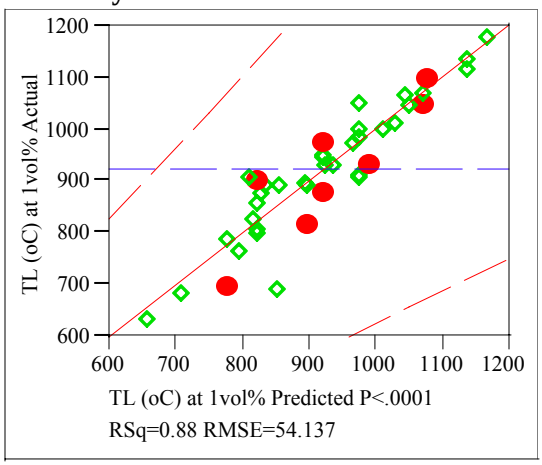

Summary of Fit

RSquare	0.880718
RSquare Adj	0.826499
Root Mean Square Error	54.13677
Mean of Response	921.9422
Observations (or Sum Wgts)	33

Analysis of Variance

Source	DF	Sum of Squares	Mean Square	F Ratio
Model	10	476067.74	47606.8	16.2437
Error	22	64477.39	2930.8	Prob > F
C. Total	32	540545.12		<.0001

Tested against reduced model: Y=mean

Lack Of Fit

Source	DF	Sum of Squares	Mean Square	F Ratio
Lack Of Fit	19	61459.674	3234.72	3.2157
Pure Error	3	3017.714	1005.90	Prob > F
Total Error	22	64477.387		0.1828
				Max RSq
				0.9944

Parameter Estimates

Term		Estimate	Std Error	t Ratio	Prob>|t|
Intercept	Zeroed	0	0	.	.
Al2O3 n		3296.4867	610.578	5.40	<.0001
B2O3 n		546.12152	484.1596	1.13	0.2715
Cr2O3 n		19937.945	9517.171	2.09	0.0479
Fe2O3 n		3975.0174	683.508	5.82	<.0001
Li2O n		-2458.438	1257.667	-1.95	0.0634
MnO n		3447.7199	1051.881	3.28	0.0034
Na2O n		-1519.361	519.2943	-2.93	0.0078
NiO n		12877.706	1626.482	7.92	<.0001
SiO2 n		200.03011	319.3821	0.63	0.5376
SrO n		-9.824355	639.3329	-0.02	0.9879
ZrO2 n		4419.7094	725.4733	6.09	<.0001

Appendix D. Model Fitting Results for T0.01 Data

Exhibit D.6: Statistical Results from the Fitting of the LMM to Each Data Grouping

Residual by Predicted Plot

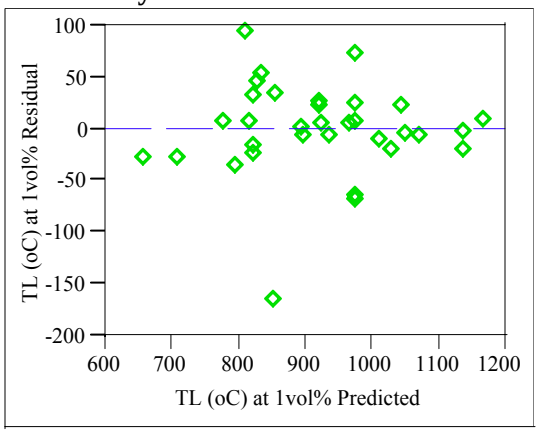

Press
186047.21088

Cr2O3 n
Leverage Plot

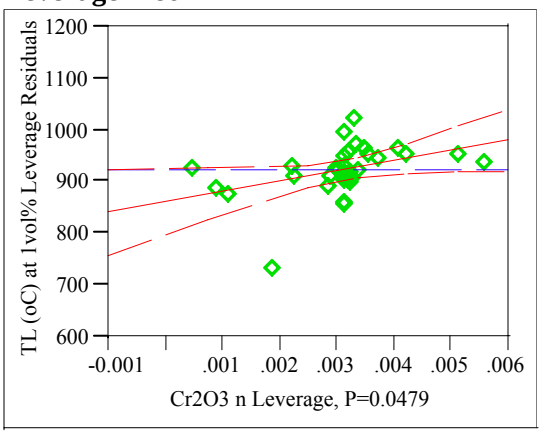

Al2O3 n
Leverage Plot

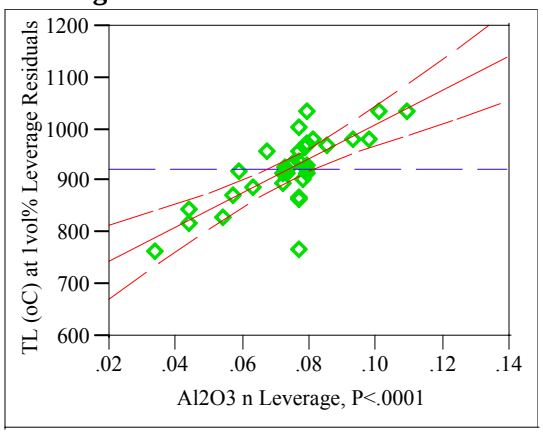

Fe2O3 n
Leverage Plot

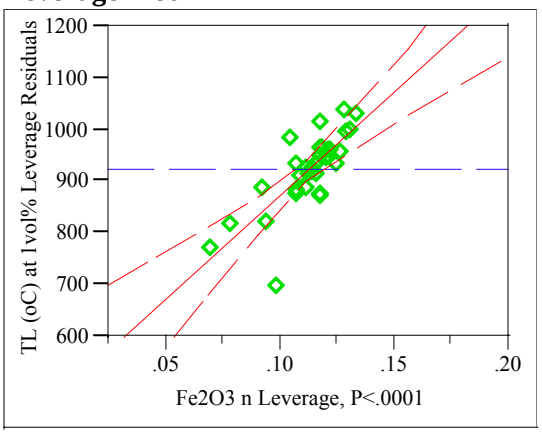

B2O3 n
Leverage Plot

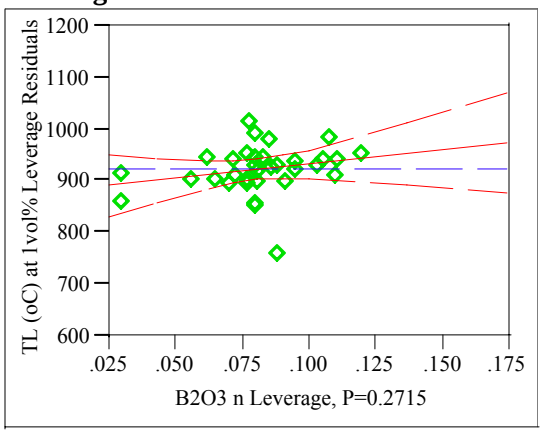

Li2O n
Leverage Plot

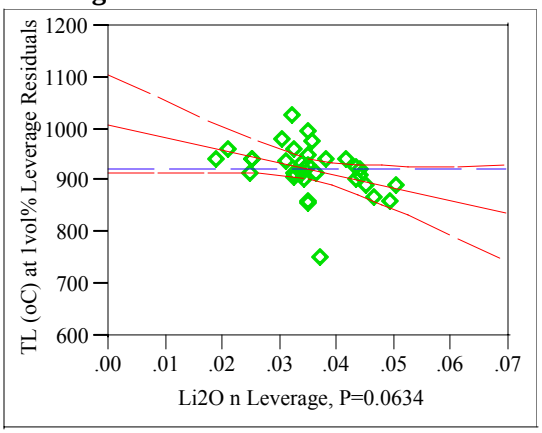

Appendix D. Model Fitting Results for T0.01 Data

Exhibit D.6: Statistical Results from the Fitting of the LMM to Each Data Grouping

MnO n
Leverage Plot

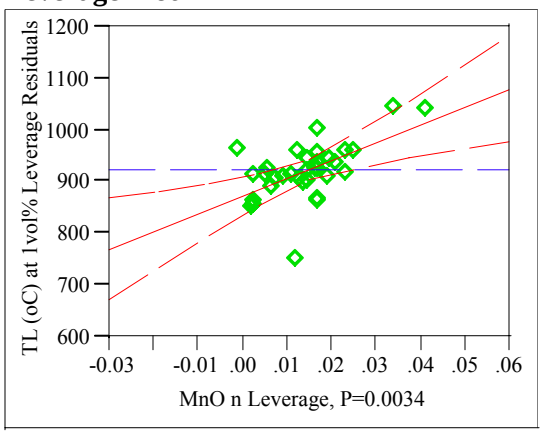

SiO2 n
Leverage Plot

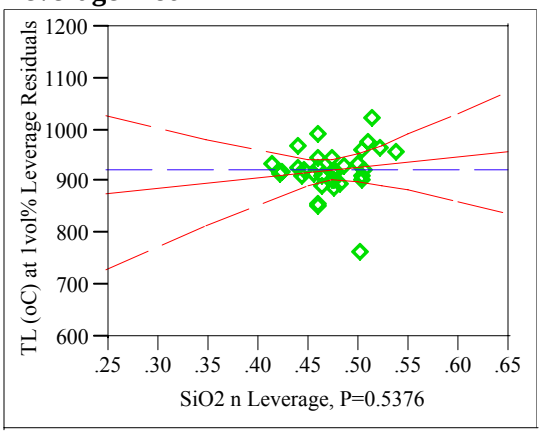

Na2O n
Leverage Plot

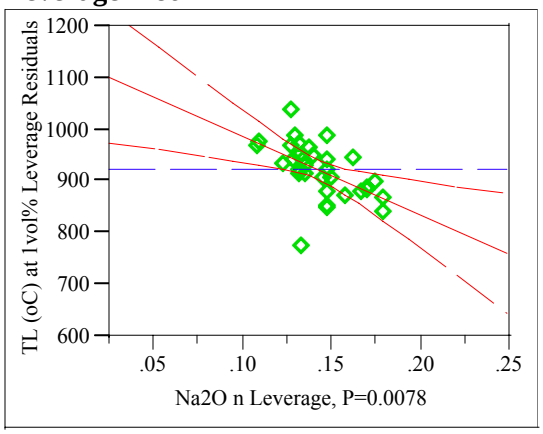

SrO n
Leverage Plot

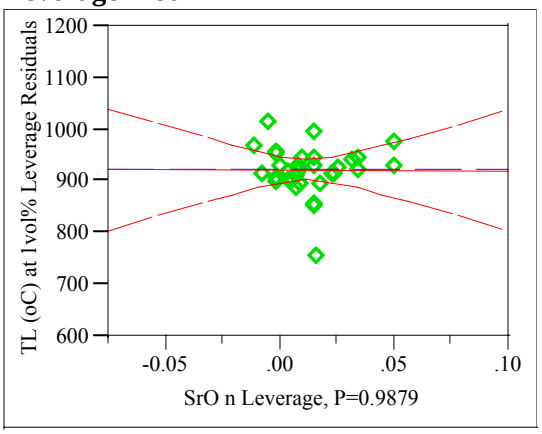

NiO n
Leverage Plot

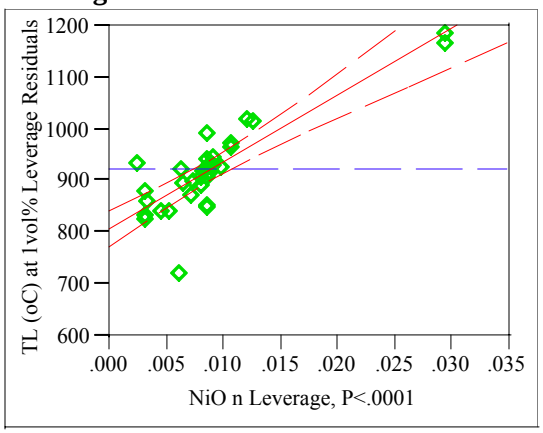

ZrO2 n
Leverage Plot

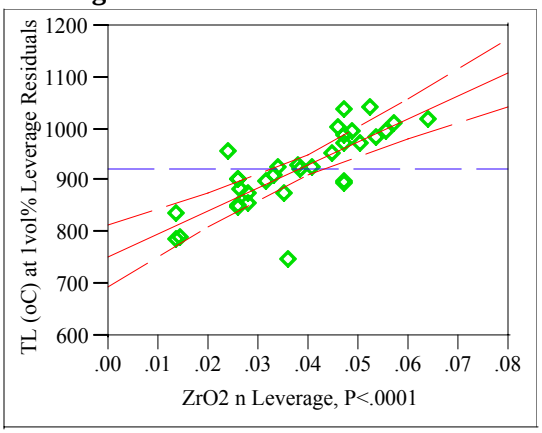

Appendix D. Model Fitting Results for T0.01 Data

Exhibit D.6: Statistical Results from the Fitting of the LMM to Each Data Grouping

Groupings=3
Response T0.01 (°C)
Singularity Details
Intercept = 0
Whole Model
Actual by Predicted Plot

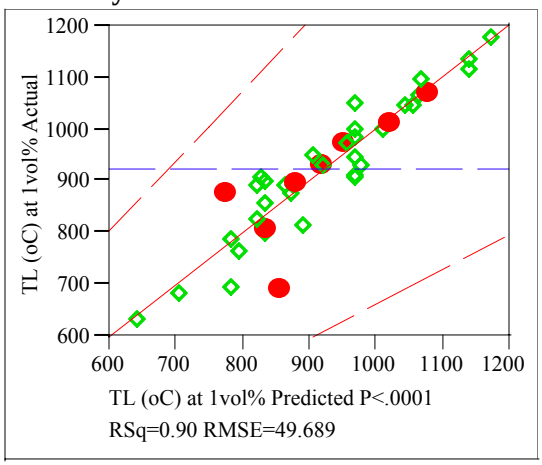

Summary of Fit

RSquare	0.901772
RSquare Adj	0.857123
Root Mean Square Error	49.68872
Mean of Response	924.3378
Observations (or Sum Wgts)	33

Analysis of Variance

Source	DF	Sum of Squares	Mean Square	F Ratio
Model	10	498655.10	49865.5	20.1969
Error	22	54317.32	2469.0	Prob > F
C. Total	32	552972.42		<.0001

Tested against reduced model: Y=mean

Lack Of Fit

Source	DF	Sum of Squares	Mean Square	F Ratio
Lack Of Fit	19	47041.790	2475.88	1.0209
Pure Error	3	7275.528	2425.18	Prob > F
Total Error	22	54317.318		0.5768
				Max RSq
				0.9868

Parameter Estimates

Term		Estimate	Std Error	t Ratio	Prob>|t|
Intercept	Zeroed	0	0	.	.
Al2O3 n		3705.3068	608.76	6.09	<.0001
B2O3 n		134.97355	493.9676	0.27	0.7872
Cr2O3 n		23518.88	7189.13	3.27	0.0035
Fe2O3 n		3573.512	550.6184	6.49	<.0001
Li2O n		-2315.934	1646.681	-1.41	0.1736
MnO n		2679.4956	784.0882	3.42	0.0025
Na2O n		-1821.937	489.5754	-3.72	0.0012
NiO n		12502.123	1415.219	8.83	<.0001
SiO2 n		443.22758	187.2641	2.37	0.0272
SrO n		-164.2151	526.4678	-0.31	0.7580
ZrO2 n		3779.368	798.334	4.73	0.0001

Appendix D. Model Fitting Results for T0.01 Data

Exhibit D.6: Statistical Results from the Fitting of the LMM to Each Data Grouping

Residual by Predicted Plot

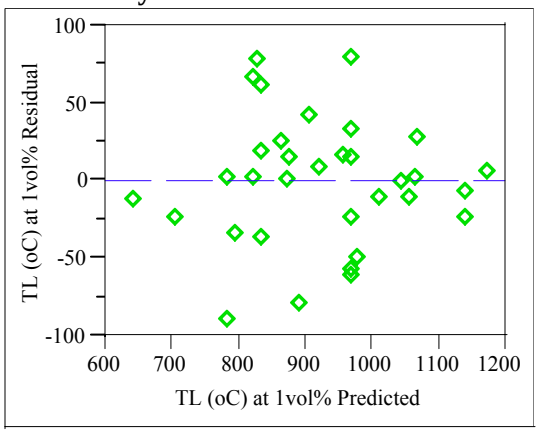

Press
125983.62763

Cr2O3 n
Leverage Plot

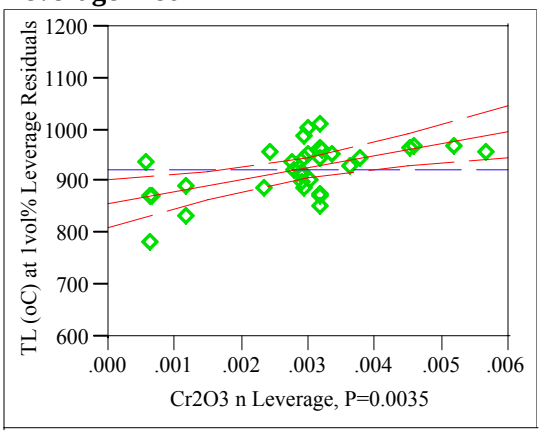

Al2O3 n
Leverage Plot

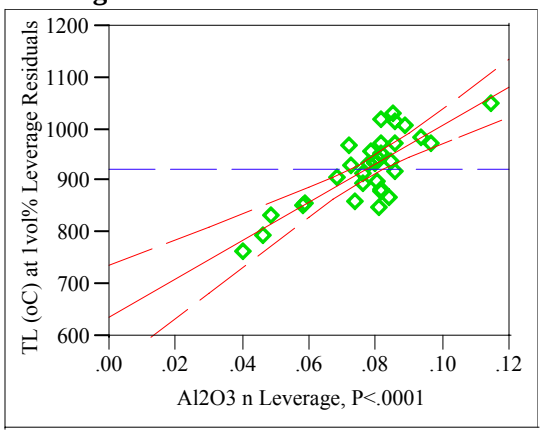

Fe2O3 n
Leverage Plot

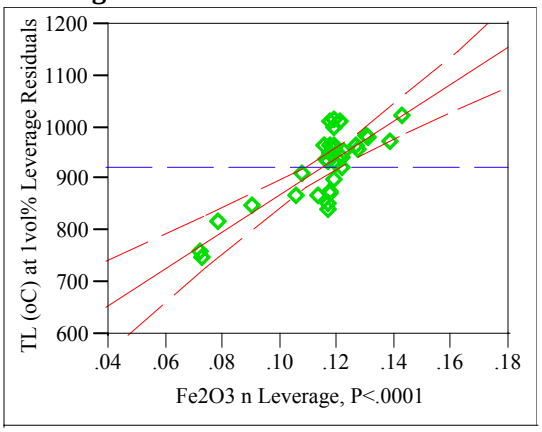

B2O3 n
Leverage Plot

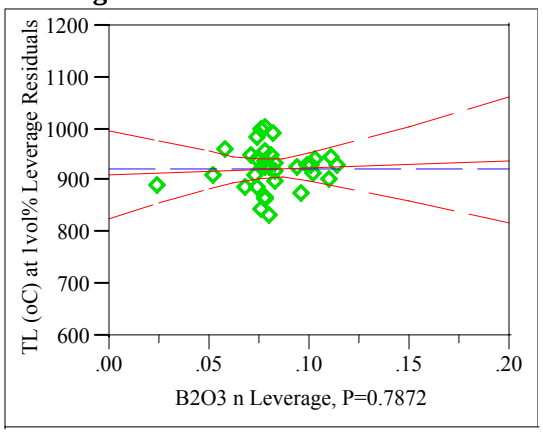

Li2O n
Leverage Plot

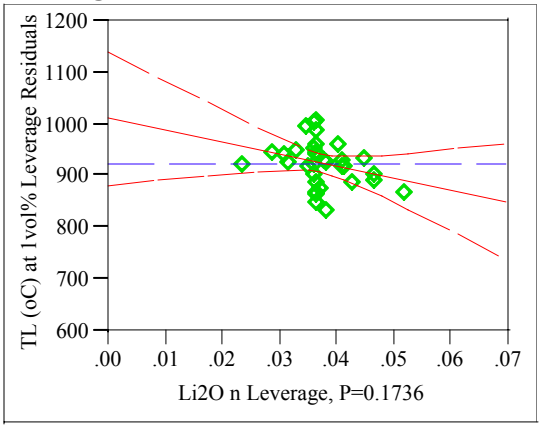

Appendix D. Model Fitting Results for T0.01 Data

Exhibit D.6: Statistical Results from the Fitting of the LMM to Each Data Grouping

MnO n
Leverage Plot

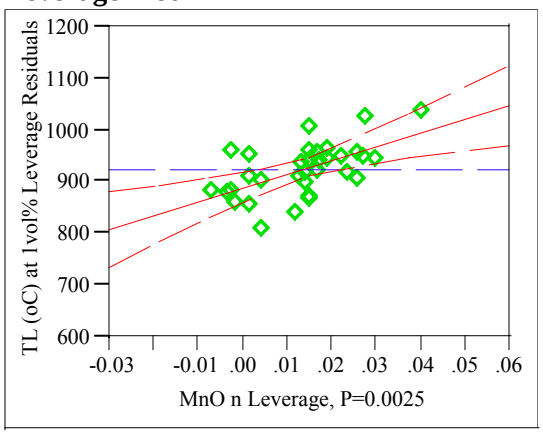

SiO2 n
Leverage Plot

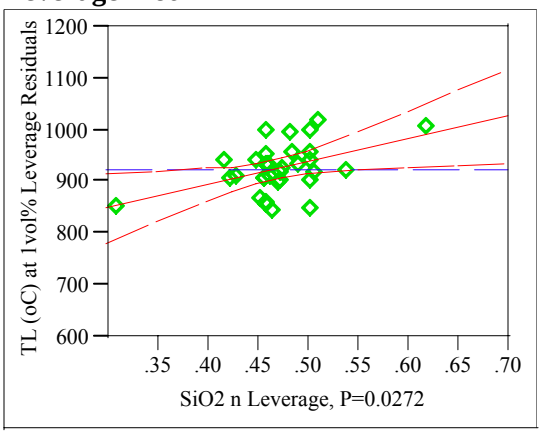

Na2O n
Leverage Plot

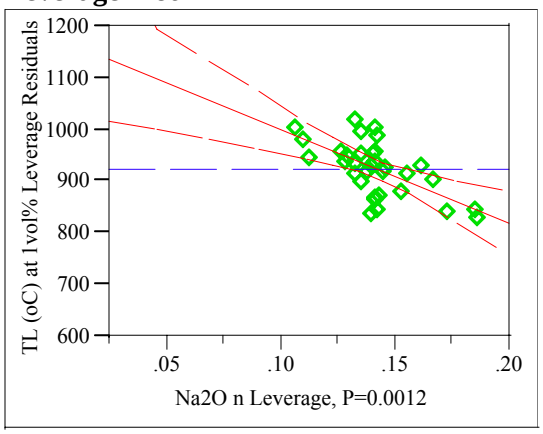

SrO n
Leverage Plot

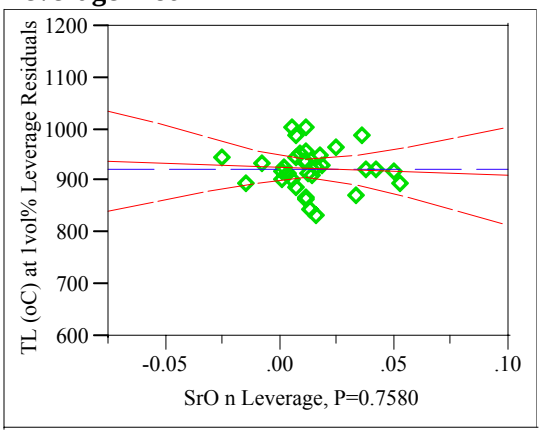

NiO n
Leverage Plot

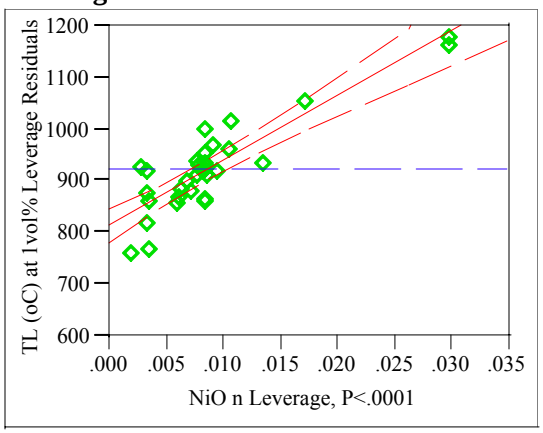

ZrO2 n
Leverage Plot

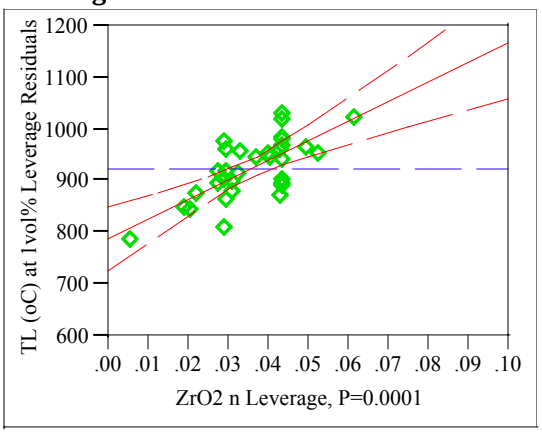

Appendix D. Model Fitting Results for T0.01 Data

Exhibit D.6: Statistical Results from the Fitting of the LMM to Each Data Grouping

Groupings=4
Response T0.01 (°C)
Singularity Details
Intercept = 0
Whole Model
Actual by Predicted Plot

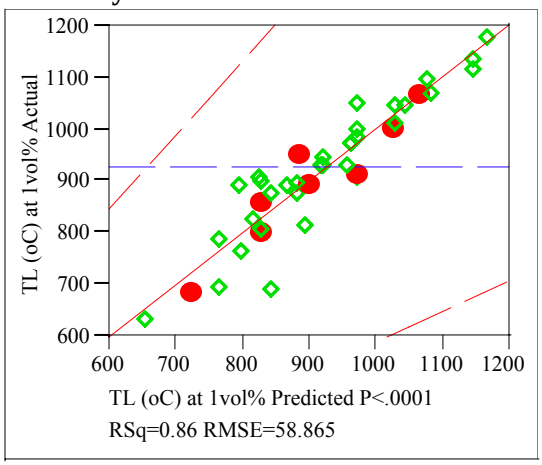

Summary of Fit

RSquare	0.861097
RSquare Adj	0.797959
Root Mean Square Error	58.86469
Mean of Response	927.1052
Observations (or Sum Wgts)	33

Analysis of Variance

Source	DF	Sum of Squares	Mean Square	F Ratio
Model	10	472575.50	47257.5	13.6383
Error	22	76231.13	3465.1	Prob > F
C. Total	32	548806.63		<.0001

Tested against reduced model: Y=mean

Lack Of Fit

Source	DF	Sum of Squares	Mean Square	F Ratio
Lack Of Fit	19	68955.606	3629.24	1.4965
Pure Error	3	7275.528	2425.18	Prob > F
Total Error	22	76231.134		0.4181
				Max RSq
				0.9867

Parameter Estimates

Term		Estimate	Std Error	t Ratio	Prob>|t|
Intercept	Zeroed	0	0	.	.
Al2O3 n		3155.4385	1029.905	3.06	0.0057
B2O3 n		532.702	539.6705	0.99	0.3343
Cr2O3 n		28570.385	9459.251	3.02	0.0063
Fe2O3 n		3603.7994	549.5	6.56	<.0001
Li2O n		-2510.31	1571.432	-1.60	0.1244
MnO n		2300.4623	1353.135	1.70	0.1032
Na2O n		-1813.821	450.0516	-4.03	0.0006
NiO n		12988.922	1670.927	7.77	<.0001
SiO2 n		433.0566	222.5289	1.95	0.0645
SrO n		-569.386	588.3748	-0.97	0.3437
ZrO2 n		3983.7683	794.5923	5.01	<.0001

Appendix D. Model Fitting Results for T0.01 Data

Exhibit D.6: Statistical Results from the Fitting of the LMM to Each Data Grouping

Residual by Predicted Plot

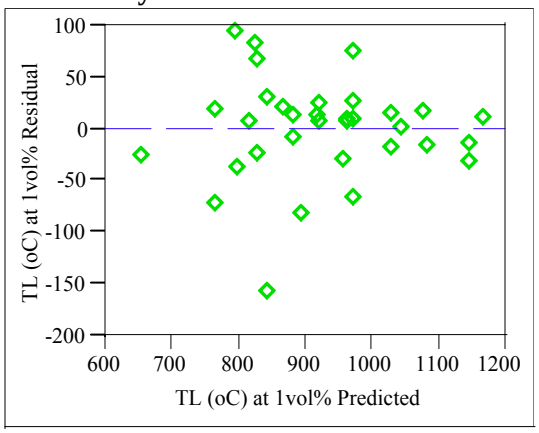

Press
160718.16535

Cr2O3 n
Leverage Plot

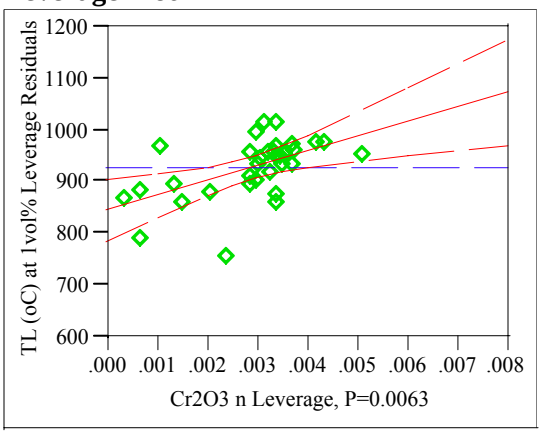

Al2O3 n
Leverage Plot

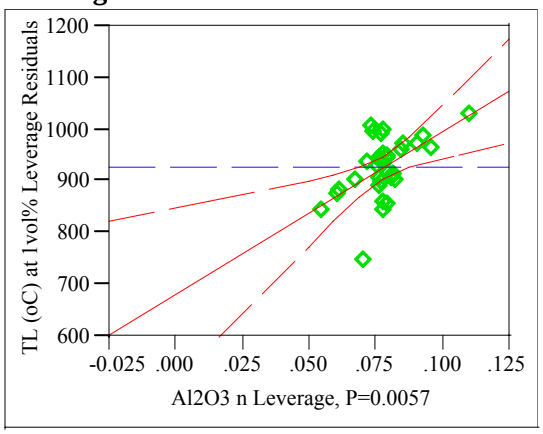

Fe2O3 n
Leverage Plot

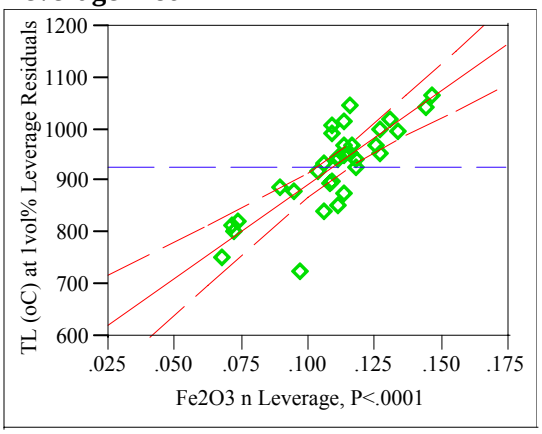

B2O3 n
Leverage Plot

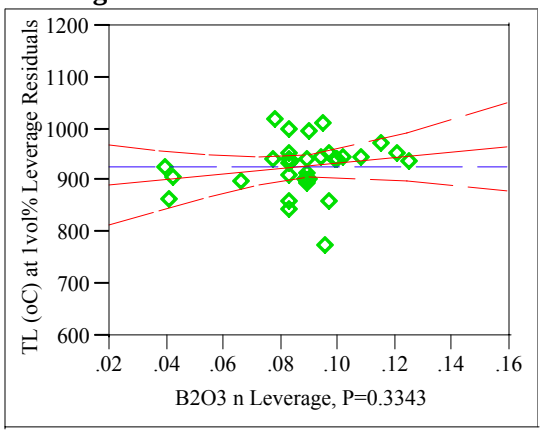

Li2O n
Leverage Plot

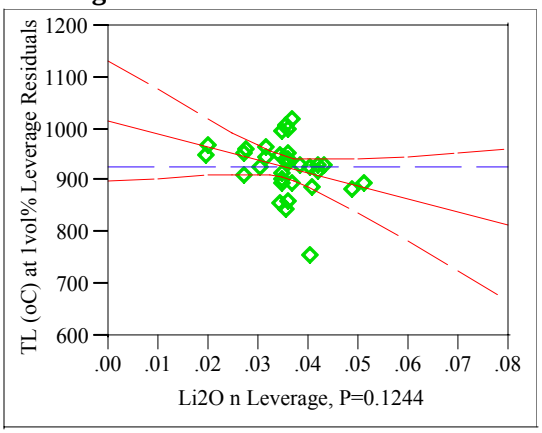

Appendix D. Model Fitting Results for T0.01 Data

Exhibit D.6: Statistical Results from the Fitting of the LMM to Each Data Grouping

MnO n
Leverage Plot

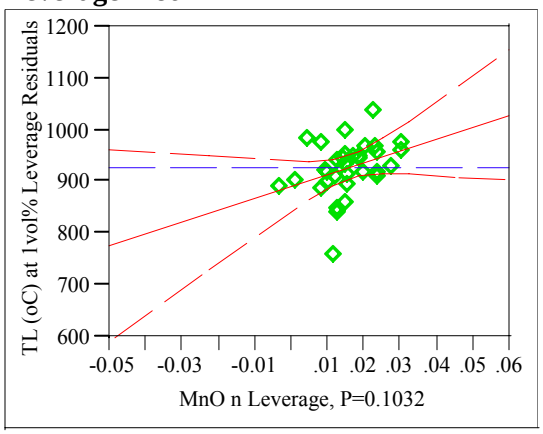

SiO2 n
Leverage Plot

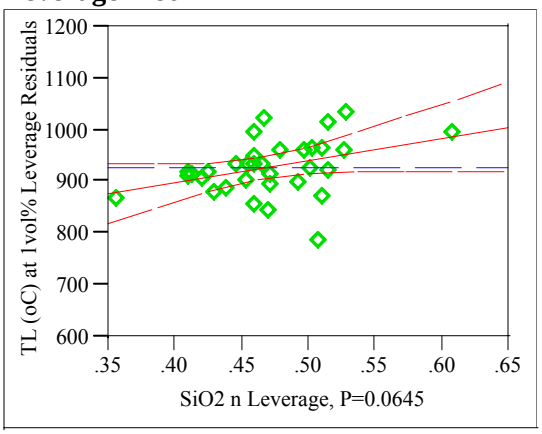

Na2O n
Leverage Plot

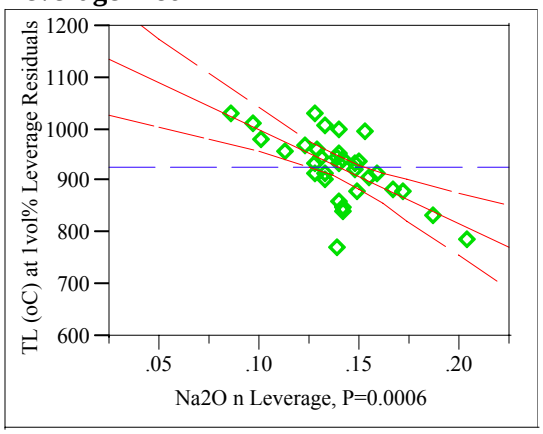

SrO n
Leverage Plot

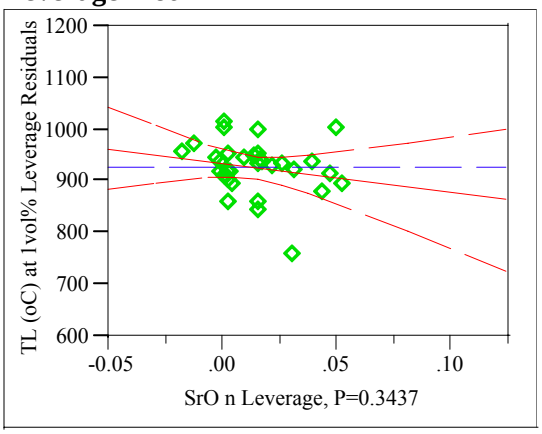

NiO n
Leverage Plot

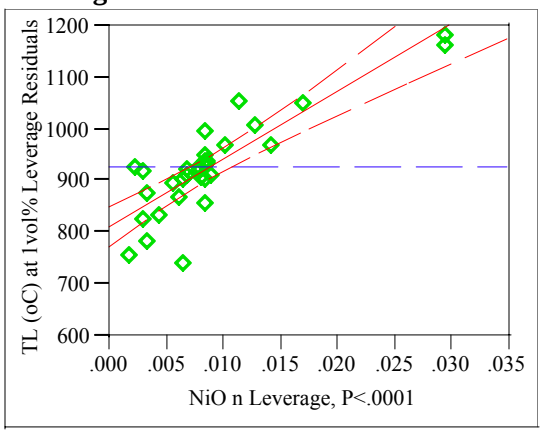

ZrO2 n
Leverage Plot

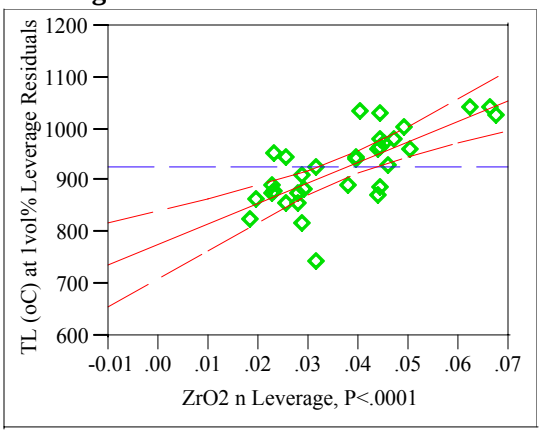

Appendix D. Model Fitting Results for T0.01 Data

Exhibit D.6: Statistical Results from the Fitting of the LMM to Each Data Grouping

Groupings=5
Response T0.01 (°C)
Singularity Details
Intercept = 0
Whole Model
Actual by Predicted Plot

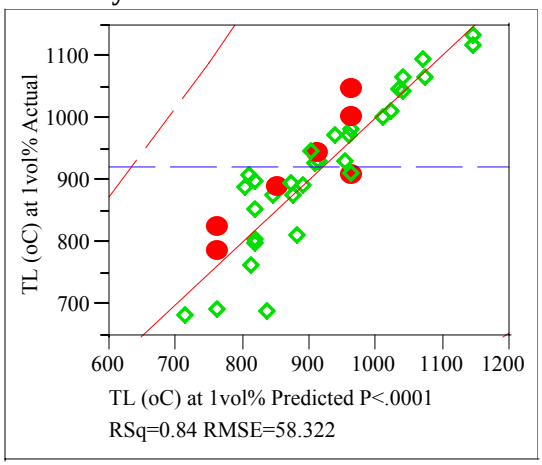

Summary of Fit

RSquare	0.842477
RSquare Adj	0.767466
Root Mean Square Error	58.32162
Mean of Response	922.9736
Observations (or Sum Wgts)	32

Analysis of Variance

Source	DF	Sum of Squares	Mean Square	F Ratio
Model	10	382025.33	38202.5	11.2314
Error	21	71429.65	3401.4	Prob > F
C. Total	31	453454.98		<.0001

Tested against reduced model: Y=mean

Lack Of Fit

Source	DF	Sum of Squares	Mean Square	F Ratio
Lack Of Fit	19	71247.733	3749.88	41.2266
Pure Error	2	181.916	90.96	Prob > F
Total Error	21	71429.648		0.0239
				Max RSq
				0.9996

Parameter Estimates

Term		Estimate	Std Error	t Ratio	Prob>|t|
Intercept	Zeroed	0	0	.	.
Al2O3 n		3112.8567	733.6917	4.24	0.0004
B2O3 n		440.21899	610.5284	0.72	0.4788
Cr2O3 n		24798.633	11734.33	2.11	0.0467
Fe2O3 n		3778.7049	774.0976	4.88	<.0001
Li2O n		-2642.672	1765.375	-1.50	0.1493
MnO n		2992.3968	1135.439	2.64	0.0155
Na2O n		-1858.229	583.243	-3.19	0.0044
NiO n		13354.067	1646.532	8.11	<.0001
SiO2 n		413.45305	254.8054	1.62	0.1196
SrO n		-722.9979	903.3614	-0.80	0.4325
ZrO2 n		4105.8967	973.8881	4.22	0.0004

Appendix D. Model Fitting Results for T0.01 Data

Exhibit D.6: Statistical Results from the Fitting of the LMM to Each Data Grouping

Residual by Predicted Plot

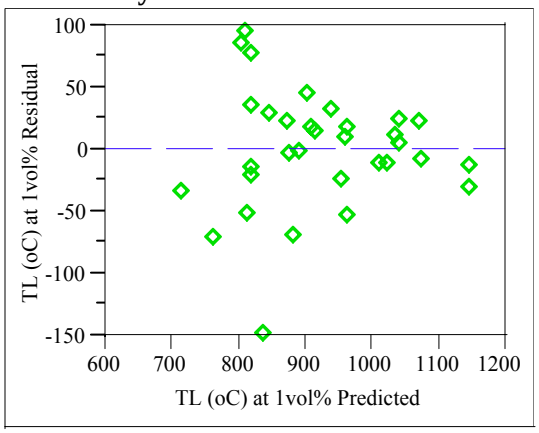

Press
207781.95856

Cr2O3 n
Leverage Plot

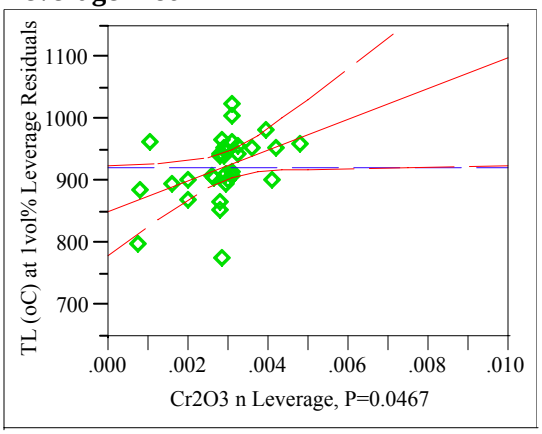

Al2O3 n
Leverage Plot

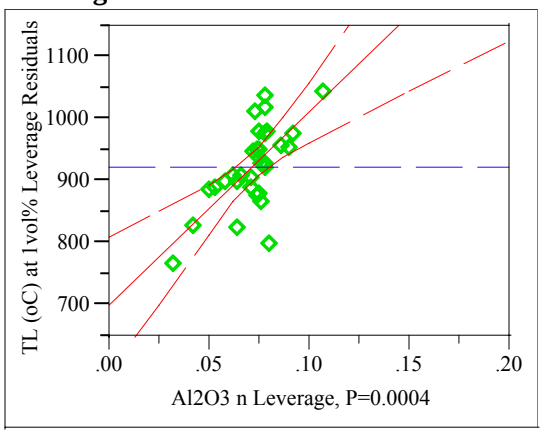

Fe2O3 n
Leverage Plot

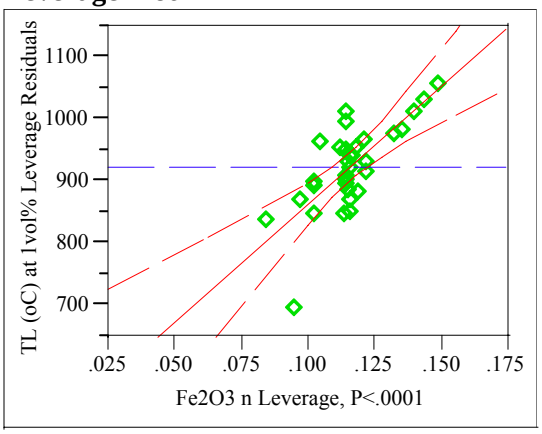

B2O3 n
Leverage Plot

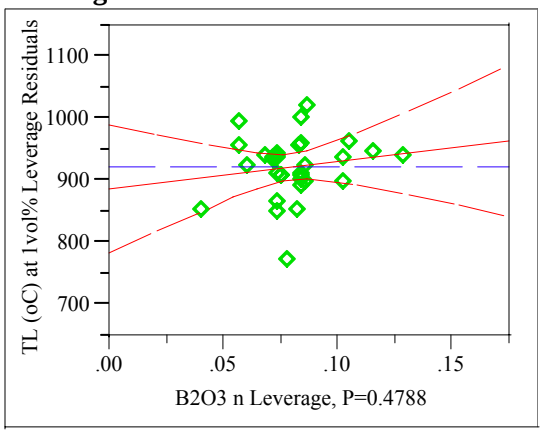

Li2O n
Leverage Plot

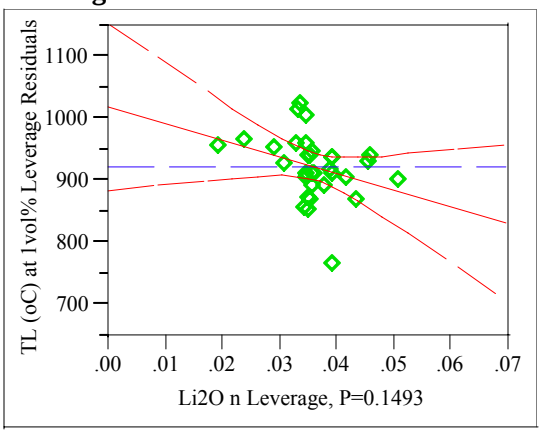

Appendix D. Model Fitting Results for T0.01 Data

Exhibit D.6: Statistical Results from the Fitting of the LMM to Each Data Grouping

MnO n
Leverage Plot

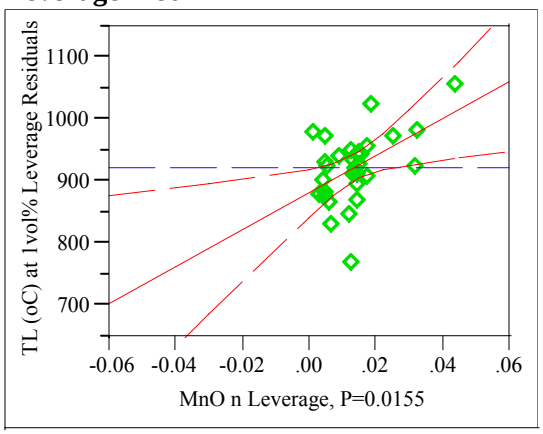

SiO2 n
Leverage Plot

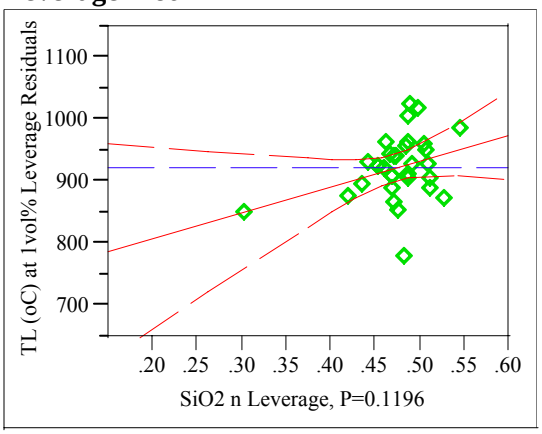

Na2O n
Leverage Plot

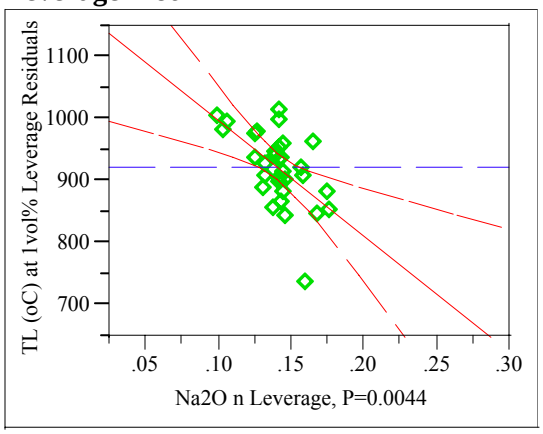

SrO n
Leverage Plot

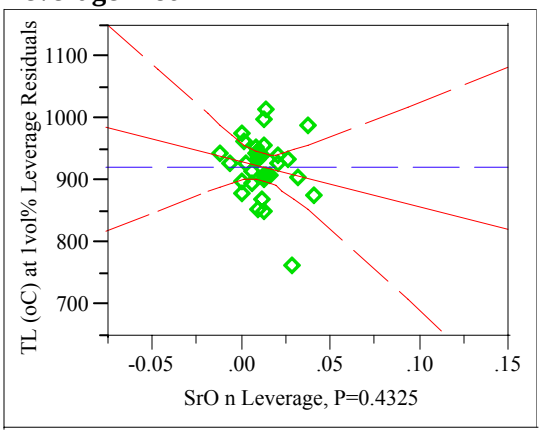

NiO n
Leverage Plot

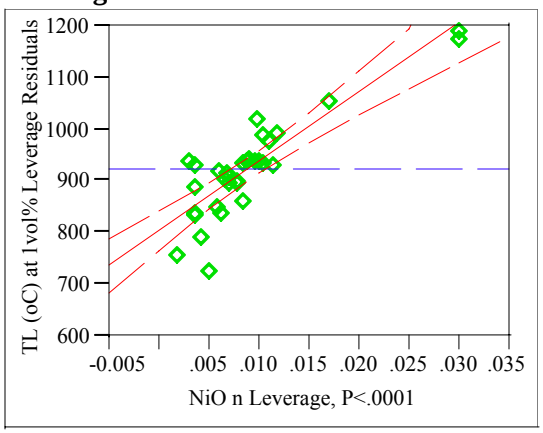

ZrO2 n
Leverage Plot

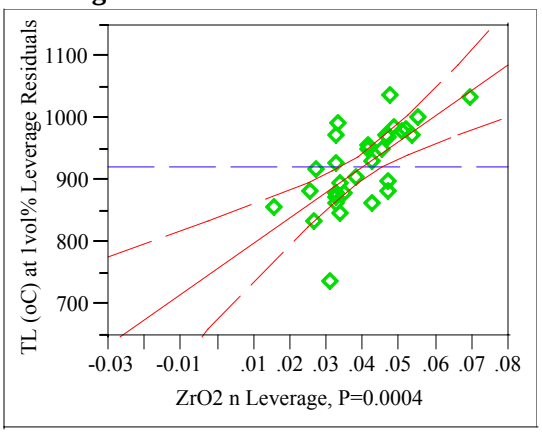

Appendix D. Model Fitting Results for T0.01 Data

Exhibit D.6: Statistical Results from the Fitting of the LMM to Each Data Grouping

Prediction Uncertainty at 95% for DWPFM By #

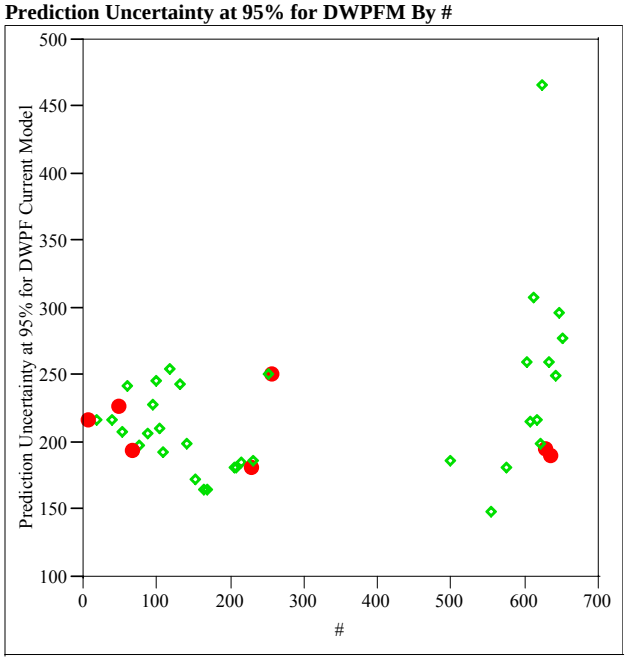

Prediction Uncertainty °C at 95% for IPM By #

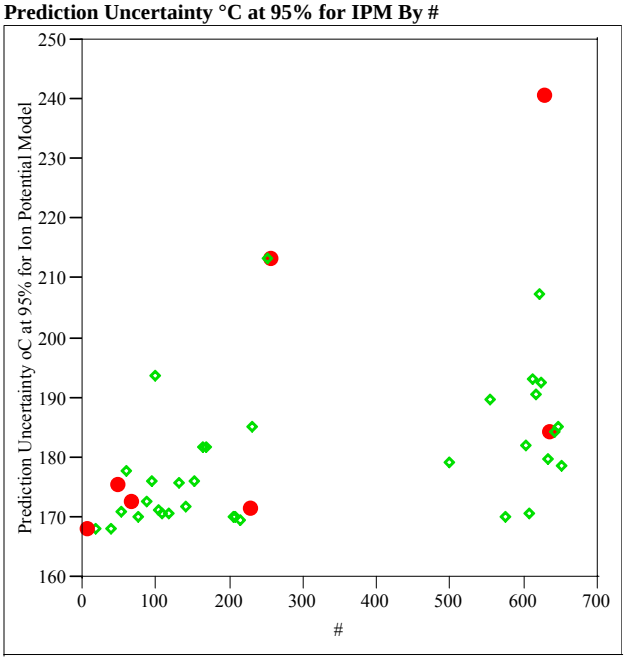

Residual °C for DWPFM By #

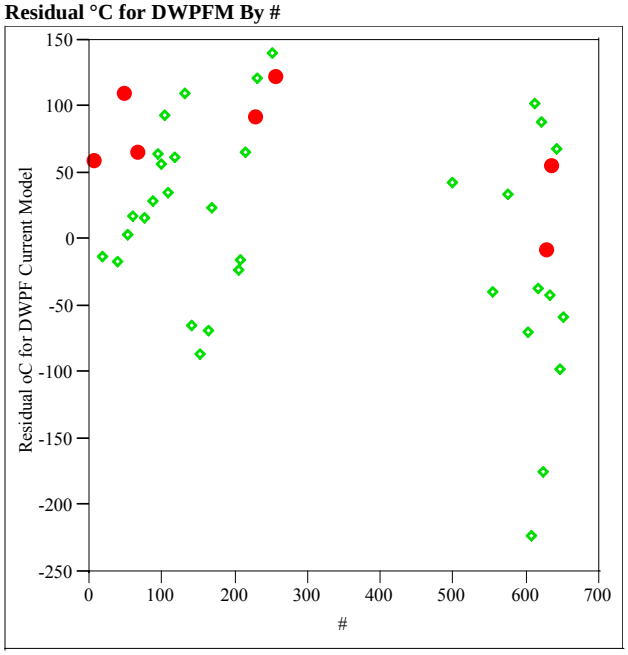

Residual °C for IPM By #

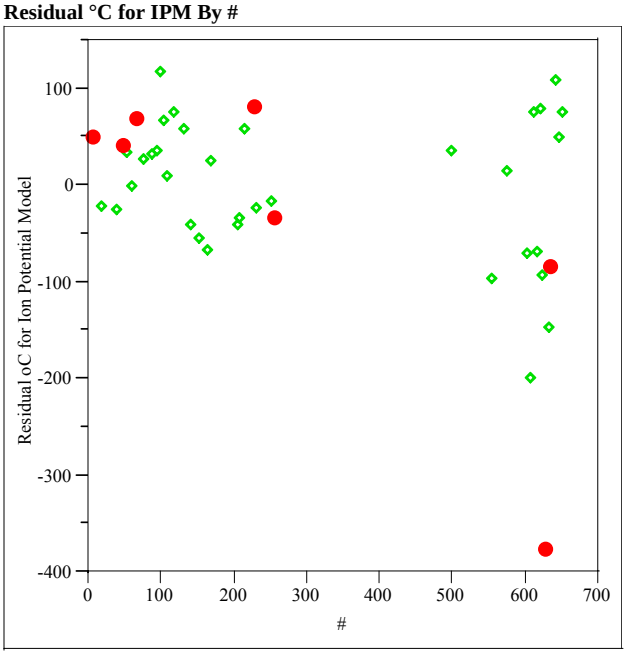

Appendix D. Model Fitting Results for T0.01 Data

Exhibit D.7: Residual and Uncertainty Plots for Data Group 1

Prediction Uncertainty at 95% in °C for SPM w Cr and By #

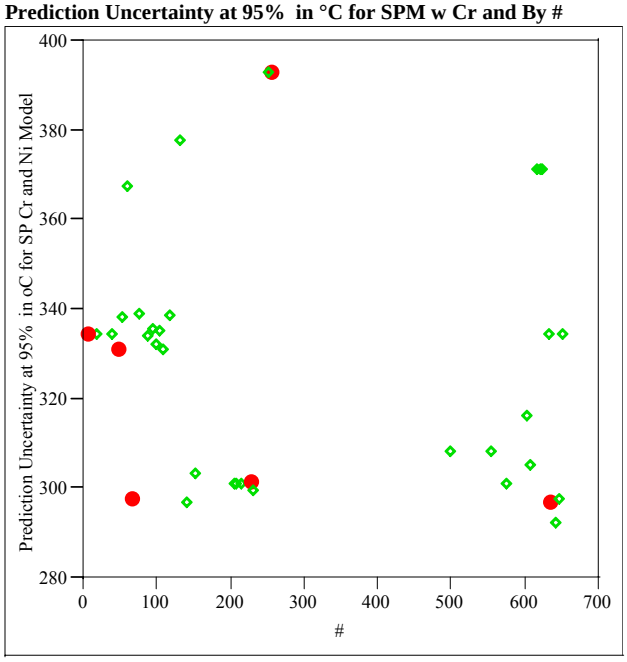

Prediction Uncertainty at 95% in °C for SPM w Ni and F By #

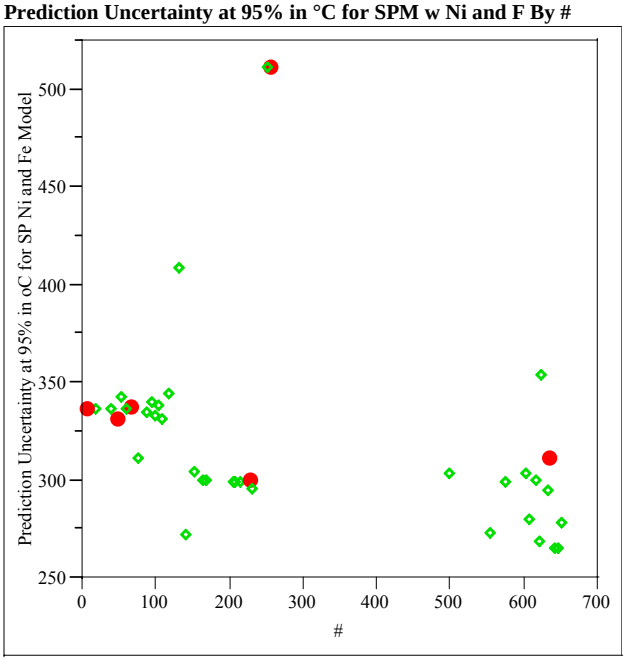

Residual °C for SPM w Cr and Ni By #

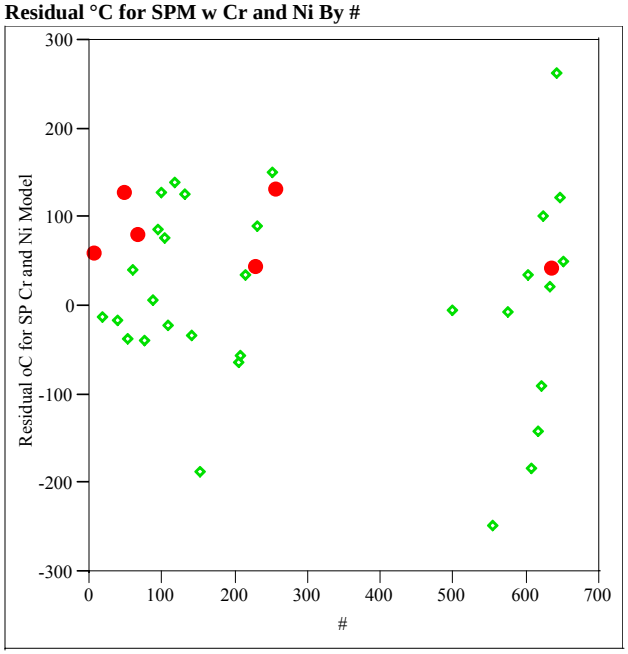

Residual °C for SPM w Ni and Fe By #

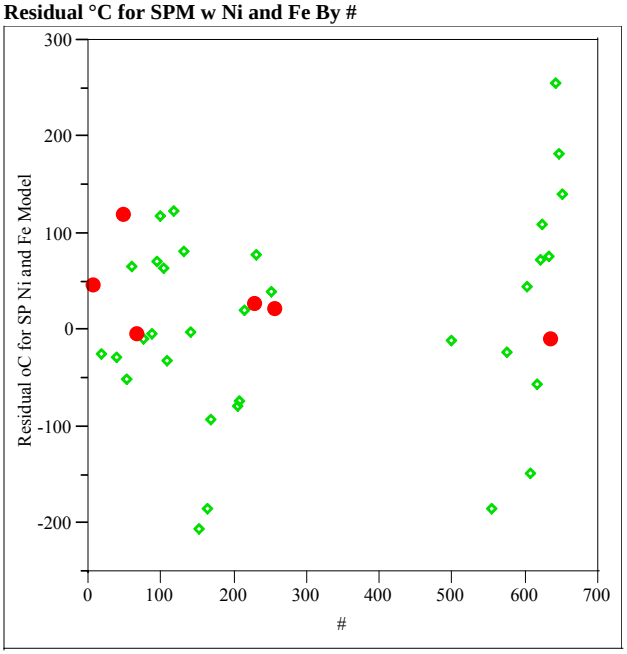

Appendix D. Model Fitting Results for T0.01 Data

Exhibit D.7: Residual and Uncertainty Plots for Data Group 1

Prediction Uncertainty at 95% in °C for SLM By #

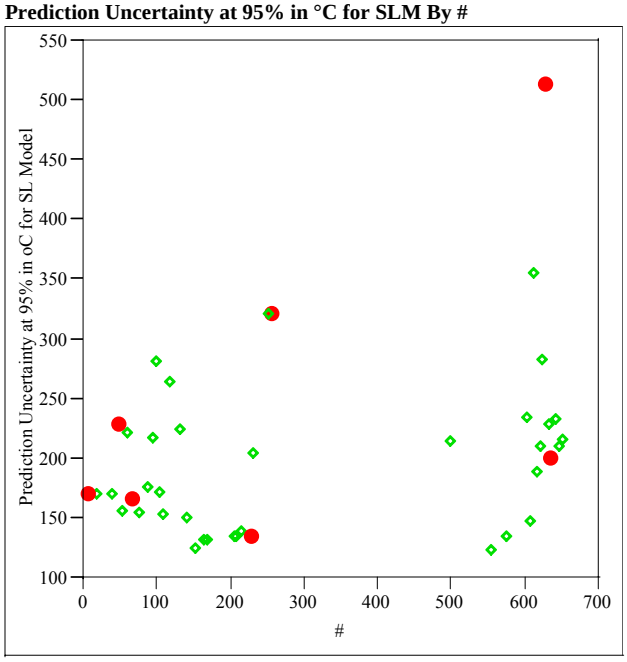

Prediction Uncertainty at 95% in °C for LMM By #

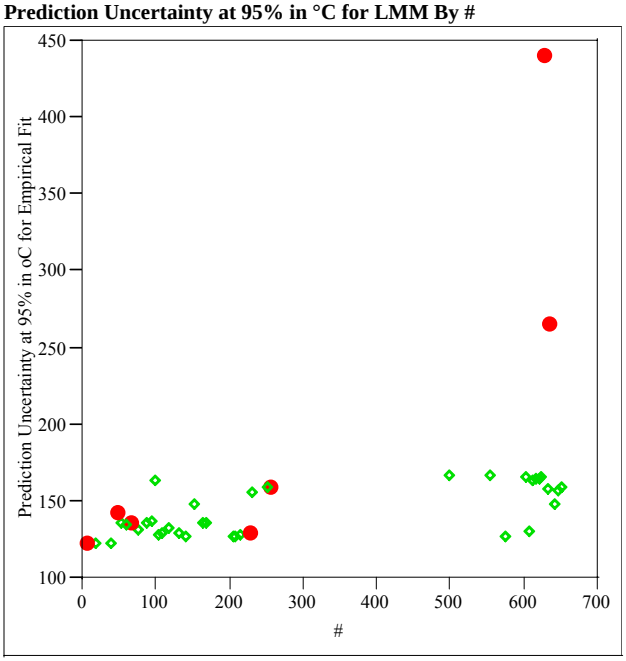

Residual °C for SLM By #

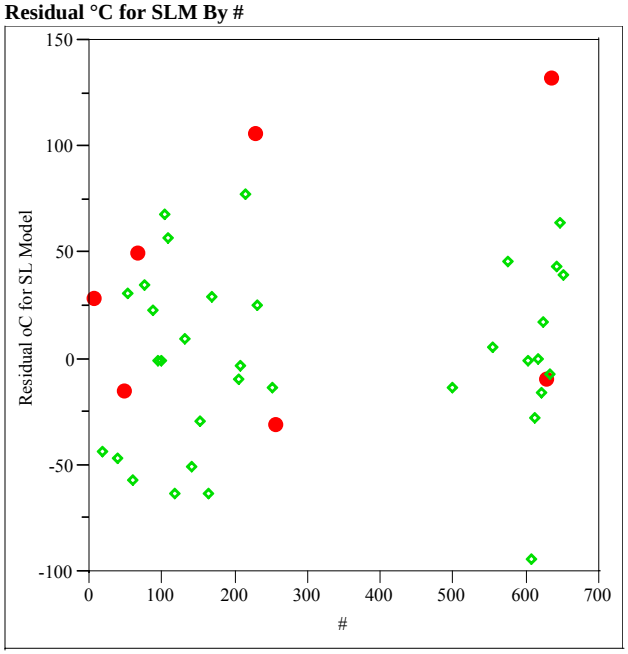

Residual °C of LMM Fit By #

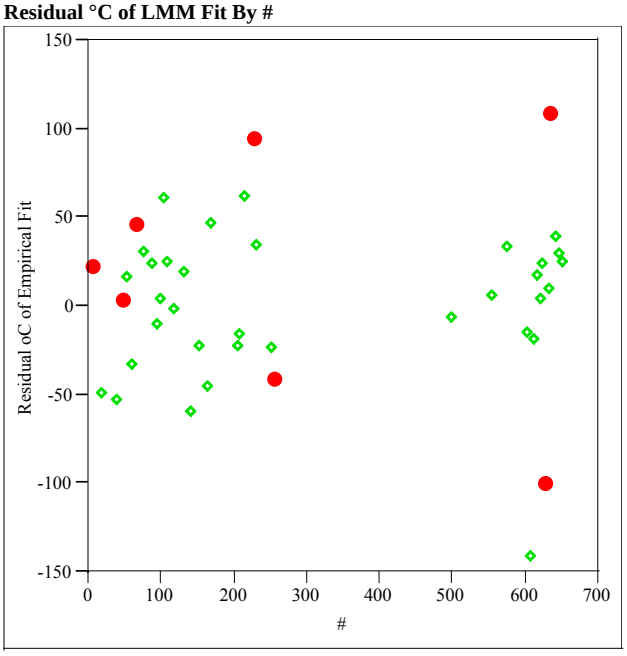

Appendix D. Model Fitting Results for T0.01 Data

Exhibit D.8: Residual and Uncertainty Plots for Data Group 2

Prediction Uncertainty at 95% in °C for DWPF Cur By #

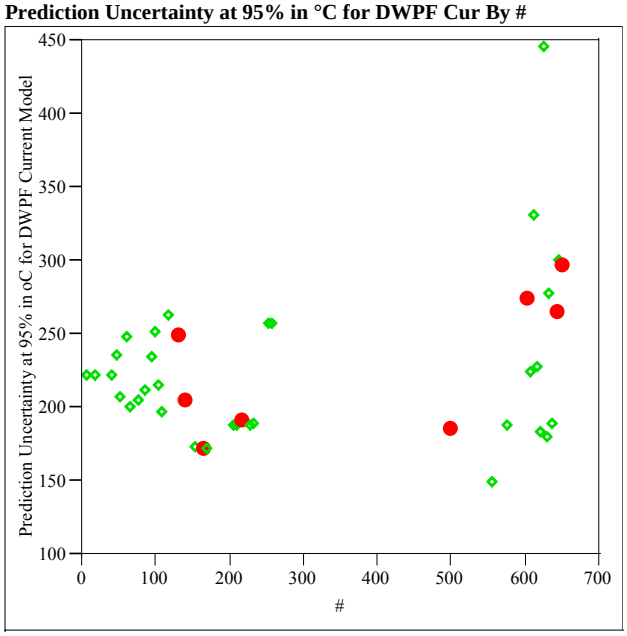

Prediction Uncertainty at 95% in °C for IPM By #

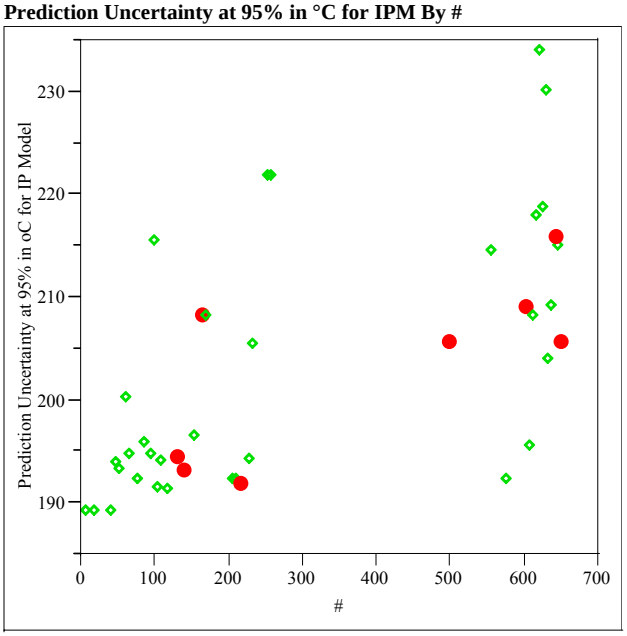

Residual °C for DWPFM By #

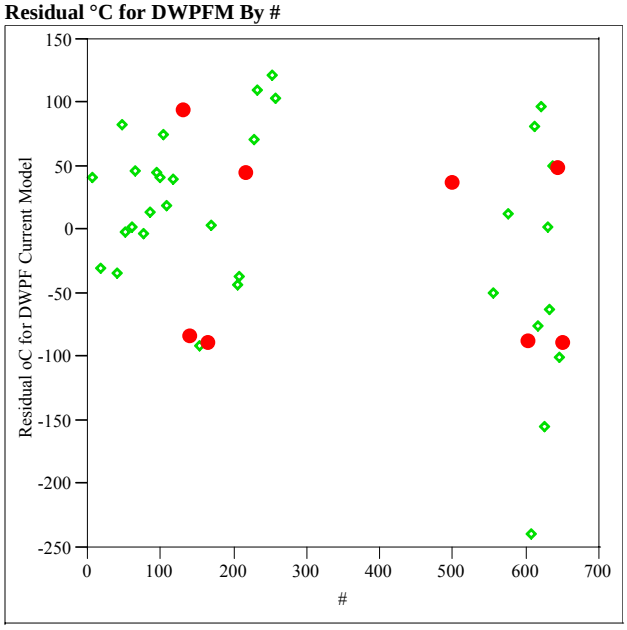

Residual °C for IPM By #

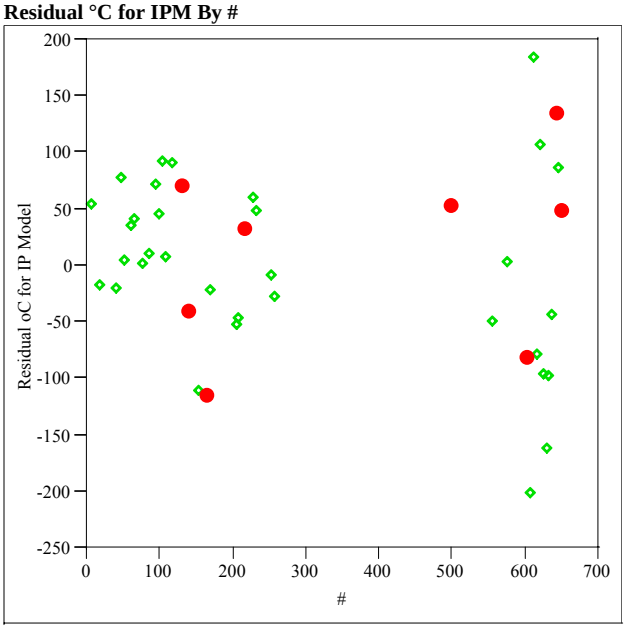

Appendix D. Model Fitting Results for T0.01 Data

Exhibit D.8: Residual and Uncertainty Plots for Data Group 2

Prediction Uncertainty at 95% in °C for SPM w Cr and N By #

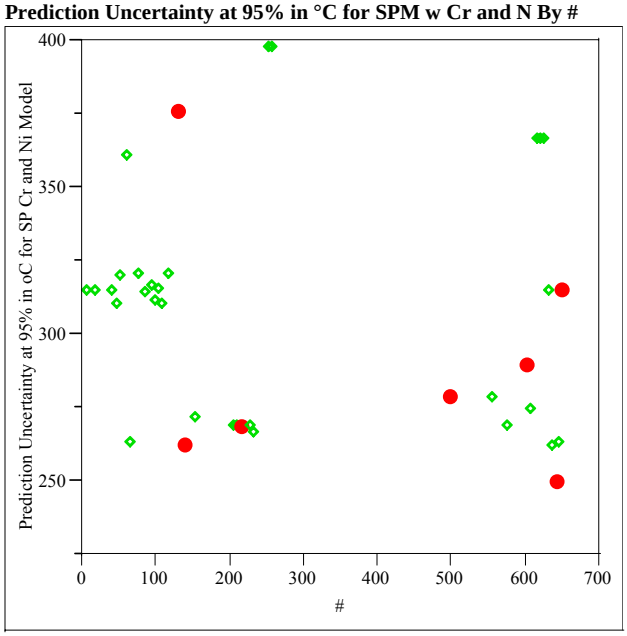

Prediction Uncertainty at 95% in °C for SPM w Ni and F By #

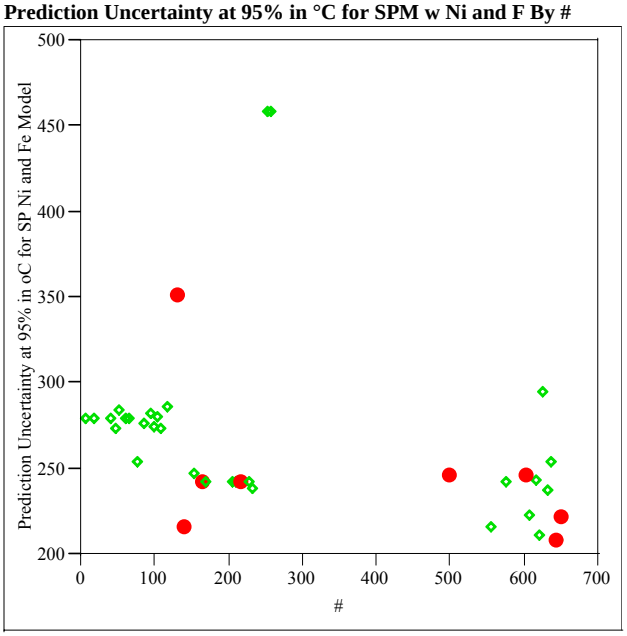

Residual °C for SPM w Cr and Ni By #

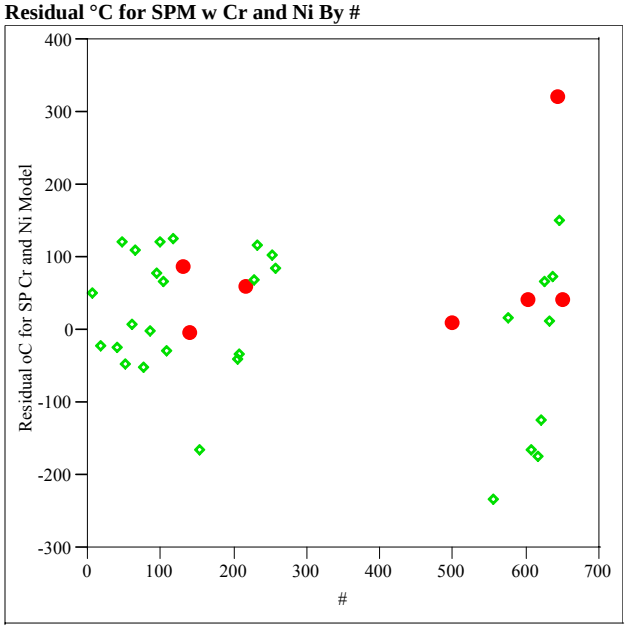

Residual °C for SPM w Ni and Fe By #

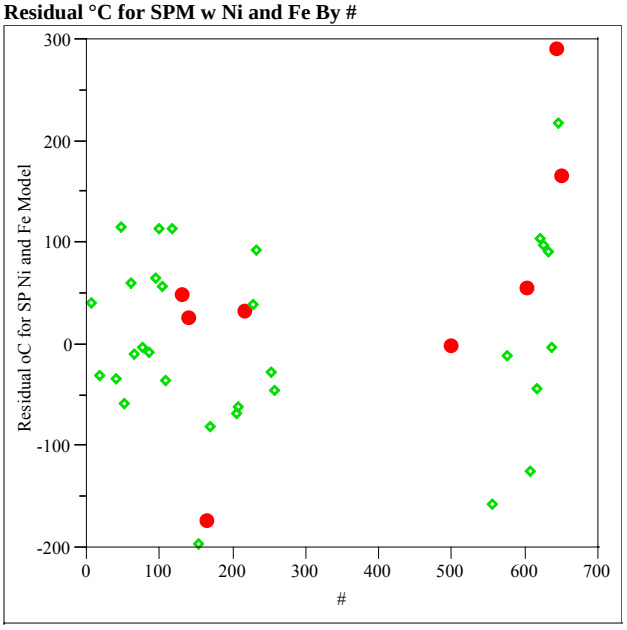

Appendix D. Model Fitting Results for T0.01 Data

Exhibit D.8: Residual and Uncertainty Plots for Data Group 2

Prediction Uncertainty in °C for SLM By #

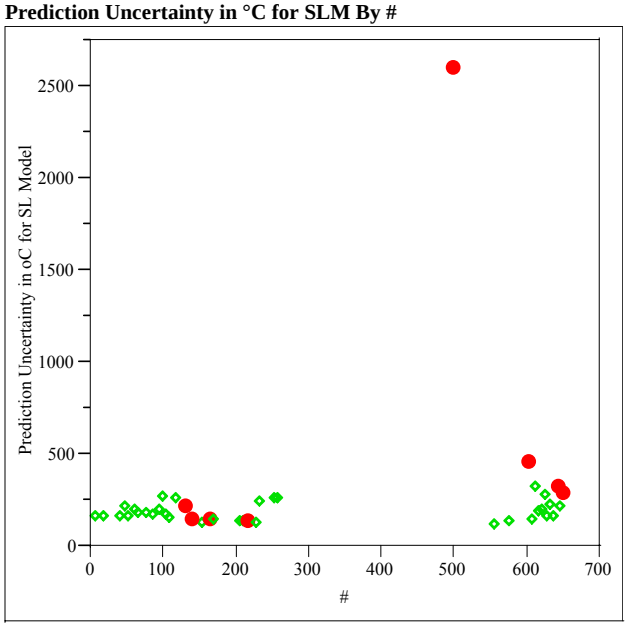

Prediction Uncertainty at 95% in °C for LMM By #

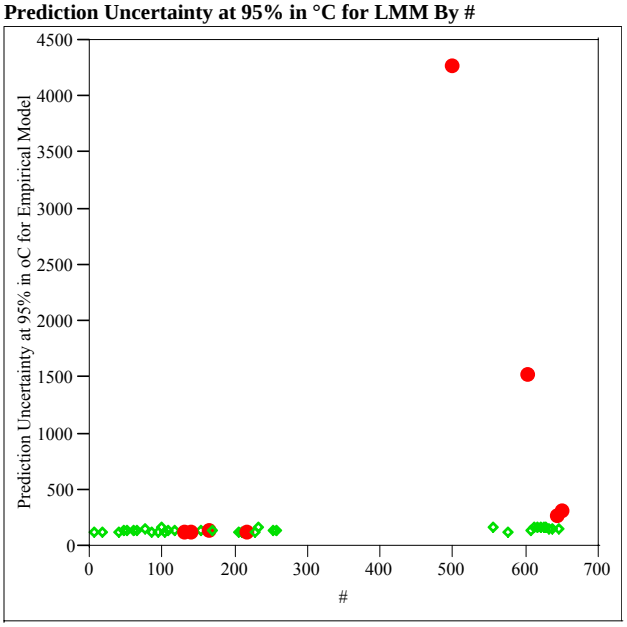

Residual °C for SLM By #

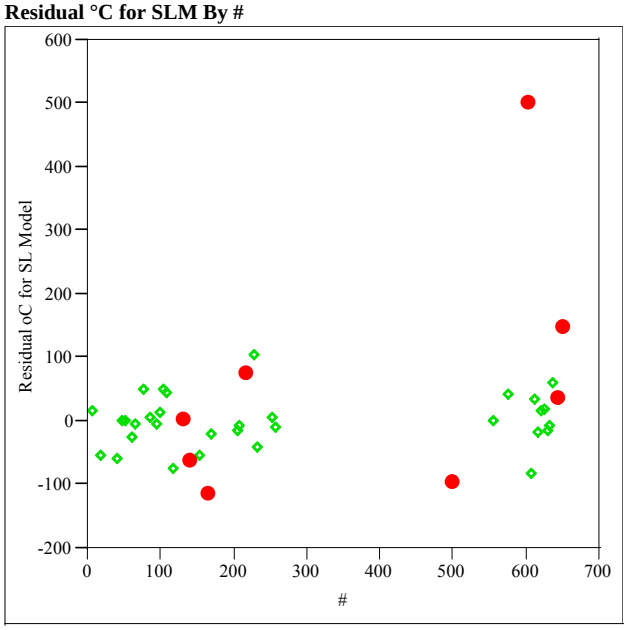

Residual °C for LMM By #

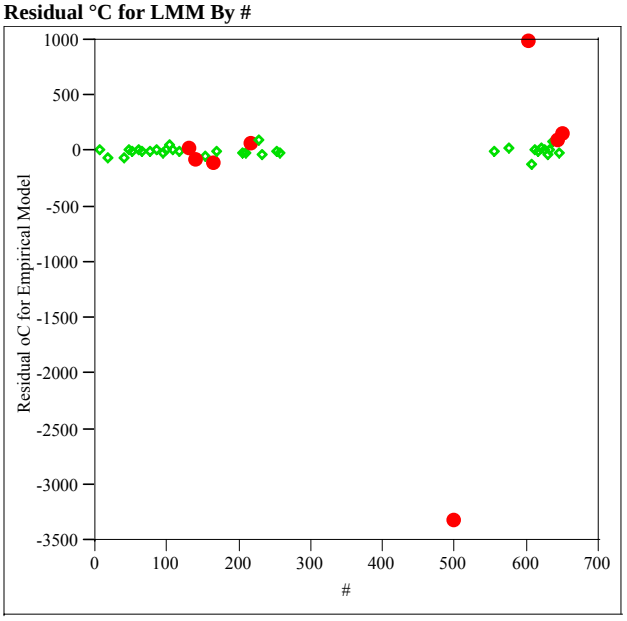

Appendix D. Model Fitting Results for T0.01 Data

Exhibit D.9: Residual and Uncertainty Plots for Data Group 3

Prediction Uncertainty °C for DWPFM By #

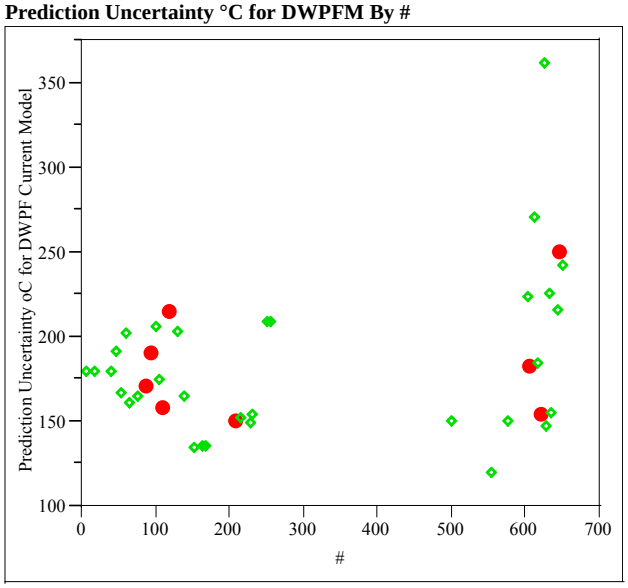

Prediction Uncertainty °C for IPM By #

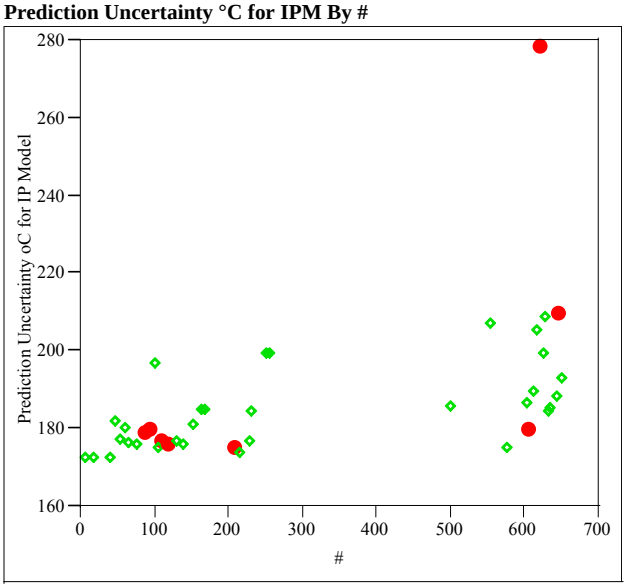

Residual °C for DWPFM By #

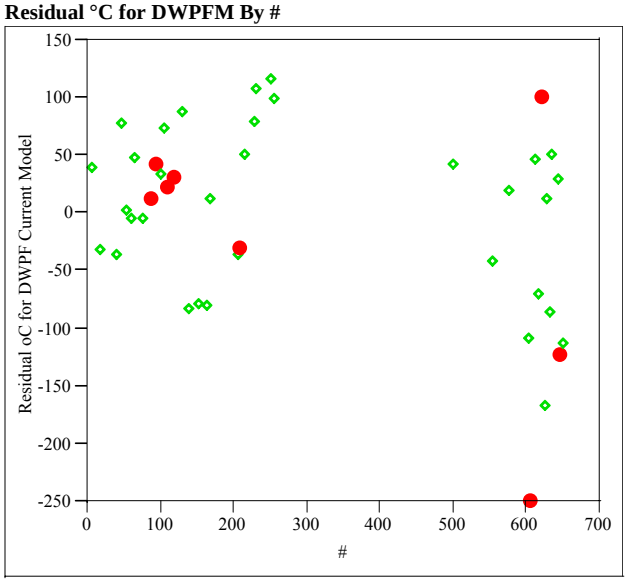

Residual °C for IPM By #

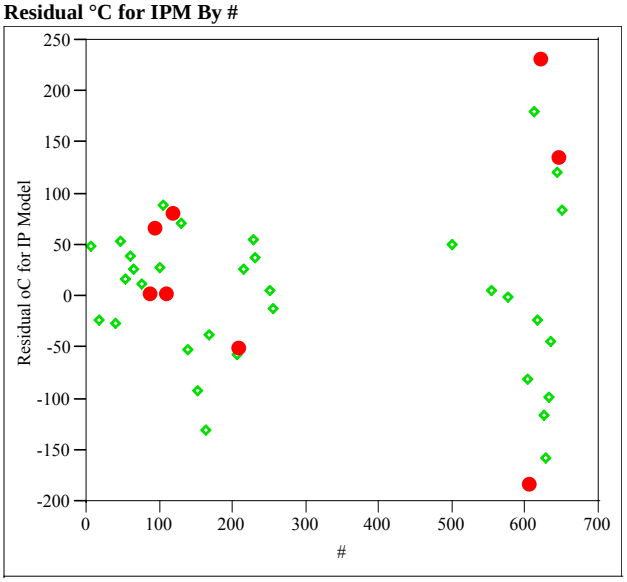

Appendix D. Model Fitting Results for T0.01 Data

Exhibit D.9: Residual and Uncertainty Plots for Data Group 3

Prediction Uncertainty °C for SPM w Cr and Ni By #

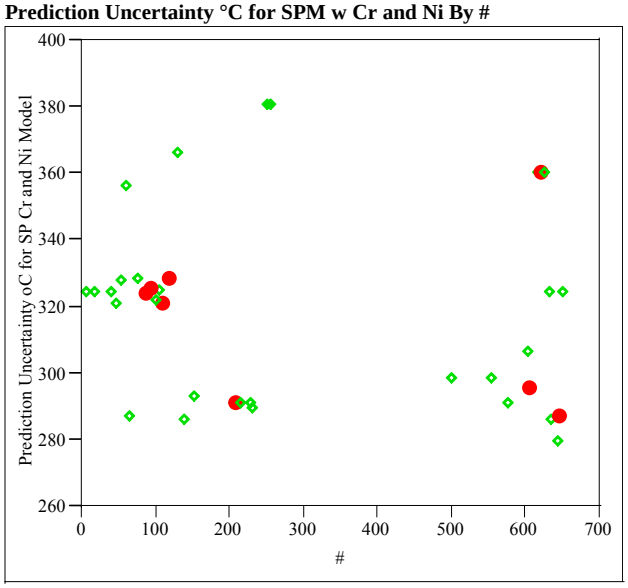

Prediction Uncertainty °C for SPM w Ni and Fe By #

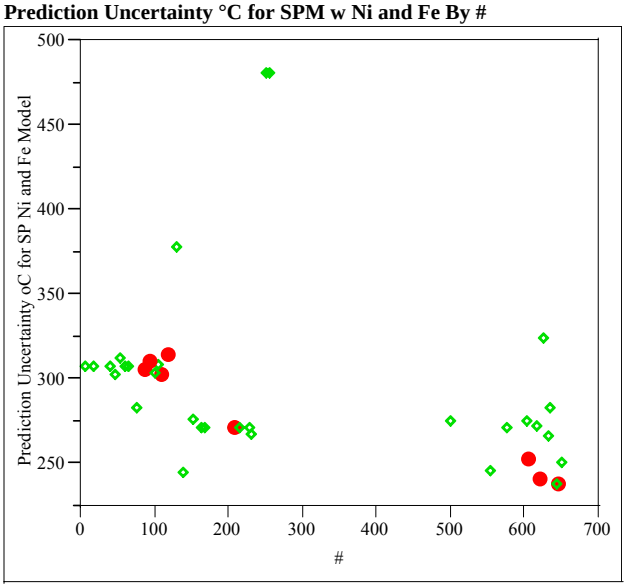

Residual °C for SPM w Cr and Ni By #

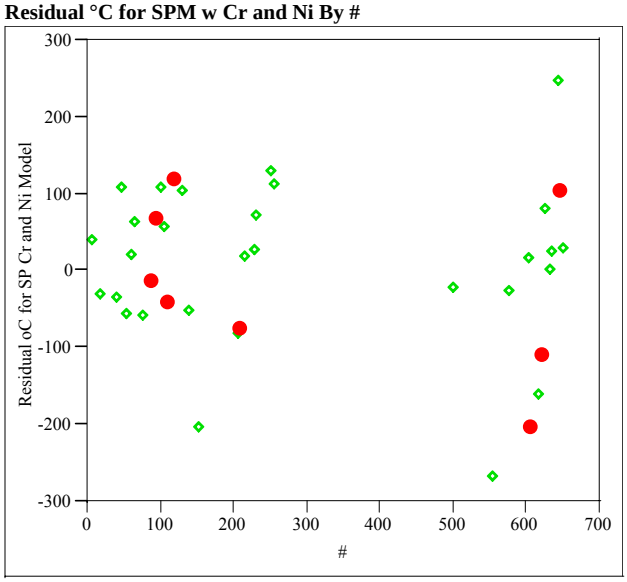

Residual °C for SPM w Ni and Fe By #

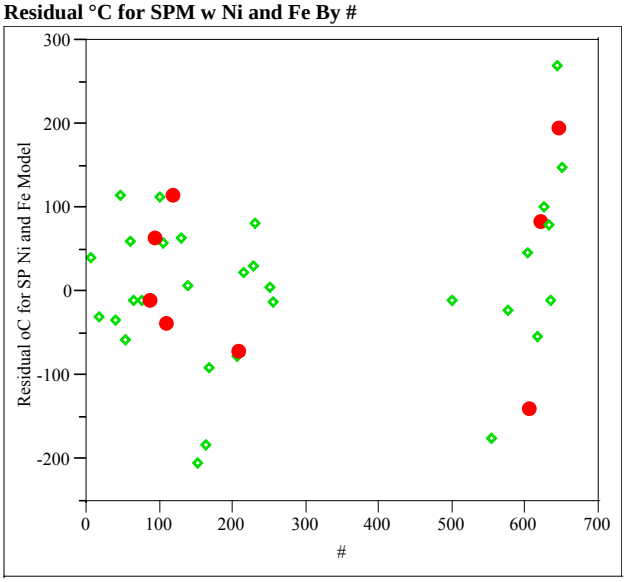

Appendix D. Model Fitting Results for T0.01 Data

Exhibit D.9: Residual and Uncertainty Plots for Data Group 3

Prediction Uncertainty °C for SLM By #

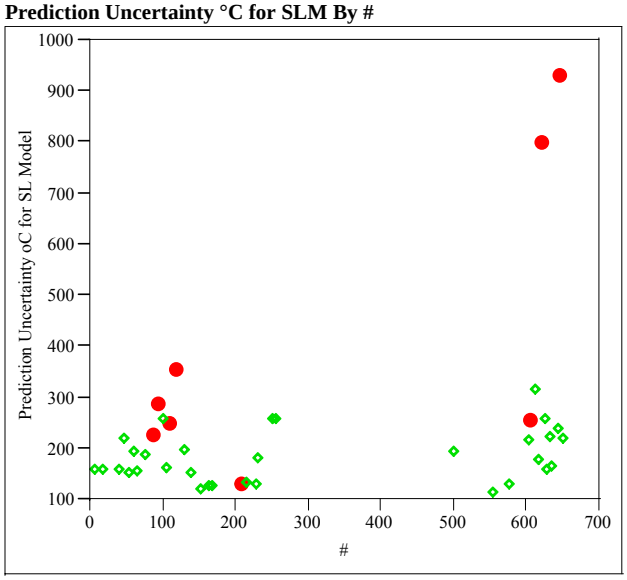

Prediction Uncertainty °C for LMM By #

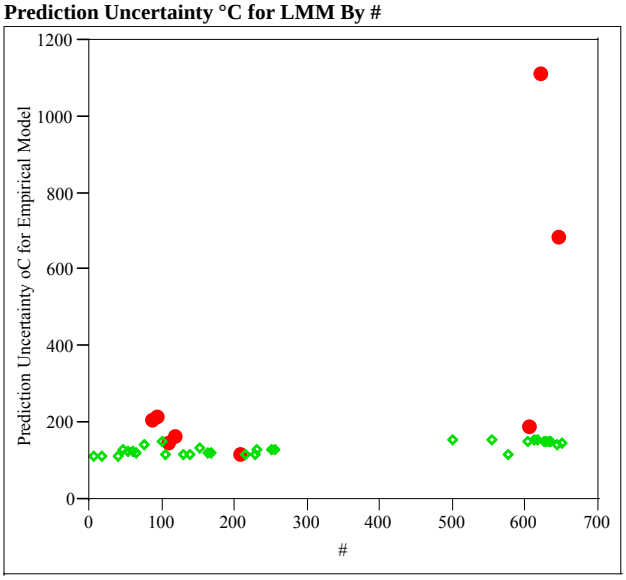

Residual °C for SLM By #

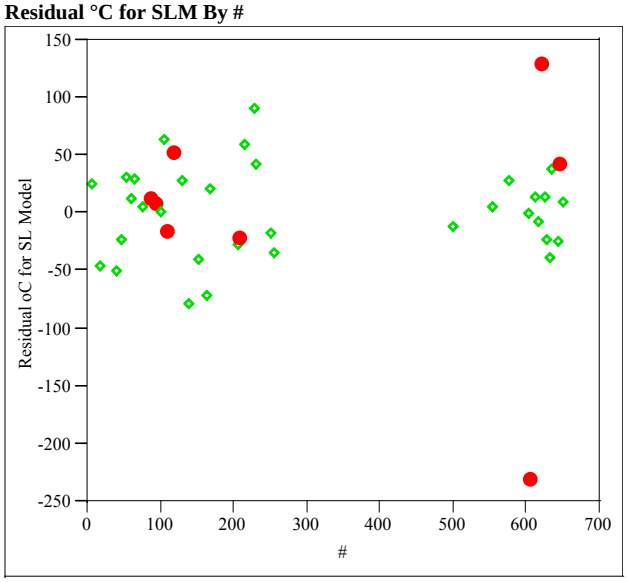

Residual °C for LMM By #

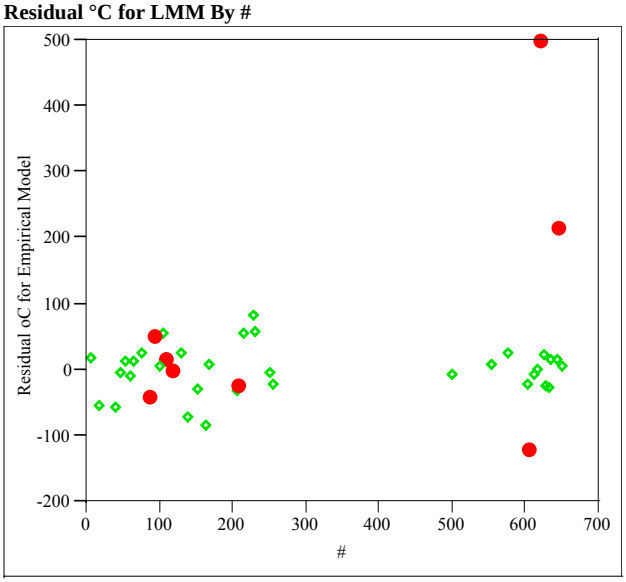

Appendix D. Model Fitting Results for T0.01 Data

Exhibit D.10: Residual and Uncertainty Plots for Data Group 4

Prediction Uncertainty °C for DWPFM By #

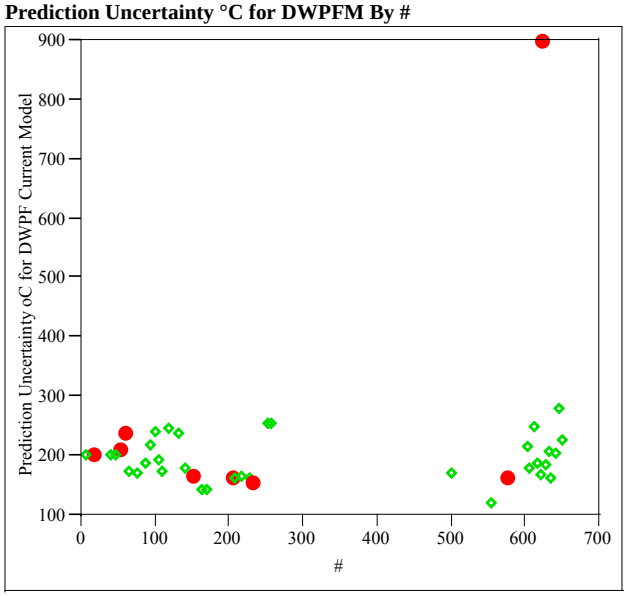

Prediction Uncertainty °C for IPM By #

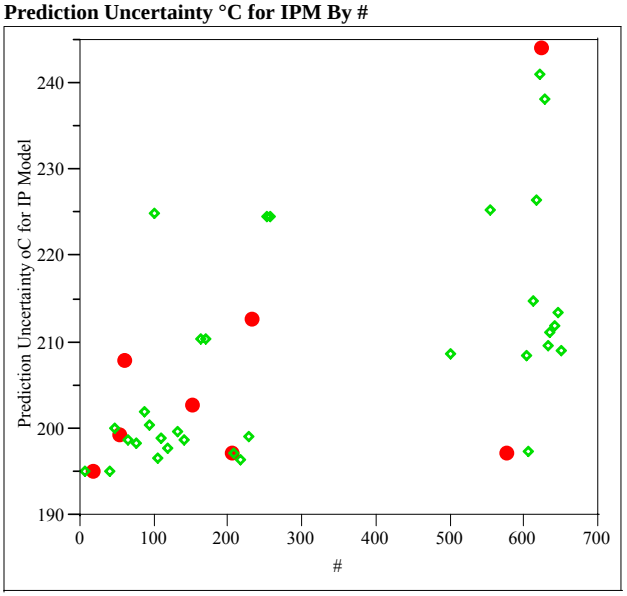

Residual °C for DWPFM By #

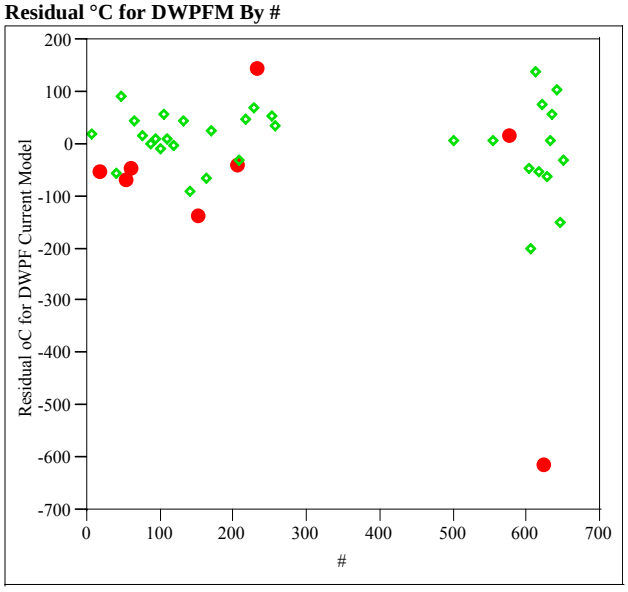

Residual °C for IPM By #

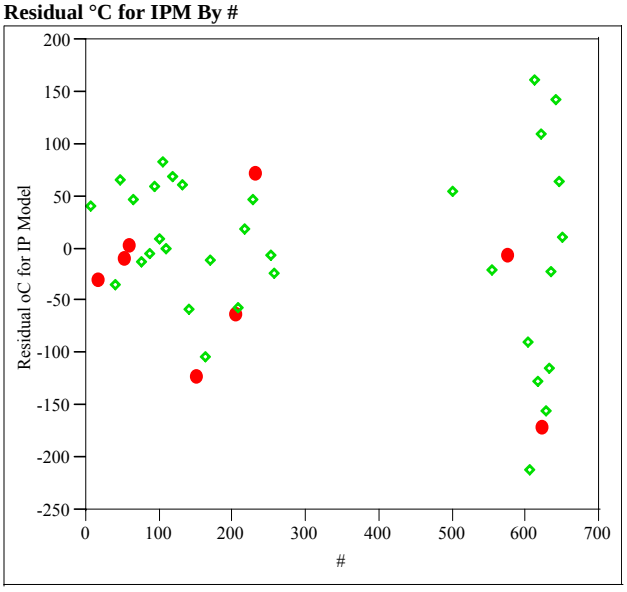

Appendix D. Model Fitting Results for T0.01 Data

Exhibit D.10: Residual and Uncertainty Plots for Data Group 4

Prediction Uncertainty °C for SPM w Cr and Ni By #

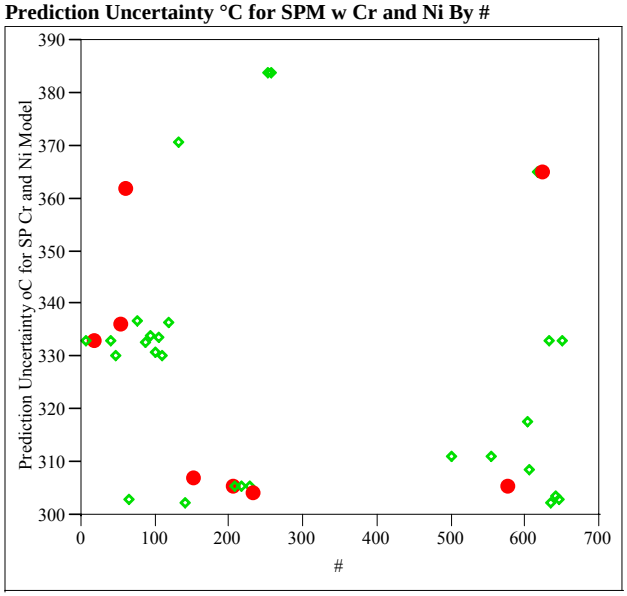

Prediction Uncertainty °C for SPM w Ni and Fe By #

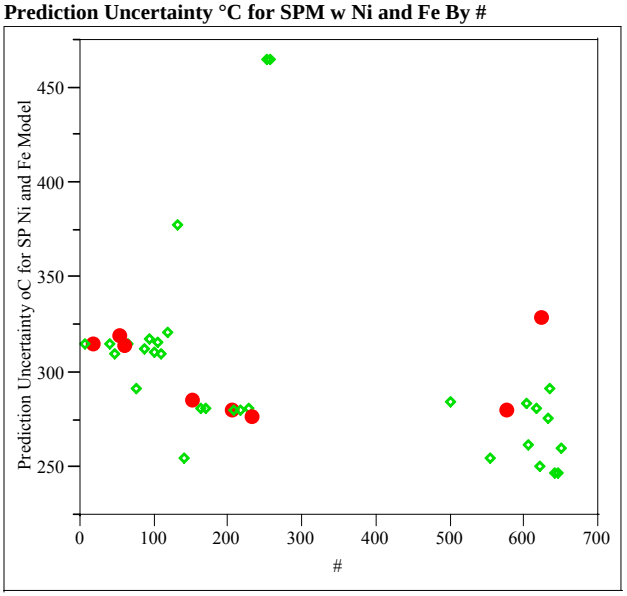

Residual °C for SPM w Cr and Ni By #

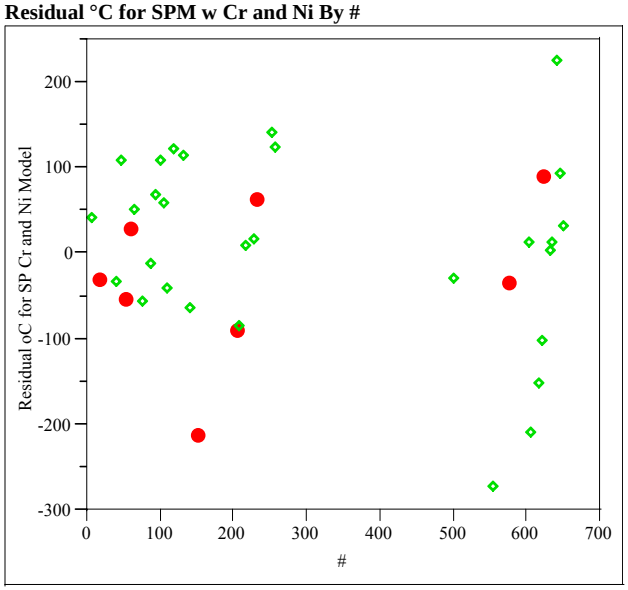

Residual °C for SPM w Ni and Fe By #

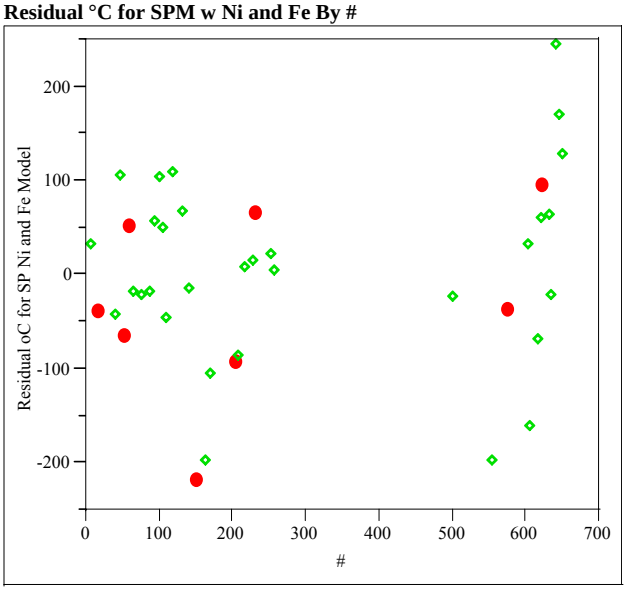

Appendix D. Model Fitting Results for T0.01 Data

Exhibit D.10: Residual and Uncertainty Plots for Data Group 4

Prediction Uncertainty °C for SLM By #

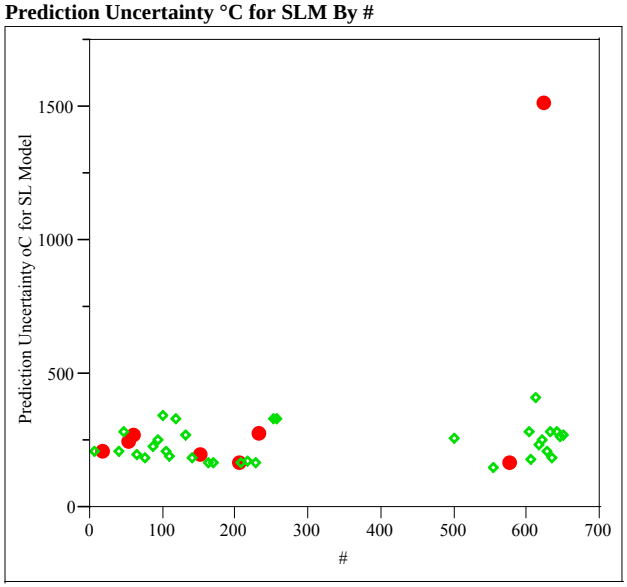

Prediction Uncertainty °C for LMM By #

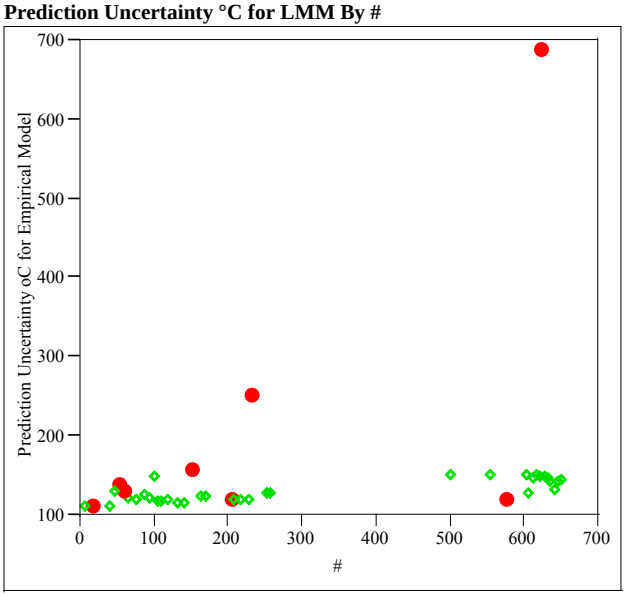

Residual °C for SLM By #

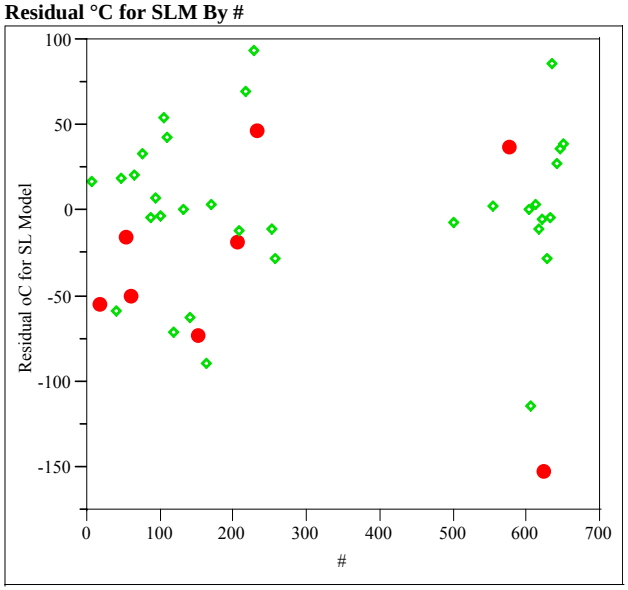

Residual °C for LMM By #

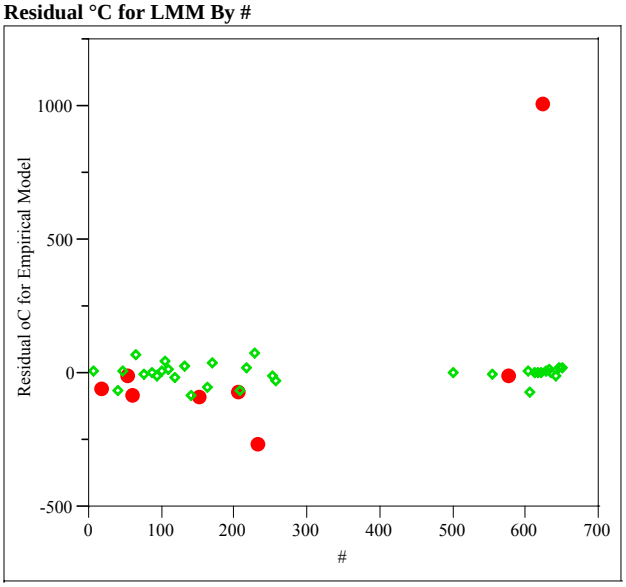

Appendix D. Model Fitting Results for T0.01 Data

Exhibit D.11: Residual and Uncertainty Plots for Data Group 5

Prediction Uncertainty °C for DWPFM By #

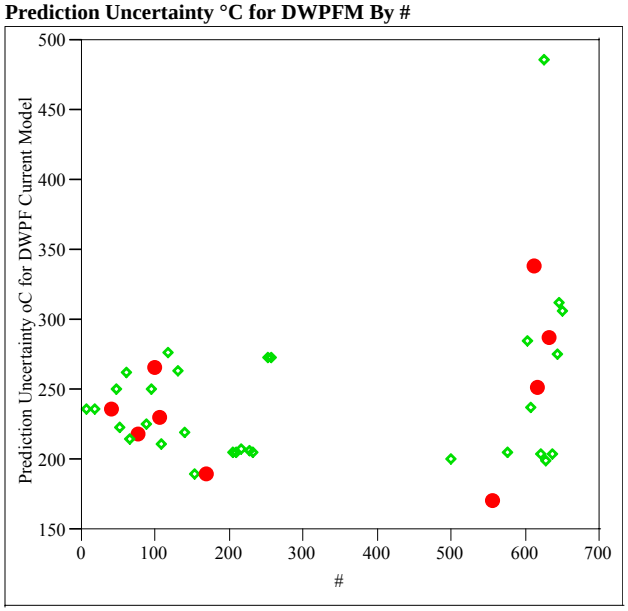

Prediction Uncertainty °C for IPM By #

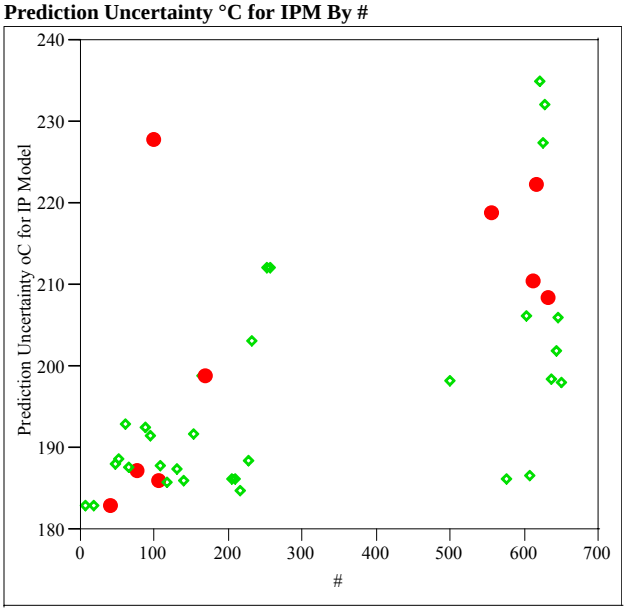

Residual °C for DWPFM By #

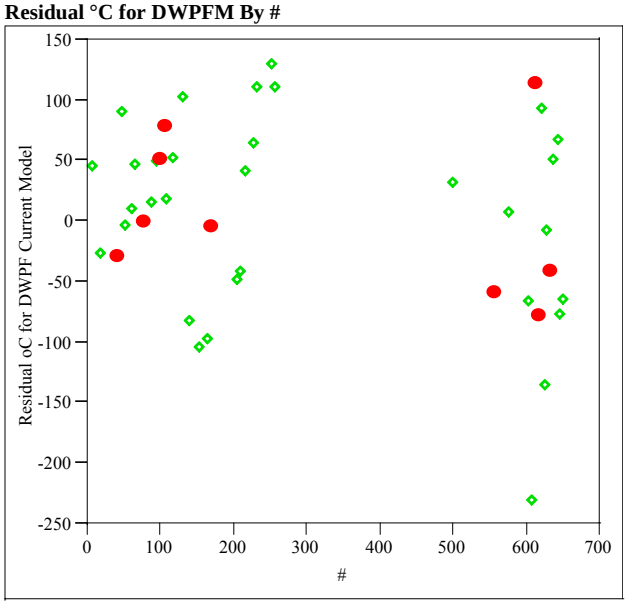

Residual °C for IPM By #

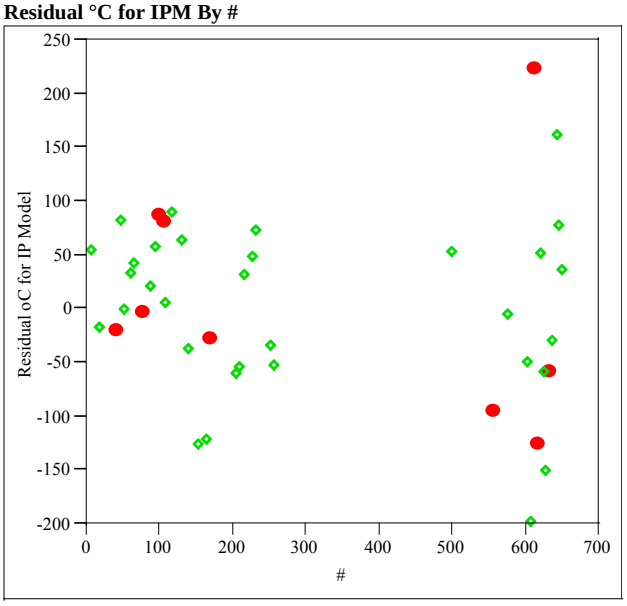

Appendix D. Model Fitting Results for T0.01 Data

Exhibit D.11: Residual and Uncertainty Plots for Data Group 5

Prediction Uncertainty °C for SPM w Cr and Ni By #

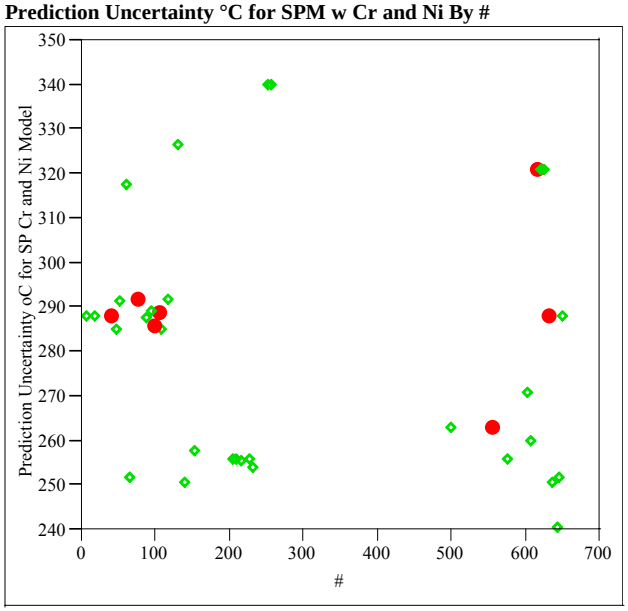

Prediction Uncertainty °C for SPM w Ni and Fe By #

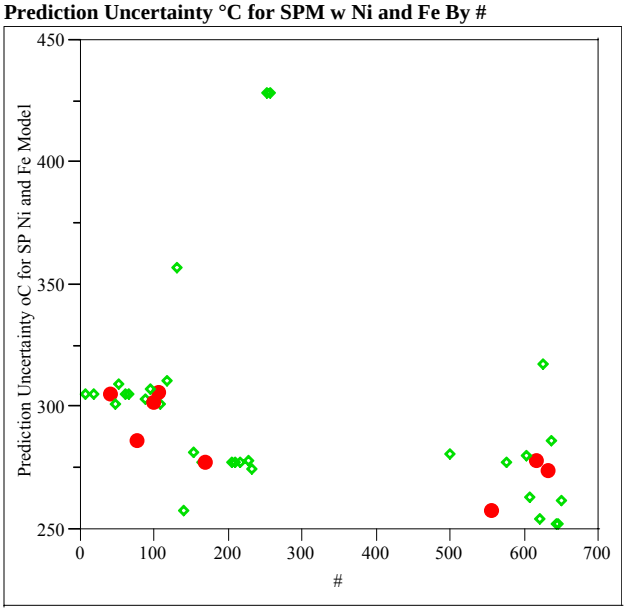

Residual °C for SPM w Cr and Ni By #

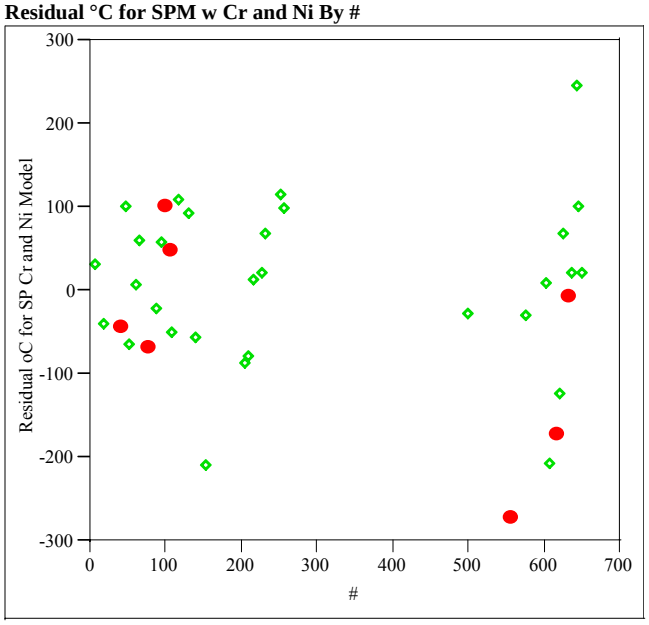

Residual °C for SPM w Ni and Fe By #

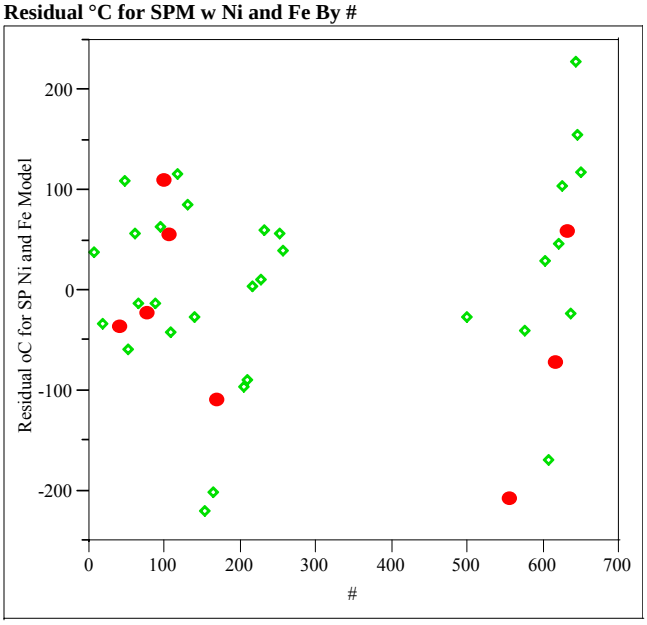

Appendix D. Model Fitting Results for T0.01 Data

Exhibit D.11: Residual and Uncertainty Plots for Data Group 5

Prediction Uncertainty °C for SLM By #

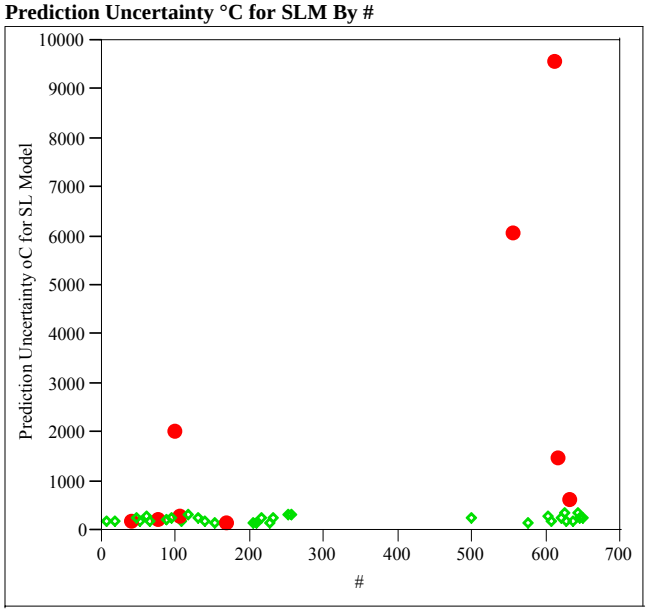

Prediction Uncertainty °C for LMM By #

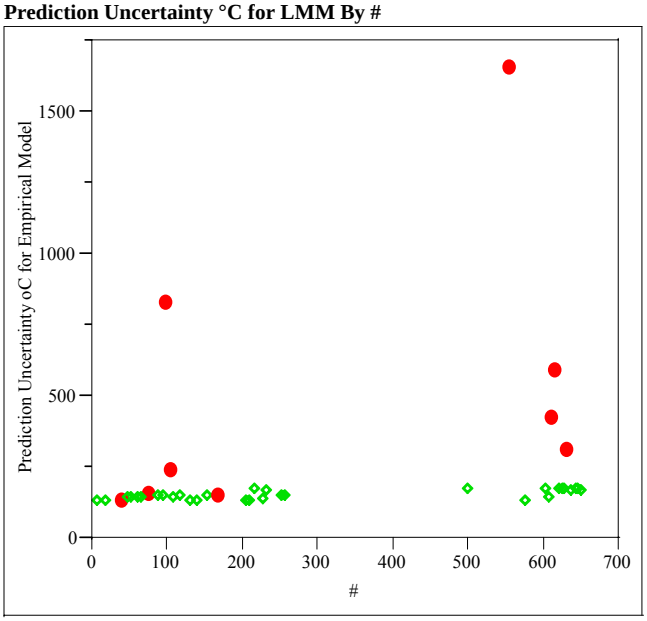

Residual °C for SLM By #

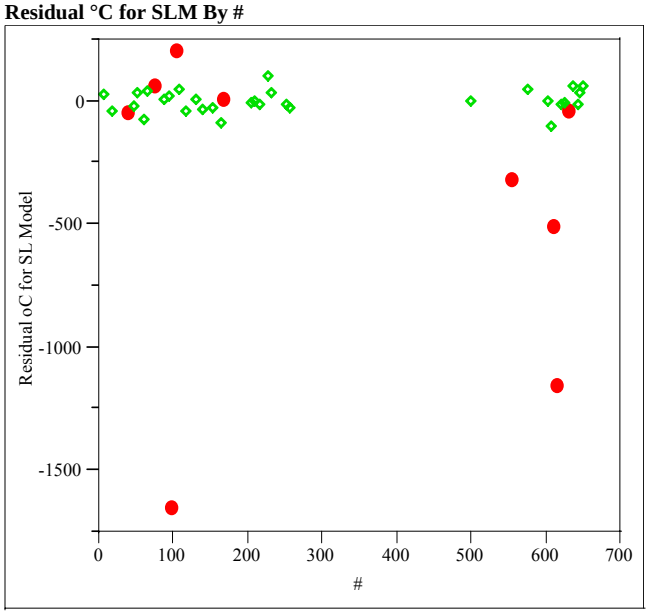

Residual °C for LMM By #

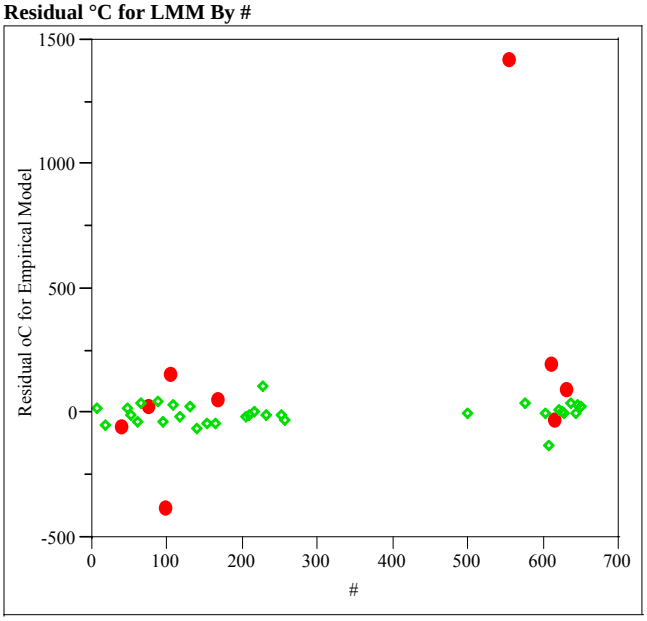

Appendix D. Model Fitting Results for T0.01 Data

Exhibit D.12: Comparisons of Performance Metrics

R2 by Data Grouping

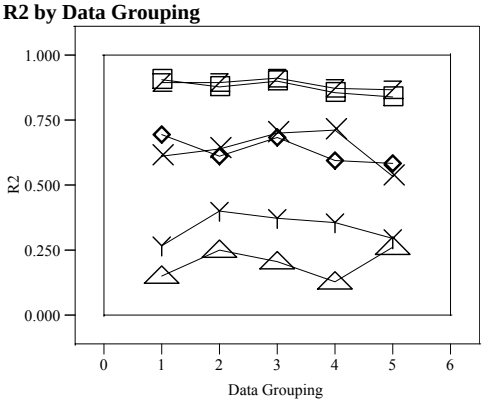

% Successfully Predicted (Model) by Data Grouping

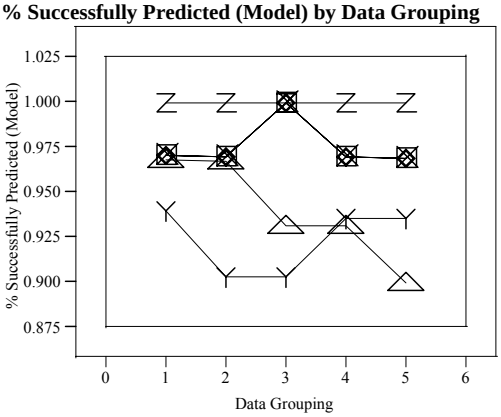

R2 val by Data Grouping

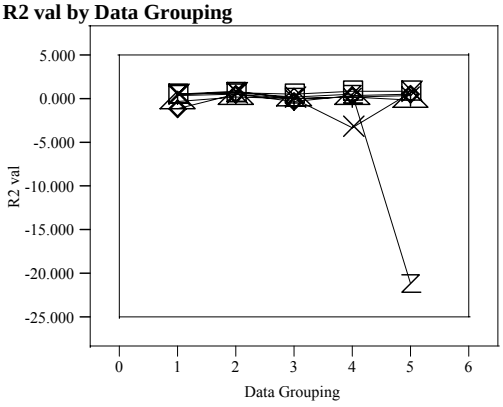

% Successfully Predicted (Valid) by Data Grouping

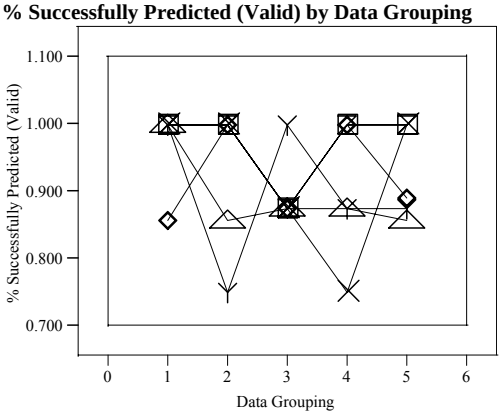

Avg Pred Uncertainty (Model) by Data Grouping

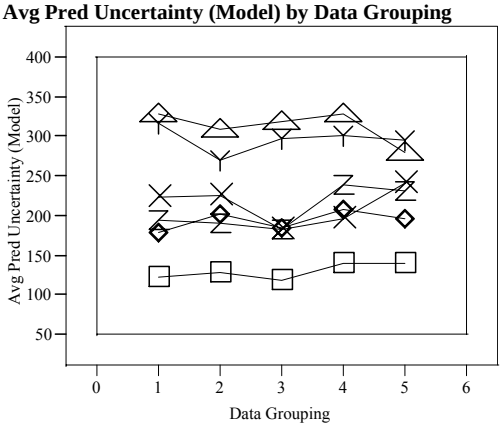

Relative, Uncertainty Weighted, Prediction Error by Data Grouping

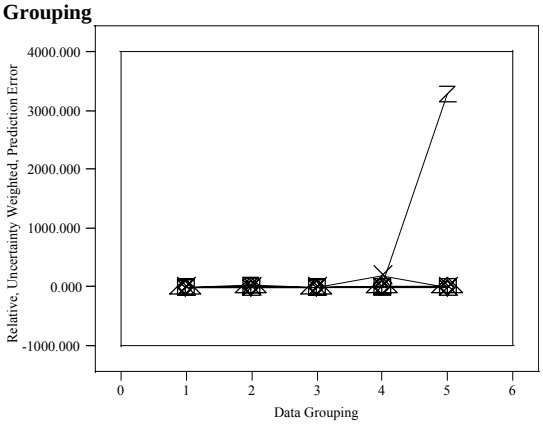

Avg Pred Uncertainty (Valid) by Data Grouping

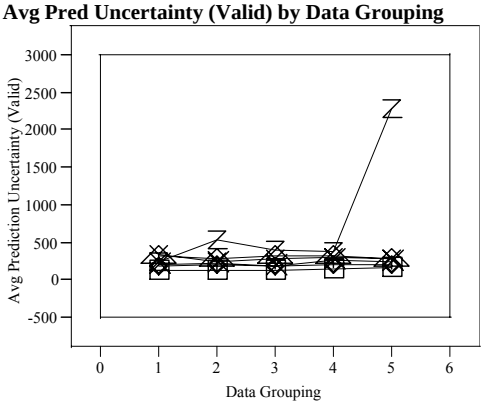

Y
- DWPF Current Model
- Empirical Linear Mixture Model
- Ion Potential Model
- Solubility Product (Cr & Ni) Model
- Solubility Product (Ni & Fe) Model
- Sub-Lattice Model

Distribution

No. of Copies

OFFSITE

4 Savannah River Technology Center

T. B. Edwards
PO Box 616, Road 1
Building 773-42A, Room 125
Aiken, South Carolina 29808

J. E. Marra
PO Box 616, Road 1
Building 773-43A
Aiken, South Carolina 29808

D. K. Peeler
Aiken County Technology Laboratory (ACTL)
PO Box 616, Road 1
999-W, Room 345
Aiken, South Carolina 29808

H. F. Sturm
PO Box 616, Road 1
Building 773-A
Aiken, South Carolina 29808

2 Vitreous State Laboratory

I. L. Pegg
The Catholic University of America
400 Hannoan, Cardinal Station
Washington, DC 20064

H. Gan
The Catholic University of America
400 Hannoan, Cardinal Station
Washington, DC 20064

No. of Copies

ONSITE

20 Battelle–Pacific Northwest Division

G. H. Beeman	K9-09
S. K. Cooley	K5-12
J. V. Crum	K6-24
P. R. Hrma	K6-24
E. O. Jones	K6-24
D. S. Kim	K6-24
D. E. Kurath	P7-28
J. Matyas	K6-24
G. F. Piepel	K5-12
B. A. Pulsipher	K5-12
D. E. Smith	K6-24
J. D. Vienna (5)	K6-24
Project Office (2)	P7-28
Information Release (2)	K1-06

6 Bechtel National, Inc.

S. M. Barnes	H4-02
J. F. Doyle	H4-02
C. A. Musick	H4-02
J. M. Perez, Jr.	H4-02
J. Reynolds	H4.02
J. H. Westsik, Jr.	H4-02